Aalborg University

Effect of Vertical Cyclic Load Characteristics on the Response of Suction Bucket Foundations

Structural and Civil Engineering
Master's thesis

Kristian Gordon Clausen

Nhivejen Thangaratnam

Redas Pilsudskis

Structural and Civil Engineering
Aalborg University
Hand in: 09-06-2022

Structural and Civil Engineering
Thomas Manns Vej 23
9000 Aalborg

AALBORG UNIVERSITY
STUDENT REPORT

Title:

Effect of Vertical Cyclic Load Characteristics on the Response of Suction Bucket Foundations

Education:

Structural and Civil Engineering

Assignment:

Master's thesis

Date for exam:

27-06-2022

Members:

Kristian Gordon Clausen 20174883
Nhivejen Thangaratnam 20191218
Redas Pilsudskis 20202089

Supervisors:

Amin Barari
Lars Bo Ibsen
Sorin Grecu

Page number: 306
Hand in: 09-06-2022

Abstract

Efficiency of current wind turbines are getting greater, letting it to harvest more wind energy which requires moving wind turbines further from the shore and wind farms are created all over the world, hence they should be able to survive several natural phenomenons. With that economical costs of conventional solutions rise along, here the suction bucket foundations on jacket structures has the possibility to become a cheaper solution.

The wind and wave forces acting on the wind turbine are converted into compressive and tensile forces through a 'push-pull' mechanism acting on the suction bucket. The understanding and knowledge of the suction bucket subjected to cyclic loading in deep waters are inadequate.

Throughout model testing this thesis aims to investigate the behaviour of the suction bucket foundation subjected to cyclic loading in dense sand. The experiments took place in a pressure tank to simulate water depth of 20 m. A variety of different cyclic loads and frequencies are tested to investigate the influence to the behaviour of the suction buckets.

It was found that force ratio and loading amplitudes has a significant impact to the way the suction bucket displace while loading frequency influence the build up of excess pore water pressure, which can lead to liquefaction of the soil. Moreover, it was noticed that cycling degrades the stiffness of the soil.

Preface

Reading guide

Tables, figures, equations are referred to in numbers, so that table 3 in chapter 1 is referred to as table 1.3. Equations are referred as following (2.3).

All references are made with the Harvard-method, ["Author","year"] and the reference list is arranged alphabetically after the authors last name. The appendix appears in the last part of the project.

The value of gravitational acceleration used in the report equals to $9.81\,\frac{\text{m}}{\text{s}^2}$.

All values for displacement are normalized by dividing with the diameter of the suction bucket, unless it is mentioned otherwise.

Aalborg University, 9th June 2022

Redas Pilsudskis
rpilsu20@student.aau.dk

Nhivejen Thangaratnam
nthang19@student.aau.dk

Kristian Gordon Clausen
kclaus17@student.aau.dk

Contents

Main Report

1 | Introduction

1.1 General

The demand of producing green energy has been in a exponential rise over last many years due to the severe climate changes, one of the most efficient ways of doing so is by harvesting wind energy through off-shore wind turbine farms, which are exposed to higher and more reliable wind throughout the year. According to [European Regional Development Fund, 2019] in 2015 the average water depth of offshore wind farms was 27.2 m and the average distance to shore was 43.3 km. in 2016, the average water depth rose to 29.2 m and the average distance to shore has also rose to 44 km. It is clear that the average water depth and distance to shore are expected to continue to increase in the future as it also can be seen in figure 1.1.

Moreover, by increasing the distance from the shore to the wind farm there is a bigger possibility of occurrence of severe natural phenomenon such as cyclones, tornado's or tsunami's which should be accounted for, while designing the turbines as they have to withstand massive loads from these events.

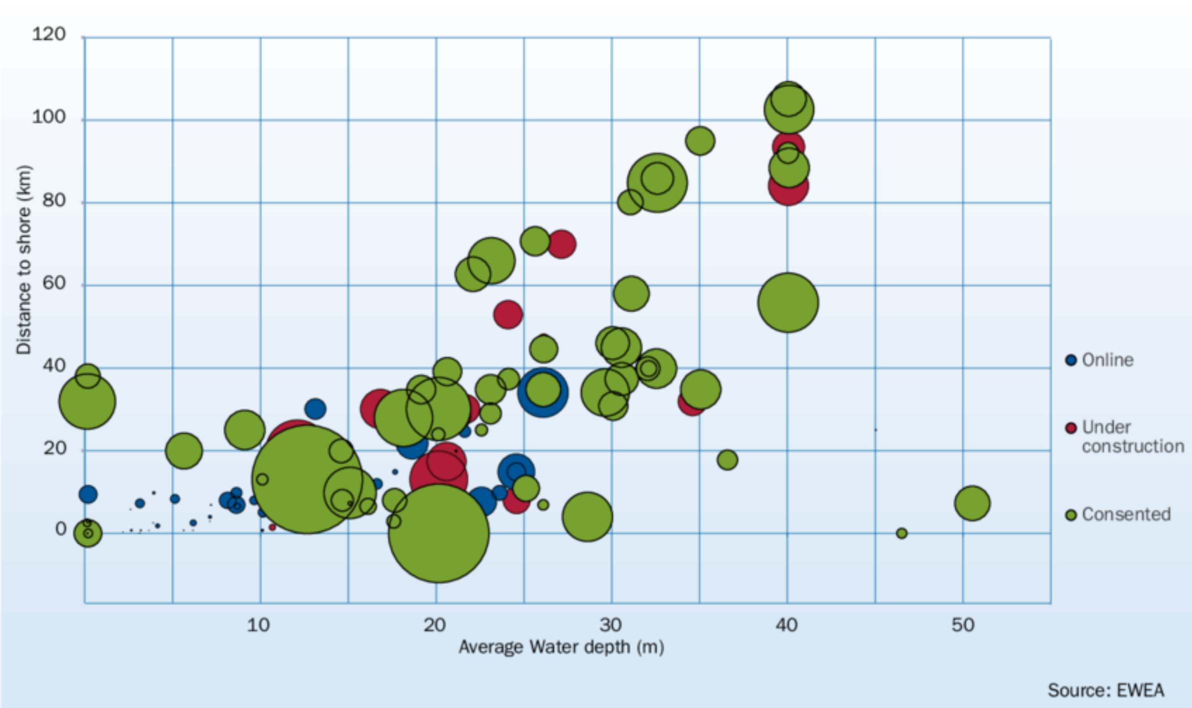

Figure 1.1: Average water depth and distance from the shore for current and planned wind farms [European Regional Development Fund, 2019]

The suction bucket could be an alternative solution for the foundation for the off-shore wind turbine in deep water, where the traditionally used monopile foundation is no longer considered to be most efficient. The suction bucket is an open bottom tube embedded in the seabed and sealed at the top. The suction bucket has various applications and has been used widely in the oil and gas industry, however it is not commonly used for wind turbines yet.

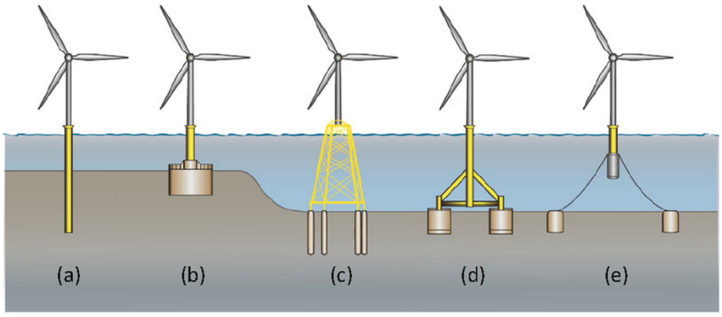

Figure 1.2: Wind turbine offshore foundations. Mono-pile (a), mono-pod (Suction bucket) (b), jacket structure (c), tripod (d) and floating wind turbine with anchors (e) [Amir M Kaynia, 2018]

As seen in figure 1.2, suction buckets have the abilities to work as a foundation at various water depths either as a rigid foundation or as an anchor to floating wind turbines.

1.2 Loading conditions

During this project example of usage of suction bucket foundations with a jacket structure is investigated. Such setup is presented in figure 1.4.

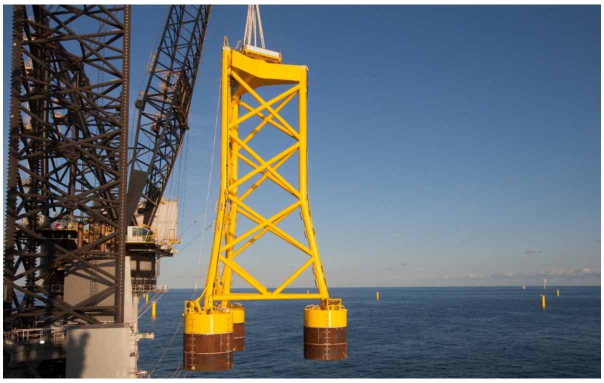

Figure 1.3: Suction bucket jacket foundation. [M.O.C., 2017]

The response to the loading of a suction bucket jacket structure is illustrated in figure 1.4

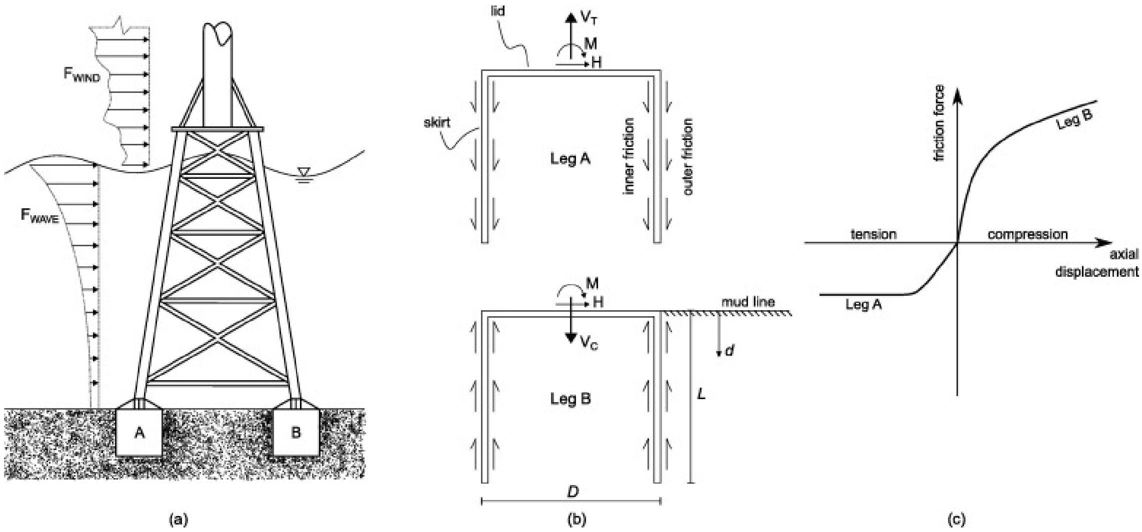

Figure 1.4: (a) Schematic elevation of a four-legged jacket structure resting on suction buckets; (b) Skin friction contribution to the stability of the system; (c) The loading direction plays a major role in the frictional behaviour of suction buckets. [Grecu et al., 2021]

As it is seen from figure 1.4 lateral environmental loads acting on the structure are converted into axial loads on the suction buckets and "push-pull" mechanism is observed.

1.3 Problem statement

The suction bucket foundation has started to be more and more interesting while designing offshore wind farms in deep waters instead of traditionally used solutions, thus a deeper understanding of its behaviour is essential. For the suction bucket in jacket structures most concerning forces are combination of tensile and compressive loads under cyclic loading, during "push-pull" mechanism, which raises the question:

"How does the behaviour of suction bucket foundations for offshore wind turbines on jacket structures in dense sand influenced by cyclic loading with different force ratios and frequencies? More specifically, is stiffness degradation due to cycling expected, which loading rate of high or low frequency is more damaging and can the initiation of soil liquefaction be expected due to build-up of excess pore water pressure if such happens at all? "

2 | Literature Review

2.1 Current knowledge

Suction bucket in offshore structures

The state of the art knowledge concerning suction bucket foundation in offshore structures, is applied from the oil and gas industry as it has been used in those structures for over 20 years [Low et al., 2020]. As Kelly et al. [2006] mentions, even though monopiles are the preferred option and are widely used, as the wind farms are moving more and more into deep waters, alternative options for the foundations are considered, hence the suction bucket on a jacket structure or tripod, as is could reduce the total cost of the installation of an off-shore wind turbine.

Opposed to the structures for the gas and oil industry, Ibsen et al. [2005] states that the structure of a wind turbine are relative light-weighted compared to their size and to the oil and gas structures, thereby the the vertical load is no longer the dominant force, instead the horizontal and overturning moments from wind and waves are the significant ones. As Kelly et al. [2006] explained that the superstructure of the turbine is very sensitive to dynamic load therefore the stiffness can be increased by used multiple footings for the support structure, the use of multiple suction bucket, for instance on a jacket structure the overturning moment is converted into a vertical 'push-pull' mechanism and as Byrne and Houlsby [2003] underlines it the variation of the vertical cyclic loading, which is most important.

Drained condition

Vaitkunaite [2016] explains that in drained conditions the tensile capacity of the suction bucket is determined by the self-weight of the entire structure and the frictional resistance of the inner and outer skirt of the bucket. Houlsby et al. [2005] also underlines that in the drained phase, it is assumed the lid of the bucket lose contact with the soil, and the tensile capacity can be calculated as a fully drained state when the tensile force is applied with a low rate.

Thieken et al. [2014] and Senders [2008] further explain that during the pull up movement a gap between the soil and lid is created, underlining the statement from above, that the resistance from the bucket solely comes from the skirt.

Vaitkunaite [2016] states that the drainage conditions of the soil depends on the size of the bucket, soil permeability and loading intensity.

Undrained condition

Opposed to the drained condition Thieken et al. [2014] explains for the perfect undrained condition the gap does not occur between the soil and lid of the bucket like in the drained condition, on the contrary a plug is formed in the bucket which affect the soil in around the bucket increasing the resistance, Senders [2008] states this increase in resistance as ´reverse end bearing´. this increased tensile capacity is far larger than the drained, but are limited by the cavitation of the pore fluid. Low et al. [2020] investigated the importance of loading frequency and drainage response, and how it influenced the capacity of the suction bucket. For a drained monotonic uplift loading he explains that the uplift capacity is low, but if the uplift happens in a higher rate relative to the pore pressure dissipation hence undrained behaviour a significantly increase in the uplift capacity is seen. he further explains that when looking at a off-shore wind turbine the limit for the uplift capacity is likely limited by cavitation.

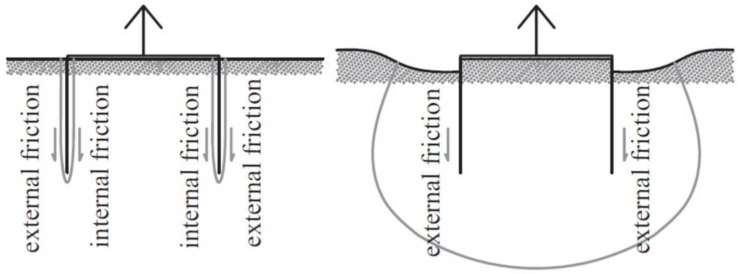

Figure 2.1: Tensile resistance in cohesionless soil: (left) drained response; (right) undrained response. [Vaitkunaite, 2016]

Influence of Cyclic loading and excess pore water pressure

Low et al. [2020] mentions when cyclic loading subjected to the bucket the reduction of the capacity can come from other mechanisms than for the monotonic. For a cyclic loading with low frequency where the pore pressure can dissipate or if it is a drained state, the maximum load subjected to the bucket are limited by drained uplift capacity or the settlement caused by reduction of the soil volume beneath the soil. Low et al. [2020] further explains for a higher frequencies the load might be limited by accumulation of pore pressure which result in shear-induced displacements. He hypothesizes that there is an intermediate zone, where the frequency allows partial drainage for some of the pore pressure to dissipate between the peaks of loading leading to a higher cyclic capacity.

Secant stiffness

G.T.Houlsby [2016] compared secant stiffness development for several scenarios of different amplitude one-way cycling. He argues it was expected that the smallest amplitude of cycling gave highest secant stiffness. However, research showed that secant stiffness increased during the cycling contrary to the conventional wisdom that cyclic degrades the performance of a soil. He argued this phenomena by medium density of sand and slight densification of the sand. This knowledge is of crucial importance since decrease or an increase of stiffness can be important while investigating resonance of the entire structure.

Pulling speed

[Tardio and Moldovan, 2021b] authors states that different failure mechanisms were observed with respect to the the change in pull-out speed. During the slow movement only a frictional failure with no visible volumetric strain were observed. However, with higher speed a so called "soil plug" were noticed which lead to significant volumetric strains. Same conclusion was made by G.T.Houlsby [2016] after he tested equivalent tests with different pulling speeds. During the test with high pull-up speed vertical stresses were way higher compared to the ones done at low speeds. He explains it as negative excess pore pressure are developed rapidly underneath the caisson, so the tensile capacity is limited by cavitation of the pore fluid underneath the caisson. These observations can be used for this project making a hypothesis that cycling with higher frequency will lead to a smaller displacements of suction bucket compared to the same cycling with lower frequency.

Effect of cyclic loading frequency

During the investigations published in [Yilmaz and Tasan, 2021] on suction bucket behaviour under cyclic axial compressive load, the effect of cyclic loading frequency was considered. One of the part of investigation was effect of cyclic loading frequency to the behaviour of suction bucket foundations. Several scenarios were performed with frequencies of 0.05 , 0.10 and 0.20 Hz while keeping the loading, soil and bucket parameters the same. It was concluded from the excess pore pressure diagrams that high cyclic load frequency results in higher pore pressure development due to less time interval for dissipation. Moreover, findings shows that the largest displacements were obtained for loading frequency of 0.20 Hz.

Effect of aspect ratio L/D

In publication [Yilmaz and Tasan, 2021] influence of the bucket diameter and skirt length to the displacement was proven. As the length of skirt decreased, the bucket response shifted towards progressive failure, whereas the long skirted bucket showed a shakedown-like behaviour. That was explained by the total load share of skin friction was increased and shares of the top plate and skirt tip were decreased as skirt was elongated.

Effect of initial relative density of the soil

During the studies published in [Yilmaz and Tasan, 2021] it was observed that initial relative density of the soil have crucial importance to the displacement behaviour. Results showed that as the relative density decreased, the bucket response shifted toward progressive failure, whereas in dense soil, it shifted towards shakedown behaviour under the same loading.

Further studies

[Yilmaz and Tasan, 2021] study is done for extreme events with large cyclic amplitudes and only with 12 cycles. Author says that such testing is not accurate for estimating behaviour for tens or hundreds of cycles, so the findings should be verified by the experimental tests. Moreover, he suggested that the effect of initial state after installation effects should also be studies

Hypothesis for further studies

- It is expected that soil stiffness is influenced by cyclic load frequency and ratio between forces.
- It is expected to obtain more severe displacements from cyclic loads with low frequencies due to dissipation of excess pore water pressure compared to loads with high frequencies.
- It is expected that certain ratio between compressive and tensile loading will lead to critical displacements.

2.2 Laboratory tests

This thesis investigates the behaviour of the suction bucket on a laboratory scale. It is important to understand and investigate other papers and their methods of testing in a laboratory.

The paper by Low et al. [2020] is based on a series of centrifuge tests simulating a prototype water depth of 24 m, performed on a suction bucket with a diameter of 80 mm, a skirt length of 40 mm and with a wall thickness of 0.5 mm. The soil samples were 'super-fine' silica sand with a relative density of 80%. After installation the testing procedure consisted of 400 cycles of ±6 kPa precycling stage with the average stress of 120 kPa to simulate the situation on the bucket before a design storm. Before starting the "severe event" and applying the cyclic load the stress was held constant at 120 kPa to allow the dissipation of induced excess pore pressure. The cyclic load history was semi randomly generated, having the larges load cycles in the middle of the history and the next largest loads on either side of the middle to simulate a ramp-up and -down situation. The maximum cyclic stress amplitude varied from 100 to 260 kPa and the frequency varied from 0.1 to 0.6 Hz. It was concluded that the displacement and stiffness response to the cyclic loading is highly dependent on the frequency and there by the drainage conditions and the average- and cyclic-stress level. The findings showed that the situations with the highest displacement and lowest stiffness occurred when the bucket were subjected to a low (quasi-drained) or high (quasi-undrained) cyclic load frequency. And additionally under favorable drainage conditions and high cavitation pressure limit the bucket could potentially withstand two-way loading with minor displacements with tension loads at approximately zero average stress.

Kelly et al. [2006] tested a suction bucket with the diameter of 280 mm, skirt length of 180 mm and a wall thickness of 3.125 mm in a pressure tank where tests were carried out at atmospheric pressure and atmospheric pressure plus 200 kPa of pressure was added to simulate 20m of water depth. Two soil types were used Redhill 110 with a relative density from 80 to 89 % and HPF5 with a relative density of 53 to 73 %, to explore the effects of drainage on the foundation. 10 cycles were used for each packet with a range of amplitudes from 10 to 80 kN, and the 3 different frequencies were used 0.1 Hz, 1.0 Hz and 10 Hz. Kelly et al. [2006] concluded that the positive pore pressure beneath the suction bucket increased when the rate of cyclic loading increased, and so does the vertical stiffness. Additionally it was found that the ambient pressure have either very little or nothing to do with the deformations during cycling, however the the ultimate tensile capacity is affected by the ambient pressure in such way that a relative pressure increase also results in higher tensile loads needed before cavitation occurs.

Vaitkunaite [2016] deals with two experimental setups in the paper, the first one also called the 'Large yellow box' two buckets were used with diameter of 1.0 m and the skirt lengths of 0.5 and 1.0 m and with a wall thickness of 3.0 mm, Aalborg University sand No. 1 was used and with a relative density of 85%. The purpose of this test was to see the behaviour of the suction bucket when subjected to axial tensile loading, and consisted of two parts. the first was a slow pull-out test which were done right after installation, with a rate of 0.002 mm/s. And the second part of the tests consisted of 20.000 - 40.000 harmonic cycles with a frequency of 0.05 to 0.1 Hz, at the end of the cyclic test a monotonic tensile load was applied to show the level of cyclic degradation. Effective stresses were added by applying a latex membrane to close the tank. In the monotonic loading tests showed that drained tensile capacity and peak resistance is reached at a upwards displacement of 10 mm. further more higher membrane pressure resulted in higher

peak resistance. [Vaitkunaite, 2016] noticed that for the cyclic tests, mean loads up to 50% of the tensile drained capacity could be applied without any significant displacements, still all the tests with a mean tensile load resulted in small upwards displacements. and the model was experiencing gradual pull-out when the peak loads reached the drained tensile capacity. For both cyclic and post cyclic tests stiffness hardening was noticed.
The second experiment was performed in a pressure tank with a suction bucket with a diameter of 0.5 m and a skirt length of 0.25 m, the same soil as the 'Large yellow box' experiment was used. The tank was pressurized until it reached 200 kPa. 15 tests were conducted with several pull-out rates from 0.01 to 152 mm/s. [Vaitkunaite, 2016] commented that tensile capacity was correlated to the pull-out rate and values for the tensile capacity were significantly larger than the drained tensile capacity from the design limit.

In paper [Houlsby et al., 2005] theory for predicting the capacity of a suction caisson in sand, when it is subjected to rapid tensile loading is compared to data obtained from conducting experiments in pressure chamber, with both atmospheric and 200 kPa pressures. The model caisson was 280 mm diameter and 180 mm skirt length. Obtained results proved that capacity depends critically on the rate of pullout and the ambient water pressure which determines whether cavitation occurs.

Scaling consideration

When performing a small scale laboratory test it is of crucial importance to be able to scale the findings to the real life model size. To do that, scaling law is needed.

An equation has been derived from 1D consolidation theory created by Kelly et al. [2006] in order to deduce the behaviour of the field test model from the small scale model. The theory accounts for parameters which influences the transient capacity (Period of loading, permeability of soil, drainage distance path). Equation (2.1) provides relations between the field model and laboratory scale model

Scaling

$$\frac{k_m}{k_p} = \frac{t_p}{t_m}(\frac{D_m}{D_p})\frac{3}{2} \tag{2.1}$$

Where:

k_m, k_p	Permeability of sand for model and prototype	[min (m/s)]
D_m, D_p	Diameter of model and prototype caissons	[mm]
t_m, t_p	Period of loading for model and prototype	[Hz]

3 | Test Preparation

This chapter consist of information regarding equipment used to perform the tests and preparation for them.

3.1 Test setup

Equipment

The testing takes place in the geotechnical engineering laboratory at the Department of the Built Environment of Aalborg University with the use of the pressure tank.

Schematic view of the pressure tank which was used during the physical experiments can be seen in figure 3.1 bellow and more detailed description of it can be found in appendix A.

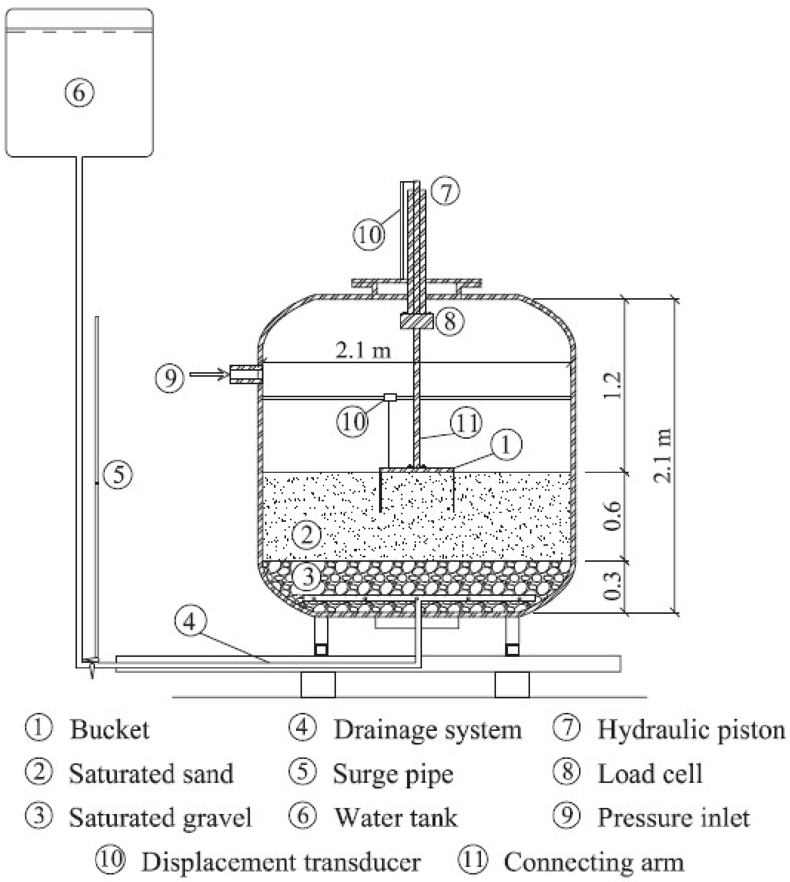

Figure 3.1: Scheme of the pressure tank

The pressure tank is filled with a 0.3 m layer of gravel which ensures a free water flow following by a filter layer and a 0.6 m thickness layer of Aalborg sand which properties can be found in appendix A.

Suction bucket which was used during this project:

- Stainless steel bucket with a skirt length L of 0.5 m and a diameter D of 0.5 m.

The bucket have two valves on the lid, which are kept open during installation in order to let the air between the inner side of the lid and sand surface dissipate. After the installation part valves were being closed. Furthermore, bucket is equipped with transducers at different level on both outer and inner sides to measure the pore water pressure which is elaborated in Section 3.2.3. Scheme view of bucket is presented in figure 3.2 below:

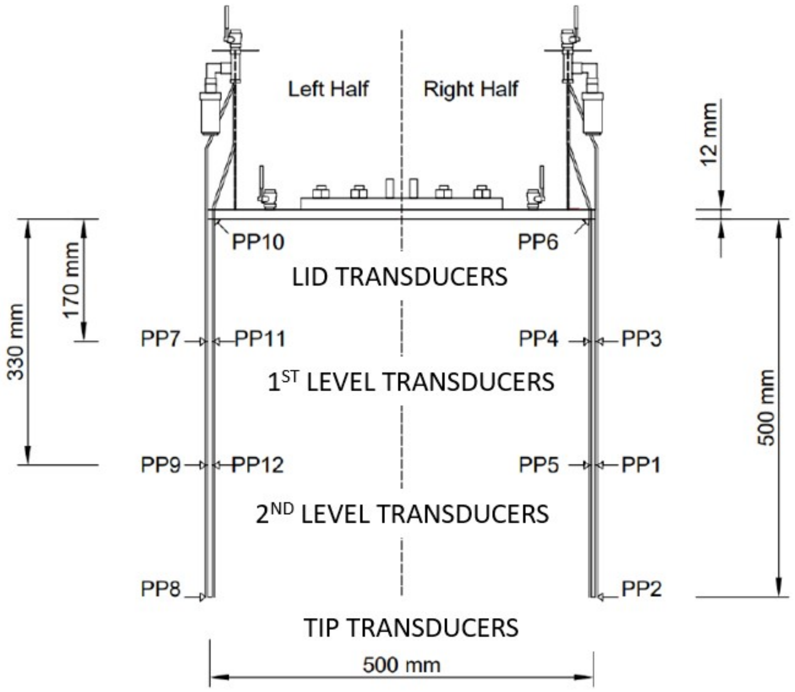

Figure 3.2: Scheme of the suction bucket

3.2 Preparation

3.2.1 Soil preparation

Soil preparation is a crucial part of the performed experiments. A paper published by ISSMGE investigate the in situ relative density (D_R) in the northern sea, using CPT data. The paper finds that the D_R is somewhat in between 60 and 110% [for Soil Mechanics and Engineering, 2016]. Furthermore, according to [Roy and Bhalla, 2017] sand with a relative density of at least 80-90 % is classified as dense sand. To keep consistency of the experiments, it is decided to work with a relative density with a average value of at least 80% for every experiment. Working with similar D_R ensures a better possibility of investigating how various frequencies, amplitudes and force changes can affect the performance of the suction bucket.

A vibration study of different possible vibration patterns in the pressure tank has been performed in order to determine a vibration pattern which provides D_R within the wanted interval. It is found that pattern of vibrating each hole next to each other gives the highest D_R after a single round of vibration. Therefore it is decided to use this pattern for further tests. Appendix B explains details and elaborate results for the performed vibration investigation.

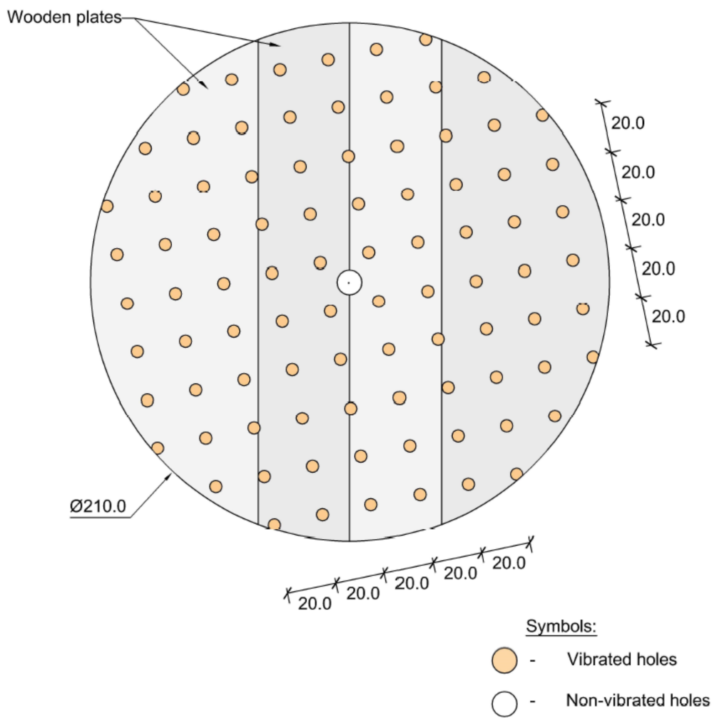

Figure 3.3: Vibration of each hole

Figure 3.4 shows the probability density of each relative density D_R for all the tested patterns. Even though CPT tests were evaluated by looking at D_R against soil depth, this comparison here was chosen for a better visual representation properties of all 4 studies.

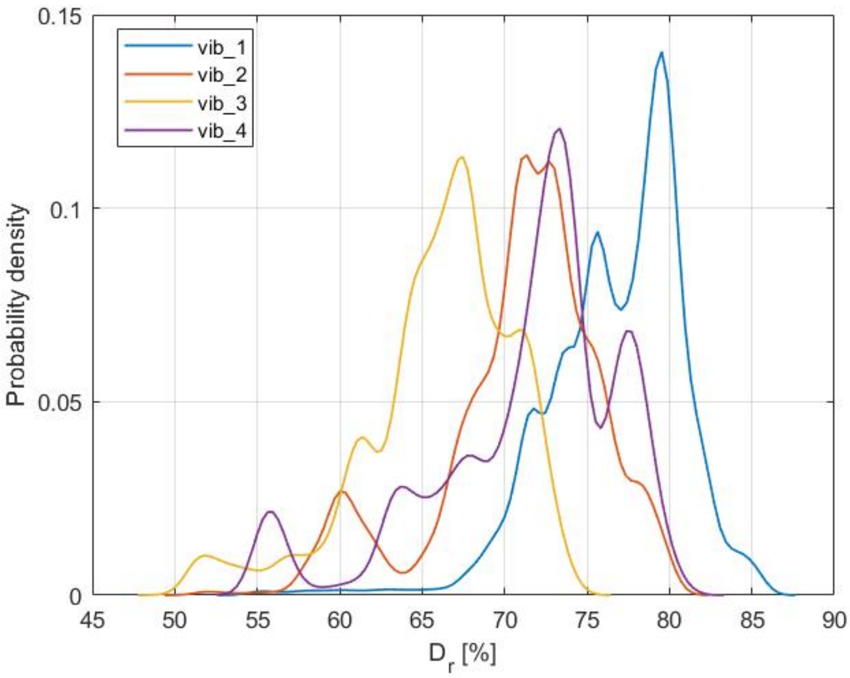

Figure 3.4: Distribution for relative density.
Vib_1: vibration of every hole once.
Vib_2: vibration of every second hole once.
Vib_3: vibration of third hole once.
Vib_4: vibration of third hole twice

As it is seen from the figure 3.4 with one round of vibration in each hole peak D_R of approximately 78 % is achieved. Therefore,it is decided to vibrate every hole twice to ensure a relative density of 80-90 %.

3.2.2 CPT

To ensure the necessary relative density of at least 80% is obtained 12 CPT tests spread over the area of the tank have been carried out. Figure 3.5 shows the exact locations of the CPT.

The tip of the CPT cones are lowered until they are just above the water and then zeroed, so only the resistance of the soil is recorded. Once the CPT's are reset they are manually lowered so the tip of the cone in submerged into the soil, as the top 70 mm of the layer of the soil is neglected due to uncertainties such as uneven soil level and loose sand.

The conventional CPT penetration rate is 20 mm/s, but as the CPT's used for the experiments are not of conventional dimensions, the formula to analyze the CPT readings where calibrated by Ibsen et al. [2009] and resulted in a penetration rate of 5 mm/s

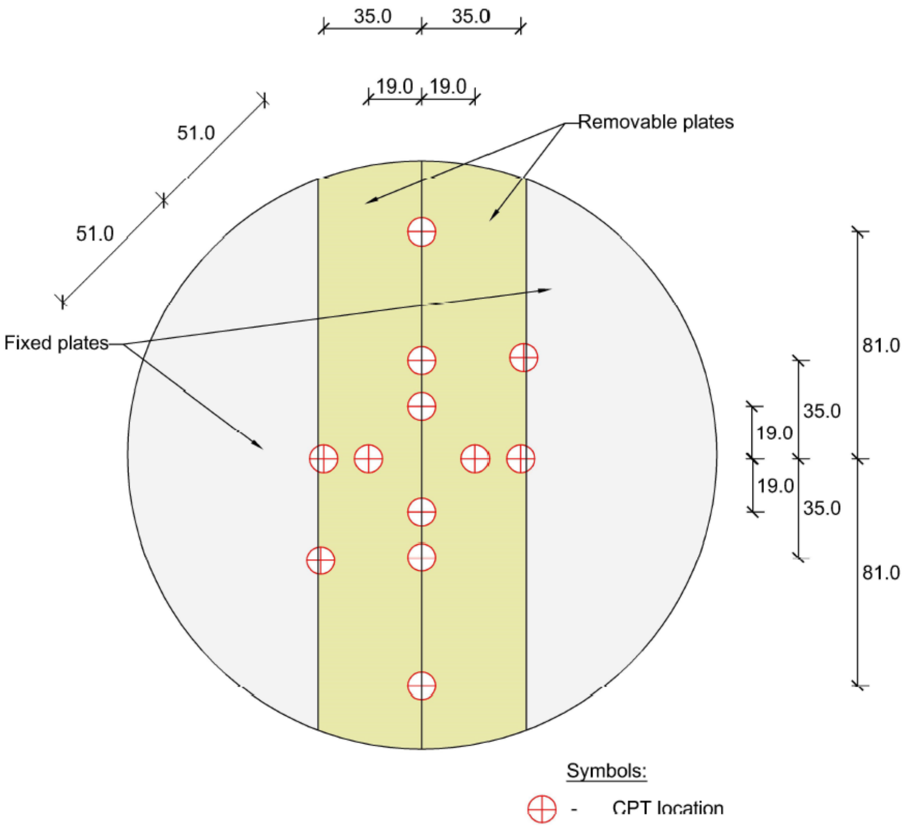

Figure 3.5: CPT locations

As seen in figure 3.5 various locations are selected for the 12 tests only restricted by the steel beams and fixed plates in the pressure tank. Most of the location are chosen to be near the bucket both in- and outside the skirt to ensure a uniform soil before a test is conducted.

Once all 12 CPT test have been performed two plots are made illustrating the distribution of the relative density and the relative density along the depth.

The peak of the distribution is wanted between 80-90% for the soil to be classified as dense, as mentioned in section 3.2

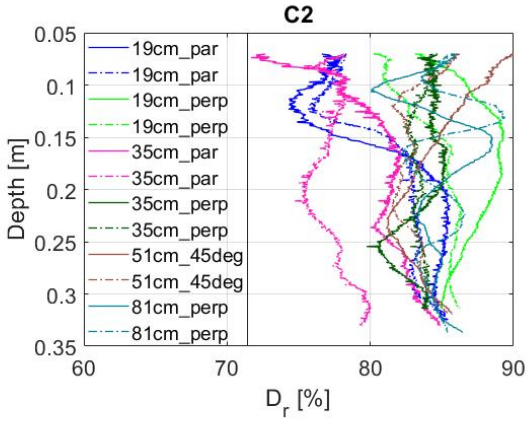

(a) Relative density over depth

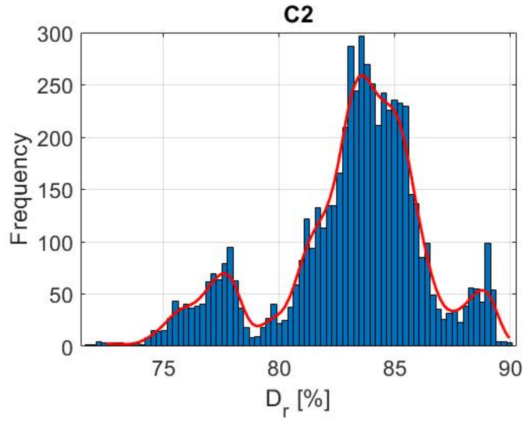

(b) Normal distribution of relative density

Figure 3.6: CPT data presenting

3.2.3 Bucket / Tank preparation

Transducers

Transducers are placed on the top of the bucket which are measuring the pore water pressure. Pipes run from the top of the bucket, above the transducer, and down along inside and outside the skirt of the bucket at different lengths and two transducers just below the lid. The exact placement of the transducers are shown in figure 3.7. Before the first test was conducted all the transducers were calibrated, the procedure for this can be seen in appendix A.8

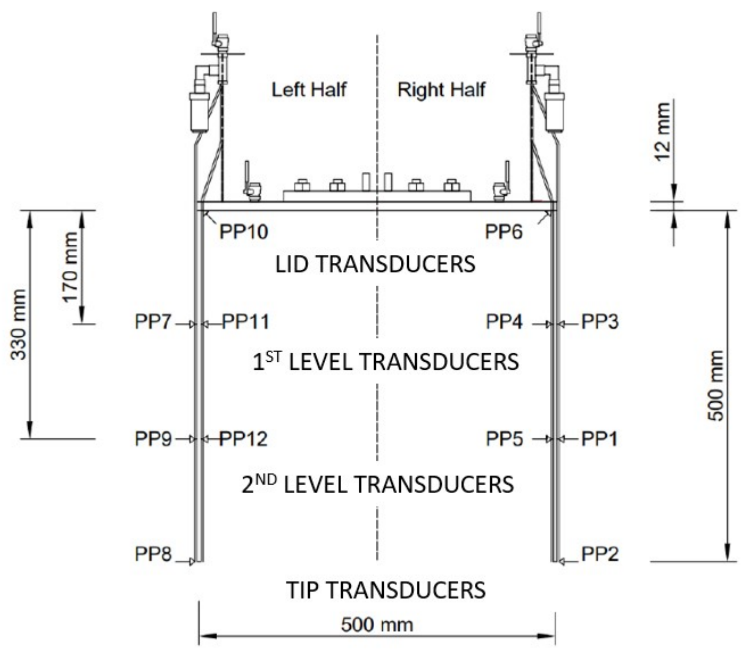

Figure 3.7: Transducers on bucket

Saturation

Once the transducers are attached, they are ready to be saturated, which is necessary to have correct readings and in that process it is checked if they are perfectly sealed on the bucket. All the valves for the transducers are opened and the bucket is submerged into water until the tip of all pipes are submerged thus water can flow through the pipes as shown in figure 3.7 and the transducers to the top end of the pipes. A transparent vacuum tube is then connected to the top end of the pipes creating the flow of water through the pipes, if any bubbles are detected in the transparent tube, the transducer needs to be re-sealed, if the transducers are perfectly sealed, the valves are closed and the saturation of the transducer is complete the bucket can be lifted into the pressure tank by crane.

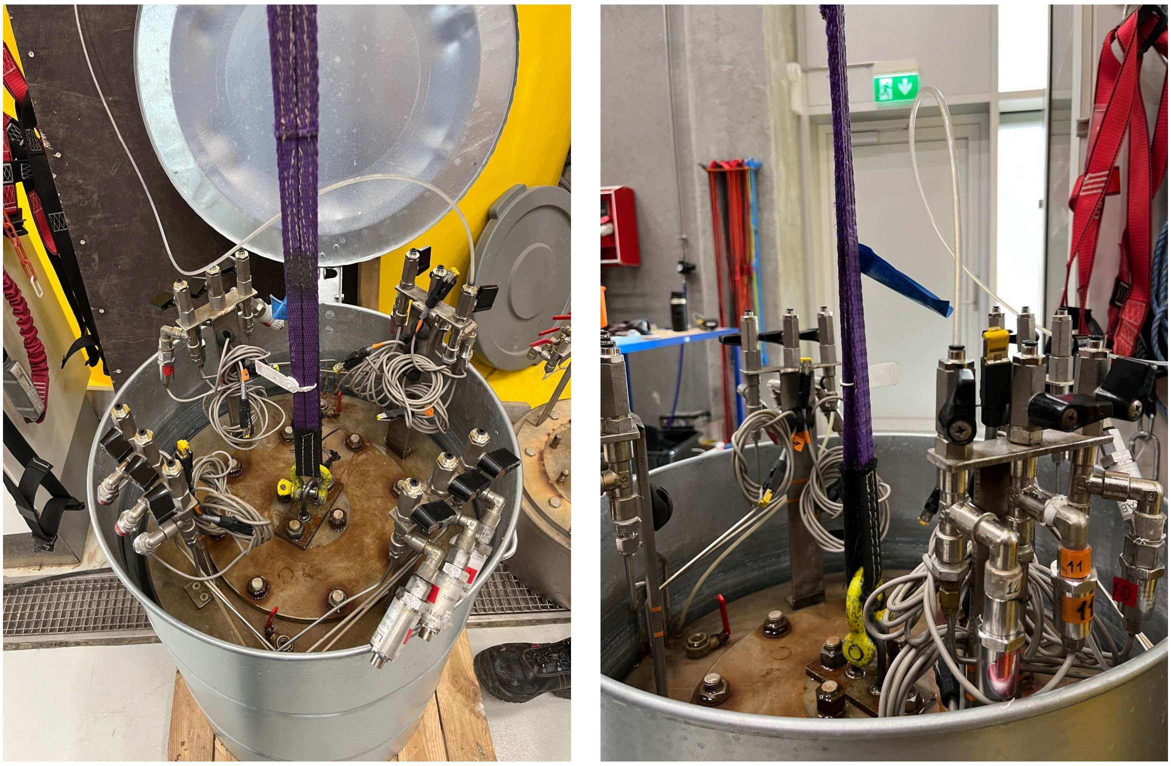

(a) Bucket submerged in water (b) vacuum tube for saturation of transducers

Figure 3.8: Transducers saturation process

Installation

After the bucket was saturated, the installation part began. The installation procedure were two fold and are explained as installation part 1 and 2.

Figure 3.9: Suction bucket

Installation Part 1

The first part of installation starts with attachment of the load cell, for that a 250 mm extension piece is attached to the piston where on the load cell is attached, to ensure the load cell is calibrated correctly a bolt is screwed on the cell and it is zeroed so the reading shows 0.0 kN, afterwards a 10 kg plate is placed on the bolt and if calibrated correctly the reading from the load cell shows −0.098 kN. The bucket is moved into the tank by crane. The footing is connected to the load cell where on the bucket can be attached. Once the footing is attached the load cell is zeroed, so only the weight of bucket is applied, when the bucket is attached the load cell should read −0.6 kN (self-weight of the steel suction bucket), before the first part of installation starts the transducers are connected and zeroed furthermore the valves on top of the bucket are open at the top to make sure air in the bucket can get out, and minimize the disturbance of the soil.

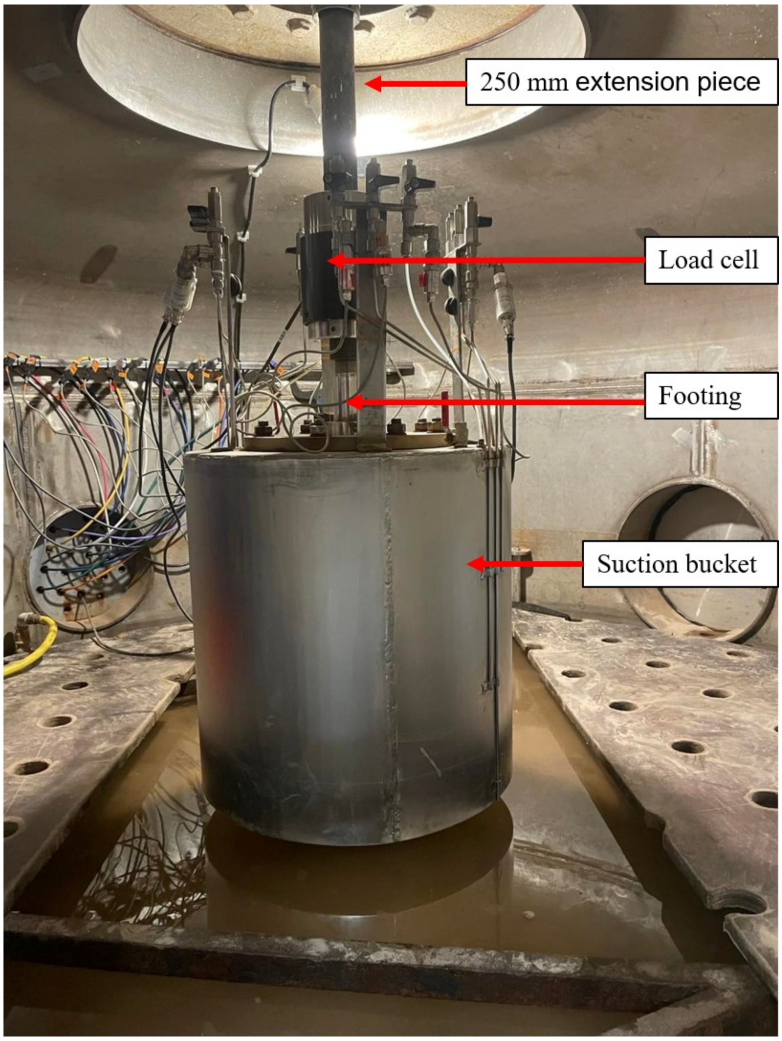

Figure 3.10: Setup before installation part 1 is started

During the first part of installation the following are connected to the piston: 250 mm extension piece, load cell, footing and bucket as seen in figure 3.10. Then the bucket was submerged into the soil as far as possible with a rate of 10 mm/s.

Installation Part 2

For the second part of installation the footing detached from the bucket and the piston is moved all the way up, and another extension of 200 mm is connected in between the load and the footing. The load cell is again zeroed before connecting it to the submerged bucket, the setup for the second part of installation can be seen in figure 3.11.

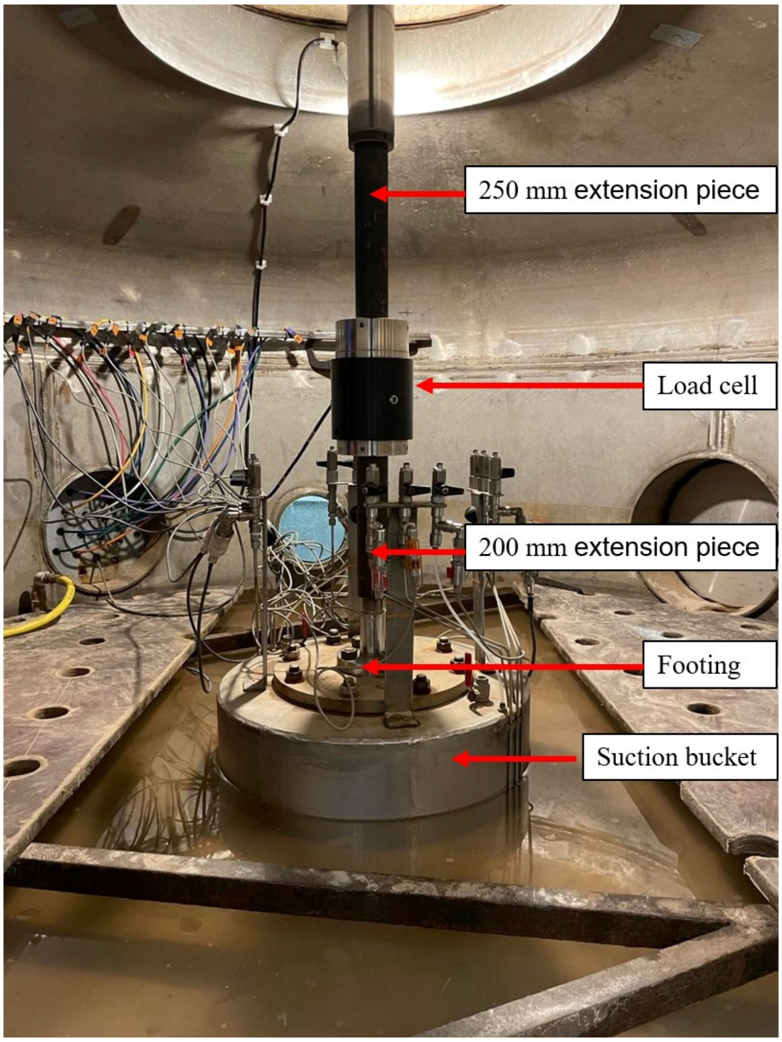

Figure 3.11: Setup before installation part 2 is started

Now the second part of the installation of the bucket can start and it is further submerged into the soil with a rate of 0.5 mm/s, this time the installation is stopped manually when the soil reaches the lid of the bucket, when this happened a sudden increase in load could be seen and sand sprayed out the valves on top of the bucket. In figure 3.12 the last 20 kN of the installation is shown, at the end of the graph the exponential increase in the load is clearly visible.

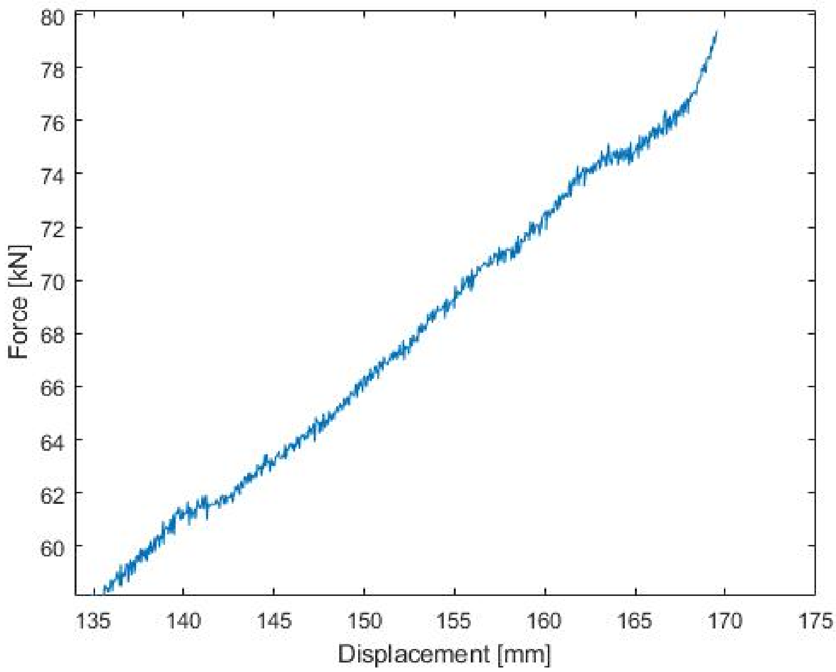

Figure 3.12: Force vs Absolute Displacement of installation part 2

Pressurizing the tank

Once the bucket is successfully installed, the transducers are checked if they respond and zeroed and the valves on top of the bucket are closed. The lid of the pressure tank is attached with a rubber seal in between to ensure a perfect seal when the bolts are screwed on. once sealed, water is filled into the tank to about 50 mm from the lowest transducer. Afterwards all the valves on the tank are closed, the transducers are checked if they are zeroed so when pressure is applied in the the tank it can be monitored from the transducers. The pressure is increased until 200 kPa is reached to simulate 20 m of water depth, once 200 kPa is reached the transducers are yet again zeroed and the setup is ready for testing.

4 | Overview

4.1 Test overview

To simplify the naming of tests a system has been made as presented in figure 4.1 which consist of 3 parts:

- Group ID + Sub-group ID - Each group consist of several sub-groups. That means that those tests has something in common, for example they might be loaded with the identical cyclic loading but loading frequency is different.
- Loading - This part shows cyclic loading amplitudes, first number is the minimum force and the second one - largest.
- Frequency - This part says the frequency of cyclic loading used for the test.

Example of such naming: **C3,-5.4+4.1,H**

C3 - 3rd sub-group test from the C group tests

-5.4+4.1 - Cyclic loading with lowest force of -5.4 kN and highest 4.1 kN

H - Cyclic loading with frequency of 1.0 Hz

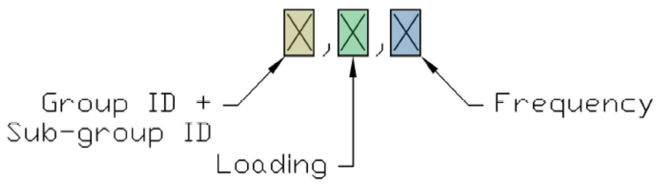

Figure 4.1: Principal scheme of test naming

Table 4.1: Group ID

A	1st group
B	2nd group
C	3rd group
D	4th group
E	5th group
F	6th group

Table 4.2: Sub-group ID

1	n'th group 1st sub-group
2	n'th group 2nd sub-group
3	n'th group 3rd sub-group

Table 4.3: Loading

-x-y	Pure tensile loading from -x kN to -y kN
x+y	Pure compressive loading from x kN to y kN
-x+y	Two-way loading from -x kN to y kN

Table 4.4: Frequency

H	High frequency - 1.0 Hz
M	Medium frequency - 0.5 Hz
L	Low frequency - 0.1 Hz

General test overview

Test name		Cycle No.	Force	Force achieved		Frequency	Loading history	Displacement*	Conclusion**
Group ID	Packet ID		[kN]	Mean compresion [kN]	Mean tensile [kN]	[Hz]			
A1,	-0.2+28.7,H	7728	-0.7 - 28	28.7	-0.2	1		+0.037	Reached lower limit
A2,	-3+35.1,H	2306	-1.1 - 28	35.1	-3	1	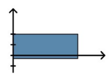	+0.015	Reached lower limit
A3,	-3+32.1,H	1619	-2.2 - 28	32.1	-3	1	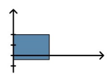	+0.013	Reached lower limit

Table 4.5: Test overview table

Test name		Cycle No.	Force	Force achieved		Frequency	Loading history	Displacement*	Conclusion**
Group ID	Packet ID		[kN]	Mean compresion [kN]	Mean tensile [kN]	[Hz]			
B1,	PRE1	10000	26.0 - 30.0	31.5	25.6	1.0	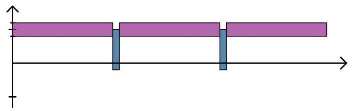	-0.024	
	2.5+29.6,H	10	-5.0 - 28.0	29.6	2.5	1.0			
	PRE2	10000	26.0 - 30.0	31.5	25.6	1.0			
	2.3+29.6,H	10	-5.0 - 28.0	29.6	2.3	1.0			
	PRE3	10000	26.0 - 30.0	31.5	25.6	1.0			
C1,	PRE1	1000	4.0 - 6.0	7.70	3.50	0.1	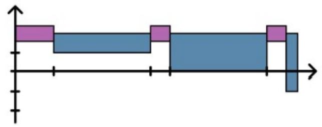	-0.042	Reached lower limit
	1.9+6.9,H	5000	2.5 - 5.0	6.90	1.90	1.0			
	PRE2	200	4.0 - 6.0	7.70	3.50	0.1			
	-0.7+7.3,H	5000	0.0 - 5.0	7.30	-0.70	1.0			
	PRE3	200	4.0 - 6.0	7.70	3.50	0.1			
	-2.9+10.0,H	1337	-2.5 - 5.0	10.0	-2.90	1.0			
C2,	PRE1	1000	4.0 - 6.0	7.60	3.50	0.1	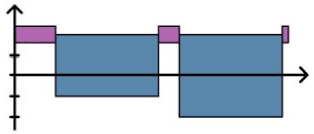	-0.04	Reached lower limit
	-2.7+6.6,H	5000	-2.5 - 5.0	6.60	-2.70	1.0			
	PRE2	200	4.0 - 6.0	7.60	3.50	0.1			
	-2.8+5.5,H	5000	-5.0 - 5.0	5.50	-2.80	1.0			
	PRE3	80	4.0 - 6.0	7.60	3.50	0.1			
C3,	PRE1	1000	4.0 - 6.0	7.6	3.50	0.1	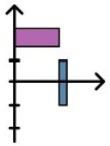	+0.220	Reached upper limit
	-4.1+3.2,H	433	-2.5 - 2.5	3.20	-4.10	1.0			

Table 4.5 Test overview table

Test name		Cycle No.	Force	Force achieved		Frequency	Loading history	Displacement*	Conclusion**
Group ID	Packet ID		[kN]	Mean compression [kN]	Mean tensile [kN]	[Hz]			
C4,	PRE1	1000	4.0 - 6.0	7.6	3.5	0.1	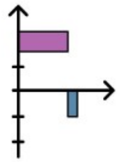	+0.238	Reached upper limit
	-4.6+0.9,H	162	-2.5 - 0.0	0.90	-4.60	1.0			
D1,	PRE1	1000	4.0 - 6.0	7.6	3.5	0.1	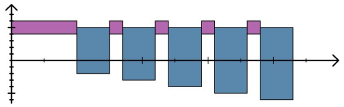	+0.064	
	-2.3+6.6,H	500	-2.0 - 5.0	6.60	-2.30	1.0			
	PRE2	200	4.0 - 6.0	7.6	3.5	0.1			
	-3.2+6.6,H	500	-3.0- 5.0	6.60	-3.20	1.0			
	PRE3	200	4.0 - 6.0	7.6	3.5	0.1			
	-3.7+6.5,H	500	-4.0 - 5.0	6.50	-3.70	1.0			
	PRE4	200	4.0 - 6.0	7.6	3.5	0.1			
	-3.2+6.4,H	500	-5.0 - 5.0	6.40	-3.20	1.0			
	PRE5	200	4.0 - 6.0	7.6	3.5	0.1			
	-4.4+5.8,H	500	-6.0 - 5.0	5.80	-4.40	1.0			
D2,	PRE1	1000	4.0 - 6.0	7.6	3.5	0.1	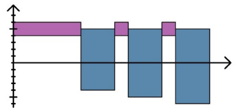	+0.092	
	-3.2+6.5,H	500	-4.0 - 5.0	6.50	-3.20	1.0			
	PRE2	200	4.0 - 6.0	7.6	3.5	0.1			
	-4.2+6.4,H	500	-5.0 - 5.0	6.40	-4.20	1.0			
	PRE3	200	4.0 - 6.0	7.6	3.5	0.1			
	-4.4+5.6,H	500	-6.0 - 5.0	5.60	-4.40	1.0			

Table 4.5 Test overview table

Test name		Cycle No.	Force	Force achieved		Frequency	Loading history	Displacement*	Conclusion**
Group ID	Packet ID		[kN]	Mean compresion [kN]	Mean tensile [kN]	[Hz]			
D3,	PRE1	1000	4.0 - 6.0	7.6	3.5	0.1	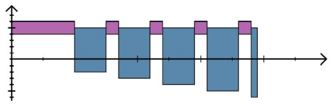	+0.256	Reached upper limit
	-2.7+6.9,L	500	-2.0 - 5.0	6.90	-2.70	0.1			
	PRE2	200	4.0 - 6.0	7.6	3.5	0.1			
	-3.7+6.9,L	500	-3.0- 5.0	6.90	-3.70	0.1			
	PRE3	200	4.0 - 6.0	7.6	3.5	0.1			
	-4.4+5.6,L	87	-4.0 - 5.0	5.60	-4.40	0.1			
E1,	PRE1	1000	4.0 - 6.0	7.6	3.5	0.1	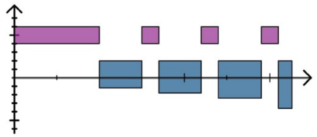	+0.236	Reached upper limit
	-1.8+4.8,L	500	-1.2 - 3.0	4.80	-1.80	0.1			
	PRE2	200	4.0 - 6.0	7.6	3.5	0.1			
	-2.4+4.8,L	500	-1.8- 3.0	4.80	-2.40	0.1			
	PRE3	200	4.0 - 6.0	7.6	3.5	0.1			
	-3.0+4.8,L	500	-2.4 - 3.0	4.80	-3.00	0.1			
	PRE4	200	4.0 - 6.0	7.6	3.5	0.1			
	-3.6+4.9,L	148	-3.0 - 3.0	4.90	-3.60	0.1			

Table 4.5 Test overview table

Test name		Cycle No.	Force	Force achieved		Frequency	Loading history	Displacement*	Conclusion**
Group ID	Packet ID		[kN]	Mean compresion [kN]	Mean tensile [kN]	[Hz]			
E2,	PRE1	1000	4.0 - 6.0	7.6	3.5	0.1	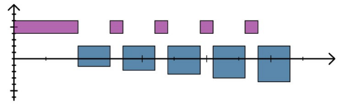	+0.004	
	-1.6+4.5,M	500	-1.2 - 3.0	4.50	-1.60	0.5			
	PRE2	200	4.0 - 6.0	7.6	3.5	0.1			
	-2.2+4.6,M	500	-1.8- 3.0	4.60	-2.20	0.5			
	PRE3	200	4.0 - 6.0	7.6	3.5	0.1			
	-2.7+4.5,M	500	-2.4 - 3.0	4.50	-2.70	0.5			
	PRE4	200	4.0 - 6.0	7.6	3.5	0.1			
	-3.2+4.5,M	500	-3.0 - 3.0	4.50	-3.20	0.5			
	PRE5	200	4.0 - 6.0	7.6	3.5	0.1			
	-3.6+4.5,M	500	-3.6 - 3.0	4.50	-3.60	0.5			
E3,	PRE1	1000	4.0 - 6.0	7.6	3.5	0.1	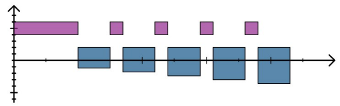	+0.040	
	-1.7+4.7,H	500	-1.2 - 3.0	4.70	-1.70	1.0			
	PRE2	200	4.0 - 6.0	7.6	3.5	0.1			
	-2.3+4.7,H	500	-1.8- 3.0	4.70	-2.30	1.0			
	PRE3	200	4.0 - 6.0	7.6	3.5	0.1			
	-2.9+4.8,H	500	-2.4 - 3.0	4.80	-2.90	1.0			
	PRE4	200	4.0 - 6.0	7.6	3.5	0.1			
	-3.4+4.6,H	500	-3.0 - 3.0	4.60	-3.40	1.0			
	PRE5	200	4.0 - 6.0	7.6	3.5	0.1			
	-3.9+4.8,H	500	-3.6 - 3.0	4.80	-3.90	1.0			

Table 4.5 Test overview table

Test name		Cycle No.	Force	Force achieved		Frequency	Loading history	Displacement*	Conclusion**
Group ID	Packet ID		[kN]	Mean compresion [kN]	Mean tensile [kN]	[Hz]			
F1,	PRE1	1000	4.0 - 6.0	7.6	3.5	0.1	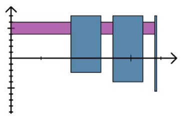	+0.238	Reached upper limit
	-3.4+8.8,L	500	-2.8 - 7.0	8.80	-3.40	0.1			
	PRE2	200	4.0 - 6.0	7.6	3.5	0.1			
	-4.9+8.9,L	500	-4.2- 7.0	8.90	-4.90	0.1			
	PRE3	200	4.0 - 6.0	7.6	3.5	0.1			
	-6.8+9.2,L	25	-5.6 - 7.0	9.20	-6.80	0.1			
F2,	PRE1	1000	4.0 - 6.0	7.6	3.5	0.1	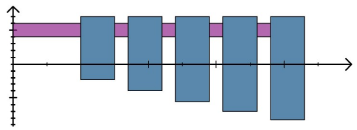	+0.086	
	-3.0+8.5,H	500	-2.8 - 7.0	8.50	-3.00	1.0			
	PRE2	200	4.0 - 6.0	7.6	3.5	0.1			
	-3.9+8.4,H	500	-4.2- 7.0	8.40	-3.90	1.0			
	PRE3	200	4.0 - 6.0	7.6	3.5	0.1			
	-4.5+8.4,H	500	-5.6 - 7.0	8.40	-4.50	1.0			
	PRE4	200	4.0 - 6.0	7.6	3.5	0.1			
	-5.0+7.6,H	500	-7.0 - 7.0	7.60	-5.00	1.0			
	PRE5	200	4.0 - 6.0	7.6	3.5	0.1			
	-5.6+6.4,H	500	-8.6 - 7.0	6.40	-5.60	1.0			

Table 4.5 Test overview table

* Displacement of the suction bucket at the end of the test. Negative value represents displacement upwards.

** Reached lower limit - means that the test stopped because bucket was pushed down to the machinery limits
Reached upper limits - means that the test stopped because bucket was pulled from the soil

Force

The compressive bearing capacity is determined from [Barari et al., 2016] with the equation found in the theorem below.

Load bearing capacity of soil in the pressure tank

$$V_{peak} = \gamma \frac{D}{2} N_\gamma (\frac{\pi D^2}{4}) + q N_q (\frac{\pi D^2}{4}) \tag{4.1}$$

Where:

γ	Unit soil weight
q	Overburden pressure
D	Diameter
N_γ	Bearing capacity factor
N_q	Bearing capacity factor

Bearing capacity factor

$$N_\gamma = c_1 \cdot [(N_q - 1) cos\phi]^{c_2} \tag{4.2}$$

Where:

c	Coefficients in for Bearing Capacity Factor	[-]
ϕ	Friction angle	[deg]

Bearing capacity factor

$$N_q = c_3 \cdot e^{c_4 \cdot \pi \cdot tan\phi} tan^2(45 + \frac{\phi}{2}) \tag{4.3}$$

Friction angle

$$\phi = 0.214 D_r + 22.86 \tag{4.4}$$

Where:

D_r	Relative density	[%]

Compressive bearing capacity for circular smooth foundations according to [Barari et al., 2016] was calculated according to relative density, D_R of the sand and presented in figure 4.2, a value of 5 % of that with $D_R = 80\%$ was chosen as it is small enough to represent loading during normal sea state. The 5% compression capacity therefore becomes 28 kN.

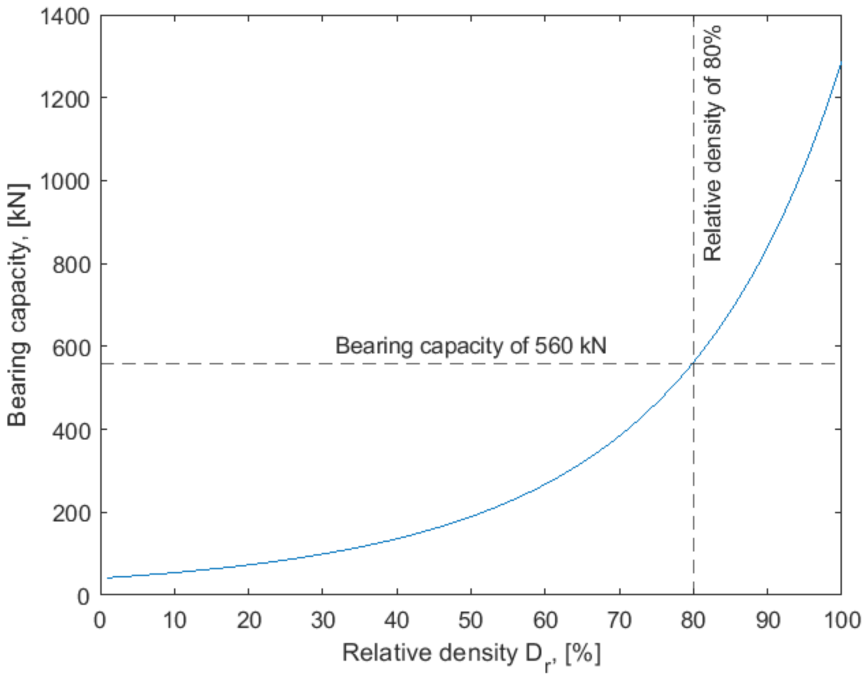

Figure 4.2: Soil bearing capacity against relative density

The tensile bearing capacity is determined for drained conditions to be $-2.2\,\mathrm{kN}$. Further explanation can be found in appendix D.1

Frequency

Even though, scaling law is considered and it is described in chapter 2 it is not proven to be completely accurate. That is why for the sake of this project it was decided to cover wide range of load frequencies from $0.1 - 1.0\,\mathrm{Hz}$. Furthermore, that gives an opportunity to investigate the influence to the behaviour of the suction bucket from the loading frequency.

4.2 Test campaign

This section contains an example of how the tests will be presented in appendix D

In order to investigate the detailed behaviour of the suction bucket foundation in various scenarios several tests with different load configurations were performed. To make the tests comparable to each other initial soil density was kept as similar as possible simulating dense sand in the Northern sea.

The parameters which will be varied for the investigation of their influence on the suction buckets behavior are listed below.

- Force ratio
- Frequency

The force ratio is investigated to get a better understating of the influence of two-way axial loading on the buckets behaviour. This particular investigation will show if there is any similarity in displacement patterns regarding the ratio between minimum and maximum loading.

Varying frequency with same loading scenario will help understand the influence of excess pore water pressure dissipation.

An example of how each individual experiment will be presented can be seen below:
Test D with all the subgroups is chosen as an example.

Test D

The experiment will be presented with a table and figure providing the general overview of the loading plan as seen in table 4.11 and figure 4.3

Table 4.11: Loading plan for 'Test D'

Packet No.	Conditions	Force command F_{min} [kN]	F_{max} [kN]	Force ratio	Cycle No.	Frequency [Hz]
1	Normal	4.0	6.0	1.50	1000	0.1
2	Severe	2.5	5.0	2.00	500	0.1, 1.0
3	Normal	4.0	6.0	1.50	200	0.1
4	Severe	0.0	5.0	-	500	0.1, 1.0
5	Normal	4.0	6.0	1.50	200	0.1
6	Severe	-2.5	5.0	-2.00	500	0.1, 1.0
7	Normal	4.0	6.0	1.50	200	0.1
8	Severe	-5.0	5.0	-1.00	500	0.1, 1.0
9	Normal	4.0	6.0	1.50	200	0.1
10	Severe	-2.5	2.5	-1.00	500	0.1, 1.0

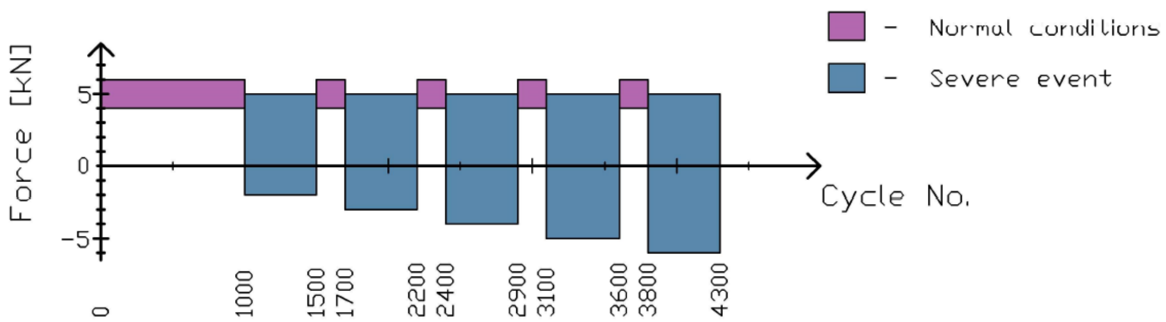

Figure 4.3: Loading plan for 'Test D'

In some cases the tests fails before running the entire plan. In such occasions the following test is started again from the failed "event". An example of such scenario can be seen in figure 4.4

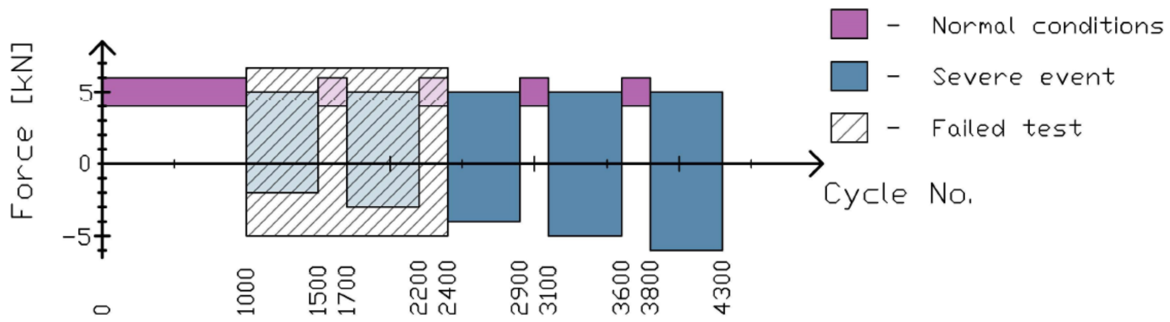

Figure 4.4: Continued test from previous failed stage

In this situation there are two main ideas behind this test:

- Investigation of two way loading for the suction bucket replicated both normal condition when the bucket is mostly exposed to the compression forces, but also a severe conditions when the bucket would be exposed to the tensile forces.
- To investigate the influence of the frequency of the cyclic loading to the behaviour of the suction bucket.

Results from the provided test will be given in following subsections, each subsection will describe the "events" investigated from given load plan.

From D1,PRE1 to D1,-4.4+5.8,H

First part of the test for which:

- Loading frequency of 0.1 Hz for precycling parts (Normal conditions) with mean compressive forces of 5.0 kN and amplitude of 1 kN were used.

- Loading frequency of 1.0 Hz for extreme event parts (Severe conditions) with varying forces from 5.0 kN to −5.0 kN were used.

Force and displacement

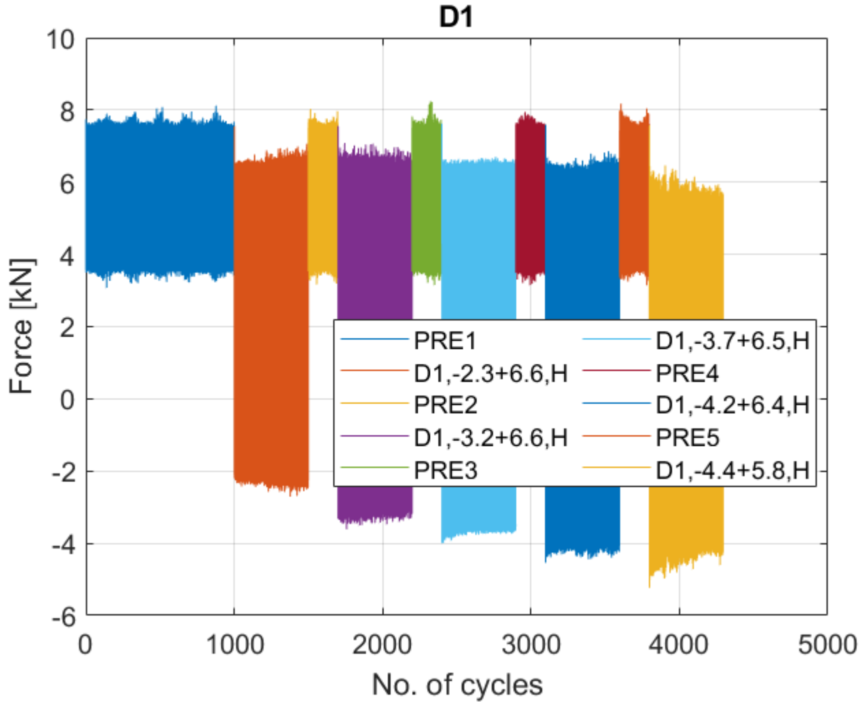

Figure 4.5: Force VS time

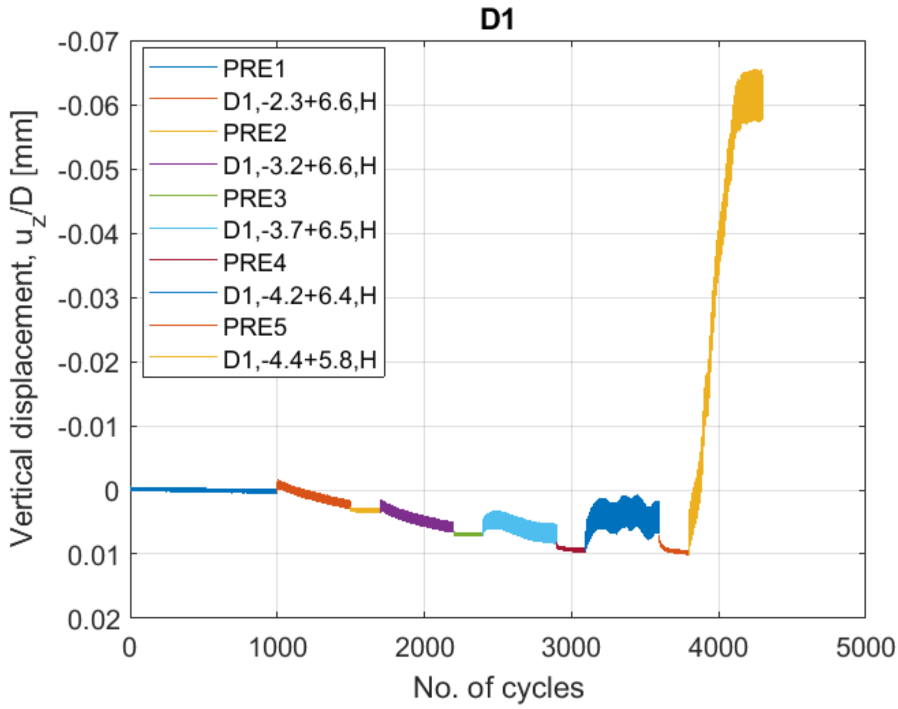

Figure 4.6: Displacement VS time

Pore pressure transducers were installed at various height on the suction bucket. Their placement can be seen in figure 4.7.

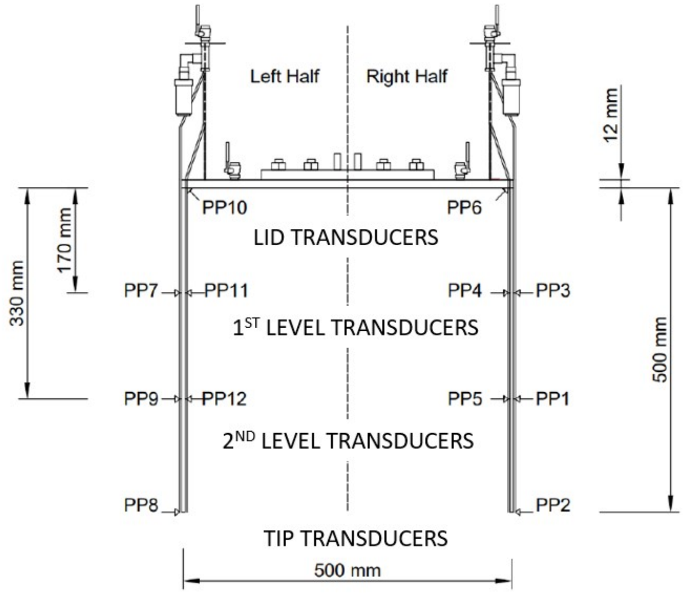

Figure 4.7: Placement of the transducers on a bucket

Lid Transducers

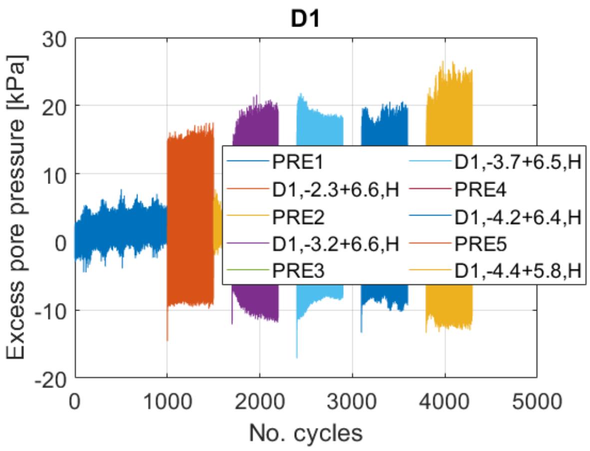

(a) Transducer P6

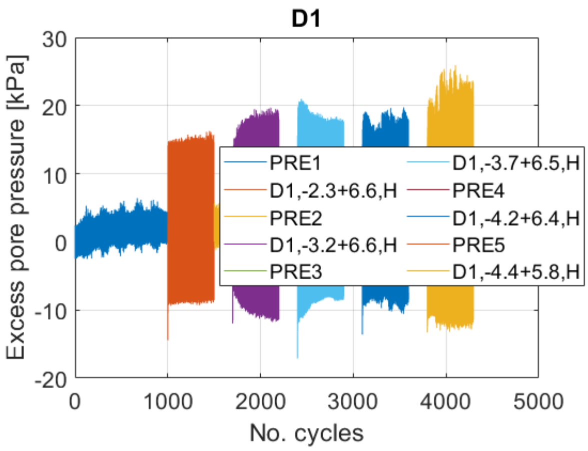

(b) Transducer P10

Figure 4.8: Pore pressure at the lid

1st Level Transducers

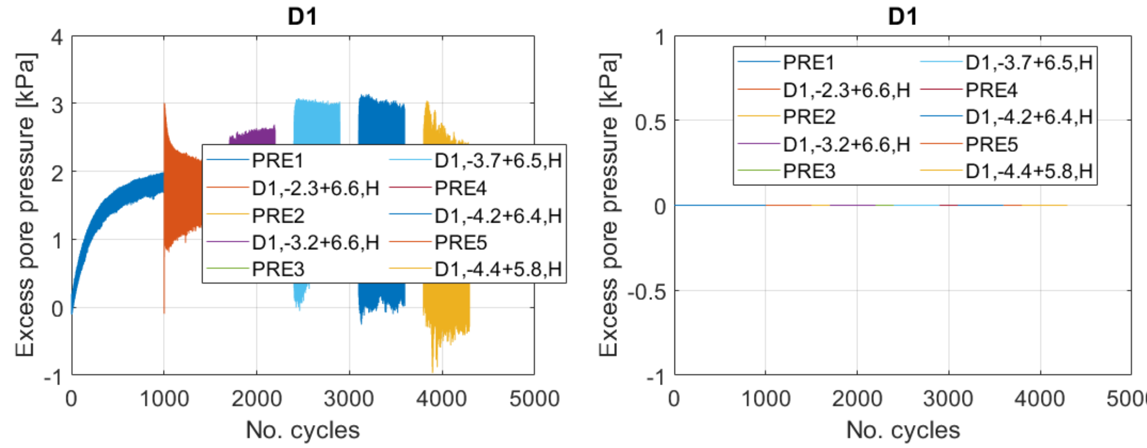

(a) Transducer P3 (b) Transducer P7

Figure 4.9: Outer pore pressure at 1st level

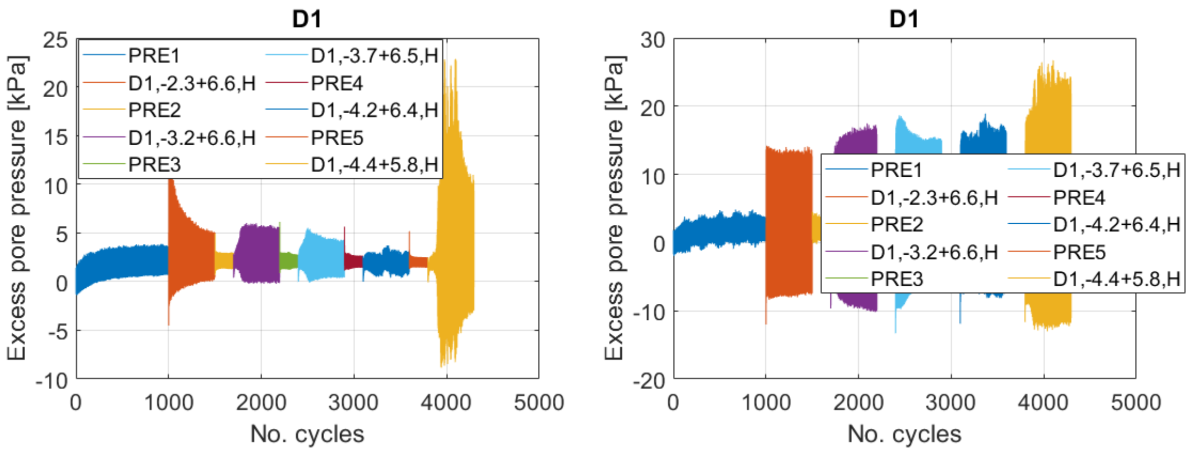

(a) Transducer P4 (b) Transducer P11

Figure 4.10: Inner pore pressure at 1st level

2nd Level Transducers

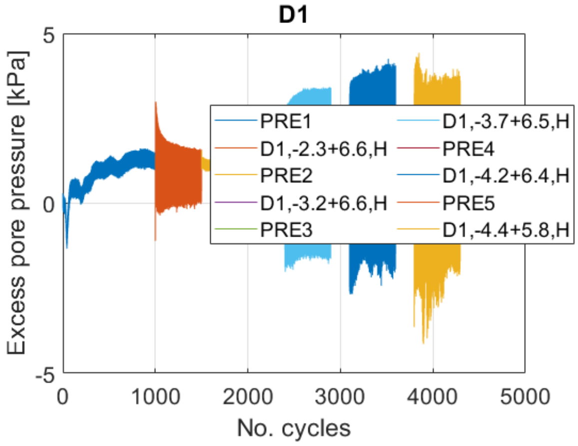

(a) Transducer P1

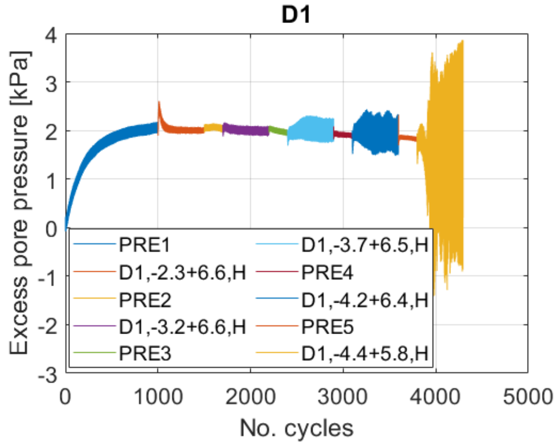

(b) Transducer P9

Figure 4.11: Outer pore pressure at 2nd level

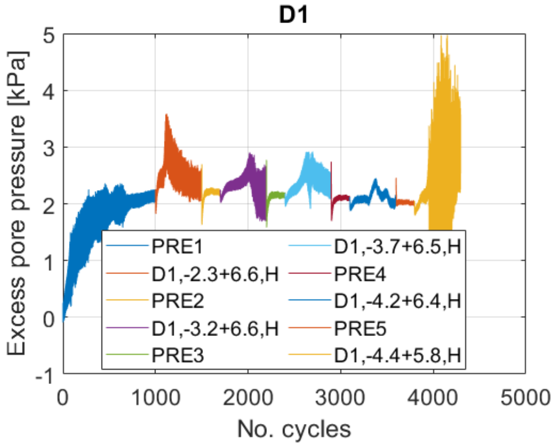

(a) Transducer P5

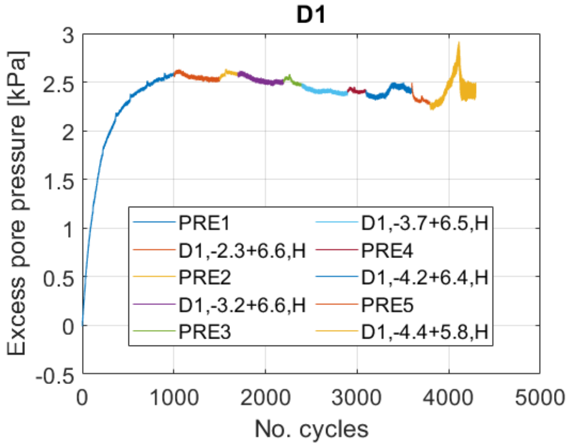

(b) Transducer P12

Figure 4.12: Inner pore pressure at 2nd level

Skirt Tip Transducers

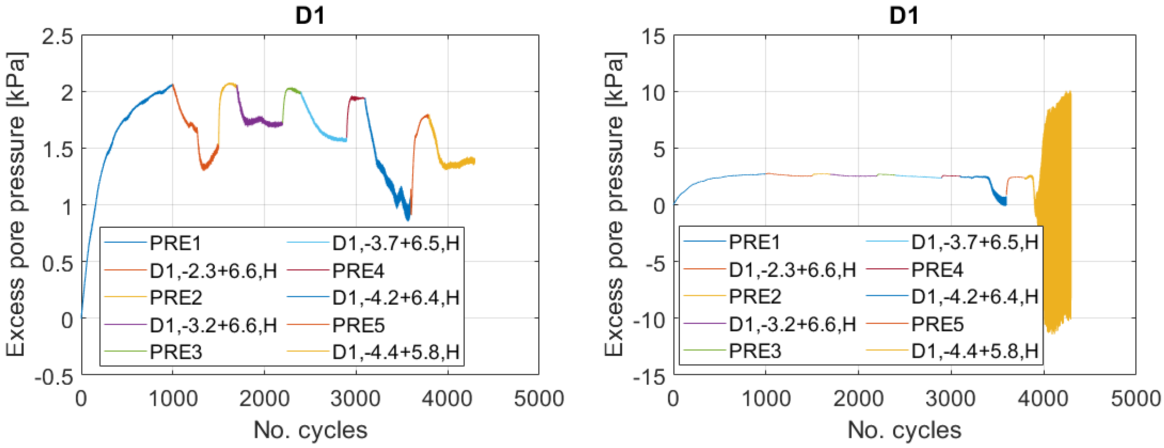

(a) Transducer P2

(b) Transducer P8

Figure 4.13: Pore pressure at the skirt tip

From D2,PRE1 to D2,-4.4+5.6,H

As it was briefly introduced in subsection 4.2 this test was done in order to verify if the odd behaviour at third extreme event loading package was cause by soil disturbance during first two severe events or not. That is why, during this experiment loading conditions were kept the same apart from first two packages of severe and normal events as it can be seen in figure 4.14 below.

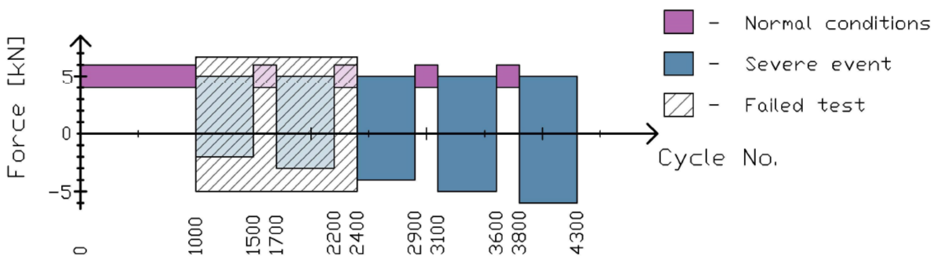

Figure 4.14: Loading plan for 'Varying 2_2 test'

The procedure will then be as previous, providing data and plots for the excess pore pressure and force displacement.

Results from all tests, with higher resolution, are presented in appendix D.

5 | Data Analysis

5.1 Data processing

To model only relevant data for this thesis the raw data is processed for various influences such as pressurisation of the tank. The procedure and equations for processing the raw data is described in this section.

5.1.1 Normalization of displacement

The displacement are normalised with equation 5.1

Normalized displacement

$$\delta = \frac{D}{D_{bucket}} \tag{5.1}$$

Where:

δ	Normalized displacement		[-]
D_{bucket}	Diameter of suction bucket	500	[mm]
D	Absolute vertical displacement		[mm]

5.1.2 Pressurisation

As mentioned in chapter 3.1, the tank is pressurised to 2.0 Bar to simulate water depth of 20 meters. However, this pressurisation will have an effect on the transducers. It is only wanted to log the relative effect of excess pore water pressure between the bucket and sand, therefore the transducers are reset to zero when the pressurisation is complete. That ensures only the relative change, during cyclic movement in excess pore water pressure.

5.1.3 Force processing

The pressurisation and submerged weight of the bucket has an influence on the force, therefore the raw data logged from the experiments are processed in means of subtracting those forces from the raw forces logged. Equation (5.2) takes that into account

Processed force

$$F_p = F_{raw} - w_{sub} - F_{LC} \tag{5.2}$$

Where:

F_p	Processed force		[kN]
F_{raw}	Raw force data		[kN]
w_{sub}	Submerged weight of the bucket	0.60	[kN]
F_{LC}	Influence of pressurization on the load cell reading	2.45	[kN]

During pressurization of the tank, the load cell readings was affected, hence an investigation of the effect the pressurization has on the load cell was performed. The experiments was run at 200 kPa and the influence on the load cell from that can be seen in figure 5.1 and is determined to be 2.45 kN at 200 kPa.

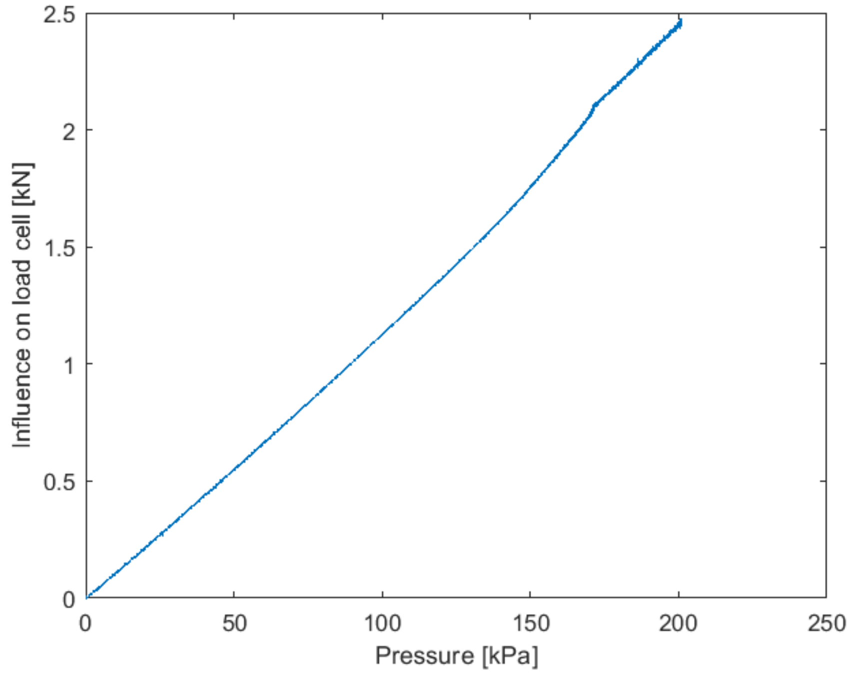

Figure 5.1: Pressurization effects on load cell

5.1.4 Excess pore pressure

The total pressure measured by the transducers consist of various components. These components are applied pressure, atmospheric pressure and hydrostatic pressure. It is only wanted to measure the relative excess pore water pressure generated by cyclic movement, therefore the known components will be subtracted as seen in equation (5.3).

Excess pore water pressure

$$P_{excess} = P_{measured} - P_{applied} - P_{hyd} - P_{atm} \tag{5.3}$$

Where:

$P_{measured}$	Measured pore pressure	[kPa]
$P_{applied}$	Applied pressure during pressurisation	[kPa]
P_{hyd}	Hydrostatic pressure	[kPa]
P_{atm}	Atmospheric pressure	[kPa]

However the excess pore pressure can also be measured simply by zeroing the transducers after pressurisation. For the matter of this thesis, the excess pore pressure is measured by this method of zeroing transducers after pressurisation.

5.2 Grouping of test results

From all 43 test carried out, it is noticed that in the end of the tests they resulted in different ways. Figure 5.2 shows all the tests in a displacement versus number of cycles plot. Since most of the tests consist of 500 cycles it is decided to use this number as an initial point for test comparison.

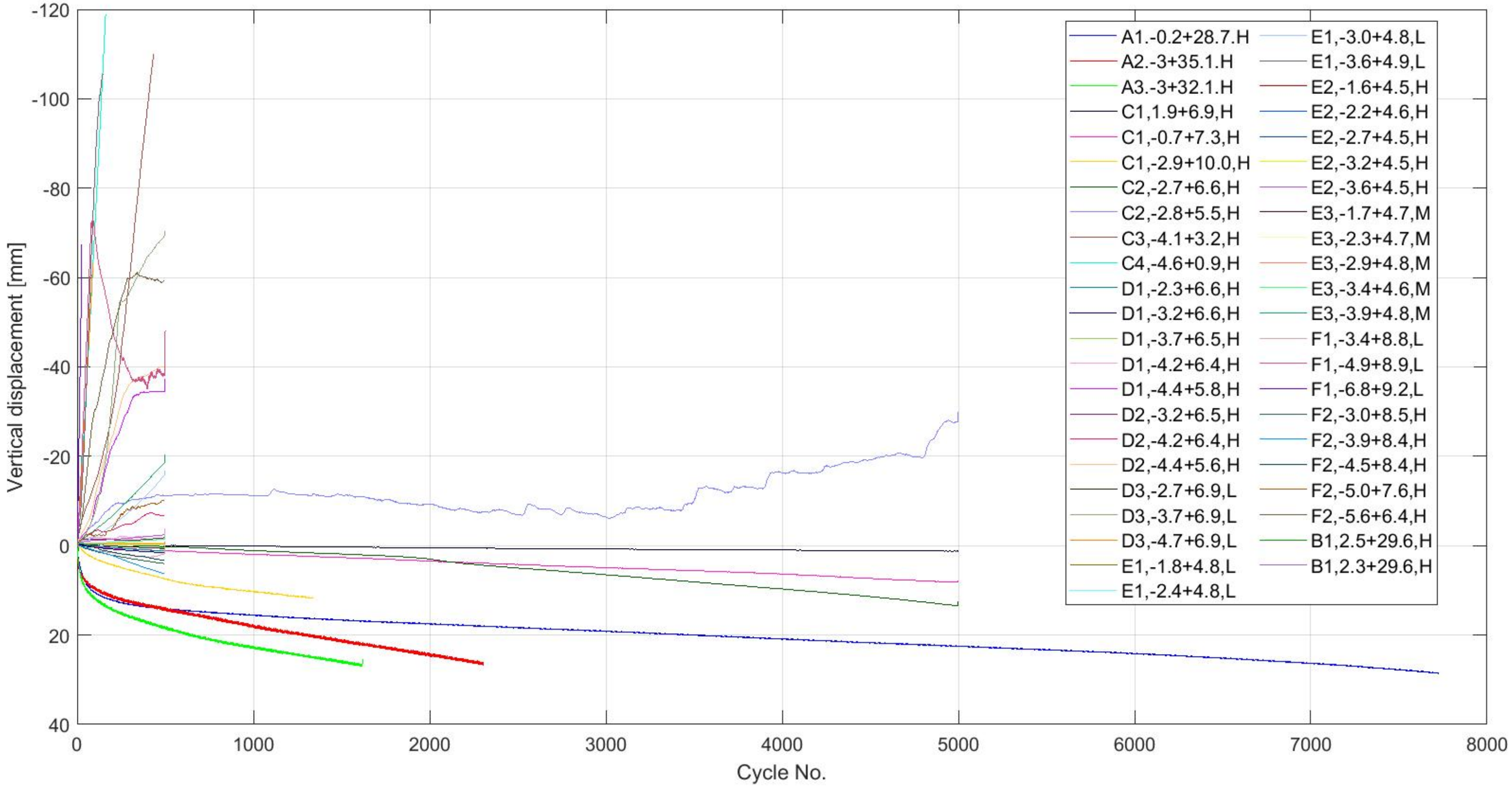

Figure 5.2: Vertical absolute displacement of all tests

The three groups are sketched out, the groups are formed from how they displace; upwards displacement, downwards displacement and minor or no displacement respectively. The groups can be seen in figure 5.3.

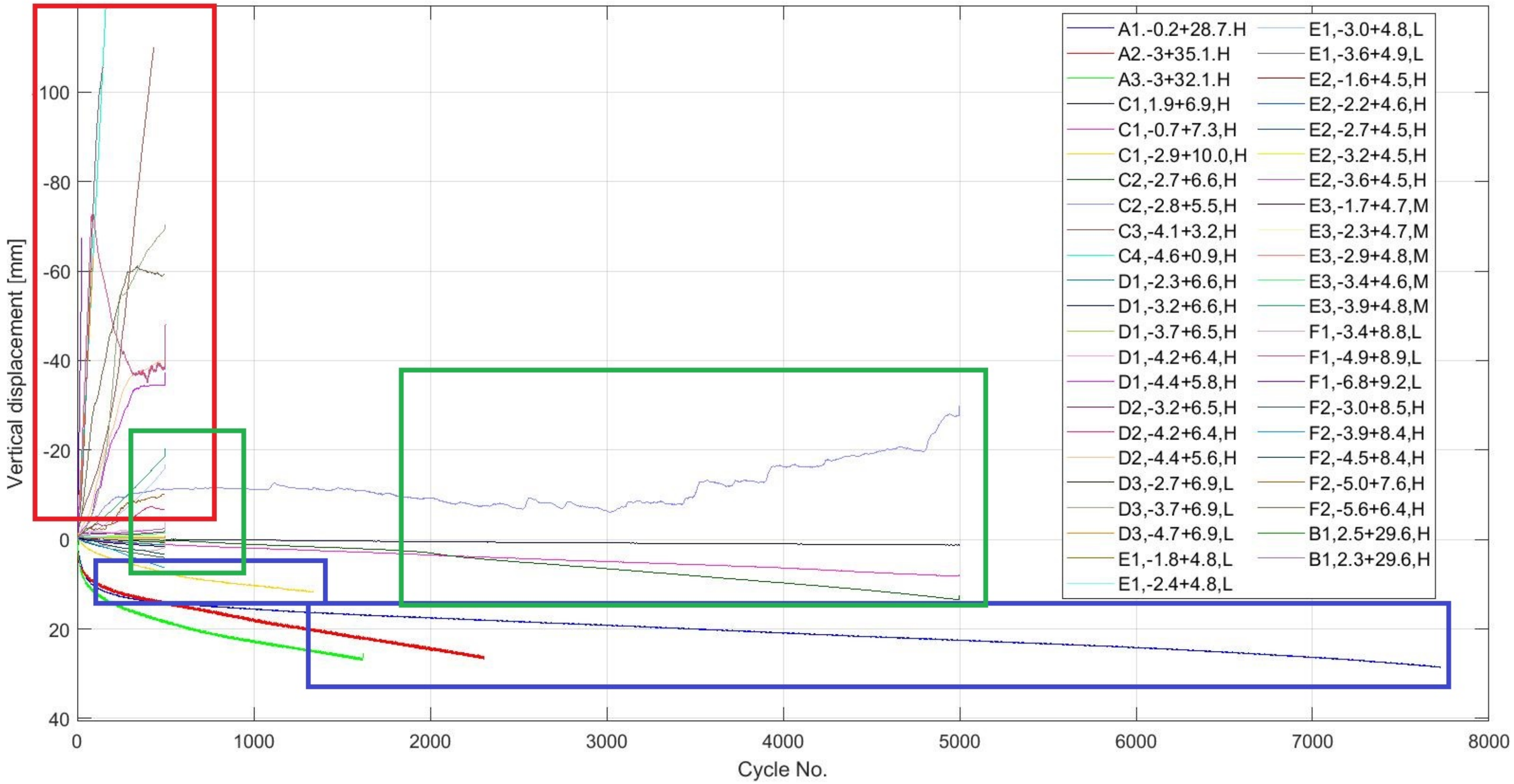

Figure 5.3: Vertical absolute displacement of all tests with the three groups

For each of these groups the frequency, force ratio and stiffness are investigated to see if a pattern can be found defining the outcome of the specific displacement. It is clear to see that test number 43 and test 8 from figure 5.3 are marked in the stable group, but should be considered in the group with upwards displacement, as it is assumed if they had been exposed to more cycles they would displace even more. In the following subsections the three groups are investigated even further.

5.2.1 Unloading/reloading stiffness of each group

The results of the laboratory tests are investigated by plotting the vertical displacement, D, in response to the applied cyclic axial loading as is presented for each of the tests separately in chapter D. This method for data extraction is outlined in figure 5.4 below and is calculated by equation (5.4). The gathered data provides information on both stiffness and displacement as function of the number of loading cycles, N. Below, in figures 5.5 and 5.6 unloading/reloading stiffness for all of the tests is presented.

Unloading/reloading stiffness

$$k = \frac{\Delta F}{\Delta D} \tag{5.4}$$

Where:

k	Unloading/reloading stiffness	[kN/mm]
ΔF	Increment in axial force	[kN]
ΔD	Increment in displacement	[mm]

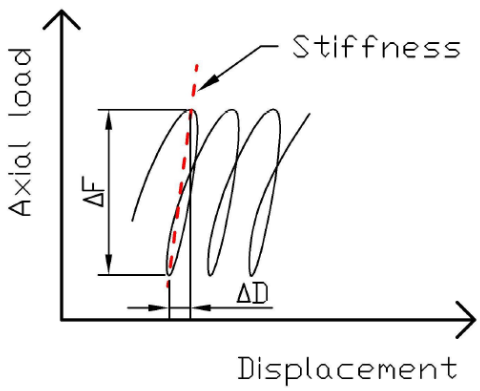

Figure 5.4: Definition of unloading/reloading stiffness

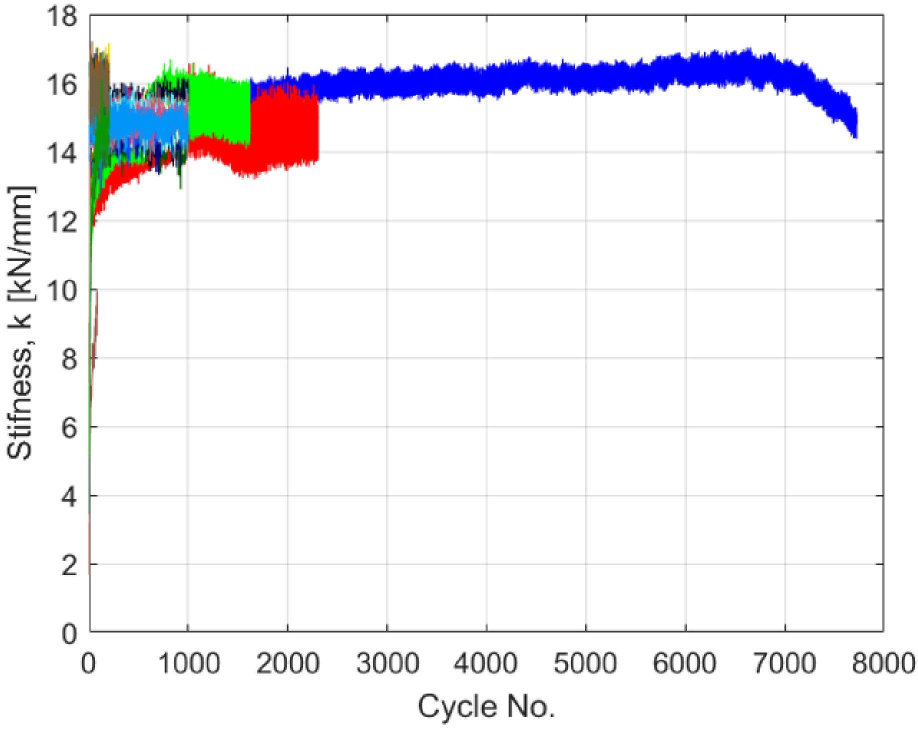

Figure 5.5: Unloading/reloading stiffness of precycling parts of each test

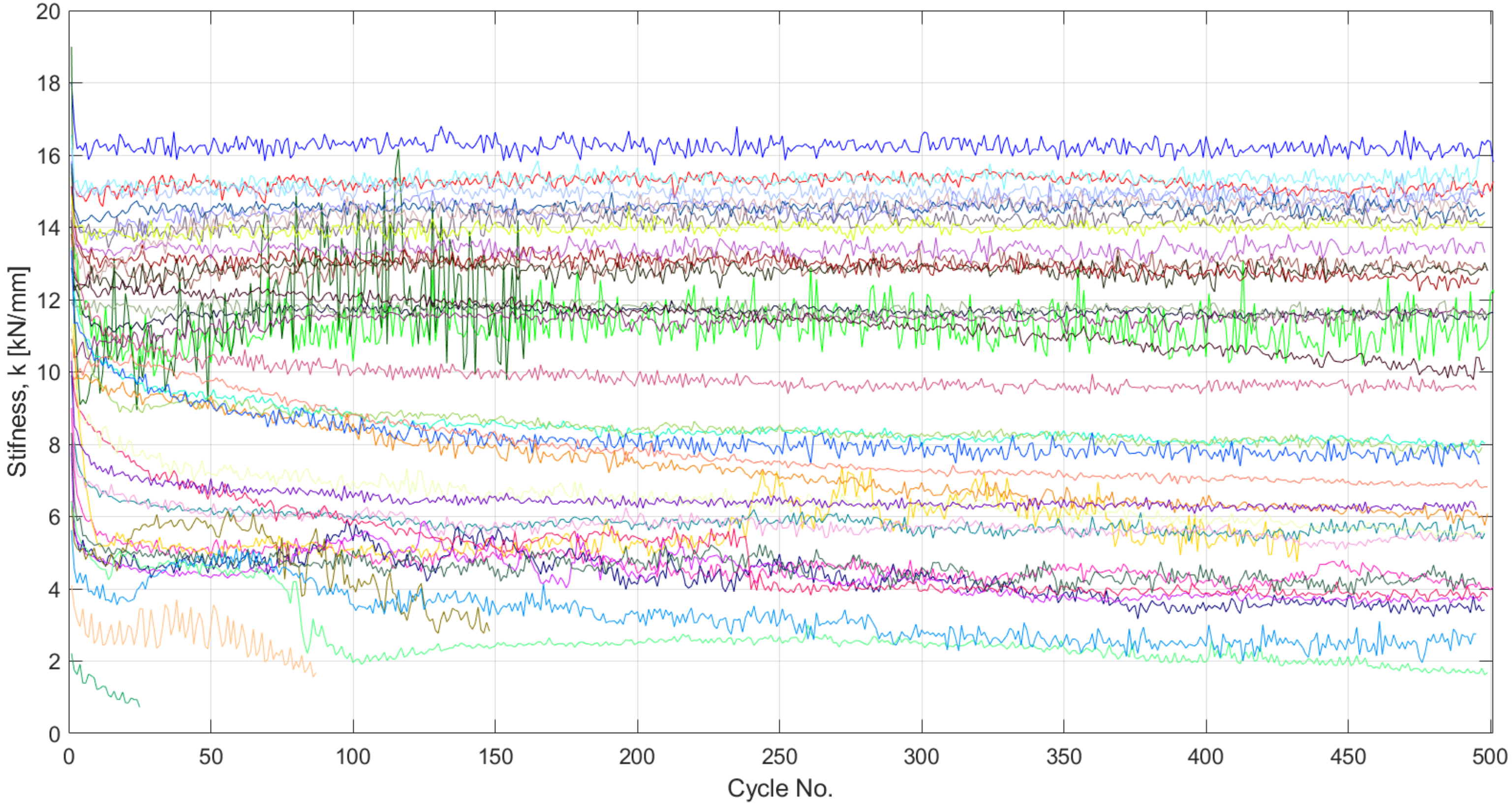

Figure 5.6: Unloading/reloading stiffness of severe events of each test

5.2.2 Development of excess pore pressure of each group

In order to present the development of excess pore water pressure for each of the group in a easily understandable way - A simplified method with combination of 4 plots were chosen. These plots are presented separately in each group's section, below example of one of them is presented in figure 5.7. This method consist of these plots:

- Max PP - Maximum value of excess pore pressure in each cycle
- Min PP - Minimum value of excess pore pressure in each cycle
- Range of PP - Range of excess pore pressure in each cycle between the maximum and minimum values.
  $Range = PP_{max} - PP_{min}$
- Ratio of PP - Ratio of excess pore pressure in each cycle between the maximum and minimum values.
  $Ratio = \frac{PP_{max}}{PP_{min}}$

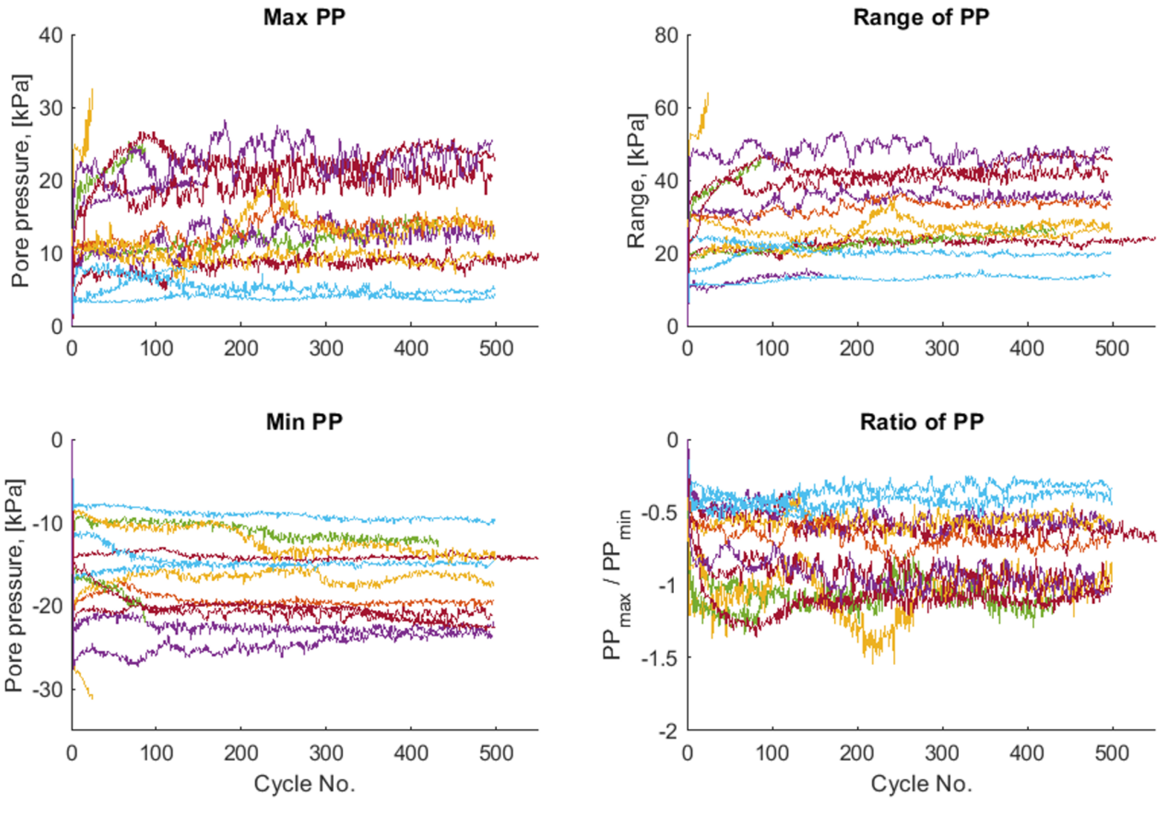

Figure 5.7: Pore pressure under the lid of the suction bucket

It is decided to present data in such way due to large number of data points in each test. Moreover, excess pore water pressure was measured at various levels on suction bucket, but only the development under the lid is presented since this is where the highest build up of pressure was observed. If entire data would be plotted together - one test would overlap other and a lot of information would be lost.

5.3 Displacement groups

5.3.1 Upwards displacement

In this section tests were the suction bucket foundation is exposed to significant upwards (pull-out) displacement is analysed as seen in figure 5.8 below:

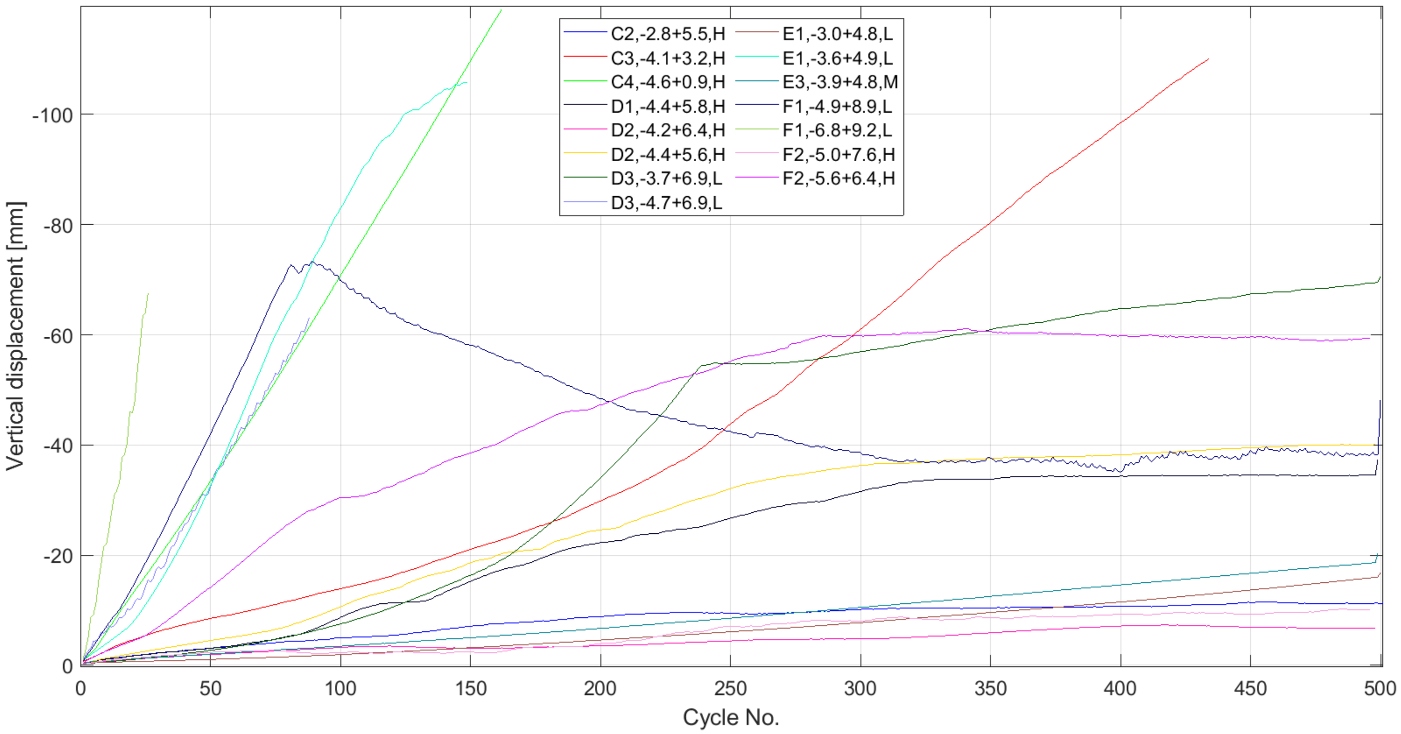

Figure 5.8: Vertical absolute displacement of tests allocated to the first group

Table 5.1: Overview of first group tests parameters

Name	Max force [kN]	Min force [kN]	Frequency [Hz]	Force ratio	Displacement
$C2, -2.8+5.5, H$	5.5	-2.8	1.0	-1.96	-0.0223(-0.059)*
$C3, -4.1+3.2, H$	3.2	-4.1	1.0	-0.78	-0.220
$C4, -4.6+0.9, H$	0.9	-4.6	1.0	-0.20	-0.236
$D1, -4.4+5.8, H$	5.8	-4.4	1.0	-1.32	-0.075
$D2, -4.2+6.4, H$	6.4	-4.2	1.0	-1.52	-0.014
$D2, -4.4+5.6, H$	5.6	-4.4	1.0	-1.27	-0.080
$D3, -3.7+6.9, L$	6.9	-3.7	0.1	-1.86	-0.141
$D3, -4.7+6.9, L$	6.9	-4.7	0.1	-1.47	-0.126
$E1, -3.0+4.8, L$	4.8	-3.0	0.1	-1.60	-0.034
$E1, -3.6+4.9, L$	4.9	-3.6	0.1	-1.36	-0.212
$E3, -3.9+4.8, M$	4.8	-3.9	0.5	-1.23	-0.041
$F1, -4.9+8.9, L$	8.9	-4.9	0.1	-1.82	-0.096
$F1, -6.8+9.2, L$	9.2	-6.8	0.1	-1.35	-0.135
$F2, -5.0+7.6, H$	7.6	-5.0	1.0	-1.52	-0.020
$F2, -5.6+6.4, H$	6.4	-5.6	1.0	-1.14	-0.119

*Displacements are shown at 500 cycles and the values in () are total displacement.

5.3.2 Stable displacement

In this section tests were the suction bucket foundation is exposed to stable displacement is analysed as seen in figure 5.9 below:

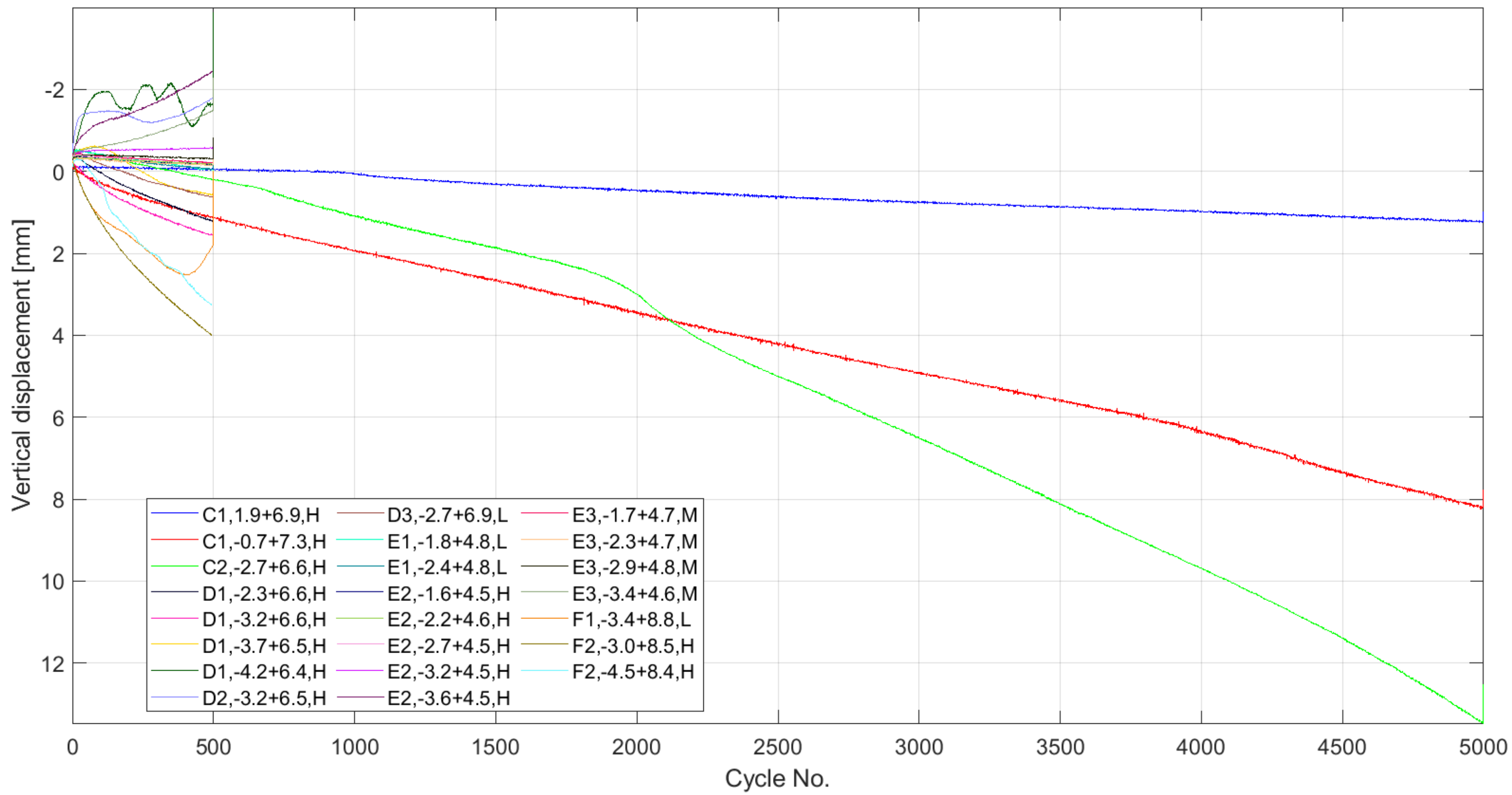

Figure 5.9: Vertical absolute displacement of tests allocated to the second group

Since a significant amount of the tests where set to run for 500 cycles, a figure with focus on the first 500 cycles can be seen in figure 5.10

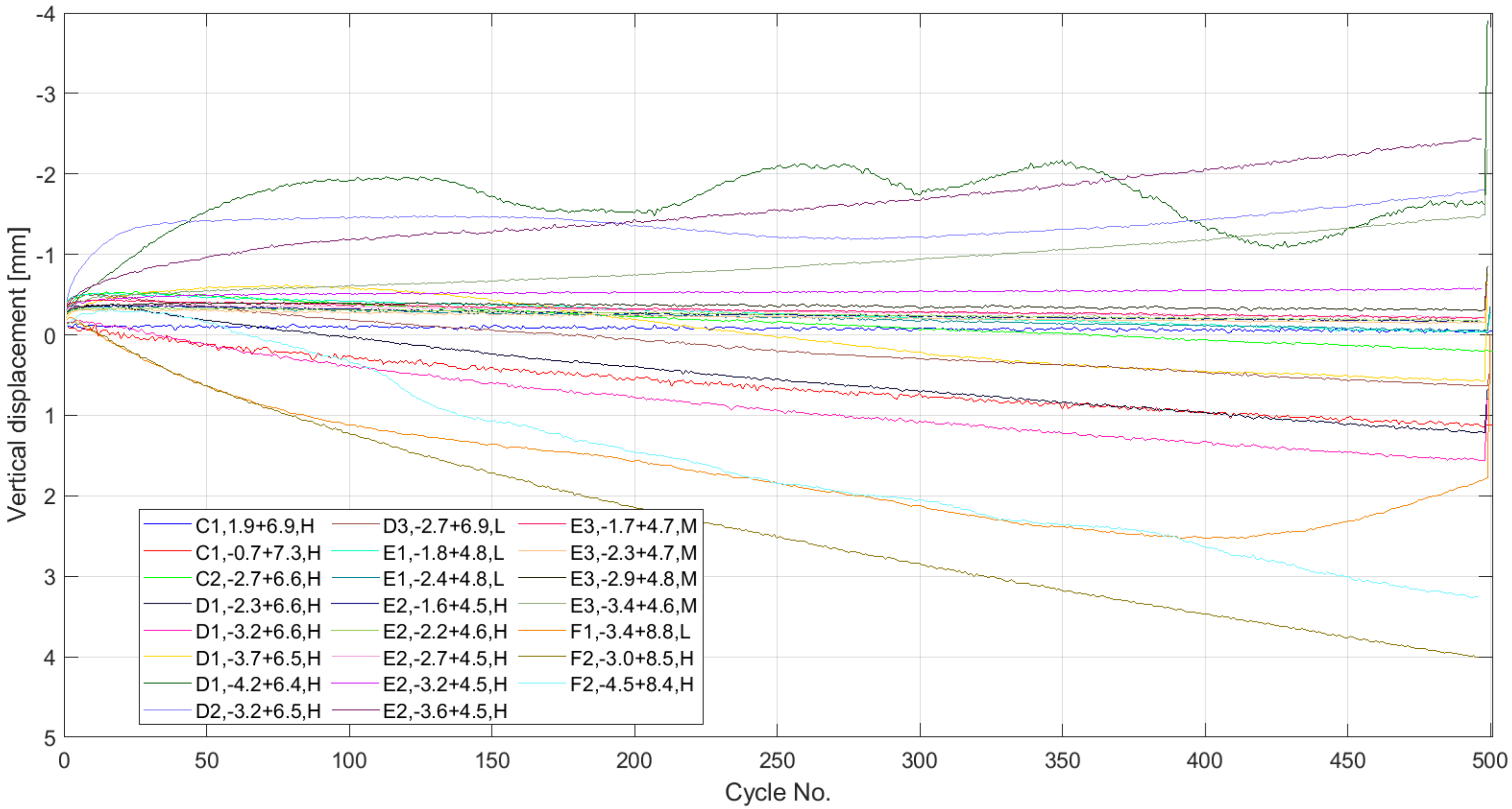

Figure 5.10: Vertical absolute displacement of tests allocated to the second group, first 500 cycles

A table with an overview of relevant parameters for the performed tests can be seen in table 5.2.

Table 5.2: Overview of second group tests parameters

Name	Max force [kN]	Min force [kN]	Frequency [Hz]	Force ratio	Displacement
C1,1.9+6.9,H	6.9	1.9	1.0	3.63	0.000(0.002)*
C1,-0.7+7.3,H	7.3	-0.7	1.0	-10.43	0.000(0.016)*
C2,-2.7+6.6,H	6.6	-2.7	1.0	-2.45	0.002(0.025)*
D1,-2.3+6.6,H	6.6	-2.3	1.0	-2.87	0.001
D1,-3.2+6.6,H	6.6	-3.2	1.0	-2.06	0.002
D1,-3.7+6.5,H	6.5	-3.7	1.0	-1.76	-0.002
D1,-4.2+6.4,H	6.4	-4.2	1.0	-1.52	-0.008
D2,-3.2+6.5,H	6.5	-3.2	1.0	-2.03	-0.002
D3,-2.7+6.9,L	6.9	-2.7	0.1	-2.56	0.001
E1,-1.8+4.8,L	4.8	-1.8	0.1	-2.67	-0.001
E1,-2.4+4.8,L	4.8	-2.4	0.1	-2.00	-0.001
E2,-1.6+4.5,H	4.5	-1.6	1.0	-2.81	0.000
E2,-2.2+4.6,H	4.6	-2.2	1.0	-2.09	0.000
E2,-2.7+4.5,H	4.5	-2.7	1.0	-1.67	0.000
E2,-3.2+4.5,H	4.5	-3.2	1.0	-1.41	-0.001
E2,-3.6+4.5,H	4.5	-3.6	1.0	-1.25	-0.005
E3,-1.7+4.7,M	4.7	-1.7	0.5	-2.77	-0.001
E3,-2.3+4.7,M	4.7	-2.3	0.5	-2.04	-0.001
E3,-2.9+4.8,M	4.8	-2.9	0.5	-1.66	-0.002
E3,-3.4+4.6,M	4.6	-3.4	0.5	-1.35	-0.005
F1,-3.4+8.8,L	8.8	-3.4	0.1	-2.59	0.000
F2,-3.0+8.5,H	8.5	-3.0	1.0	-2.83	0.008
F2,-4.5+8.4,H	8.4	-4.5	1.0	-1.87	0.007

*Displacements are shown at 500 cycles and the values in () are total displacement.

Since most of the tests were exposed to 500 cycles, it is wanted in the following to compare data at this exact cycle count. For the tests running for more than 500 cycles (C1,1.9+6.9,H , C1,-0.7+7.3,H and C2,-2.7+6.6,H), the data which will be compared is thereby extracted at their 500 cycle count.

5.3.3 Downwards displacement

In this section tests were the suction bucket foundation is exposed to significant downwards (pushed-down) displacement is analysed as seen in figure 5.11 below:

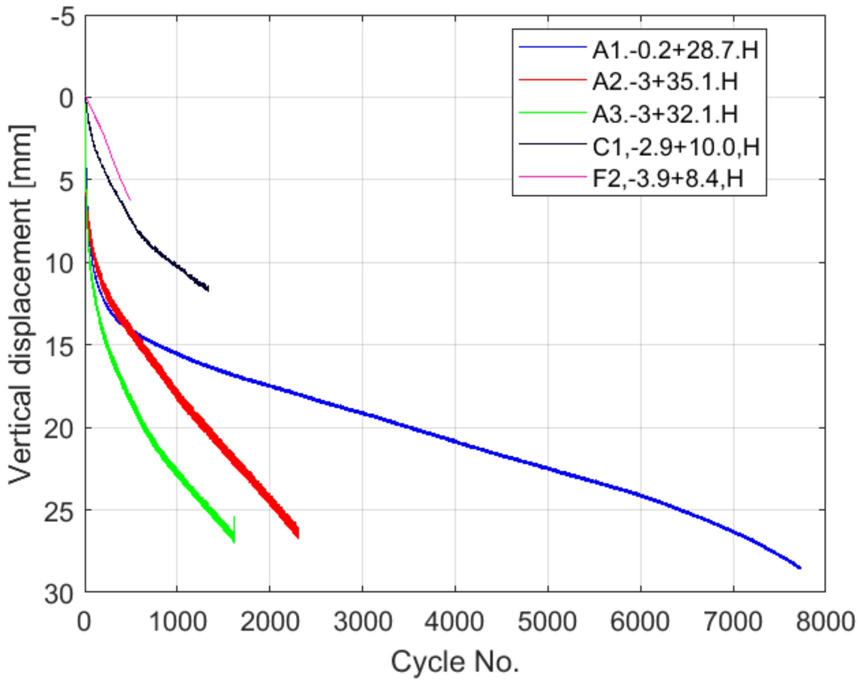

Figure 5.11: Vertical absolute displacement of tests allocated to the third group

The amount of cycles varied a lot in between the tests shown, therefore like the two sections above, the comparison between the tests are made at 500 cycles. The displacement at 500 cycles are shown in figure 5.12

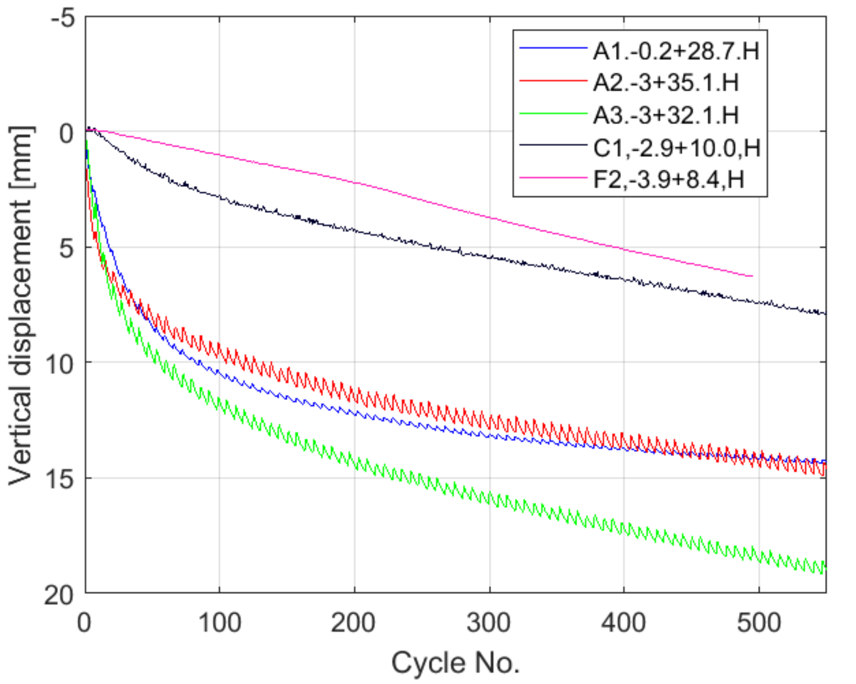

Figure 5.12: Vertical absolute displacement of tests allocated to the third group, first 500 cycles

In the zoomed version of the tests in figure 5.12, it is clear to see the bucket have a shake-down behaviour, which could be a sign of the bucket is exposed to cyclic force with a high compressive force resulting in a downwards displacement.

Table 5.3: Overview of third group tests parameters

Name	Max force [kN]	Min force [kN]	Frequency [Hz]	Force ratio	Displacement
A1,-0.2+28.7.H	28.7	-0.20	1.0	-143.5	0.028 (0.057)*
A2,-3.0+35.1.H	35.1	-3.00	1.0	-11.7	0.029 (0.053)*
A3,-3.0+32.1.H	32.1	-3.00	1.0	-10.7	0.037 (0.054)*
C1,-2.9+10.0,H	10.0	-2.90	1.0	-3.44	0.015 (0.024)*
F2,-3.9+8.4,H	8.40	-3.90	1.0	-2.15	0.013

*Displacements are shown at 500 cycles and the values in () are total displacement.

5.4 Comparison of the results

5.4.1 Stiffness comparison

Unloading/reloading stiffness of tests appointed to a specific group are presented below. By looking at figures 5.13, 5.14 and 5.16 some tendencies can be observed:

- Generally for the 1st group which was exposed to the upwards-displacement a degradation of stiffness is observed. Even though, during one of the test an odd behaviour in changes of stiffness was observed as it can be seen from the figure 5.13, majority of the tests shows a clear visible degradation path.
- For the 2nd group it was observed that the stiffness remains approximately the same during all 500 loading cycles. On the other hand, as it is seen from figure 5.14 that some of the tests showed stiffness degradation during very few loading cycles. More detailed investigation should be done to find the reasons for such behaviour but it might be because of the initial soil conditions before the tests.
- For the 3rd group no common tendency can be seen. As it was mentioned earlier this group consist of only 5 tests which can be argued as a very small number to make some kind of conclusions, so more tests should be performed. In this case, 4 out of 5 performed tests showed stiffness hardening, for 3 of those 4 hardening was significant, on the other hand, those 3 tests had been loaded with a huge compression loading. The last test from of this group showed stiffness degradation.

Displacing upwards (1st group)

Figure 5.13 contains information about unloading/reloading stiffness of the 1st group. One of the tests in this group consist of 5.000 cycles a plot with entire data set can be seen in appendix G in figure G.1, in this section only the first 500 cycles are presented.

By looking at the plot below a common tendency of stiffness degradation can be observed. These changes in stiffness could explain why the suction bucket resulted in upwards displacement.

However, test - C4,-4.6+0.9,H was the only test which showed different behaviour in stiffness. It can be seen that for approximately first 100 cycles soil experienced stiffness hardening and after that - stiffness degradation started to happen. This odd behaviour should be detailed investigated before making conclusions but it can be argued that the reason for that might be loading conditions, since this test is subjected to the lowest compression forces from the entire group, leading to a significant displacement before reaching upper limits of the laboratory equipment capabilities at just 162 loading cycles, as it can be seen in figure 5.8, making equation 5.4 used for unloading / reloading stiffness calculations invalid.

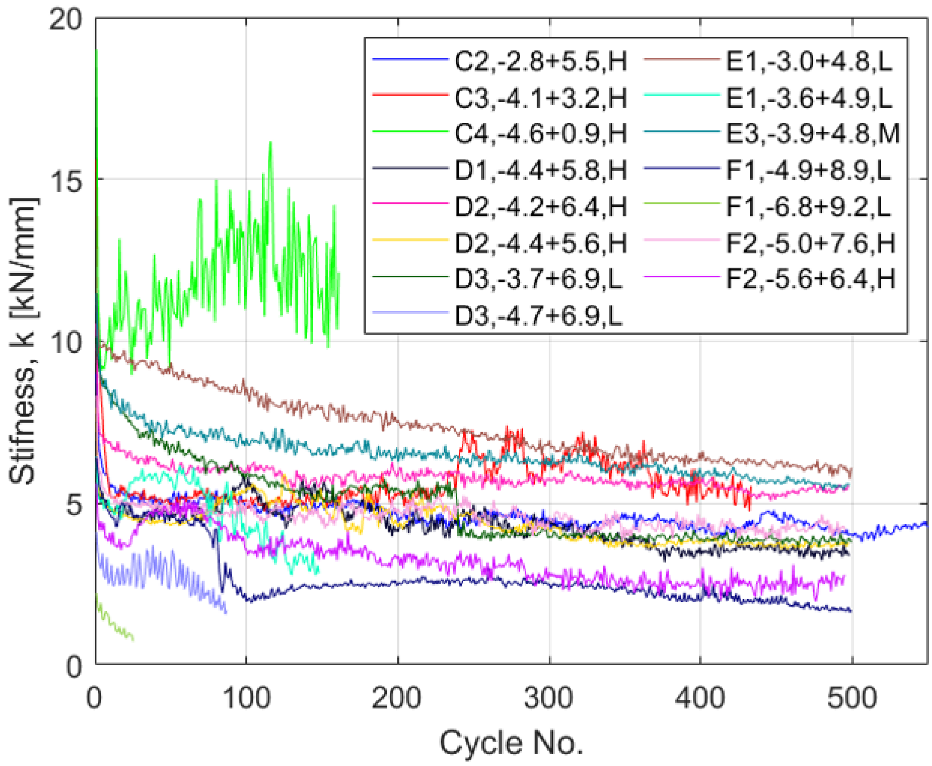

Figure 5.13: Unloading/reloading stiffness of first group of tests of first 500 cycles

Stable (2nd group)

Figure 5.14 contains information about unloading/reloading stiffness of the 2nd group. Again, information with all of the cycles can be seen in appendix G in figure G.2.

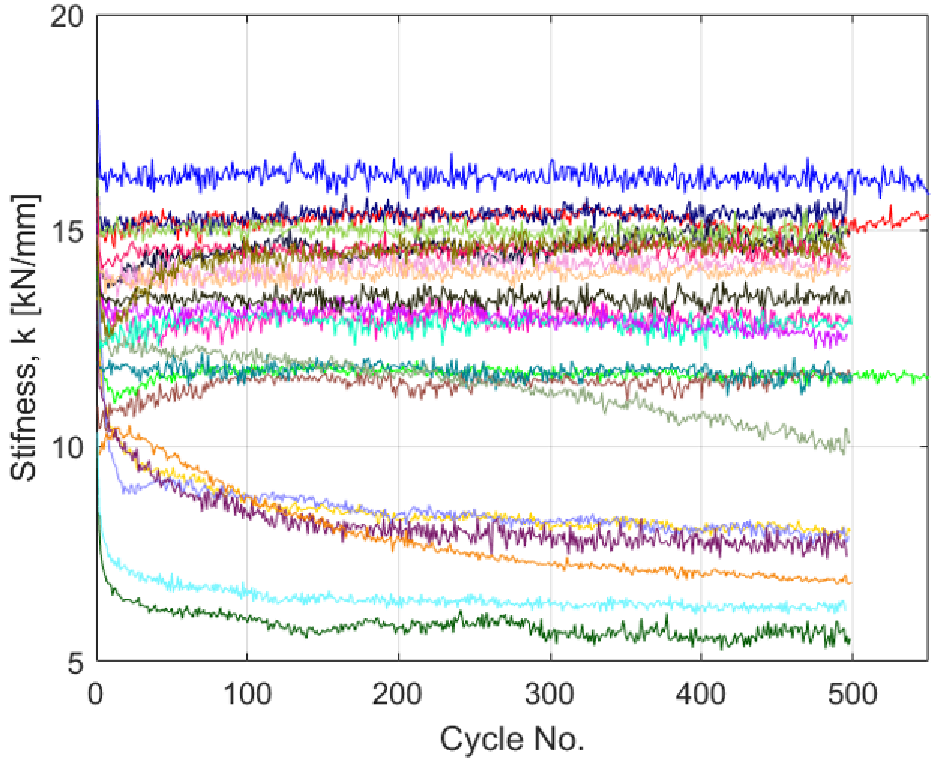

Figure 5.14: Unloading/reloading stiffness of second group of tests of first 500 cycles

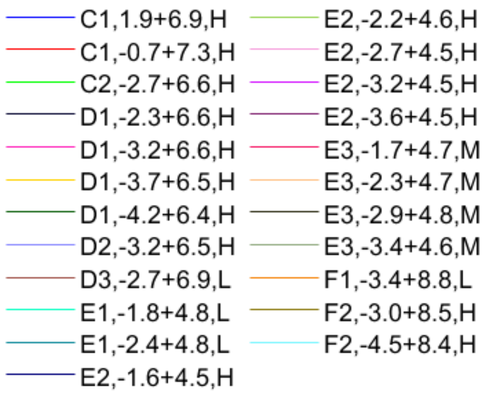

Figure 5.15: Legend for unloading/reloading stiffness of second group of tests in 5.14

Even though the displacement of these experiments in the second group seems quite small and in general fluctuating around the neutral axis, the same can not be said regarding the stiffness development. There are some experiments with neutral stiffness development, however for

- D1,-3.7+6.5,H
- D1,-4.2+6.4,H
- D2,-3.2+6.5,H
- E2,-3.6+4.5,H
- F1,-3.4+8.8,L
- F2,-4.5+8.4,H

The stiffness degrades with a significant rate for the first ≈ 50 cycles and then seems to stabilize. Those 6 experiments are also the ones with the largest displacement in the second group for the first 500 cycles. However, the displacements are relatively small compared to the stiffness degradation. Elaborated results from the 6 experiments exposed to stiffness degradation during small strain development can be found in appendix D. By investigating their individual displacement pattern a clear tendency is visible. For experiment D1,-3.7+6.5,H, D1,-4.2+6.4,H, E2,-3.6+4.5,H, F2,-4.5+8.4,H it appears that these experiments are located in the "transient" zone which is when the displacement is going from downwards to upwards. This change in displacement could affect the soil grains and induce relocation of those grains resulting in rapid stiffness degradation in the first cycles. Regarding experiment D2,-3.2+6.5,H and F2,-4.5+8.4,H it is not clear that they also are within this "transient" zone, since the previous and following tests does not conclude them being in the transient zone like for the first four tests, however their displacement pattern indicates it could be a possibility. Further investigation of this behaviour with stiffness degradation during small strain development should be performed.

Displacing downwards (3rd group)

Figure 5.16 contains information about unloading/reloading stiffness of the 3rd group. Like the two previous groups data set from entire test can be seen in G.3.

Since the bucket is displacing downwards an increase of stiffness can be seen for the tests lasting over 500 cycles, which is expected since the soil is being compressed by the bucket, hence the increasing in stiffness, test $F2,-3.9+8.4,H$ do not follow this trend, it is also the only test which do not exceed 500 cycles, and the stiffness is somewhat stable for that test when looking at figure 5.16 but still decreasing unlike the other 4 tests, it is also worth to remember that this test was included in the pushed down tests since it has a steep displacement curve, and is assumed to displace more if the test continued for more cycles, this could be the reason for the test not following the tendencies as the other tests. $C1,-2.9+10.0,H$ also diverges from the other tests, this also makes sense since, tests $A1.-0.2+28.7.H$, $A2.-3+35.1.H$ and $A3.-3+32.1.H$ have significantly higher forces compared to the other two, as seen in table 5.3. But it is important to notice that the pushed down tests unlike the pulled-up tests do not show a clear tendency of behaviour of soil stiffness. That could also be explained as the number of tests in this group is insufficient.

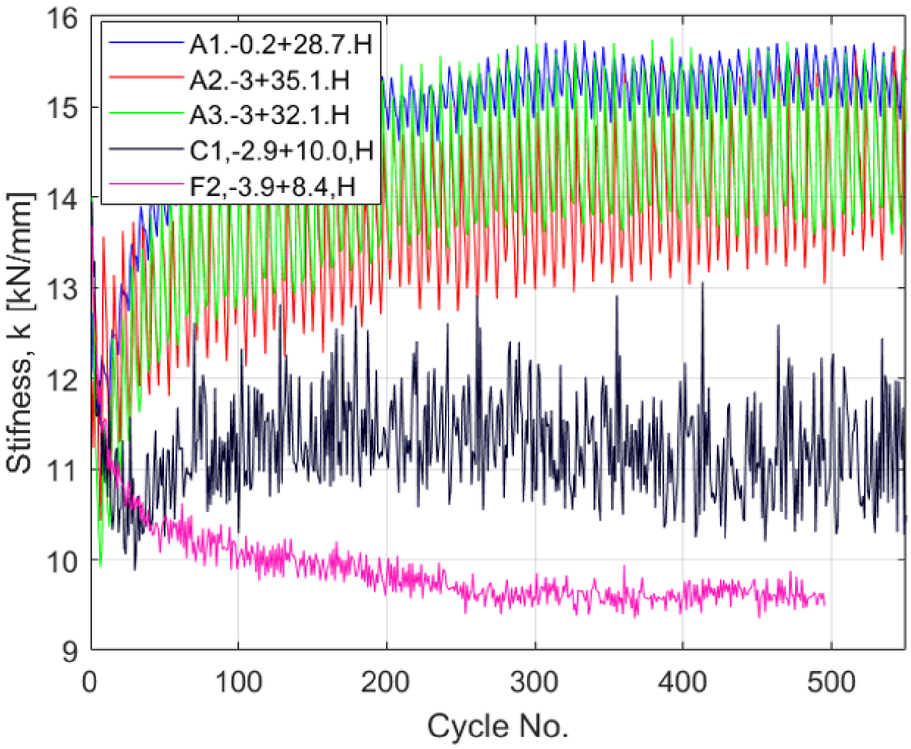

Figure 5.16: Unloading/reloading stiffness of third group of tests of first 500 cycles

5.4.2 Excess pore pressure development comparison

A summary of the tables provided in appendix F with changes in excess pore water pressure is presented in table 5.4 below. This table consist of average values of changes expressed in percentage between the values at 1st and 500th cycle.

Some tendencies can be clearly seen from this table:

- Maximum pore pressure decrease over time for tests exposed to downwards displacement, while insignificant build-up of pressure is seen for the tests which remained stable over entire test. Finally, higher than double of its origin pore pressure can be seen over 500 cycles in the tests exposed to upwards displacement
- Minimum pore pressure decreased for both the stable and pushed-down tests while small build-up was observed for the pulled-up tests. It is worth to mention that both maximum and minimum pore pressure decreased in a similar way for 3rd group while no correlation can be seen for 1st group.
- The ratio of pore pressure increased almost by 100 % for the 1st group meaning that build-up of maximum pore pressure caused by compressive loads were significantly higher than the build-up of minimum pore pressure caused by tensile loads. Opposite behaviour can be seen for the 3rd group.

On the other hand, no statistical analysis were done for this comparison, so the results should not be taken for granted and a more detailed investigation with a sufficient amount of specimens to perform statistical analysis should be executed. Especially that is important for the 3rd group, exposed to downwards displacement, because as it can be seen in appendix D where results of each of the test presented separately, during 3 out of 5 tests the pipes for pressure transducers got clocked meaning that results might be unreliable.

Table 5.4: Comparison of changes in EPP for all three groups of tests

Group	Δ Max PP [%]	Δ Min PP [%]	Δ Range of PP [%]	Δ Ratio of PP [%]
Pulled-upwards	109.0	11.9	31.7	99.3
Stable	13.0	-10.4	0.1	29.2
Pushed-down	-29.4	-29.8	-33.7	-30.3

Displacing upwards (1st group)

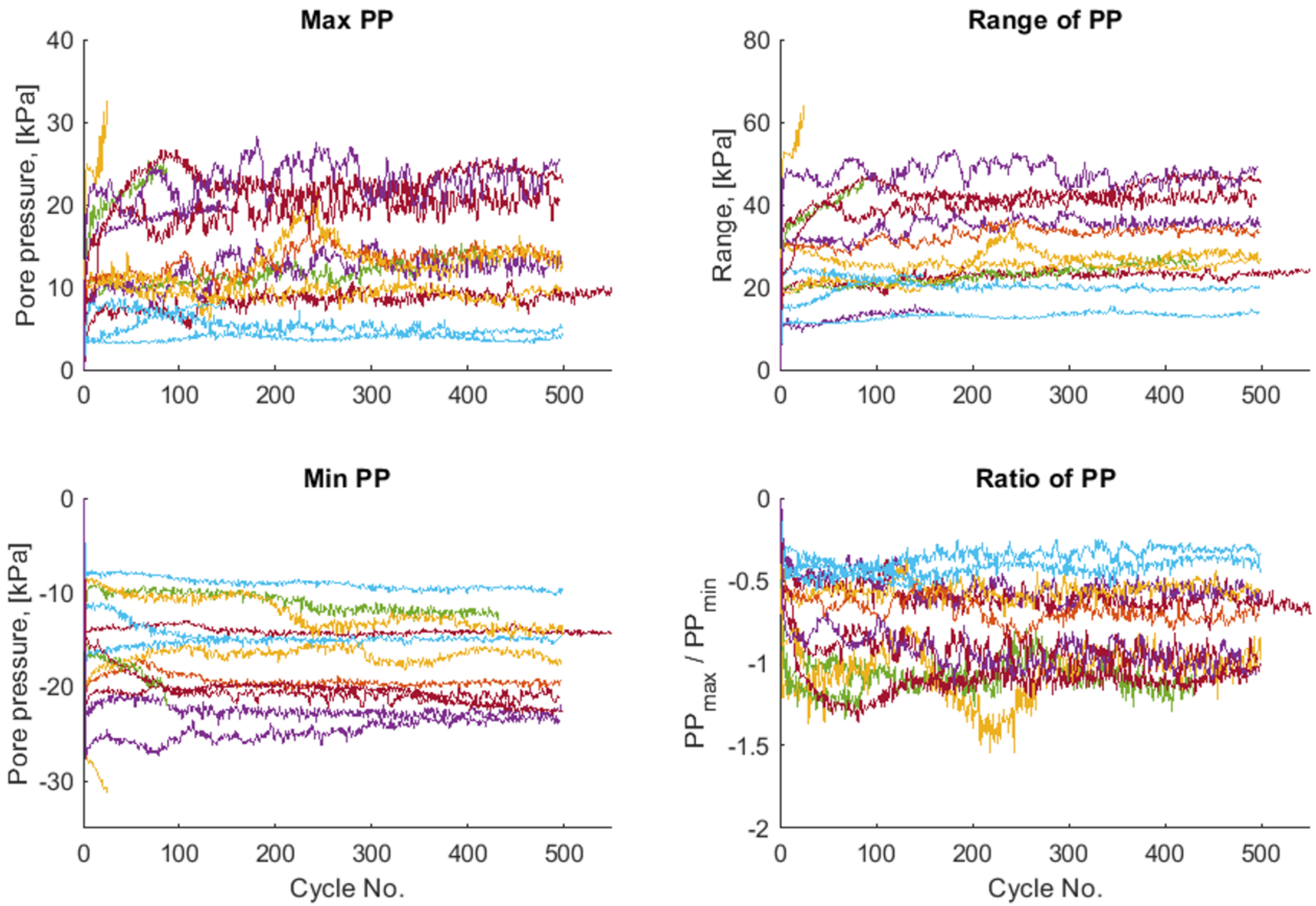

Figure 5.17: Pore pressure under the lid of the suction bucket

Stable (2nd group)

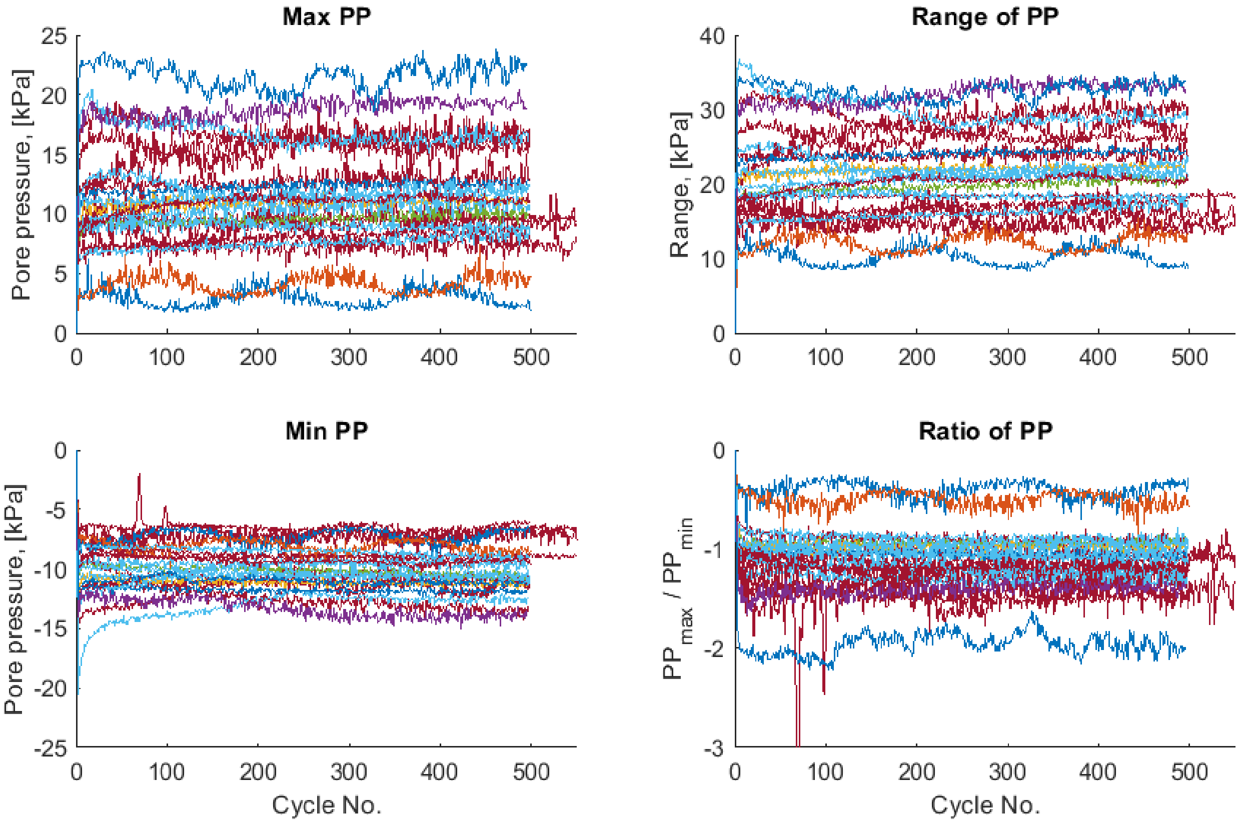

Figure 5.18: Pore pressure under the lid of the suction bucket

Displacing downwards(3rd group)

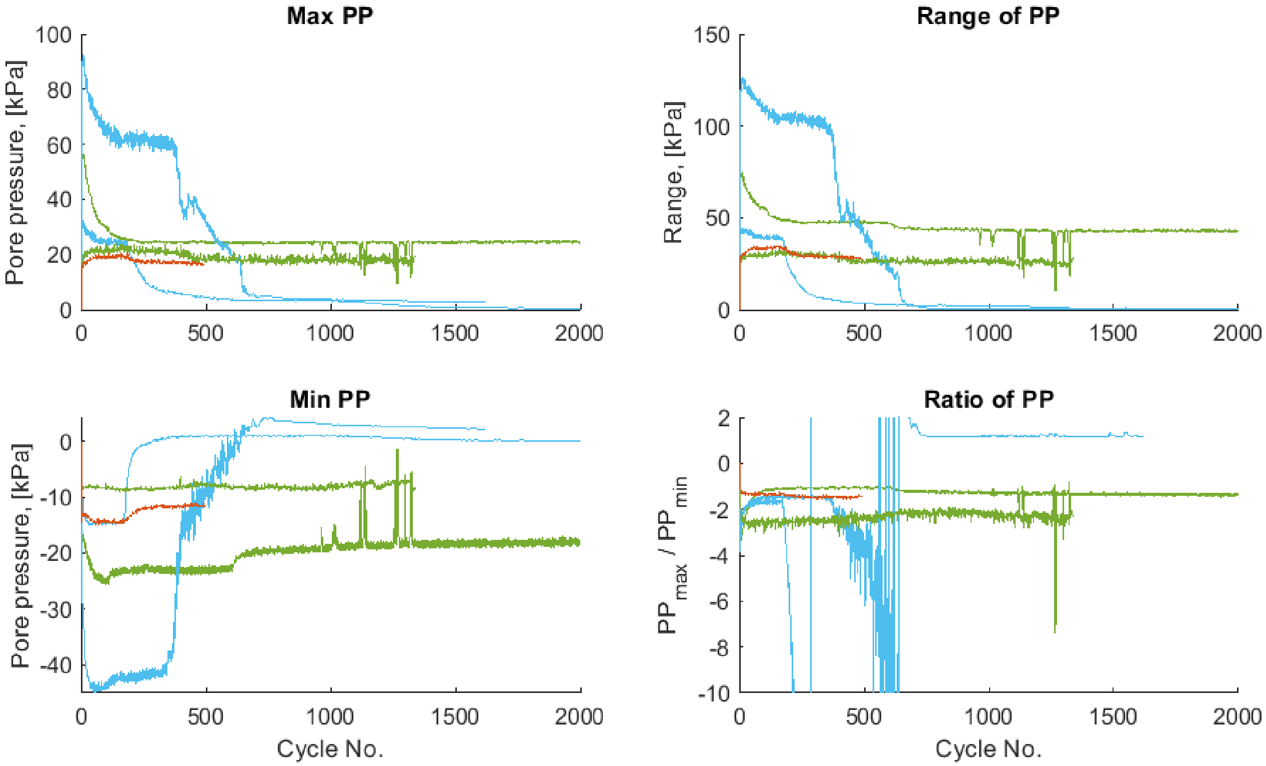

Figure 5.19: Pore pressure under the lid of the suction bucket

Effective overburden pressure

When designing foundations situated on sand deposits there is a potential for instability caused by the development of excess pore pressure as a result of cyclic loading. If the build-up of excess pore pressure exceeds the overburden pressure the soil might be exposed to initial liquefaction.

The effective overburden pressure is calculated as stated in equation (5.5)

Effective overburden pressure

$$\sigma'_v = \sigma_v - u \tag{5.5}$$

Where:

σ'_v	Effective overburden pressure	[kPa]
σ_v	Total overburden pressure	[kPa]
u	Excess pore pressure	[kPa]

The build-up of effective overburden pressure is investigated from 1st cycle to 500th cycle. Furthermore the values chosen as representative excess pore pressure is the ones obtained when the force is maximum, zero and minimum as illustrated in figure 5.20

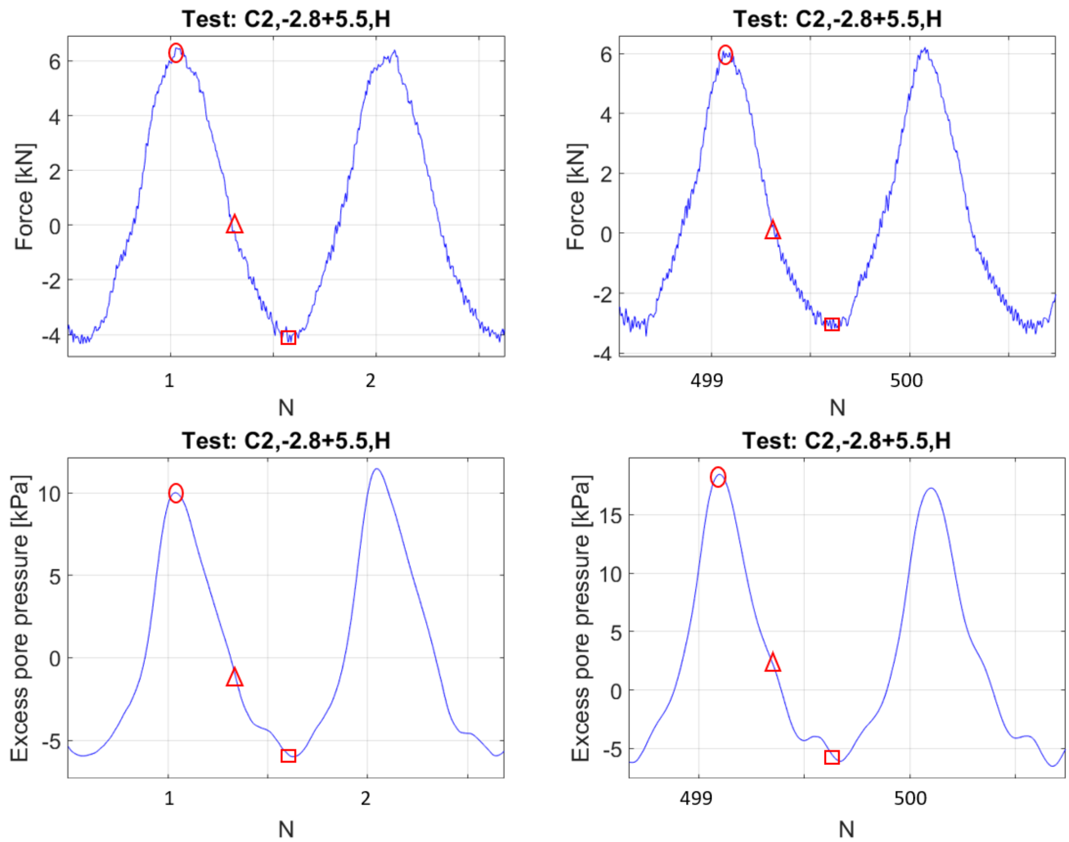

Figure 5.20: Force cycle compared to excess pore pressure at lid, transducer 6, for 1st (Left) cycle and 500th (right) cycle

Equation (5.5) is used to calculate the effective overburden pressure and the build up from 1st to 500th cycle for the three scenarios (Maximum force, zero force and minimum force) as illustrated in figure 5.21. It is noted that there might already be initiation of liquefaction in the 1st cycle, however there is a significant build up of excess pore pressure from the 1st to 500th cycle for both the excess pore pressure obtained at maximum force and minimum force. The initiation of liquefaction almost covers the entire skirt length of the bucket during 500th cycle. It could indicate that the soil grains are loosened and allows the water to flow more freely which in other words means that the bucket is "pushing" more water and thereby a build up of excess pore pressure is present.

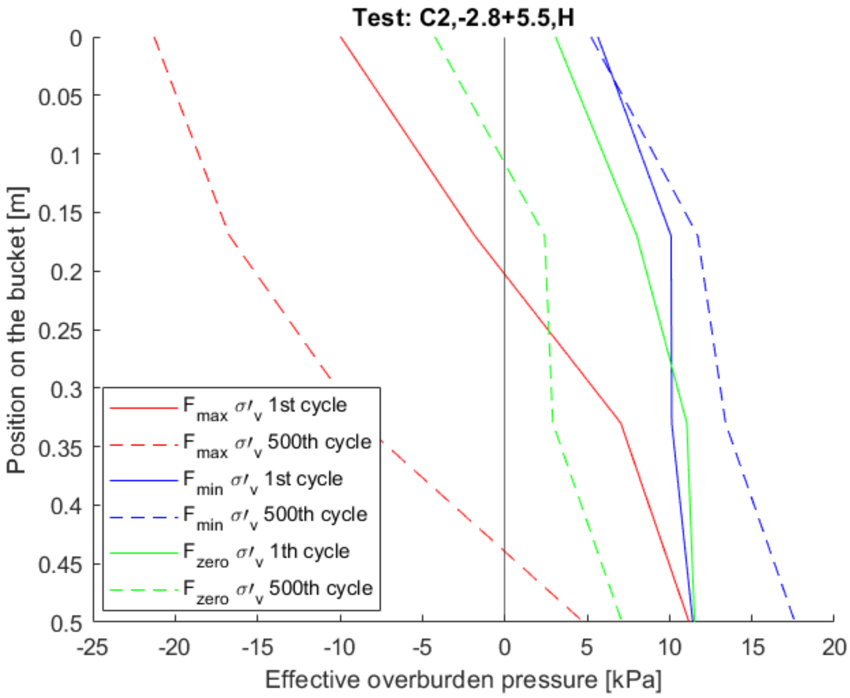

Figure 5.21: Overburden pressure build op from 1st to 500th cycle

For every test the build-up of excess pore pressure is investigated and the results can be found in appendix F the average buil-up or decrease for the three test groups are shown in table 5.4 on page 57.

5.4.3 Comparison of input parameters

All three groups of tests were summarized and the mean values with their standard deviations were compared and presented in table 5.5 and figure 5.22 below. Even though the performed tests differ quite widely from each other some tendencies can be seen:

- Average of maximum (compression) forces were lowest during the tests which were exposed to upwards displacement (pulled-up). Slightly higher compression forces were observed for tests which did not show any significant displacement and the highest forces were used during tests when the suction bucket was pushed deeper into the soil (downwards displacement). Opposite situation can be seen for minimum (tension) forces, for the tests exposed to a upwards displacement the highest tensile forces were used and vice versa for tests subjected to downwards displacement.
- As a continuation to just mention influence of forces to the displacements similar relationship with force ratio and displacements can be observed. From the obtained

results it is clear to see that tests exposed to upwards displacement had the smallest force ratio, while the highest was for tests exposed to pushed-down displacement.
- From the figure 5.22 it can be seen that majority of tests resulted to a insignificant displacement tests and all of tests subjected to upwards displacement significantly exceeds tensile capacity for drained conditions.

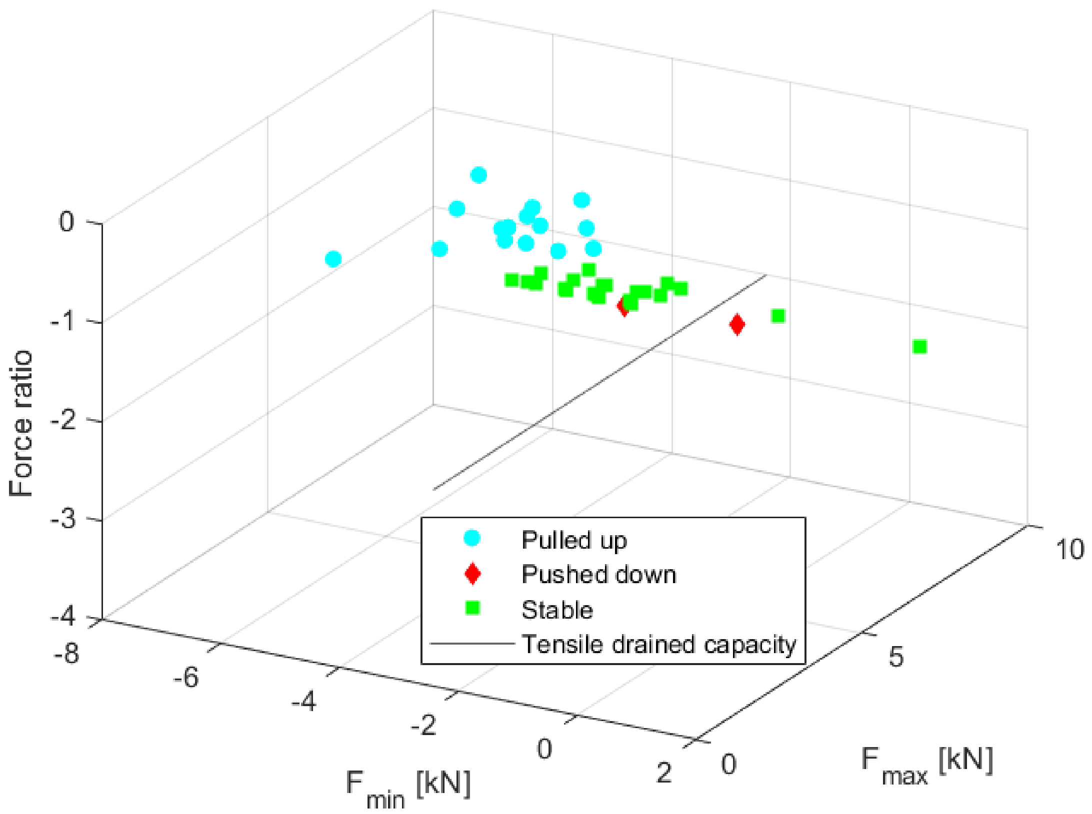

Figure 5.22: Comparison of three test groups

Table 5.5: Comparison of three groups

Group	Max force [kN]	Min force [kN]	Force ratio	Displacement
Pulled-up	5.85(2.02)	-4.38(0.97)	-1.36(0.43)	-0.105(0.130)
Stable	5.96(1.41)	-2.59(1.28)	-2.22(2.16)	0.001(0.007)
Pushed-down	22.86(11.35)	-2.60(1.25)	-34.30(54.73)	0.024(0.009)

- All the values are given as the average from the entire corresponding group
- Values presented in parenthesis are the standard deviations

Frequency

It was noticed that the loading frequency has a significant influence on the behaviour of suction bucket:

- 40.0 % of 1st group were loaded with a frequency of 0.1 Hz compared to 17.4 % and 0.0 % respectively for the 2nd and 3rd groups. The rest of the tests were loaded with higher frequencies either 0.5 or 1.0 Hz.

- All of the tests in the 3rd group were exposed to a pushed-down displacement were loaded with frequency of 1.0 Hz

That could be explained by the higher concentration of excess pore water pressure for a higher frequency loading, which happens due to the fact that permeability of the soil is unaffected by the loading rate and therefore water has less time to dissipate and significantly higher build up of excess pore water pressure is expected as it is described in [Arora, 2009] . This build up of pressure acts as a resisting force to the applied tensile load, which leads to the fact that higher tensile force is needed to overcome the resistance and pull the suction bucket out of the soil.

The hypothesis mentioned above about the influence of loading frequency to a build up of excess pore water pressure can be supported by results obtained from this project. Figure 5.23 compares tests D1,-2.3+6.6,H with D3,-2.7+6.9,L which were loaded with very similar forces except for the loading frequency were the first test is 1.0 Hz while the frequency of the second test is 0.1 Hz. Due to used machinery precision identical loads were not obtained for different frequencies even though used command forces in software were identical. The lines in the plot below represents maximum and minimum values of EPP in each of the cycle.

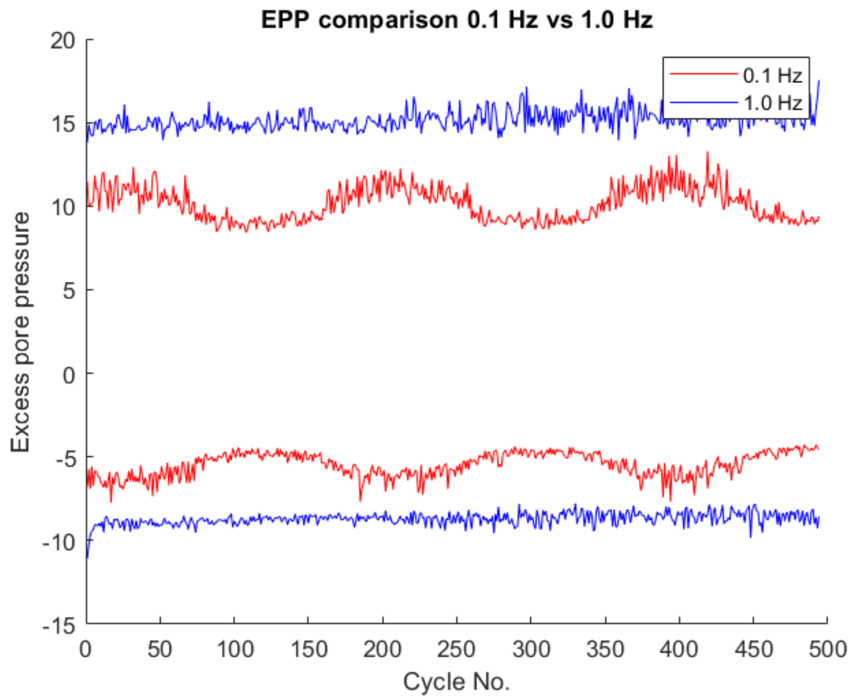

Figure 5.23: Comparison of EPP for the two tests with different loading frequencies

Moreover, another test which is not yet discussed was performed to analyse loading frequency influence. This displacement based test is detailed described in E but the idea behind the test is to investigate pore pressures at different loading frequencies for the same constant cyclic displacement (±2 mm displacement). Results can be seen in figure 5.24 where build-up of excess pore water pressure with the increasing loading frequency can be seen clearly.

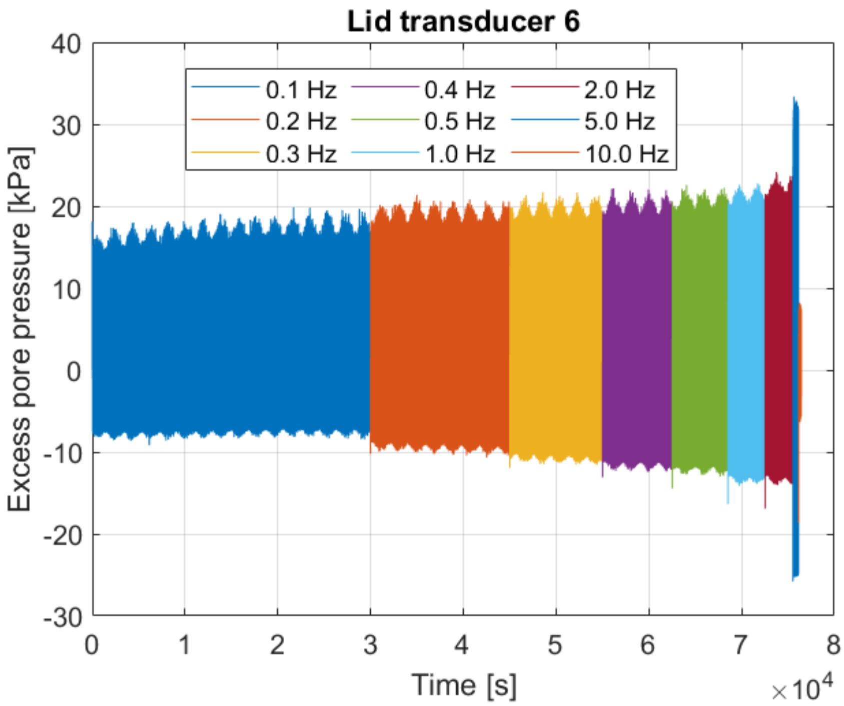

Figure 5.24: EPP under the lid of the suction bucket during displacement based test

Displacing upwards (1st group)

By sorting the results presented in table 5.1 according to the cyclic load frequency, 3 groups were made.

The two groups(FREQ1.1 and FREQ1.3) consists of tests with wide variety of force ratios, it can be seen that the average displacement for FREQ1.1 with loading frequency of 0.1 Hz is −0.124 mm has a standard deviation (SD) of 0.058 mm while the second group, FREQ1.3, with loading frequency of 1.0 Hz subjected to average displacement of −0.096 mm with standard deviation of 0.077 mm. Even though, both groups show a relatively high spread in displacement, FREQ1.1 were affected by higher displacements than FREQ1.3, that could mean that cyclic loading with lower frequency is more damaging than the one with high frequency. Since there is only one test with a frequency of 0.5 Hz no conclusion has been made.

Table 5.6: First group tests sorted according to the frequency

Group	Name	Max force [kN]	Min force [kN]	Frequency [Hz]	Force ratio	Displacement	Mean D	SD
FREQ1.1	D3,-3.7+6.9,L	6.9	-3.7	0.1	-1.86	-0.141	-0.124	0.058
	D3,-4.7+6.9,L	6.9	-4.7	0.1	-1.47	-0.126		
	E1,-3.0+4.8,L	4.8	-3.0	0.1	-1.60	-0.034		
	E1,-3.6+4.9,L	4.9	-3.6	0.1	-1.36	-0.212		
	F1,-6.8+9.2,L	9.2	-6.8	0.1	-1.35	-0.135		
	F1,-4.9+8.9,L	8.9	-4.9	0.1	-1.82	-0.096		
FREQ1.2	E3,-3.9+4.8,M	4.8	-3.9	0.5	-1.23	-0.041		
FREQ1.3	C2,-2.8+5.5,H	5.5	-2.8	1.0	-1.96	-0.023(-0.059)*	-0.096	0.077
	C3,-4.1+3.2,H	3.2	-4.1	1.0	-0.78	-0.220		
	C4,-4.6+0.9,H	0.9	-4.6	1.0	-0.20	-0.236		
	D1,-4.4+5.8,H	5.8	-4.4	1.0	-1.32	-0.075		
	D2,-4.2+6.4,H	6.4	-4.2	1.0	-1.52	-0.014		
	D2,-4.4+5.6,H	5.6	-4.4	1.0	-1.27	-0.080		
	F2,-5.0+7.6,H	7.6	-5.0	1.0	-1.52	-0.020		
	F2,-5.6+6.4,H	6.4	-5.6	1.0	-1.14	-0.119		

*Displacements are shown at 500 cycles and the values in () are total displacement.

Stable (2nd group)

By sorting results presented in table 5.2 according to the loading rate 3 groups were made.

Table 5.7: Frequency order of second group tests

Group	Name	Max force [kN]	Min force [kN]	Frequency [Hz]	Force ratio	Displacement	Mean D	SD
FREQ2.1	C1,1.9+6.9,H	6.9	1.9	1.0	3.63	-0.000(0.001)*	0.000	0.003
	C1,-0.7+7.3,H	7.3	-0.7	1.0	-10.43	0.000(0.015)*		
	C2,-2.7+6.6,H	6.6	-2.7	1.0	-2.45	0.002(0.025)*		
	D1,-2.3+6.6,H	6.6	-2.3	1.0	-2.87	0.001		
	D1,-3.2+6.6,H	6.6	-3.2	1.0	-2.06	0.001		
	D1,-3.7+6.5,H	6.5	-3.7	1.0	-1.76	-0.001		
	D1,-4.2+6.4,H	6.4	-4.2	1.0	-1.52	-0.007		
	D2,-3.2+6.5,H	6.5	-3.2	1.0	-2.03	-0.002		
	E2,-1.6+4.5,H	4.5	-1.6	1.0	-2.81	-0.000		
	E2,-2.2+4.6,H	4.6	-2.2	1.0	-2.09	-0.000		
	E2,-2.7+4.5,H	4.5	-2.7	1.0	-1.67	-0.000		
	E2,-3.2+4.5,H	4.5	-3.2	1.0	-1.41	-0.001		
	E2,-3.6+4.5,H	4.5	-3.6	1.0	-1.25	-0.004		
	F2,-3.0+8.5,H	8.5	-3.0	1.0	-2.83	0.008		
	F2,-4.5+8.4,H	8.4	-4.5	1.0	-1.87	0.006		
FREQ2.2	E3,-1.7+4.7,M	4.7	-1.7	0.5	-2.77	-0.001	-0.002	0.001
	E3,-2.3+4.7,M	4.7	-2.3	0.5	-2.04	-0.001		
	E3,-2.9+4.8,M	4.8	-2.9	0.5	-1.66	-0.001		
	E3,-3.4+4.6,M	4.6	-3.4	0.5	-1.35	-0.004		
FREQ2.3	F1,-3.4+8.8,L	8.8	-3.4	0.1	-2.59	0.000	-0.000	0.000
	D3,-2.7+6.9,L	6.9	-2.7	0.1	-2.56	0.000		
	E1,-1.8+4.8,L	4.8	-1.8	0.1	-2.67	-0.000		
	E1,-2.4+4.8,L	4.8	-2.4	0.1	-2.00	-0.000		

*Displacements are shown at 500 cycles and the values in () are total displacement.

As this is the group of tests which resulted in insignificant displacements it is difficult to relate the influence of the loading frequency to the displacement. However, this group consist of 23 tests in total and: 15 of them are loaded with the frequency of 1.0 Hz, 4 tests with the frequency of 0.5 Hz and 4 tests with the frequency of 0.1 Hz. It could be argued as an indication that tests with higher frequency requires higher loads to be subjected to any kind of displacement.

Displacing downwards (3rd group)

The frequency for the pushed-down test are not compared since they are all with a frequency of 1.0 Hz, it could be argued that loading with a high frequency needs higher tensile forces to have an up-wards displacement.

Loading

Generally, the tests performed during this project varies a lot from each other so it is difficult to observe right tendencies with relative small amount of specimens even though, some tendencies can be seen in figure 5.25 for each of the groups when talking about loading settings for the tests:

- The 3rd group subjected to downwards displacement were exposed to the highest compressive forces, while the 1st and 2nd groups shares very similar compressive forces.
- 1st group subjected to upwards displacement were expose to the highest tensile forces.
- Even though all three groups shares a very similar force ratios but it can be seen that the 3rd group has the largest force ratio values and the 1st group has slightly smaller force ratios compared to the 2nd group. It is worth to mention that it should have been investigated in a more detailed level because the number of tests is not sufficient enough.
- A correlation between displacement and force ratio was noticed, from the tests made, the tests with low force ratios had had the highest displacement and vice verse, the figures can be seen in appendix H.

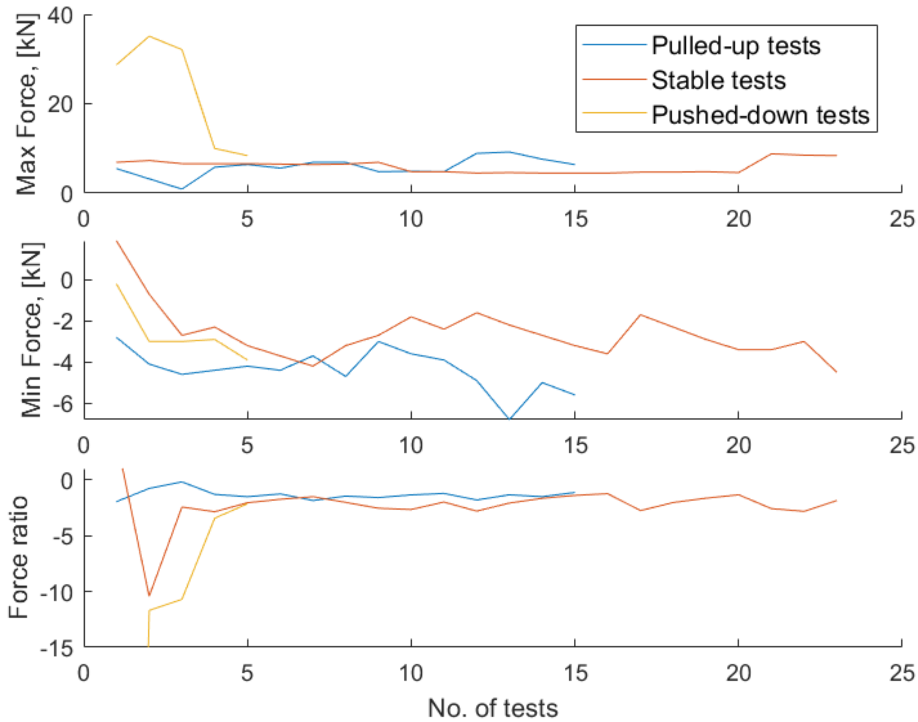

Figure 5.25: Comparison of loading parameters for each of the group

Pulled-up tests

By sorting the results presented in table 5.1 according to the force ratio 4 groups with a similar ratios were made.

For each of the groups the average displacement (Mean D) and standard deviation (SD) were calculated. It can be stated that the groups *FR1.1*, *FR1.2* and *FR1.3* with the force ratio ranges of (-0.20) ,$(-0.78$: -1.32) and $(-1.35: -1.52)$ respectively were subjected to the largest average displacements. Looking purely from this point of view it is possible to make an assumption that the least damaging forces should be in the range of $(-1.60: -1.96)$, even though the standard deviation of the displacements is quite significant in these groups, which means that the data is quite stochastic. It is important to highlight that this assumption should be tested more detailed before making a conclusion.

Table 5.8: First group tests sorted according to the force ratio

Group	Name	Max force [kN]	Min force [kN]	Frequency [Hz]	Force ratio	Displacement	Mean D	SD
FR1.1	C4,-4.6+0.9,H	0.9	-4.6	1.0	-0.20	-0.236	-0.236	
FR1.2	C3,-4.1+3.2,H	3.2	-4.1	1.0	-0.78	-0.219	-0.106	0.056
	F2,-5.6+6.4,H	6.4	-5.6	1.0	-1.14	-0.118		
	E3,-3.9+4.8,M	4.8	-3.9	0.5	-1.23	-0.040		
	D2,-4.4+5.6,H	5.6	-4.4	1.0	-1.27	-0.080		
	D1,-4.4+5.8,H	5.8	-4.4	1.0	-1.32	-0.074		
FR1.3	F1,-6.8+9.2,L	9.2	-6.8	0.1	-1.35	-0.135	-0.101	0.075
	E1,-3.6+4.9,L	4.9	-3.6	0.1	-1.36	-0.211		
	D3,-4.7+6.9,L	6.9	-4.7	0.1	-1.47	-0.126		
	F2,-5.0+7.6,H	7.6	-5.0	1.0	-1.52	-0.020		
	D2,-4.2+6.4,H	6.4	-4.2	1.0	-1.52	-0.013		
FR1.4	E1,-3.0+4.8,L	4.8	-3.0	0.1	-1.60	-0.039	-0.073	0.048
	F1,-4.9+8.9,L	8.9	-4.9	0.1	-1.82	-0.096		
	D3,-3.7+6.9,L	6.9	-3.7	0.1	-1.86	-0.141		
	C2,-2.8+5.5,H	5.5	-2.8	1.0	-1.96	-0.022(-0.058)*		

*Displacements are shown at 500 cycles and the values in () are total displacement.

Stable tests

By sorting results presented in table 5.2 according to the force ratio 5 groups were made.

Table 5.9: Force ratio order of second group tests

Group	Name	Max force [kN]	Min force [kN]	Frequency [Hz]	Force ratio	Displacement	Mean D	SD
FR2.1	C1,-0.7+7.3,H	7.3	-0.7	1.0	-10.43	0.000(0.015)*	0.000	0
FR2.2	D1,-2.3+6.6,H	6.6	-2.3	1.0	-2.87	0.001	0.001	0.002
	F2,-3.0+8.5,H	8.5	-3.0	1.0	-2.83	0.008		
	E2,-1.6+4.5,H	4.5	-1.6	1.0	-2.81	-0.000		
	E3,-1.7+4.7,M	4.7	-1.7	0.5	-2.77	-0.001		
	E1,-1.8+4.8,L	4.8	-1.8	0.1	-2.67	-0.000		
	F1,-3.4+8.8,L	8.8	-3.4	0.1	-2.59	0.000		
	D3,-2.7+6.9,L	6.9	-2.7	0.1	-2.56	0.000		
	C2,-2.7+6.6,H	6.6	-2.7	1.0	-2.45	0.002(0.025)*		
FR2.3	E2,-2.2+4.6,H	4.6	-2.2	1.0	-2.09	-0.000	0.000	0.002
	D1,-3.2+6.6,H	6.6	-3.2	1.0	-2.06	0.001		
	E3,-2.3+4.7,M	4.7	-2.3	0.5	-2.04	-0.002		
	D2,-3.2+6.5,H	6.5	-3.2	1.0	-2.03	-0.002		
	E1,-2.4+4.8,L	4.8	-2.4	0.1	-2.00	-0.000		
	F2,-4.5+8.4,H	8.4	-4.5	1.0	-1.87	0.006		
	D1,-3.7+6.5,H	6.5	-3.7	1.0	-1.76	-0.001		
FR2.4	E2,-2.7+4.5,H	4.5	-2.7	1.0	-1.67	-0.000	-0.003	0.002
	E3,-2.9+4.8,M	4.8	-2.9	0.5	-1.66	-0.001		
	D1,-4.2+6.4,H	6.4	-4.2	1.0	-1.52	-0.007		
	E2,-3.2+4.5,H	4.5	-3.2	1.0	-1.41	-0.001		
	E3,-3.4+4.6,M	4.6	-3.4	0.5	-1.35	-0.004		
	E2,-3.6+4.5,H	4.5	-3.6	1.0	-1.25	-0.004		
FR2.5	C1,1.9+6.9,H	6.9	1.9	1.0	3.63	-0.000(0.001)*	-0.000	0

*Displacements are shown at 500 cycles and the values in () are total displacement.

From the obtained results it is difficult to predict any tendency relating force ratio with the displacement of the suction bucket, that is because this group covers a wide range of force ratios starting with $FR = 3.63$ and ending with $FR = -10.43$ and yet all of the test are not exposed to any significant displacement.

Pushed-down tests

By sorting results presented in table 5.3 according to the force ratio 3 groups with a similar ratios were made. The three groups are shown in table 5.10.

Table 5.10: Third group tests sorted according to the force ratio

Group	Name	Max force [kN]	Min force [kN]	Frequency [Hz]	Force ratio	Displacement
FR3.1	A1.-0.2+28.7.H	28.7	-0.20	1.0	-143.5	0.028 (0.057)*
FR3.2	A2.-3+35.1.H	35.1	-3.00	1.0	-11.7	0.028 (0.053)*
	A3.-3+32.1.H	32.1	-3.00	1.0	-10.7	0.037 (0.053)*
FR3.3	C1,-2.9+10.0,H	10.0	-2.90	1.0	-3.44	0.014 (0.023)*
	F2,-3.9+8.4,H	8.40	-3.90	1.0	-2.15	0.012

*Displacements are shown at 500 cycles and the values in () are total displacement.

By sorting results presented in table 5.10 according to the force ratio 3 groups were made.

Three groups have been formed, when the tests are compared with the force ratios, it is clear from table 5.10 that group $FR3.1$ and $FR3.2$ have significant larger displacements compared to $FR3.3$. When looking purely at the force ratio, it can be assumed that the force ratio do not have a significant influence when they are that large, since $FR3.1$ and $FR3.2$ have quite similar displacements even though the ratio between the force ratios are 13 times bigger. However looking at $FR3.2$ and $FR3.3$ it can be assumed that the force ratio starts to have an influence when values are lower, since there is quite some difference in displacements between these groups.

6 | Discussion

Key findings

- **Stiffness development** - It was observed that the unloading/reloading stiffness development for each group were quite different, various scenarios of stress reversal were observed due to the variety of different amplitude forces which were used. One of the reasons for that could be that with each repeated cyclic loading, there is a gradual change in strength due to stress reversal in two-ways loading so the rapid generation of excess pore pressure and large strains can be observed at this moment leading to the changes in soil stiffness.
  For the first group, which displaced upwards a clear degradation in the stiffness was noticed, it could corresponds with the statement mentioned above, that for each cycle a gradual decrease in stiffness is noticed as the excess pore water pressure increases, resulting with the soil "loosing the grip" on the suction bucket under the cyclic loading and could be a sign of the initiation of liquefaction occurring.
  For the second group the displacements were quite insignificant for the 500 cycles applied, the stiffness for these tests remained approximately unchanged, which corresponds with the displacing behaviour. However 6 tests experienced a significant stiffness degradation during their first 50 cycles. During their remaining 450 cycles the stiffness remained stable. The reason for this could be because it was observed that majority of these tests where just before the ending of this transient zone where the displacement of the suction bucket goes from downwards to upwards.
- **Excess pore pressure development** - It was found that ratio between tensile and compressive forces plays a significant role in displacement pattern and development of excess pore pressure when comparing the development of the 1st with the 500th cycle.
  The first group (Pulled-upwards) was exposed to the relative biggest increase for both maximum and minimum excess pore pressure. It could be because the tensile forces exceeds the tensile bearing capacity resulting in upwards displacement which during each cycle loosened the soil grains and allowing the water to flow more freely between the grains. This results in a build-up of excess pore pressure from the 1st to 500th cycle. Even at the 1st cycle there is a potential initiation of liquefaction, however it is significantly larger at the 500th cycle. It indicates that the bucket is pushing more water and a relative large build-up of excess pore pressure is expected. Moreover, findings from the third group (Pushed-down) shows decrease in both maximum and minimum EPP during increasing number of cycles. It can be argued that it happened due to the fact that while the bucket was displacing downwards, soil on the same time was being more and more compressed leading towards drained behaviour of it with smaller EPP. However, there are only 5 tests in this group with quite different loading characteristics so amount of specimens might not be sufficient enough to analyse the results.
- **Influence of frequency** - It was found that the loading frequency plays a significant role to the development of the displacement. In total 44 tests were performed during the research, 10 of them were loaded with frequency of 0.1 Hz, 5 with 0.5 Hz and 29 with 1.0 Hz. A group of 15 tests subjected to large up-wards displacements consist of 6 out of 10 of those tests which were tested with a low frequency were found in this group. That could be a good indication about the influence of frequency to the displacement of the

suction bucket. This relationship can be explained by the time needed for excess pore water pressure to dissipate ([Arora, 2009]). Permeability of the soil is not affected by the loading rate meaning that dissipation of EPP is only limited by time between the cycles. Due to that, higher concentration of it can be expected when loading frequency is high. Build up of this pressure acts as a additional resisting force which needs to be surpassed before causing any displacement for the suction bucket. Worth to mention that current understanding of loading rate dependence is in "grey" area. Paper [Byrne and Houlsby, 2015] states that loading rate has little effect of the transient response. However, [Low et al., 2020] findings supports our results confirming that cyclic at low frequency lead to additional settlement or uplift, while cycling at higher frequency leads to greater pore pressure generation.

- **Number of cycles** - The obtained results showed the importance of number of loading cycles. Even though, most of the tests were performed with only 500 cycles to represent severe conditions in the sea, it was noticed that neither the displacement, stiffness or EPP shows any signs of convergence over time. Moreover, some of the tests were subjected to a significantly larger amount of loading cycles, still, no convergence of the results were noticed. However, it is worth to mention that the smallest difference over time was observed in unloading / reloading stiffness of the soil compared to the displacement and EPP. Here significant influence was noted during very first cycles, while later the difference was insignificant.
- **Design criterion** - Results discussed in section 5.4.3 on page 62 provided an insight for design of suction bucket foundations during "push-pull" mechanism failure. All of the tests which resulted in upwards displacement and majority of tests resulted in stable displacement were subjected to significantly higher tensile forces then soil tensile drained capacity limit which was investigated during research and discussed in D.1 . So it can be argued that design according to drained bearing capacity is a very safe against being pulled-up and no additional safety factors should be used.

Unexpected results

Unexpected odd results were not avoided during the project. During $C4,-4.6+0.9,H$ test from the 1st group, stiffness hardening were observed when other tests in the group resulted in degradation of stiffness. Furthermore, different behaviour of suction bucket were seen for 3rd group subjected to the downwards displacement. 3 of those tests experienced stiffness hardening, the next test experienced no significant change in stiffness and for the last the stiffness decreased. These stiffness developments were unexpected. Even though, minority of the tests showed odd results it is still a good indication that results are highly influenced by the initial soil conditions and loading parameters and deeper investigation should be done.

The investigated topic is very wide making it extremely difficult and time consuming to cover every aspect of it. Due to limited resources some limitations which requires detailed studies were faced:

Limitations

The third group (Pushed-down) only consisted of five experiments which is an insufficient amount of data sample for a reliable data analysis and thereby the tendencies for downwards displacement can not be concluded.

Another limitation during this project was related to the technical issues of the equipment used during tests. During some of the tests there were discrepancy between command forces stated in the software and actual forces. As a consequence to that some of the tests with identical theoretical loading conditions ended up being loaded with different loads making them difficult to compare in between.

Sources of errors and limitations

- **Over- and undershooting of the piston:**
  During load extrapolation, the actual loads (induced by the piston) did not correspond to the command loads (input in the program) as seen in figure 6.1. The value of the over- and undershooting was different from test to test, it was tried to manipulate the the command load so the actual load would read the wanted load, this was not possible which can be seen in the presentation of the results, as the actual load differs from the load plan.

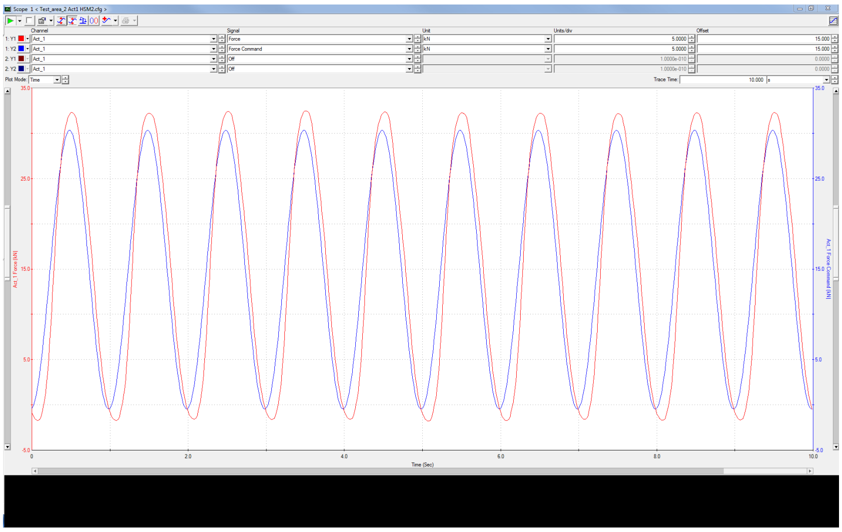

Figure 6.1: Actual force red - force command blue

- **Vibrations of the piston:**
  Odd behaviour of the hydraulic piston was noticed as it was vibrating some time. Exact reason for that was not determined but warming up the hydraulic system and calibration of the system input parameters before running the test reduced the vibrations at that time. On the other hand, it was not a permanent solution as these vibrations occurred quite randomly, meaning that it could also occur during the test affecting the results.
- **Load cell:**
  Two load cell were used, one which could withstand a load up to 250 kN and 100 kN for the other. Their precision where not specified and could only be determined by calibration from manufacturer. When checking correct calibration of the load cell with a 10 Kg steel plate the load cell should show 0.98 kN however readings where fluctuating.
- **CPT:**
  CPT locations where initially specified however manually positioned. If a CPT cone where to penetrate at a vibration hole or near one, the readings would be affected and perhaps untrustworthy. The water where not transparent enough to determine positions of vibration holes.

- **Transducers calibration:**
  The calibration factor for each transducer were done manually, by taking the average of three values since they fluctuated, this leads to some uncertainty since more values could have been chosen.
- **Clogging of transducers pipes:**
  It was noticed that during some of the tests the pipes running from the transducers along the suction bucket skirt got clogged by the sand grains effecting the measurement of excess pore pressure. Highly effected results were neglected completely but partial clog which was not taken into consideration could have happened.
- **Sealing of the transducers:**
  Before mounting transducers to the suction bucket they were sealed with sealing tape and tested by submerging them into the water and looking for air bubbles coming from the connection. However, it can be argued that such sealing does not ensure complete seal and air leak effecting excess pore pressure measurements could be expected.
- **Transducers limitations:**
  Transducers are limited to withstand a maximum pressure of 2 bar which limits the pressurisation of the tank hence limit the simulate of water depth to maximum of 20 m.
- **Depth limitations:**
  Tests were done in the pressure tank with limited space inside. After installation of the suction bucket there were approximately 20 – 30 mm space below the bucket until reaching the displacement limits, due to that some of the tests stopped earlier than planned. Furthermore, it can be argued that influence from the boundaries of the pressure tank could effect the behaviour of the suction bucket.

Follow up studies and restatement

As it is mentioned earlier due to limited resources it was impossible to cover every aspect of the problem, so follow-up studies are suggested:

During this project it was chosen to work with a narrow range of relative density of sand between 80 - 90 % . However, different soil conditions can be expected to be faced while designing a offshore wind farm, that is why future work could consist of wider spectrum of relative density and results could be compared in order to investigate the influence of Dr to the behaviour of suction bucket foundations subjected to a axial cyclic loading.

Moreover the group of tests subjected to down-wards displacement showed very different results, reason for that could be that there were only 5 tests with different loading situations. No conclusions were made about this group due to this fact so the behaviour of suction bucket subjected to down-ward displacements remains in "grey" area. Further studies could be done in order to investigate it and compare with other groups subjected to up-wards or minor displacements.

The results highlighted the dependency of axial cyclic loading frequency, amplitude and number of cycles to the performance of suction bucket foundations in dense sand in deep waters. As it is seen from the results, behaviour of suction bucket was effected significantly, so it is of crucial importance to take into consideration these parameters while designing such foundations for a offshore wind park.

7 | Conclusion

As off-shore wind parks are being installed in deeper and deeper waters and traditional usage of monopile foundations becomes less economical efficient, and so it is important to look for alternatives. One of such alternatives could be the suction bucket foundations. This project deals with the very first step of this investigation - performance of suction bucket foundation on a jacket structure subjected to different cases of axial cyclic loading.

By testing scaled model of suction bucket foundation subjected to different scenarios of axial cyclic loading evidence of relationship between the behaviour of the bucket and loading were observed by assigning results according to how the bucket displaced in three groups:

- 1st group of tests resulted in upwards displacements.
- 2nd group of tests resulted in minor displacements.
- 3rd group of tests resulted in downwards displacements.

Clear tendency of stiffness degradation was observed for majority of the tests subjected to an upwards displacement. Moreover, tests during which the bucket displacement were negligibly small changes in unloading / reloading stiffness were insignificant. However, no pattern of stiffness development were found for the 3rd group tests due to small amount of specimens and relatively high stochastic spread of the results. Furthermore, it is worth to mention that greatest changes in stiffness happened in first 100 loading cycles

Like the stiffness there were a clear difference in the development of excess pore pressure and influence of the loading frequency for each of the group. Similarly to the [Low et al., 2020] findings, results from this project showed that cycling at lower frequency tends to lead to a significant upwards displacements while cyclic at high frequency leads to the greater build up of excess pore water pressure.

Moreover, it was proved that in order to displace upwards suction bucket needs to be exposed to significantly higher tensile forces than the soil drained tensile bearing capacity. Due to that, it is a safe method to design such type of structure according to drained bearing capacity.

Finally, it must be mentioned that this research covers narrow spectrum of different scenarios so future work with more specimens should be done focusing on a specific displacement group or by varying one of the used loading parameters such as: frequency or amplitude.

Literature

Amir M Kaynia, 2018. Amir M Kaynia. *Wind turbine foundation.* `https://www.researchgate.net/figure/Common-foundation-types-used-in-offshore-wind-turbine-design-mono-pile-a-mono-pod_fig1_324954841`, *2018. Downloaded: 03-03-2022.*

Arora, 2009. DR. K.R. Arora. *SOIL MECHANICS AND FOUNDATION ENGINEERING. STANDARD PUBLISHER DIST., 2009. ISBN: 978-8180141126.*

Barari et al., 2016. A. Barari, L. B. Ibsen, A. Taghavi Ghalesari and K. A. Larsen. *Embedment Effects on Vertical Bearing Capacity of Offshore Bucket Foundations on Cohesionless Soil. Aalborg University, 2016.*

Byrne and Houlsby, 2003. Byrne and Houlsby. *Foundations for offshore wind turbines. University of Oxford, 2003.*

Byrne and Houlsby, 2015. Byron W. Byrne and Guy T. Houlsby. *Experimental Investigations of Response of SuctionCaissons to Transient Vertical Loading. Universidad Politecnica De Valencia, 2015.*

Claus Hindsgaul, 2005. Claus Hindsgaul. *Wind resource map for Denmark.* `https://www.researchgate.net/figure/Wind-resource-map-for-Denmark-height-above-terrain-sea-level-75-m-based-on-EMD-ConWx_fig21_325295428`, *2005. Downloaded: 03-03-2022.*

Cornwall Insight, 2019. Cornwall Insight. *Wind resource map for Denmark.* `https://www.renewableenergyworld.com/wind-power/report-says-offshore-wind-could-beat-onshore-wind-on-cost/#gref`, *2019. Downloaded: 03-03-2022.*

Danish Wind Industry Association, 2003. Danish Wind Industry Association. *Wind Map of Western Europe.* `http://www.xn--drmstrre-64ad.dk/wp-content/wind/miller/windpower%20web/en/tour/wres/euromap.htm`, *2003. Downloaded: 03-03-2022.*

EarthLabs, 2020. EarthLabs. *Wind turbine foundation.* `https://serc.carleton.edu/eslabs/corals/4b.html`, *2020. Downloaded: 03-03-2022.*

European Regional Development Fund, 2019. European Regional Development Fund. *Future Energy Indrustry Trends.* `https://bit.ly/3zc9e4r`, *2019. Downloaded: 31-05-2022.*

European Union's Horizon, 2022. European Union's Horizon. *i4offshore, 2022. Downloaded: 20-05-2022.*

for Soil Mechanics and Engineering, 2016. International Society for Soil Mechanics and Geotechnical Engineering. *Relative densities and void ratios derived from CPT data using in situ field calibration. Australian Geomechanics Society, 2016. ISBN: 978-0-9946261-1-0.*

Grecu et al., 2021. Sorin Grecu, Lars Bo Ibsen and Amin Barari. *Soils and Foundations. Department of civil engineering Aalborg university, 2021. Adresse: https://www.sciencedirect.com/science/article/pii/S0038080620337525.*

G.T.Houlsby, 2016. G.T.Houlsby. *Interactions in offshore foundation design. Department of Engineering Science, University of Oxford, 2016.*

Houlsby et al., 2005. Guy T. Houlsby, Richard B. Kelly and Byron W. Byrne. *The tensile capacity of suction cassions in sand under rapid loading. Department of Engineering Science, Oxford University, 2005.*

Ibsen et al., 2005. Lars Bo Ibsen, Morten Liingaard and Søren A. Nielsen. *Bucket foundation, a status. Department of civil engineering Aalborg university, 2005.*

Ibsen et al., 2009. Lars Bo Ibsen, Mats Hanson, T. Hjort and M. Thaarup. *MC-Parameter Calibration of Baskarp Sand No. 15. Department of civil engineering Aalborg university, 2009.*

Kelly et al., 2006. R. B. Kelly, G. T. Houlsby and B. W. Byrne. *Transient vertical loading of model suction caissons in a pressurechamber. Geotechnique, 2006.*

Low et al., 2020. H. E. Low, F. Zhu, H. Mohr and C. Erbrich. *CYCLIC LOADING OF OFFSHORE WIND TURBINE SUCTION BUCKET FOUNDATIONS IN SAND: THE IMPORTANCE OF LOADING FREQUENCY. Bureau of Safety and Environmental Enforcement (BSEE), U.S., 2020.*

M.O.C., 2017. M.O.C. *Suction Bucket Jacket Foundations. https://marineoffshoreconsultants.com/marine-warranty-survey-borkum-riffgrund-2-owf-suction-bucket-jacket-foundations/, 2017. Downloaded: 03-03-2022.*

Roy and Bhalla, 2017. Surendra Roy and Sanjeev Kumar Bhalla. *Role of Geotechnical Properties of Soil on Civil Engineering Structures. Resources and Environment, 2017.*

Senders, 2008. M. Senders. *SUCTION CAISSONS IN SAND AS TRIPOD FOUNDATIONS FOR OFFSHORE WIND TURBINES. The University of Western Australia, 2008.*

Society, 2001. Danish Geotechnical Society. *Laboratoriehaandbogen. STANDARD PUBLISHER DIST., 2001. ISBN: 87-89833-12-0.*

Tardio and Moldovan, 2021a. Carolina Andrea Vial Tardio and Elena-Ioana Moldovan. *Monotonic Tensile Loading of Suction Bucket Foundation Model in a Pressure Tank, 2021a.*

Tardio and Moldovan, 2021b. Carolina Andrea Vial Tardio and Elena-Ioana Moldovan. *Monotonic Tensile Loading of Suction Bucket Foundation Model in a Pressure Tank. Department of civil engineering Aalborg university, 2021b.*

Thieken et al., 2014. K. Thieken, M. Achmus and C. Schröder. *On the behavior of suction buckets in sand under tensile loads. Geotechnical Engineering, Leibniz University Hannover, 2014.*

Vaitkunaite, 2016. Evelina Vaitkunaite. *Physical Modelling of Bucket Foundations Subjected to Axial Loading. Department of civil engineering Aalborg university, 2016.*

Wind Europe, 2020. Wind Europe. *Wind turbine foundation. https://orsted.com/en/our-business/offshore-wind/wind-technology/suction-bucket-jacket-foundations, 2020. Downloaded: 03-03-2022.*

Yilmaz and Tasan, 2021. S.Alp Yilmaz and H.Ercan Tasan. *A study on the behaviour of offshore suction bucket foundations under cyclic axial compressive loading. Department of Civil Engineering, Middle East Technical University, Universiteler Mahallesi, Cankaya Ankara, Turkey, 2021.*

II

Appendix

Appendix A | Test Set-up

In this chapter a more detailed explanation of the equipment from the Department of the Built Environment of Aalborg University which was used for the experiments is provided.

A.1 Pressure tank

Pressure tank which is used for all the experiments described in this project is approximately 2.1 m x 2.1 m x 2.1 m size steel container with a cylindrical shape. Schematic view of the pressure tank with all the accessories is presented below in figure A.1 in a same way as it is presented in 3.1.

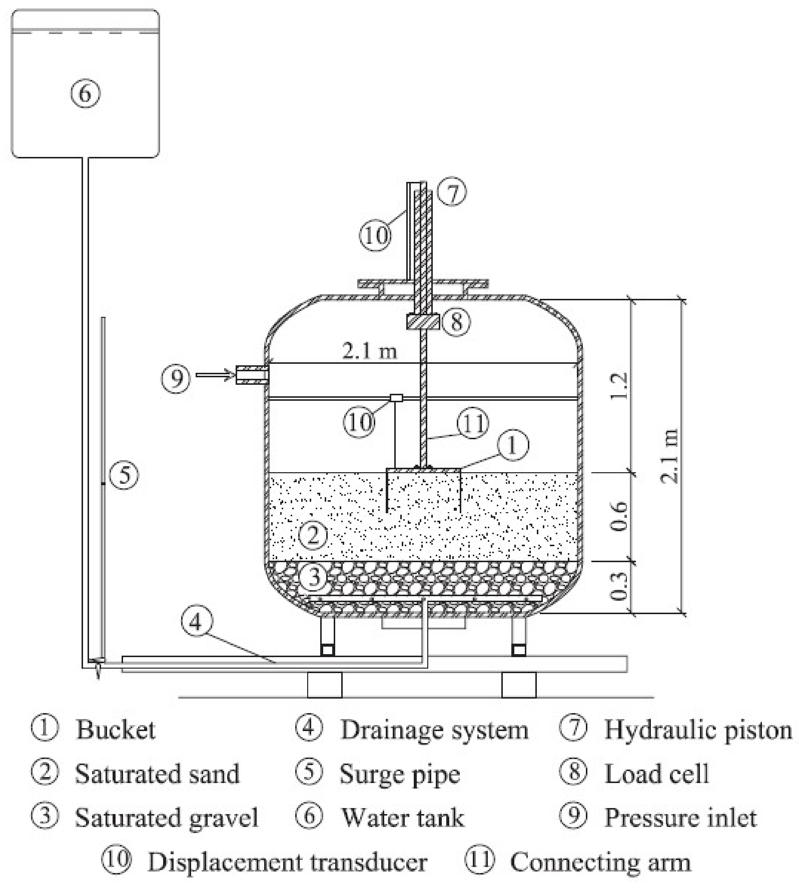

Figure A.1: Scheme of the pressure tank

Fully sealed this pressure tank can safely withstand a maximum of 2.0 bar pressure, which is enough to simulate real life situations with water depth up to 20 m. Tank itself is pressurizing by opening pressure inlet after closing all the drainage system valves and sealing the entrance lid as presented in figures A.2:

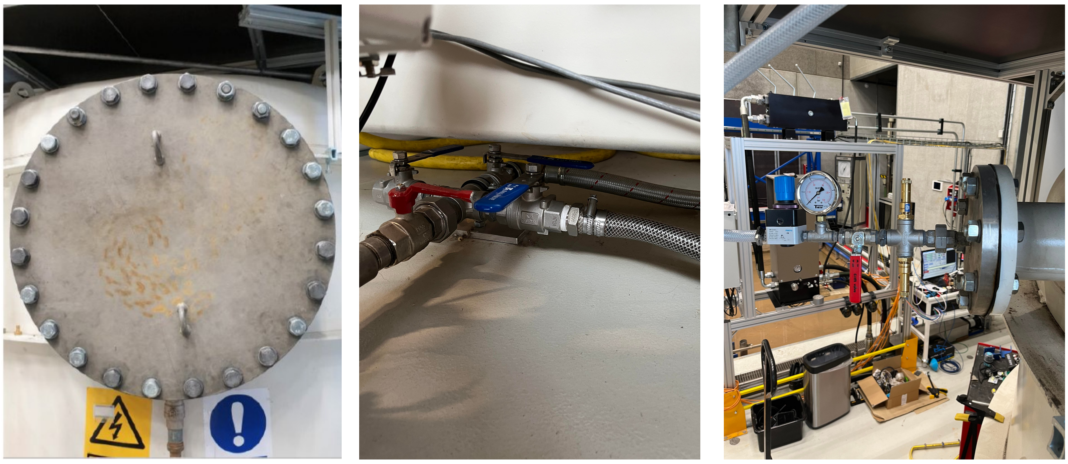

(a) Closed lid (b) Drainage valve (c) Valve for pressurizing

Figure A.2: Procedure for pressurizing the tank

Just after installing the entrance lid pressure tank is filled with extra water from the water tank to ensure that after pressurizing it the suction bucket is going to be be fully submerged into the water. This is done by opening valve on a pressure tank, as shown in figure A.3. External water tank is placed in a laboratory at 7.0 m height in order to have a consistent flow to a pressure tank without using extra equipment.

Figure A.3: Valve for adding water

Furthermore, inside the pressure tank there is connection to a hydraulic system which is fixed to outer side of the tank. This connection is used to attach a connection arm, load cell and a suction bucket to it. Example of such setup and hydraulic system are presented in figures A.4:

(a) Hydraulic system (b) Example of setup attached to the system

Figure A.4: Hydraulic system and its connection inside the tank

In order to use the transducers which are attached to the suction bucket and discussed later in this project some connections are installed and fixed inside the pressure tank. These connections can be seen in figure A.5:

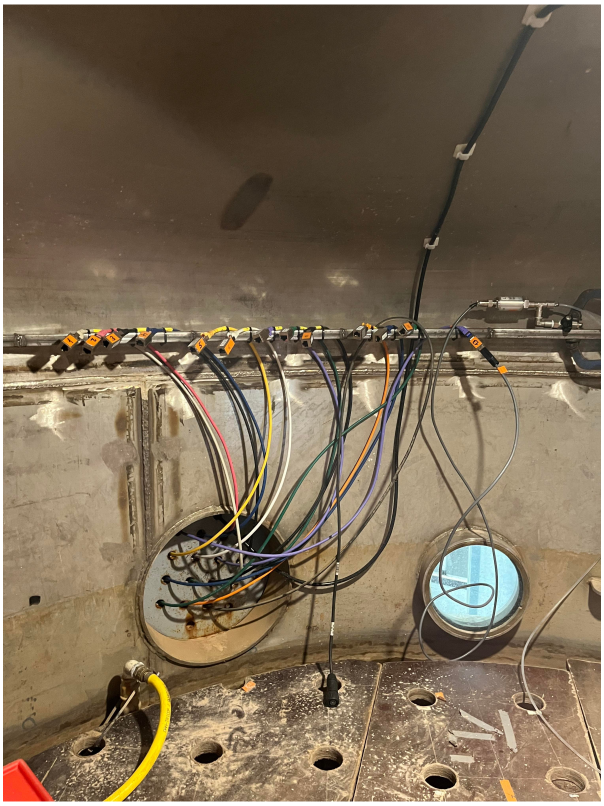

Figure A.5: Connections for sensors

A.2 Suction buckets

As it is briefly mentioned in 3.1 the suction buckets used during this project:

Suction bucket - Stainless steel bucket with a skirt length L of 0.5 m and a diameter D of 0.5 m

The bucket has two valves on the lid, which are kept open during installation in order to let the air between the inner side of the lid and sand surface dissipate. After the installation part valves were being closed. Furthermore, the bucket are equipped with sensors at different level on both outer and inner sides to measure the pore water pressure. Schematic drawing of a cross-section of the bucket with placement positions of pore pressure transducers is presented in A.6a while the bucket are seen in figure A.6b

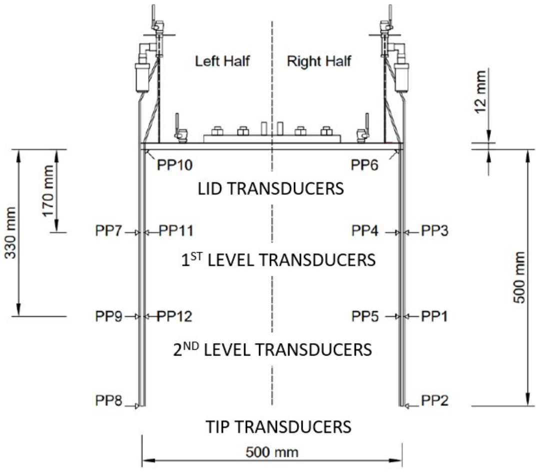

(a) Cross-section drawing of bucket

(b) Bucket A and B

Figure A.6: Schematic view of bucket

The bucket has a connections to fix the pore pressure transducers, which can be seen in A.7. They are welded approximately 25.0 cm above the lid of the bucket in order to keep the connections dry during the experiments when the bucket is fully emerged into the water.

Figure A.7: Connections for sensors on the bucket

A.3 Soil

From the A.1 it can be seen that pressure tank is filled with 0.3 m and 0.6 m layers of gravel and Aalborg sand respectively.

Gravel is used to ensure free water flow and it is seperated from the sand by the use of membrane layer, which allows water to flow without mixing the sand with gravel. Further, as a main material in which bucket is installed - Aalborg University Sand No.1 is used, which has been tested according to Danish Geotechnical Society [2001] characteristics are summarized in A.1:

Table A.1: Properties of Aalborg University Sand No.1

Parameter	Notation	Value
Specific Gravity	G_s	2.640
Minimum Void Ratio	e_{min}	0.549
Maximum Void Ratio	e_{max}	0.858
50% Quantile [mm]	d_{50}	0.140
Uniformity Coefficient	U	1.780

A.4 Pore pressure transducers

During the test 12 transducers were fixed to the bucket to measure pore pressure development through out the test. This number consist of two different type of sensors:

A - "Small" sensors with ethernet cable attached to them and with the range of 5.0 bar

B - "Big" sensors with separate ethernet cable and with the range of 2.0 bar

Due to pressure tank limitations maximum pressure of 2.0 bar were used which ensures that sensors were suitable for tests described in this project. Moreover, sensors are calibrated with the procedure described in A.8 before each test to ensure trustworthy readings.

(a) Sensor A (b) Sensor B

Figure A.8: Sensors A and B used for tests

A.5 Equipment for saturation

In order to saturate transducers with the procedure described in 3.2.3 vacuum pump were used to which plastic pipe were attached which other end later was attached to the sensor which were about to be saturated. Moreover, barrel filled with water was used in which bucket was emerge during saturation procedure. Equipment used during saturation can be seen in A.9:

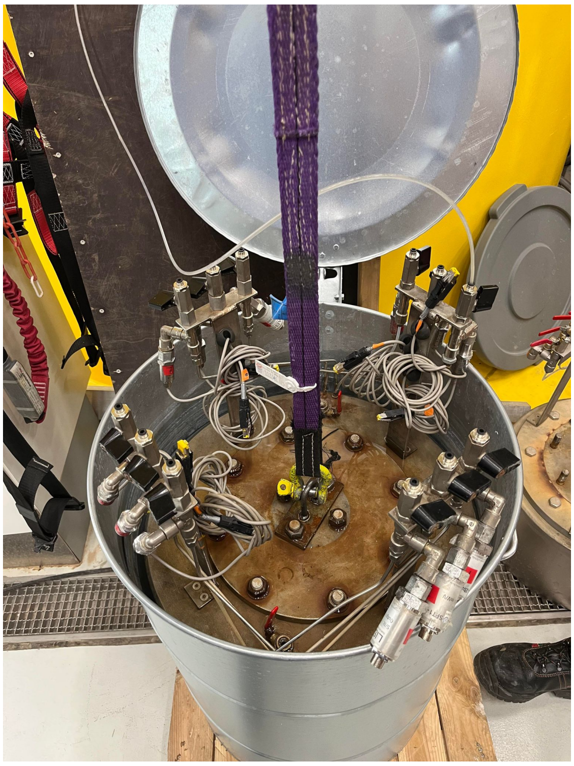

(a) Bucket submerged in water

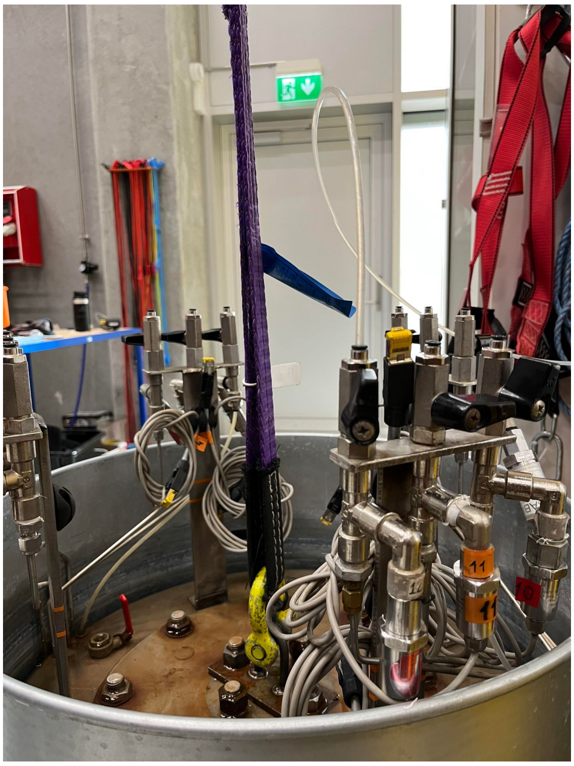

(b) Vacuum tube for saturation of transducers

Figure A.9: Transducers saturation process

A.6 Soil vibrators

To densify the soil 2 industrial concrete vibrators "ENAR" as seen in A.10 were used .

Figure A.10: Soil vibrators

A.7 CPT

To perform the Cone Penetration Tests (CPT) rectangular profile steel beam were attached to the hydraulic piston. Moreover, on the same beam two CPT cones were attached in order to obtain two sets of data at different locations inside the tank from the same test. CPT cones and whole setup can be seen in figures below:

(a) CPT rods

(b) CPT setup inside the tank

Figure A.11: CPT setup

A.8 Transducer calibration

The available transducers needs to be calibrated in order to show correct readings. This section will provide explanation of the procedure for transducer calibration.

The set-up is as seen in figure A.12 and A.13

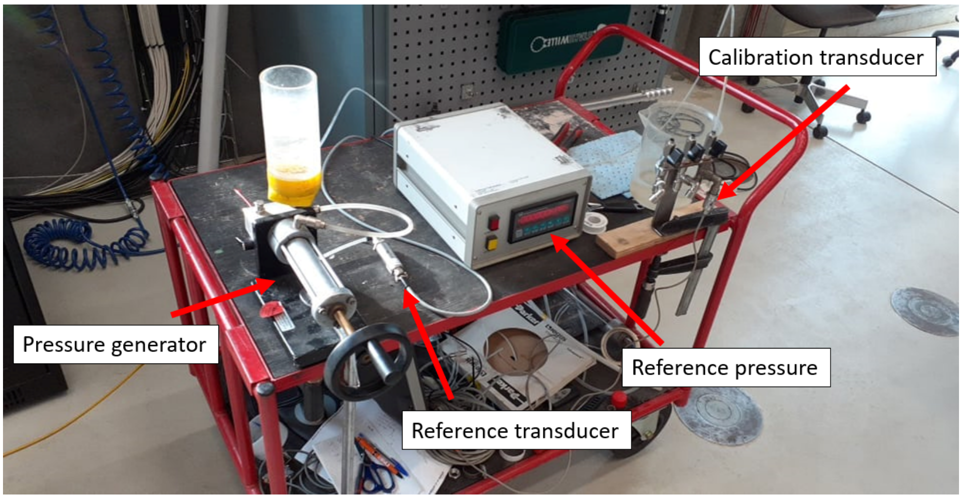

Figure A.12: Transducer calibration set-up

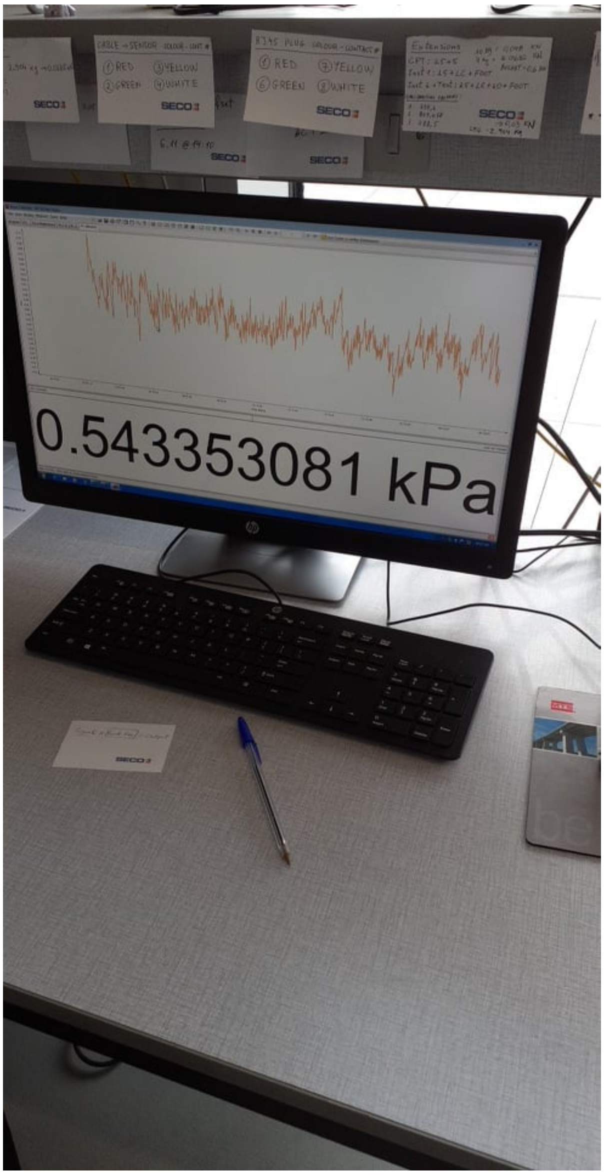

Figure A.13: Transducer reading from MTS software

As seen from the set-up a reference transducer is used to measure the applied pressure and then compare that reading to the pressure measured by the transducer connected to MTS software. In order to calibrate reference transducer with the readings from MTS software scaling factor was introduced and calculated as shown in equation (A.1).

Scale factor

$$K = \frac{p_{reference}}{p_{MTS}} \tag{A.1}$$

Where:

K	scale factor	[-]
$P_{reference}$	Reference pressure	[kPa]
P_{MTS}	MTS transducer reading	[kPa]

When calculating the scale factor an average of three readings are used in order to even out the difference in between each average calculated scale factor. 13 transducers are calibrated and their scale factor is provided in table A.2

Table A.2: Transducer scale factor

Transducer ID	Scale factor
16092502	5158.3
16092508	5603
16092505	5175.68
12116048-001A	17955.45
12116048-004A	18147.14
12126215-006A	17987.3
12126215-002A	21428.57
16092506	5294.67
12126215-008A	18157.99
12116048-005A	17995.95
12126215-012A	21422.9
12126215-013A	27594.2
16092507	5305.18

Appendix B | Vibration Study

The purpose of this chapter is to illustrate and explain how the most efficient vibration pattern and procedure is found to obtain the sufficient relative density.

When a test is conducted, the same initial state of the soil before testing is wanted, that can be controlled by the relative density, which is obtained by vibration of the soil. The soil is vibrated manually hence a lot of human errors can occur, which is why a specific procedure is wanted to minimize the errors and at the same time obtain the same soil state for each test.

Before the soil is vibrated, the same loose state of the soil is wanted. This is obtained by loosening of the soil with water pressure, by forcing a pipe with high water flow down through the soil at different locations. Four different vibration patterns are investigated; vibration in each hole, in every second hole, every third hole and lastly every third hole twice. The patterns are illustrated in figures B.1 and B.2 once the vibration is done for one pattern, 12 CPT tests are made at various locations which can be seen in figure B.2

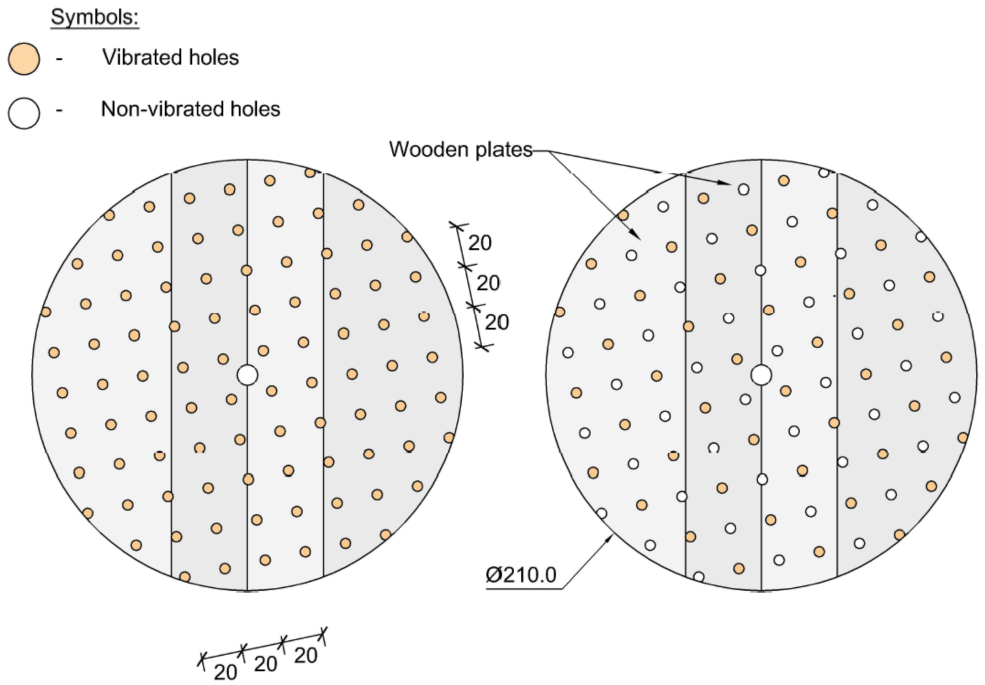

Figure B.1: Vibration patterns for every and every 2nd hole

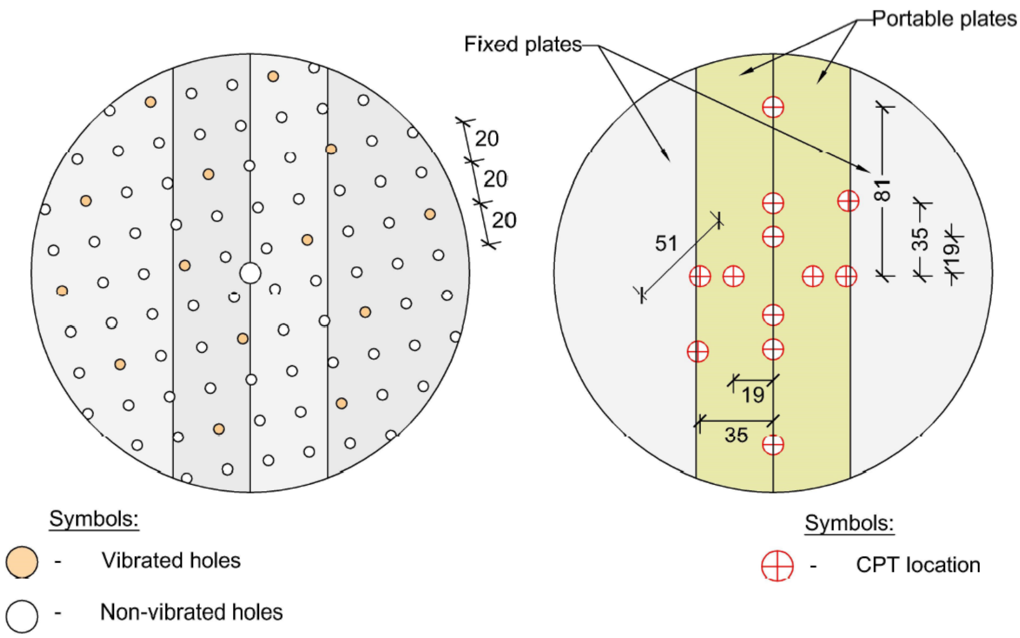

Figure B.2: Vibration pattern for every 3rd hole and CPT's locations

The value of the relative density is preferred to be between 80-90% if the value is below, the pattern is not sufficient enough, and thereby it is easy to compare which procedure gives the best result, in this case vibration for every hole gives the highest relative density and with the best distribution. And thereby it is concluded that vibration of the soil is done in every hole before all experiments twice.

Appendix C | Cone Penetration Test (CPT)

This chapter contains equations, based on [Ibsen et al., 2009], used to calculate relative density, D_R, of the soil by using results obtained from the CPT's. This is needed because after vibrating the soil and before installation of the suction bucket it had to be checked if D_R of the soil is in wanted range so that results of the experiments could be comparable with others.

Ibsen et al. [2009] states that density index of Aalborg University Sand No.1 in the pressure tank can be determined by using equation (C.1) below:

Relative density

$$D_R = 5.14\left(\frac{\sigma'_{v0}}{(q_c)^{0.75}}\right)^{-0.42} \tag{C.1}$$

Where:

σ'_{v0}	Vertical effective stress	[MPa]
q_c	Cone resistance	[MPa]

$$q_c = \frac{1000 \cdot q_{c,measured}}{A_{cone}} \tag{C.2}$$

Where:

$q_{c,measured}$	Measured cone resistance	[kN]
A_{cone}	Area of the cone tip	[mm^2]

$$A_{cone} = \pi r^2 \tag{C.3}$$

Where:

r	Radius of the cone	7.5	[mm]

$$\sigma'_{v0} = \frac{\gamma' d}{1000} \tag{C.4}$$

Where:

γ'	Effective unit weight of saturated soil	[kN/m^3]
d	Soil depth	[m]

Effective unit weight of saturated soil γ' is calculated by using void ratio e which is obtained by iteration procedure. It starts by guessing $e = e_{min}$ until acceptable e is being found as presented in equation (C.2):

$$\gamma' = \frac{G_s - 1}{1 + e}\gamma_w \tag{C.5}$$

Where:

G_s	Specific gravity	2.64	[-]
e	Void ratio		[-]
γ_w	Unit weight of water	9.81	[kN/m^3]

$$D_R = \frac{e_{max} - e}{e_{max} - e_{min}} \tag{C.6}$$

Where:

e_{max}	Maximum void ratio	0.549	[-]
e_{min}	Minimum void ratio	0.854	[-]

Appendix D | Test Results

This chapter consists of brief description of each test together with results obtained during those tests. Comments about errors or explanation of the results might be added for a specific tests

D.1 Tensile bearing capacity

This test was done in order to determine the tensile bearing capacity of the soil. Furthermore, in order to verify the results they were compared with similar test done by [Tardio and Moldovan, 2021a].

Before the test, the sand was densified as it is presented in appendix B. After the bucket was installed into the sand with a compression force between 50 and 70 kN as it can be seen in figure D.1 it was pulled out with a constant speed of 0.5 mm/s. The peak of tensile force during pull-out phase is taken as a tensile bearing capacity. It is assumed that the drained conditions can be considered because valves on top of the bucket were opened which allowed excess pore water pressure to dissipate.

After the bucket was pulled out, procedure was repeated two more times. The only difference between the first test and other twos is that the soil was not densified. The bucket was slowly lowered into the soil and pulled out again.

Results from "test 2" and "test 3" corresponds well with the results obtained by [Tardio and Moldovan, 2021a], while results from "test 1" are higher. This could be explained by the fact that the sand was very well densified and not disturbed for the first test. Moreover, it is decided to use value of −2.2 kN as an average value from second and third tests as it is seen in D.2.

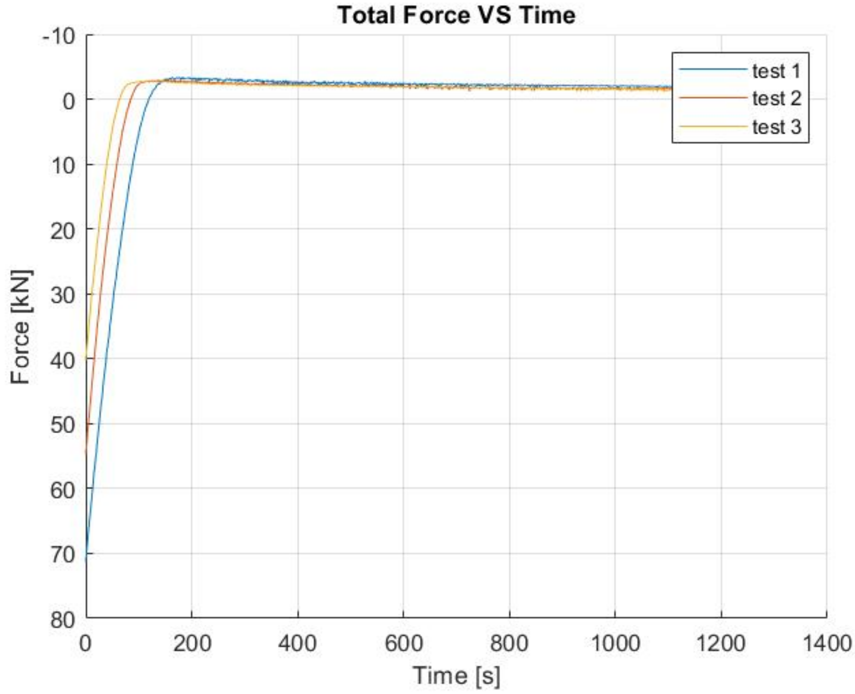

Figure D.1: Force vs Time. Test - Tensile bearing capacity

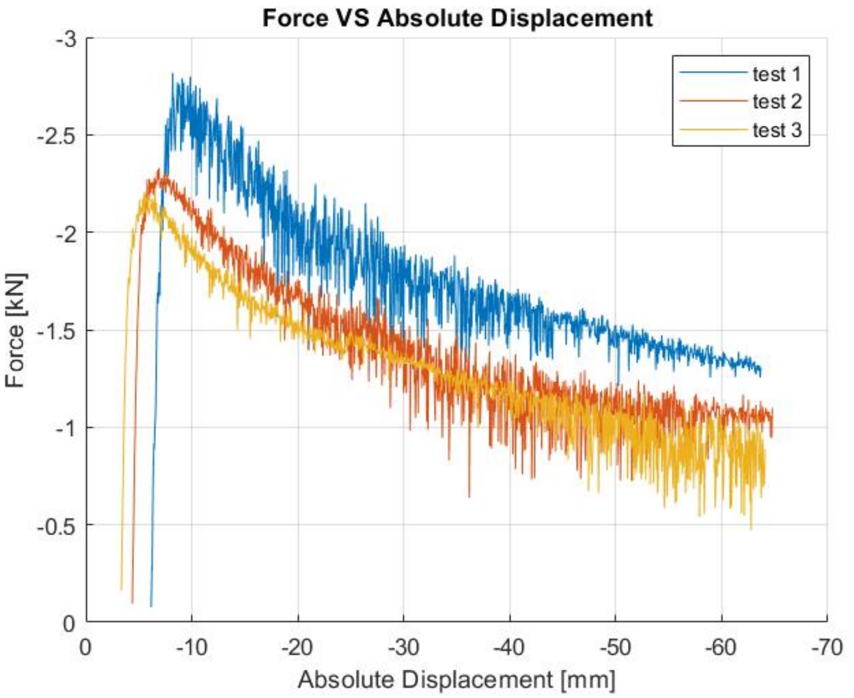

Figure D.2: Force vs Displacement. Test - Tensile bearing capacity

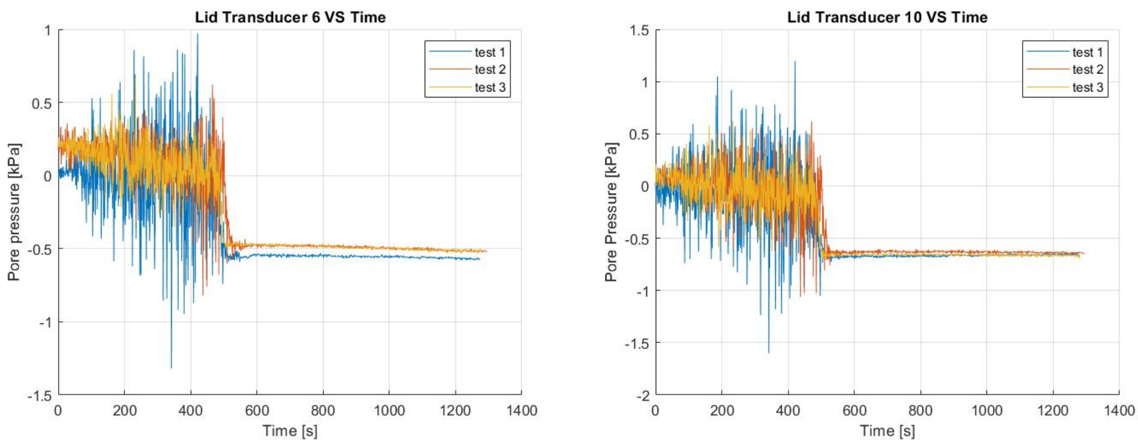

Figure D.3: Lid transducers 6 and 10

CPT

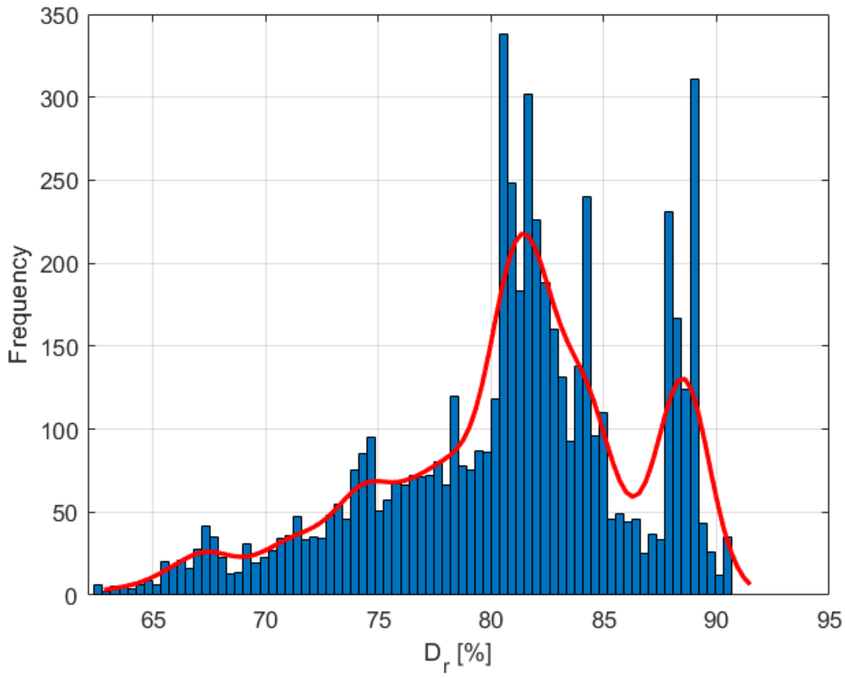

Figure D.4: Dr distribution histogram. Test - Tensile bearing capacity

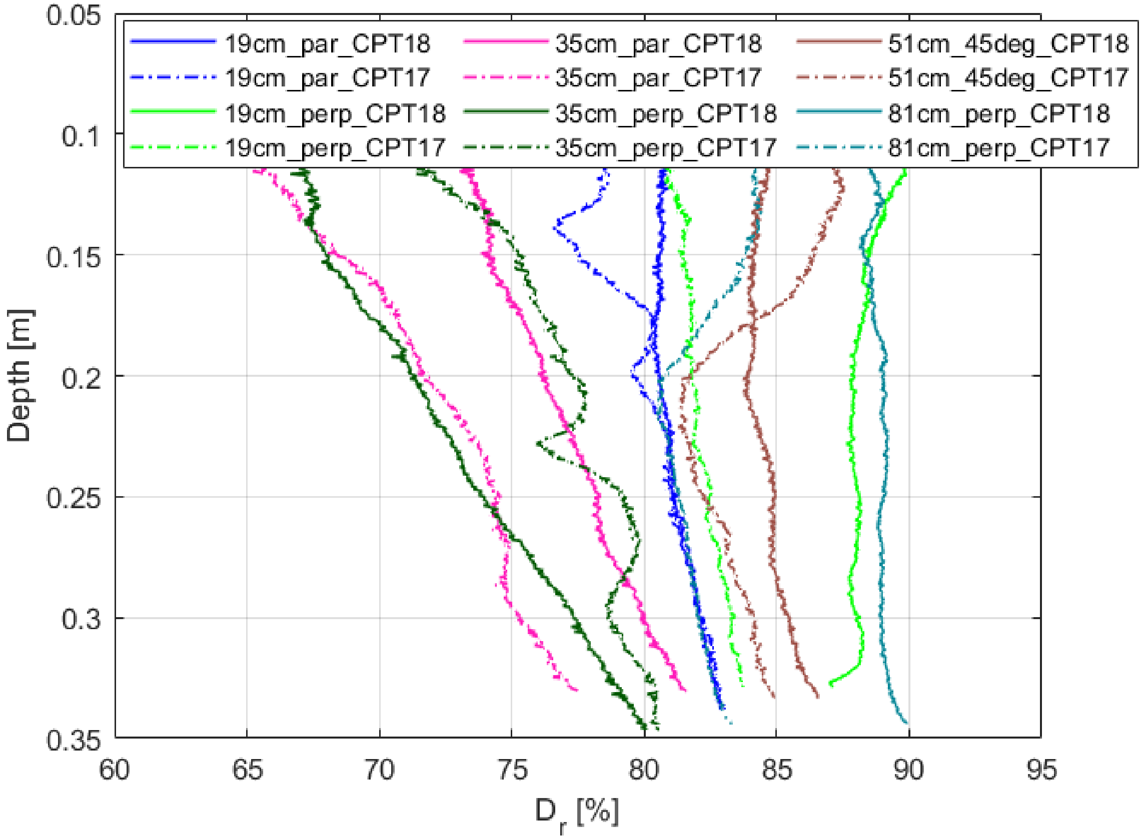

Figure D.5: Test-specific Dr results. Test - Tensile bearing capacity

D.2 Test group A

It was decided to perform series of tests to investigate the limit of tensile bearing capacity of soil obtained in D.1 via several two-way loading scenarios. The compression capacity is determined from [Barari et al., 2016] and then taken as the 5% of that found value. The compression capacity therefore becomes 28 kN.

Frequency of cyclic loading is taken as 1.0 Hz.

This series of tests consist of three parts with the only difference in tensile loading:

- During the first test it is decided to take 30 % of tensile bearing capacity which is 0.7 kN.
- During the second test it is decided to take 50 % of tensile bearing capacity which is 1.1 kN
- During the third test it is decided to take 100 % of tensile bearing capacity which is 2.2 kN

D.2.1 Test subgroup A1

Loading plan with all the parameters which were used can be seen in both table D.1 and figure D.6 below, while the actual loading can be seen in D.7

Table D.1: Loading plan for 'Test group A1 - 30 %'

Compressive force [kN]	Tensile force [kN]	Frequency [Hz]	Cycle No.
28.0	-0.7	1.0	10000

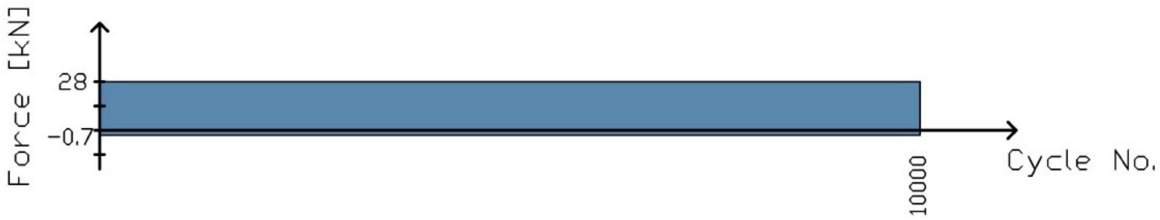

Figure D.6: Loading plan for 'Test group A1 - 30 %'

Figure D.7: Actual loading plan for 'Test group A1 - 30 %'

Even though it was planned to run the test with 10000 cycles, bucket was pushed down to the lower limit of our experiment set-up capabilities and test stopped after 7728 cycles.

CPT

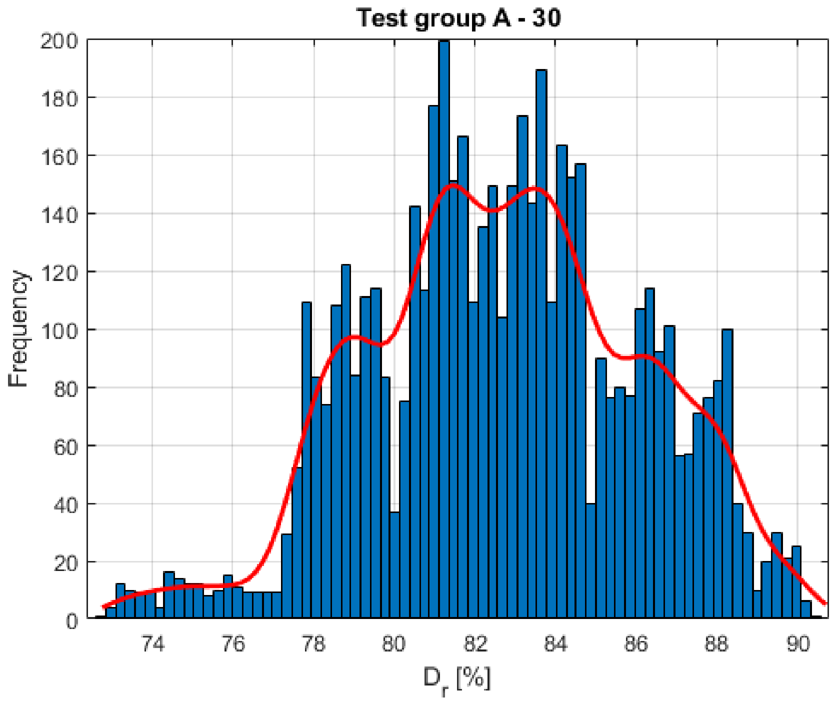

Figure D.8: Dr histogram with distribution fit for CPT test subgroup A1

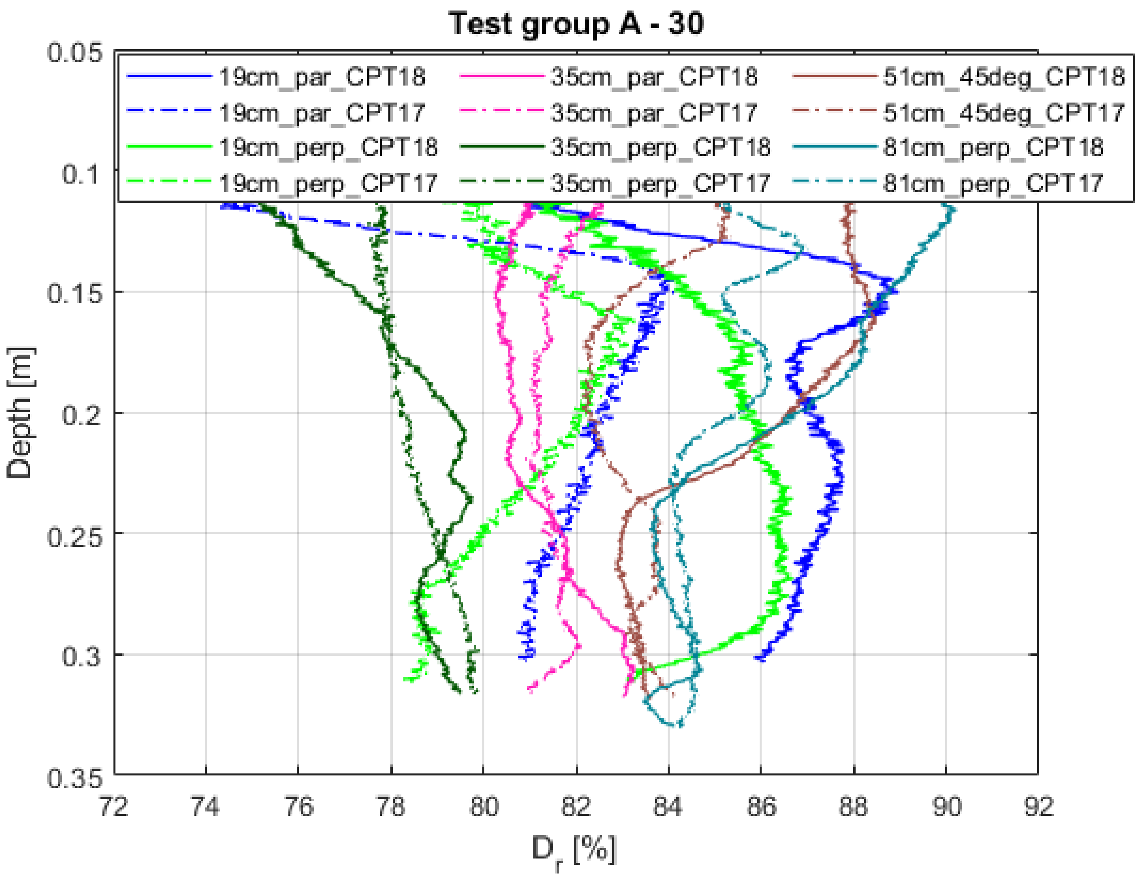

Figure D.9: Test-specific Dr results for CPT test subgroup A1

Force and displacement

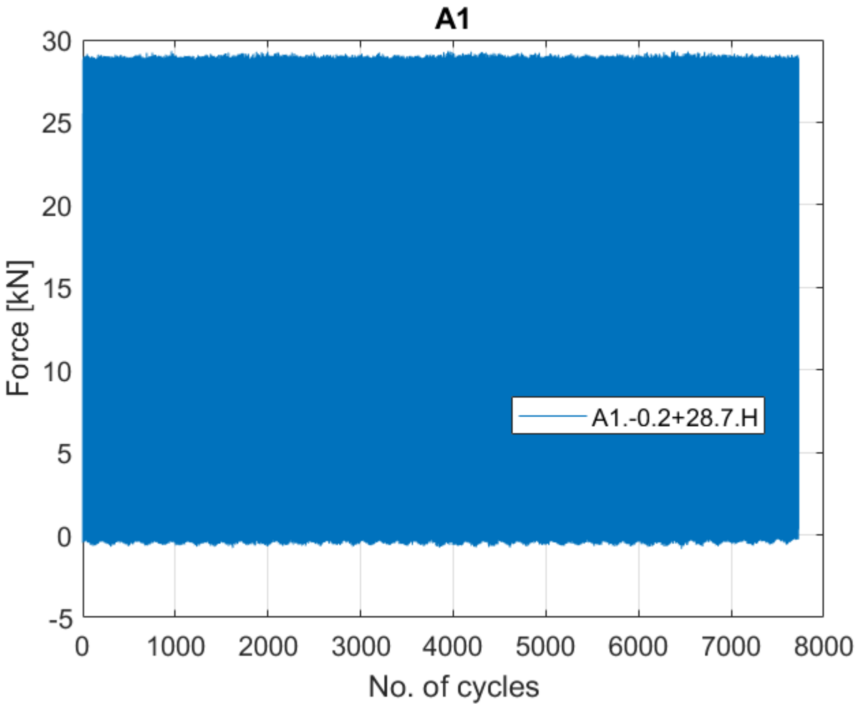

Figure D.10: Force VS No. of cycles

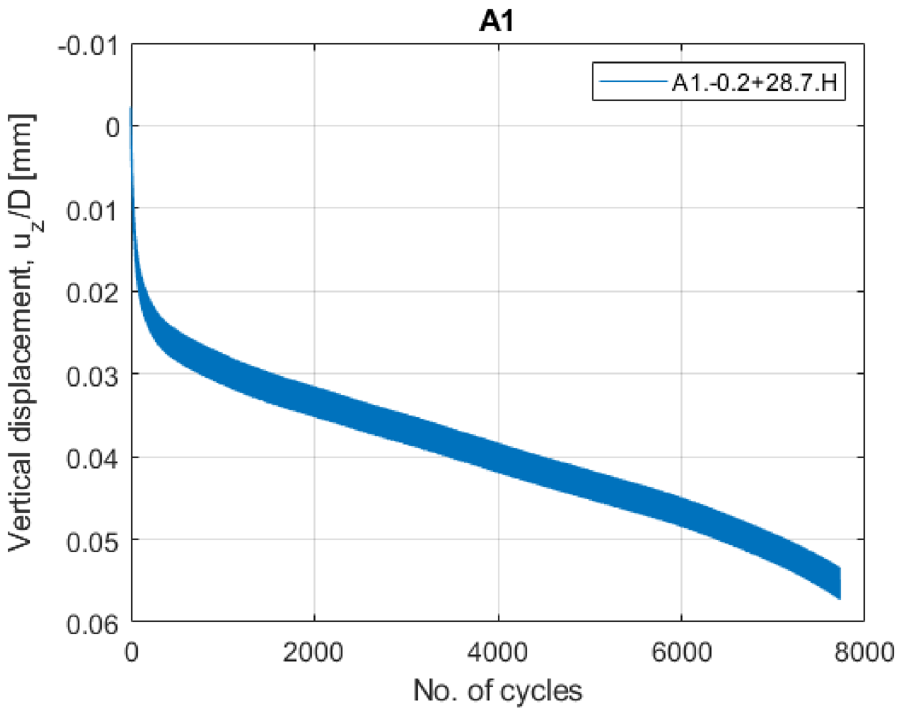

Figure D.11: Displacement VS No. of cycles

Lid Transducers

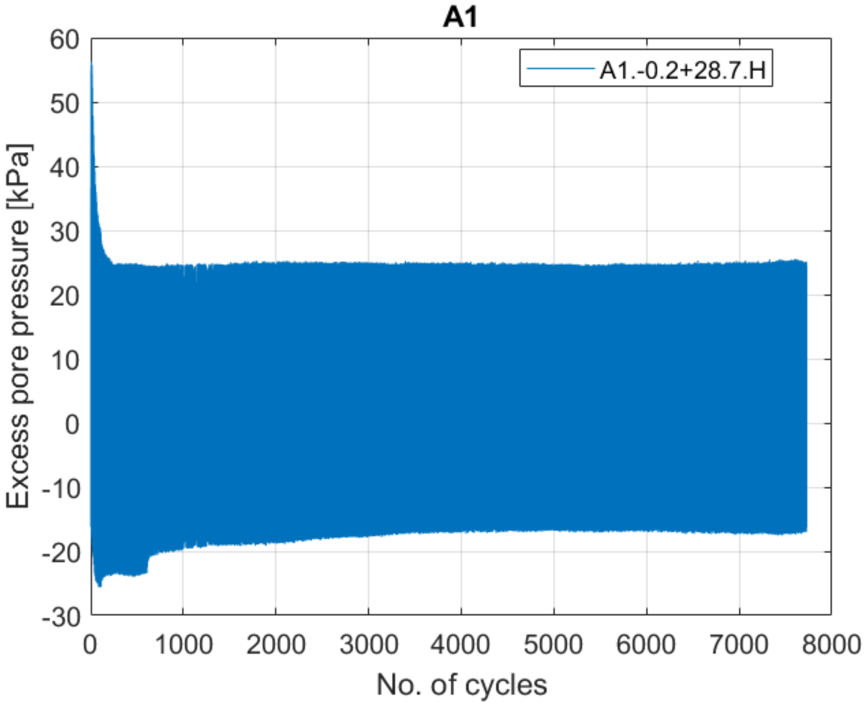

Figure D.12: Pore pressure at lid transducer P6

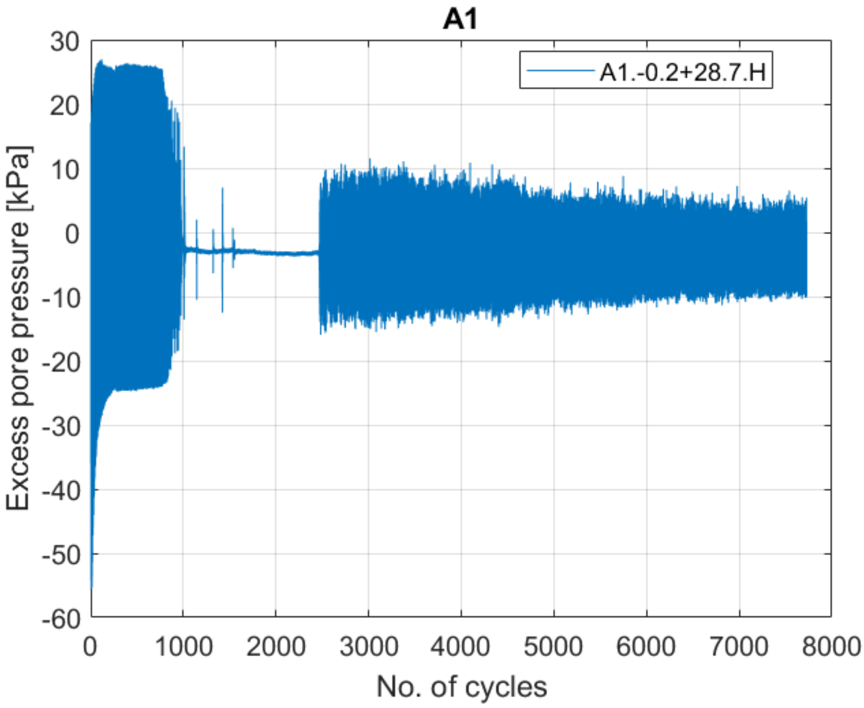

Figure D.13: Pore pressure at lid transducer P10

1st Level Transducers

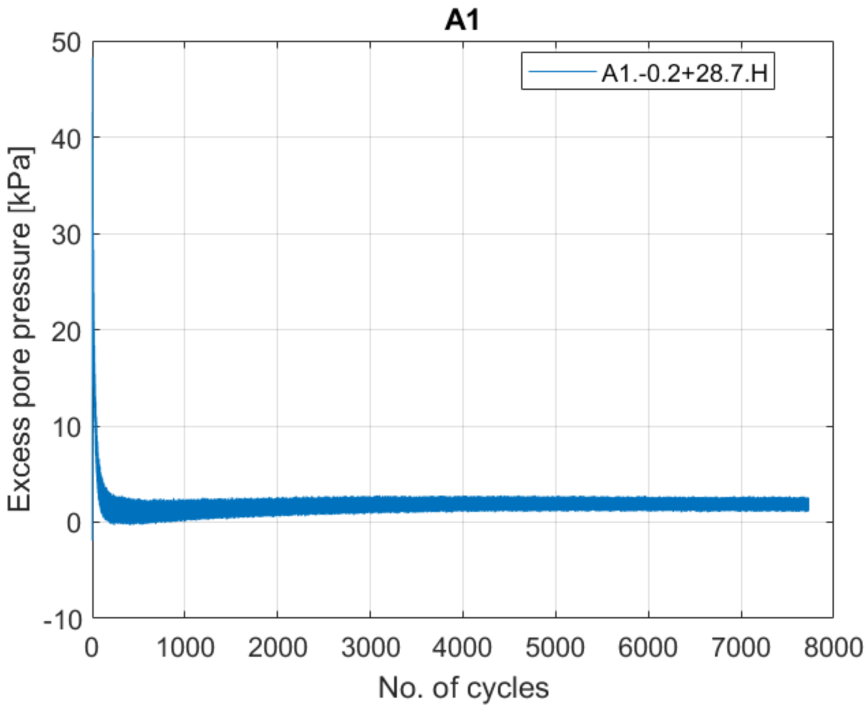

Figure D.14: Pore pressure at 1st level inner side transducer P4

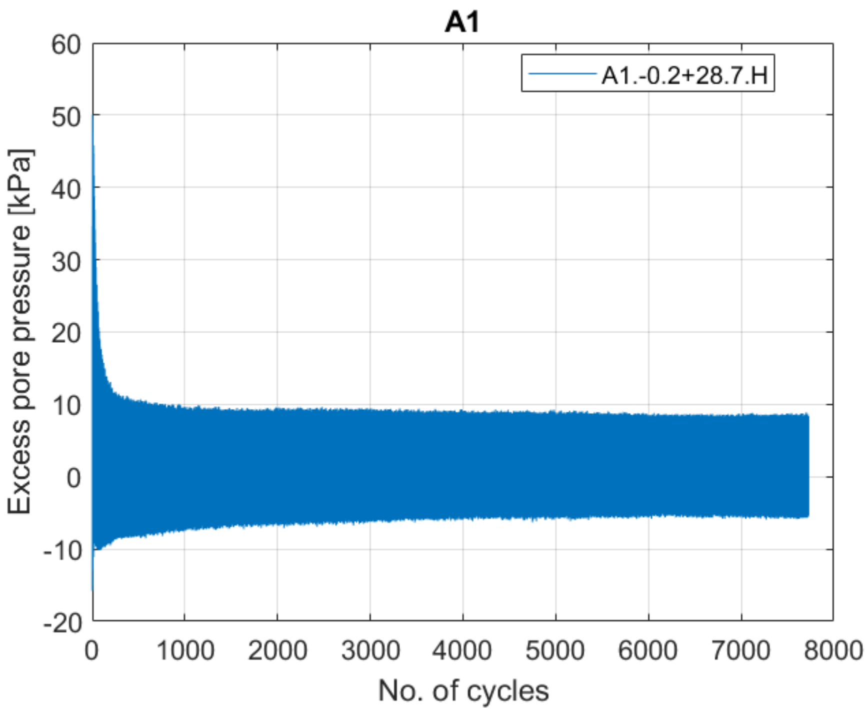

Figure D.15: Pore pressure at 1st level inner side transducer P11

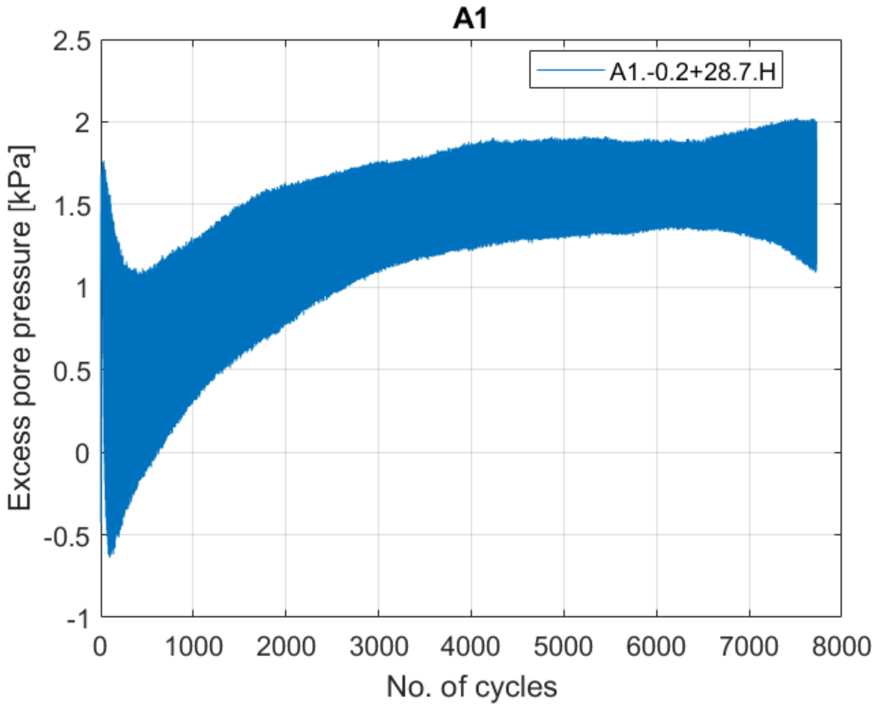

Figure D.16: Pore pressure at 1st level outer side transducer P3

2nd Level Transducers

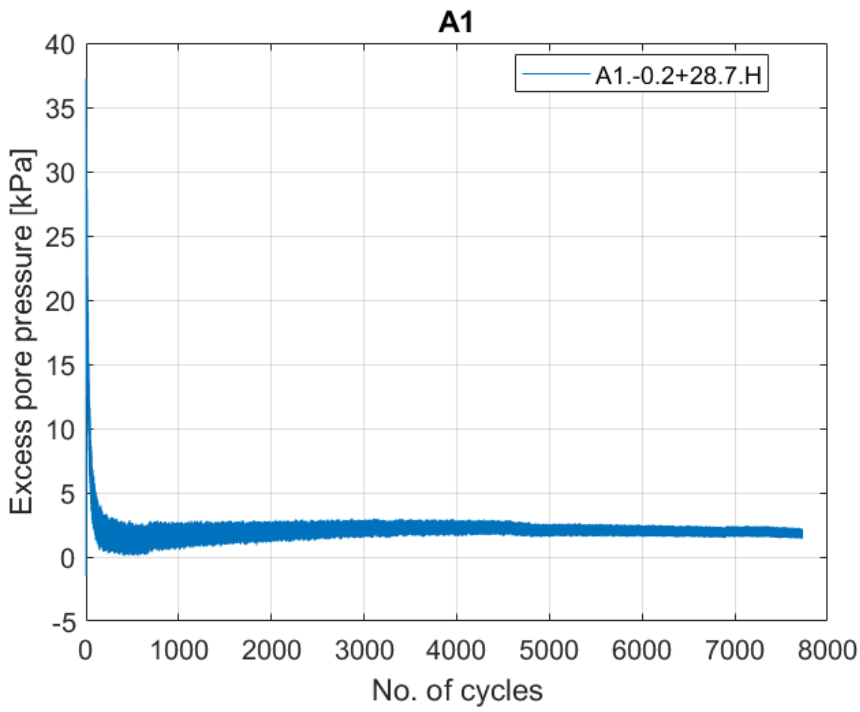

Figure D.17: Pore pressure at 2nd level inner side transducer P5

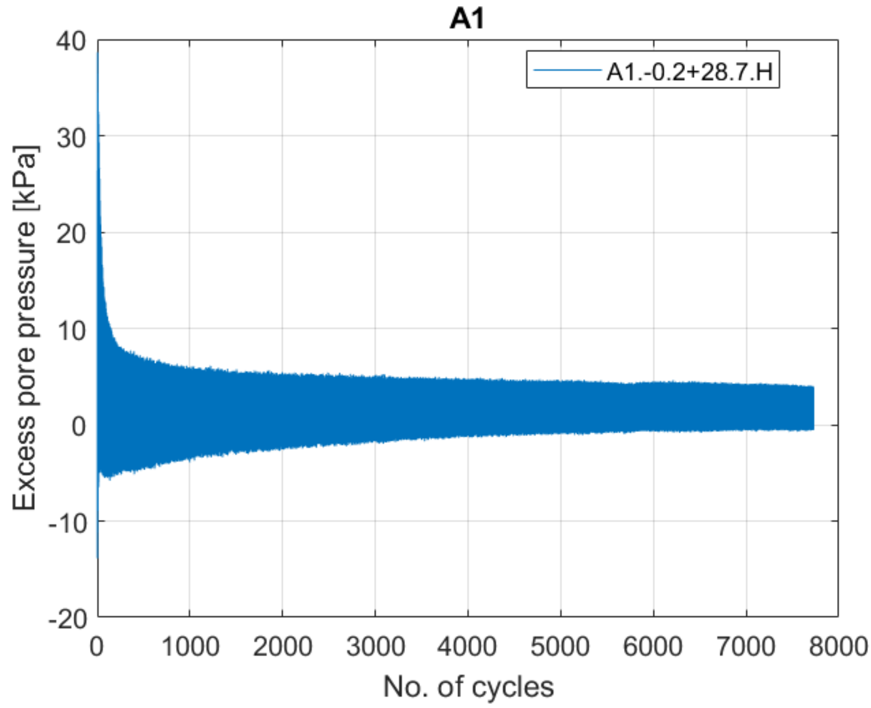

Figure D.18: Pore pressure at 2nd level inner side transducer P12

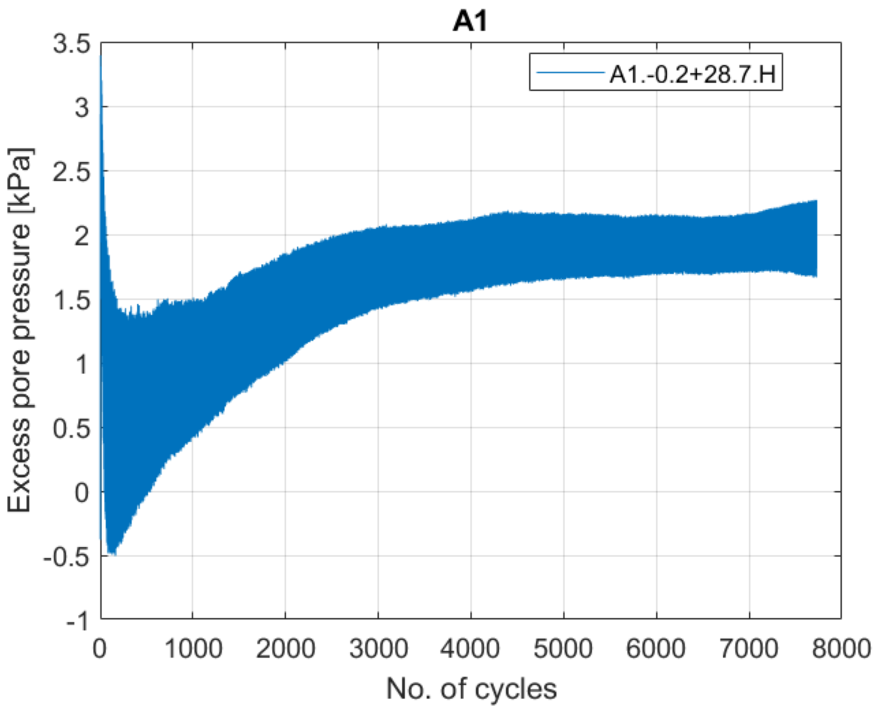

Figure D.19: Pore pressure at 2nd level outer side transducer P1

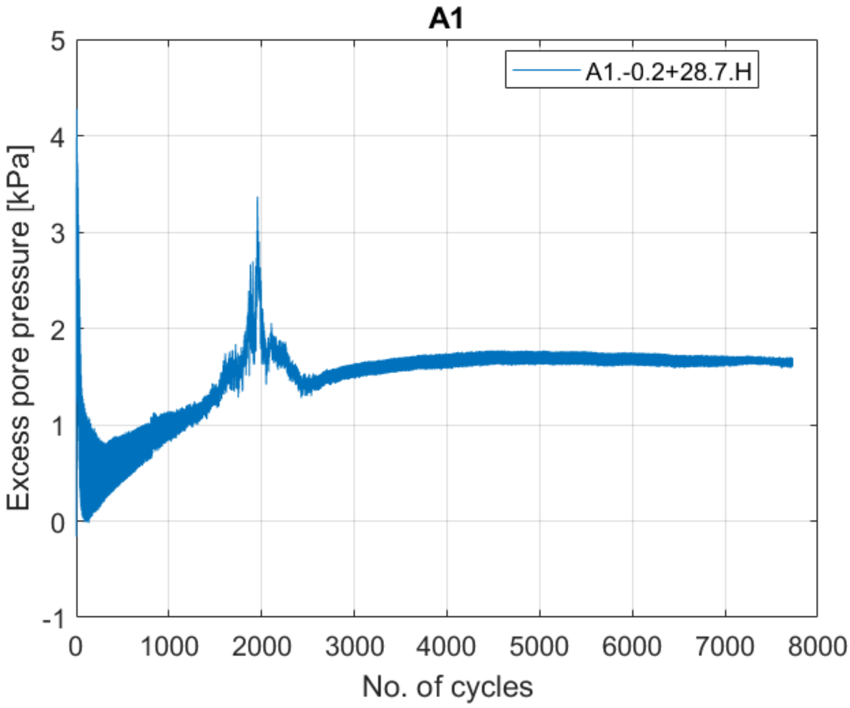

Figure D.20: Pore pressure at 2nd level outer side transducer P9

Skirt Tip Transducers

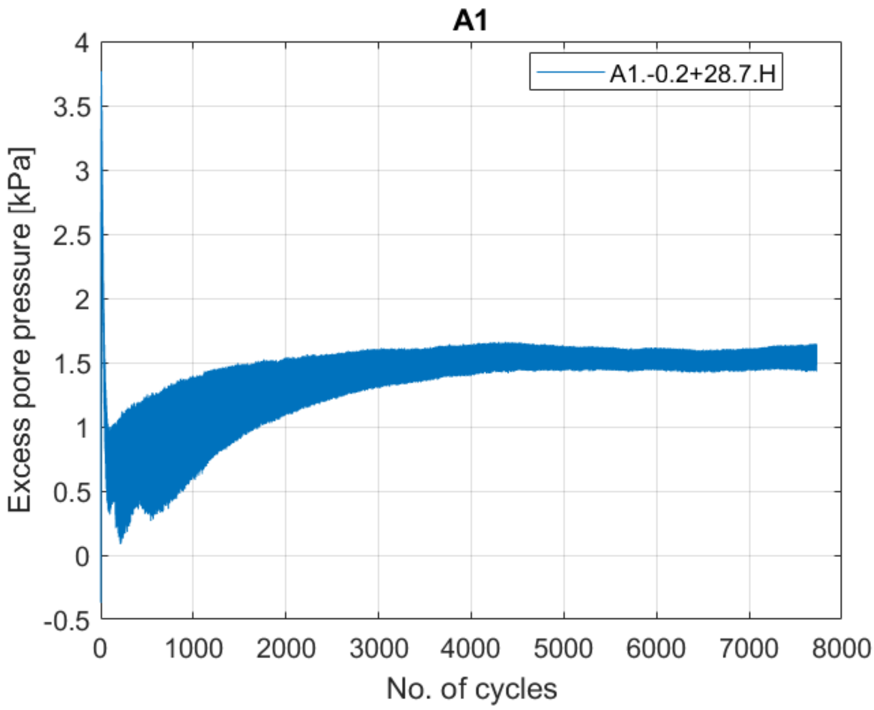

Figure D.21: Pore pressure at tip transducer P2

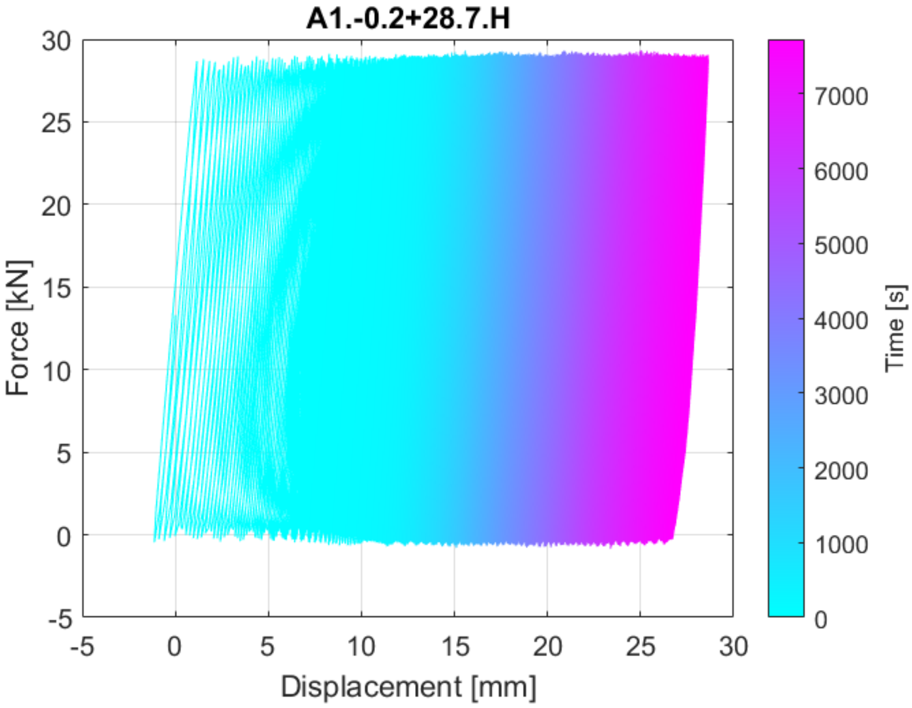

Figure D.22: Force VS absolute displacement

D.2.2 Test subgroup A2

Loading plan with all the parameters which were used can be seen in both table D.2 and figure D.23 below, while the actual loading can be seen in D.24.

Table D.2: Loading plan for 'Test group A2 - 50 %'

Compressive force [kN]	Tensile force [kN]	Frequency [Hz]	Cycle No.
28.0	-1.1	1.0	10000

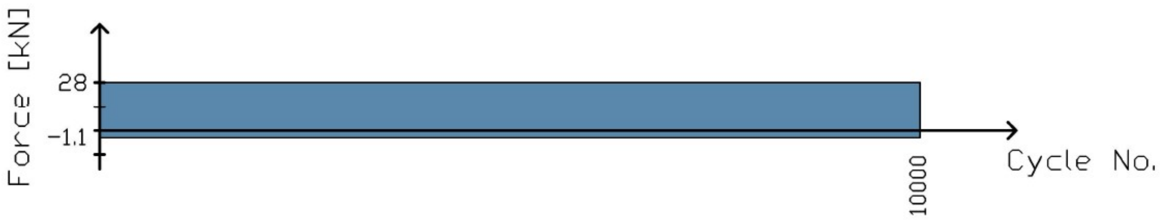

Figure D.23: Loading plan for 'Test group A2 - 50 %'

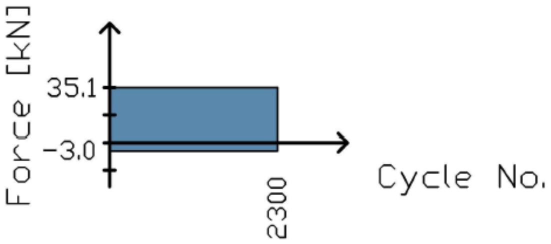

Figure D.24: Actual loading plan for 'Test group A2 - 50 %'

Even though it was planned to run the test with 10000 cycles, bucket was pushed down to the lower limit of our experiment set-up capabilities and test stopped after 2300 cycles.

CPT

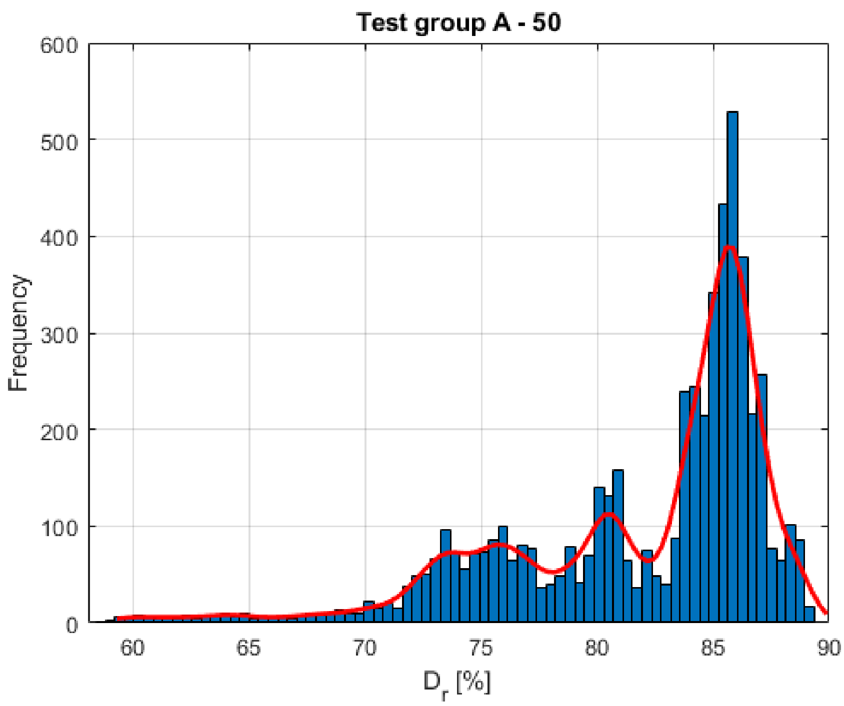

Figure D.25: Dr histogram with distribution fit for CPT test subgroup A2

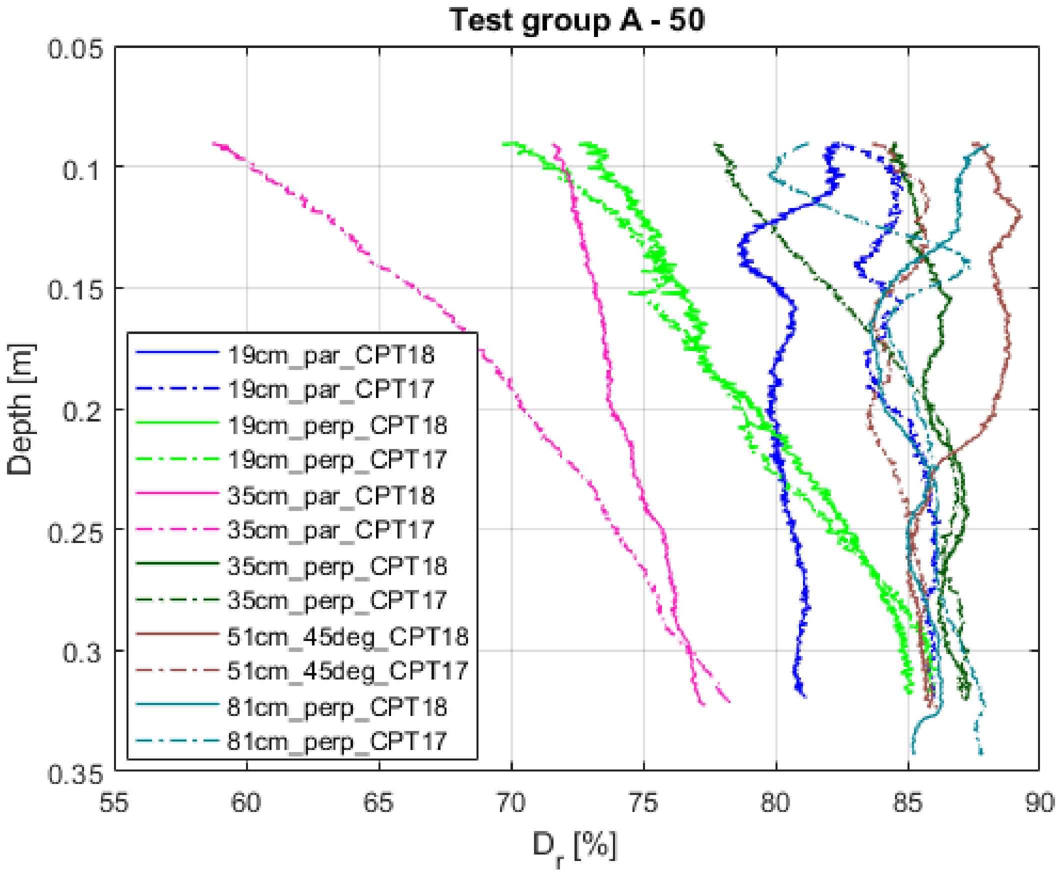

Figure D.26: Test-specific Dr results for CPT test subgroup A2

Force and displacement

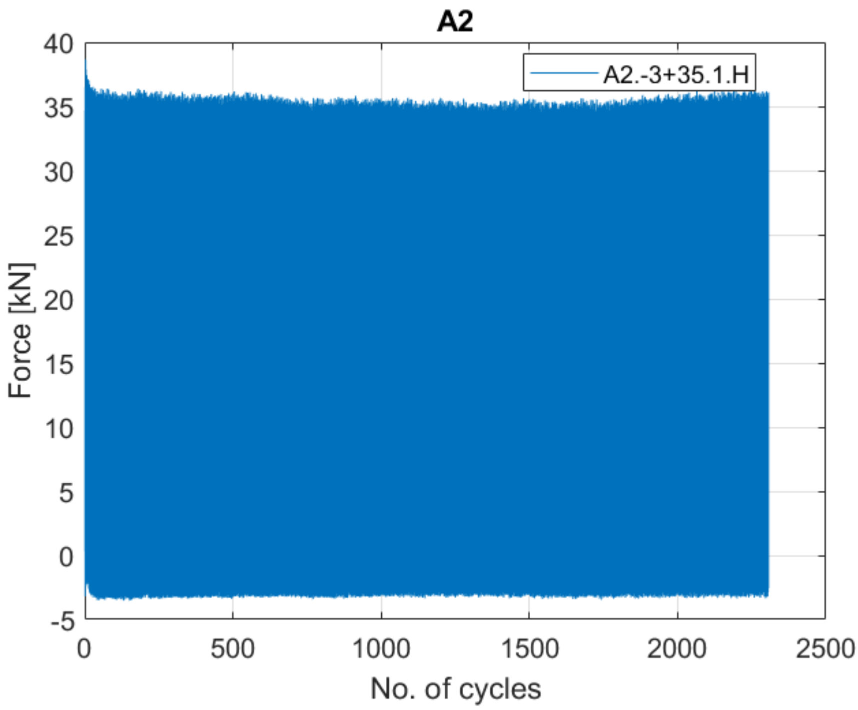

Figure D.27: Force VS No. of cycles

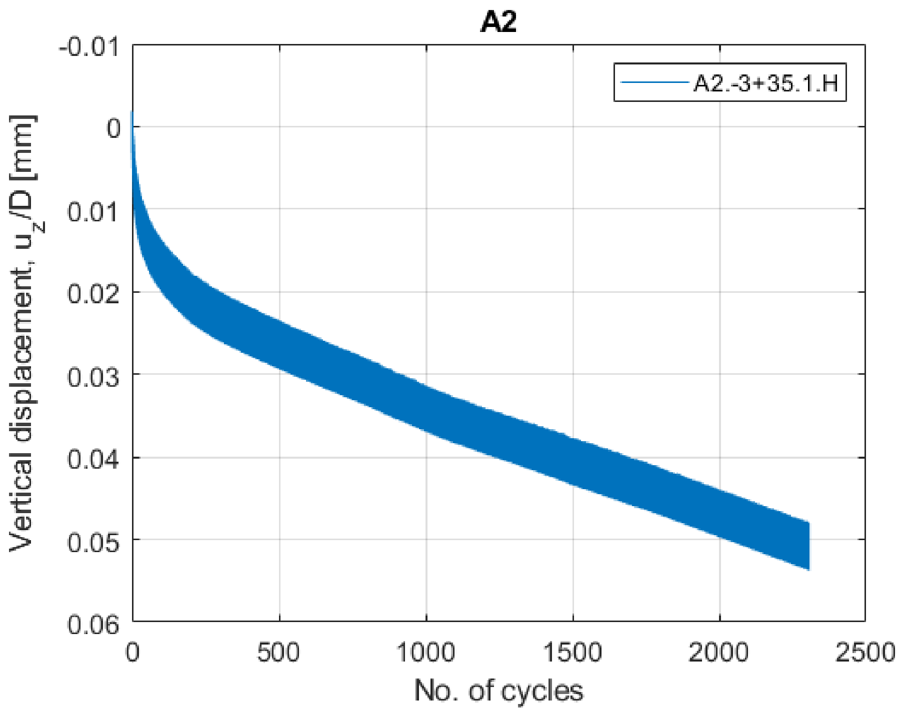

Figure D.28: Displacement VS No. of cycles

Lid Transducers

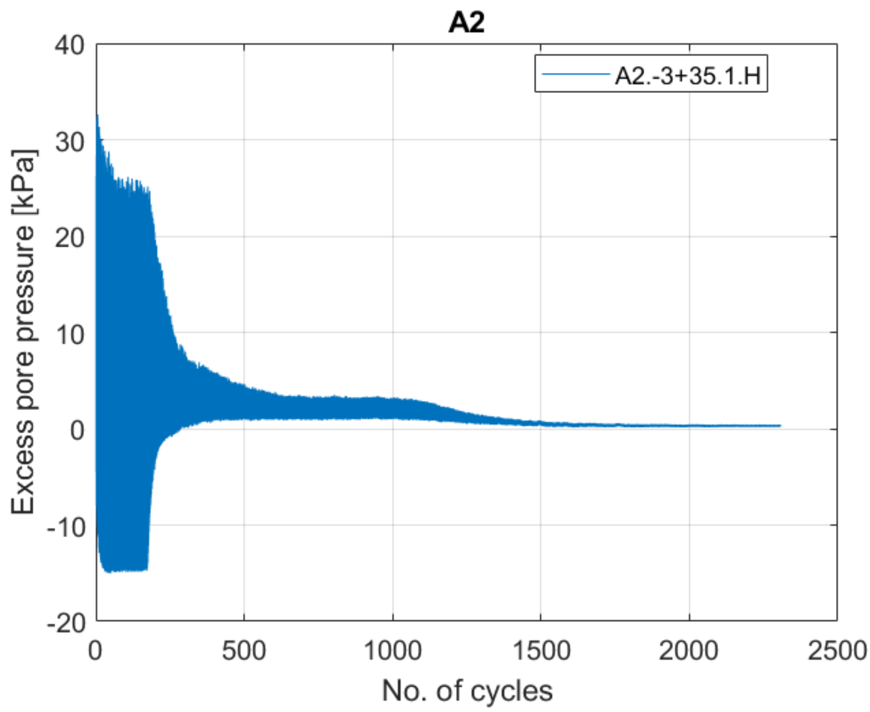

Figure D.29: Pore pressure at lid transducer P6

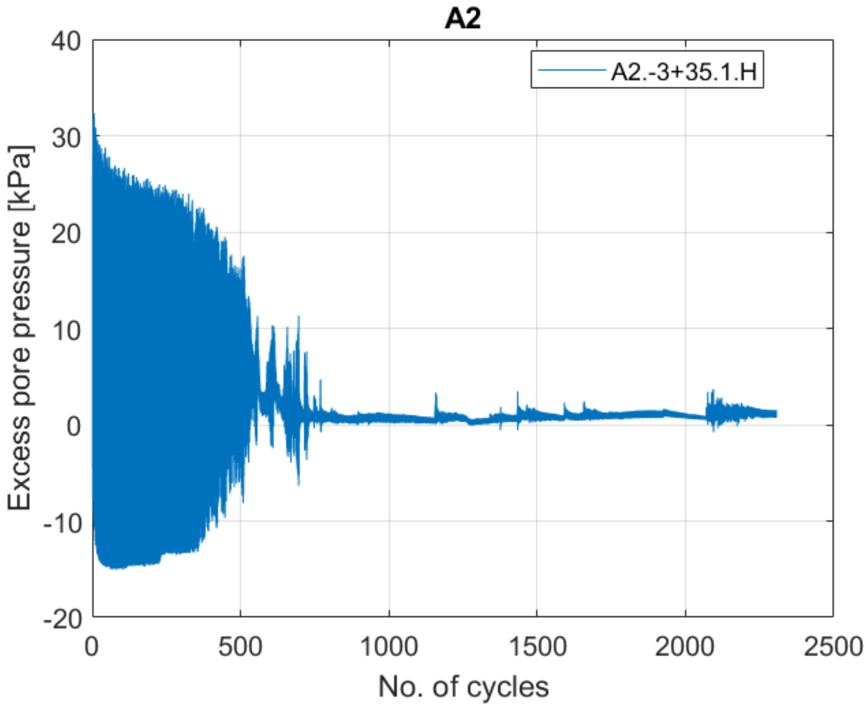

Figure D.30: Pore pressure at lid transducer P10

1st Level Transducers

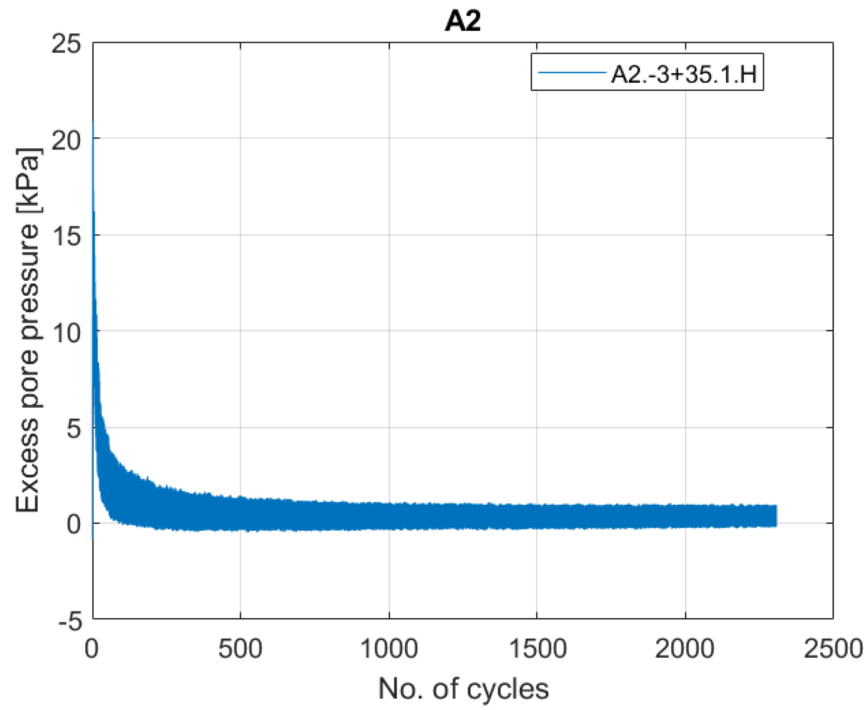

Figure D.31: Pore pressure at 1st level inner side transducer P4

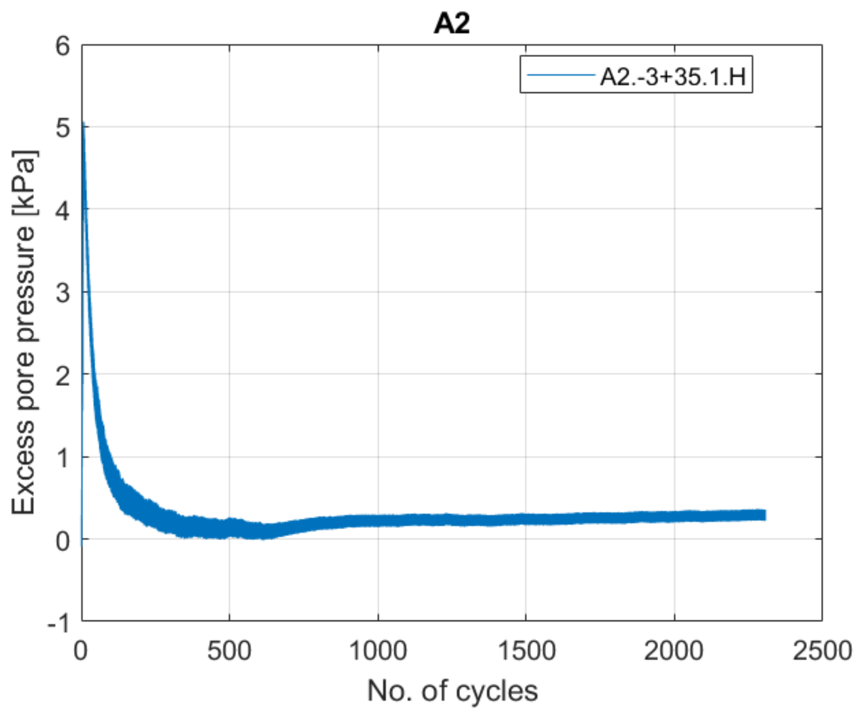

Figure D.32: Pore pressure at 1st level inner side transducer P11

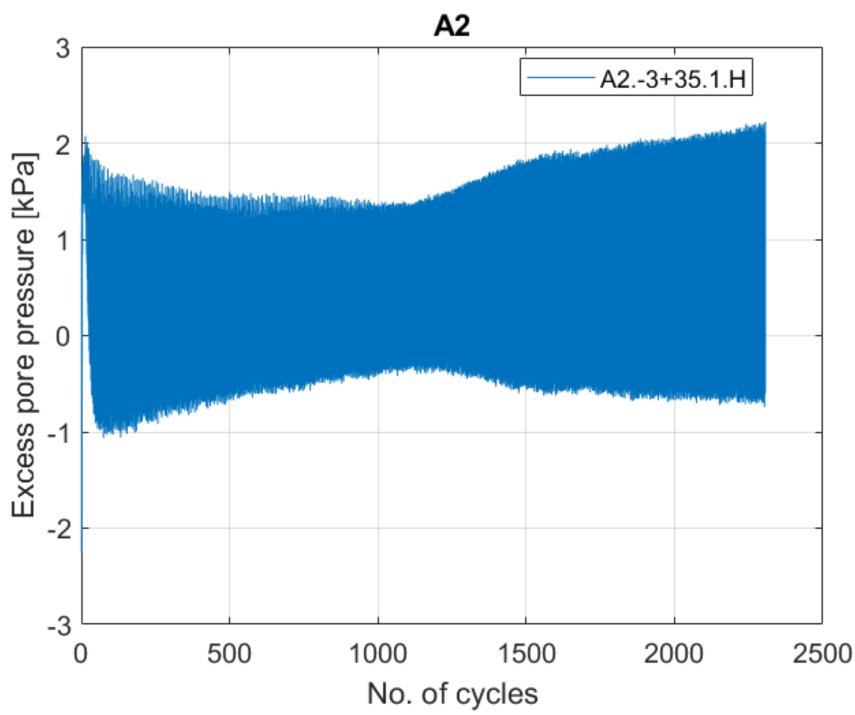

Figure D.33: Pore pressure at 1st level outer side transducer P3

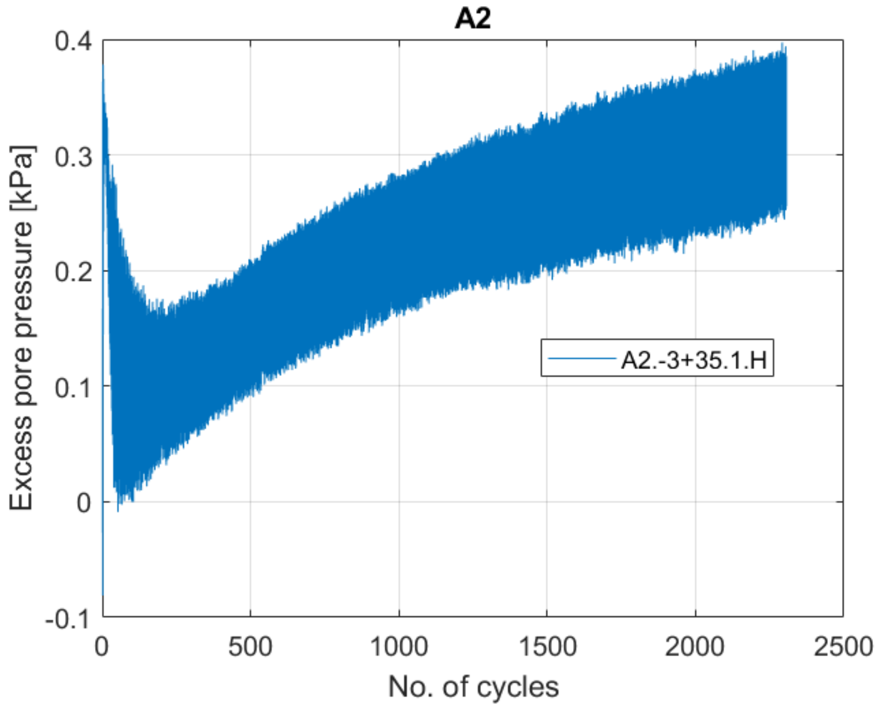

Figure D.34: Pore pressure at 1st level outer side transducer P7

2nd Level Transducers

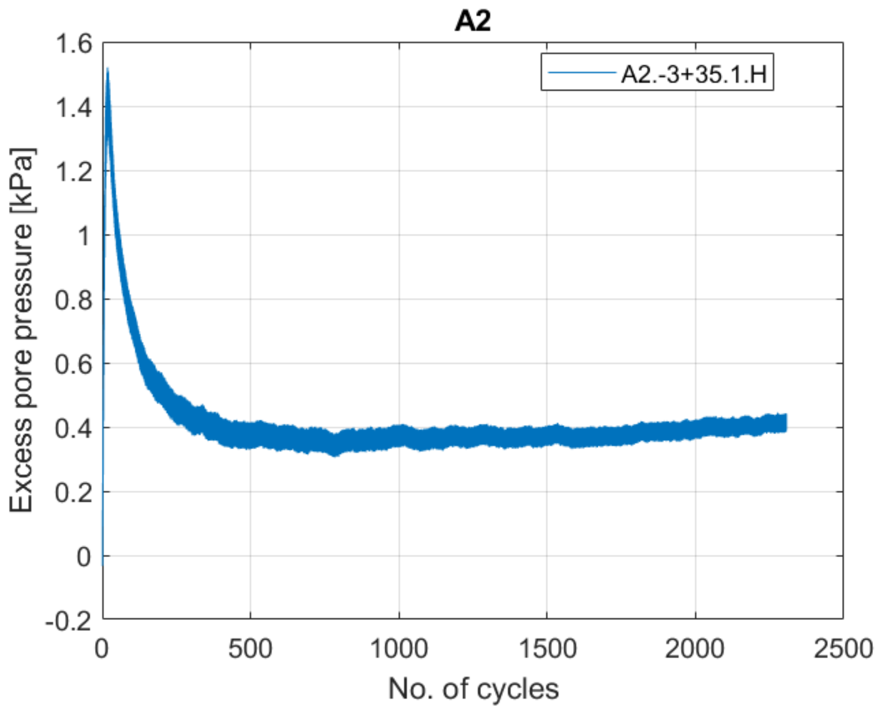

Figure D.35: Pore pressure at 2nd level inner side transducer P5

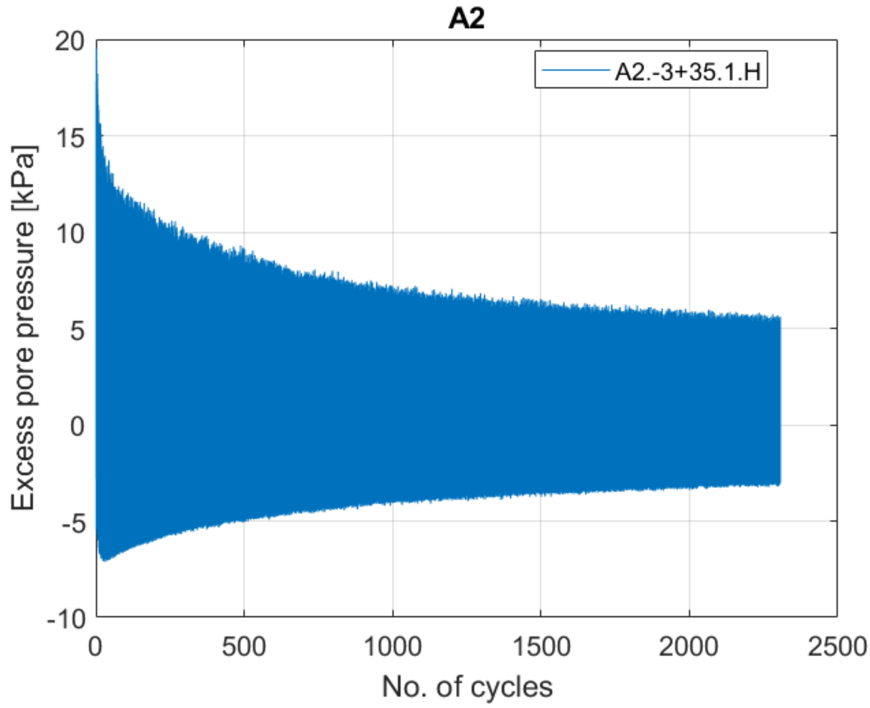

Figure D.36: Pore pressure at 2nd level inner side transducer P12

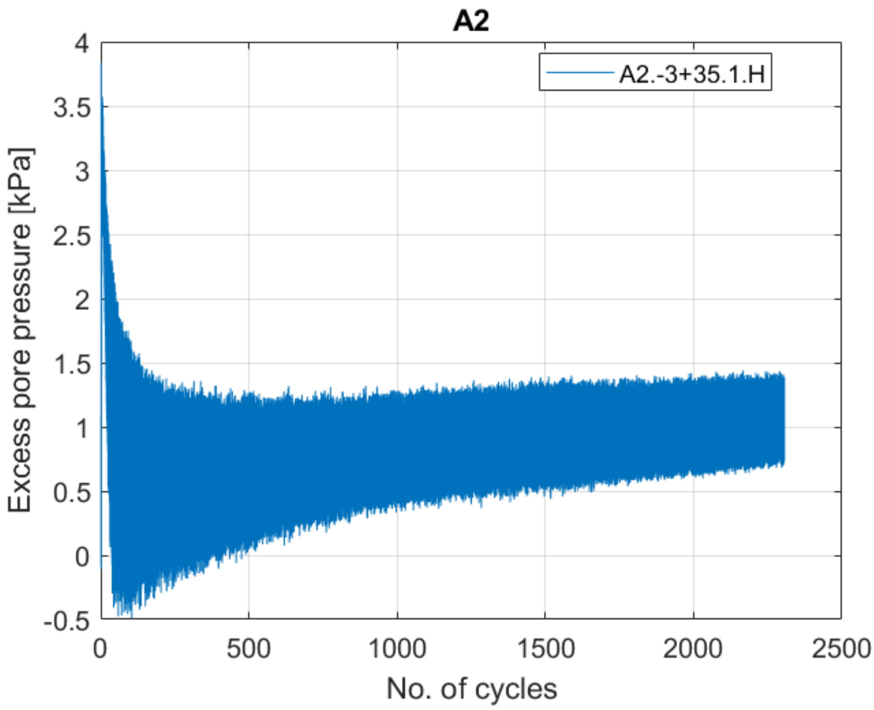

Figure D.37: Pore pressure at 2nd level outer side transducer P9

Skirt Tip Transducers

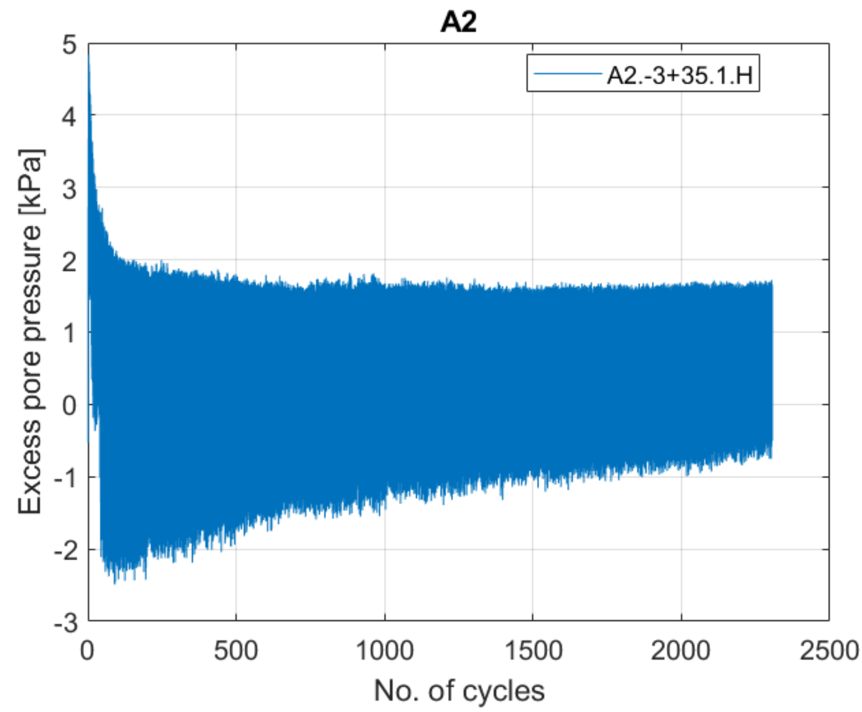

Figure D.38: Pore pressure at tip transducer P2

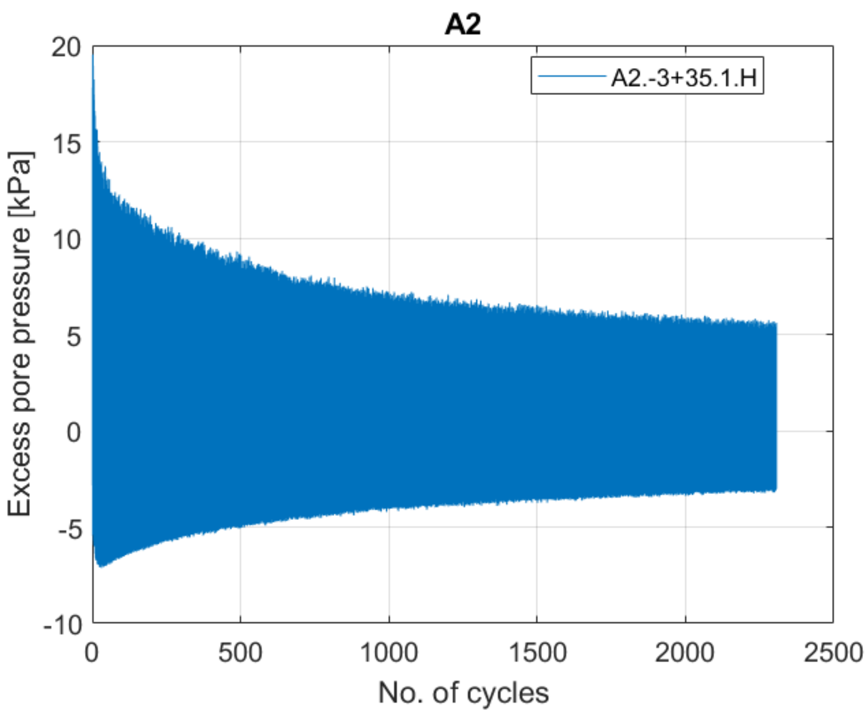

Figure D.39: Pore pressure at tip transducer P8

Force vs displacement

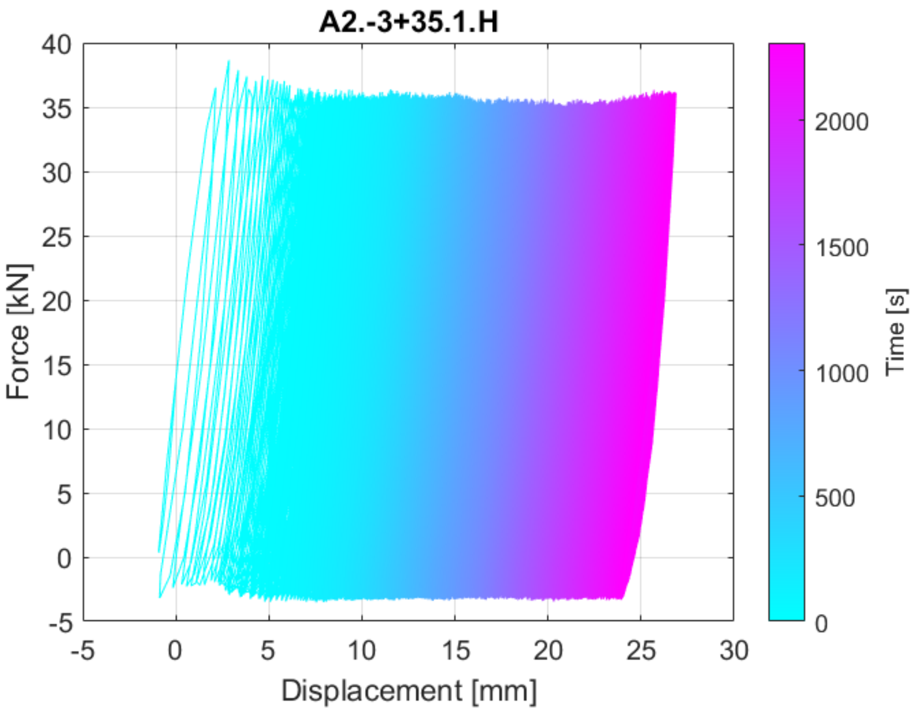

Figure D.40: Force VS absolute displacement

D.2.3 Test subgroup A3

Loading plan with all the parameters which were used can be seen in both table D.3 and figure D.41 below, while actual loading can be seen in D.42

Table D.3: Loading plan for 'Test group A3 - 100 %'

Compressive force [kN]	Tensile force [kN]	Frequency [Hz]	Cycle No.
28.0	-1.1	1.0	10000

Figure D.41: Loading plan for 'Test group A3 - 100 %'

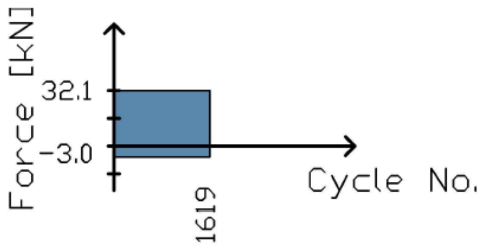

Figure D.42: Actual loading plan for 'Test group A3 - 100 %'

Even though it was planned to run the test with 10000 cycles, bucket was pushed down to the lower limit of our experiment set-up capabilities and test stopped after 1619 cycles.

CPT

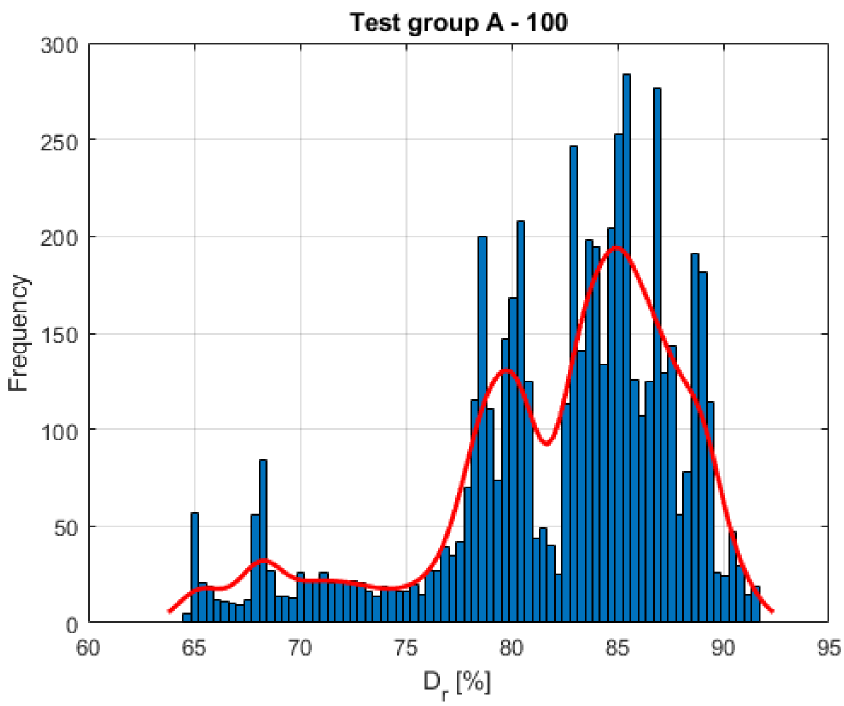

Figure D.43: Dr histogram with distribution fit for CPT test subgroup A3

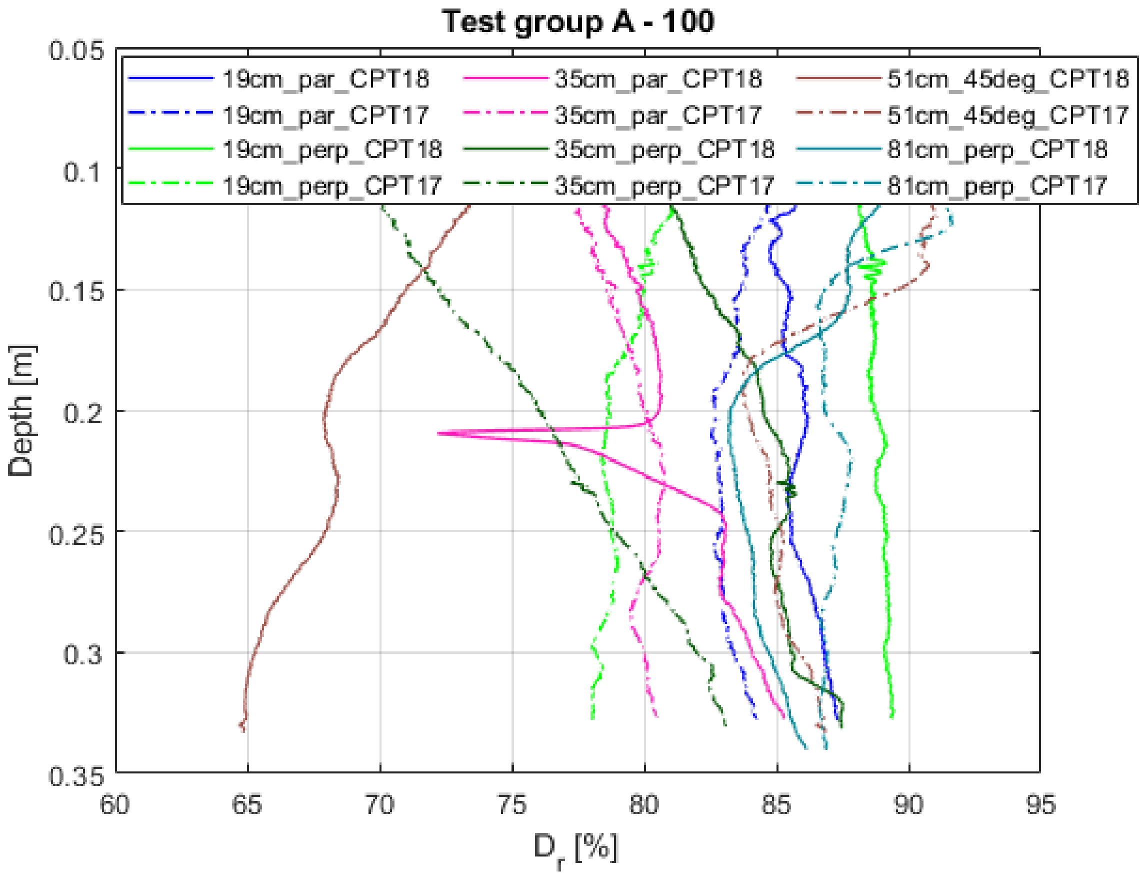

Figure D.44: Test-specific Dr results for CPT test subgroup A3

Force and displacement

During the test odd behavior of the test equipment were noticed. Force command defined in the software used for control of the test did not correspond to actual readings of the force. Due to this fact test did not went as planned, obtained actual forces can be seen in D.45 while planned loading scenario is seen in table D.3 and figure D.41.

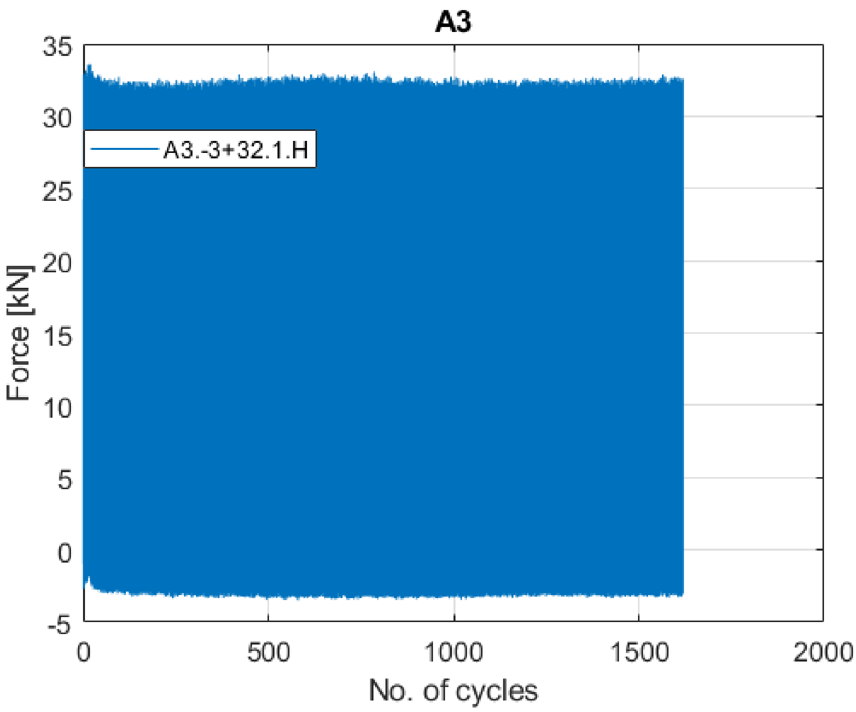

Figure D.45: Force VS No. of cycles

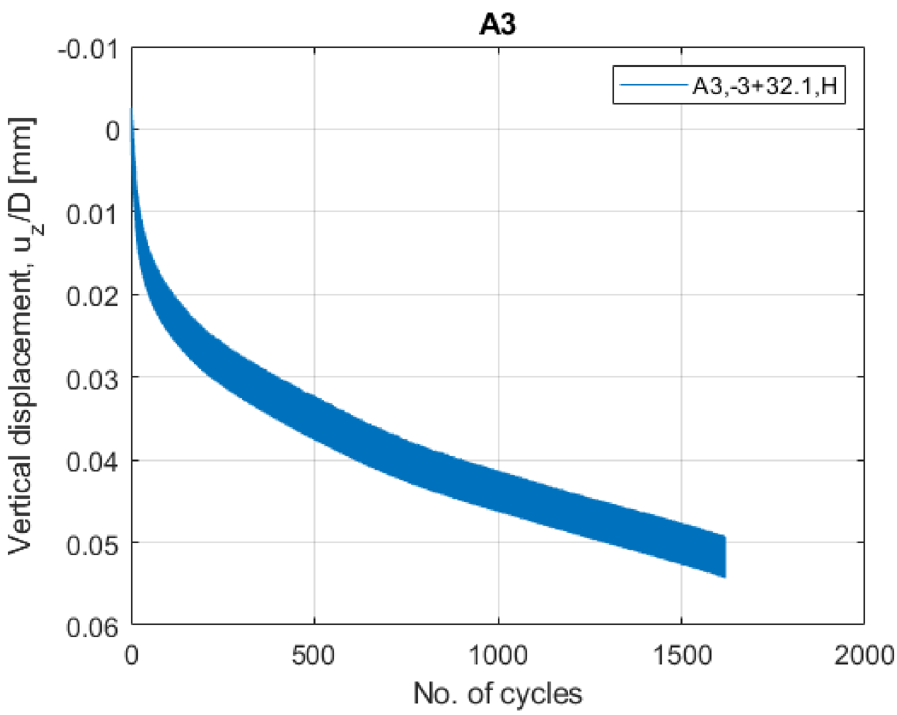

Figure D.46: Displacement VS No. of cycles

Lid Transducers

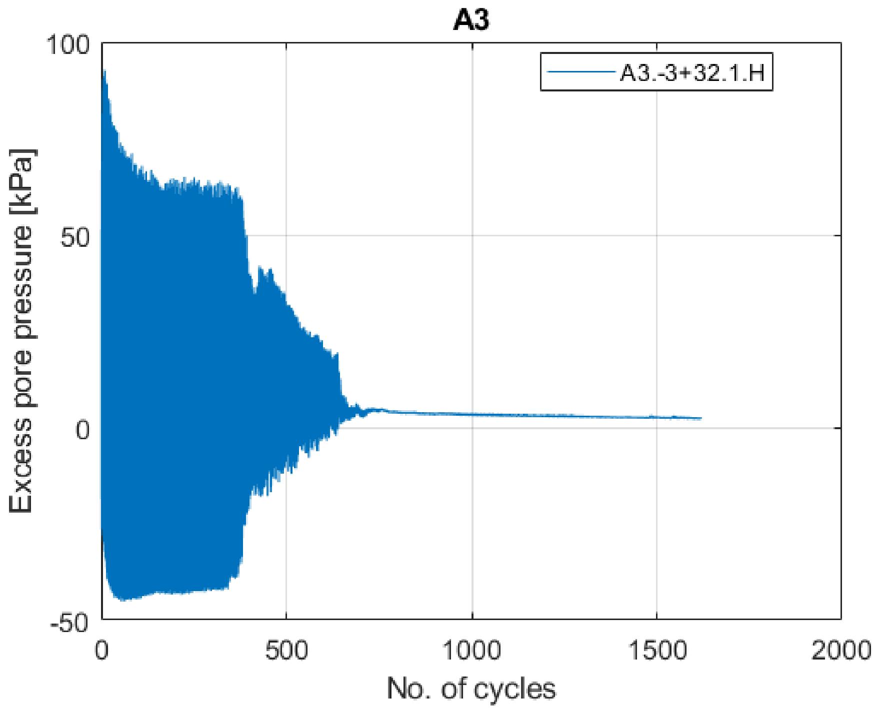

Figure D.47: Pore pressure at lid transducer P6

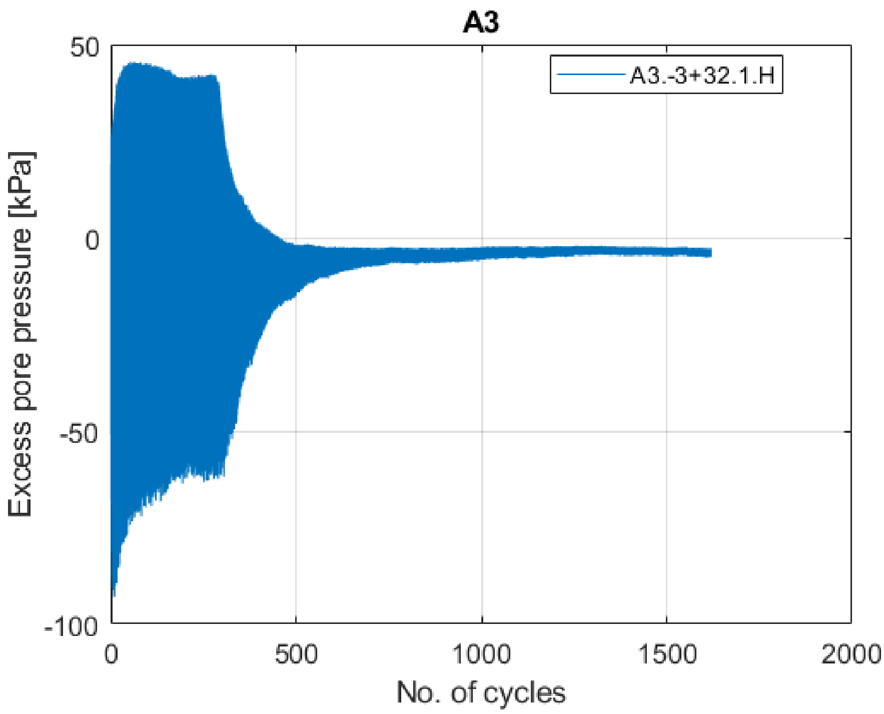

Figure D.48: Pore pressure at lid transducer P10

1st Level Transducers

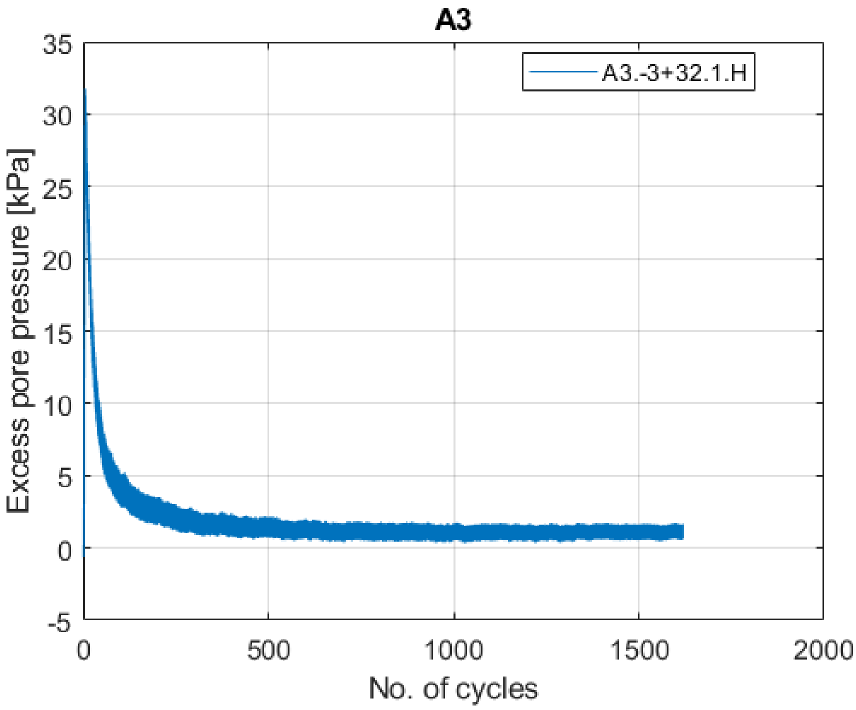

Figure D.49: Pore pressure at 1st level inner side transducer P4

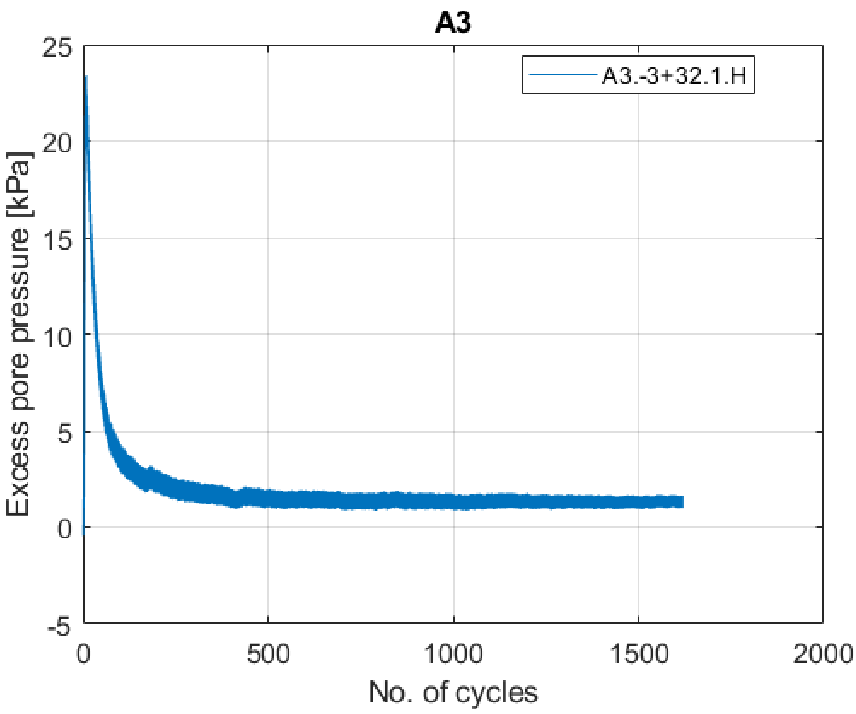

Figure D.50: Pore pressure at 1st level inner side transducer P11

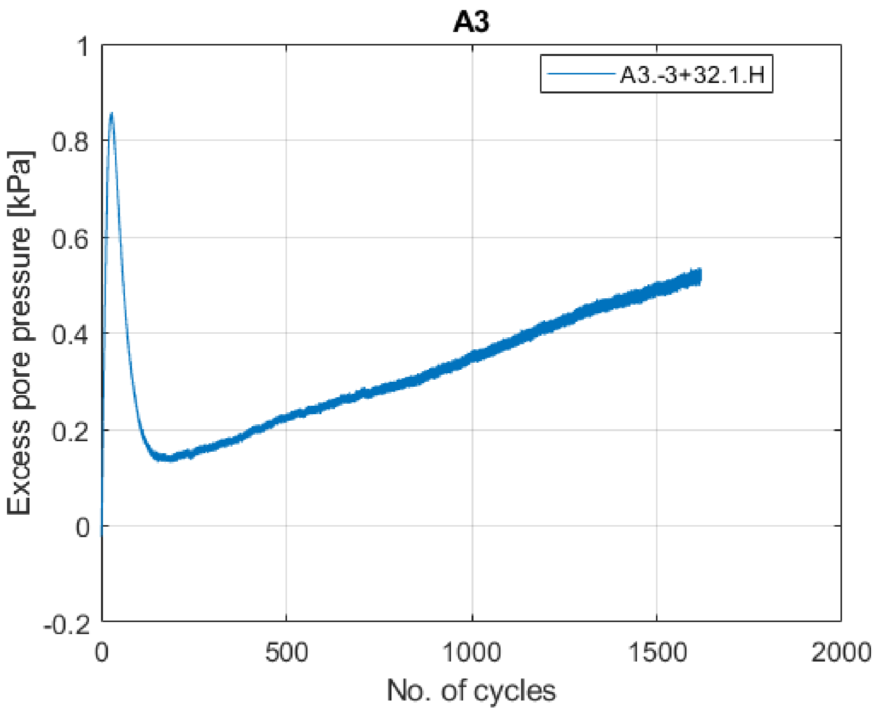

Figure D.51: Pore pressure at 1st level outer side transducer P3

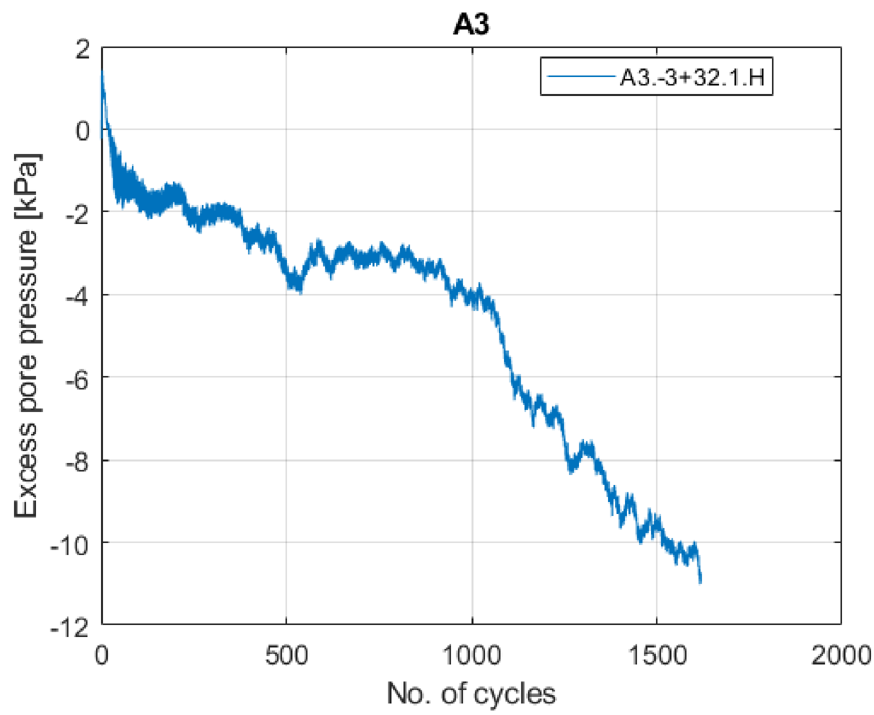

Figure D.52: Pore pressure at 1st level outer side transducer P7

2nd Level Transducers

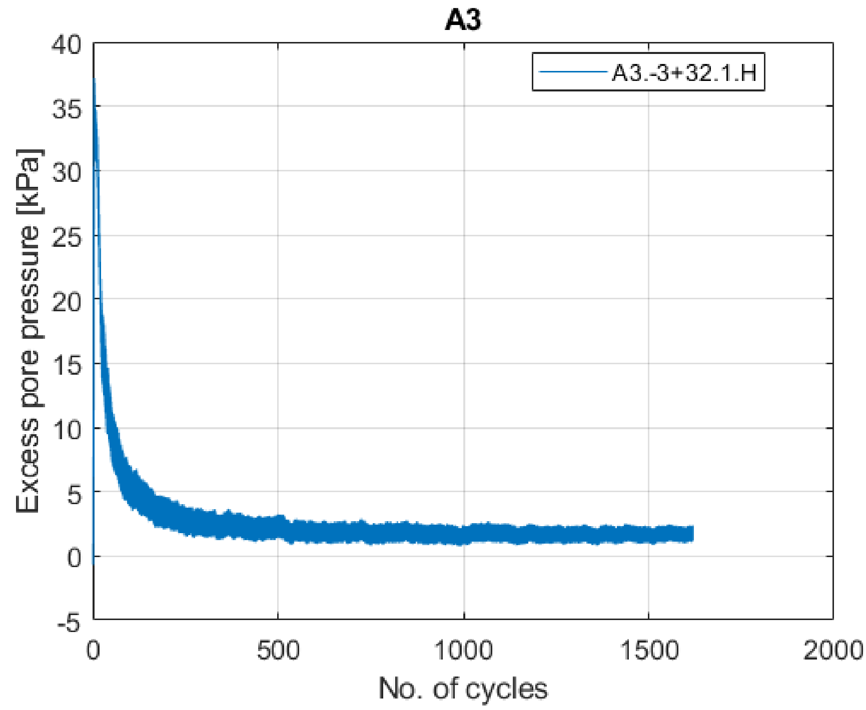

Figure D.53: Pore pressure at 2nd level inner side transducer P5

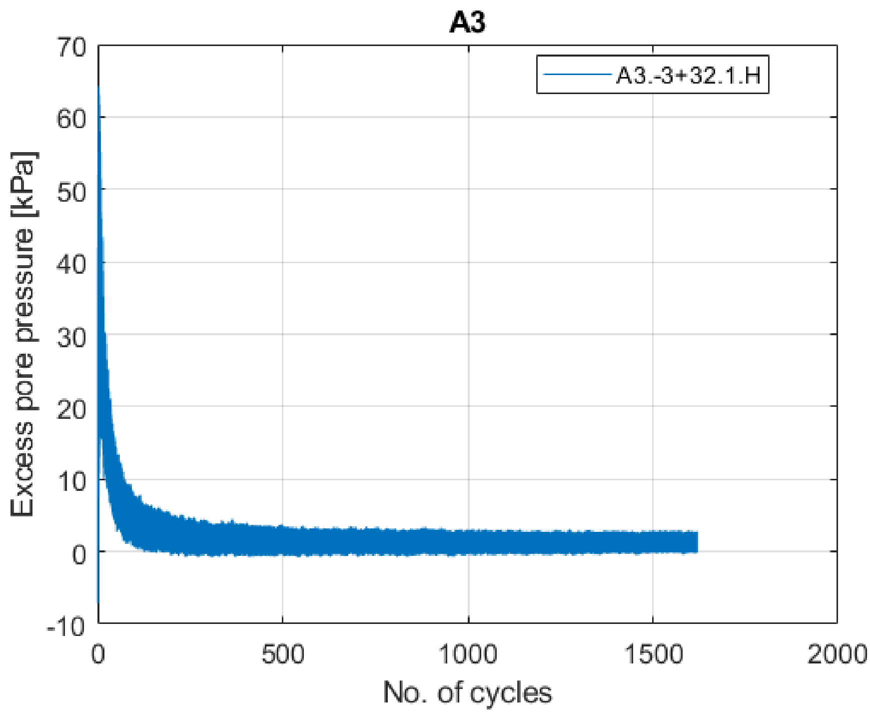

Figure D.54: Pore pressure at 2nd level inner side transducer P12

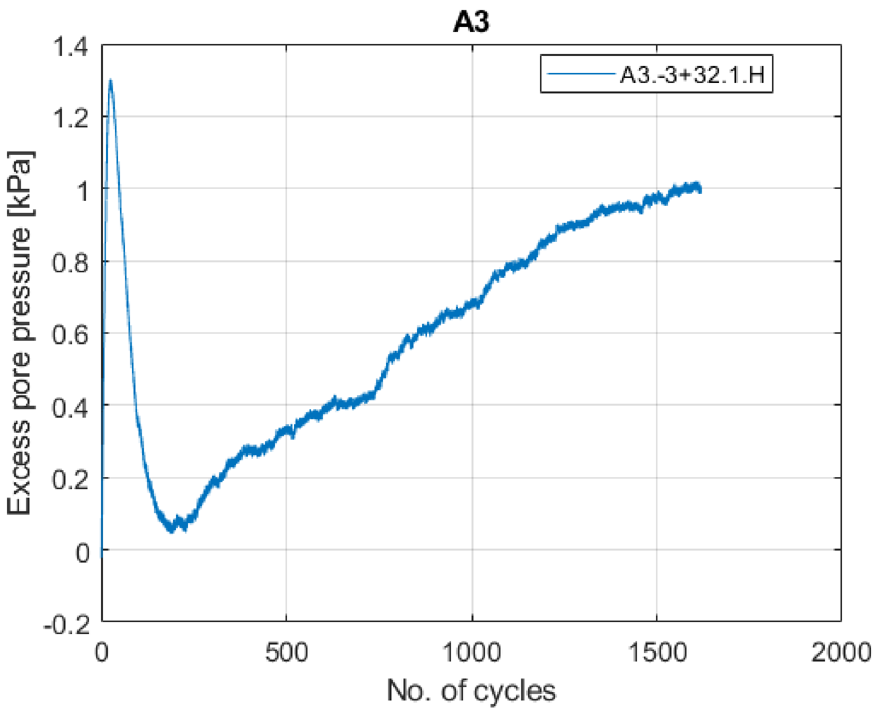

Figure D.55: Pore pressure at 2nd level outer side transducer P1

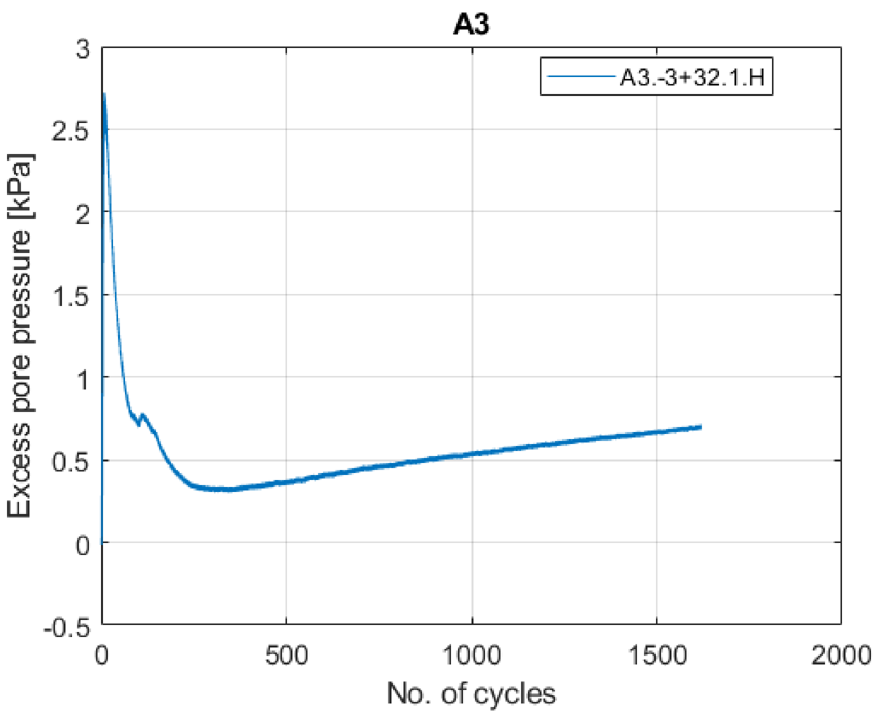

Figure D.56: Pore pressure at 2nd level outer side transducer P9

Skirt Tip Transducers

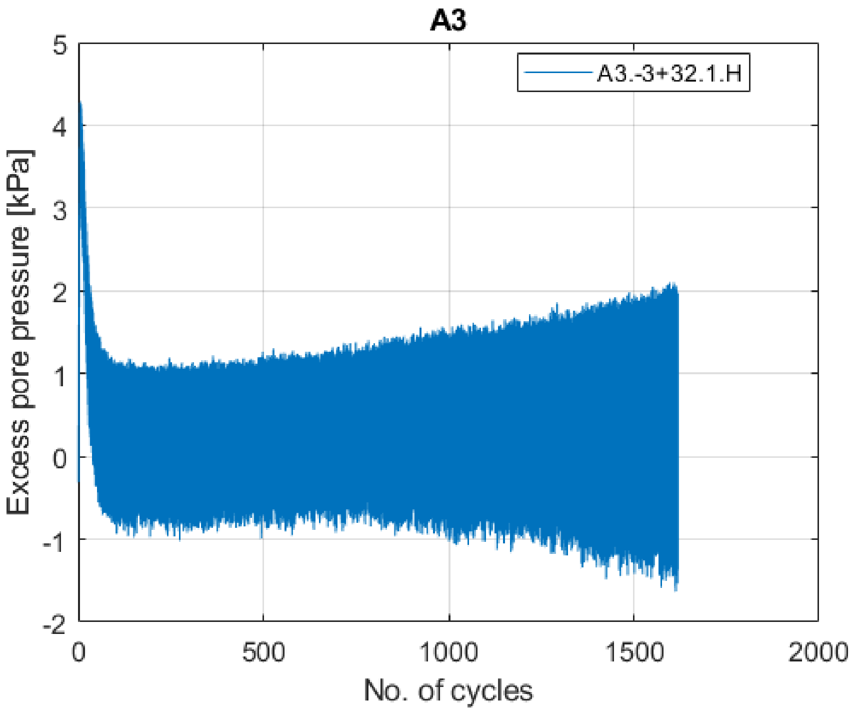

Figure D.57: Pore pressure at tip transducer P2

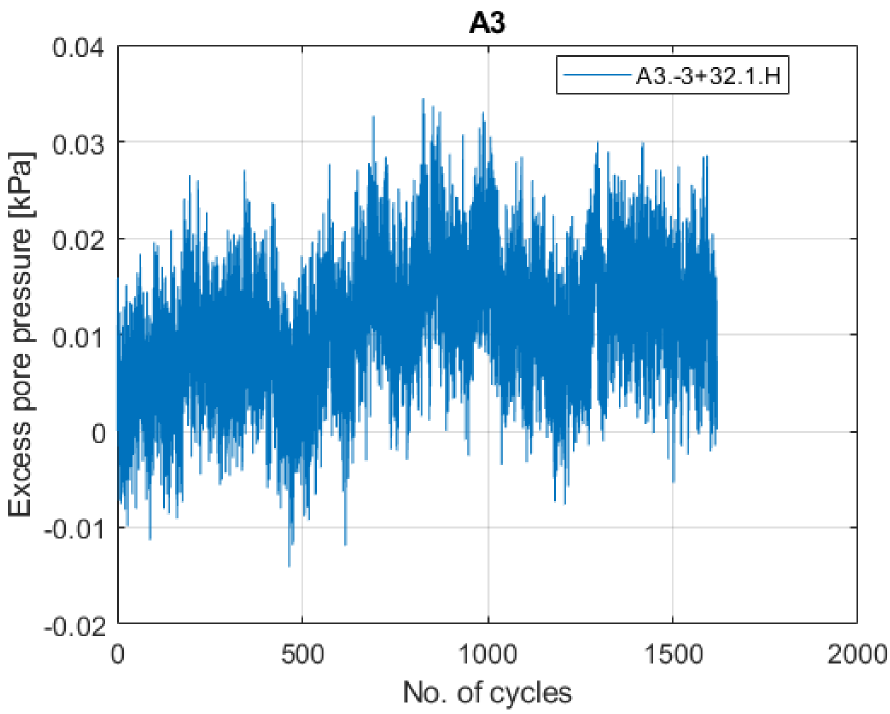

Figure D.58: Pore pressure at tip transducer P8

Force vs displacement

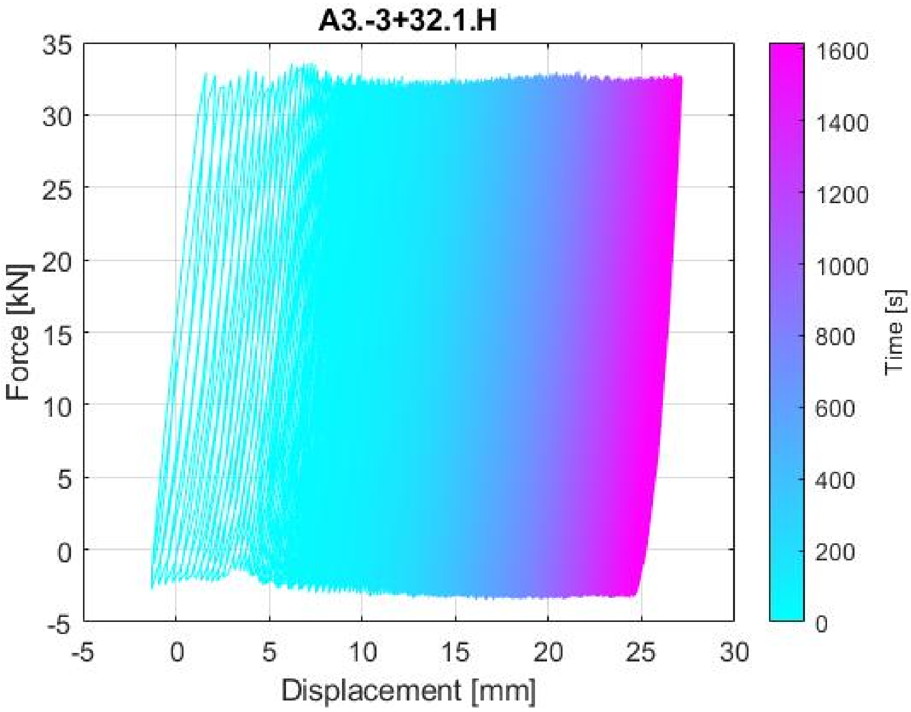

Figure D.59: Force VS absolute displacement

D.3 Test group B

Table D.4: Loading plan for 'Test group B'

Packet No.	Conditions	Force command		Force ratio	Cycle No.	Frequency
		F_{min} [kN]	F_{max} [kN]			[Hz]
1	Normal	25.6	31.5	1.23	10000	1.0
2	Severe	2.5	29.6	11.84	10	1.0
3	Normal	25.6	31.5	1.23	10000	1.0
4	Severe	2.3	29.6	12.87	10	1.0
5	Normal	25.6	31.5	1.23	10000	1.0

D.3.1 CPT

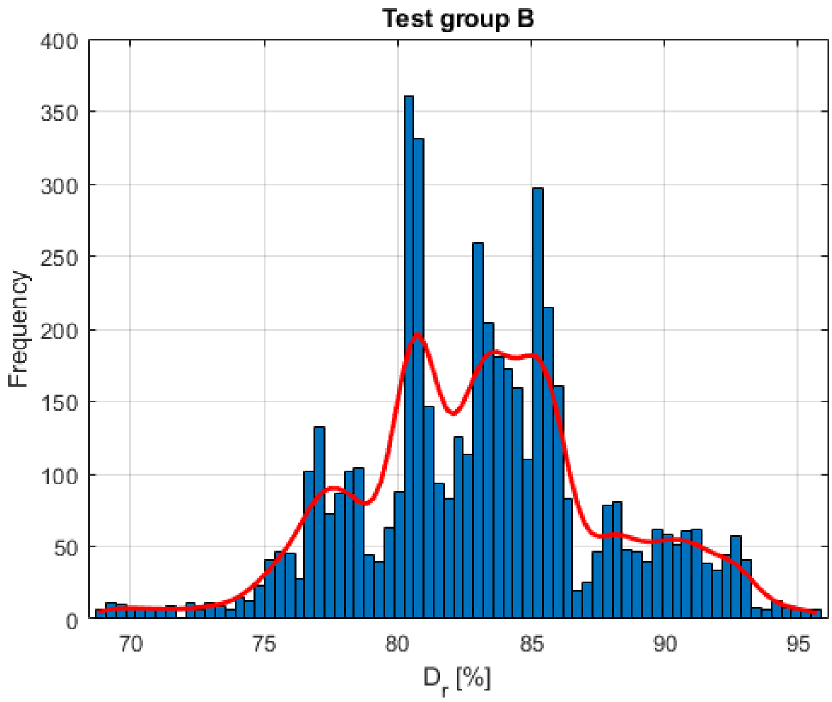

Figure D.60: Dr histogram with distribution fit for test group B

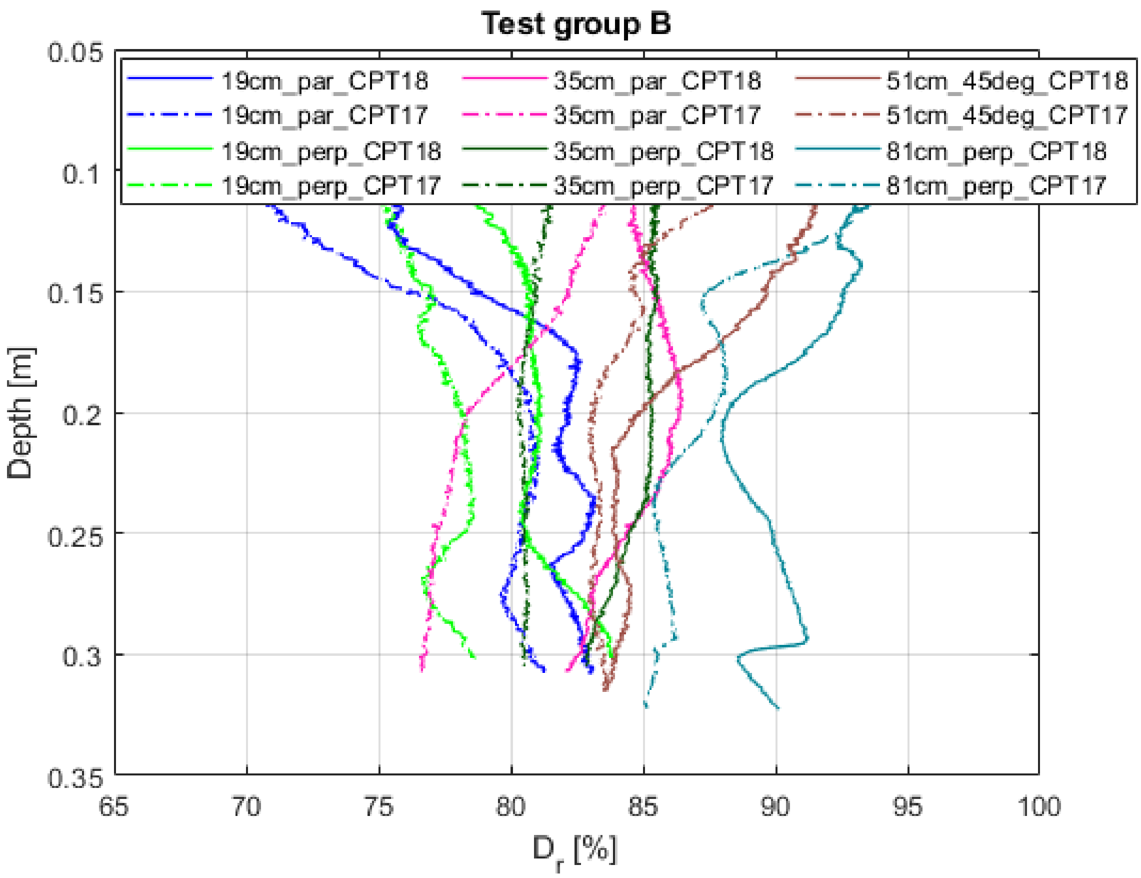

Figure D.61: Test-specific Dr results for CPT test group B

D.3.2 Test group B1 results

Idea behind this test is to try and replicate loads which acts on a wind turbine during normal conditions. Test consist of 5 parts:

- PRE1;PRE2;PRE3 - 10000 cycles of compression forces with max force load of 31.5 kN and minimum force load of 25.6 kN representing normal conditions

-B1,2.5+29.6,H ; B1,2.3+29.6,H - 10 cycles of two ways loading with sudden increase in loading amplitude from max compression force load of 29.6 kN to approximately 50 % of tensile drained bearing capacity which according to D.1 is 2.2 kN. Representing severe conditions which could be explained as loads during heavy storm.

Forces for all parts during test were applied with frequency of 1.0 Hz

Loading time history can be seen in figure D.62.

Sudden jump in all pore pressure measurements at a time approximately $0.8 \cdot 10^4$ cycle can be explained due to the fact that during the test there was an pressure leak from one of the valves which was fixed and pressure in the pressure tank increased by 2-3 kPa.

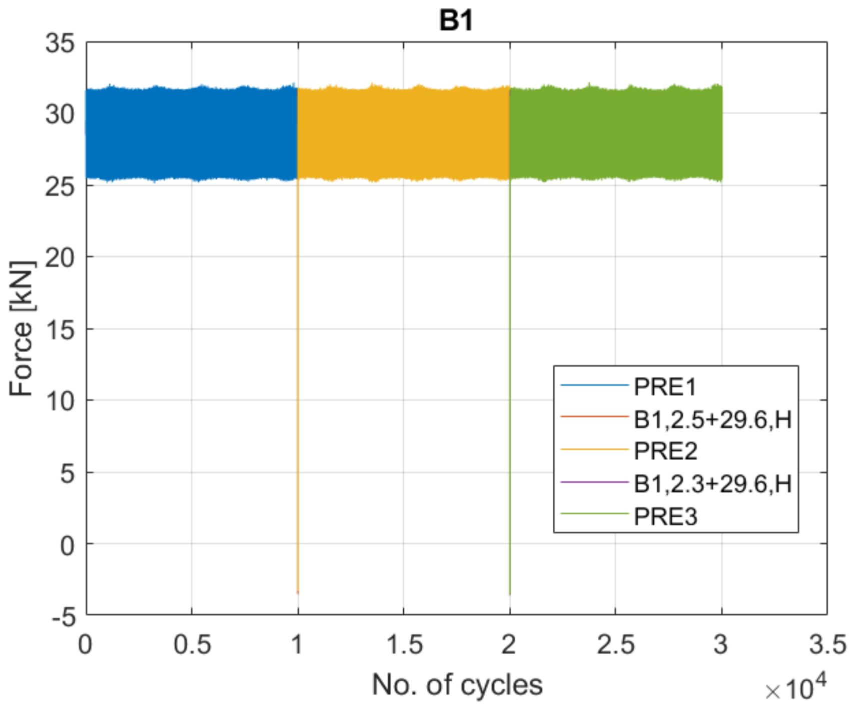

Figure D.62: Force vs No. of cycles

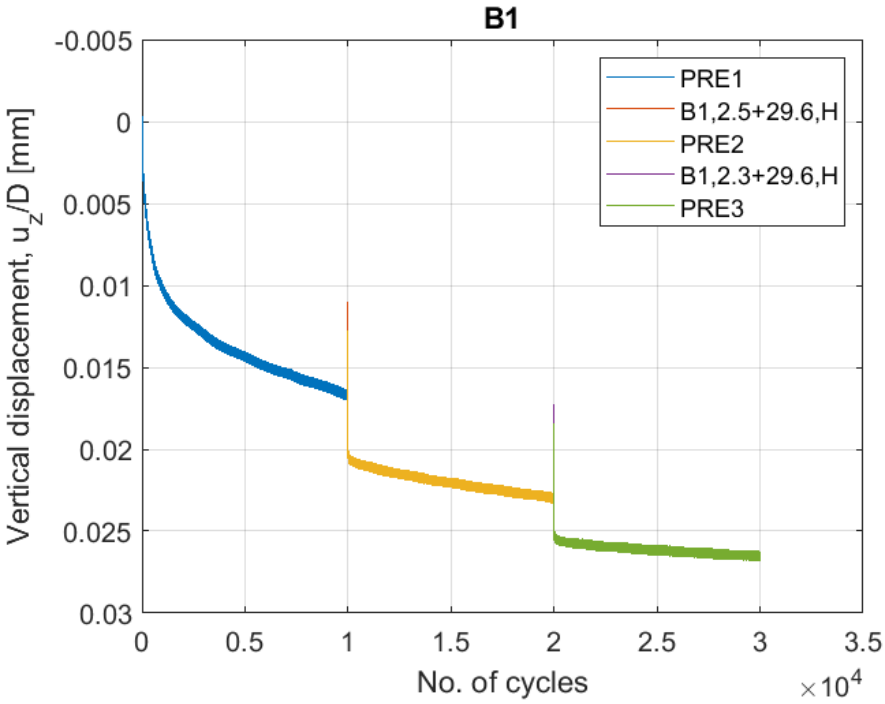

Figure D.63: Displacement VS No. of cycles

D.3.3 Lid transducers

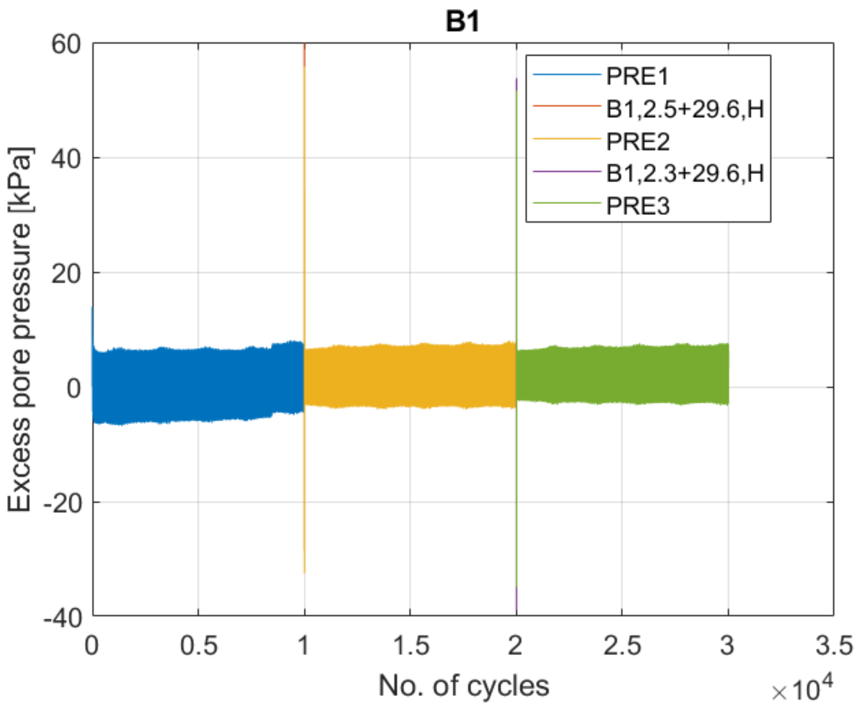

Figure D.64: Lid Transducer 6

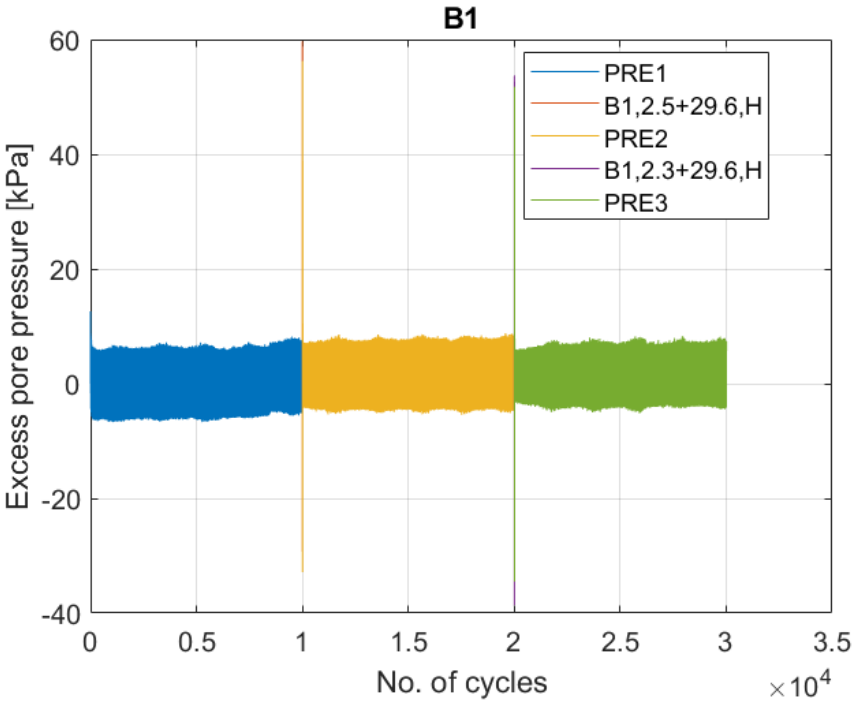

Figure D.65: Lid Transducer 10

D.3.4 Level 1 transducers

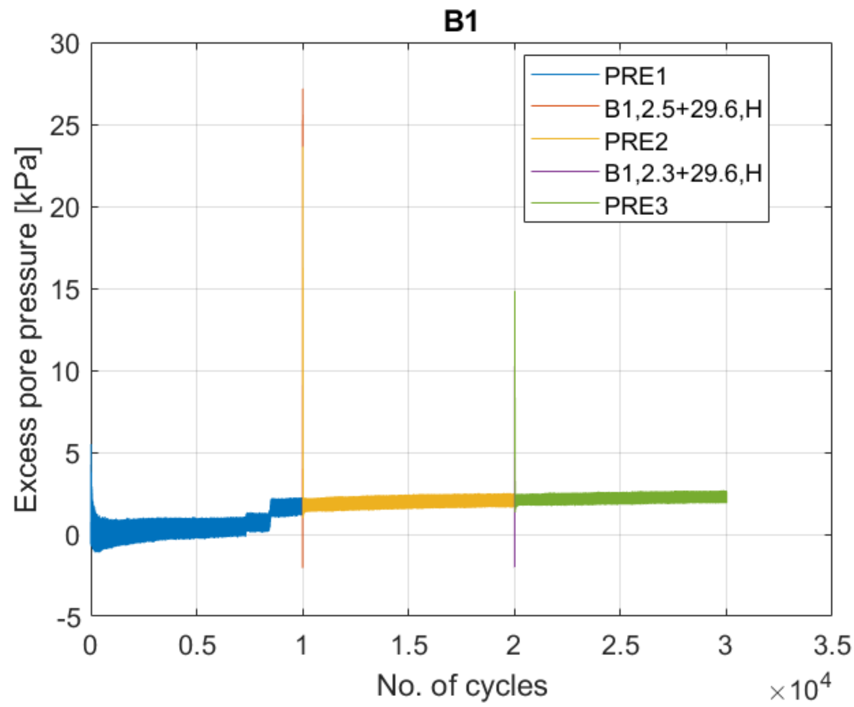

Figure D.66: Level 1 Transducer 4

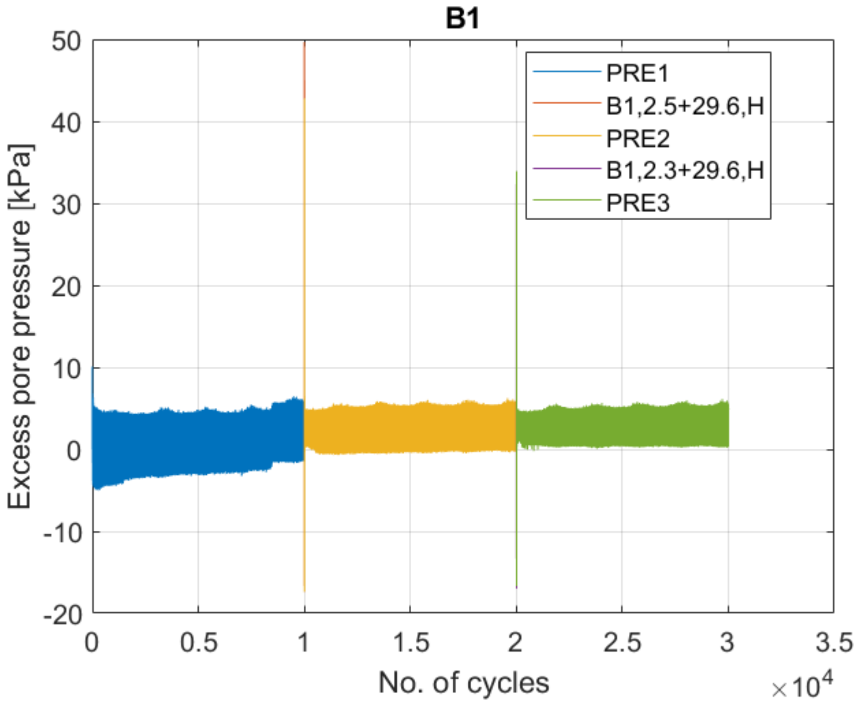

Figure D.67: Level 1 Transducer 11

D.3.5 Level 2 transducers

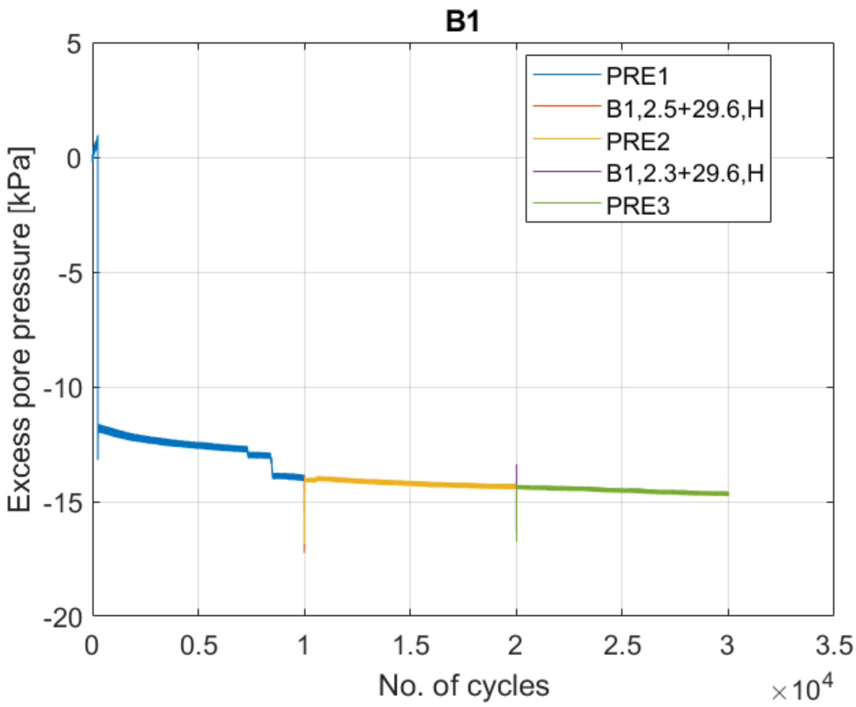

Figure D.68: Level 2 Transducer 1

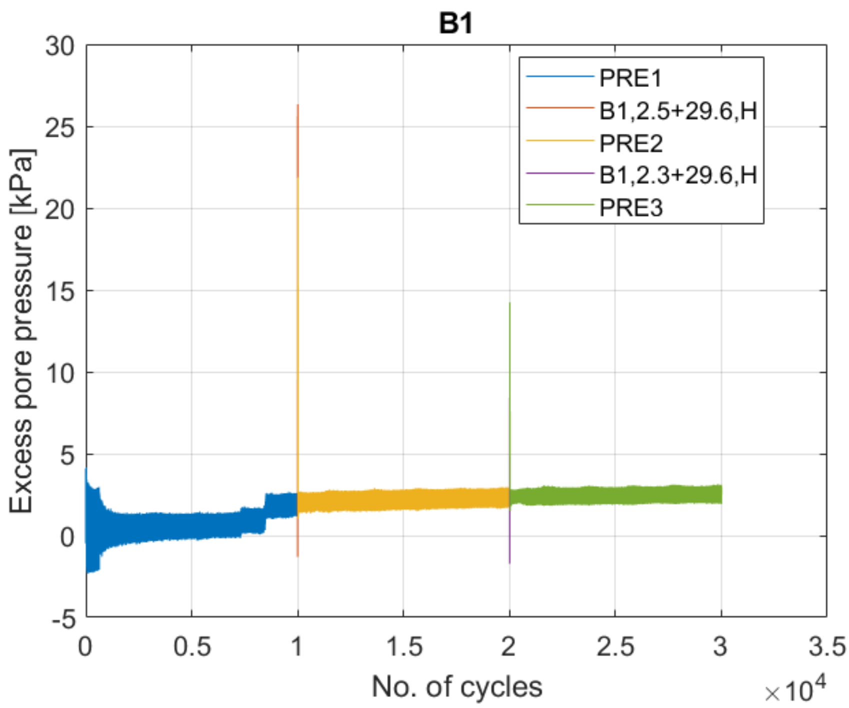

Figure D.69: Level 2 Transducer 5

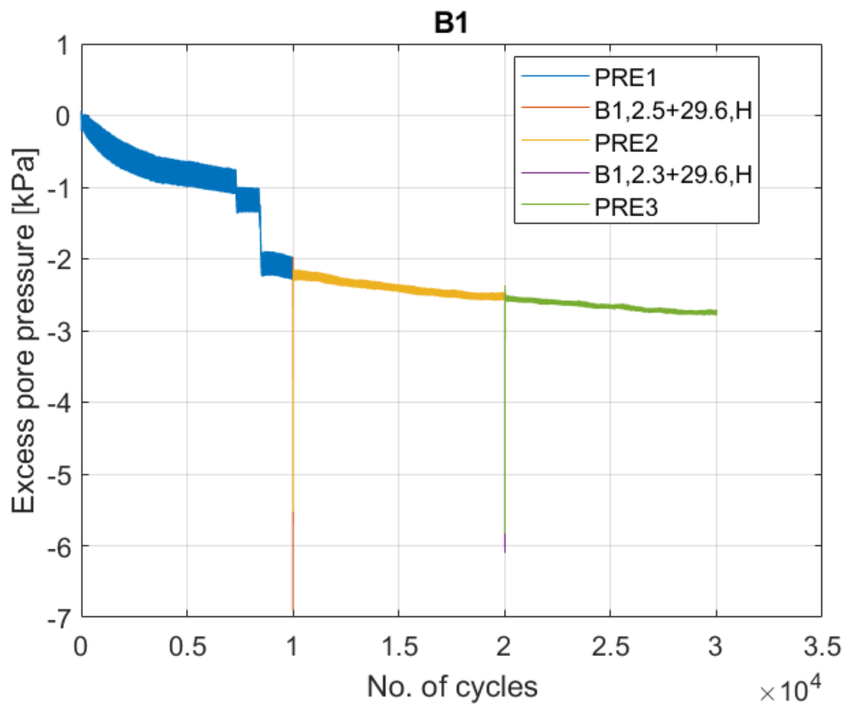

Figure D.70: Level 2 Transducer 9

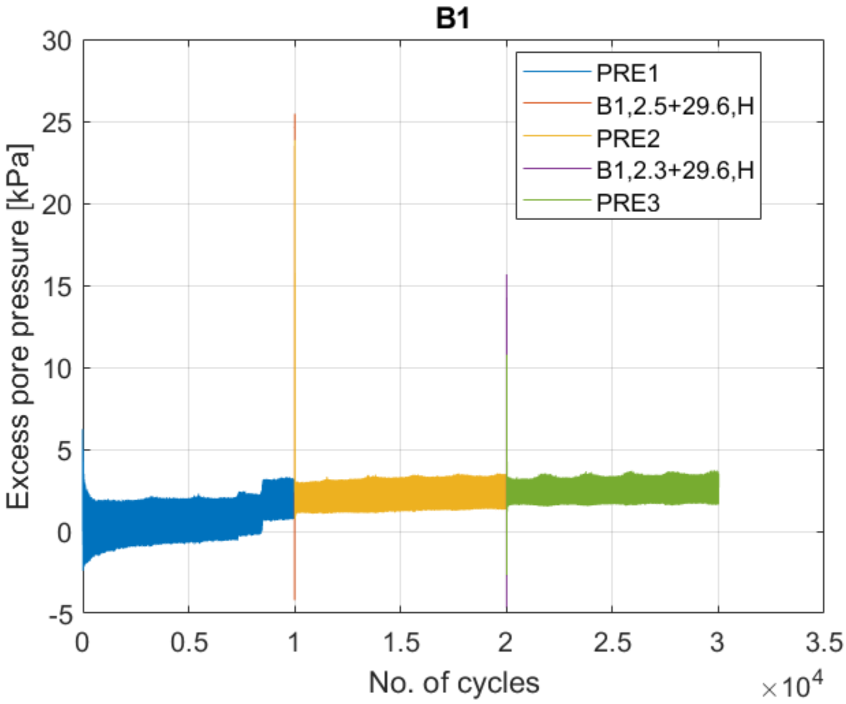

Figure D.71: Level 2 Transducer 12

D.3.6 Skirt tip transducers

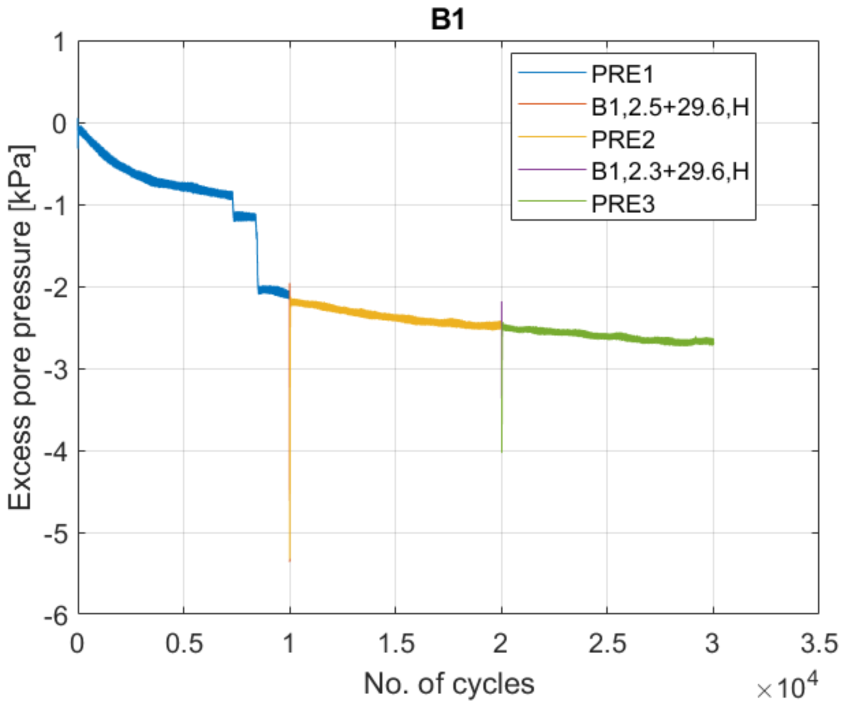

Figure D.72: Skirt tip Transducer 2

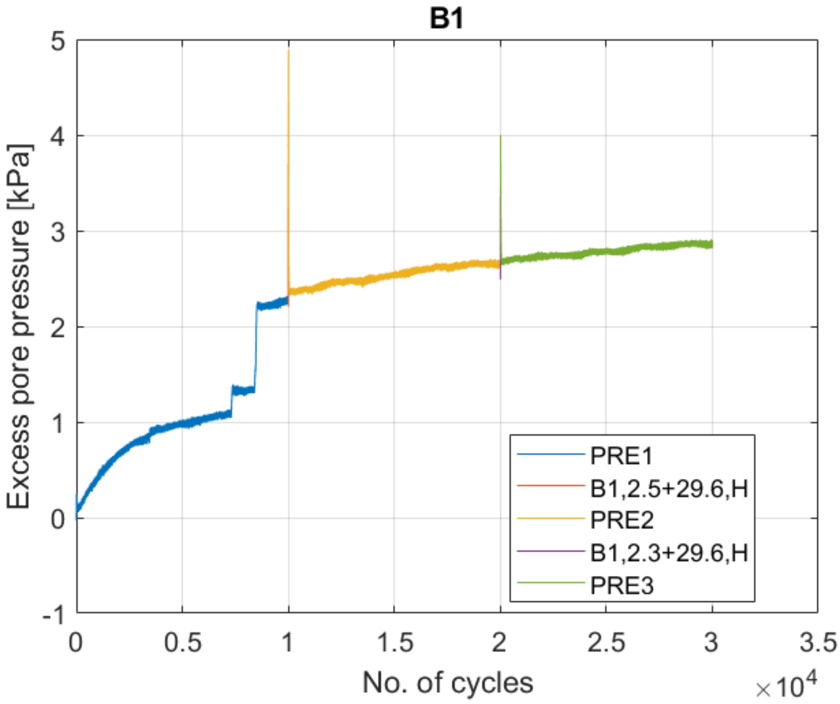

Figure D.73: Skirt tip Transducer 8

Force VS displacement

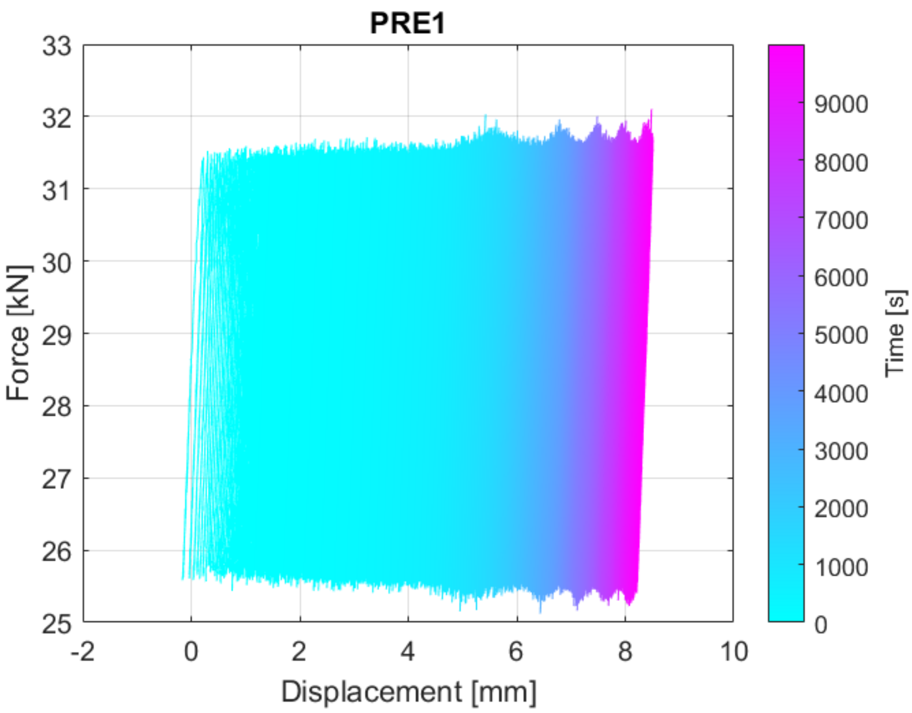

Figure D.74: Force VS absolute displacement

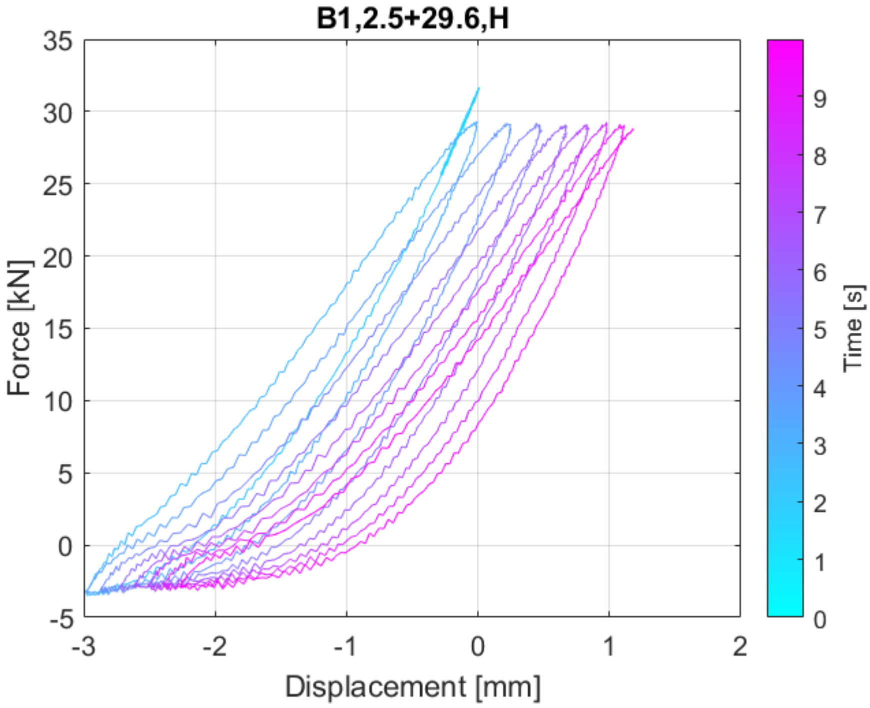

Figure D.75: Force VS absolute displacement

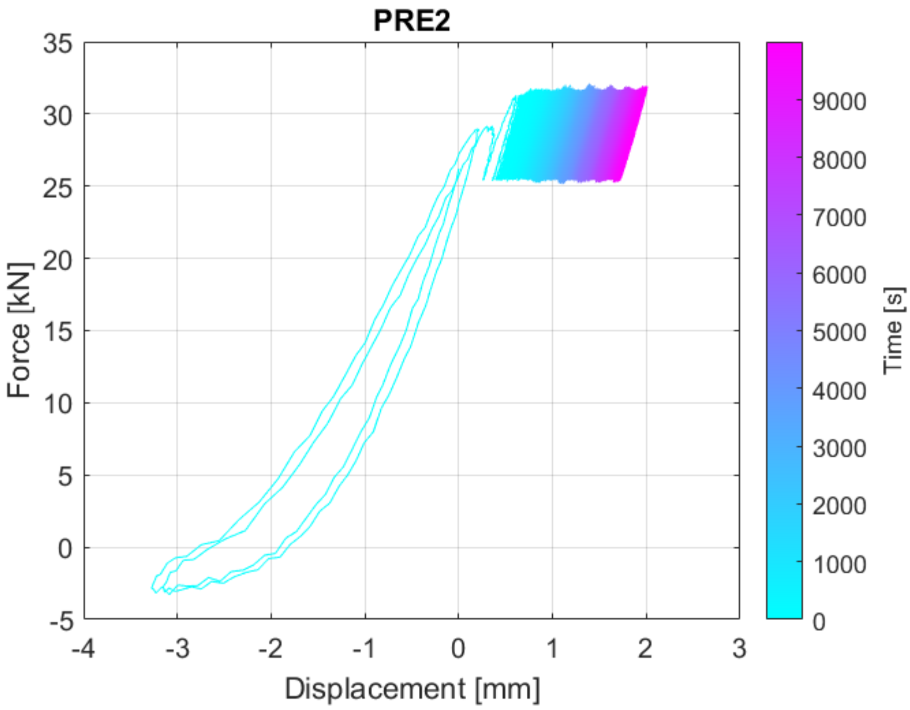

Figure D.76: Force VS absolute displacement

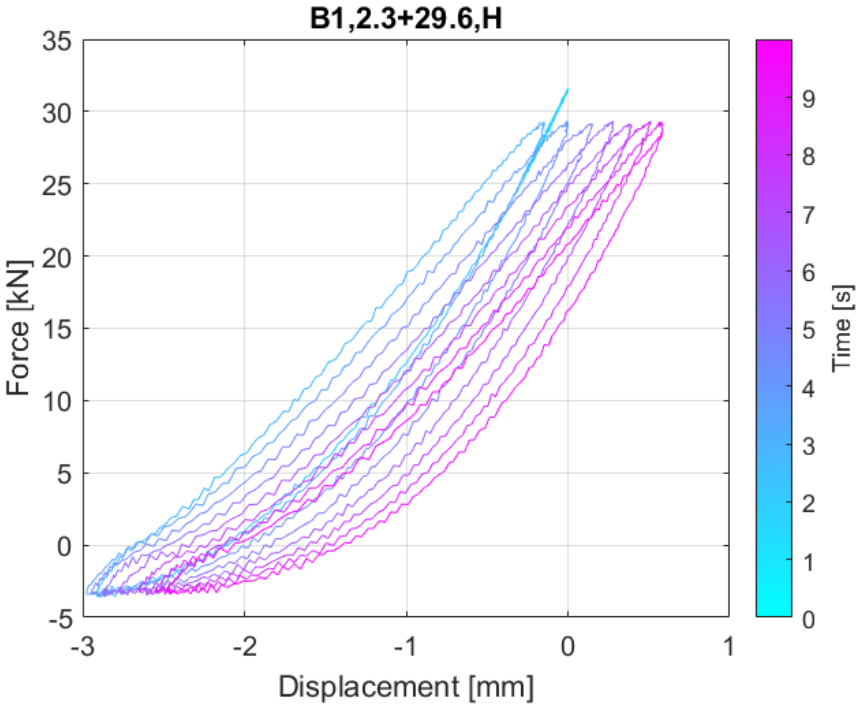

Figure D.77: Force VS absolute displacement

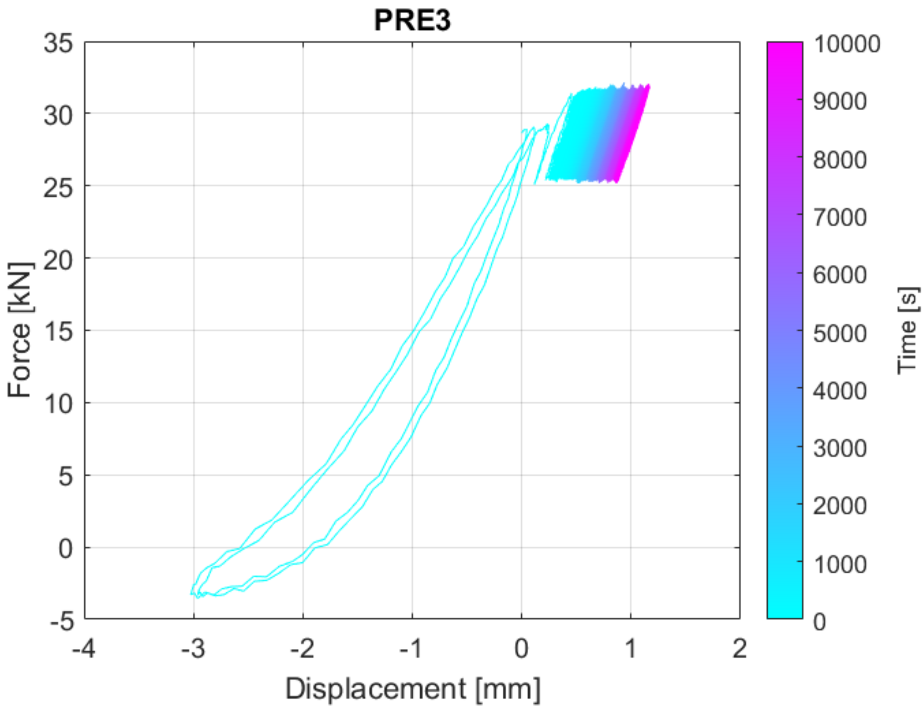

Figure D.78: Force VS absolute displacement

D.4 Test group C

The test is performed as two way loading. In the following results the compression force is kept at 5 kN for the first 4 "events" with increasing tensile force. Afterwards the remaning 2 "events" the tensile is kept at −2.5 kN and compression decreases. The ratio between tensile and compression for each event is increased to investigate the influence on the bucket from tensile loading. 6 "event" tests have been carried out where the following frequencies are used 1 Hz. Precycle is kept with a frequency of 0.1 Hz. The loading plan for all tests are shown in table D.5 as well as in figure D.79.

Table D.5: Loading plan for 'Test group C'

Packet No.	Conditions	Force command F_{min} [kN]	F_{max} [kN]	Force ratio	Cycle No.	Frequency [Hz]
1	Normal	4.00	6.00	0.67	1000	0.1
2	Severe	2.50	5.00	0.50	5000	1.0
3	Normal	4.00	6.00	0.67	200	0.1
4	Severe	0.00	5.00	-	5000	1.0
5	Normal	4.00	6.00	0.67	200	0.1
6	Severe	-2.50	5.00	-0.50	5000	1.0
7	Normal	4.00	6.00	0.67	200	0.1
8	Severe	-5.00	5.00	-1.00	5000	1.0
9	Normal	4.00	6.00	0.67	200	0.1
10	Severe	-2.50	2.5	-1.00	5000	1.0
11	Normal	4.00	6.00	0.67	200	0.1
12	Severe	0.00	2.50	-	5000	1.0

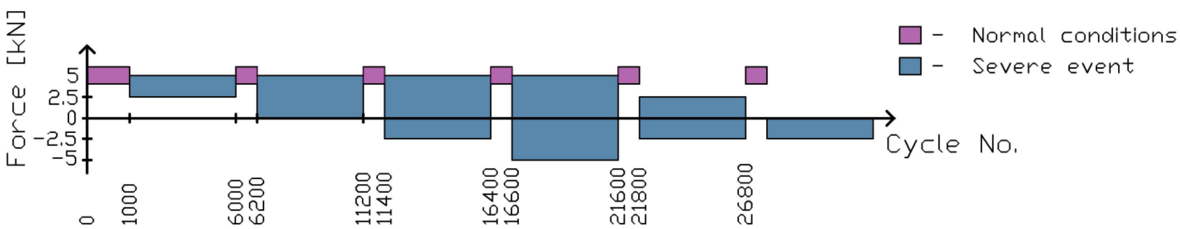

Figure D.79: Scheduled loading plan for Test group C

D.4.1 Test subgroup C1 - 1 Hz

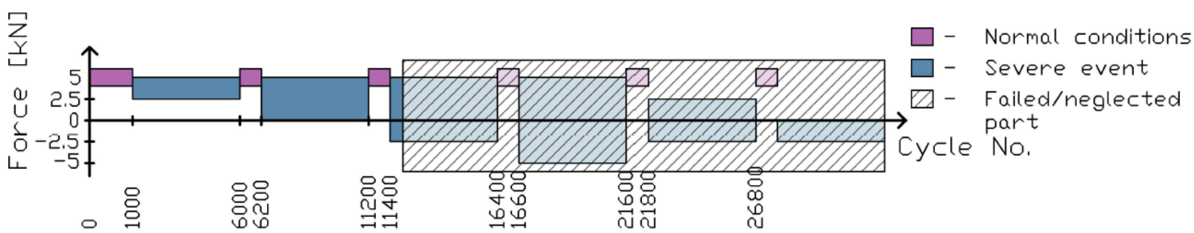

Figure D.80: Actual loading plan for Test subgroup C1

CPT

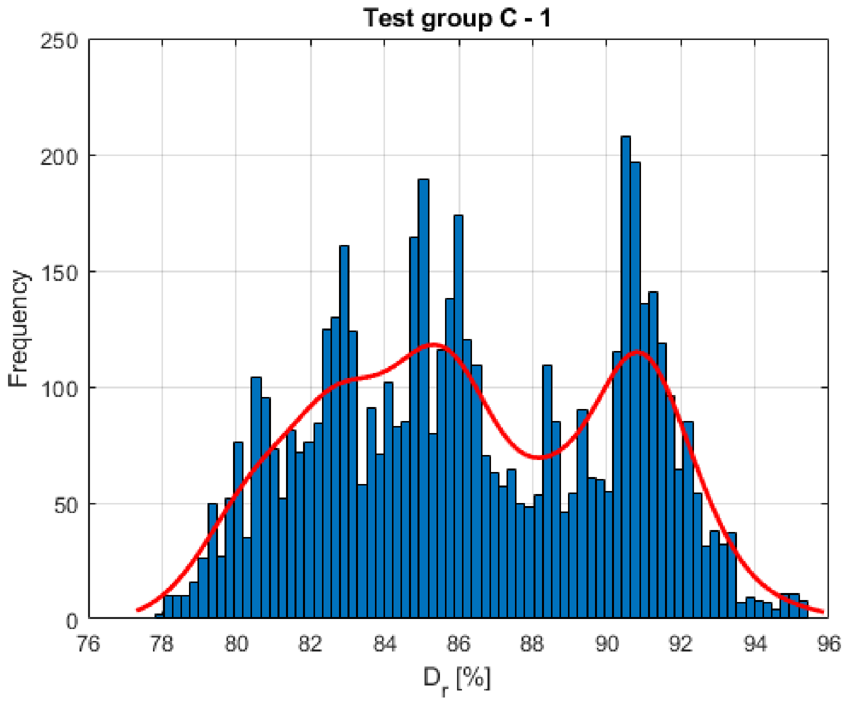

Figure D.81: Dr histogram with distribution fit for test subgroup C1

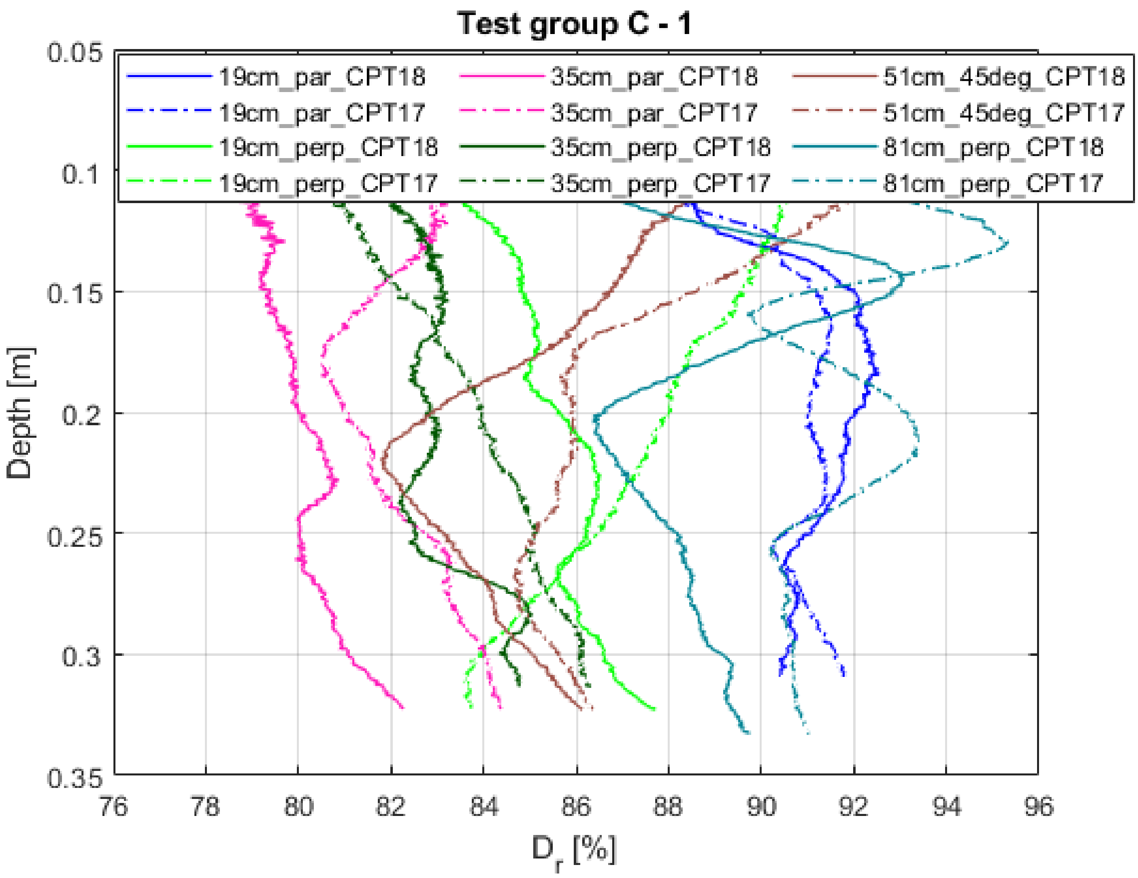

Figure D.82: Test-specific Dr results for CPT test subgroup C1

Force and displacement

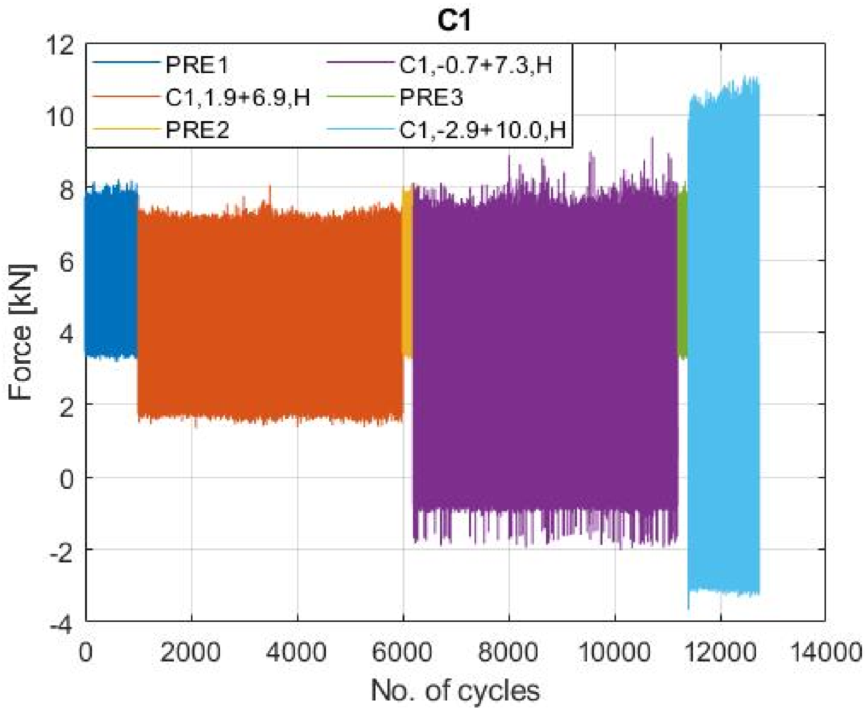

Figure D.83: Force VS no. of cycles

Looking at the amplitude and maximum and minimum forces from D.83, and comparing it to table D.5, its clear to see, that the loading exceeds the planned loading for the test. For the precycle and load cycles at some points it reaches a value of 2 kN higher than wanted. That might be explained by precision of the machinery. These loads used during the test are relatively small compared to the load transducer with capability of 100 kN which was used for the test, so errors between command and actual force are expected.

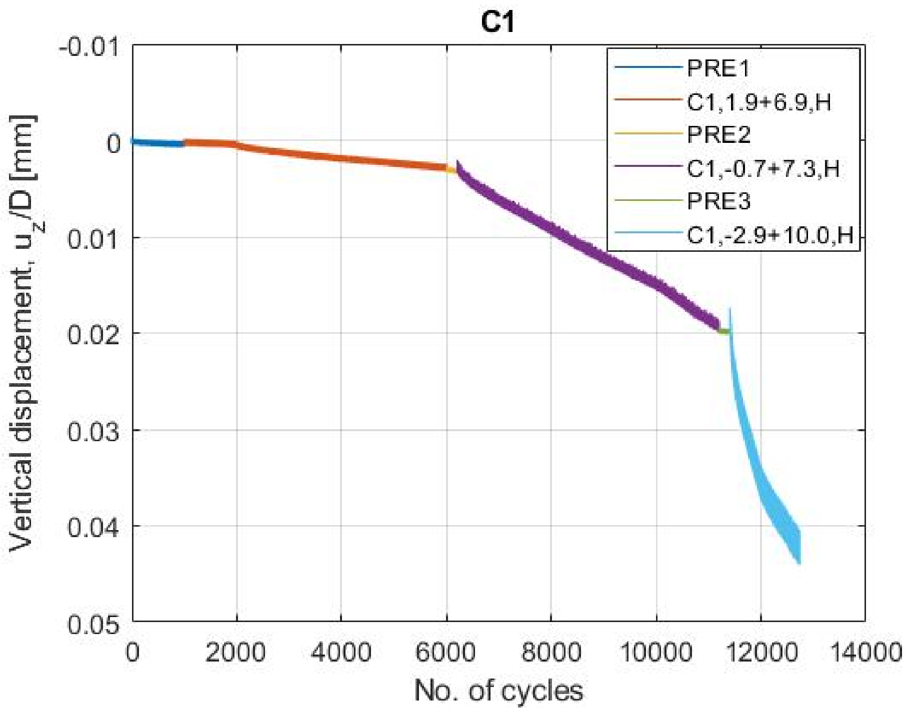

Figure D.84: Displacement VS No. of cycles

From the plot above, it is clear that the bucket does not settle significantly in the first load cycle where as in the second cycle, the soil starts to lose its strength, and loses the grip of the bucket and it moves downwards, and in the third cycle the soil complete loses the strength and reaches the lower limit, which is an downward displacement of 21 mm from the starting position.

Lid Transducers

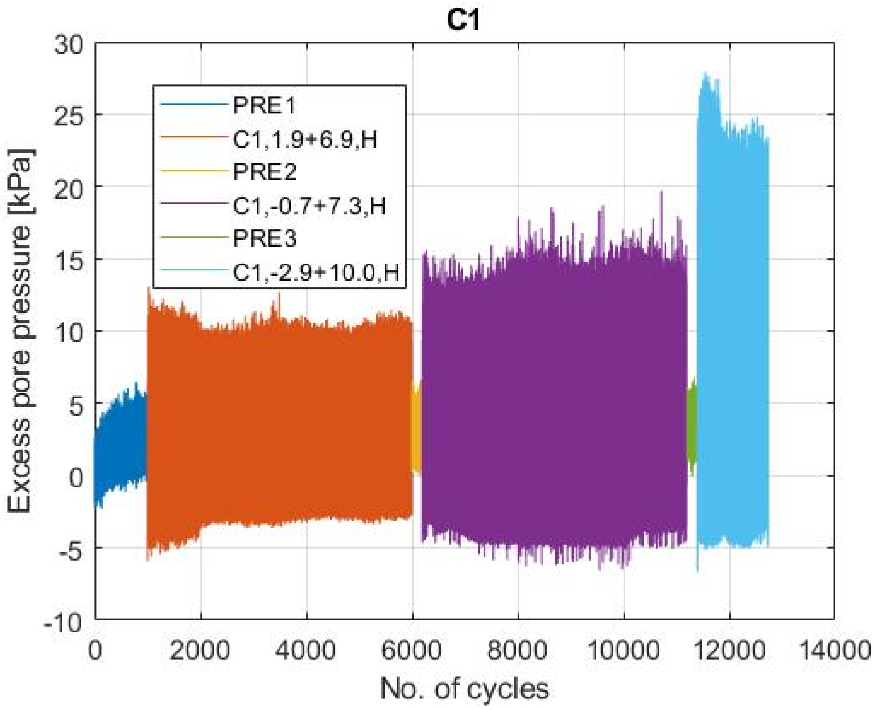

Figure D.85: Pore pressure at lid transducer P6

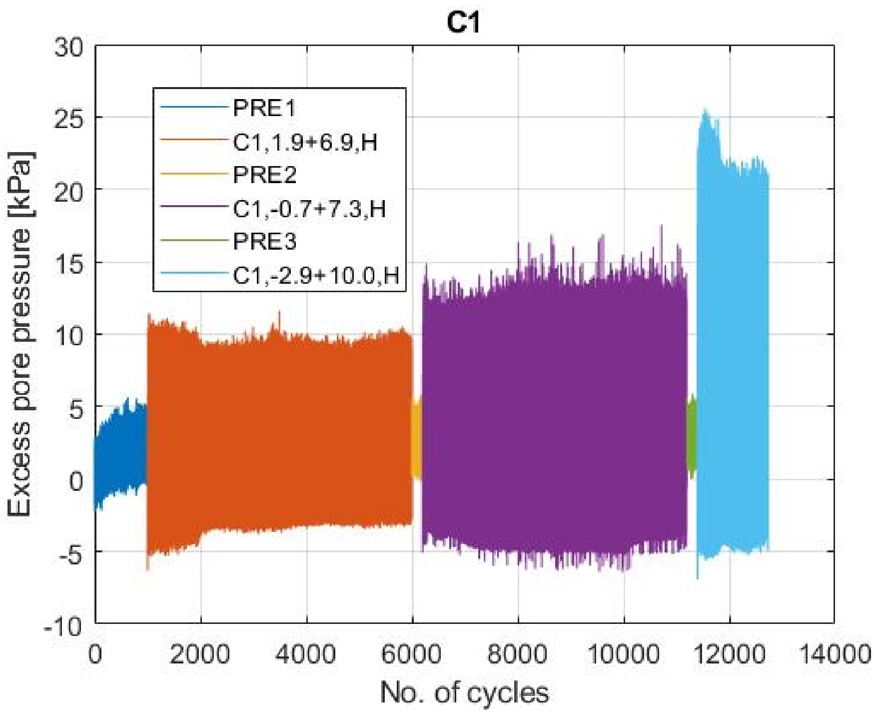

Figure D.86: Pore pressure at lid transducer P10

1st Level Transducers

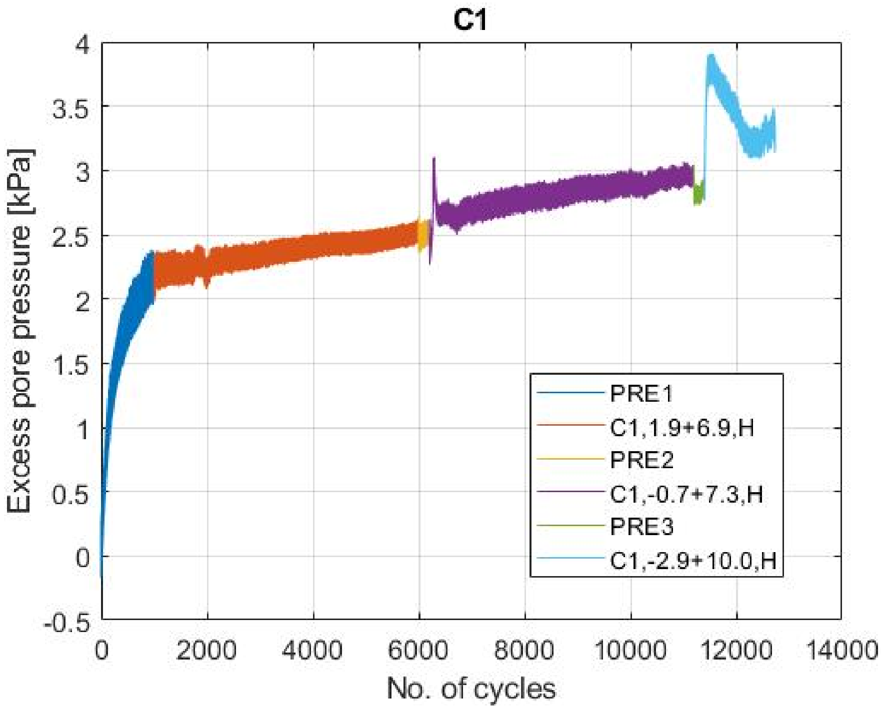

Figure D.87: Pore pressure at 1st level inner side transducer P11

2nd Level Transducers

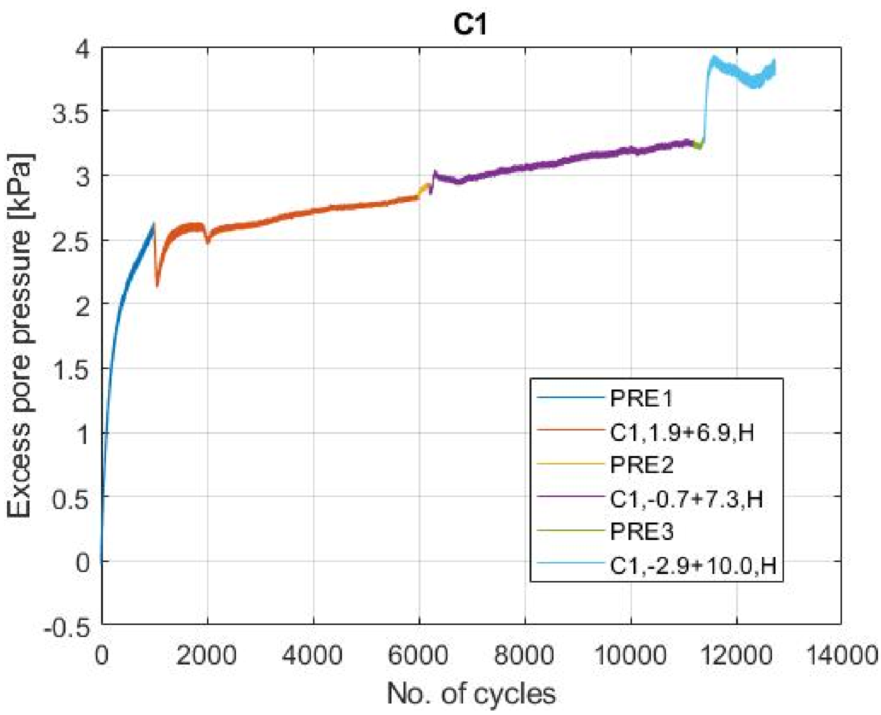

Figure D.88: Pore pressure at 2nd level inner side transducer P5

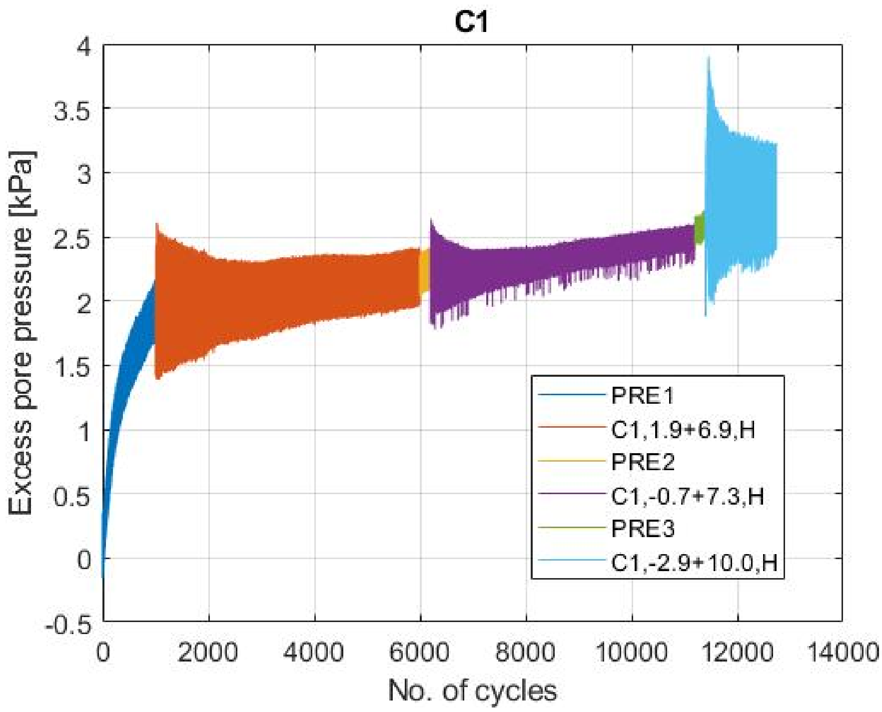

Figure D.89: Pore pressure at 2nd level outer side transducer P9

Skirt Tip Transducers

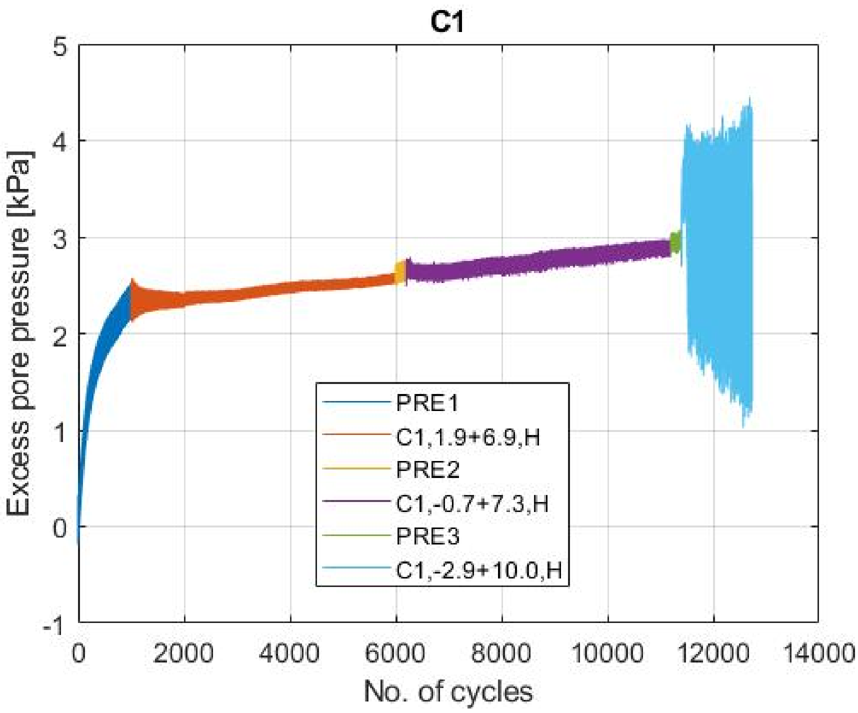

Figure D.90: Pore pressure at tip transducer P2

Soil pore pressure at 50 cm depth

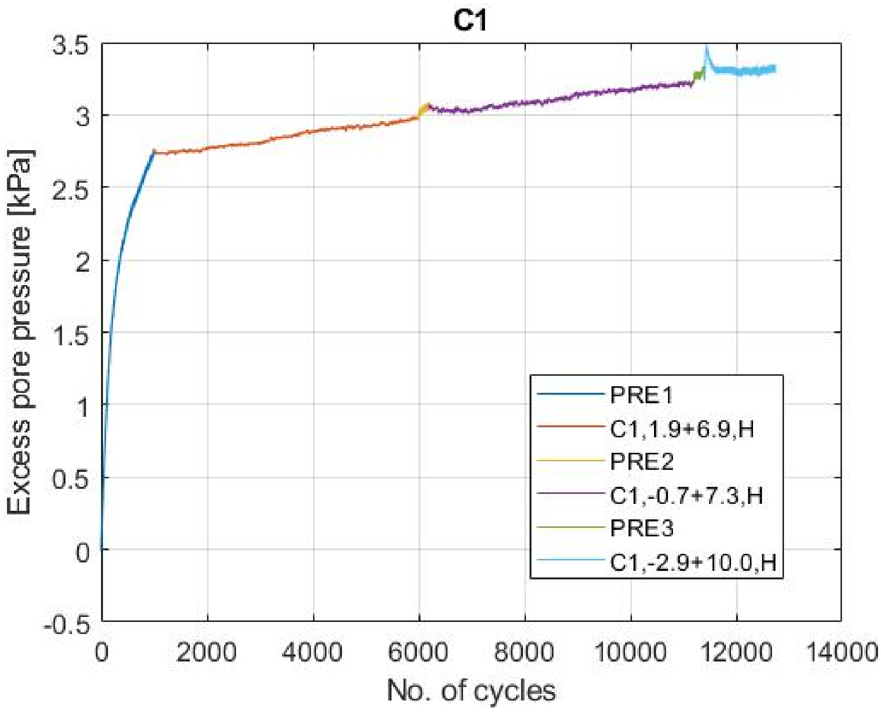

Figure D.91: Pore pressure transducer P13

Force vs displacement

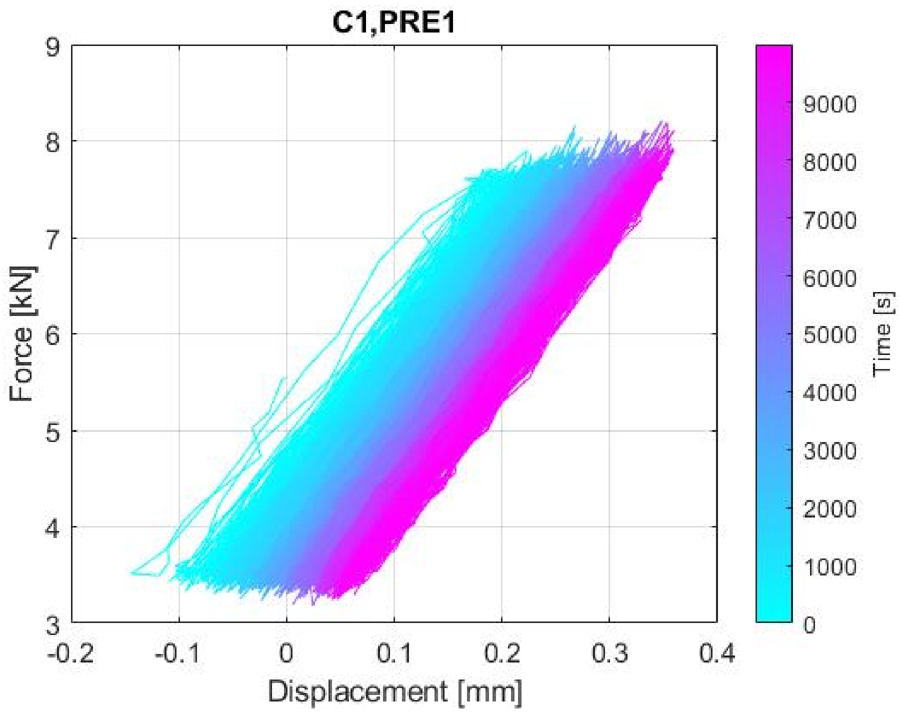

Figure D.92: Force VS absolute displacement

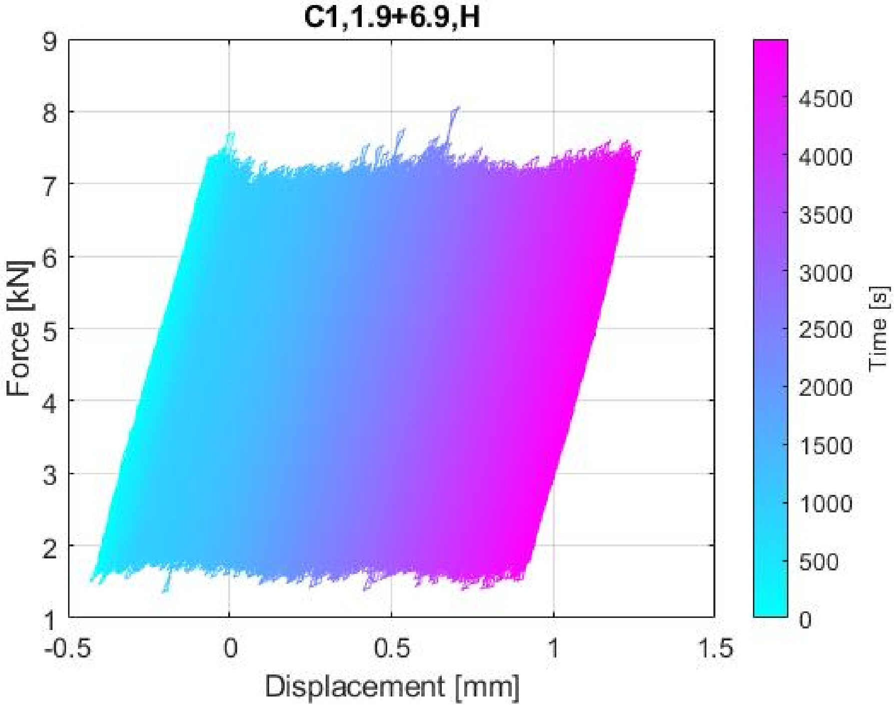

Figure D.93: Force VS absolute displacement

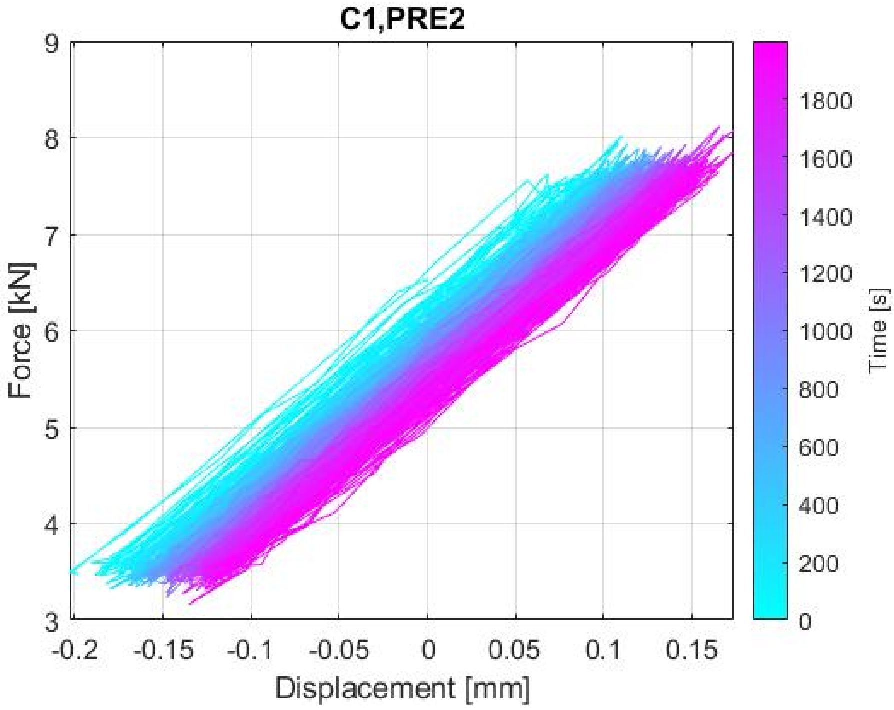

Figure D.94: Force VS absolute displacement

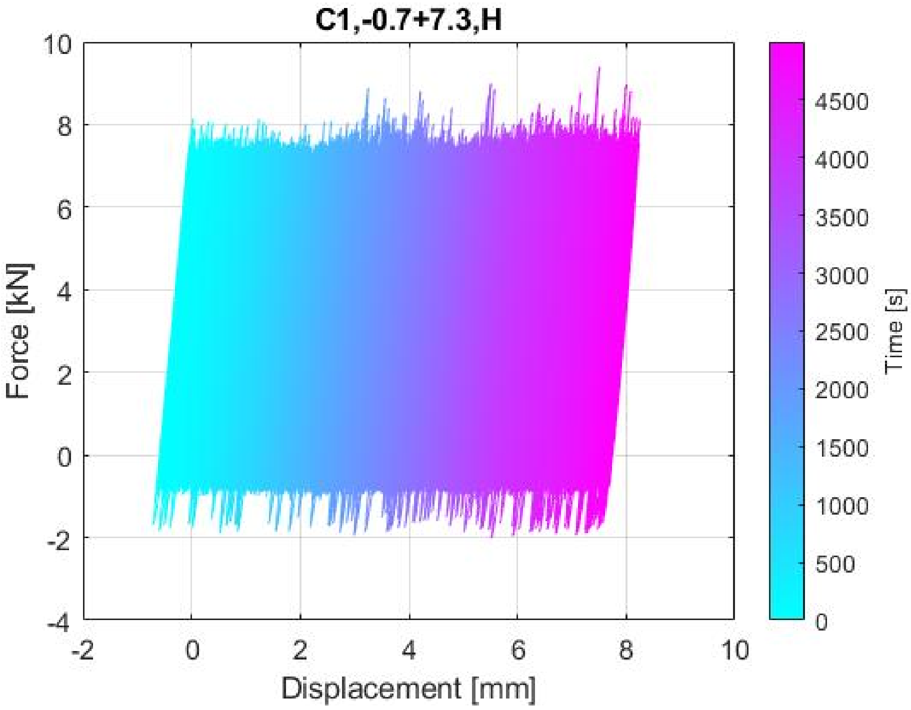

Figure D.95: Force VS absolute displacement

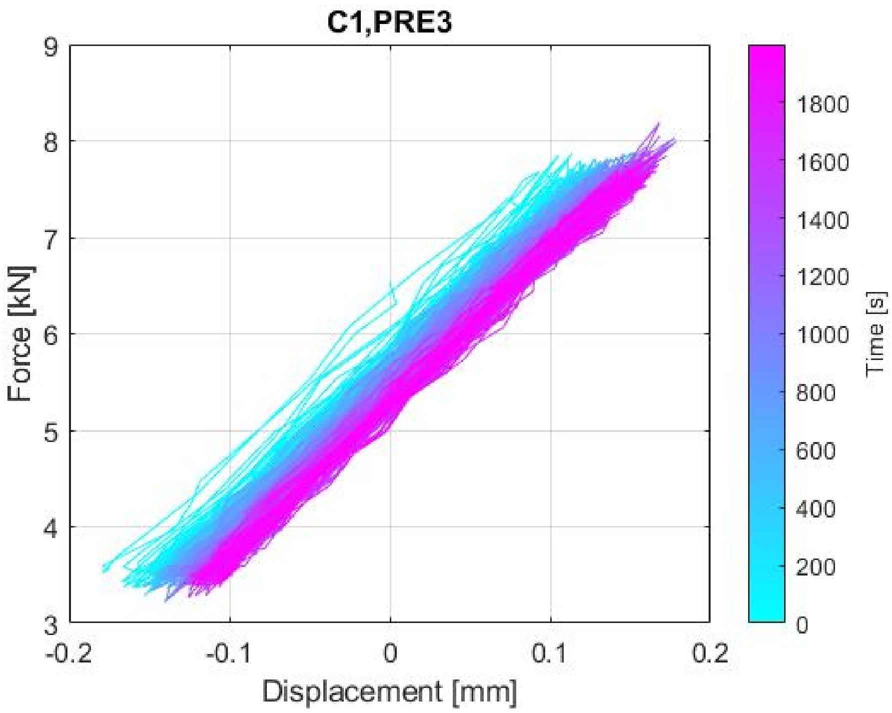

Figure D.96: Force VS absolute displacement

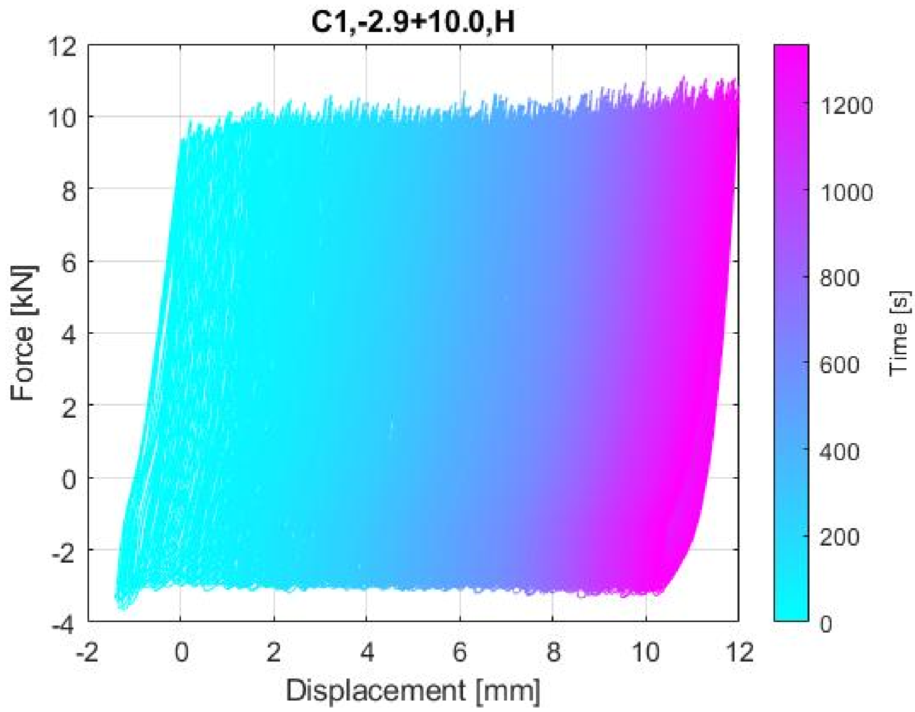

Figure D.97: Force VS absolute displacement

D.4.2 Test subgroup C2 - 1.0 Hz

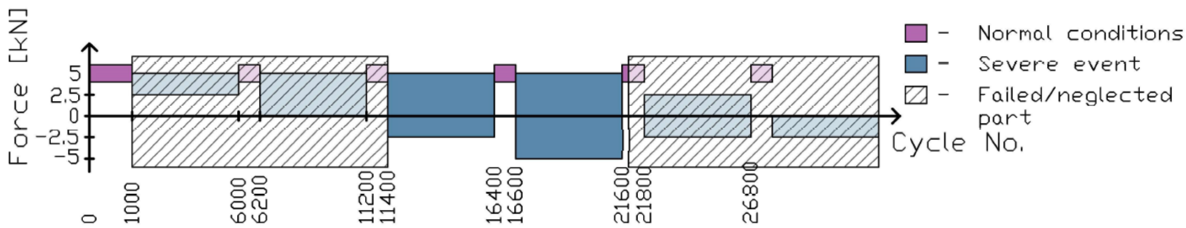

Figure D.98: Actual loading plan for Test subgroup C2

CPT

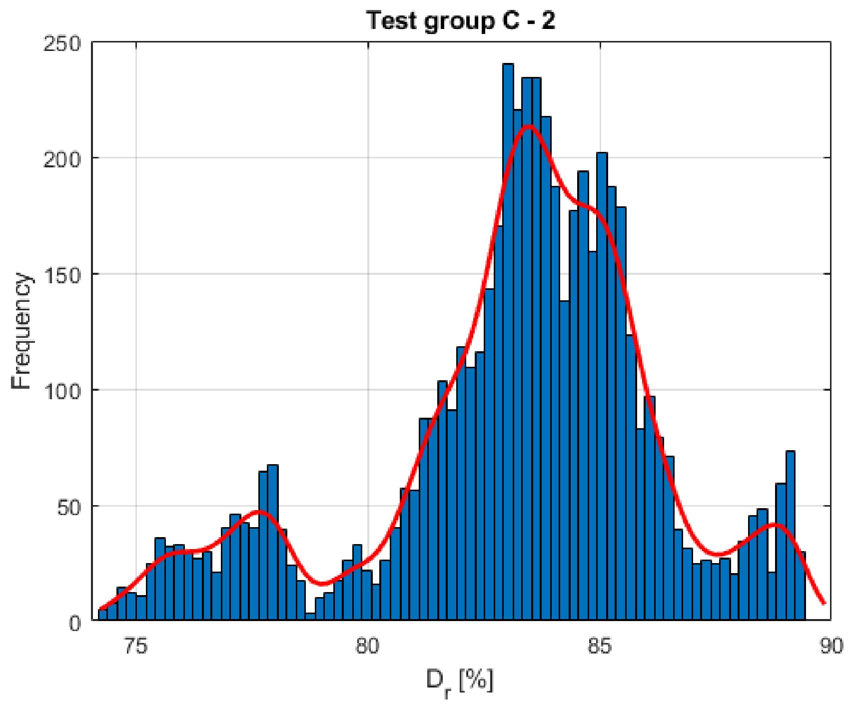

Figure D.99: Dr histogram with distribution fit for test subgroup C2

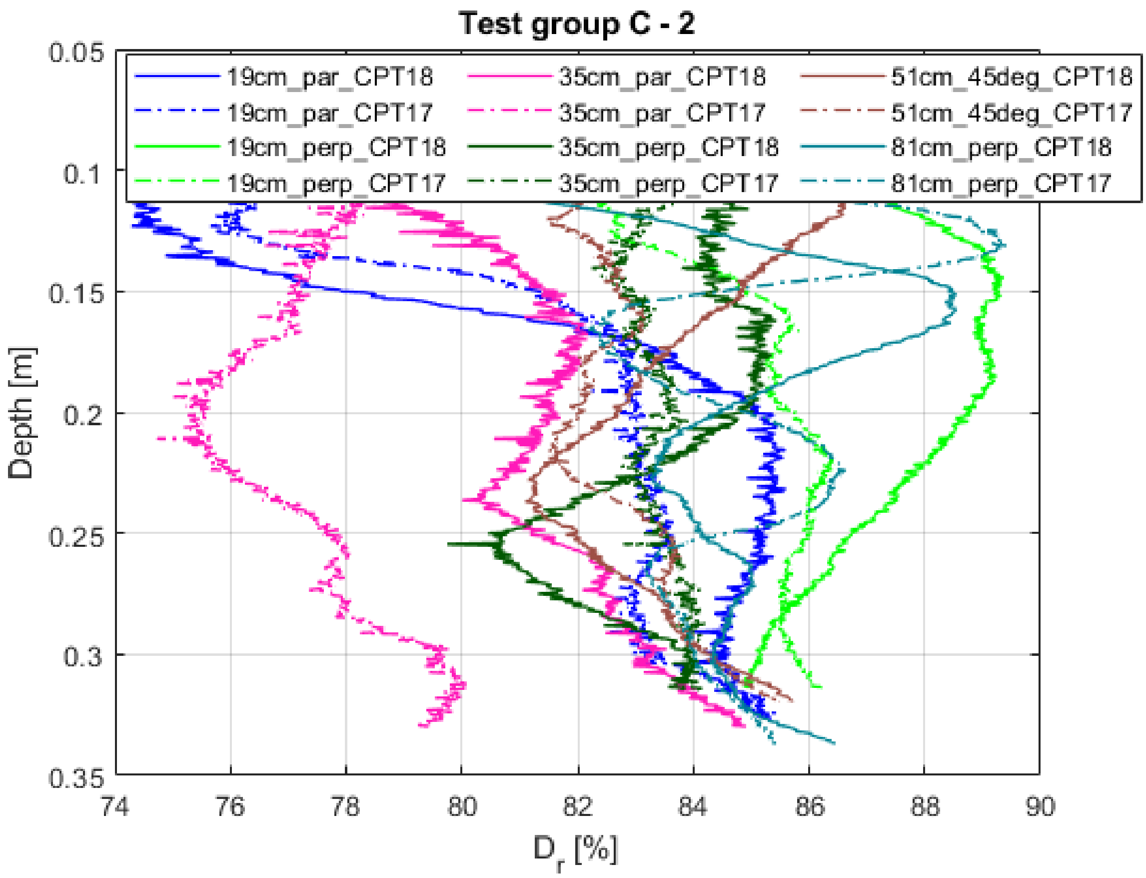

Figure D.100: Test-specific Dr results for CPT test subgroup C2

Force and displacement

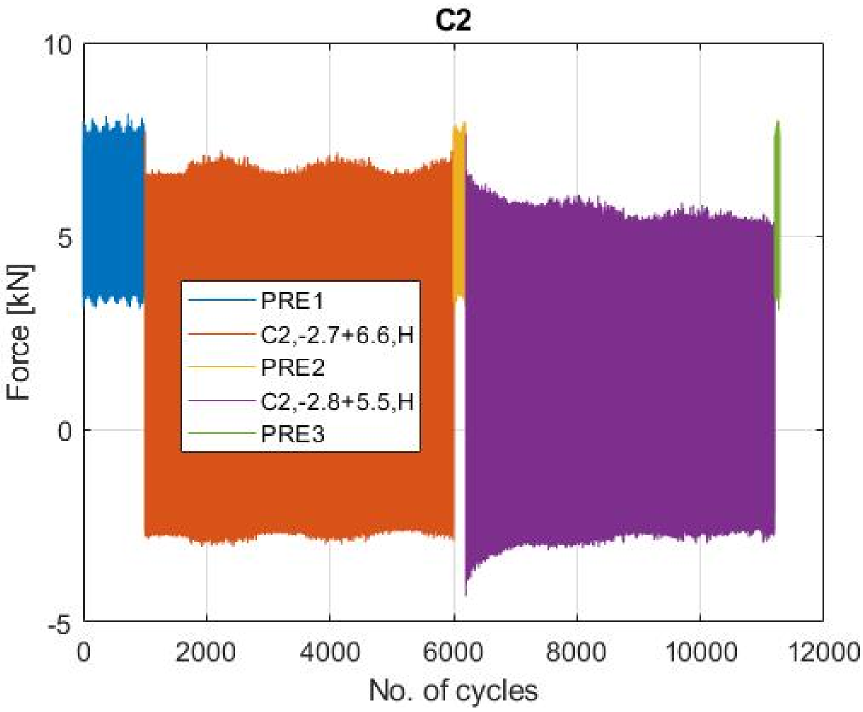

Figure D.101: Force VS No. of cycles

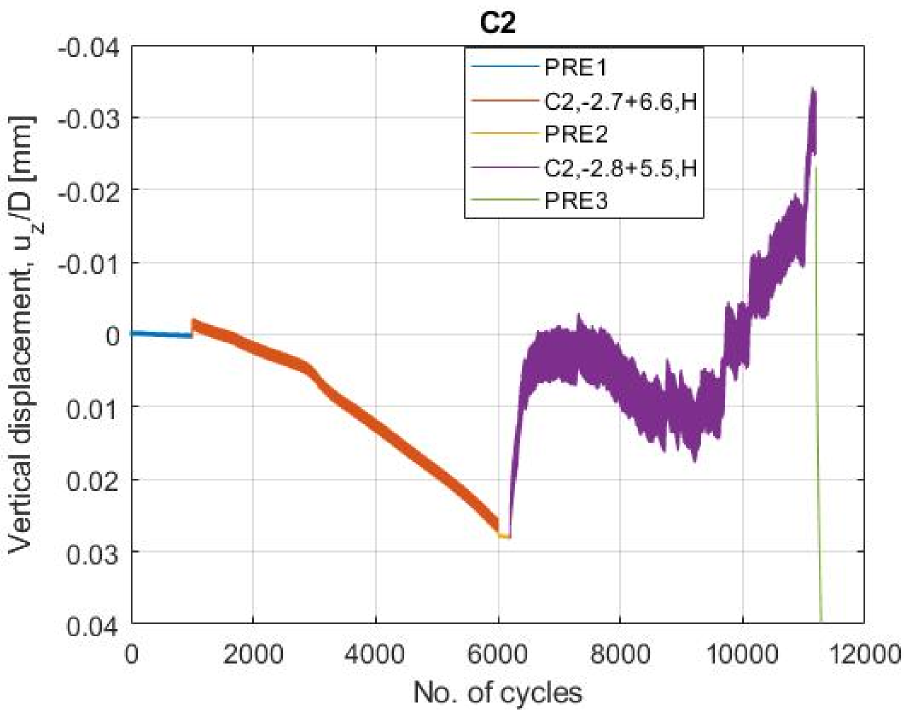

Figure D.102: Displacement VS No. of cycles

Lid Transducers

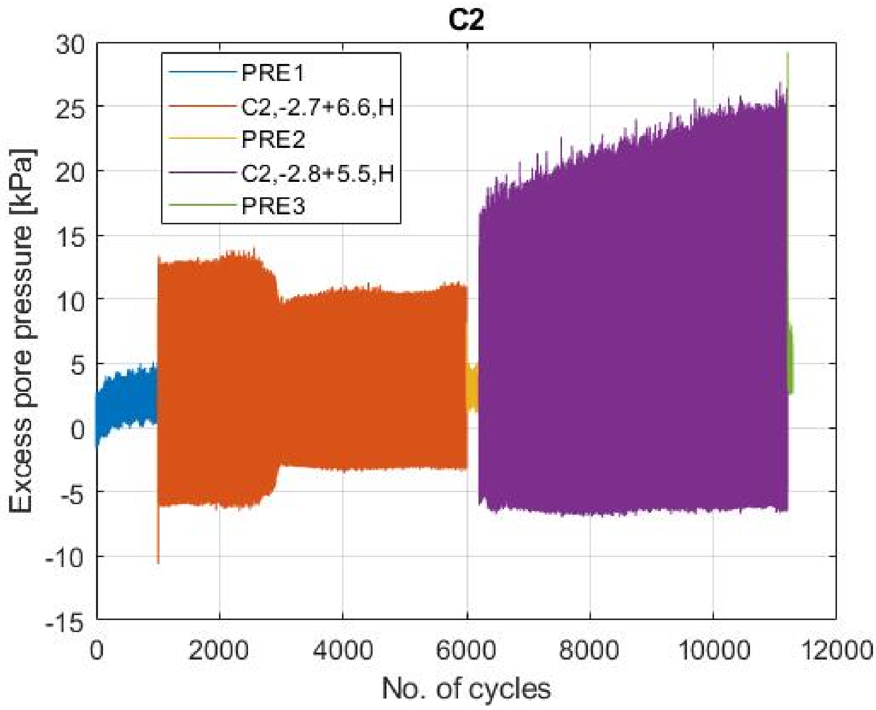

Figure D.103: Pore pressure at lid transducer P6

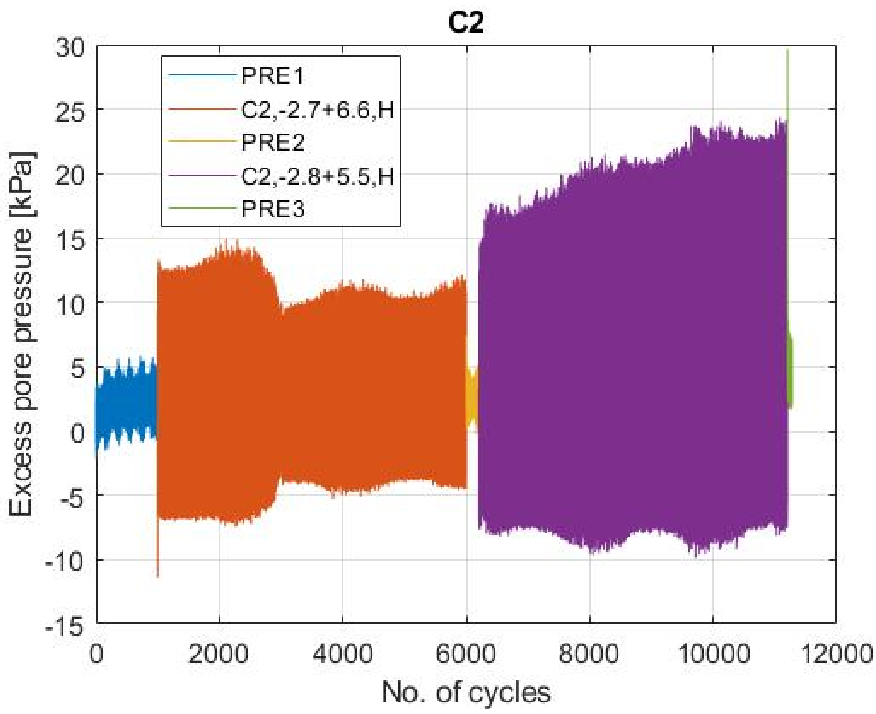

Figure D.104: Pore pressure at lid transducer P10

1st Level Transducers

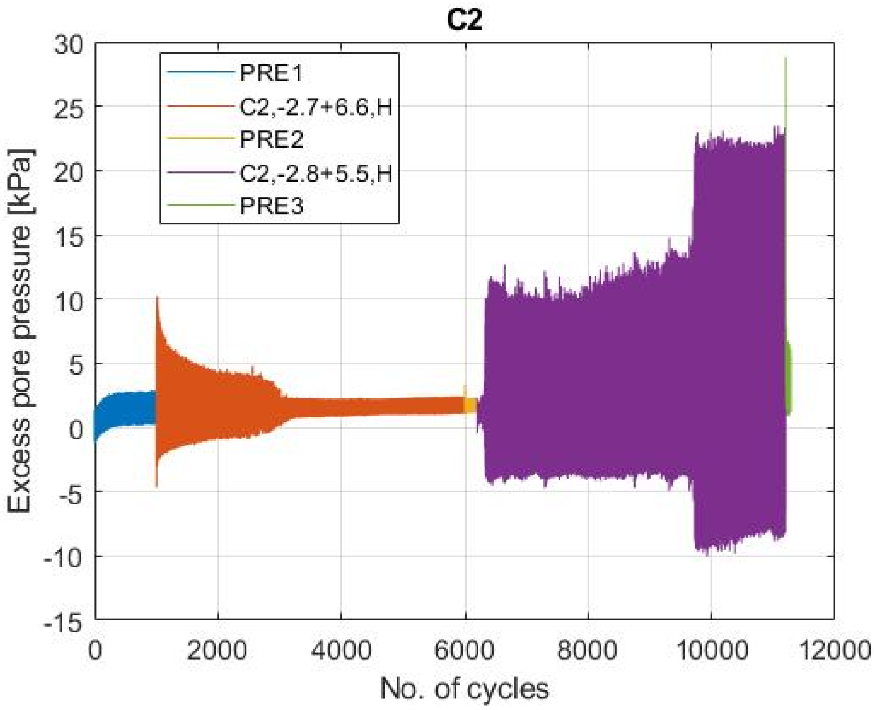

Figure D.105: Pore pressure at 1st level inner side transducer P4

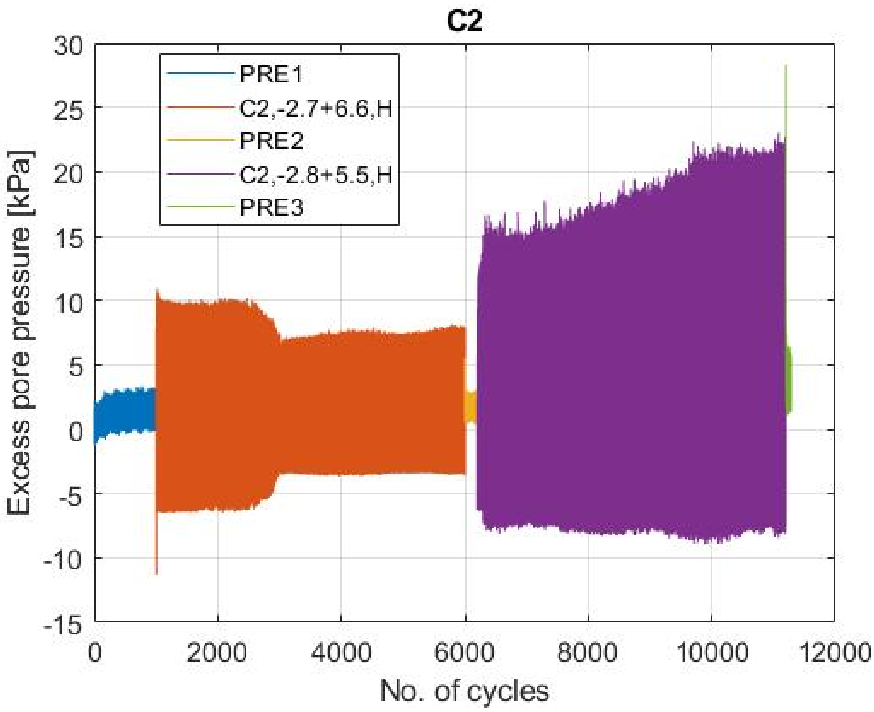

Figure D.106: Pore pressure at 1st level inner side transducer P11

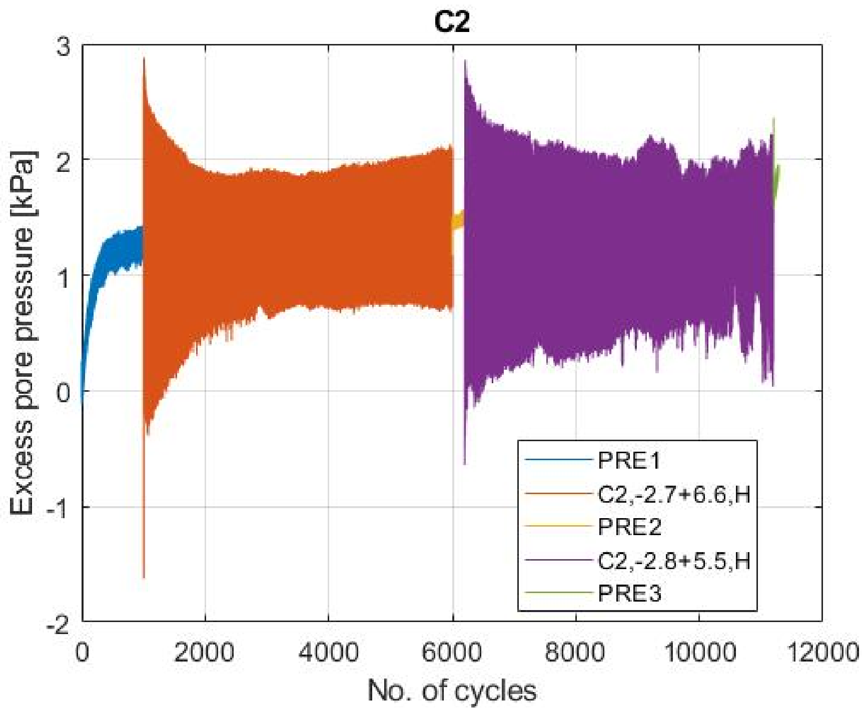

Figure D.107: Pore pressure at 1st level outer side transducer P3

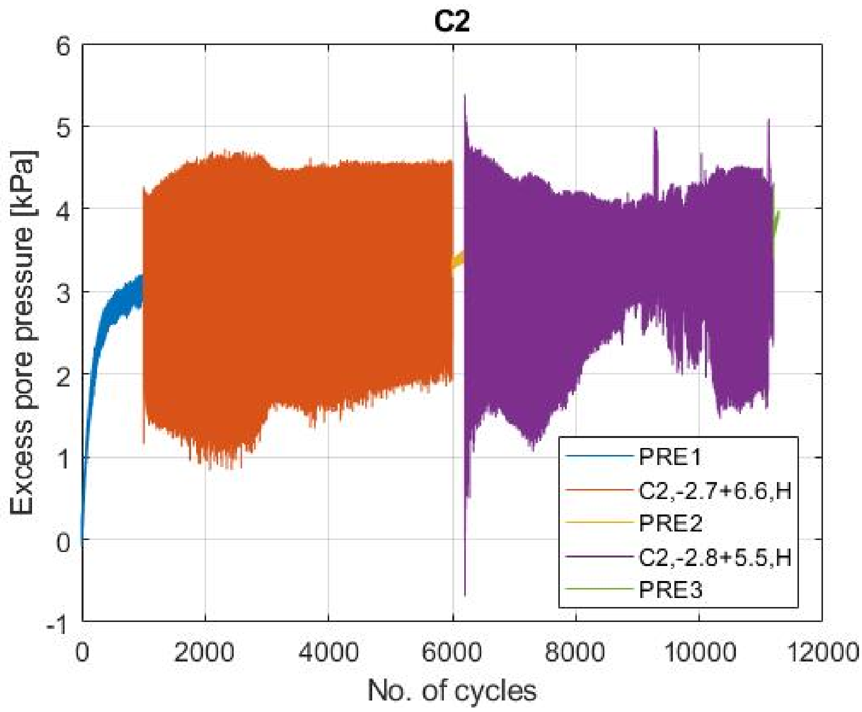

Figure D.108: Pore pressure at 1st level outer side transducer P7

2nd Level Transducers

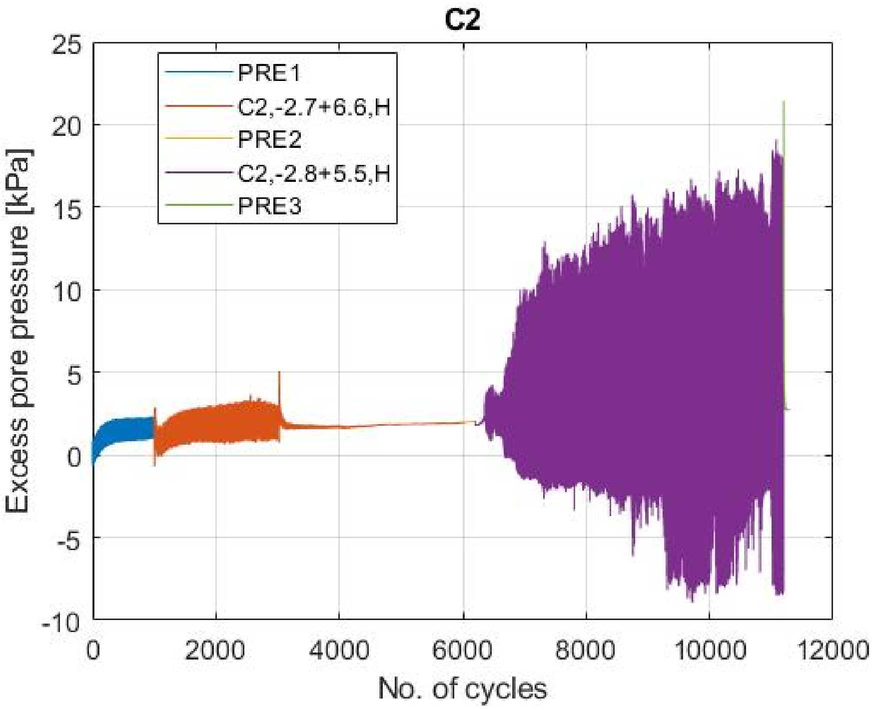

Figure D.109: Pore pressure at 2nd level inner side transducer P5

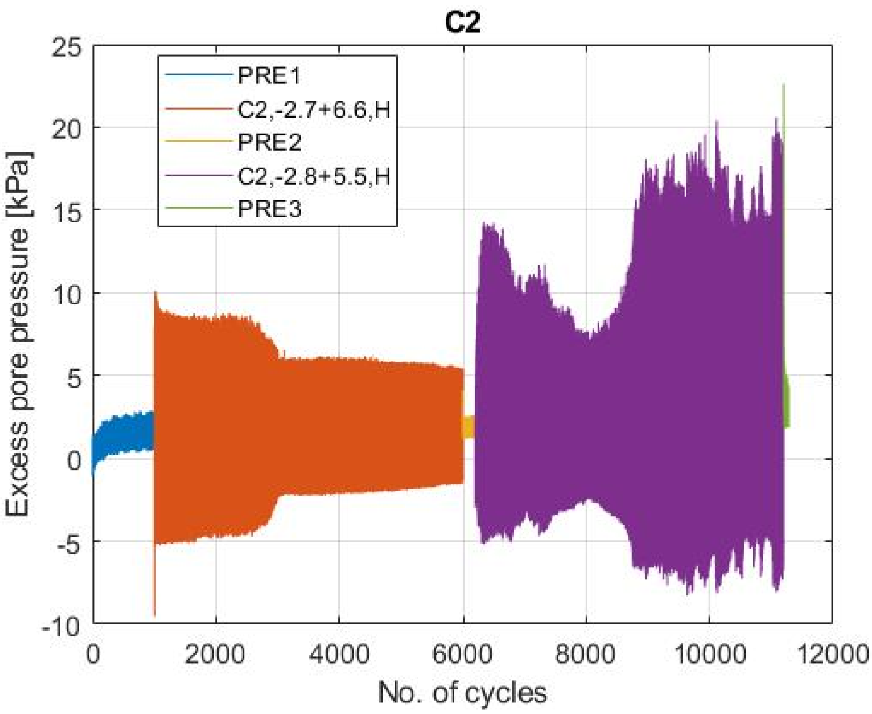

Figure D.110: Pore pressure at 2nd level inner side transducer P12

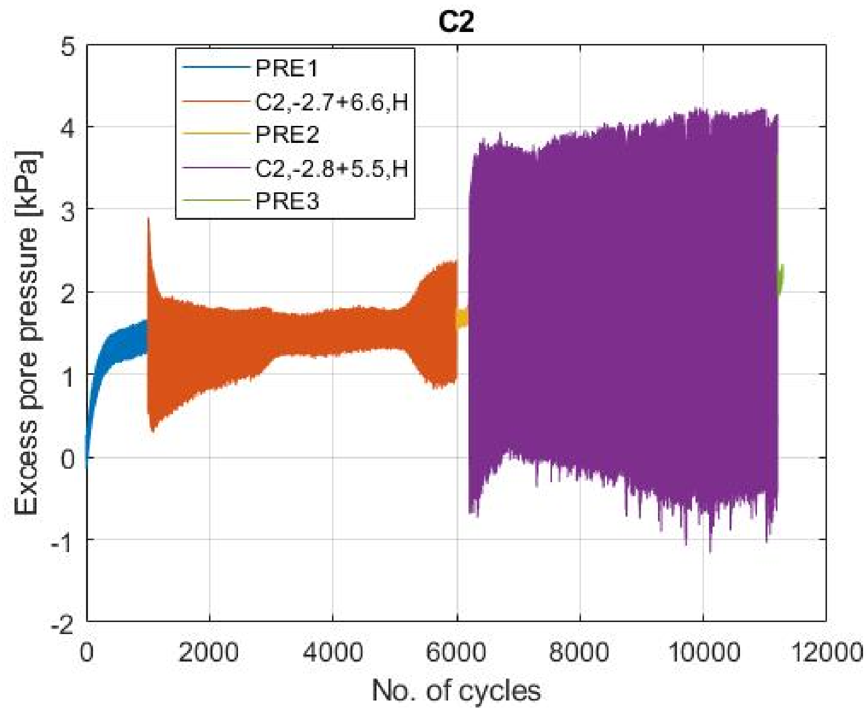

Figure D.111: Pore pressure at 2nd level outer side transducer P9

Skirt Tip Transducers

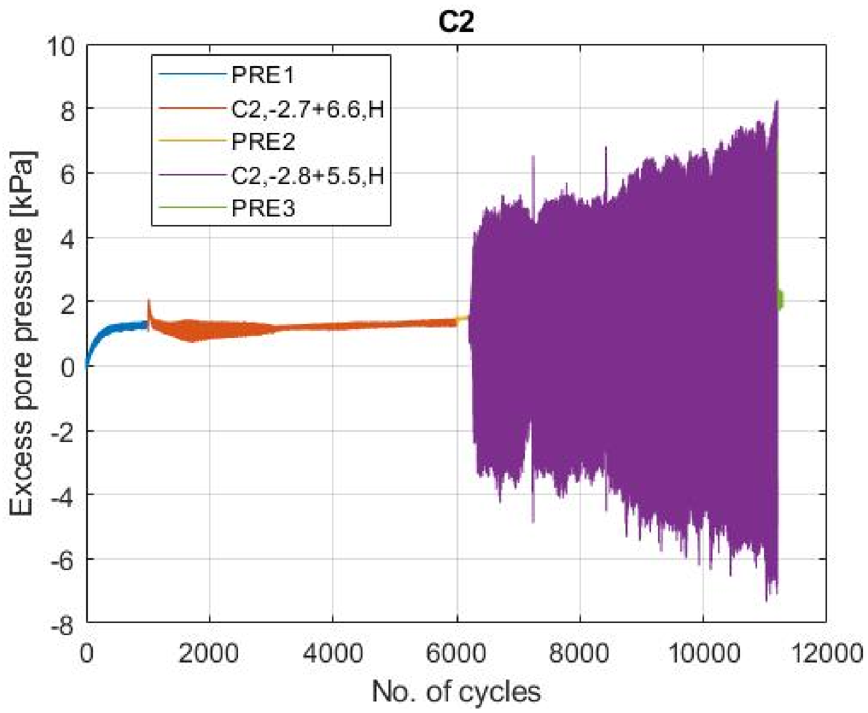

Figure D.112: Pore pressure at tip transducer P2

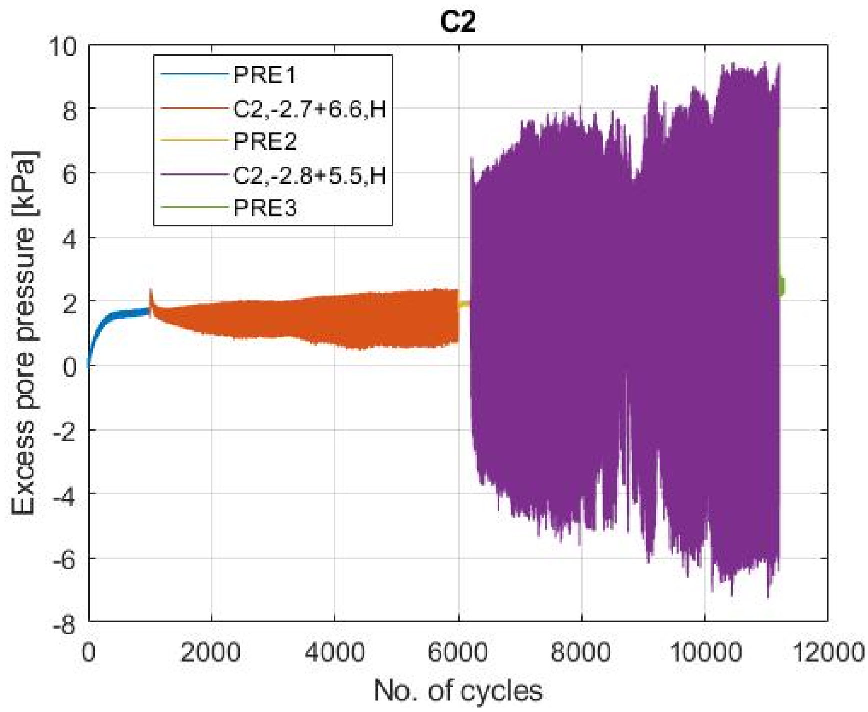

Figure D.113: Pore pressure at tip transducer P8

Force vs displacement

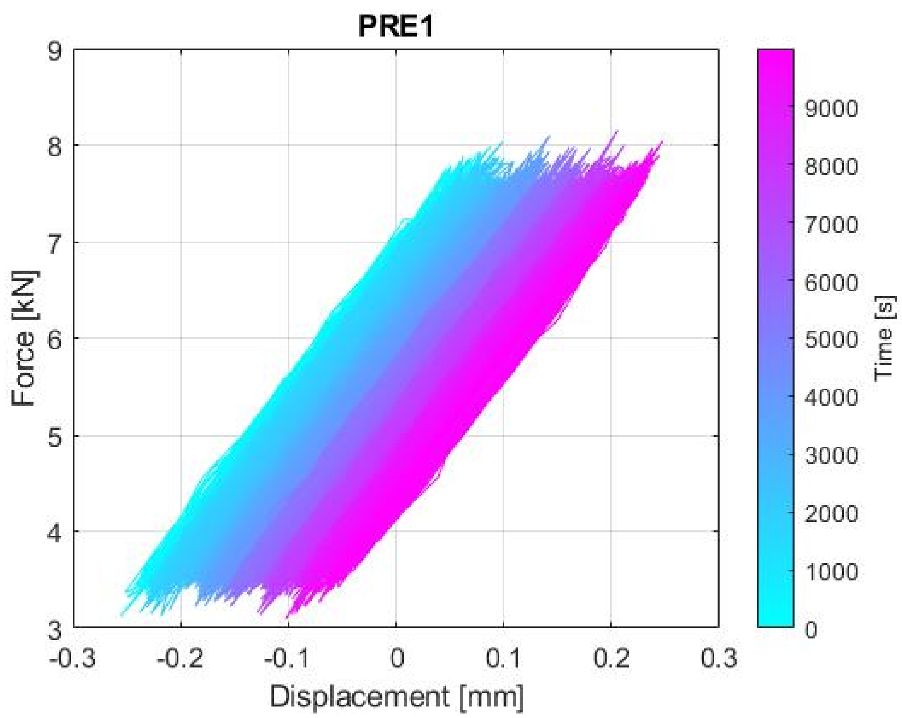

Figure D.114: Force VS absolute displacement

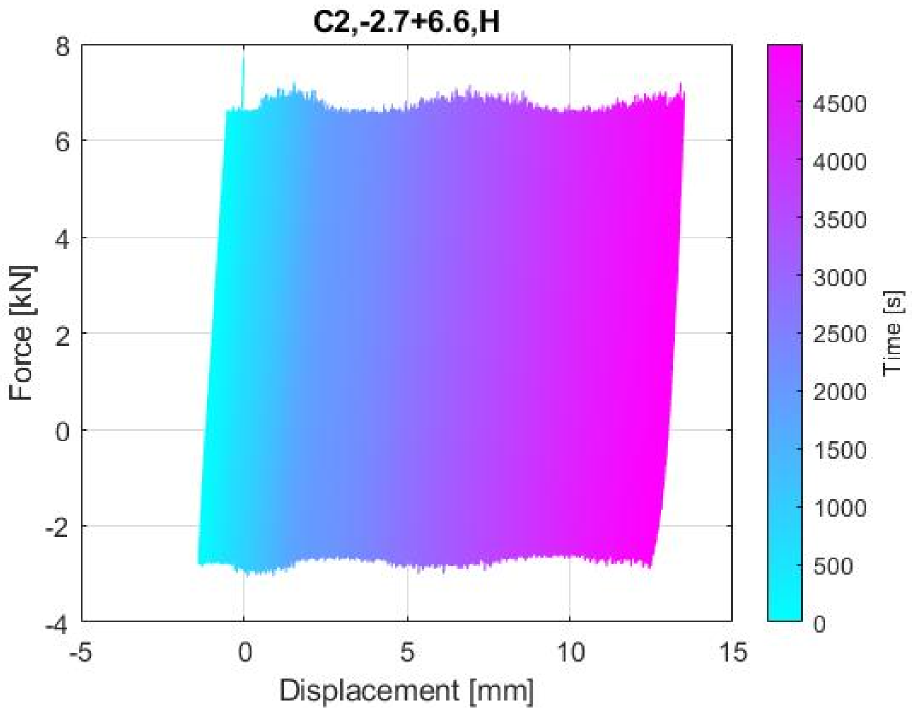

Figure D.115: Force VS absolute displacement

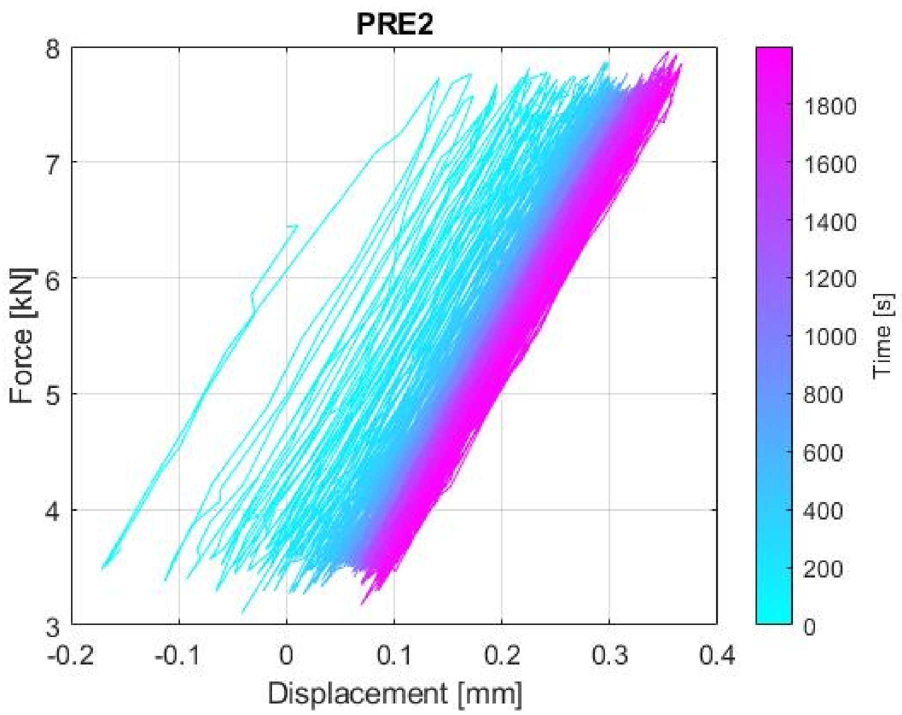

Figure D.116: Force VS absolute displacement

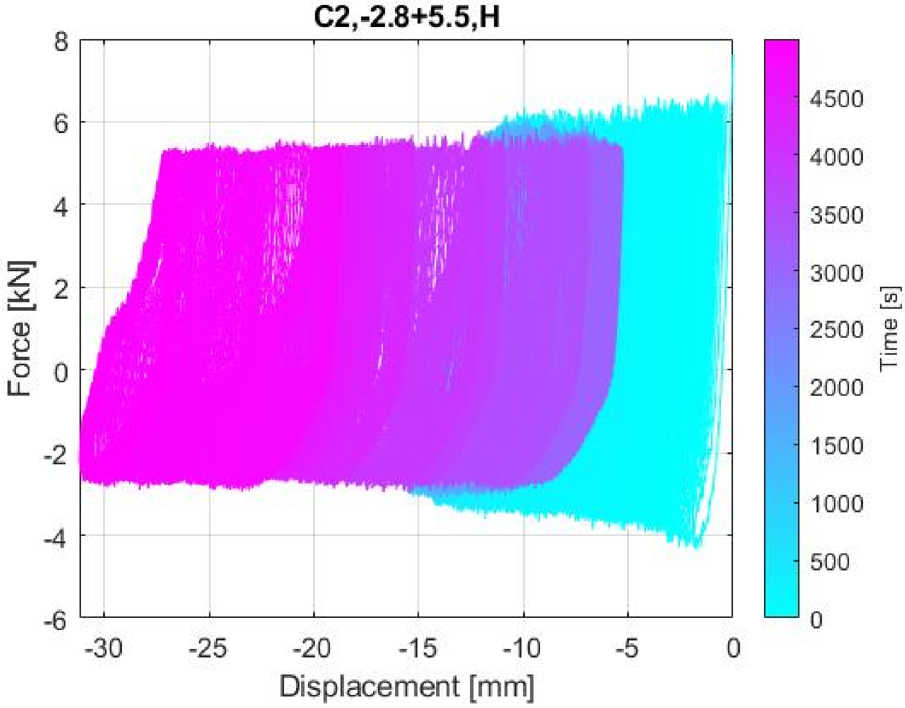

Figure D.117: Force VS absolute displacement

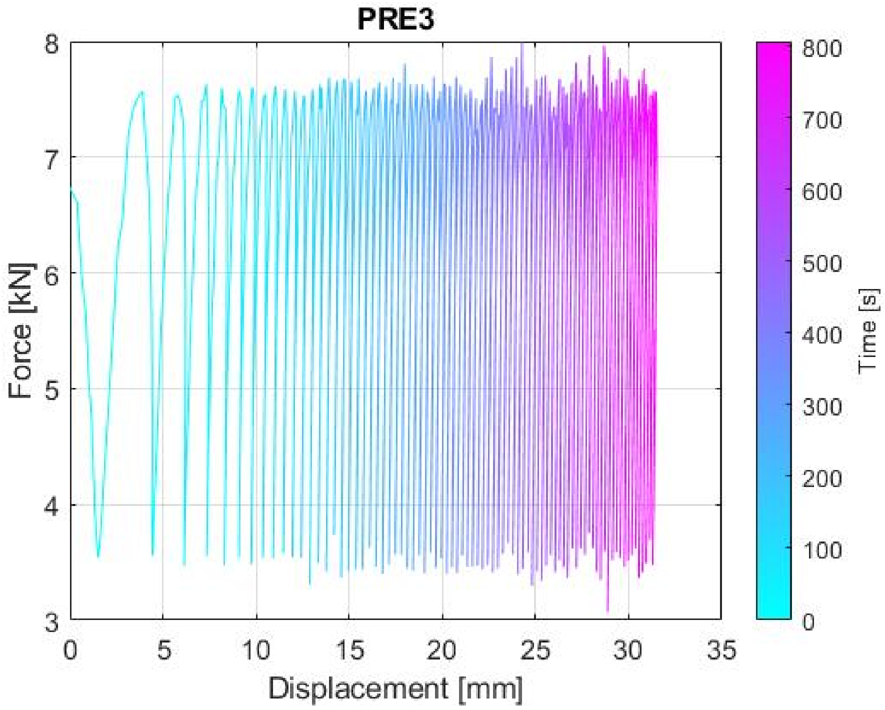

Figure D.118: Force VS absolute displacement

D.4.3 Test subgroup C3 - 1 Hz

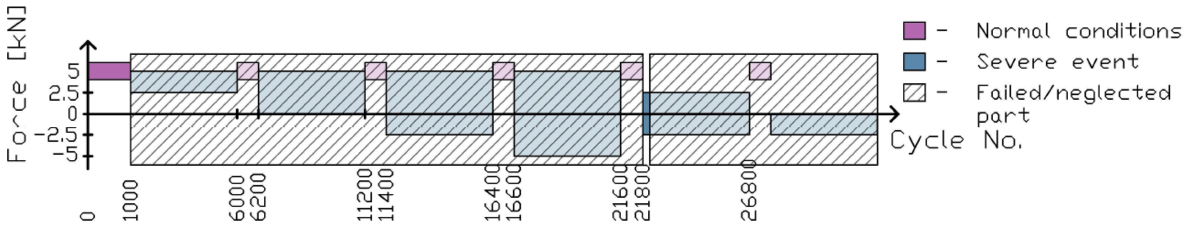

Figure D.119: Actual loading plan for Test subgroup C3

CPT

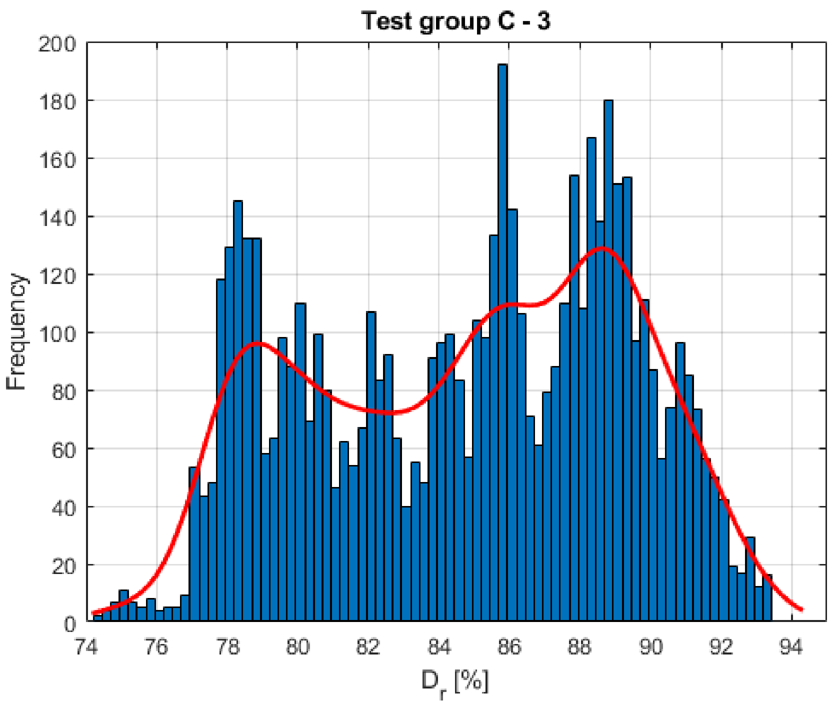

Figure D.120: Dr histogram with distribution fit for test subgroup C3

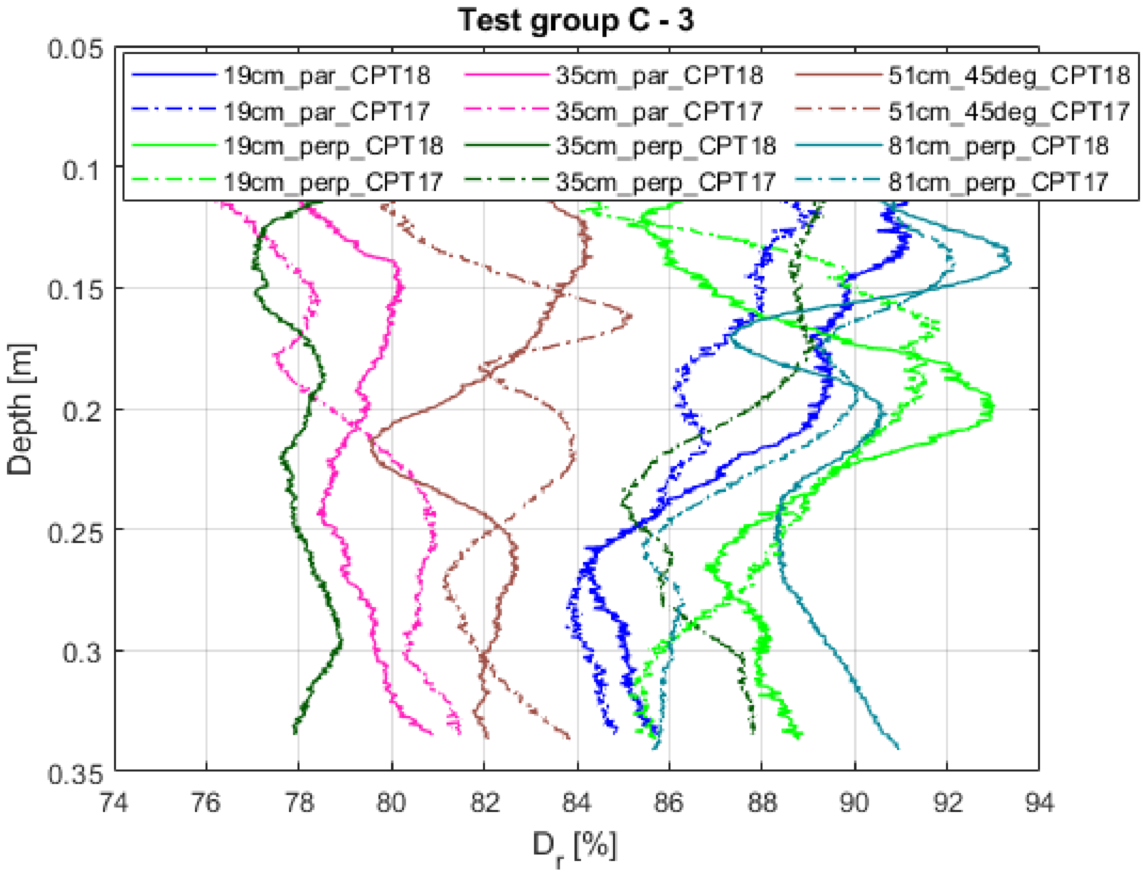

Figure D.121: Test-specific Dr results for CPT test subgroup C3

Force and displacement

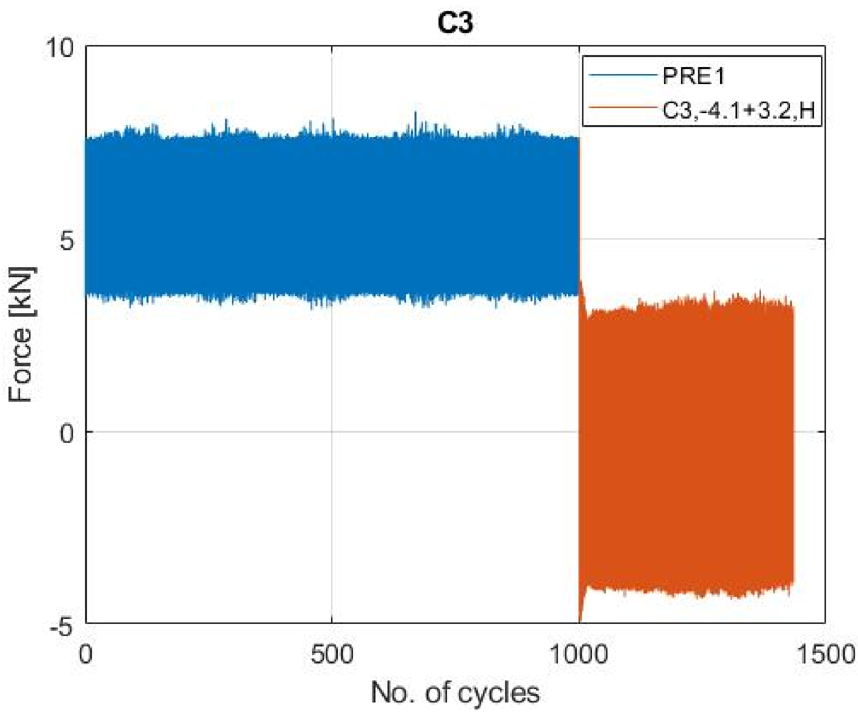

Figure D.122: Force VS No. of cycles

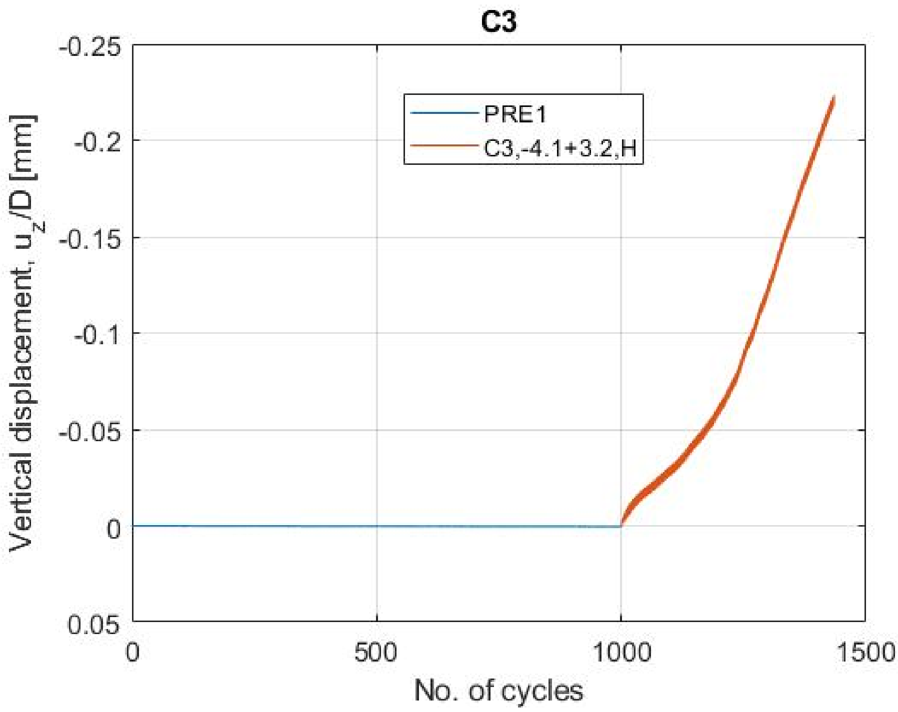

Figure D.123: Displacement VS No. of cycles

Lid Transducers

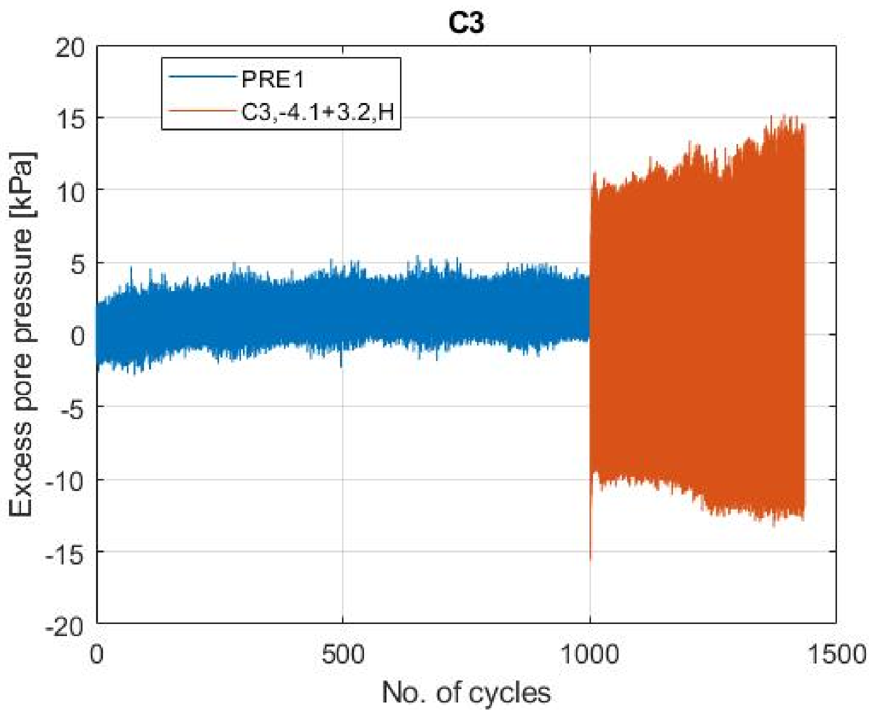

Figure D.124: Pore pressure at lid transducer P6

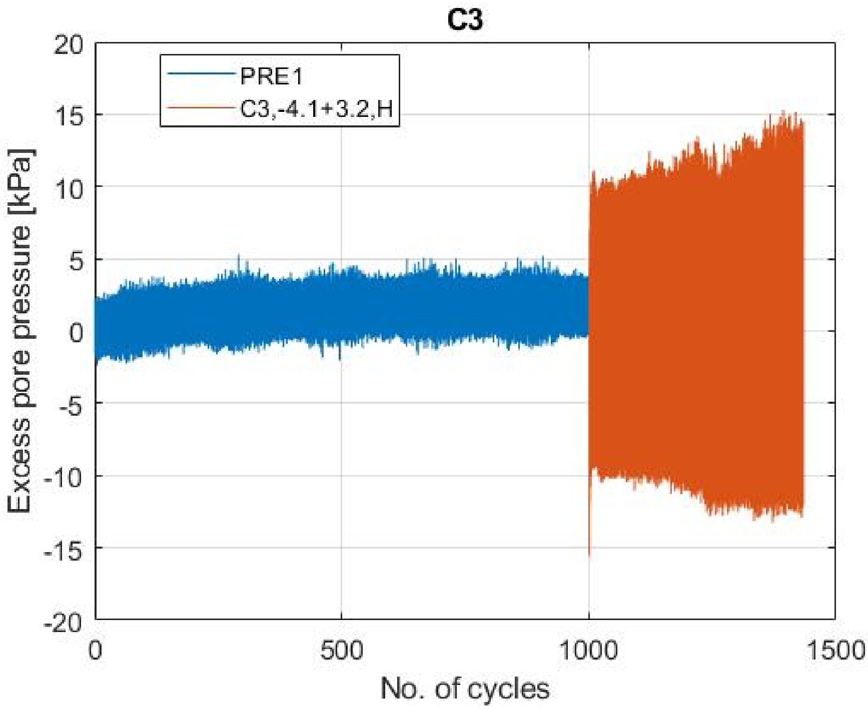

Figure D.125: Pore pressure at lid transducer P10

1st Level Transducers

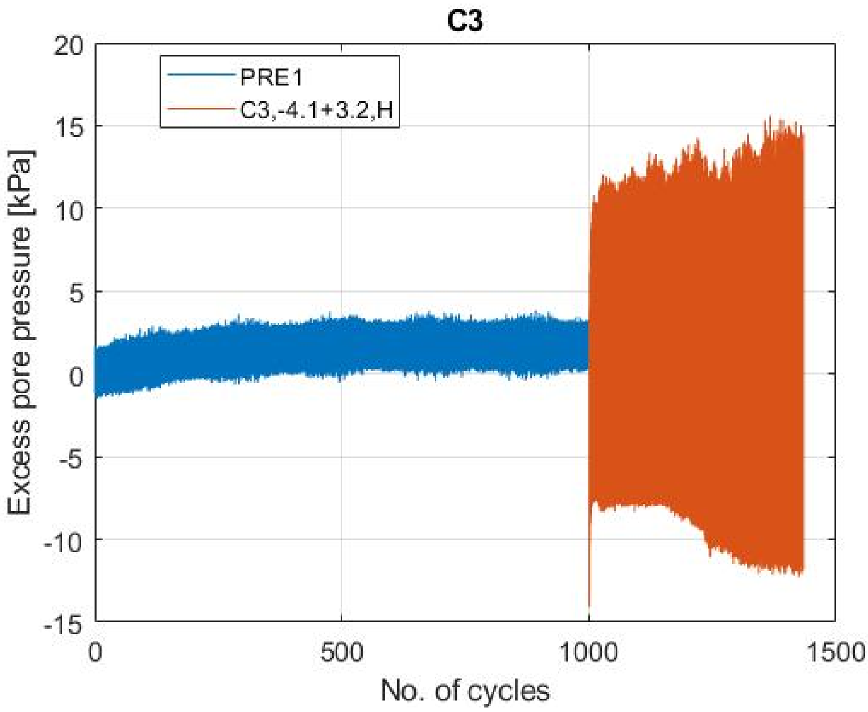

Figure D.126: Pore pressure at 1st level inner side transducer P4

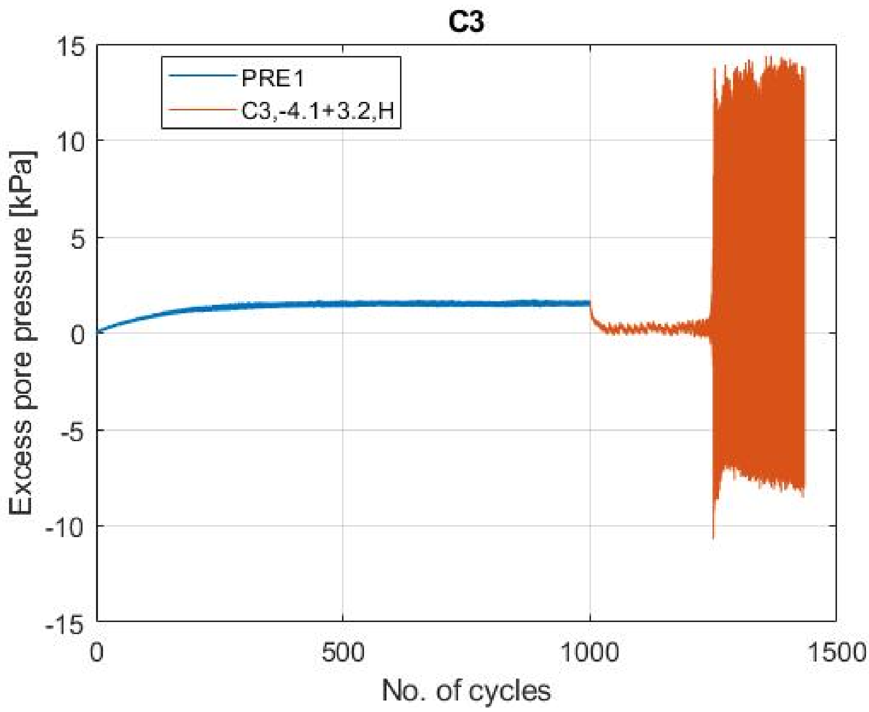

Figure D.127: Pore pressure at 1st level inner side transducer P11

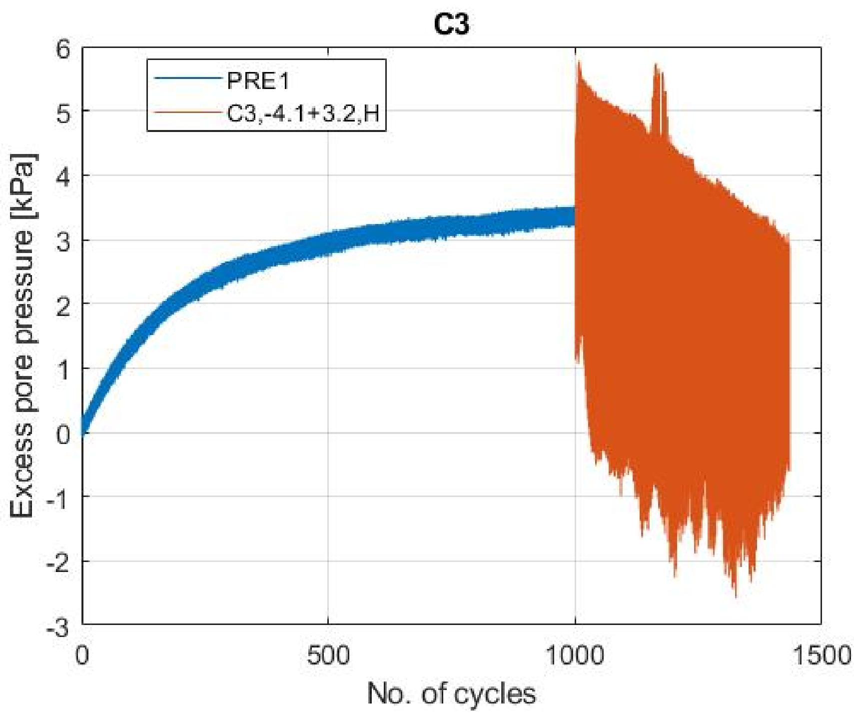

Figure D.128: Pore pressure at 1st level outer side transducer P7

2nd Level Transducers

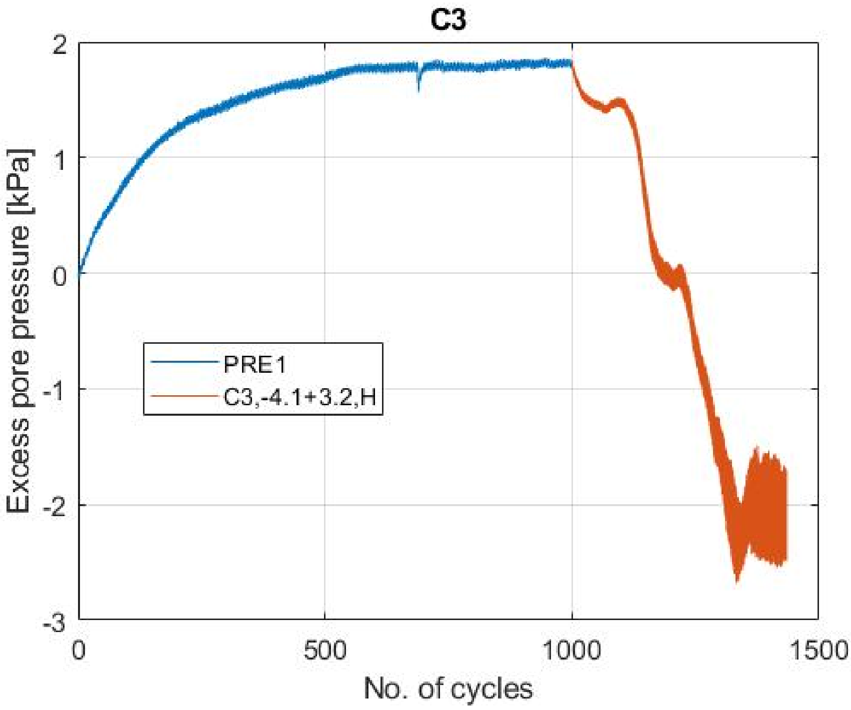

Figure D.129: Pore pressure at 2nd level inner side transducer P5

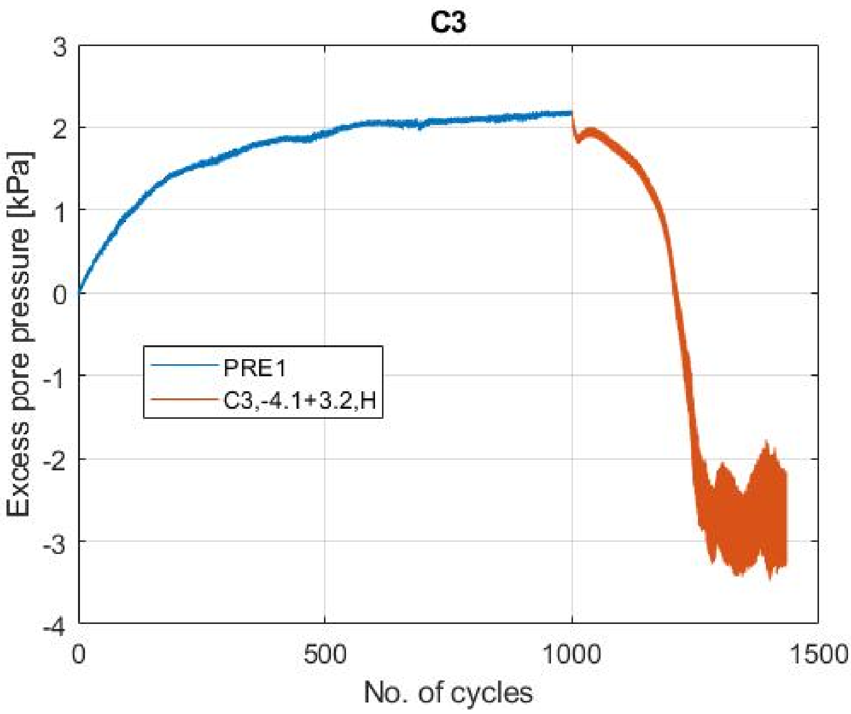

Figure D.130: Pore pressure at 2nd level inner side transducer P12

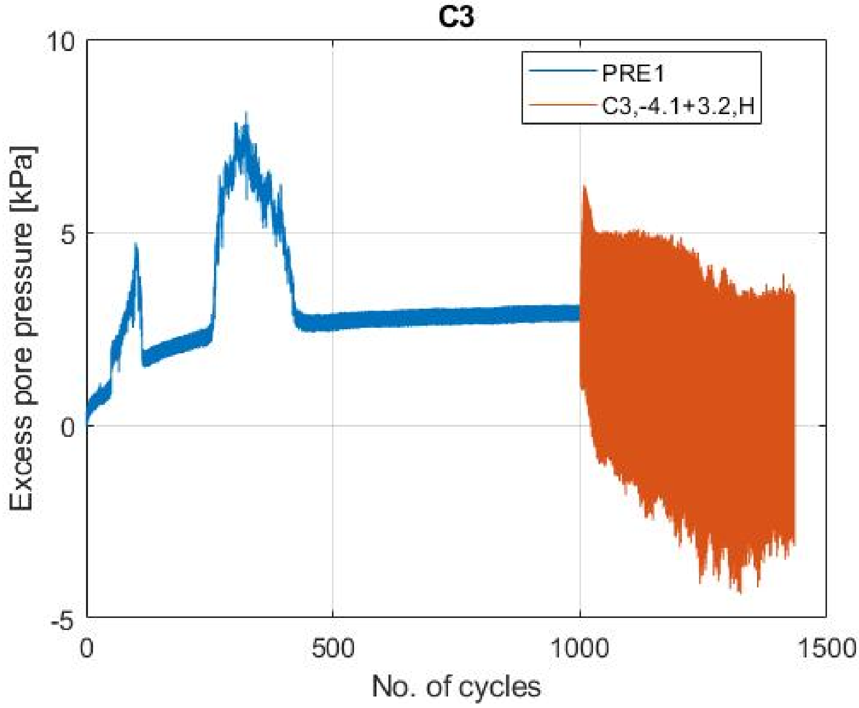

Figure D.131: Pore pressure at 2nd level outer side transducer P9

Skirt Tip Transducers

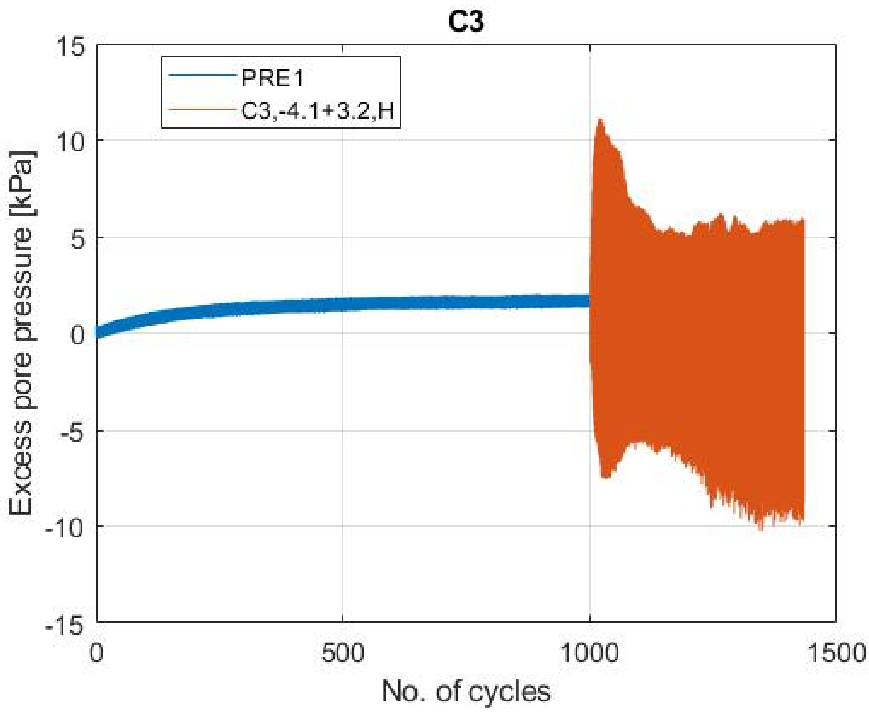

Figure D.132: Pore pressure at tip transducer P2

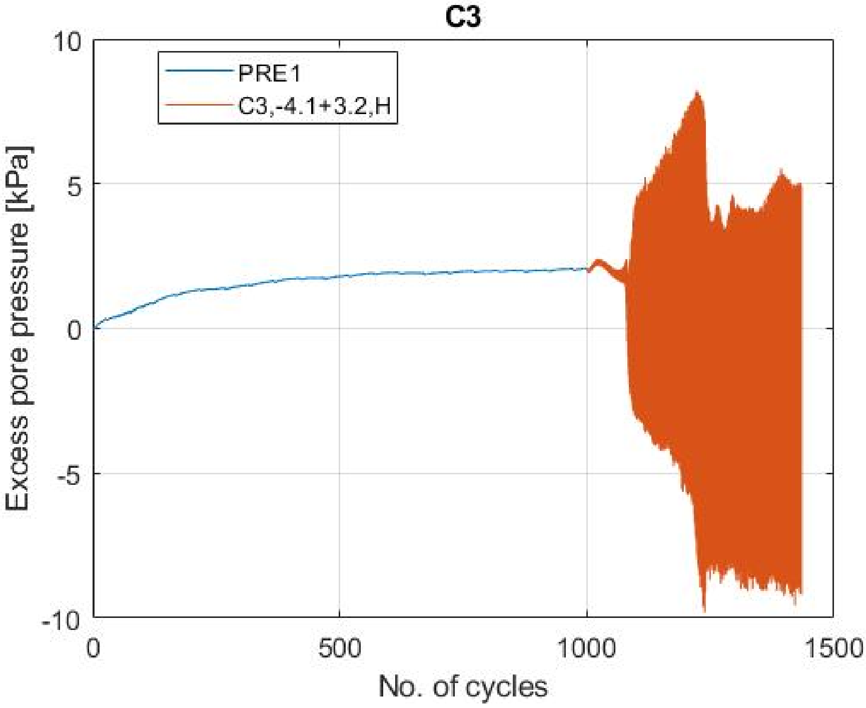

Figure D.133: Pore pressure at tip transducer P8

Soil pore pressure at 50 cm depth

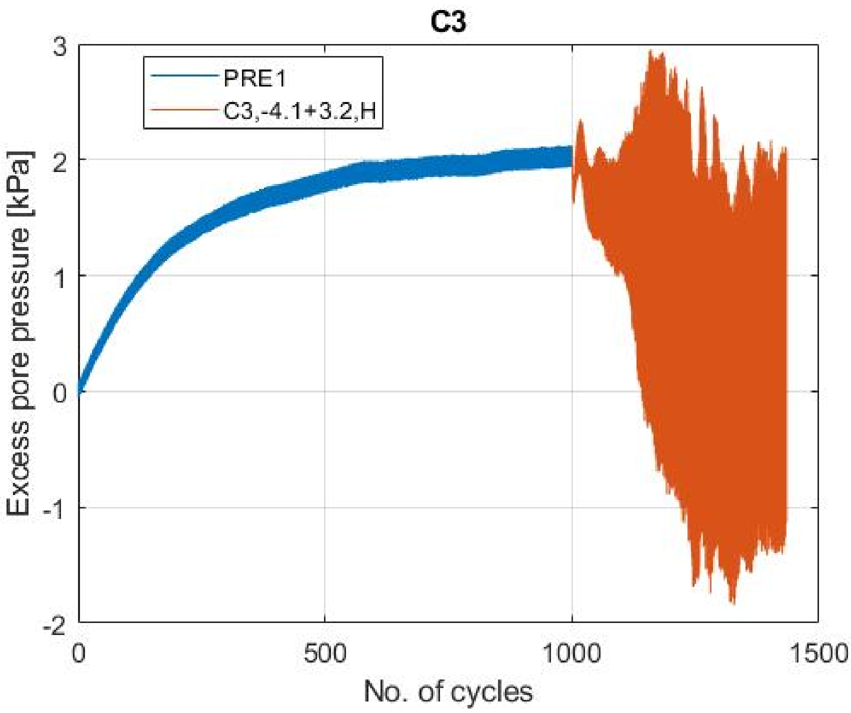

Figure D.134: Pore pressure transducer P13

Force vs displacement

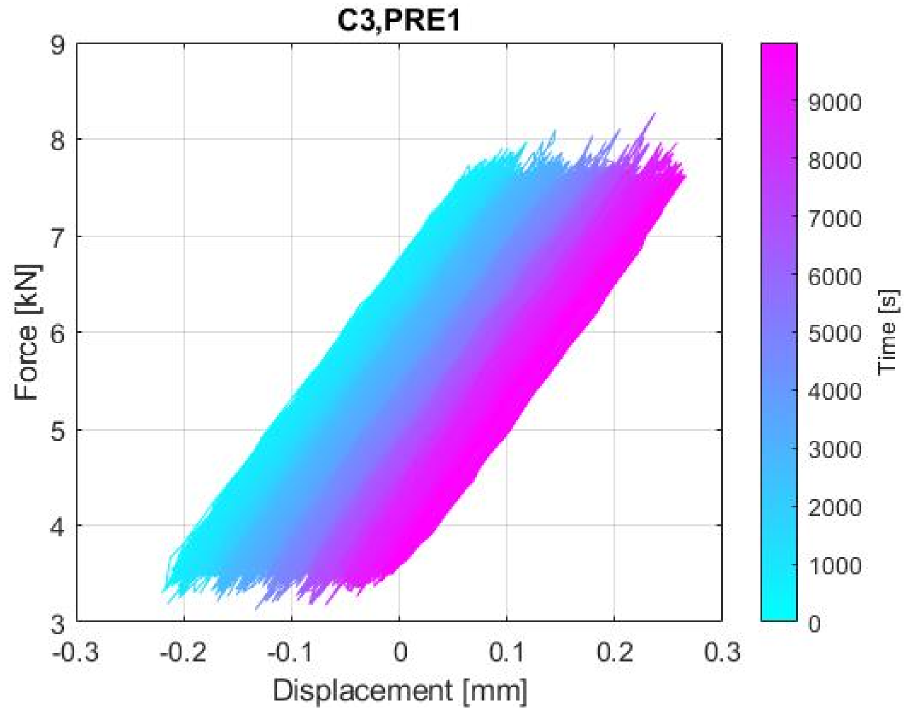

Figure D.135: Force VS absolute displacement

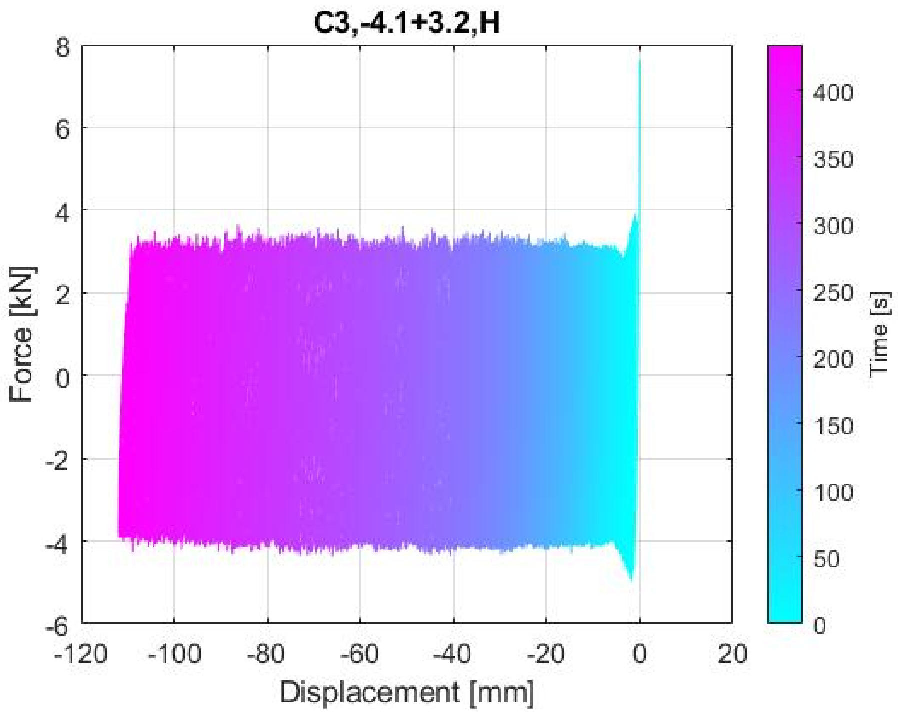

Figure D.136: Force VS absolute displacement

D.4.4 Test subgroup C4 - 1 Hz

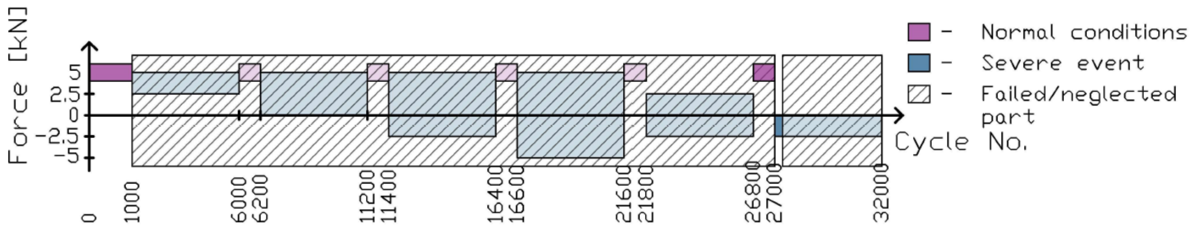

Figure D.137: Actual loading plan for Test subgroup C4

CPT

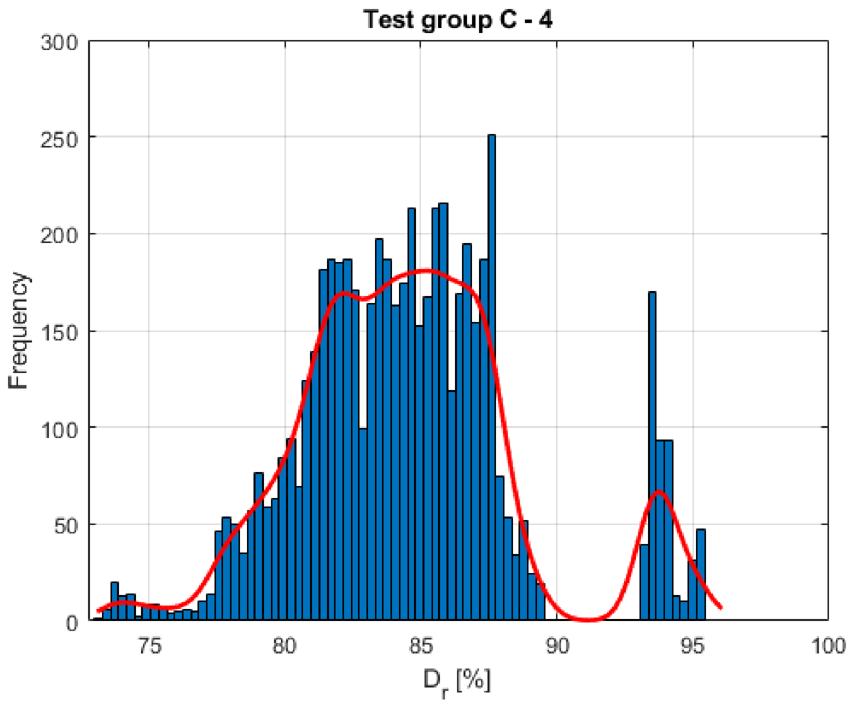

Figure D.138: Dr histogram with distribution fit for test subgroup C4

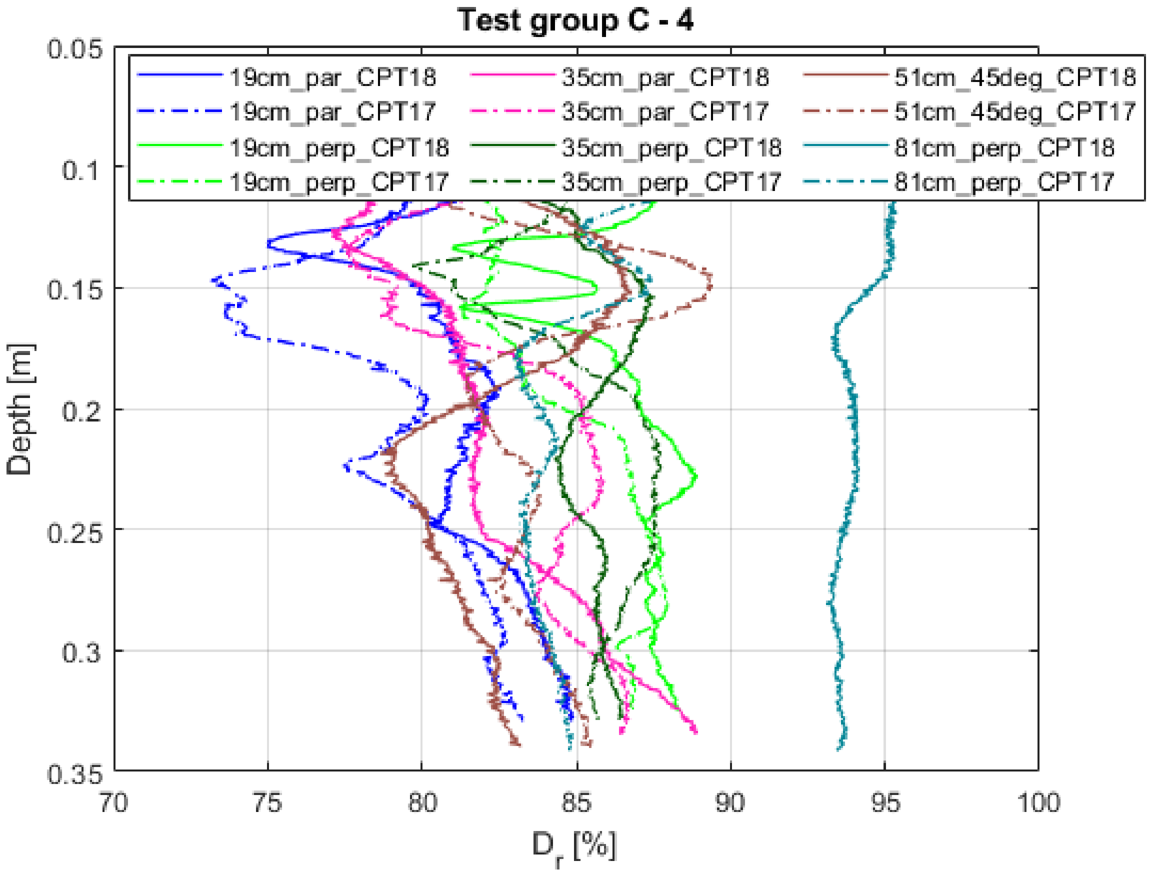

Figure D.139: Test-specific Dr results for CPT test subgroup C4

Force and displacement

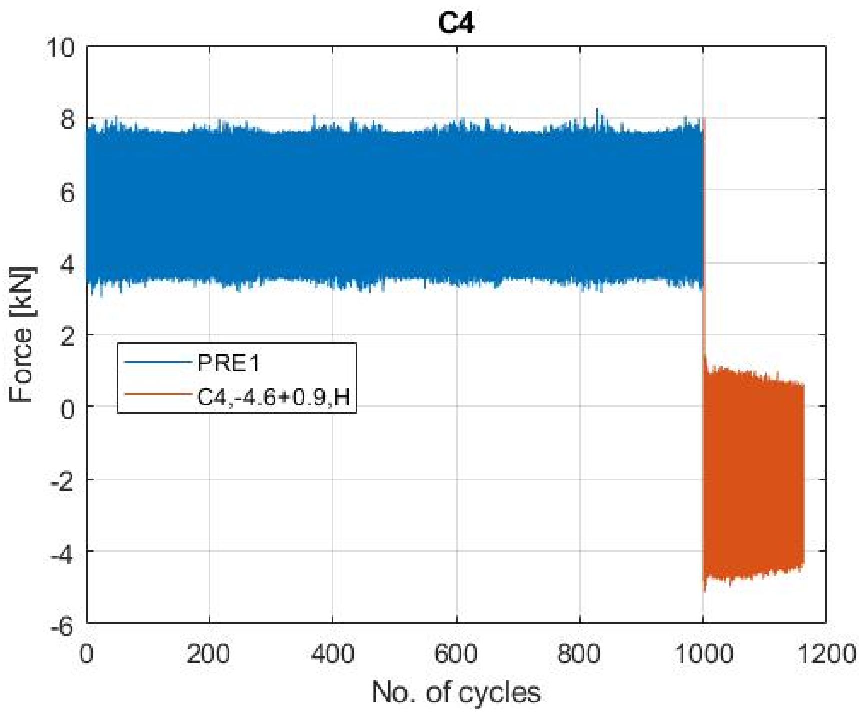

Figure D.140: Force VS No. of cycles

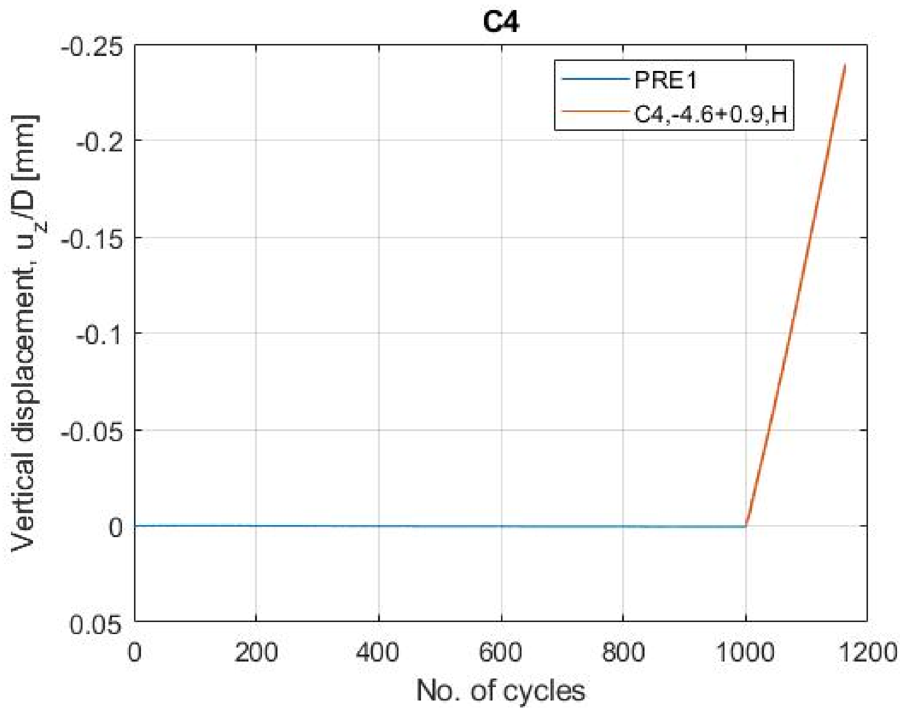

Figure D.141: Displacement VS No. of cycles

Lid Transducers

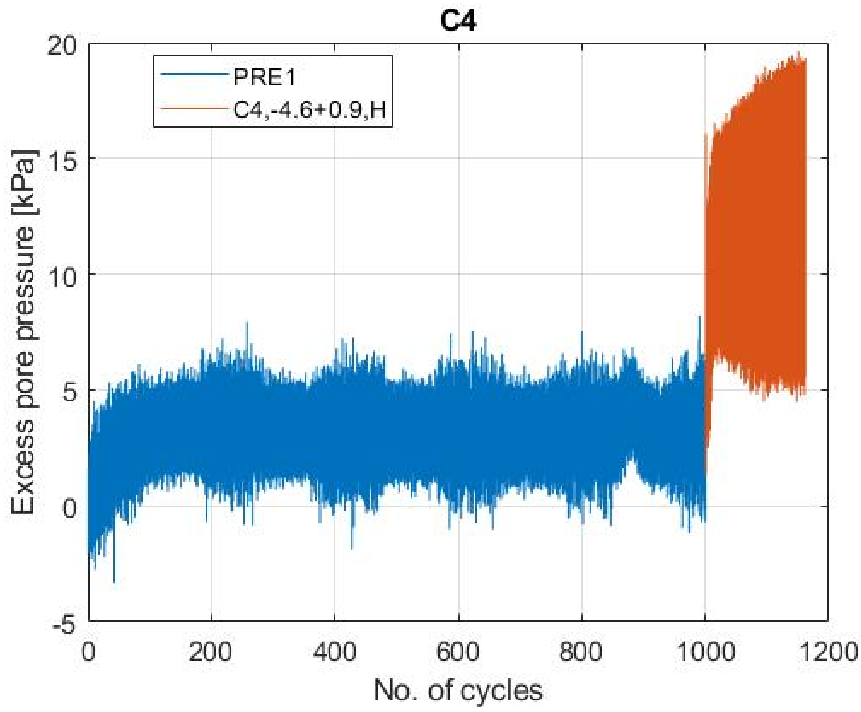

Figure D.142: Pore pressure at lid transducer P6

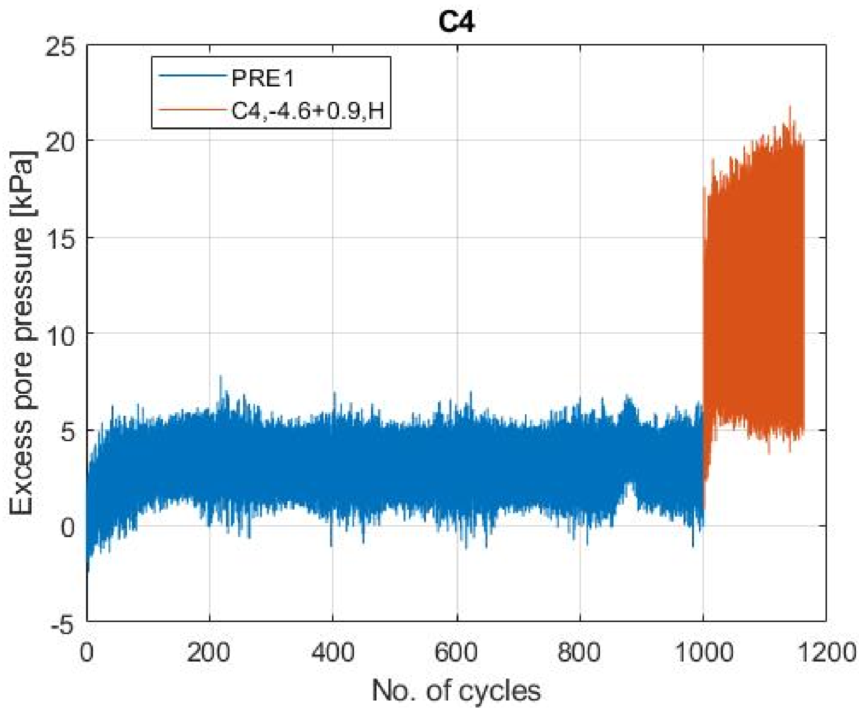

Figure D.143: Pore pressure at lid transducer P10

1st Level Transducers

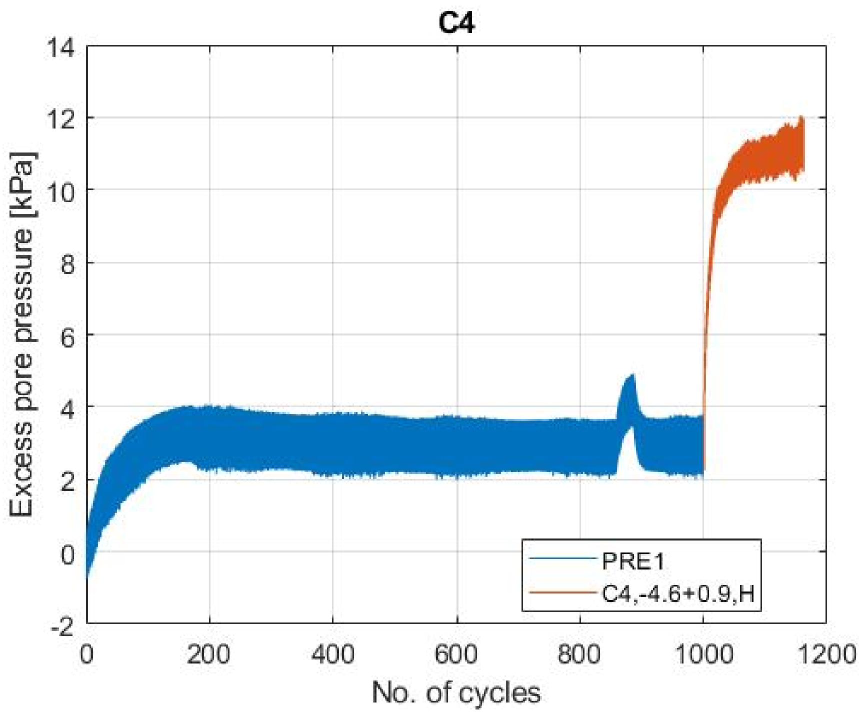

Figure D.144: Pore pressure at 1st level inner side transducer P4

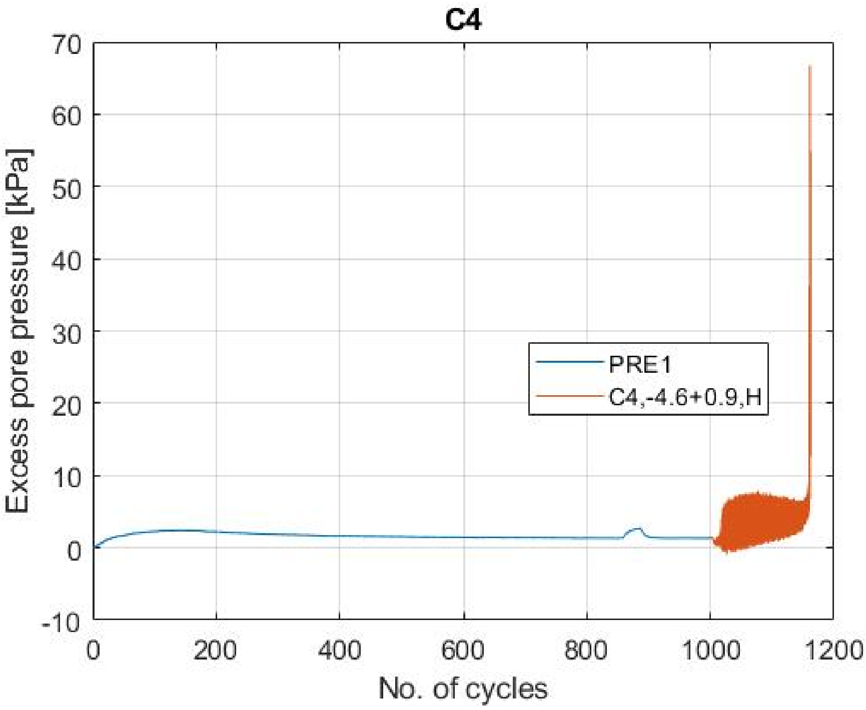

Figure D.145: Pore pressure at 1st level outer side transducer P7

2nd Level Transducers

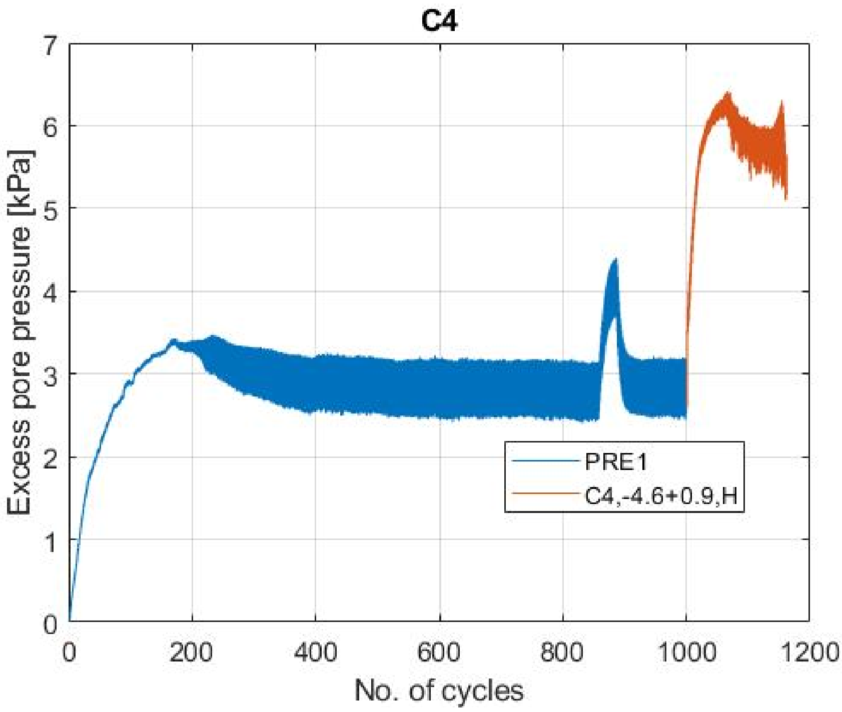

Figure D.146: Pore pressure at 2nd level inner side transducer P5

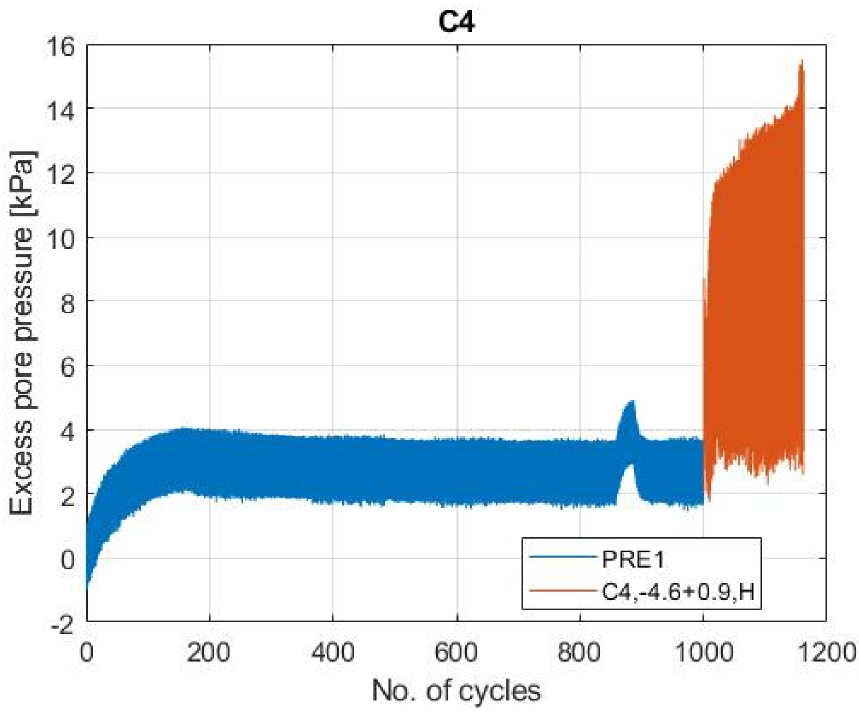

Figure D.147: Pore pressure at 2nd level inner side transducer P12

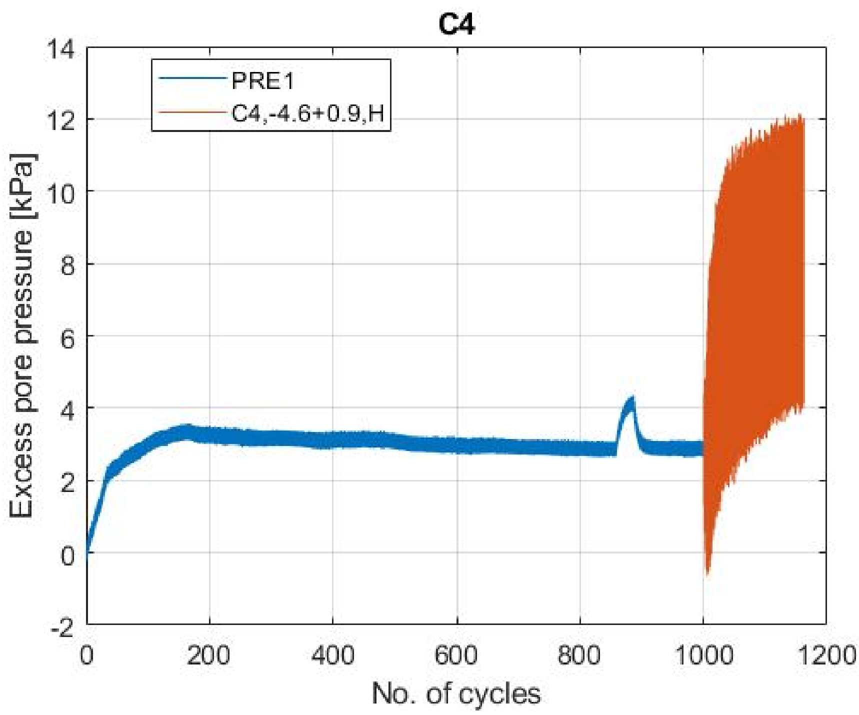

Figure D.148: Pore pressure at 2nd level outer side transducer P9

Skirt Tip Transducers

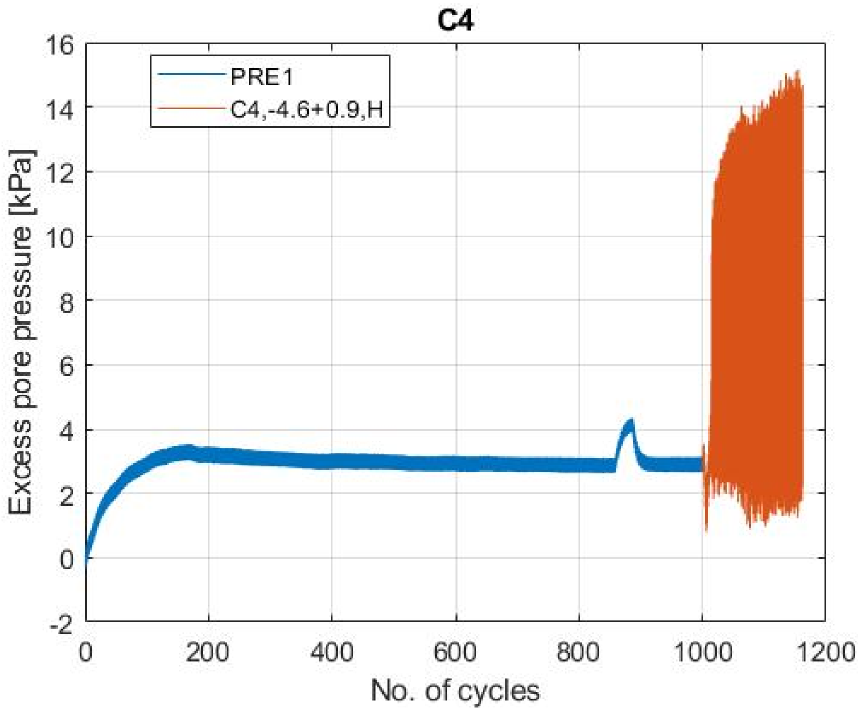

Figure D.149: Pore pressure at tip transducer P2

Force vs displacement

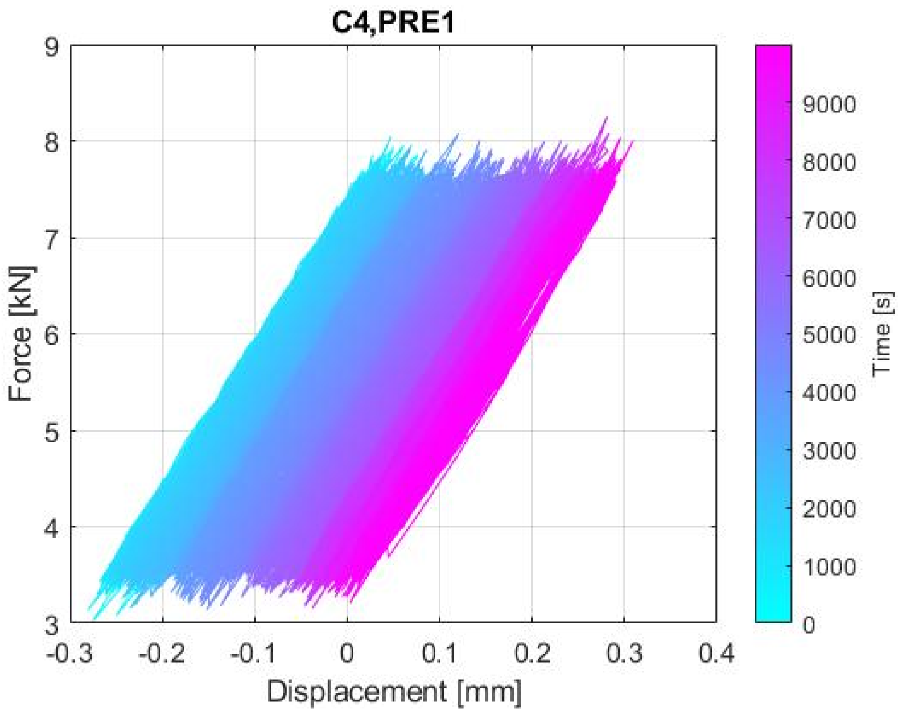

Figure D.150: Force VS absolute displacement

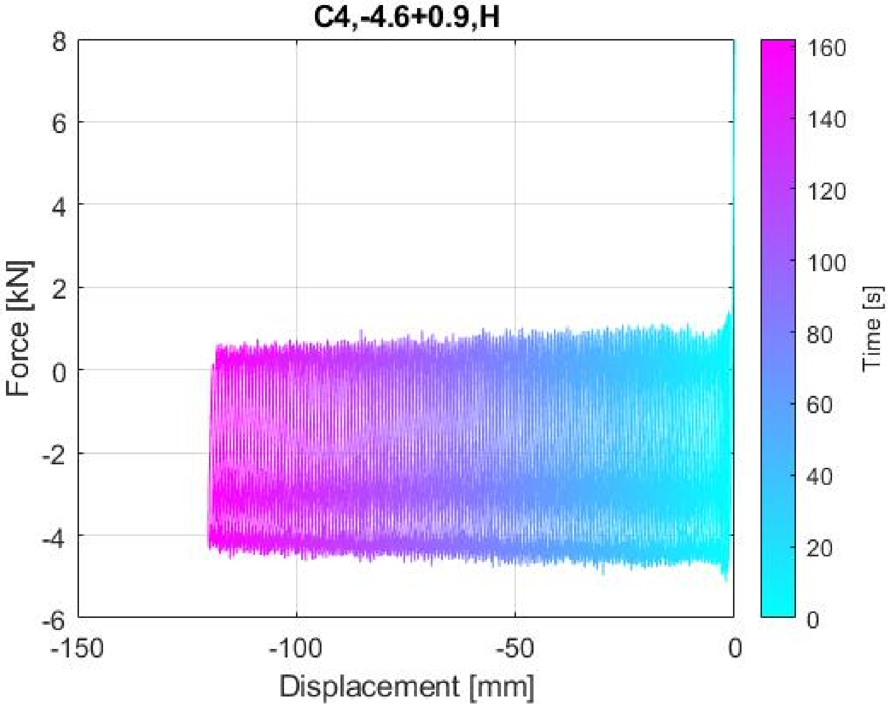

Figure D.151: Force VS absolute displacement

D.5 Test group D

There are two main ideas behind these tests:

1 - Similarly to the test described in section D.2 it was a big concern to investigate two way loading for the suction bucket replicated both normal conditions, when the bucket is mostly exposed to the compression forces, but also a severe conditions when the bucket would be exposed to the tensile forces.

2 - To investigate the influence of the frequency of the cyclic loading to the behaviour of the suction bucket.

Differently, than in previously mentioned test described in section D.2 compressive loads are no longer taken as a 5.0 % of compression bearing capacity of the sand. This time experience from the "i4Offshore" project by [European Union's Horizon, 2022] was used. In the preliminary stage of the project it was stated that the compressive bearing capacity of the suction bucket with the skirt length and diameter of $d = L = 6.0m$ was $F_{capacity} = 966MN$ while the characteristic environmental forces during normal conditions were $F_{characteristic} = 8.5MN$. Due to the fact that during this project scaled model was investigated so the different values with same ratio were used:

$$\frac{F_{characterisctic}}{F_{capacity}} = 0.0088$$

Compressive bearing capacity of suction bucket used in this project was calculated using 4.1 suggested by [Barari et al., 2016] as discussed in 4 and all the final values are presented in table D.6 and figure D.152 below.

Table D.6: Loading plan for 'Test group D'

Packet No.	Conditions	Force command F_{min} [kN]	F_{max} [kN]	Force ratio	Cycle No.	Frequency [Hz]
1	Normal	4.0	6.0	0.67	1000	0.1
2	Severe	2.5	5.0	0.50	500	0.1, 1.0
3	Normal	4.0	6.0	0.67	200	0.1
4	Severe	0.0	5.0	-	500	0.1, 1.0
5	Normal	4.0	6.0	0.67	200	0.1
6	Severe	-2.5	5.0	-0.50	500	0.1, 1.0
7	Normal	4.0	6.0	0.67	200	0.1
8	Severe	-5.0	5.0	-1.00	500	0.1, 1.0
9	Normal	4.0	6.0	0.67	200	0.1
10	Severe	-2.5	2.5	-1.00	500	0.1, 1.0

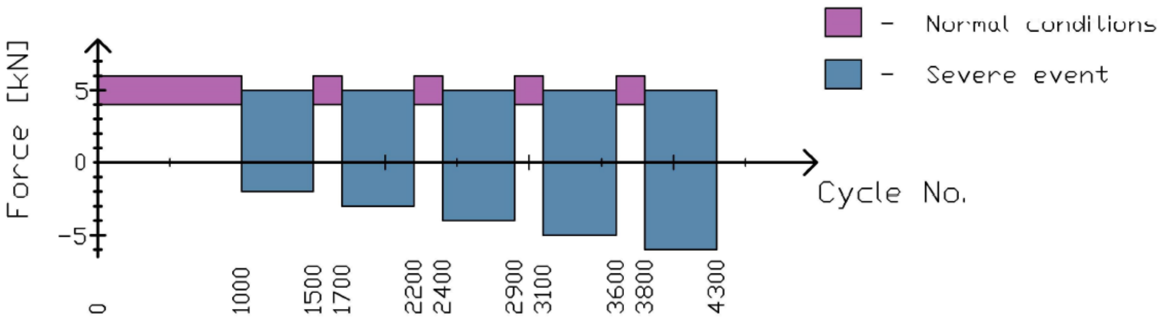

Figure D.152: Scheduled loading plan for 'Test group D'

D.5.1 **Test subgroup D1 -** 1.0 Hz

First part of the test for which:

- Loading frequency of 0.1 Hz for precycling parts (Normal conditions) with mean compressive forces of 5.0 kN and amplitude of 1 kN were used.

- Loading frequency of 1.0 Hz for extreme event parts (Severe conditions) with varying forces from 5.0 kN to −5.0 kN were used.

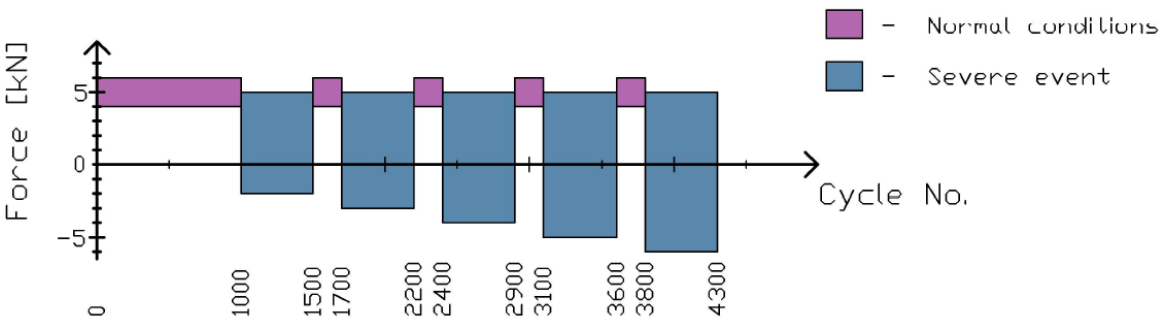

Figure D.153: Actual loading plan for Test subgroup D1

CPT

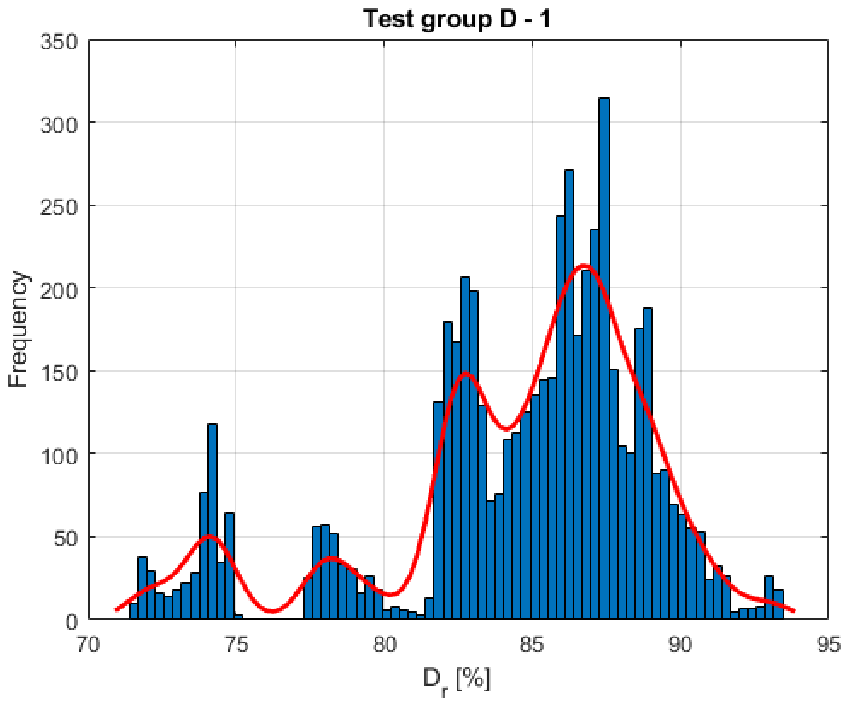

Figure D.154: Dr histogram with distribution fit for test subgroup D1

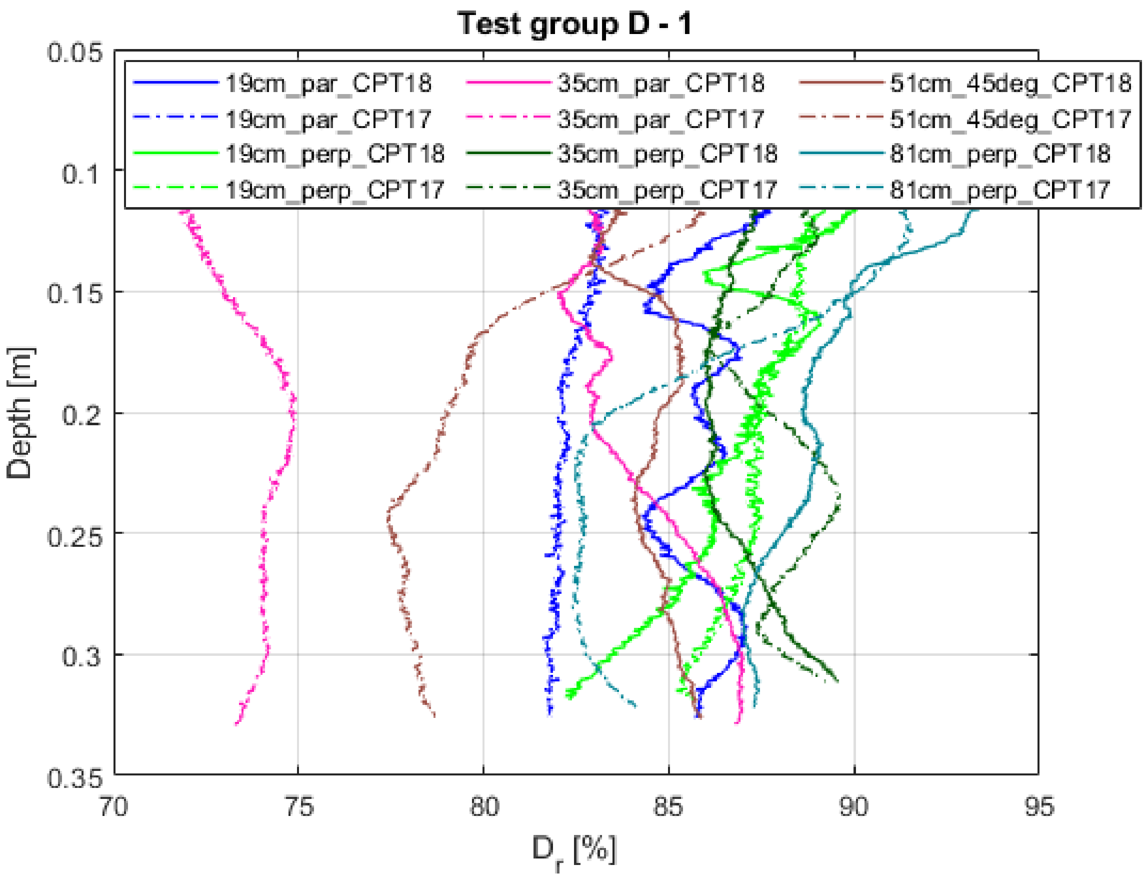

Figure D.155: Test-specific Dr results for CPT test subgroup D1

Force and displacement

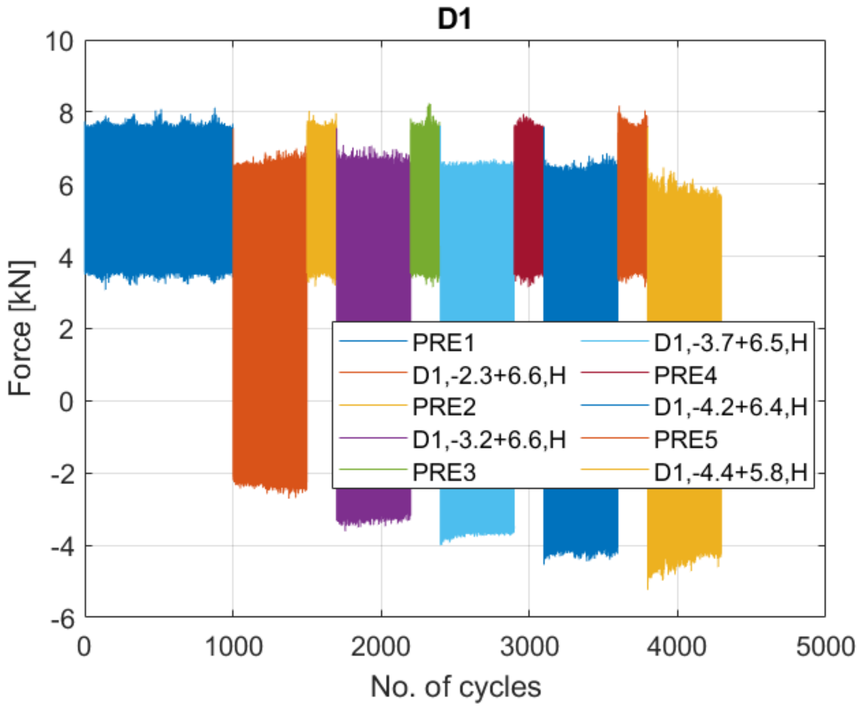

Figure D.156: Force VS no. of cycles

As it is seen from figure D.156 actual forces acting on a suction bucket are not exactly the same as was planned and presented in table D.6.

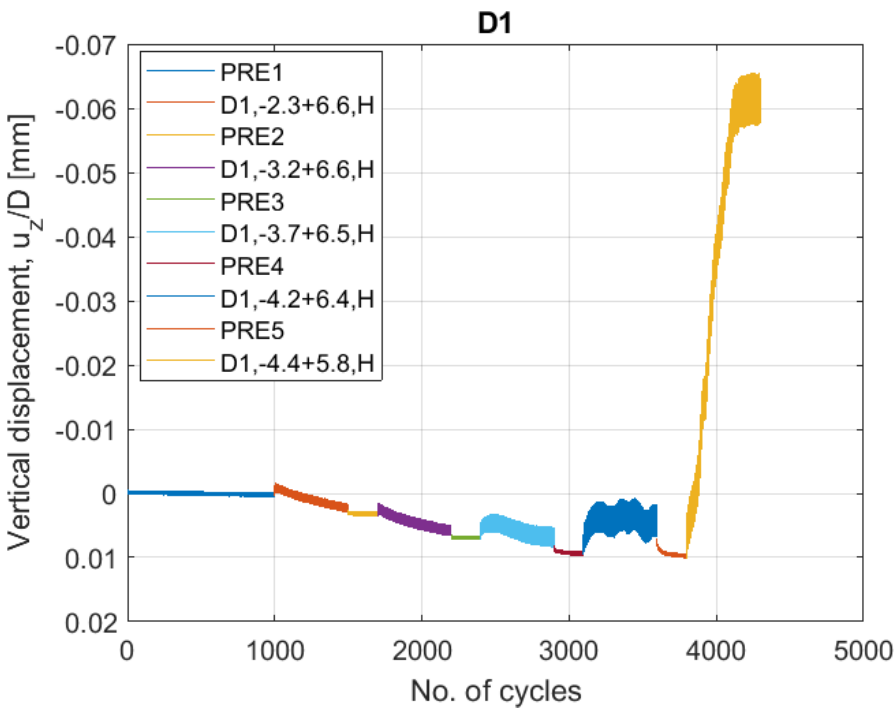

Figure D.157: Displacement VS no. of cycles

Even though, loading for severe events are relatively similar to each other from the figure D.157 it can be seen a different behaviour of soil response to the loading of 3 last extreme events compared to the first 2. To investigate the reasons behind this sudden change in behaviour it was decided to perform another experiment which would start with PRE1 event following by D1,-3.7+6.5,H to check if the reason for this odd behaviour could be disturbance of the soil in first two extreme events. This test is described more detailed in subsection D.5.2.

Moreover,it is seen that pore pressure increase significantly during last stage of the loading so the outstanding displacement could be caused by the liquefaction of the soil. To investigate if it might be related to relatively high loading frequency used during the severe events it was decided to perform another experiment described in D.5.2. It is similar experiment just with loading frequency of 0.1 Hz for both precycling and extreme event parts.

Lid Transducers

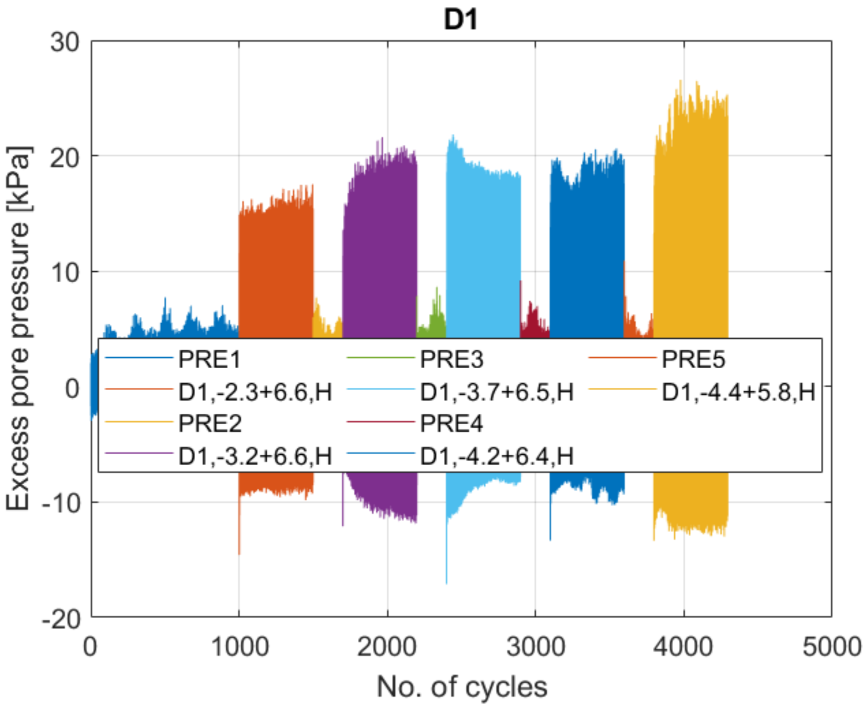

Figure D.158: Pore pressure at lid transducer P6

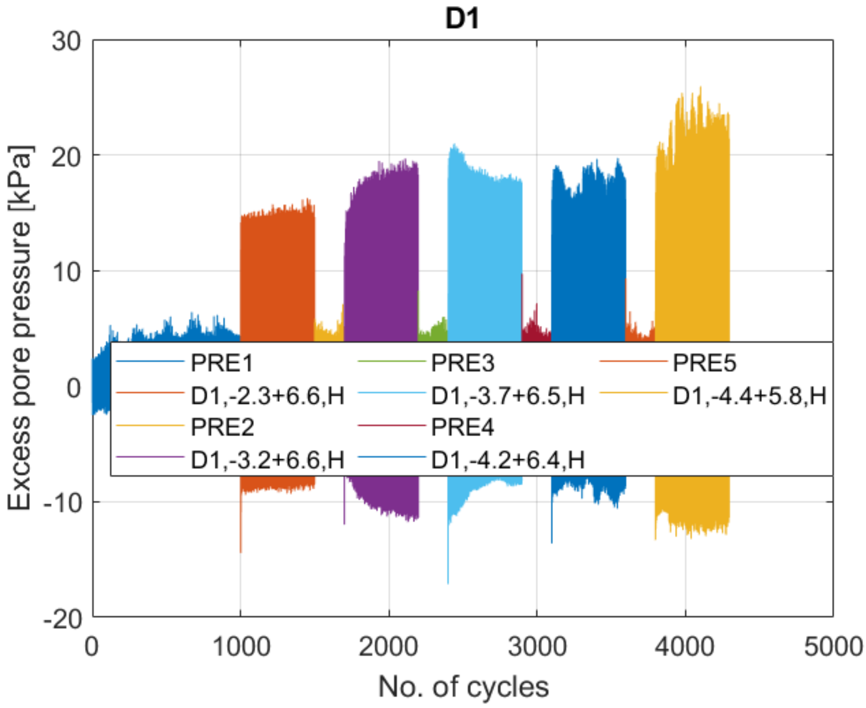

Figure D.159: Pore pressure at lid transducer P10

1st Level Transducers

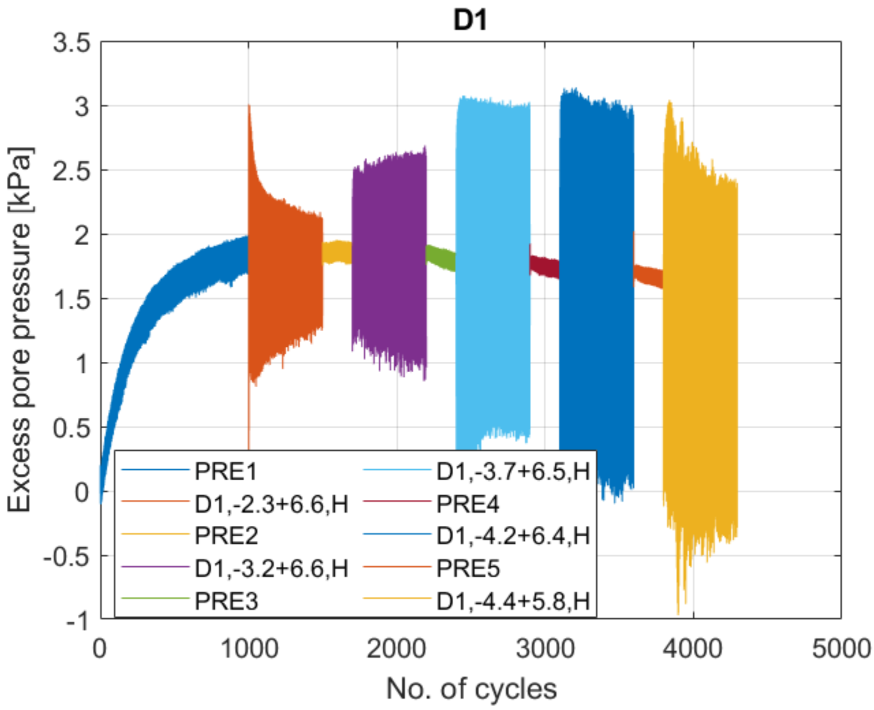

Figure D.160: Pore pressure at 1st level outer side transducer P3

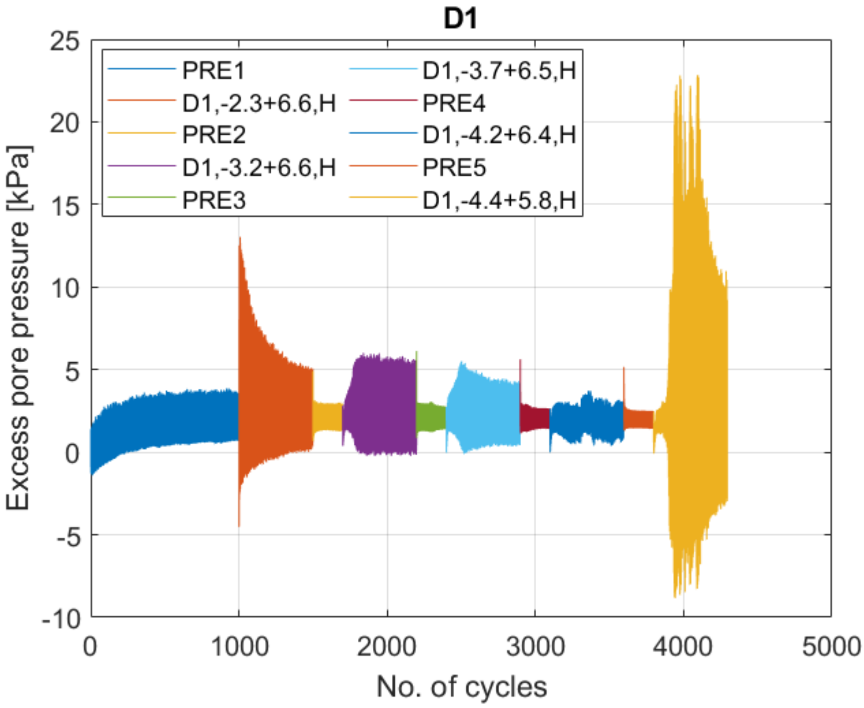

Figure D.161: Pore pressure at 1st level inner side transducer P4

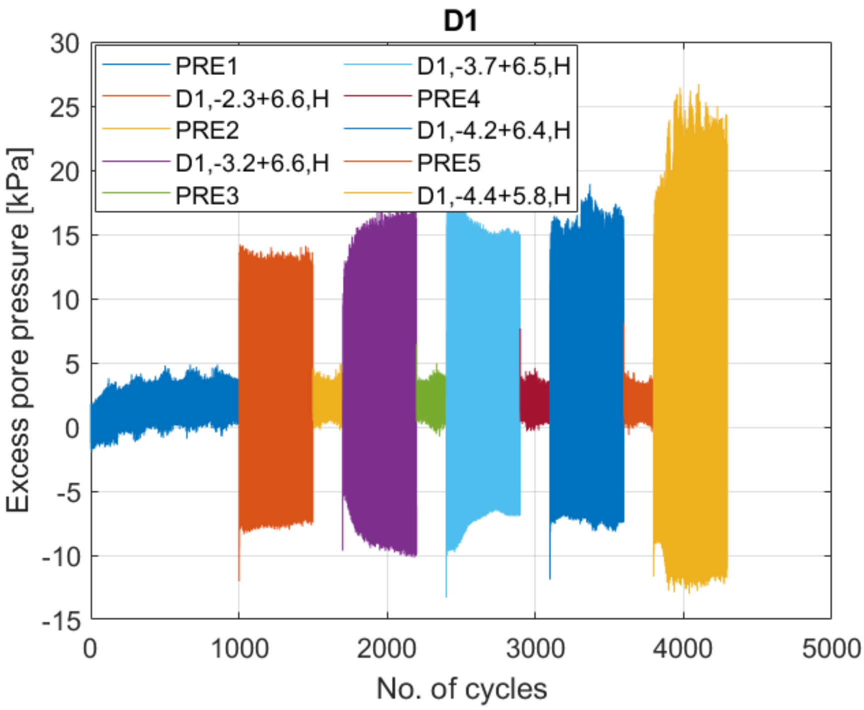

Figure D.162: Pore pressure at 1st level inner side transducer P11

2nd Level Transducers

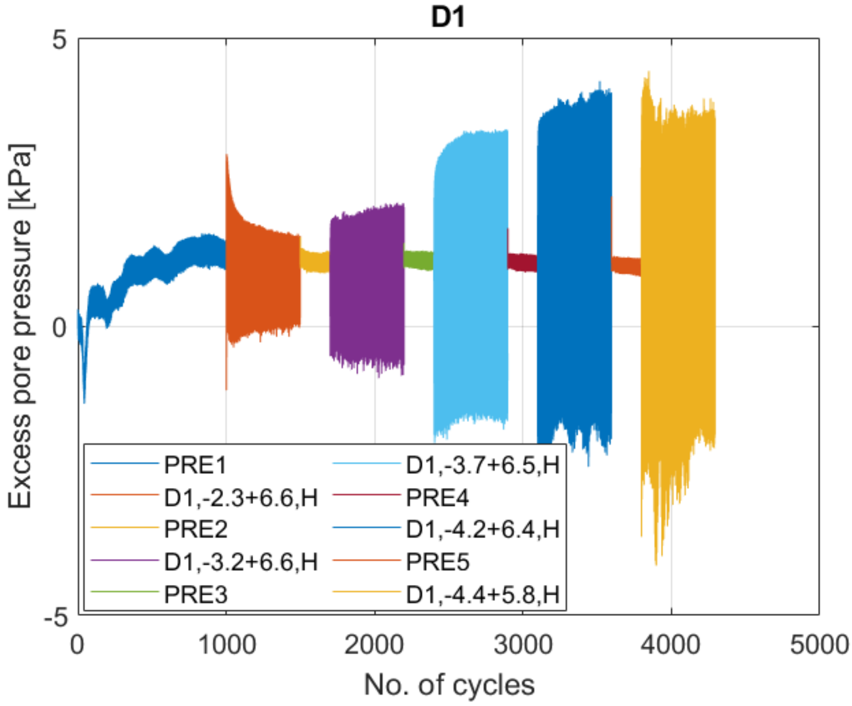

Figure D.163: Pore pressure at 2nd level outer side transducer P1

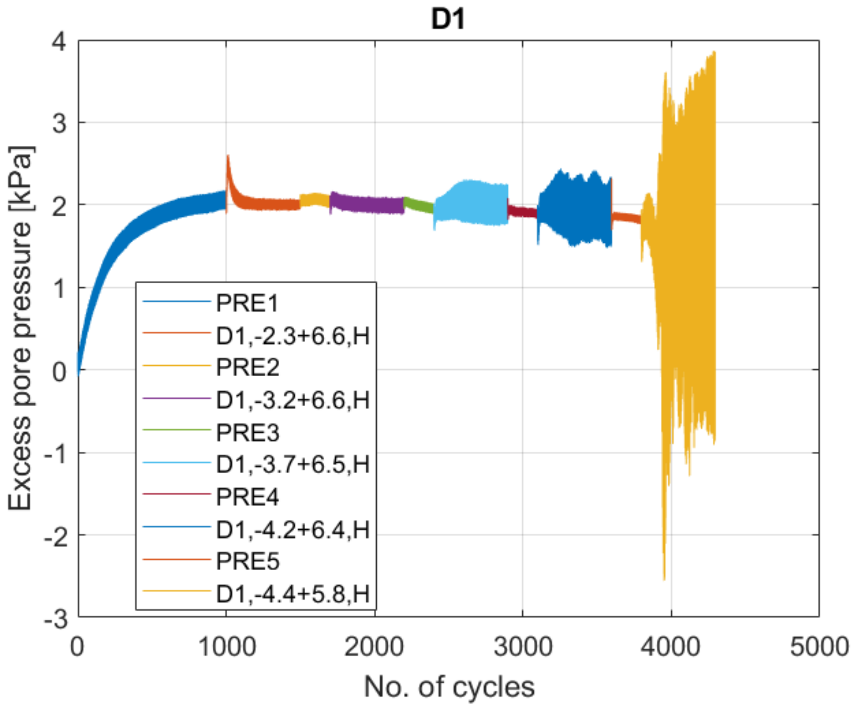

Figure D.164: Pore pressure at 2nd level outer side transducer P9

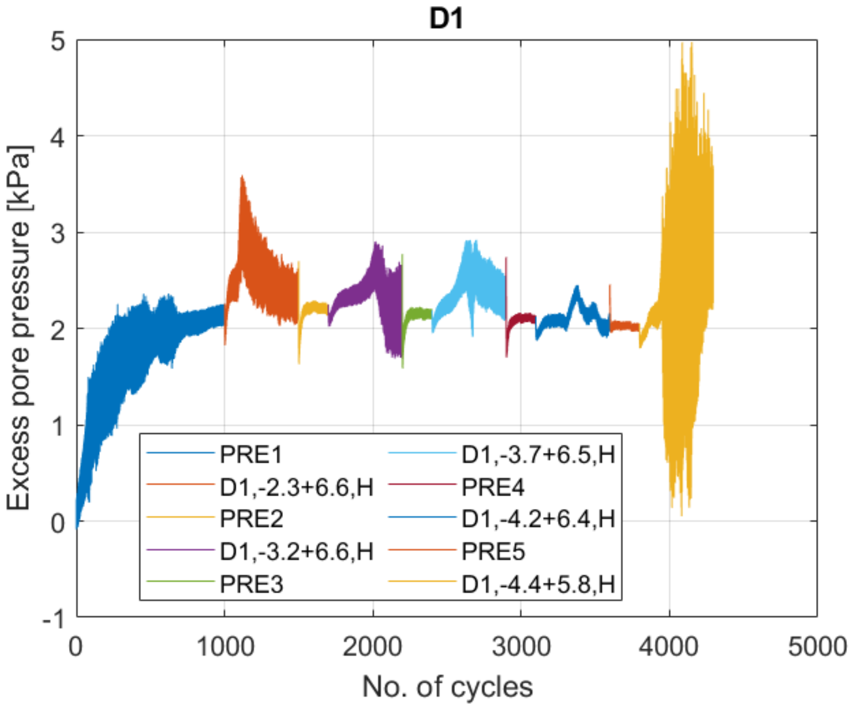

Figure D.165: Pore pressure at 2nd level inner side transducer P5

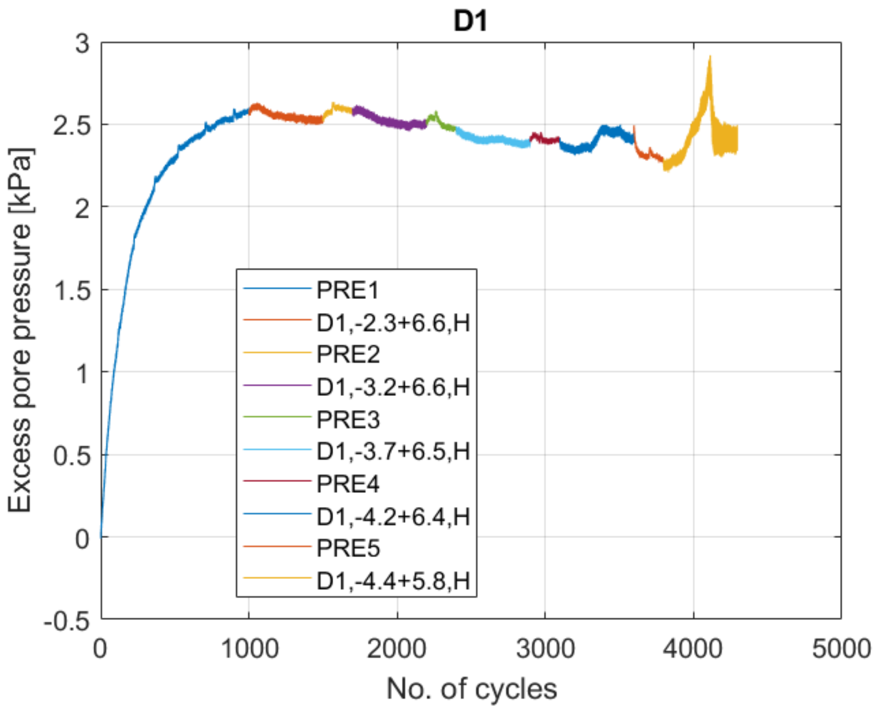

Figure D.166: Pore pressure at 2nd level inner side transducer P12

Skirt Tip Transducers

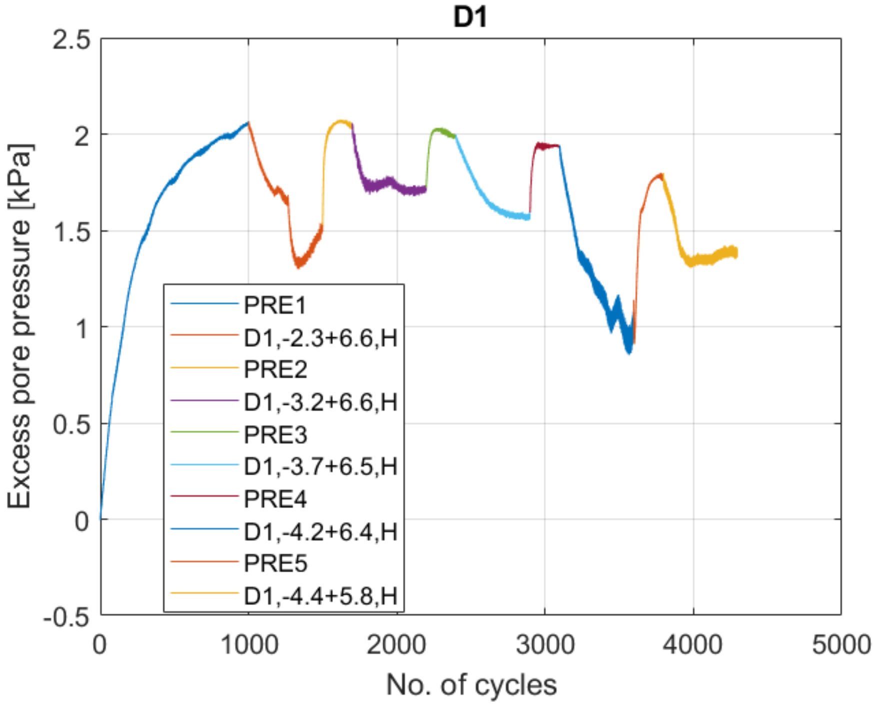

Figure D.167: Pore pressure at tip transducer P2

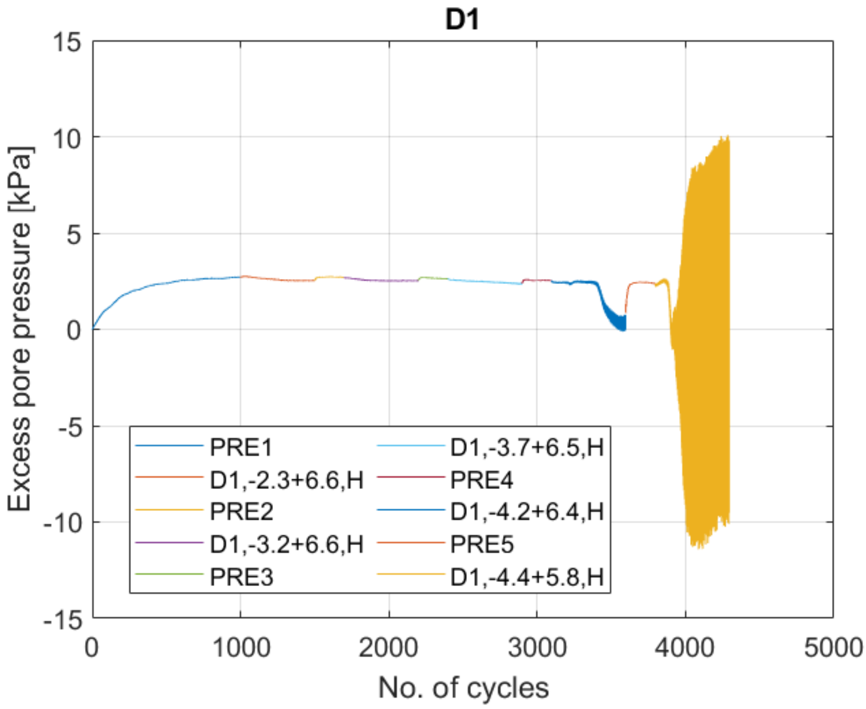

Figure D.168: Pore pressure at tip transducer P8

Force vs displacement

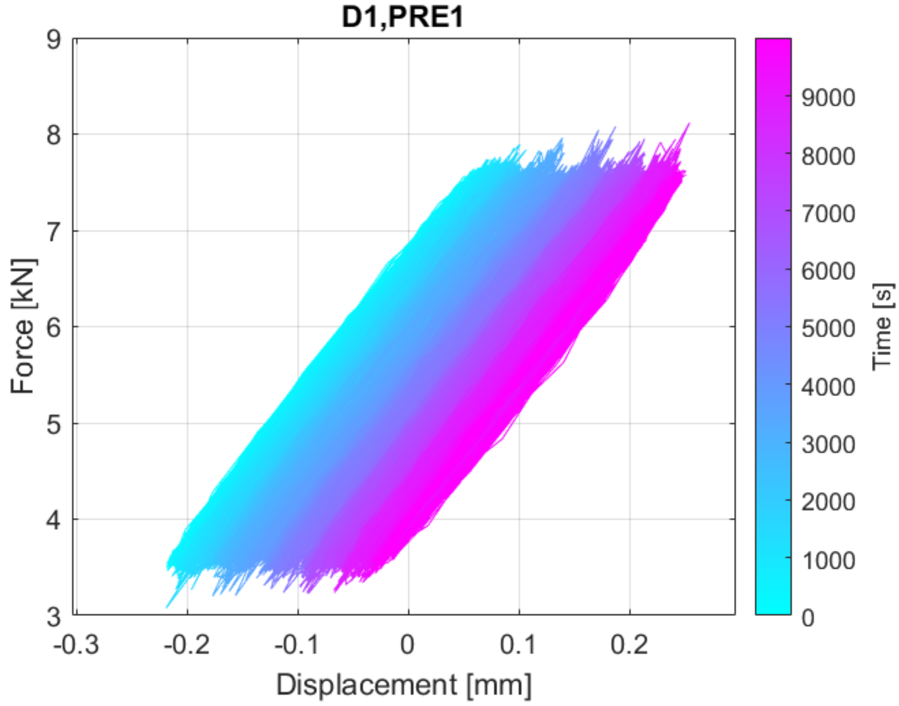

Figure D.169: Force VS absolute displacement

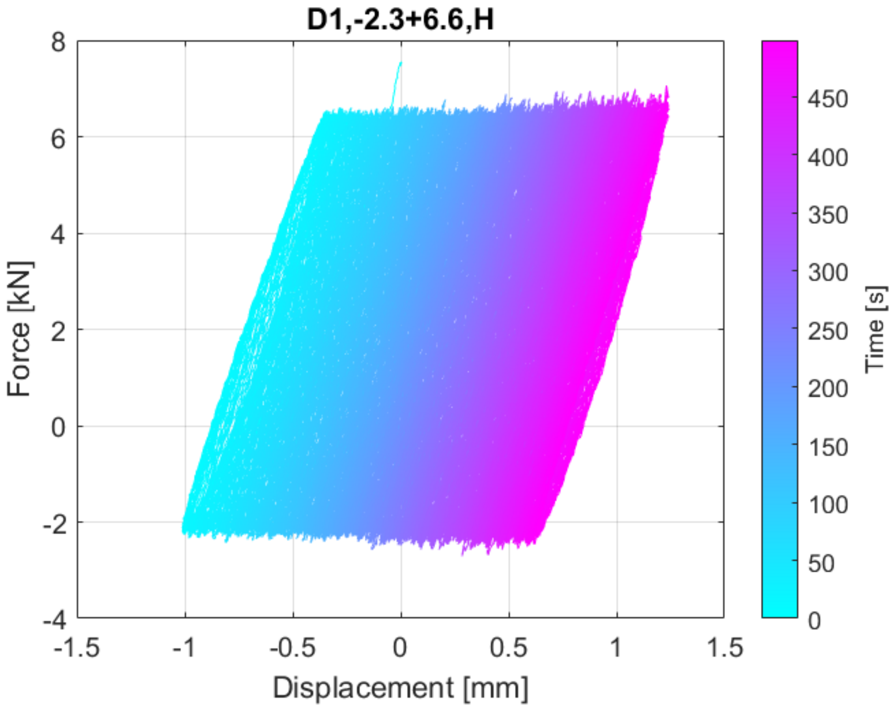

Figure D.170: Force VS absolute displacement

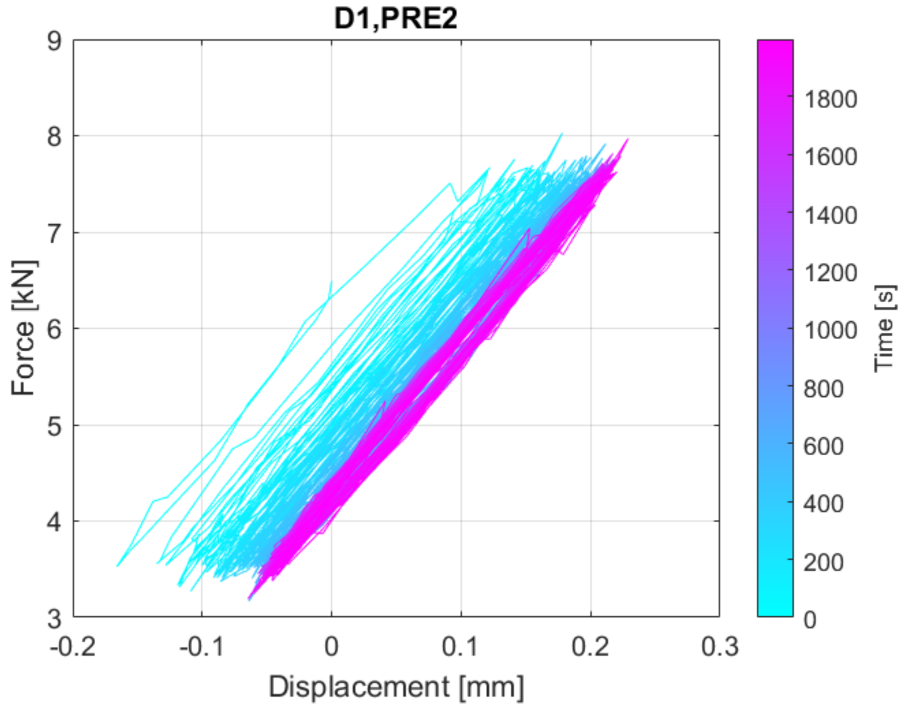

Figure D.171: Force VS absolute displacement

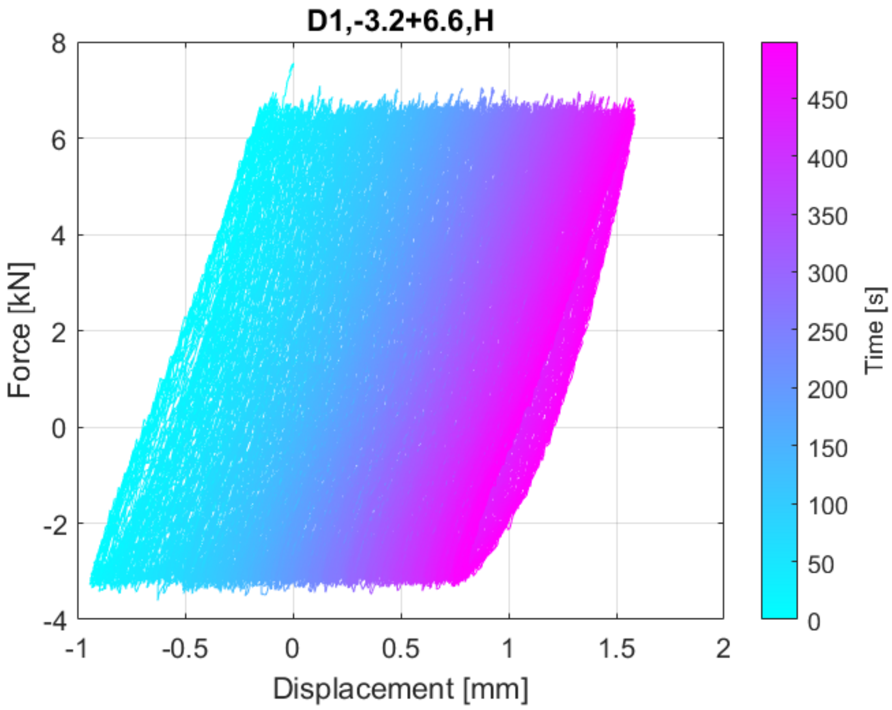

Figure D.172: Force VS absolute displacement

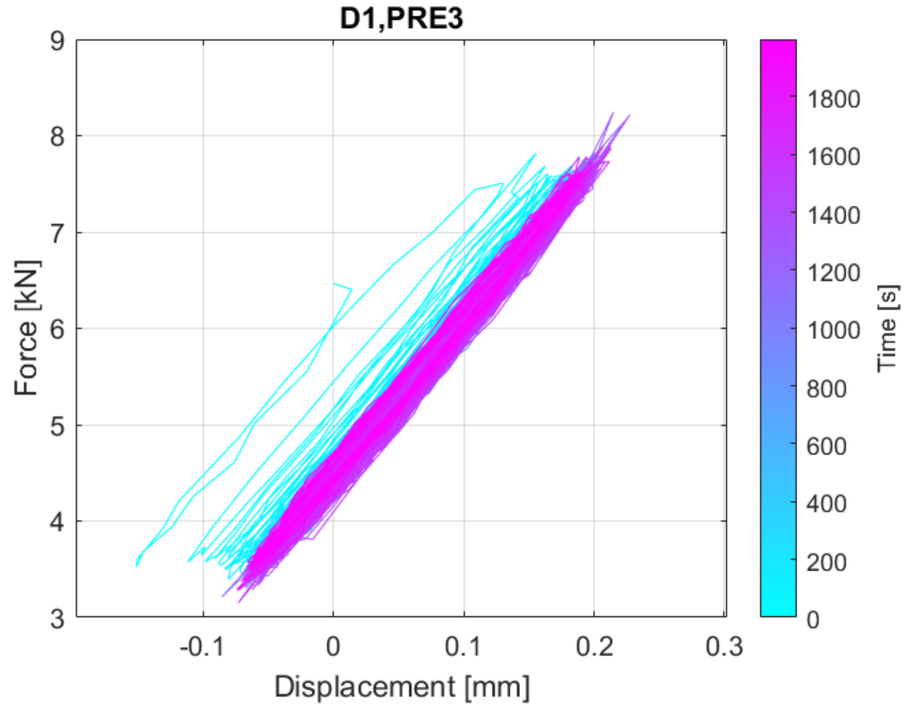

Figure D.173: Force VS absolute displacement

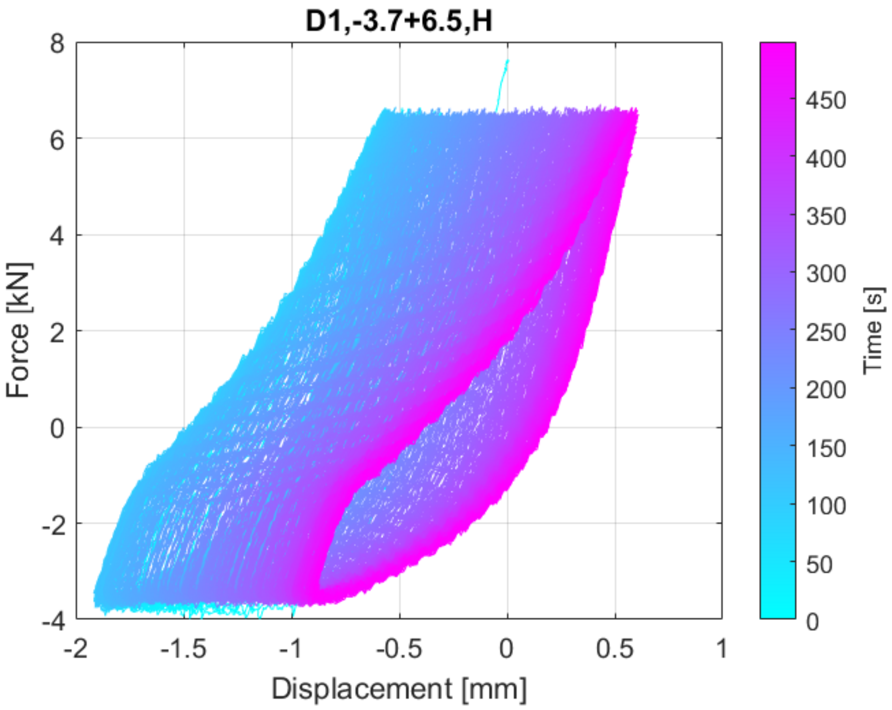

Figure D.174: Force VS absolute displacement

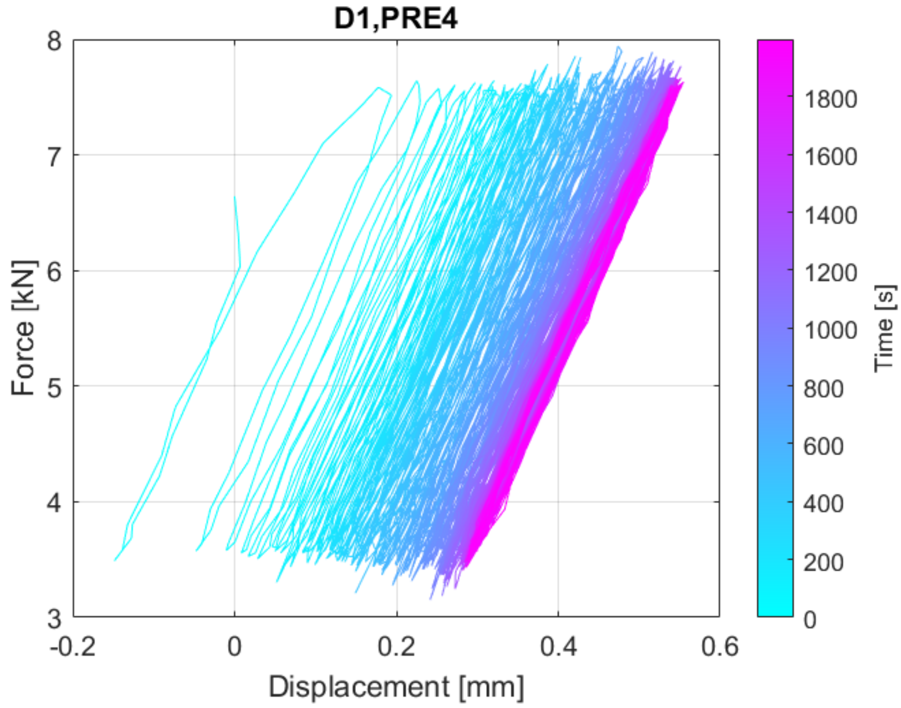

Figure D.175: Force VS absolute displacement

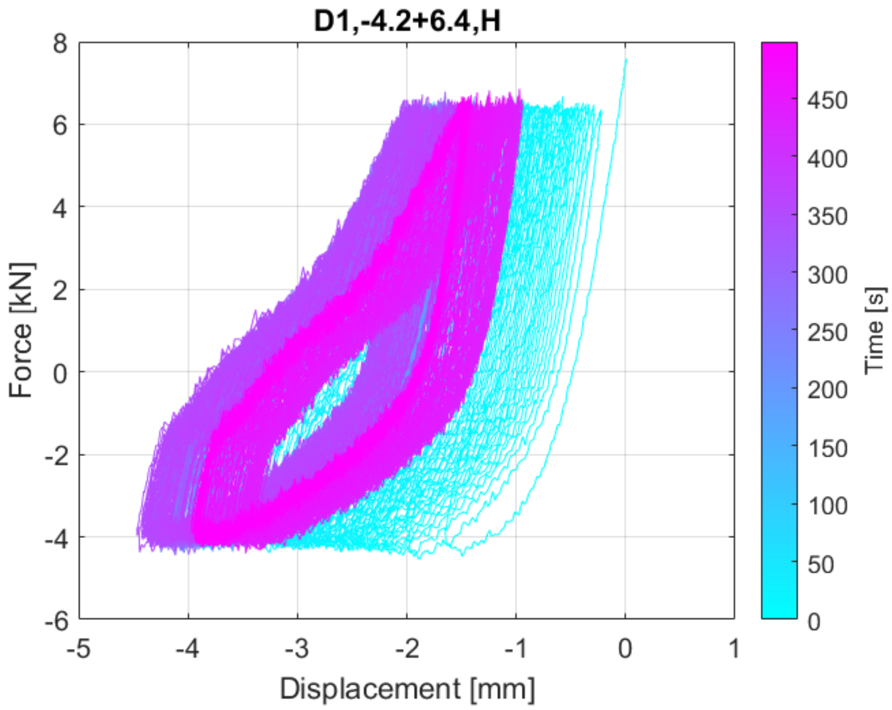

Figure D.176: Force VS absolute displacement

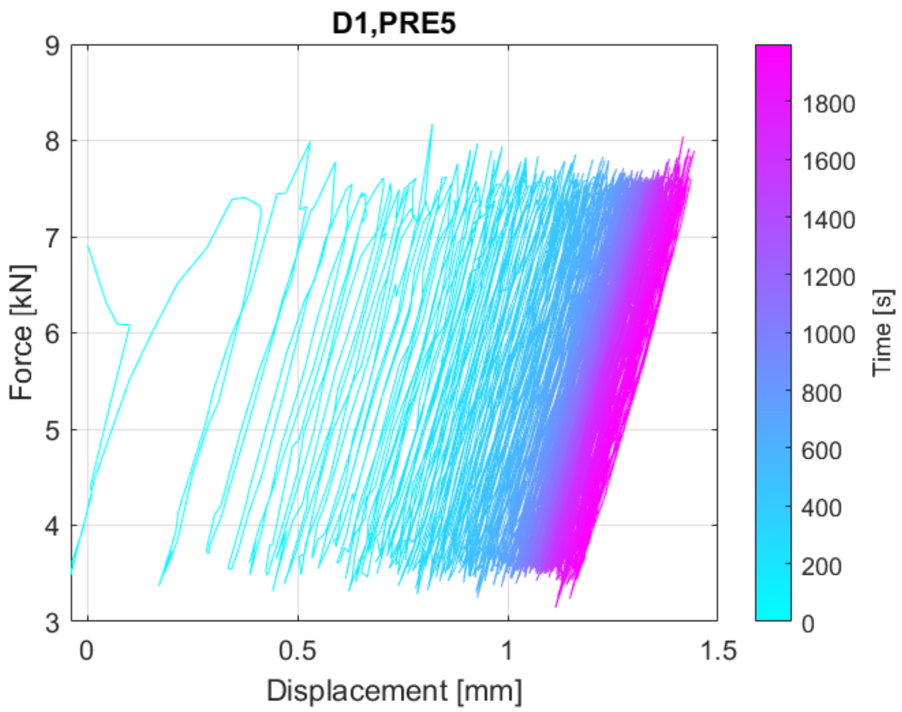

Figure D.177: Force VS absolute displacement

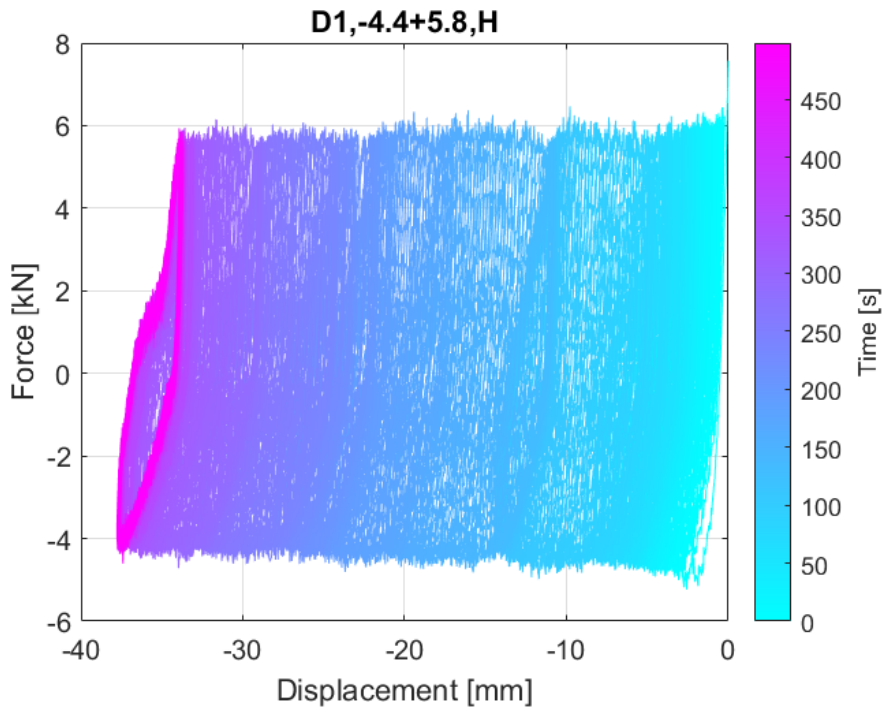

Figure D.178: Force VS absolute displacement

D.5.2 Test subgroup D2 - 1.0 Hz

As it was briefly introduced in subsection D.5.1 this test was done in order to verify if the odd behaviour at third extreme event loading package was cause by soil disturbance during first two severe events or not. That is why, during this experiment everything was kept the same apart from first two packages of severe and normal events as it can be seen in figure D.179 below.

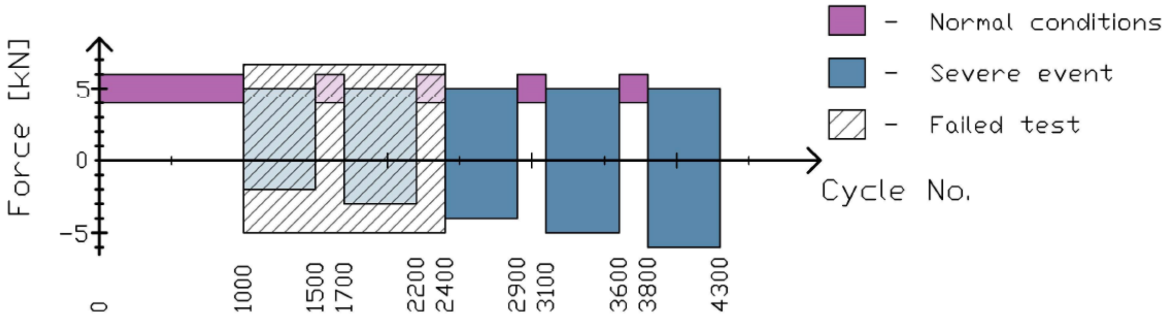

Figure D.179: Actual loading plan for test subgroup D2

CPT

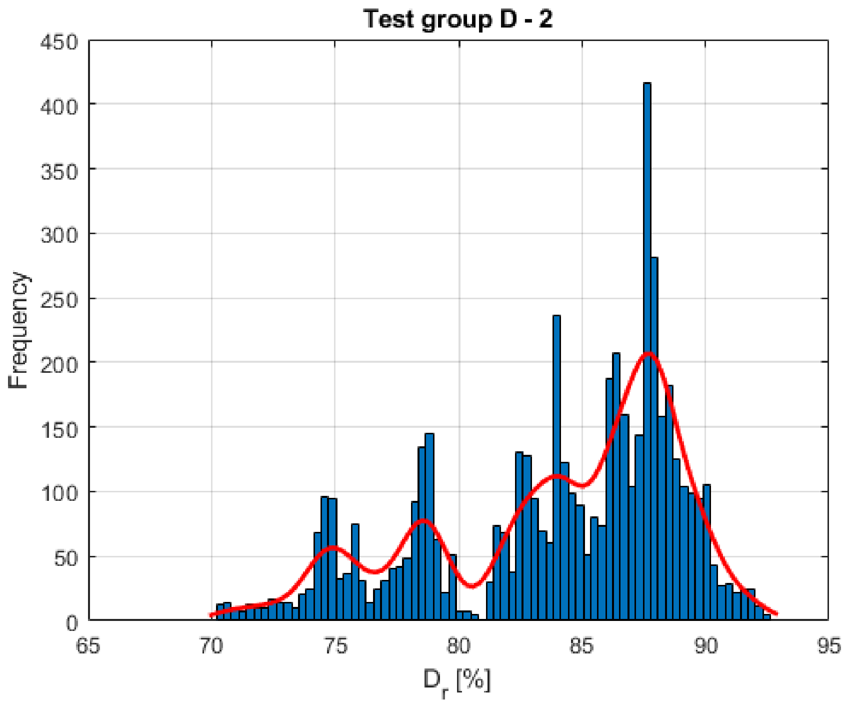

Figure D.180: Dr histogram with distribution fit for test subgroup D2

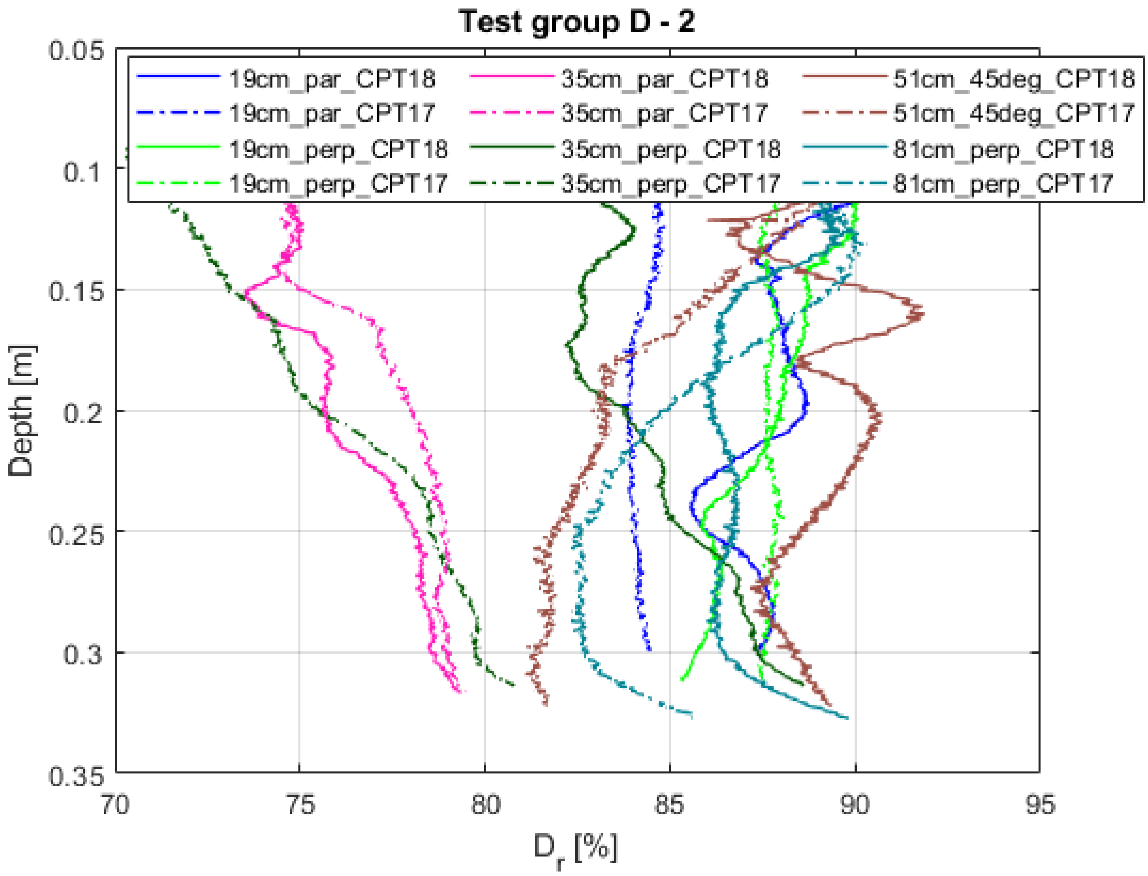

Figure D.181: Test-specific Dr results for CPT test subgroup D2

Force and displacement

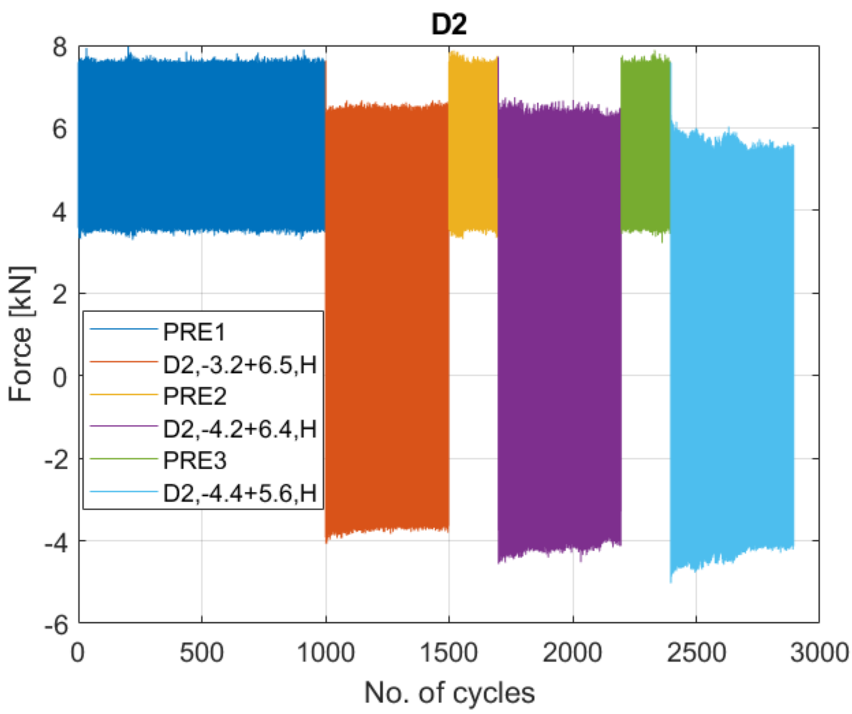

Figure D.182: Force VS no. of cycles

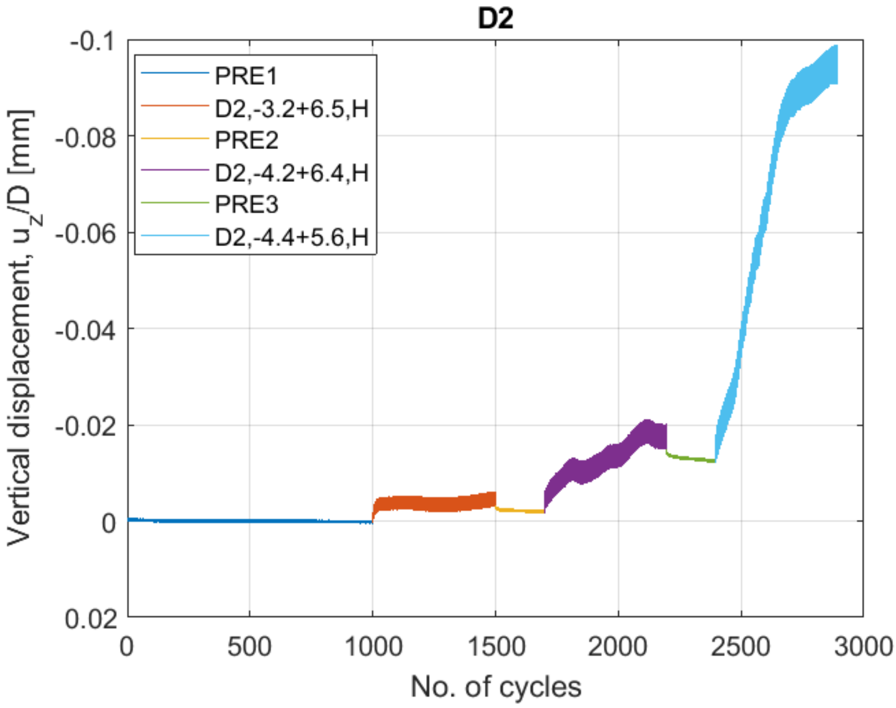

Figure D.183: Displacement VS no. of cycles

Even though, loading conditions presented in figure D.182 are similar for all extreme events, different soil behaviour can be seen for each of those events in figure D.183. Acting tensile forces tends to pull the suction bucket up, starting with relatively small displacement in the first extreme event and finishing with significant displacement in the final event.

Lid Transducers

Both transducers 6 and 10 placed on the lid of the suction bucket corresponds to each other very well so it can be concluded that these results are trustworthy.

Furthermore, it can be seen significant build up of both negative (from the tensile forces) and positive (from the compressive forces) excess pore water pressure during extreme loading. It can be argued that this pressure exceeds effective stress under the lid and liquefaction occured. That might be one of the reasons leading to significant displacement of the suction buckets. On the other hand, pore pressures at all 3 events are quite similar while the displacement varies extremely for each of the event as presented earlier.

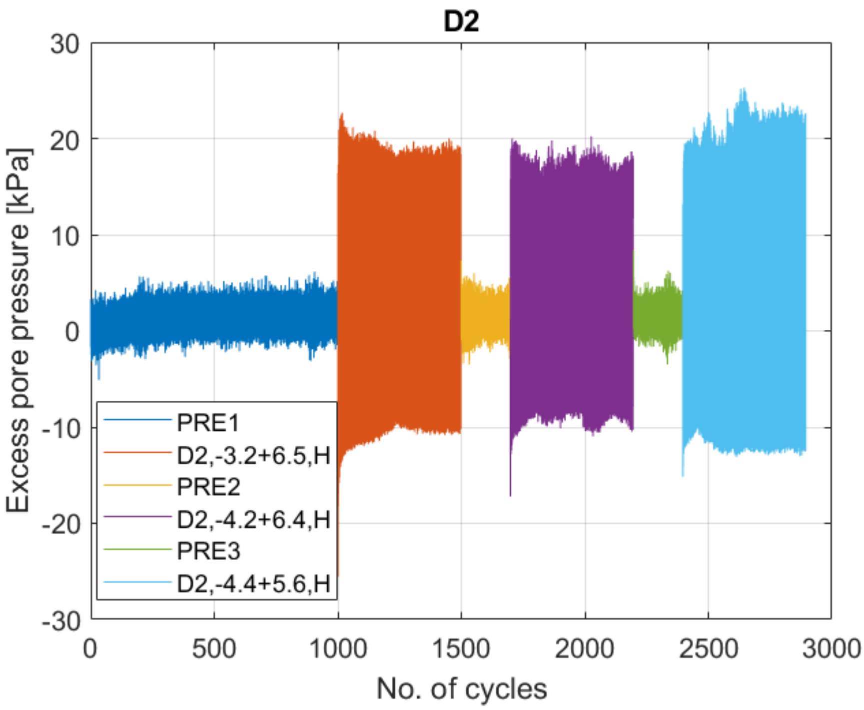

Figure D.184: Pore pressure at lid transducer P6

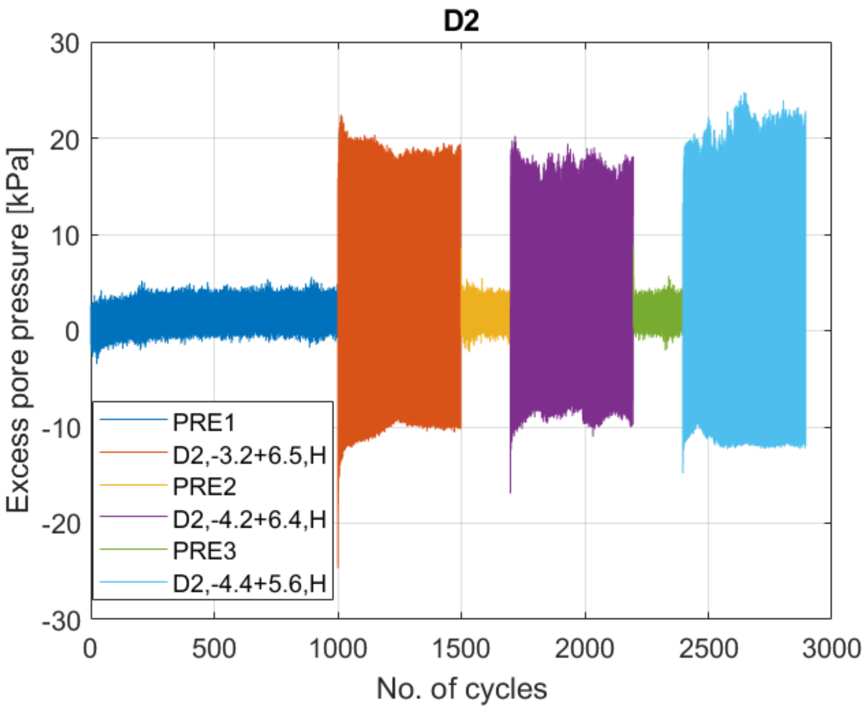

Figure D.185: Pore pressure at lid transducer P10

1st Level Transducers

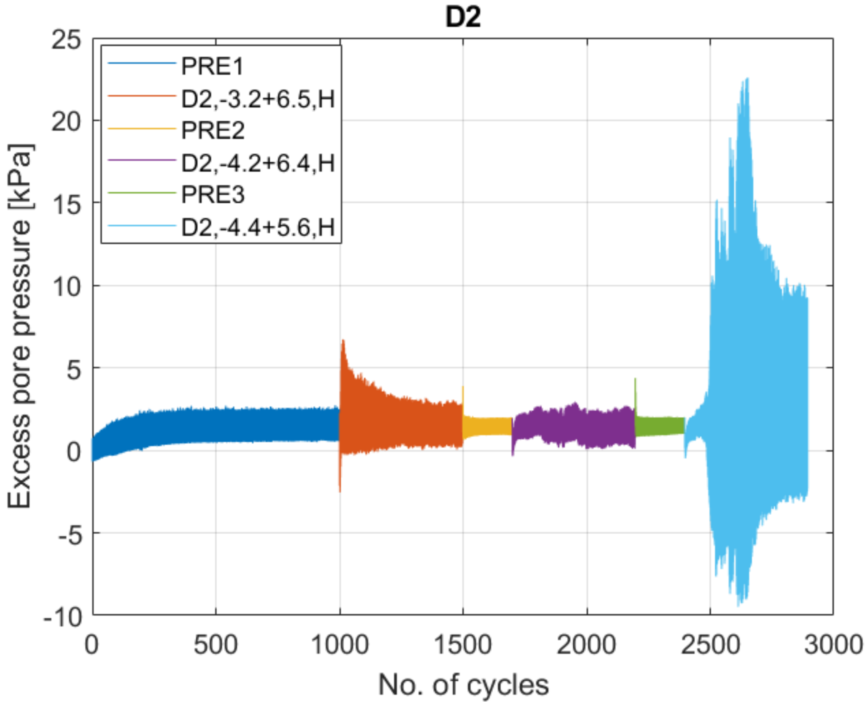

Figure D.186: Pore pressure at 1st level inner side transducer P4

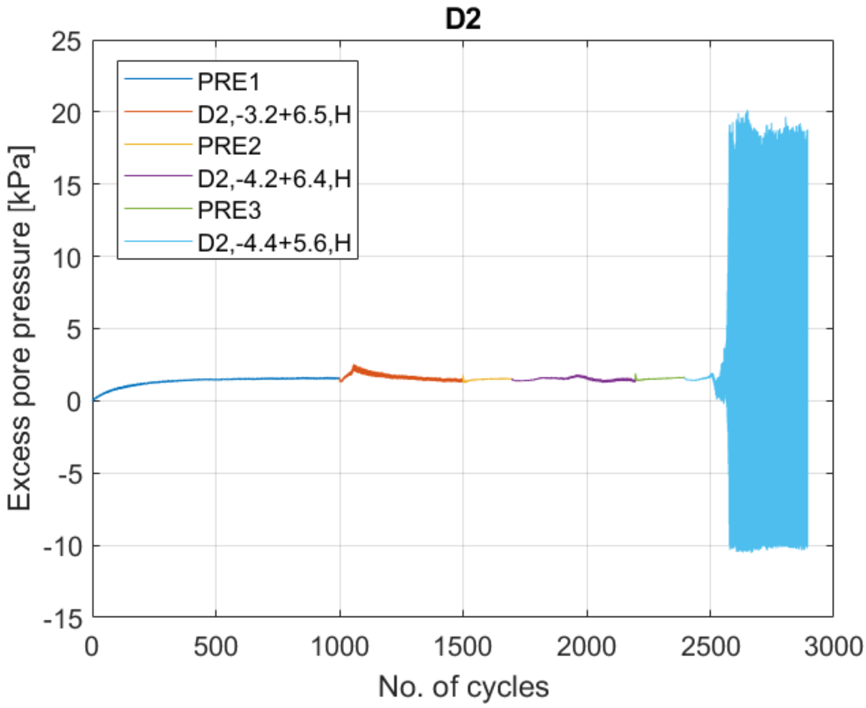

Figure D.187: Pore pressure at 1st level inner side transducer P11

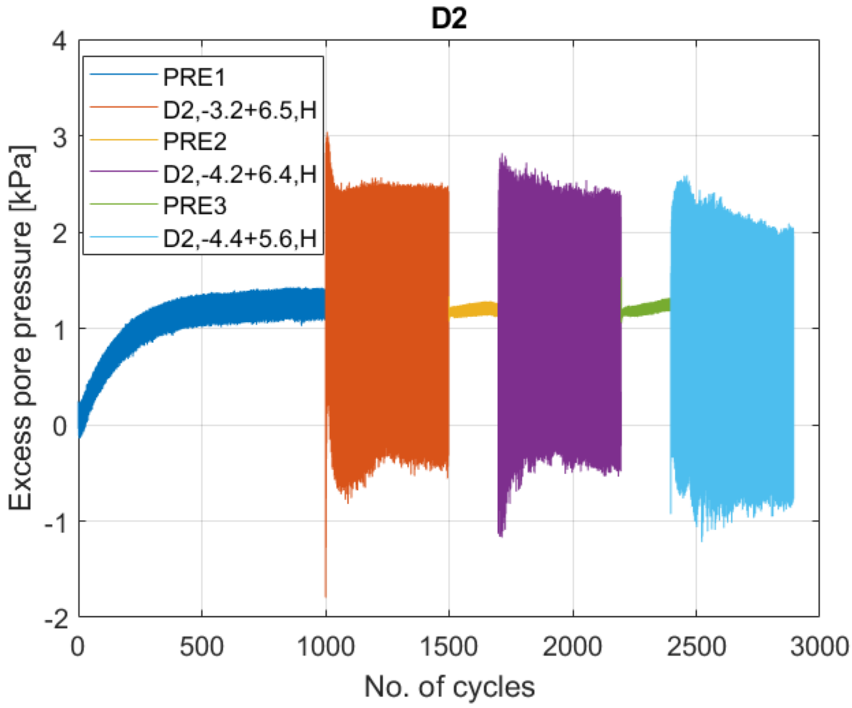

Figure D.188: Pore pressure at 1st level outer side transducer P3

2nd Level Transducers

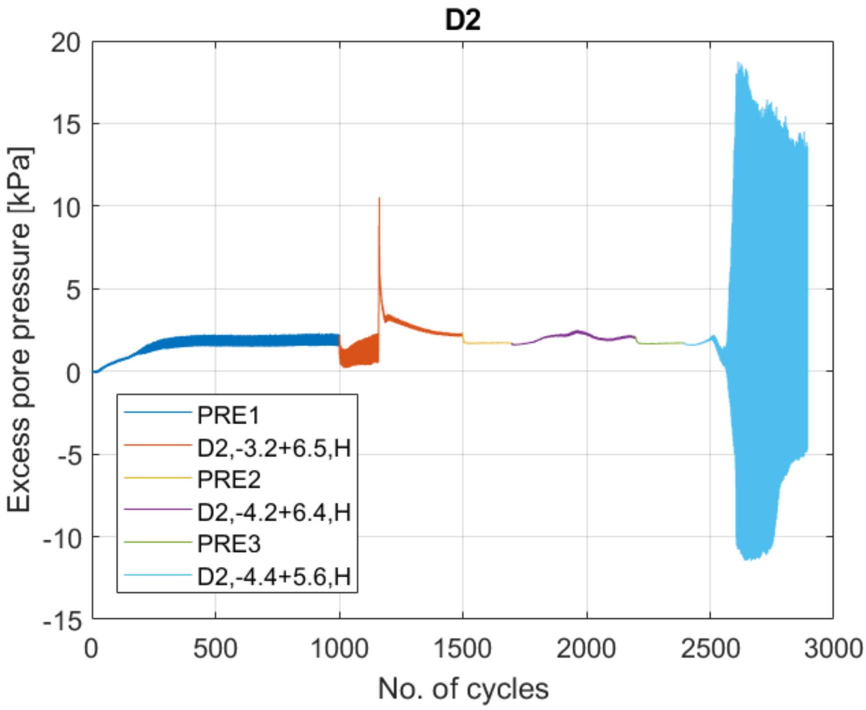

Figure D.189: Pore pressure at 2nd level inner side transducer P5

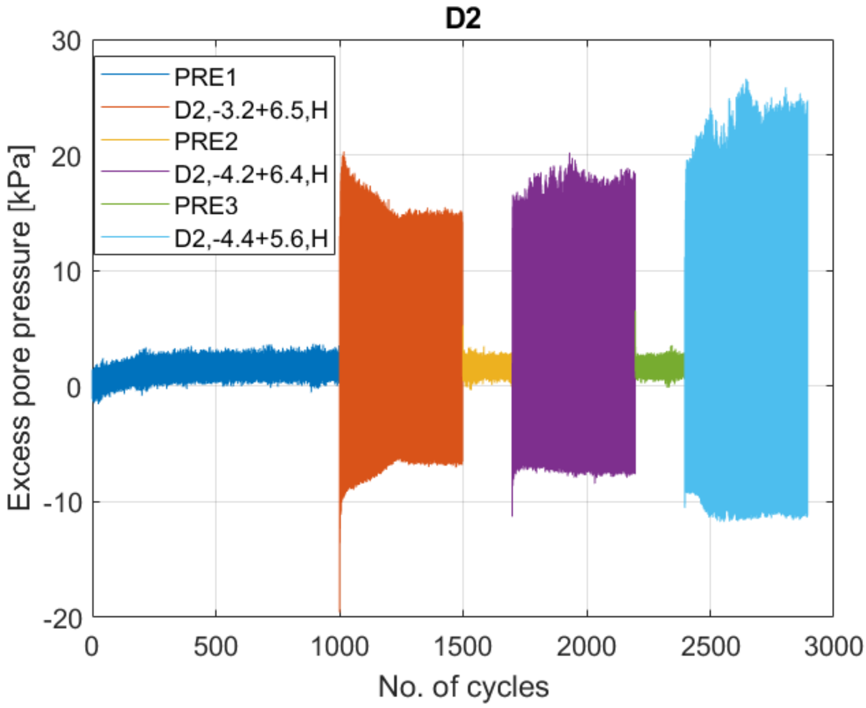

Figure D.190: Pore pressure at 2nd level inner side transducer P12

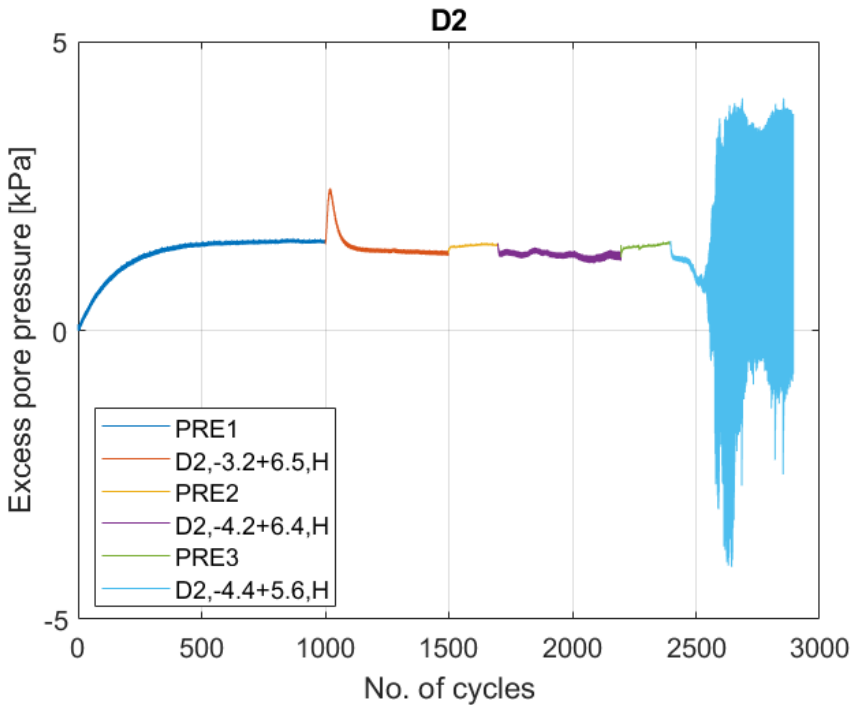

Figure D.191: Pore pressure at 2nd level outer side transducer P9

Skirt Tip Transducers

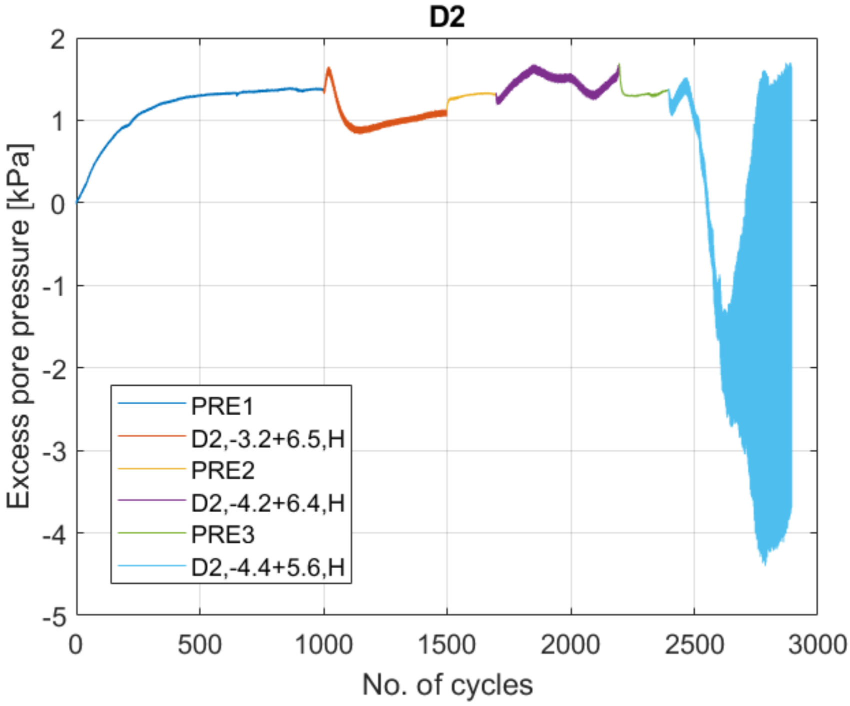

Figure D.192: Pore pressure at tip transducer P2

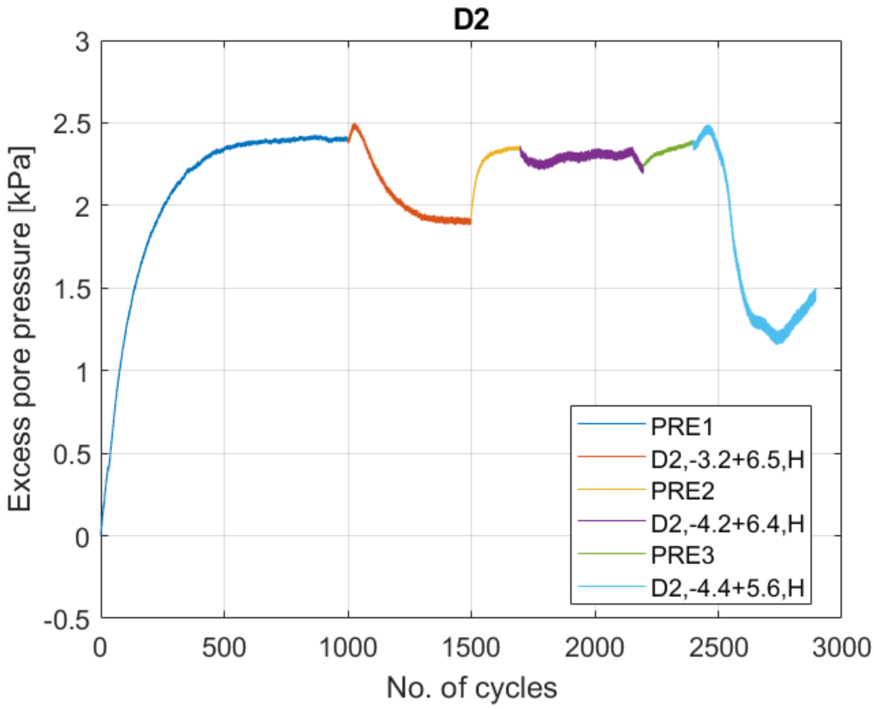

Figure D.193: Pore pressure at tip transducer P8

Force VS displacement

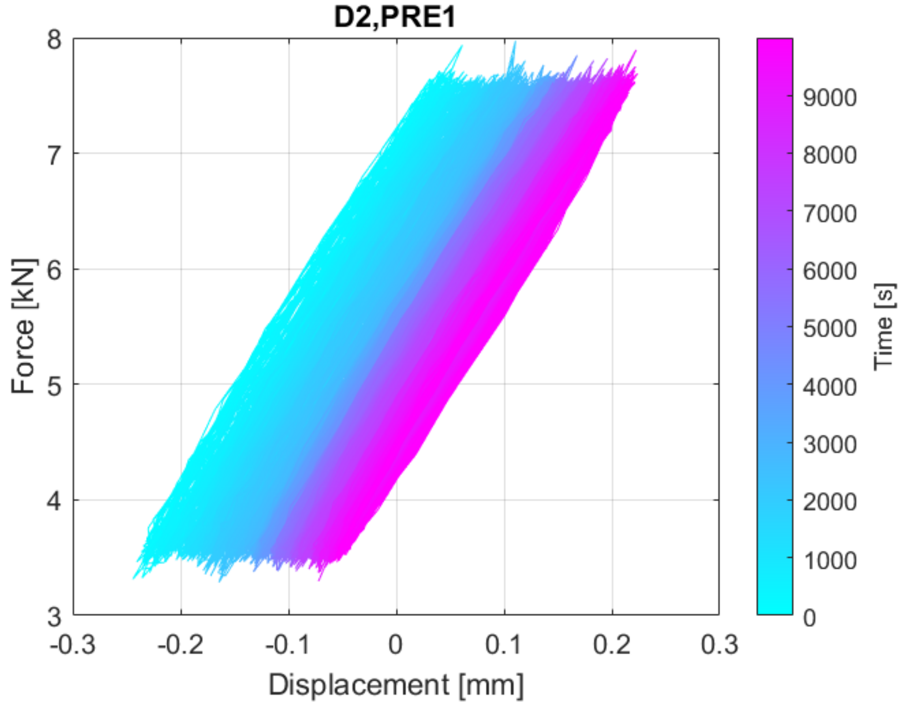

Figure D.194: Force VS absolute displacement

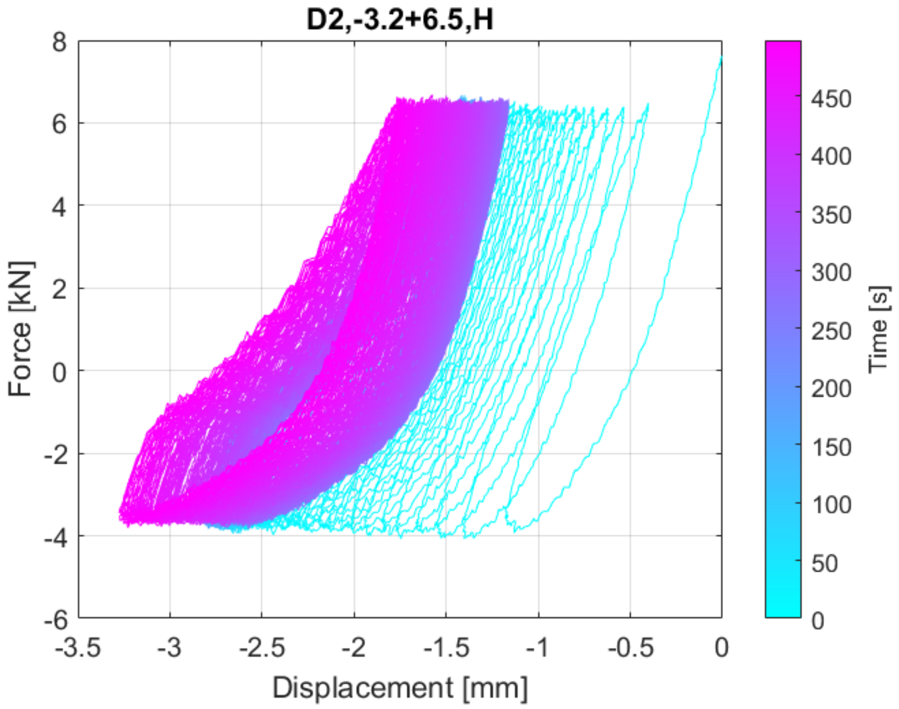

Figure D.195: Force VS absolute displacement

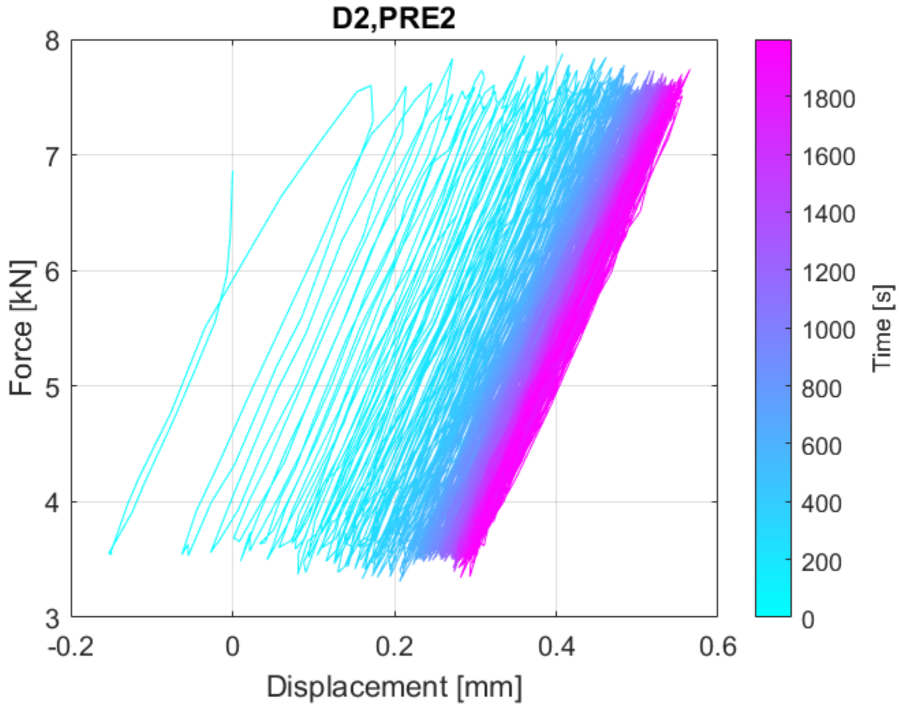

Figure D.196: Force VS absolute displacement

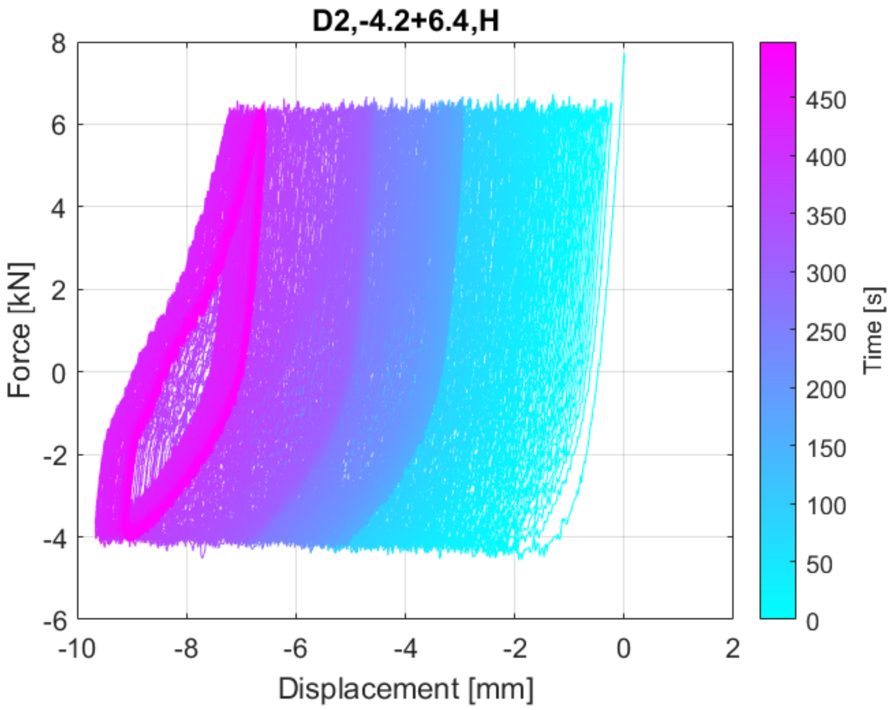

Figure D.197: Force VS absolute displacement

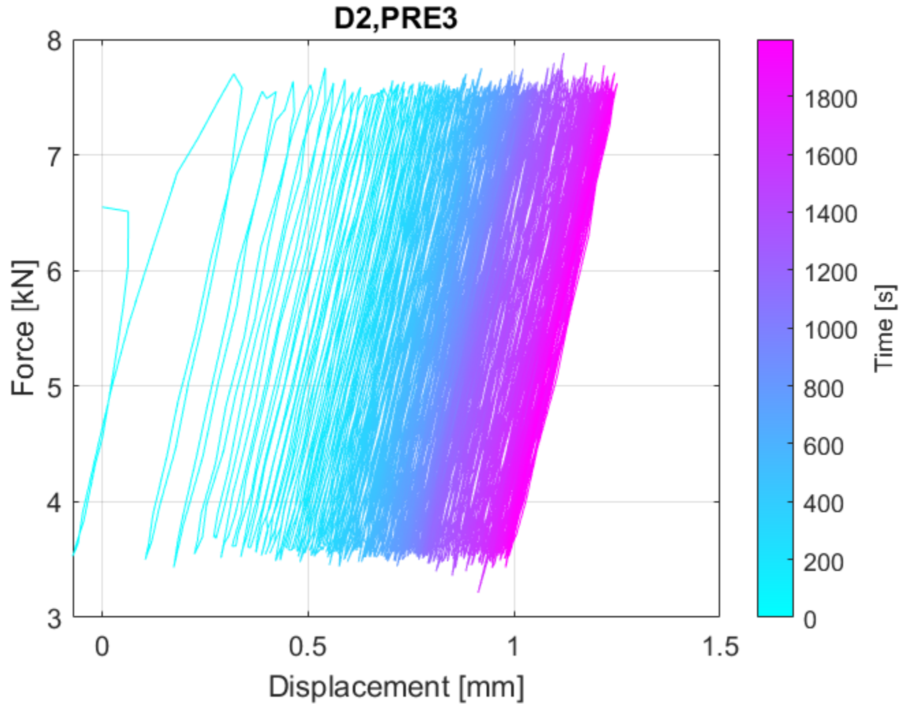

Figure D.198: Force VS absolute displacement

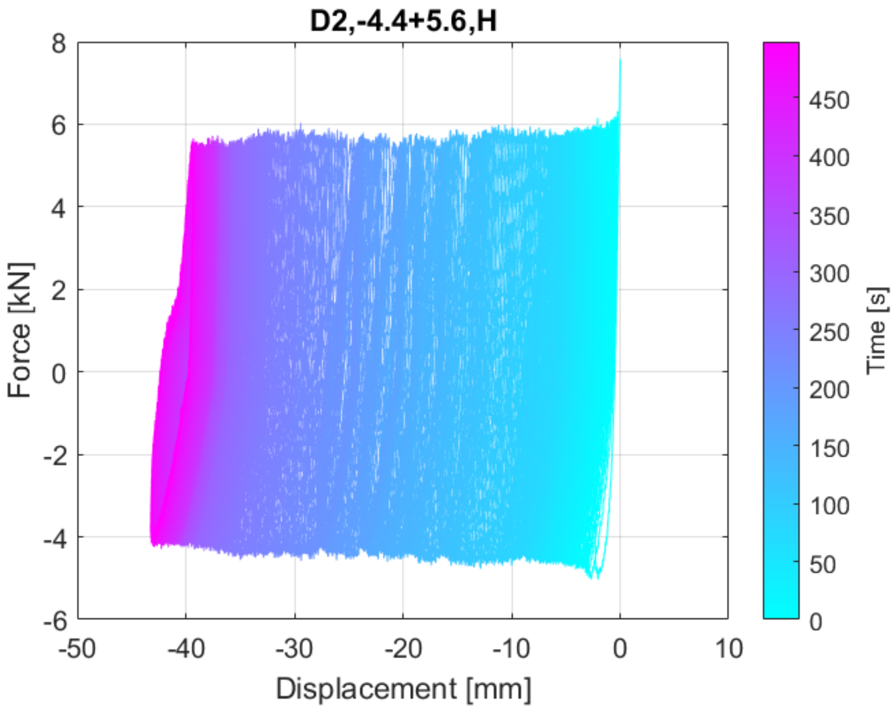

Figure D.199: Force VS absolute displacement

D.5.3 Test subgroup D3 - 0.1 Hz

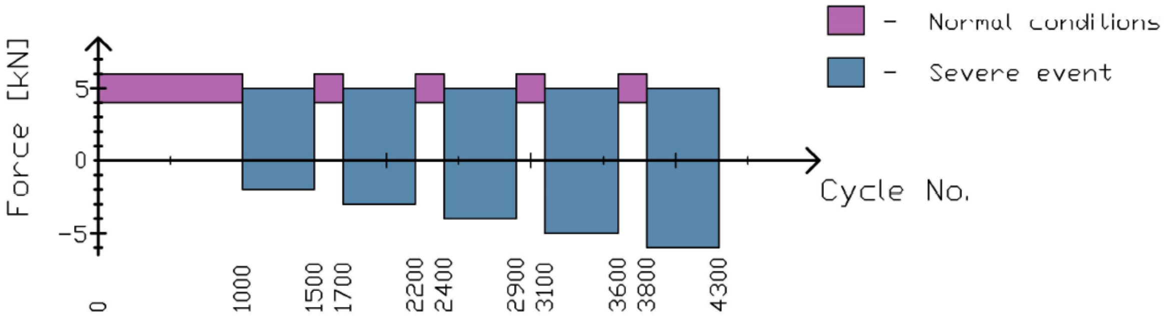

Figure D.200: Actual loading plan for Test subgroup D3

CPT

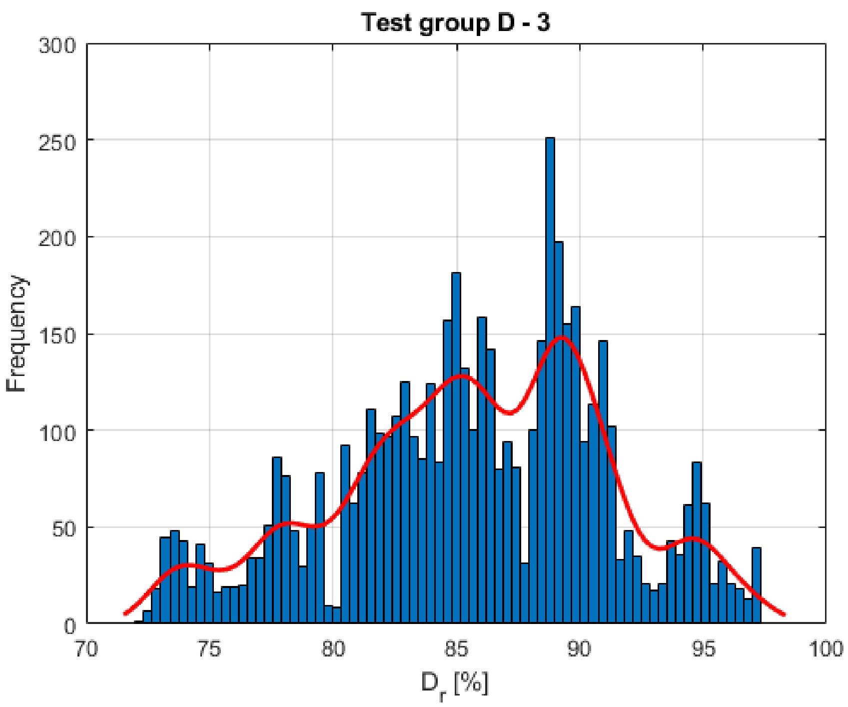

Figure D.201: Dr histogram with distribution fit for test subgroup D3

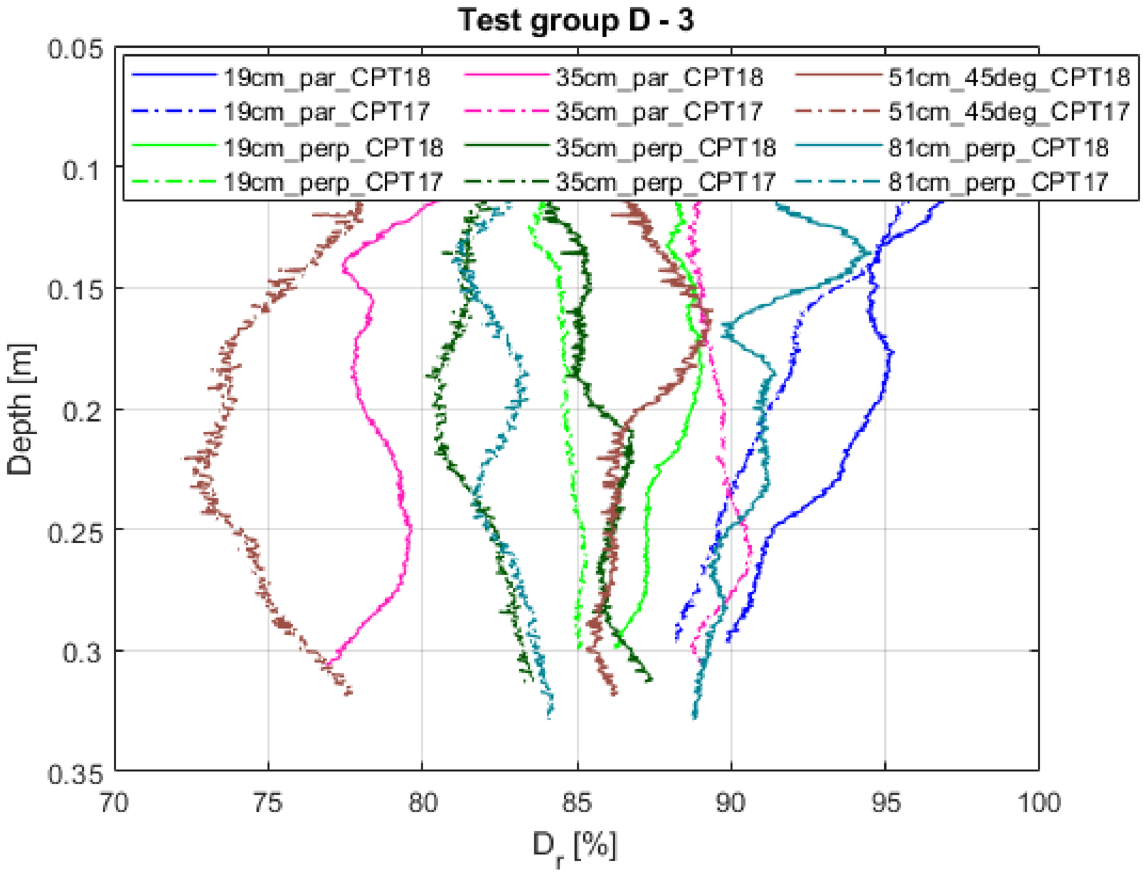

Figure D.202: Test-specific Dr results for CPT test subgroup D3

Force and displacement

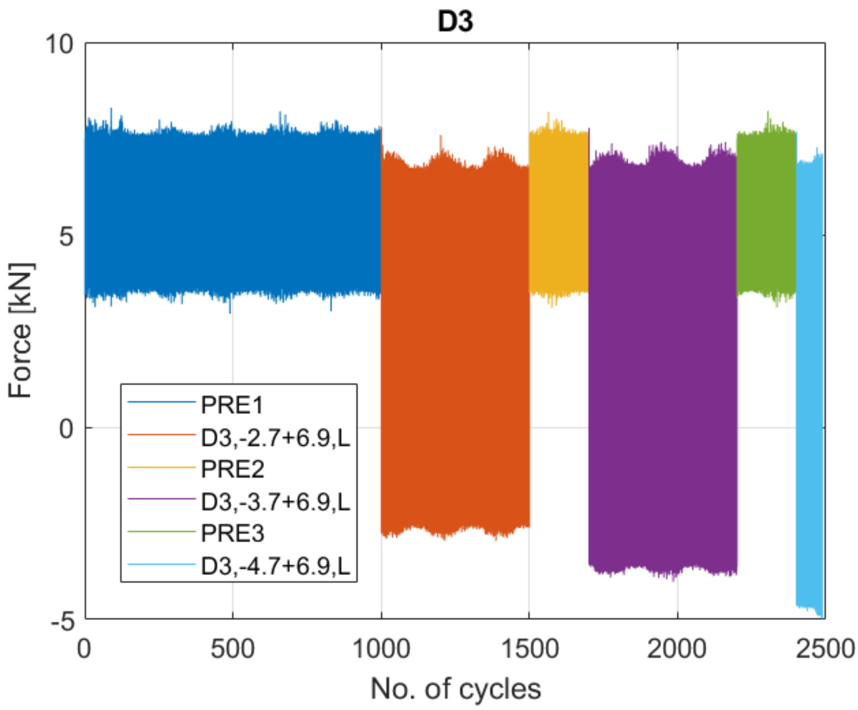

Figure D.203: Force VS no. of cycles

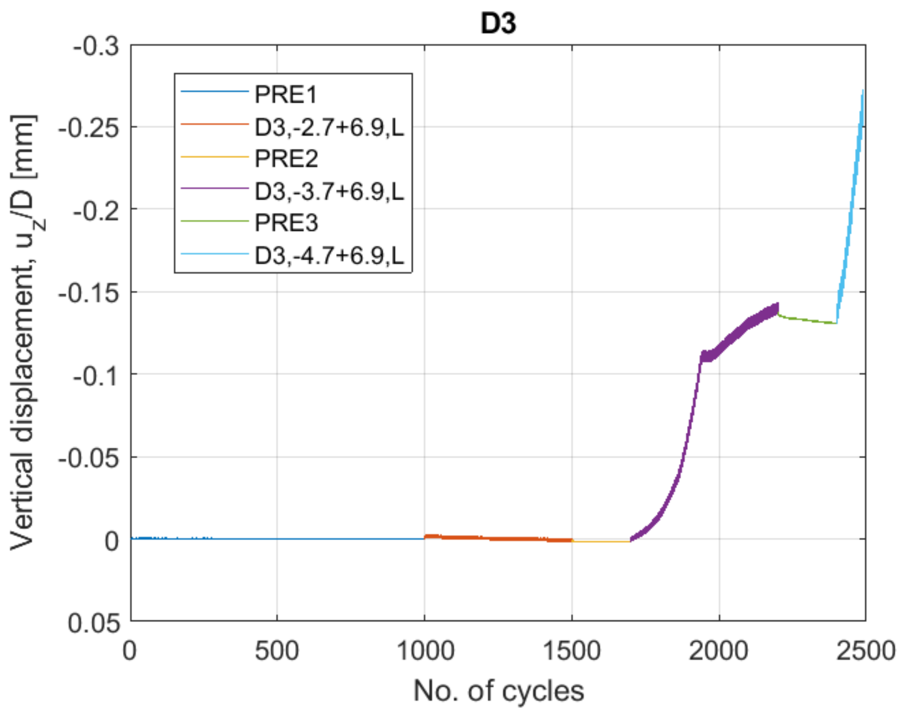

Figure D.204: Displacement VS no. of cycles

Lid Transducers

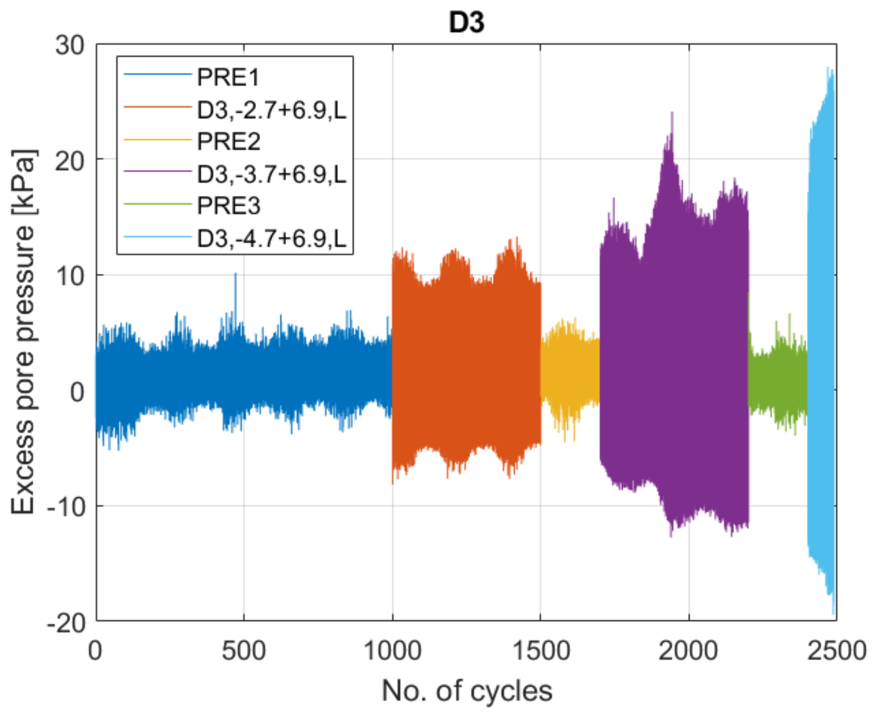

Figure D.205: Pore pressure at lid transducer P6

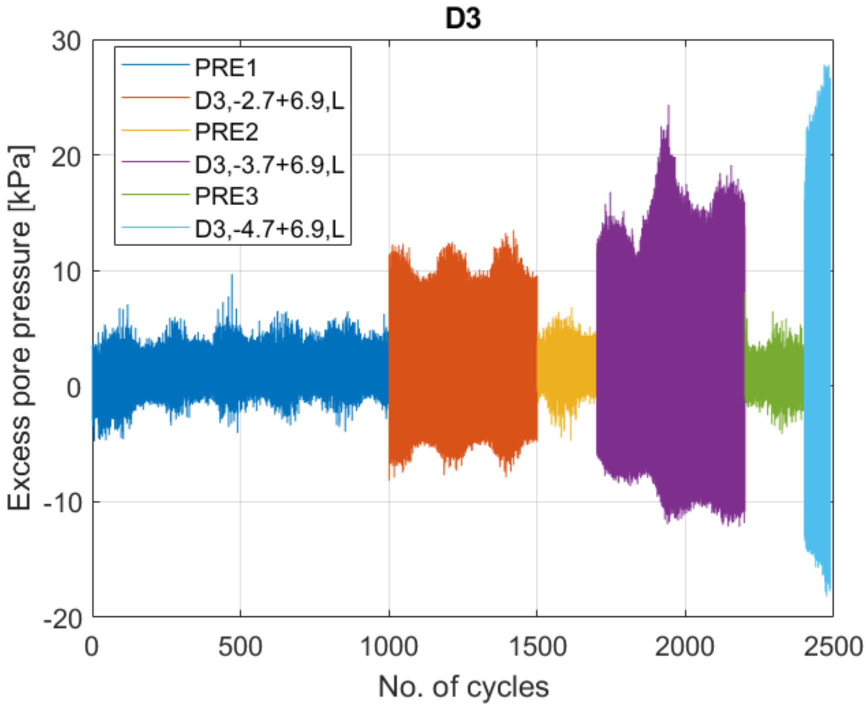

Figure D.206: Pore pressure at lid transducer P10

1st Level Transducers

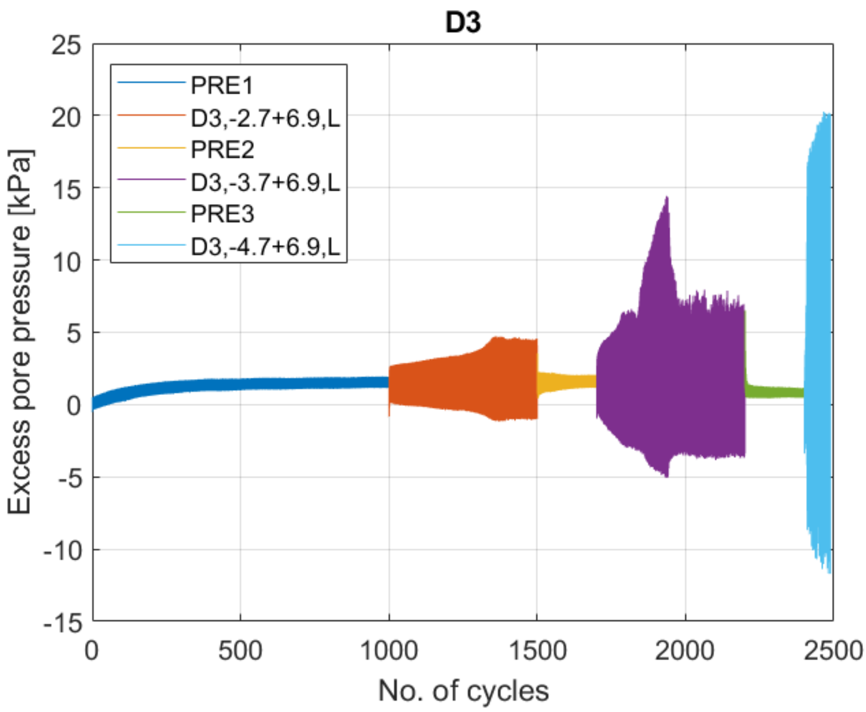

Figure D.207: Pore pressure at 1st level inner side transducer P4

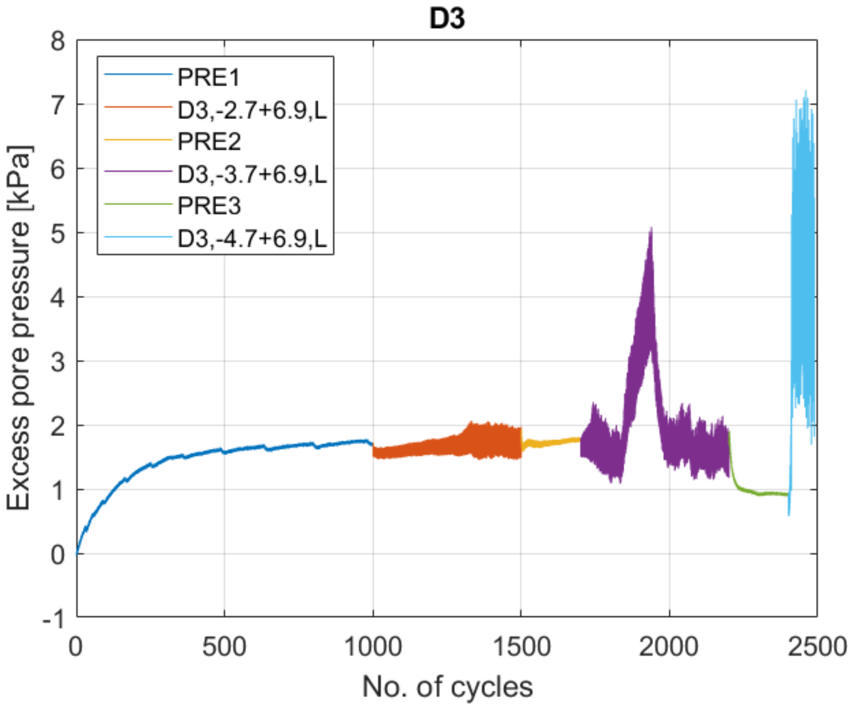

Figure D.208: Pore pressure at 1st level inner side transducer P11

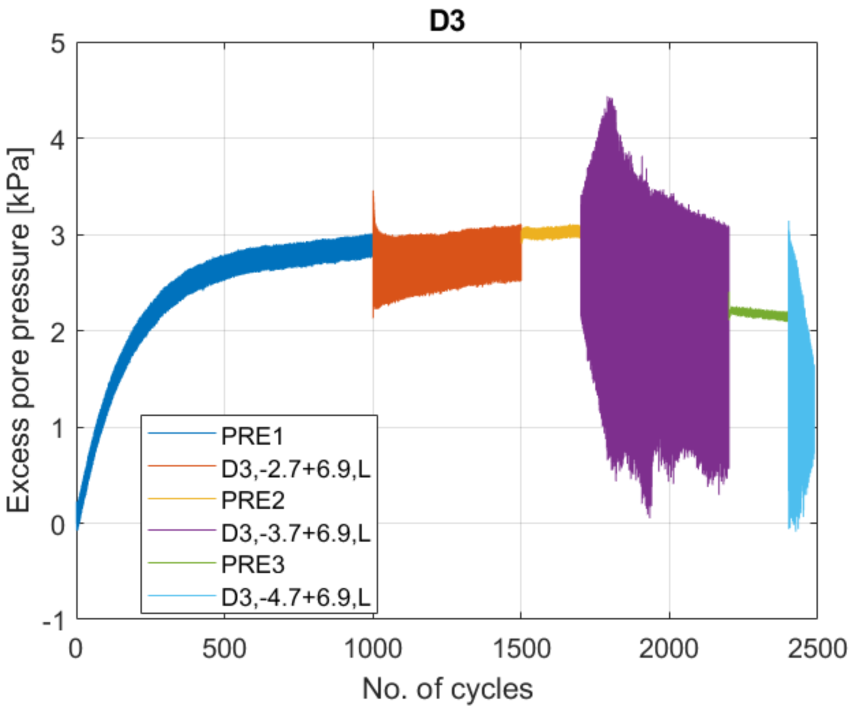

Figure D.209: Pore pressure at 1st level outer side transducer P7

2nd Level Transducers

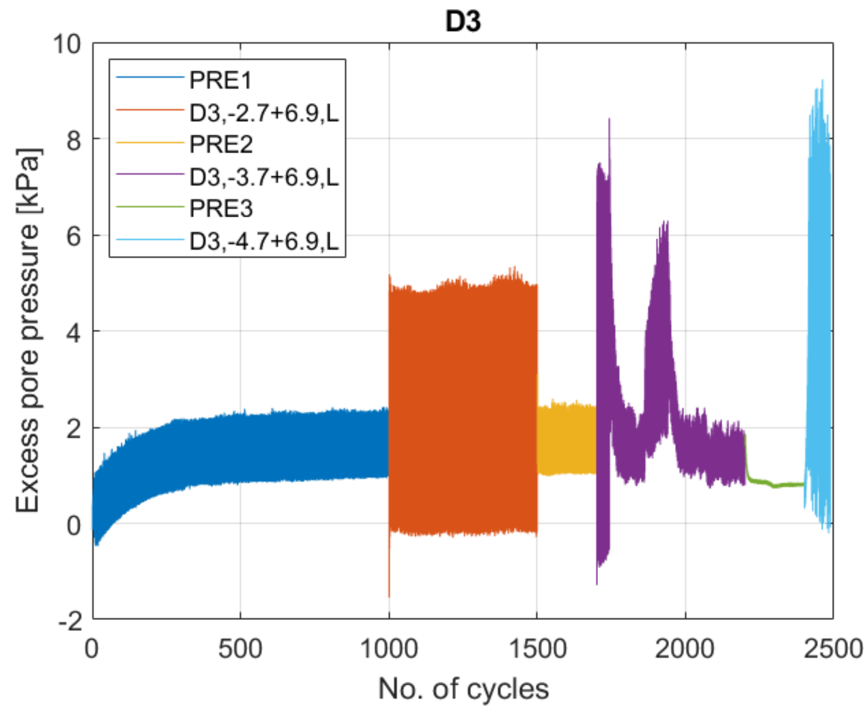

Figure D.210: Pore pressure at 2nd level inner side transducer P5

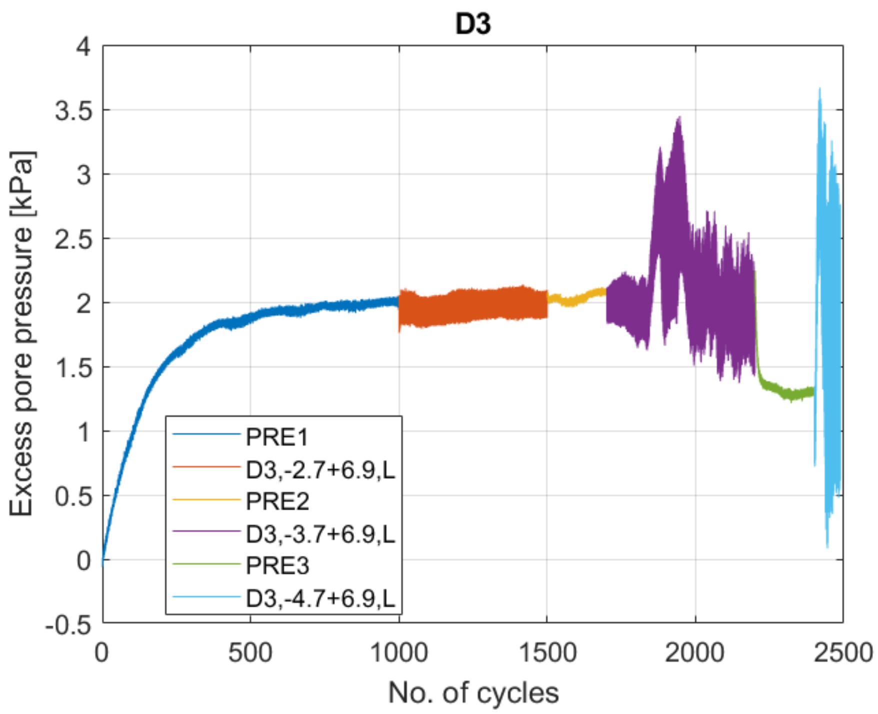

Figure D.211: Pore pressure at 2nd level inner side transducer P12

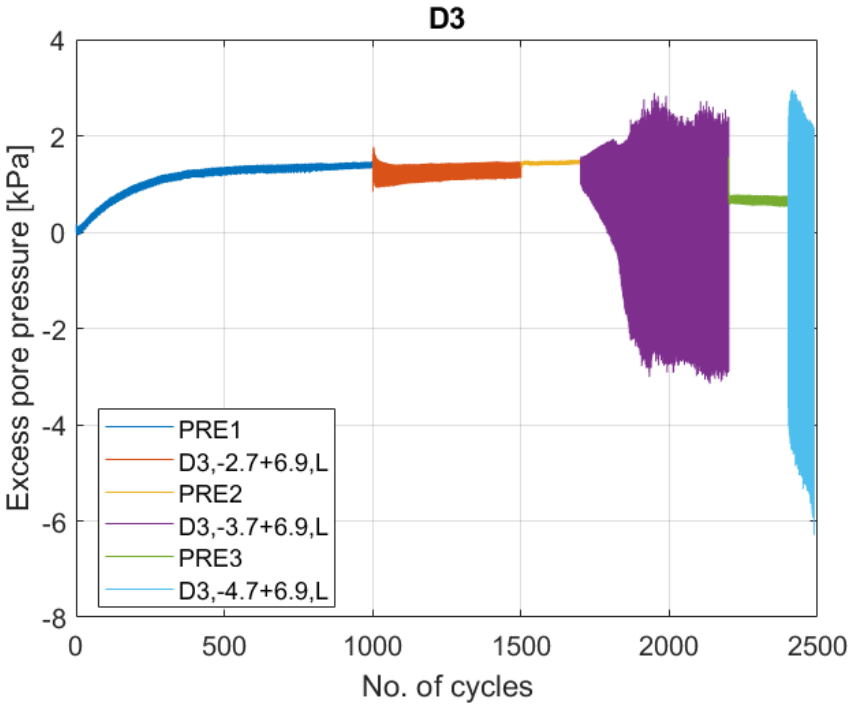

Figure D.212: Pore pressure at 2nd level outer side transducer P9

Skirt Tip Transducers

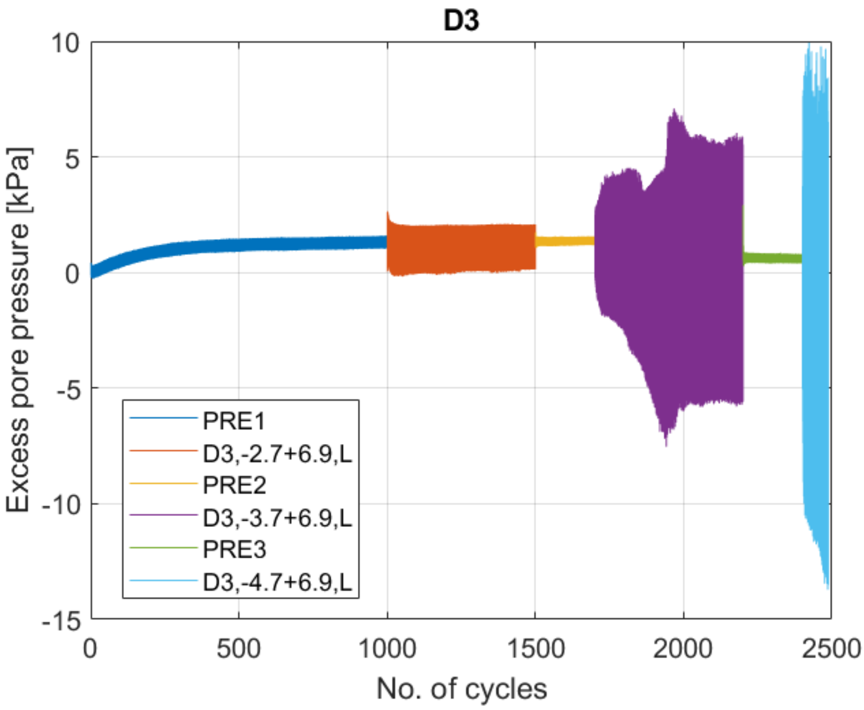

Figure D.213: Pore pressure at tip transducer P2

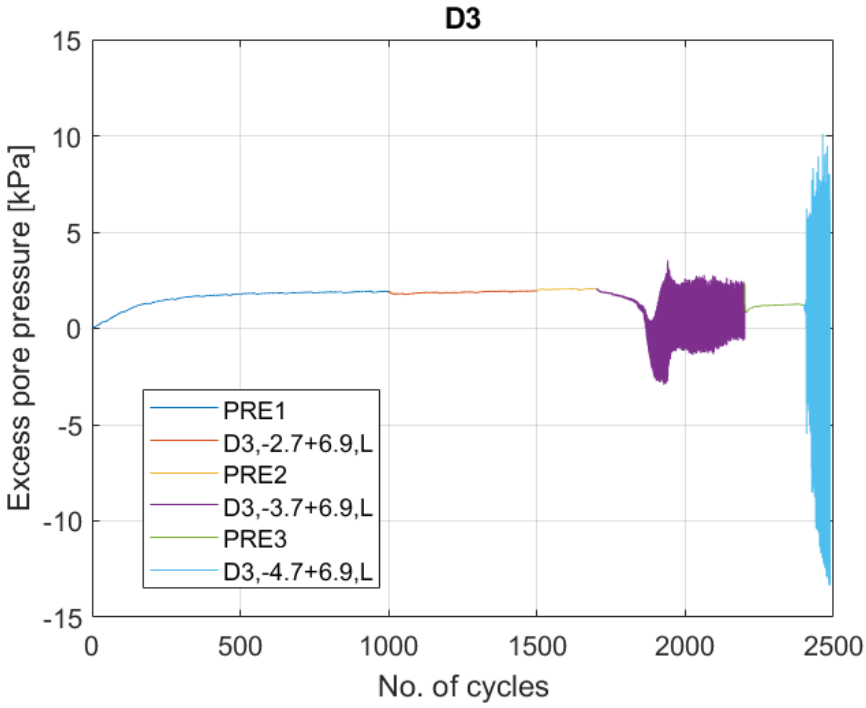

Figure D.214: Pore pressure at tip transducer P8

Force VS displacement

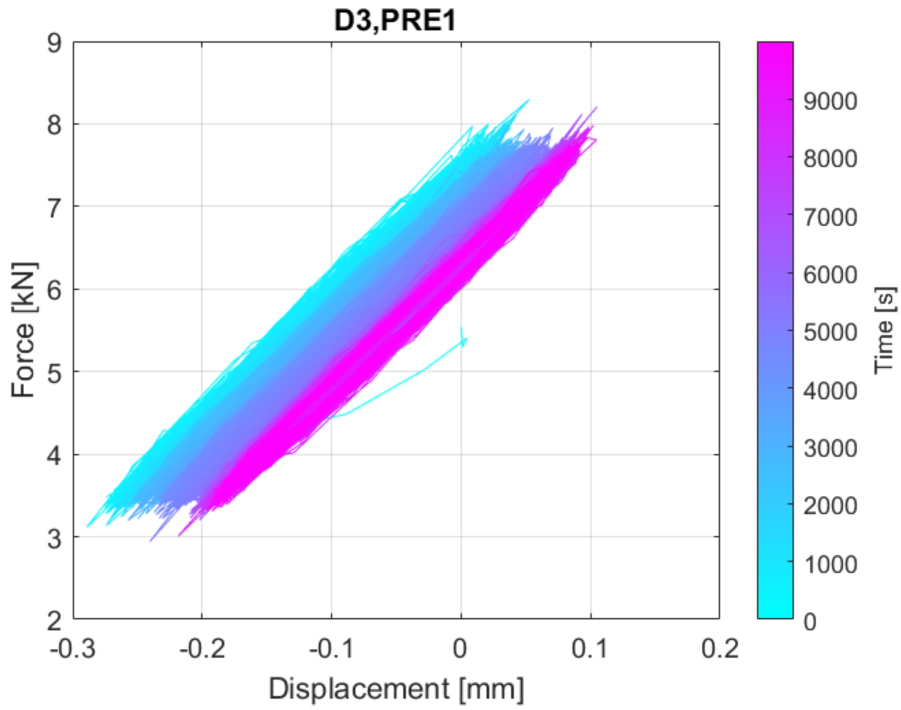

Figure D.215: Force VS absolute displacement

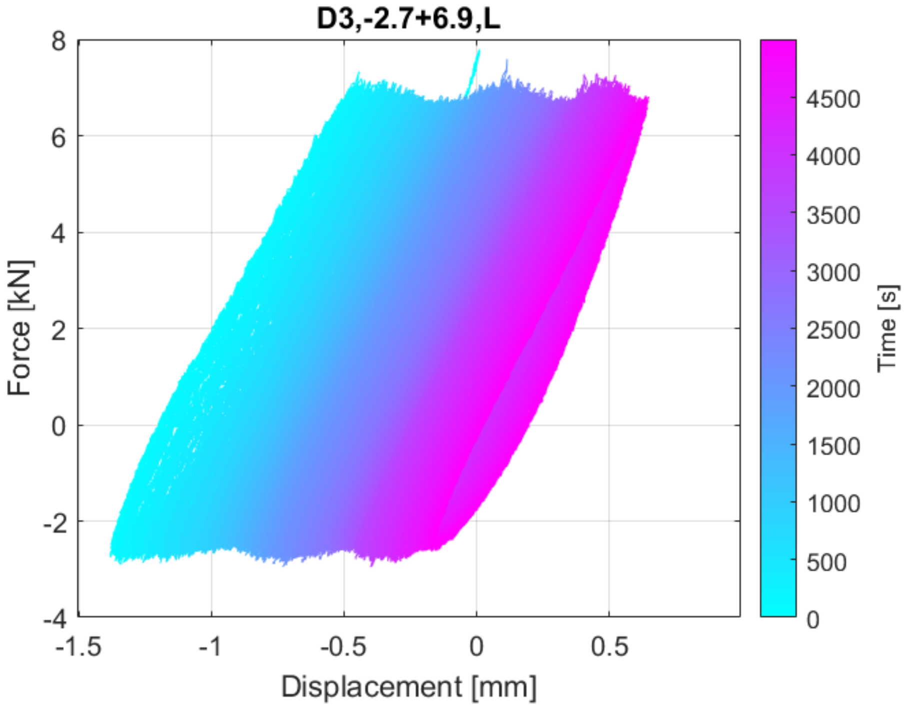

Figure D.216: Force VS absolute displacement

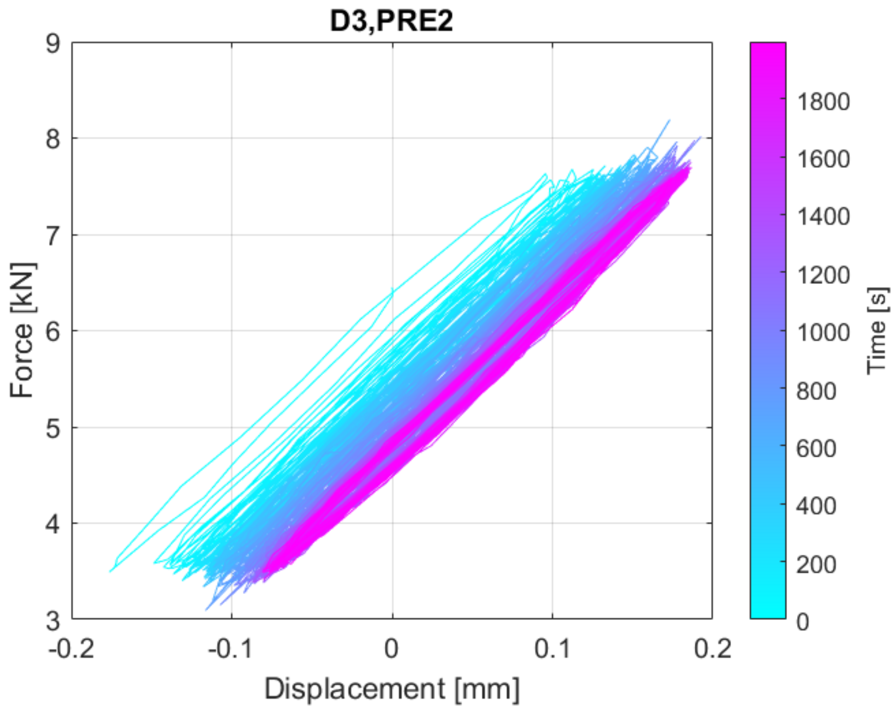

Figure D.217: Force VS absolute displacement

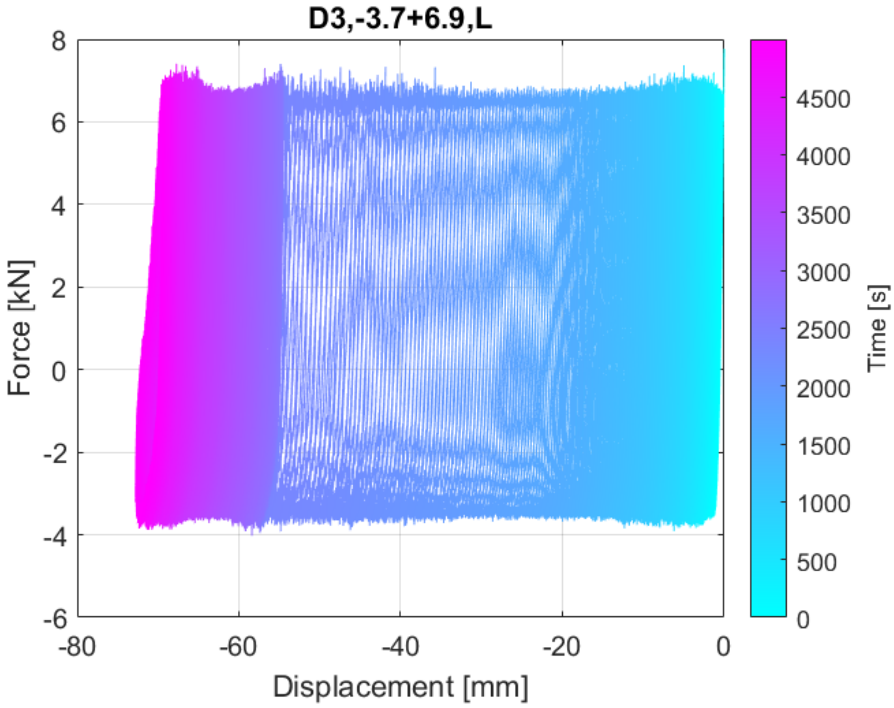

Figure D.218: Force VS absolute displacement

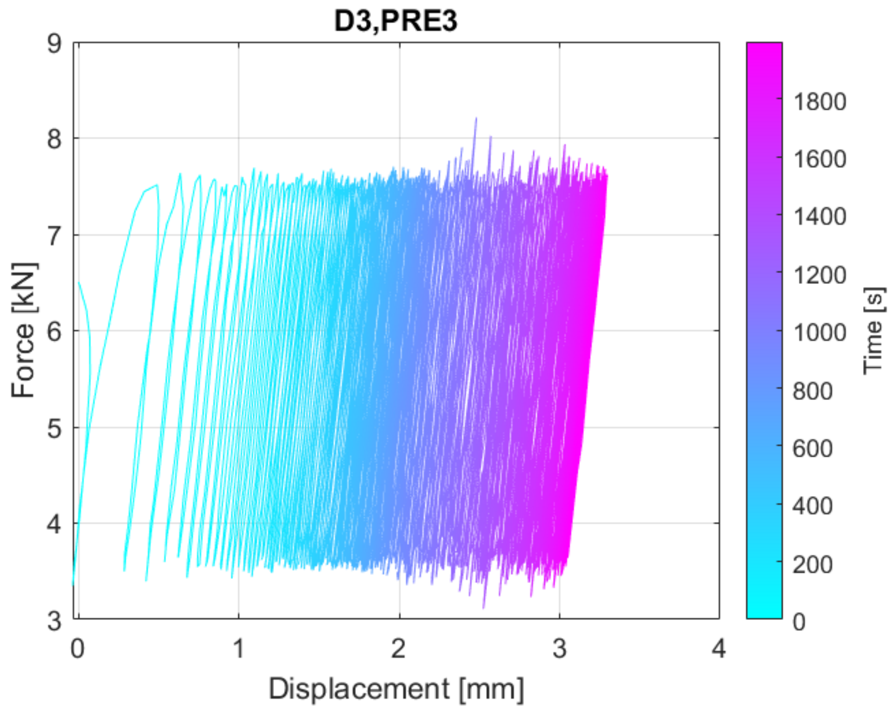

Figure D.219: Force VS absolute displacement

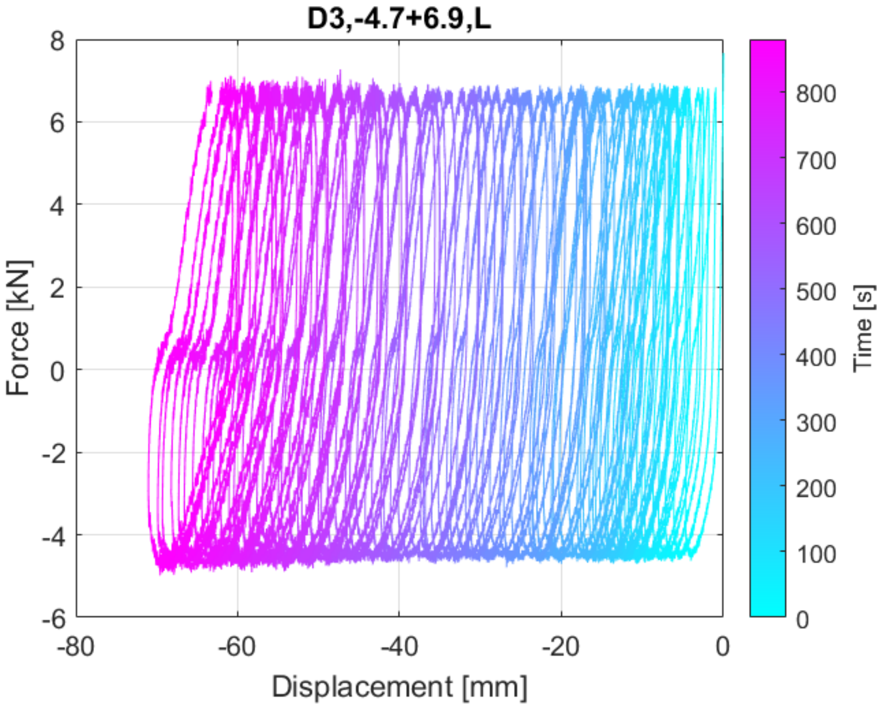

Figure D.220: Force VS absolute displacement

D.6 Test group E

Similar to the test conducted in section D.5 two way loading is tested. In the following results the compression force is changed to 3 kN, and ratio between tensile and compression for each event is kept as D.5 to investigate if the force has an influence on the bucket. 3 tests have been carried out where the following frequencies are used 0.1 Hz, 1 Hz and 0.5 Hz, the precycle is kept with a frequency of 0.1 Hz. The loading plan for all three tests are shown in table D.7 as well as in figure D.221.

Table D.7: Loading plan for 'Test group E'

Packet No.	Conditions	Force command F_{min} [kN]	F_{max} [kN]	Force ratio	Cycle No.	Frequency [Hz]
1	Normal	4.0	6.0	0.67	1000	0.1
2	Severe	-1.2	3.0	-0.40	500	0.1, 0.5, 1.0
3	Normal	4.0	6.0	0.67	200	0.1
4	Severe	-1.8	3.0	-0.60	500	0.1, 0.5, 1.0
5	Normal	4.0	6.0	0.67	200	0.1
6	Severe	-2.4	3.0	-0.80	500	0.1, 0.5, 1.0
7	Normal	4.0	6.0	0.67	200	0.1
8	Severe	-3.0	3.0	-1.00	500	0.1, 0.5, 1.0
9	Normal	4.0	6.0	0.67	200	0.1
10	Severe	-3.6	3.0	-1.20	500	0.1, 0.5, 1.0

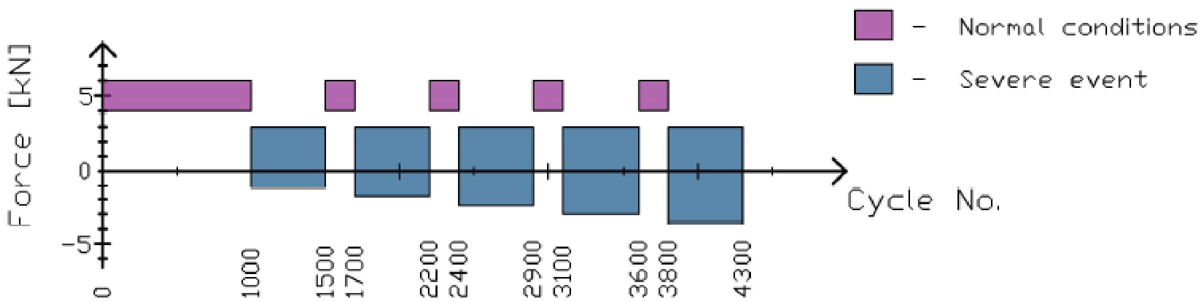

Figure D.221: Scheduled loading plan for Test group E

D.6.1 Test subgroup E1 - 0.1 Hz

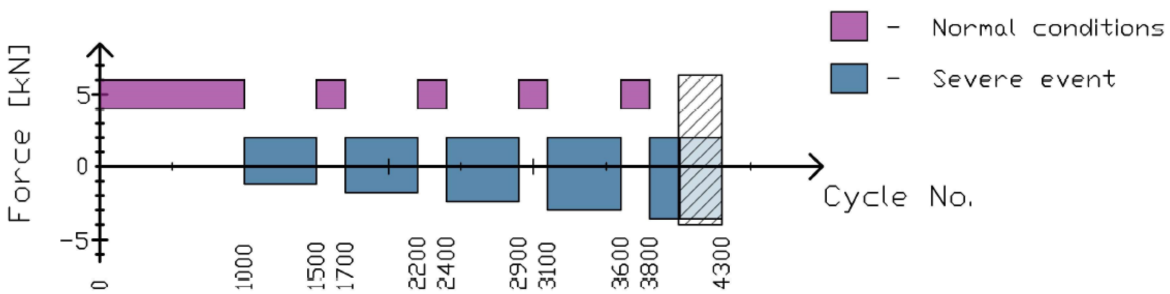

Figure D.222: Actual loading plan for Test subgroup E1

CPT

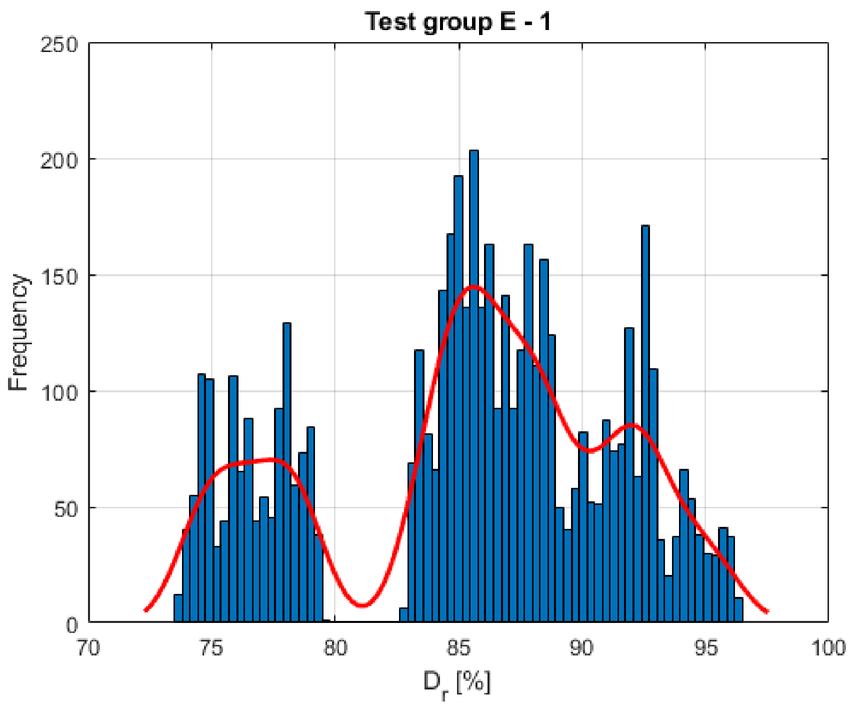

Figure D.223: Dr histogram with distribution fit for test subgroup E1

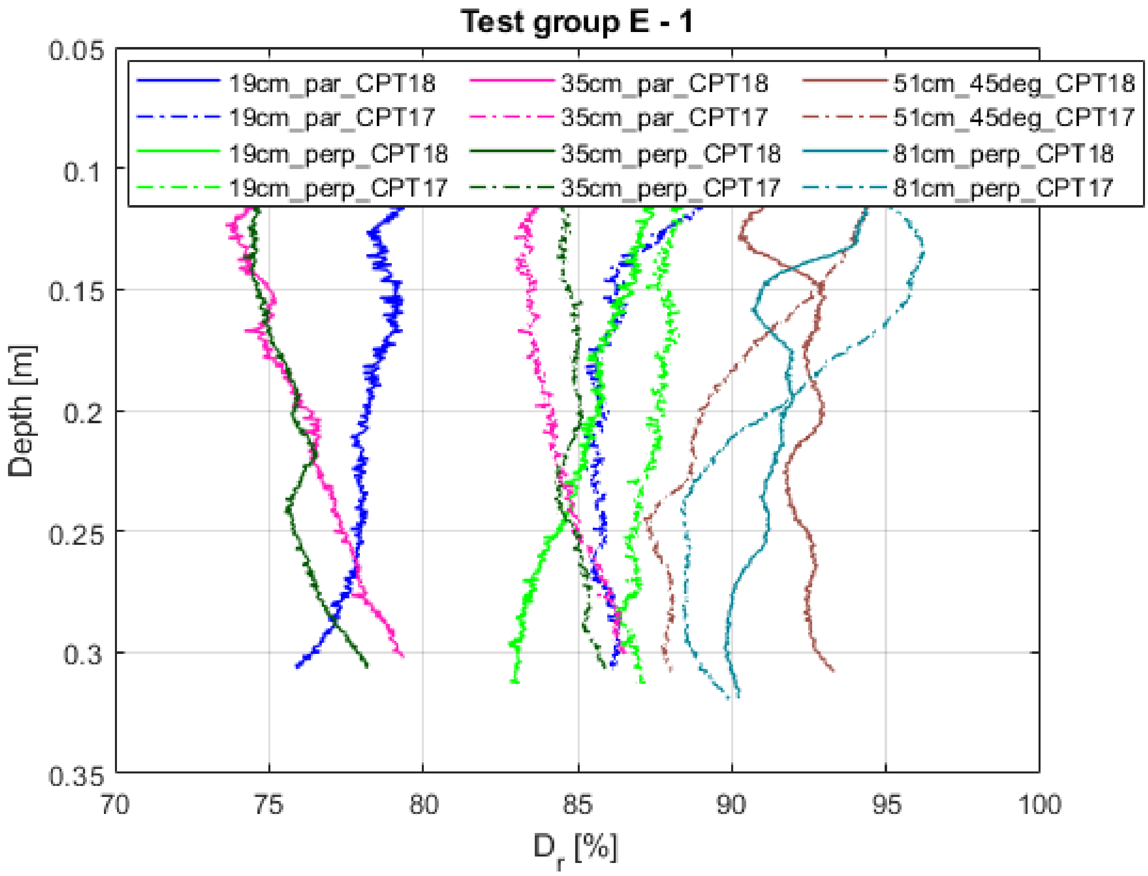

Figure D.224: Test-specific Dr results for CPT test subgroup E1

Force and displacement

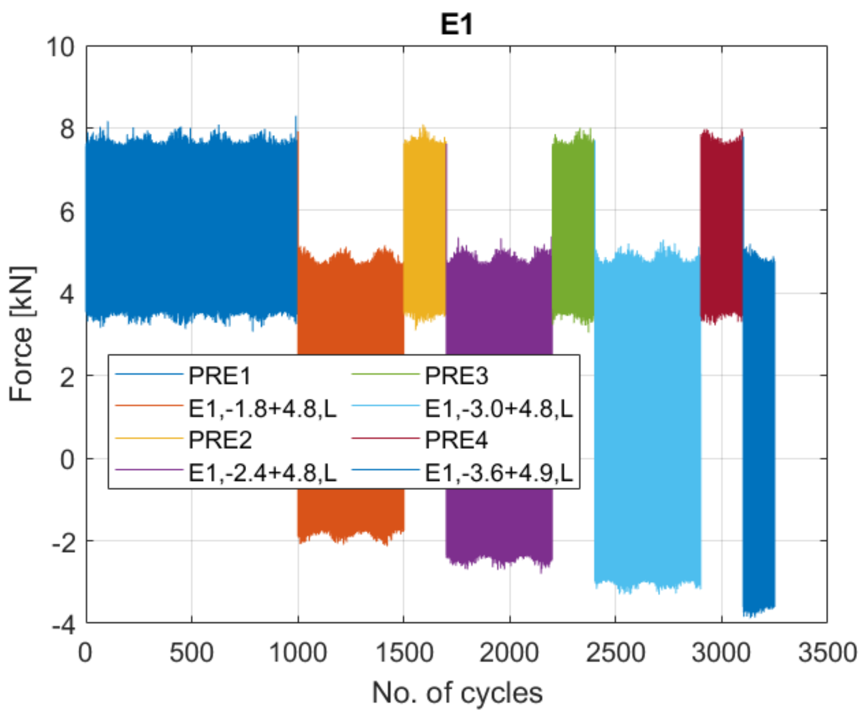

Figure D.225: Force VS No. of cycles

Looking at the amplitude and maximum and minimum forces from D.225, and comparing it to table D.7, its clear to see, that the loading exceeds the planned loading for the test. For the precycle and load cycles at some points it reaches a value of 2 kN higher than wanted. That might be explained by precision of the machinery. These loads used during the test are relatively small compared to the load transducer with capability of 100 kN which was used for the test, so errors between command and actual force are expected.

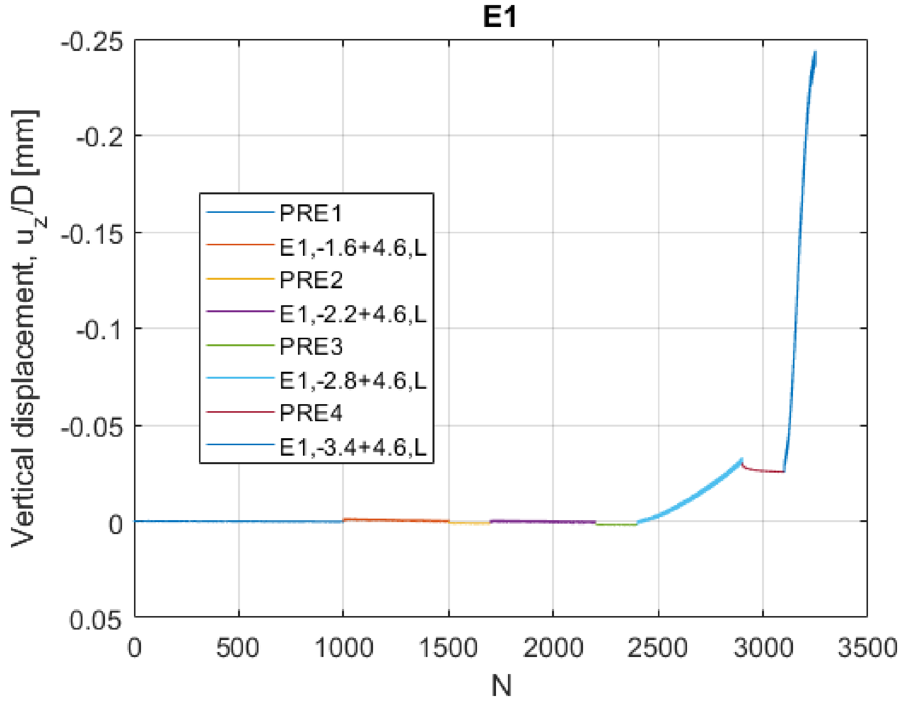

Figure D.226: Displacement VS No. of cycles

From the plot above, it is clear that the bucket does not settle significantly in the first two load cycles where as in the third cycle, the soil starts to lose its strength, and loses the grip of the bucket and it moves upwards, and in the forth cycle the soil complete loses the strength and reaches the upper limit, which is an upward absolute displacement of 120 mm from the starting position.

Lid Transducers

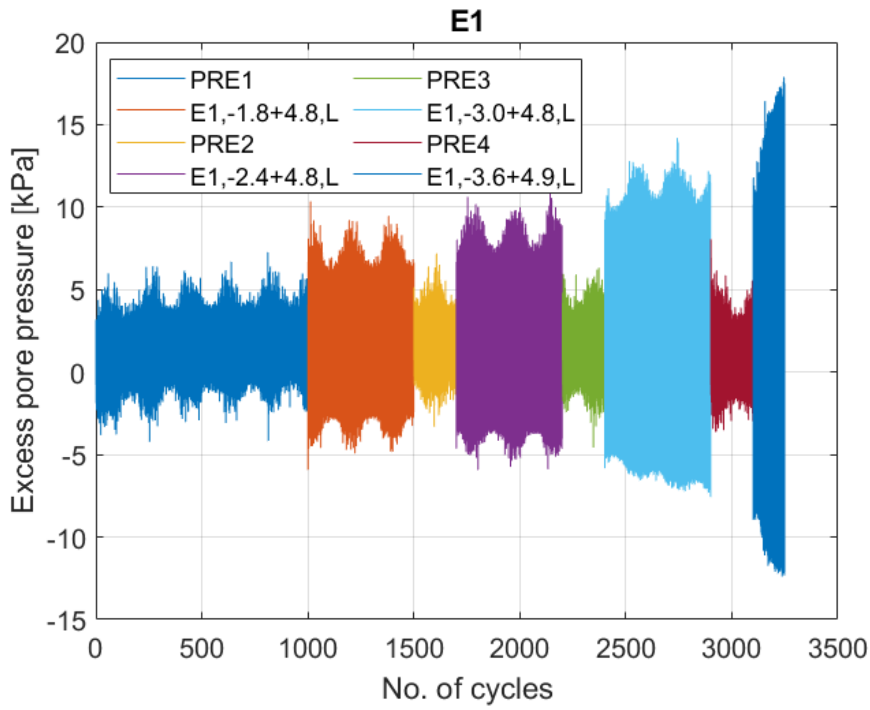

Figure D.227: Pore pressure at lid transducer P6

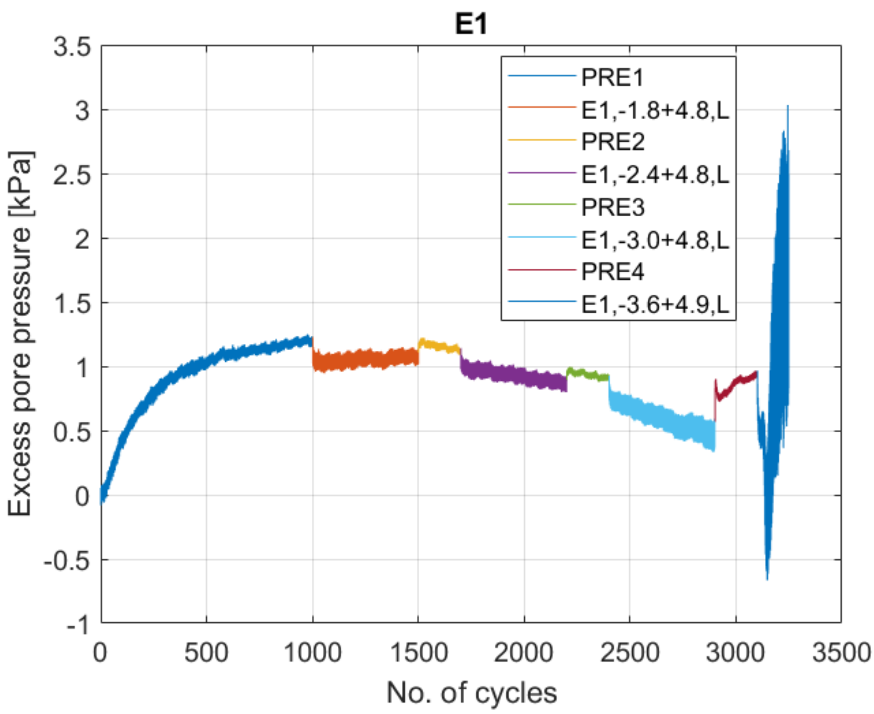

Figure D.228: Pore pressure at lid transducer P10

1st Level Transducers

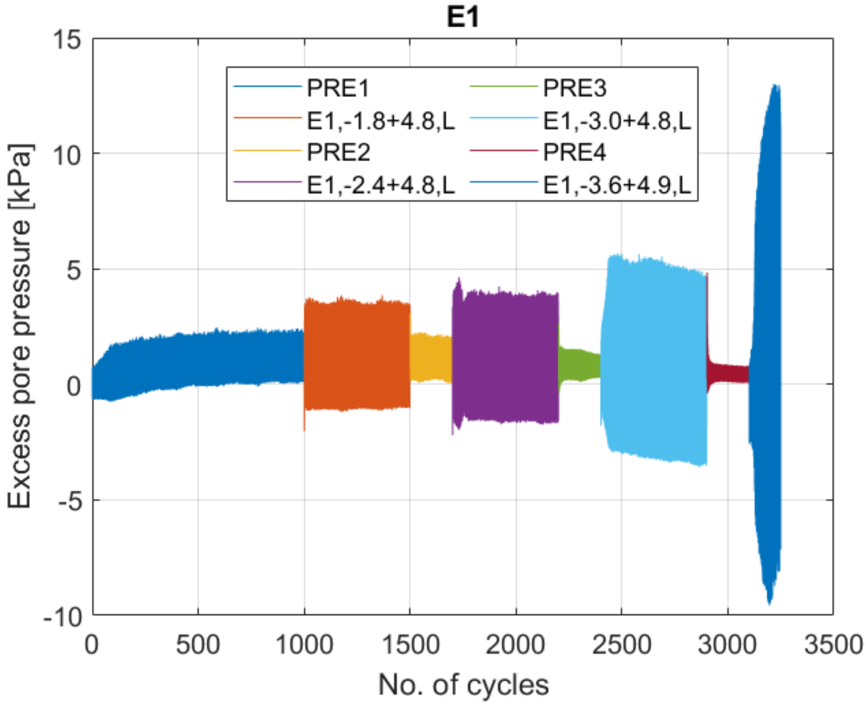

Figure D.229: Pore pressure at 1st level inner side transducer P4

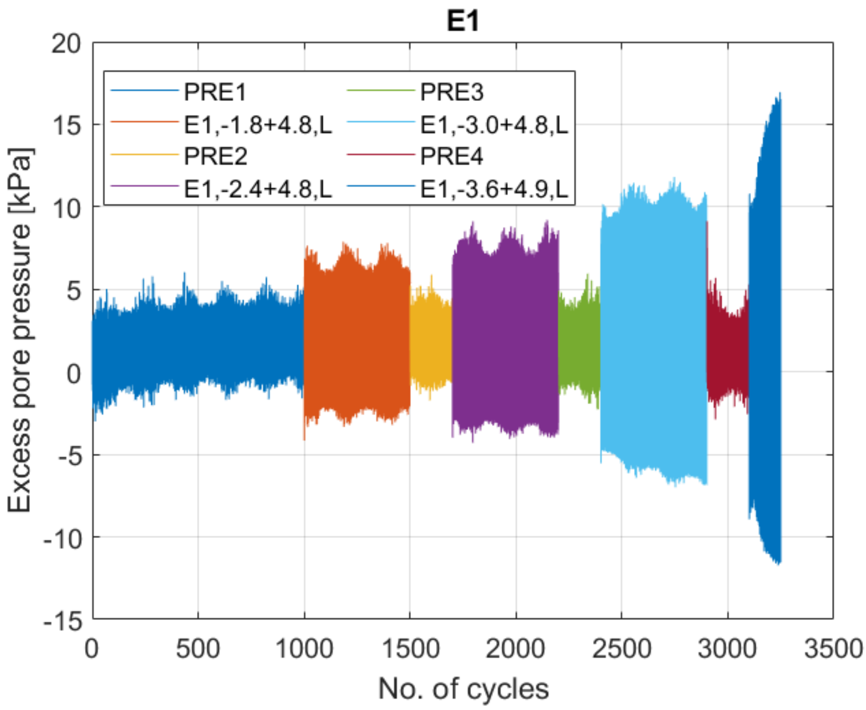

Figure D.230: Pore pressure at 1st level inner side transducer P11

2nd Level Transducers

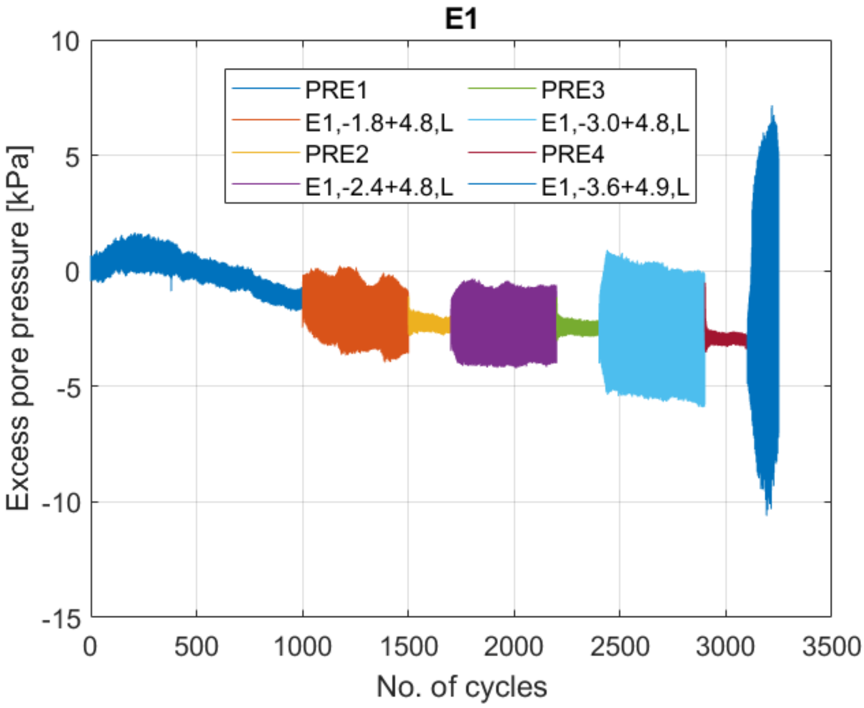

Figure D.231: Pore pressure at 2nd level inner side transducer P5

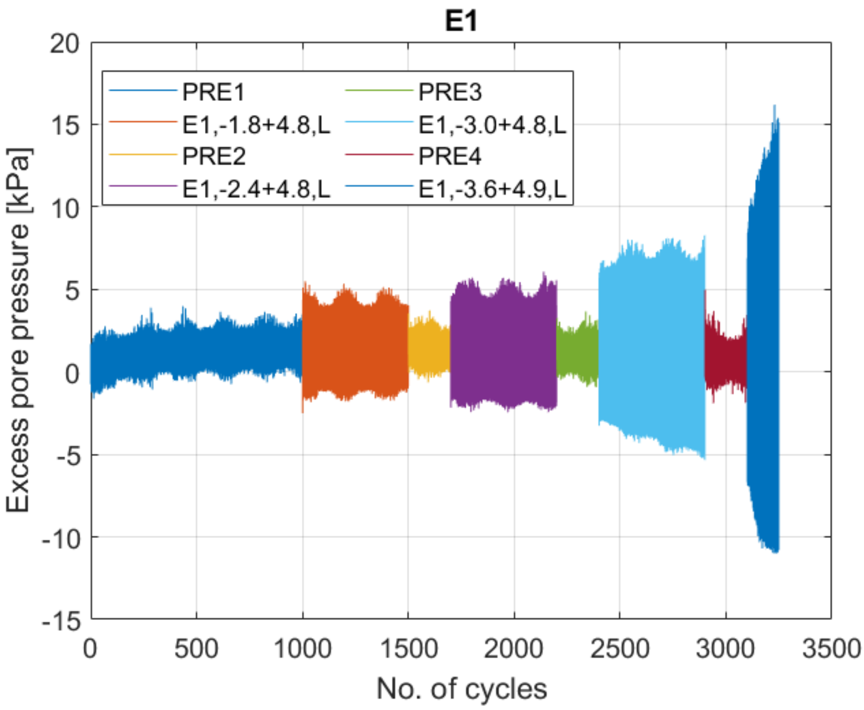

Figure D.232: Pore pressure at 2nd level inner side transducer P12

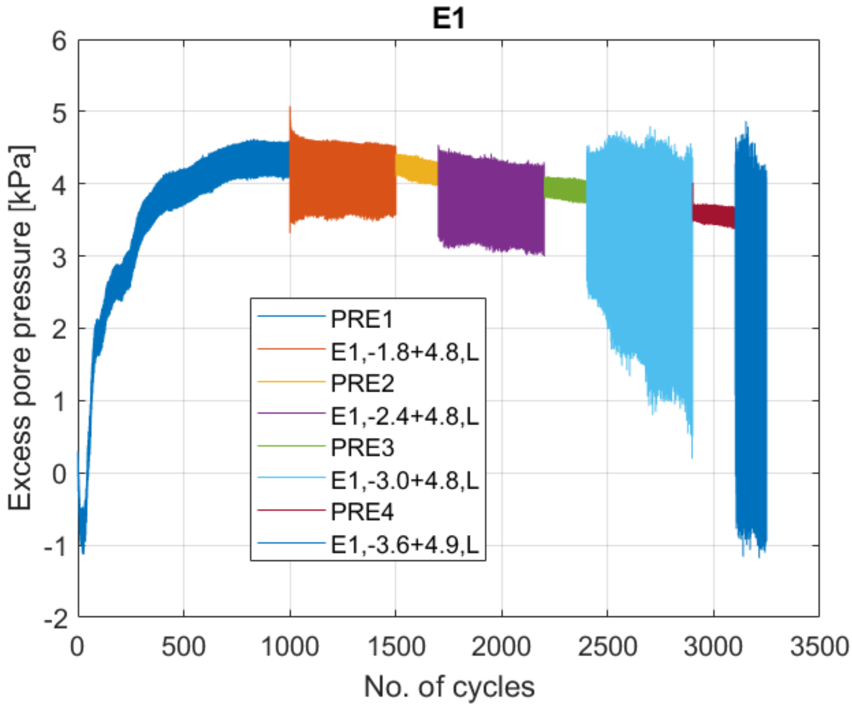

Figure D.233: Pore pressure at 2nd level outer side transducer P1

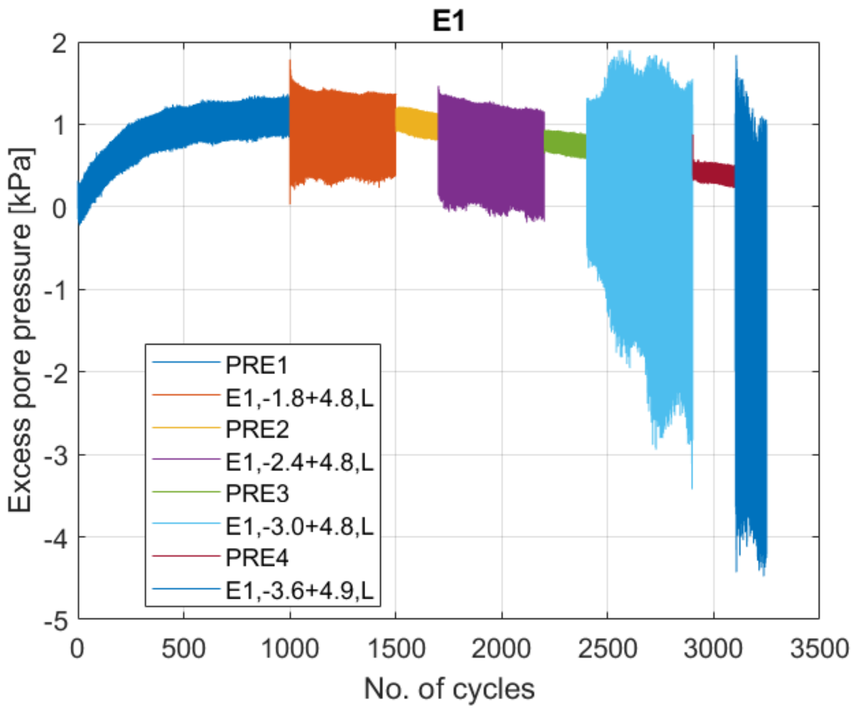

Figure D.234: Pore pressure at 2nd level outer side transducer P9

Skirt Tip Transducers

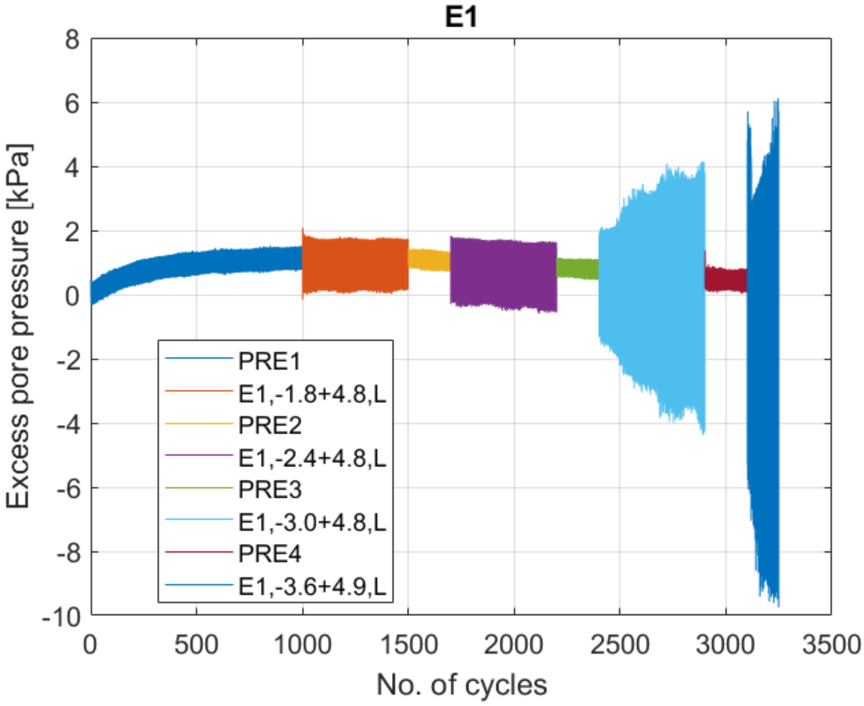

Figure D.235: Pore pressure at tip transducer P2

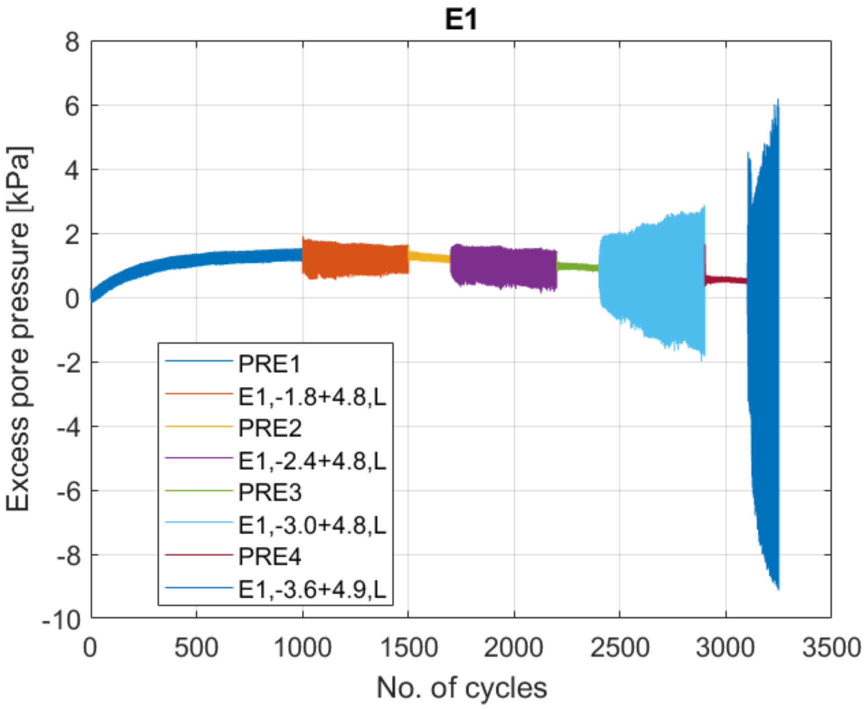

Figure D.236: Pore pressure at tip transducer P8

Force VS displacement

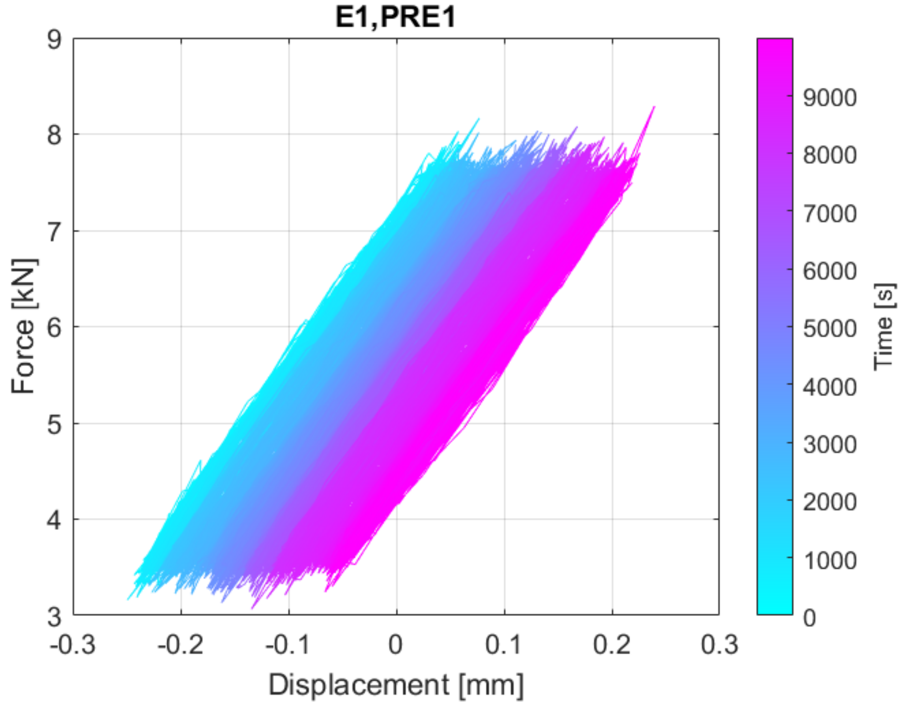

Figure D.237: Force VS absolute displacement

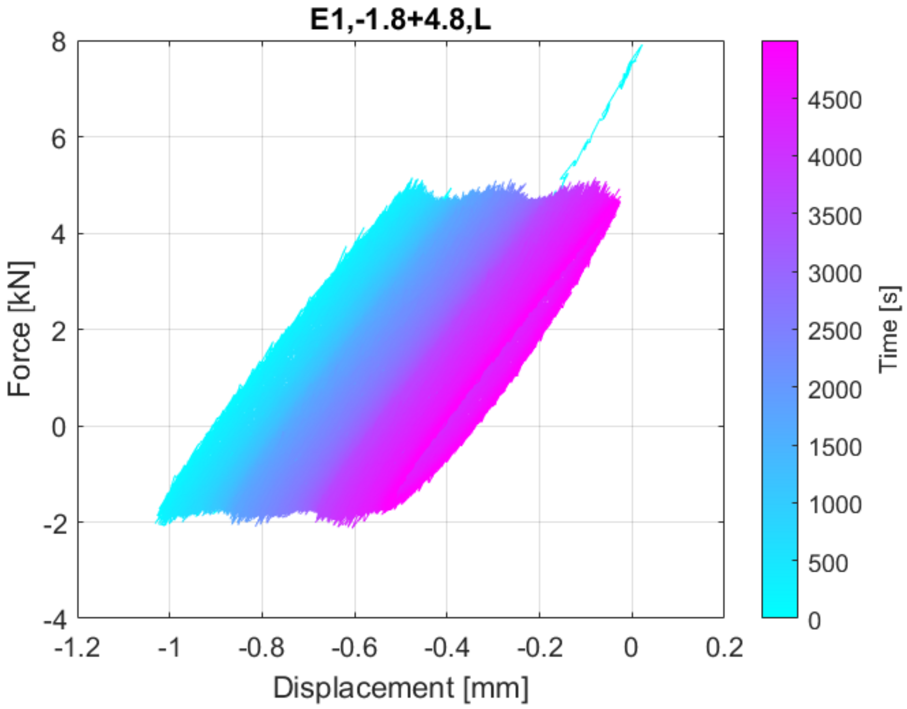

Figure D.238: Force VS absolute displacement

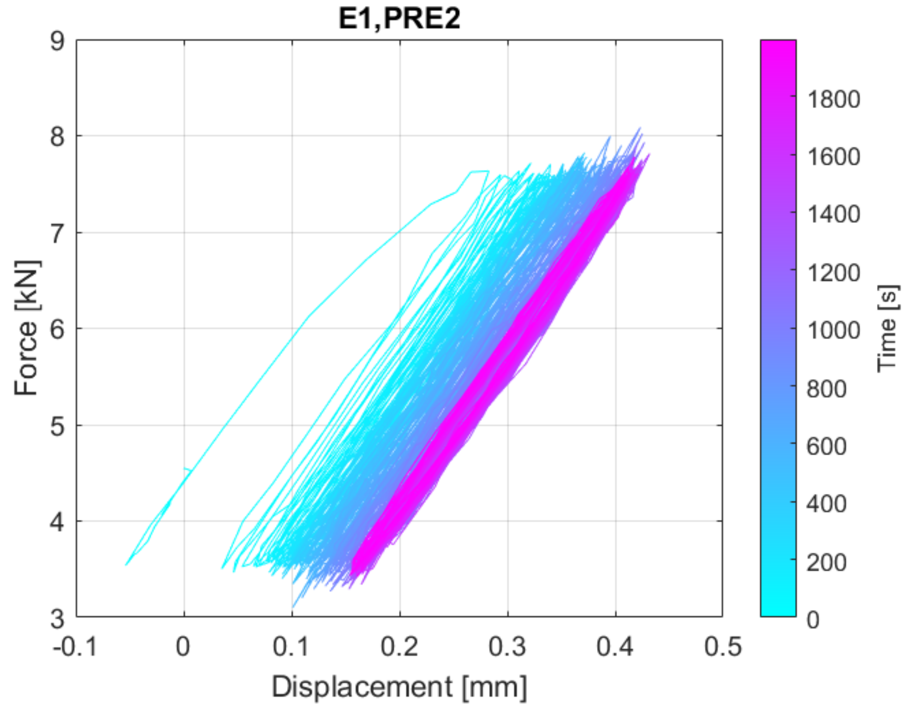

Figure D.239: Force VS absolute displacement

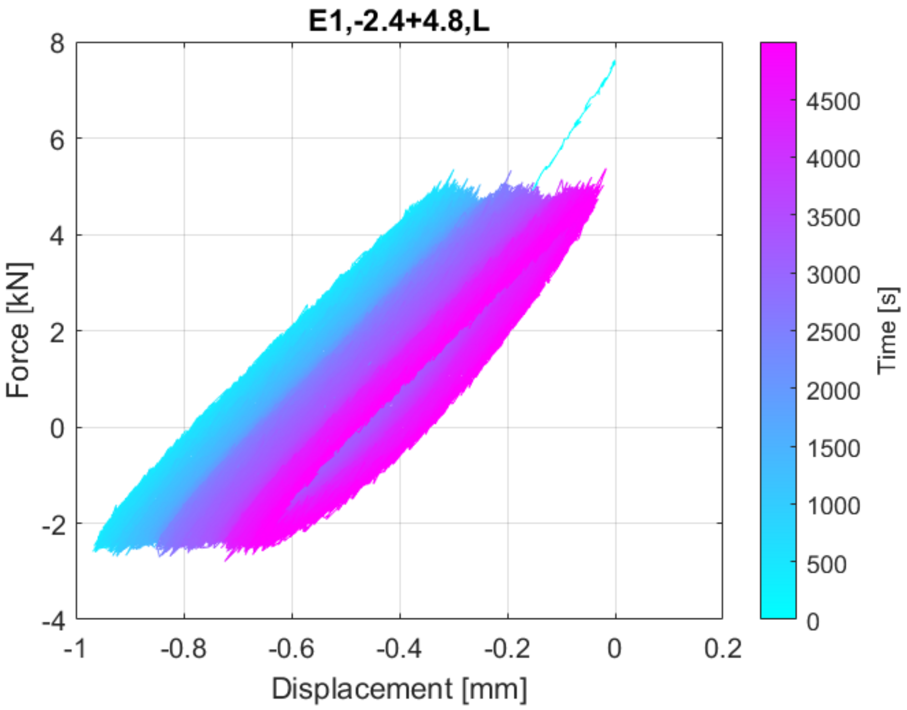

Figure D.240: Force VS absolute displacement

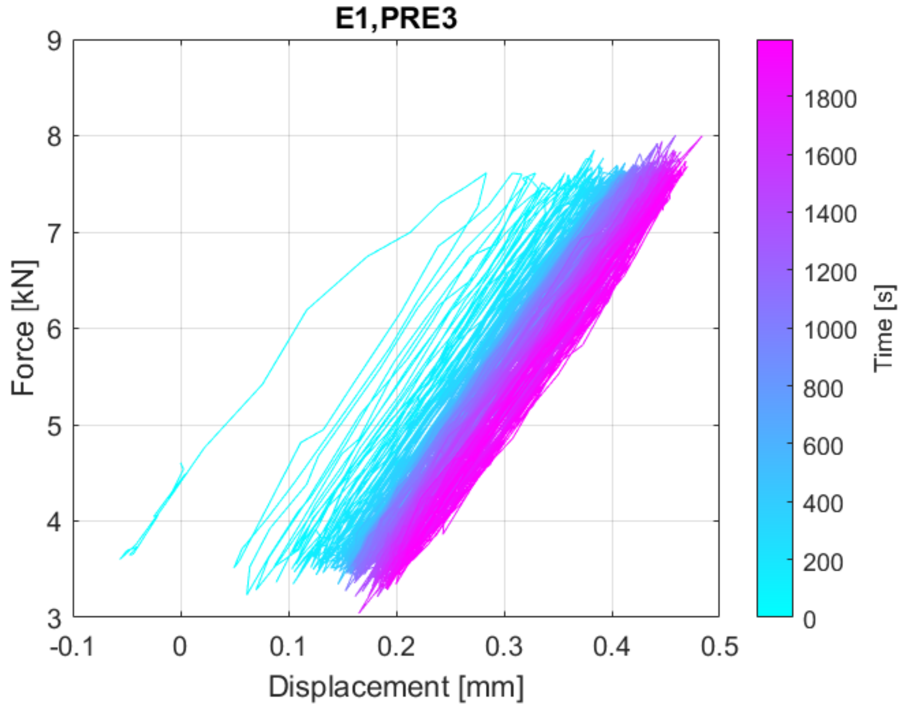

Figure D.241: Force VS absolute displacement

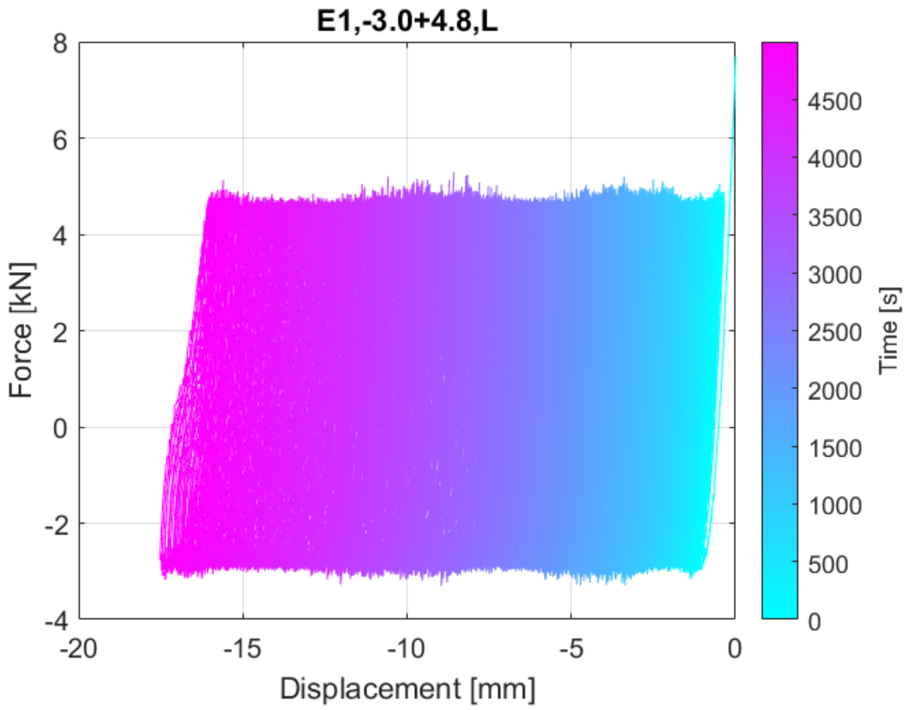

Figure D.242: Force VS absolute displacement

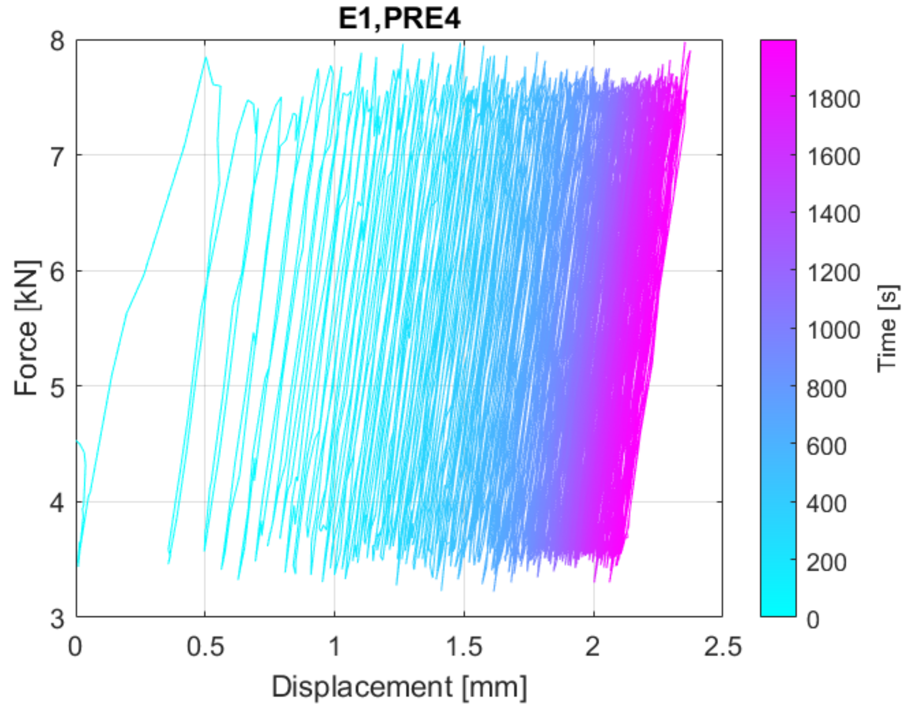

Figure D.243: Force VS absolute displacement

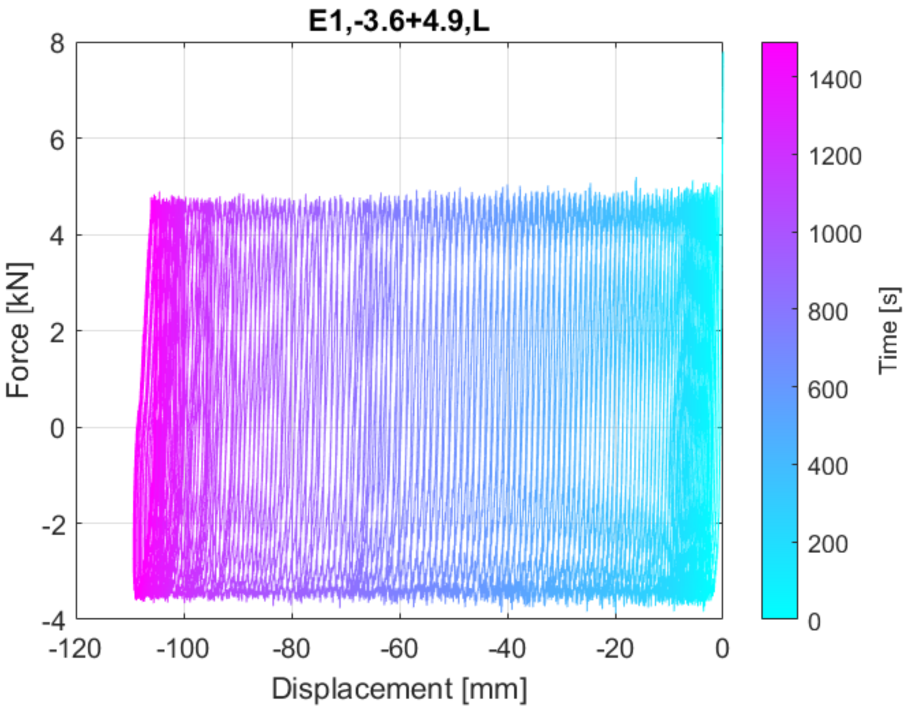

Figure D.244: Force VS absolute displacement

D.6.2 Test subgroup E2 - 1.0 Hz

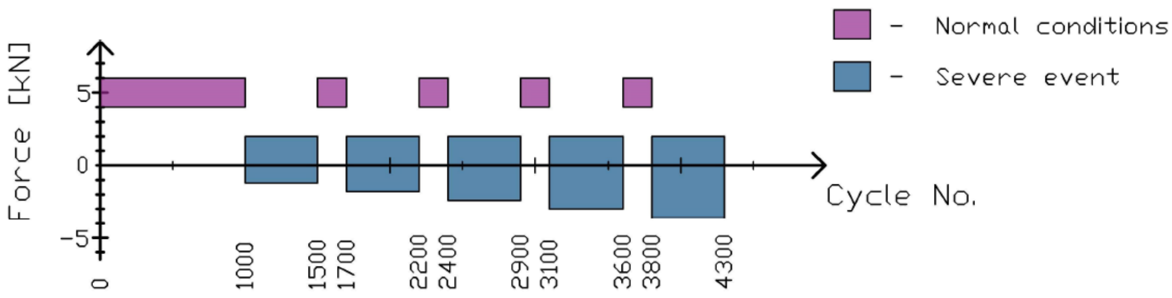

Figure D.245: Actual loading plan for Test subgroup E2

CPT

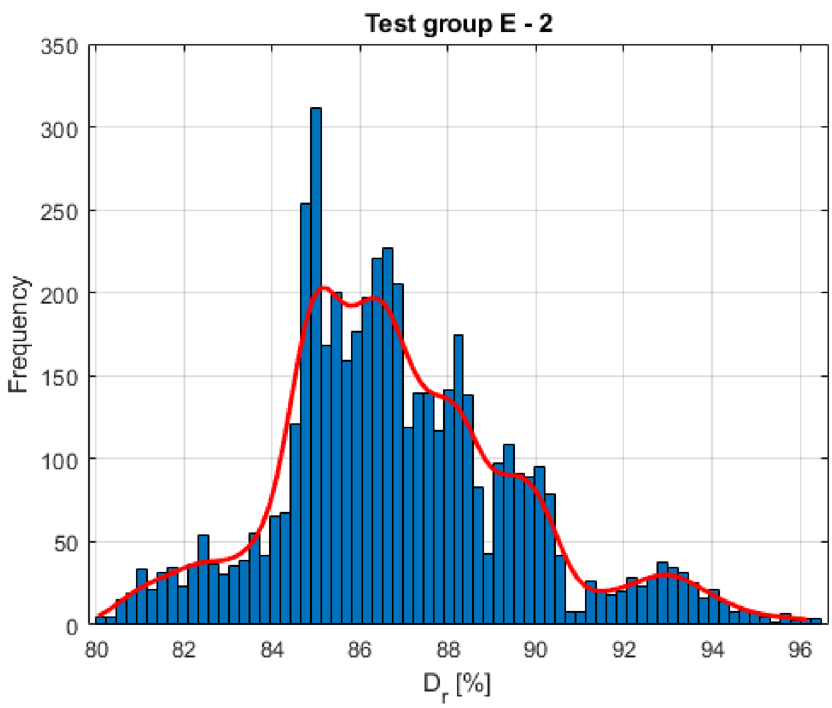

Figure D.246: Dr histogram with distribution fit for test subgroup E2

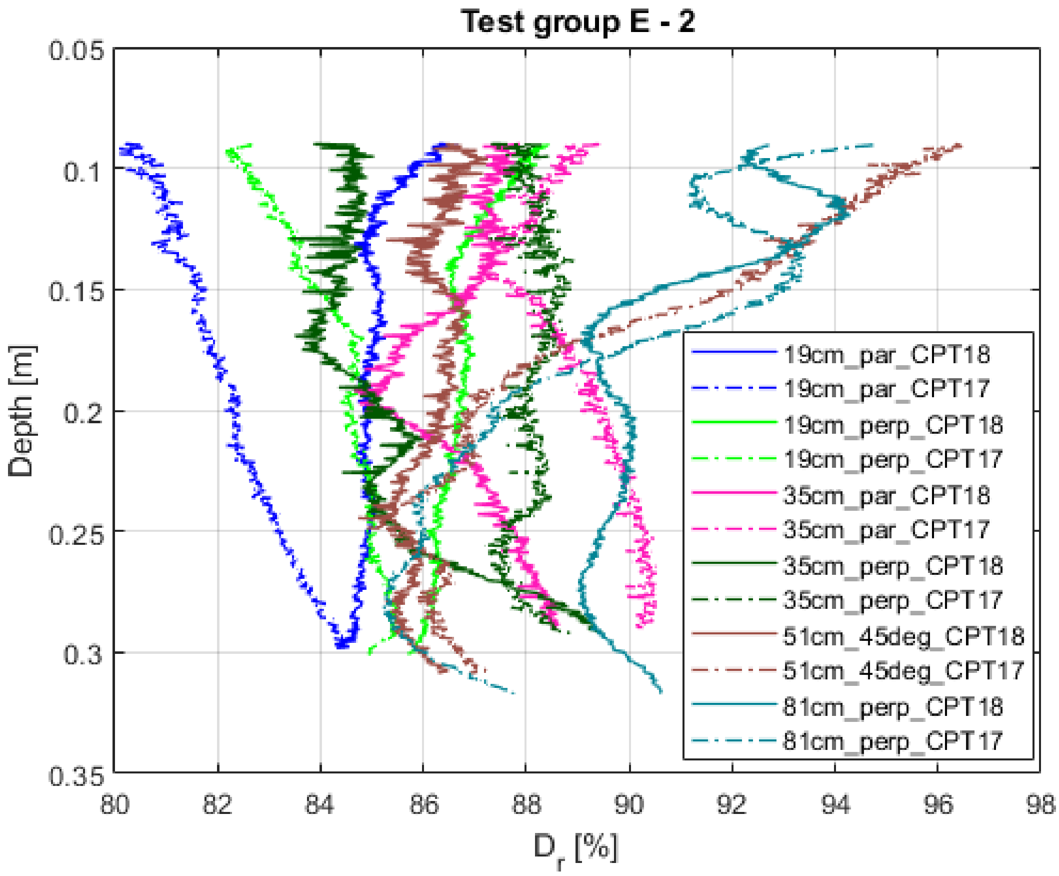

Figure D.247: Test-specific Dr results for CPT test subgroup E2

Force and displacement

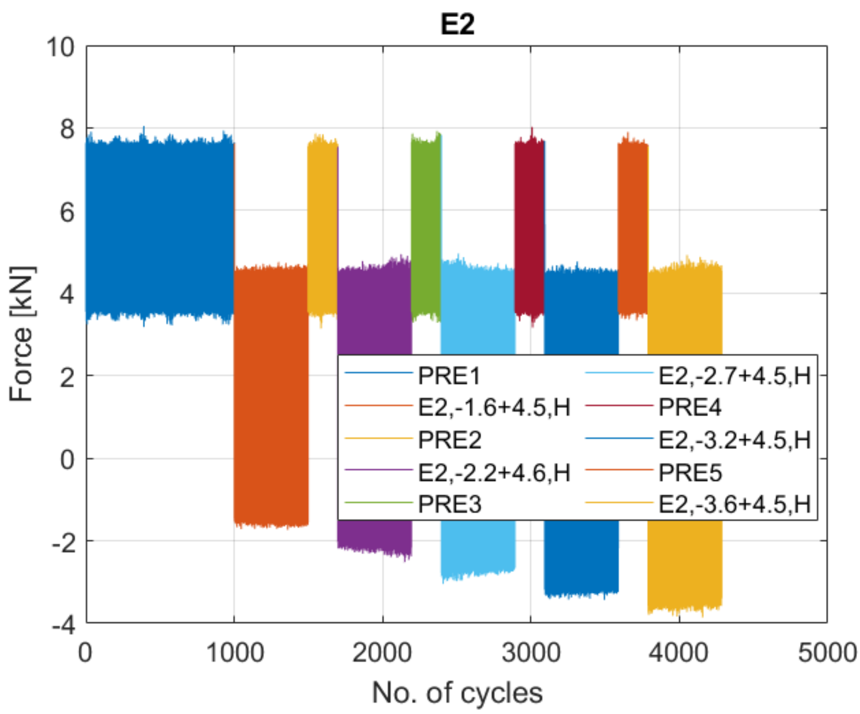

Figure D.248: Force VS No. of cycles

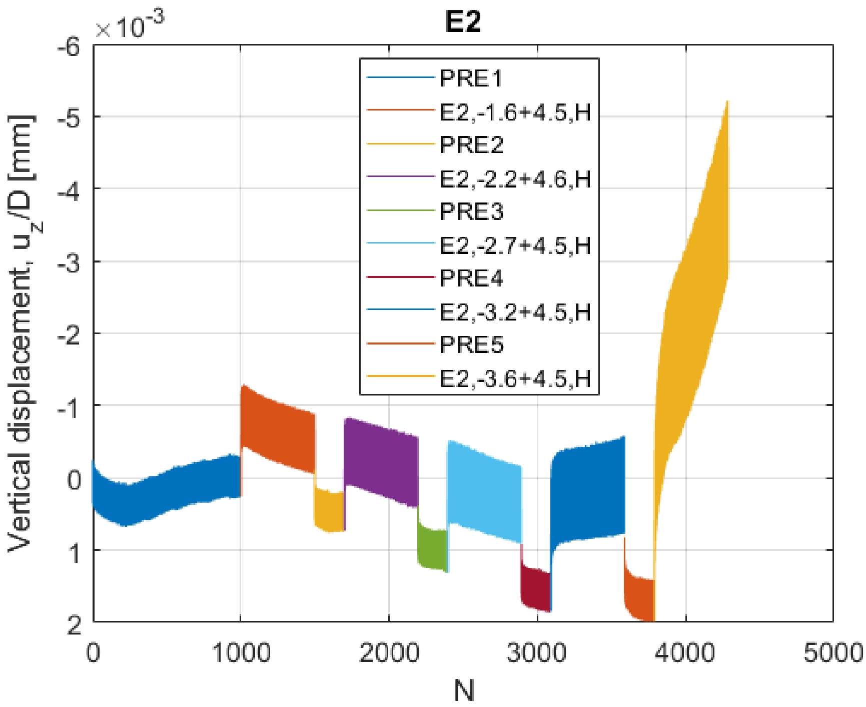

Figure D.249: Displacement VS No. of cycles

Lid Transducers

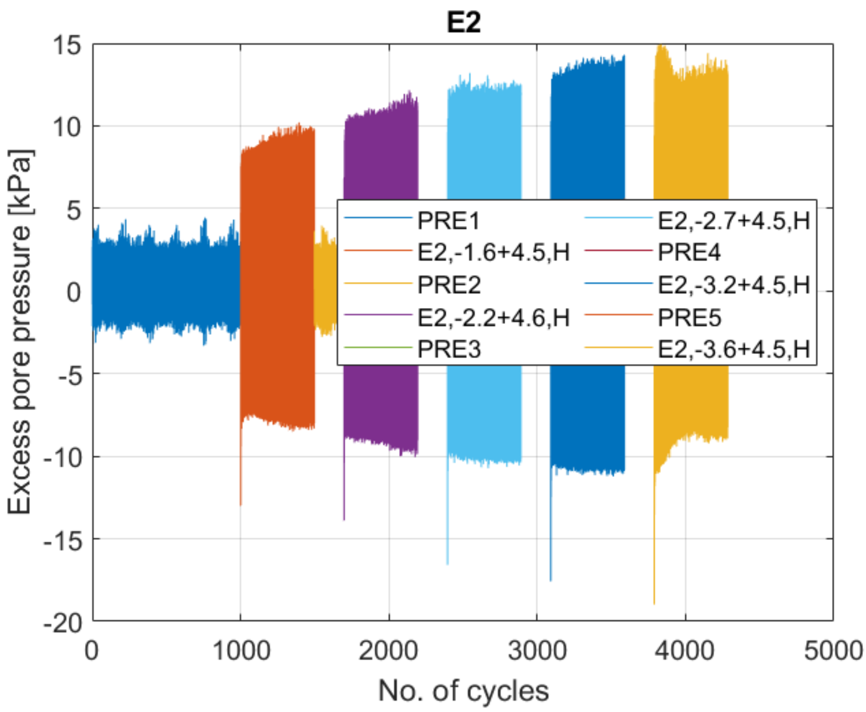

Figure D.250: Pore pressure at lid transducer P6

1st Level Transducers

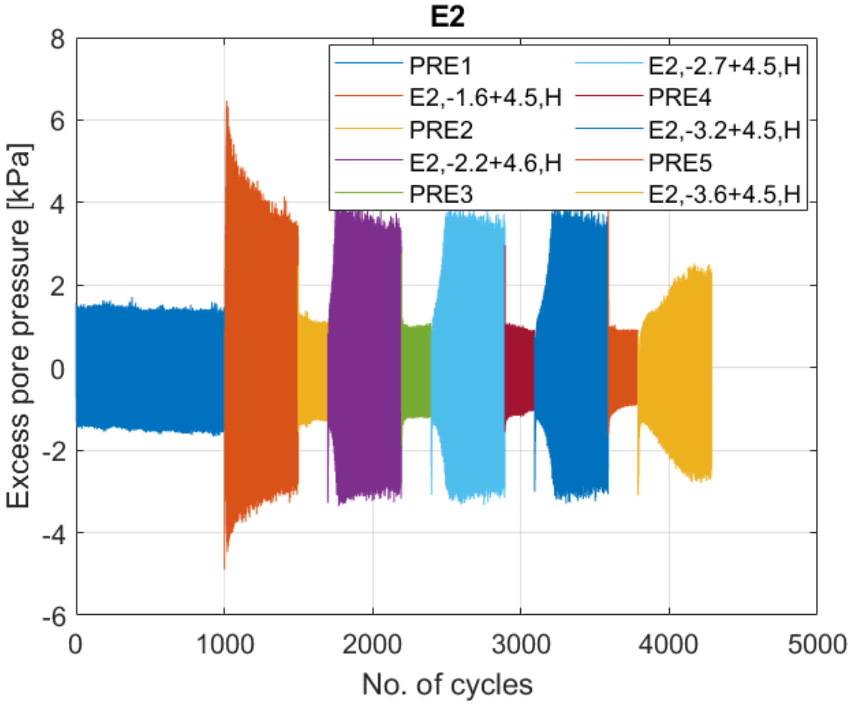

Figure D.251: Pore pressure at 1st level inner side transducer P4

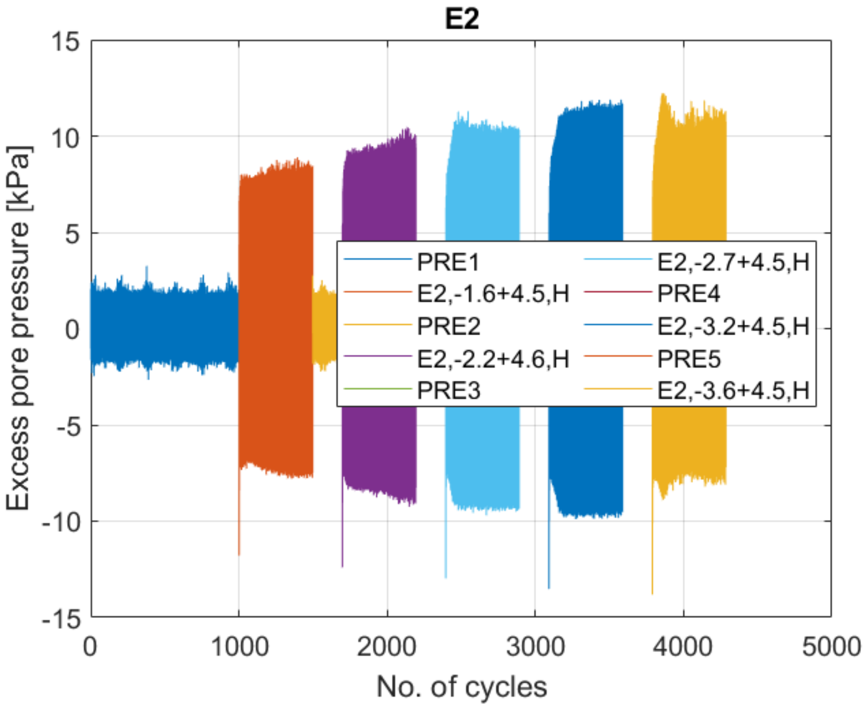

Figure D.252: Pore pressure at 1st level inner side transducer P11

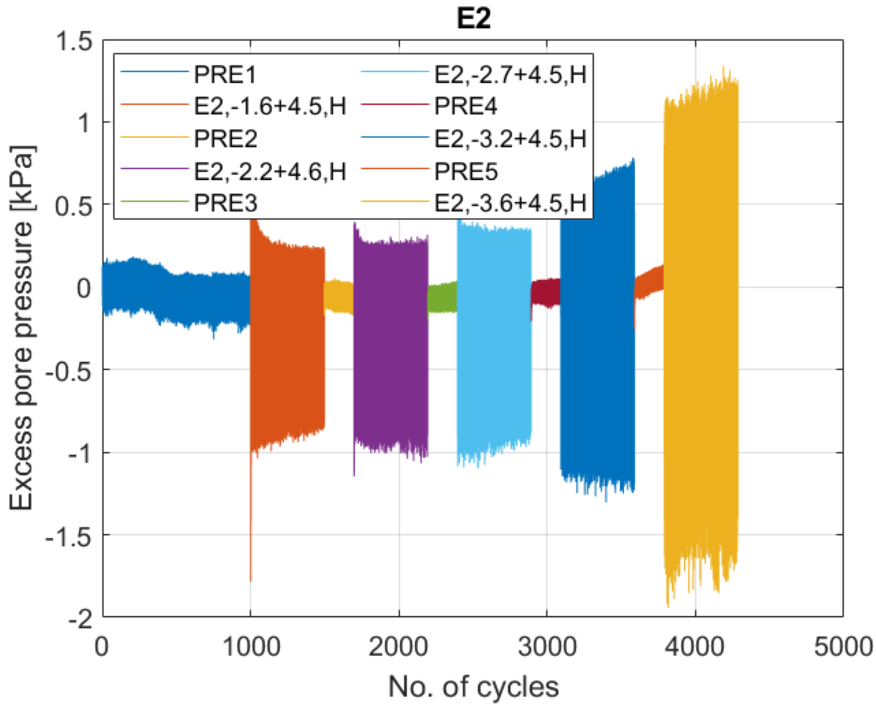

Figure D.253: Pore pressure at 1st level outer side transducer P3

2nd Level Transducers

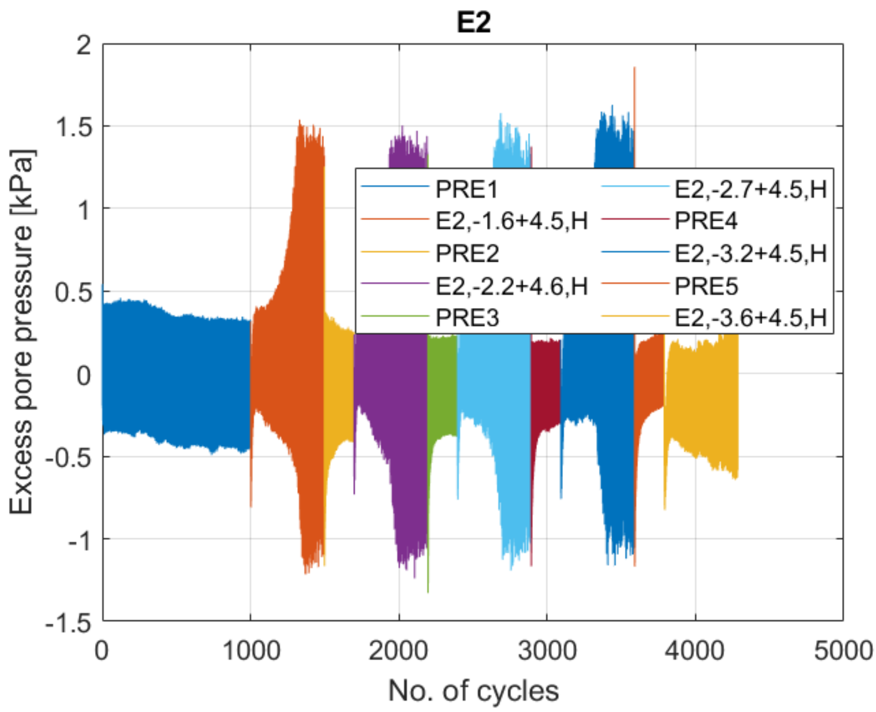

Figure D.254: Pore pressure at 2nd level inner side transducer P5

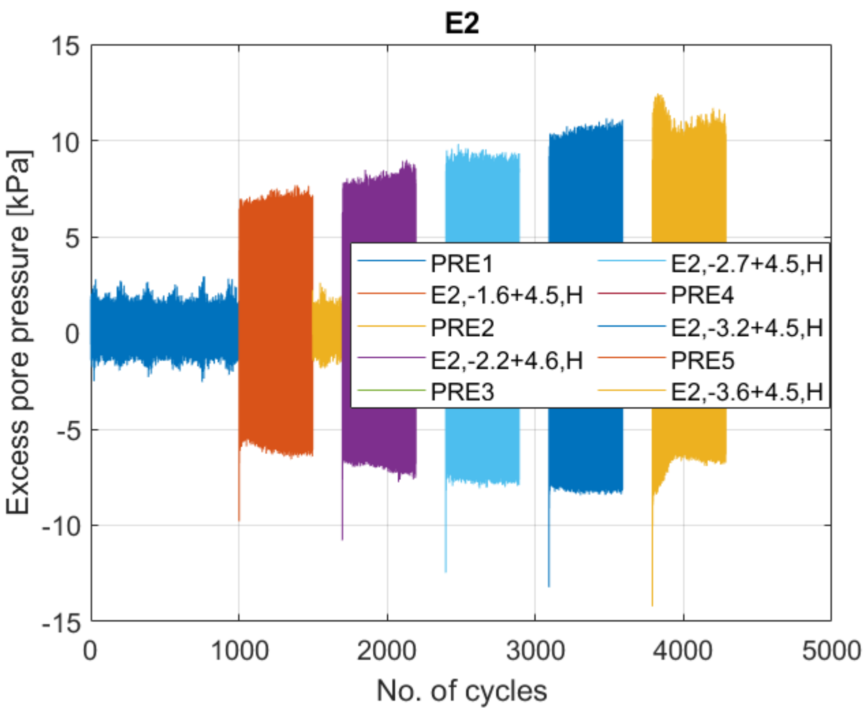

Figure D.255: Pore pressure at 2nd level inner side transducer P12

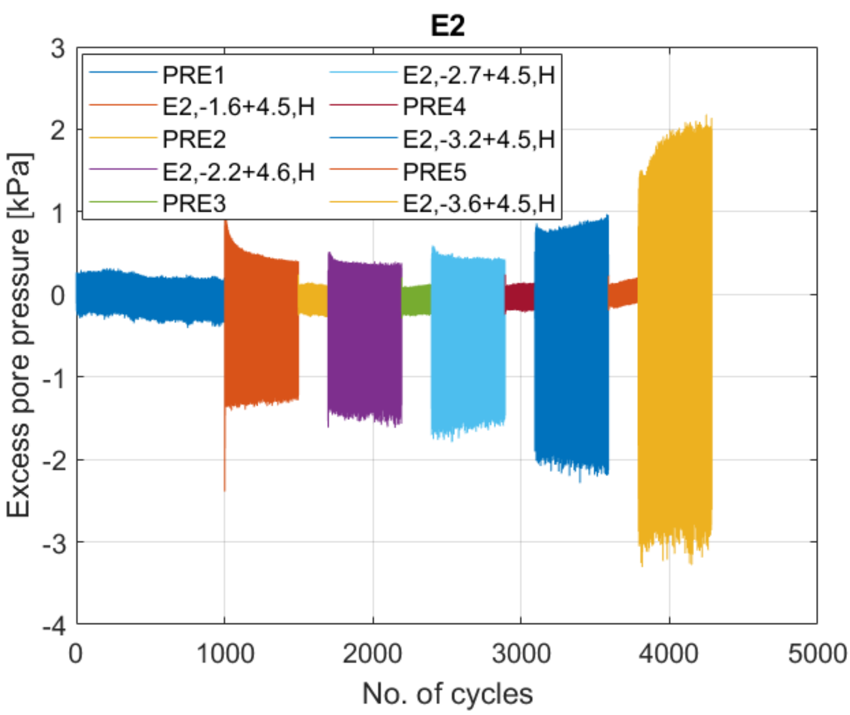

Figure D.256: Pore pressure at 2nd level outer side transducer P1

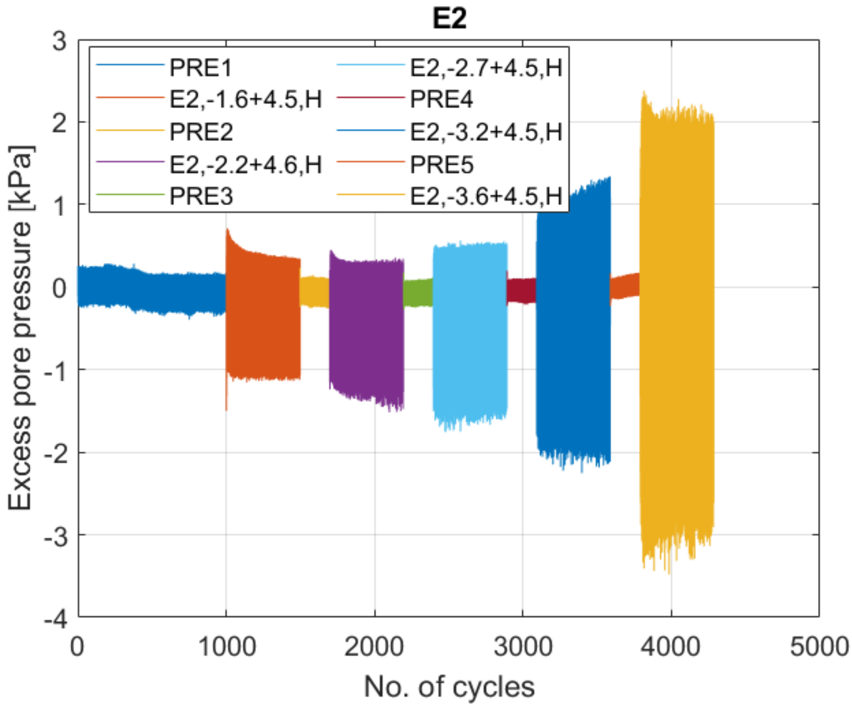

Figure D.257: Pore pressure at 2nd level outer side transducer P9

Skirt Tip Transducers

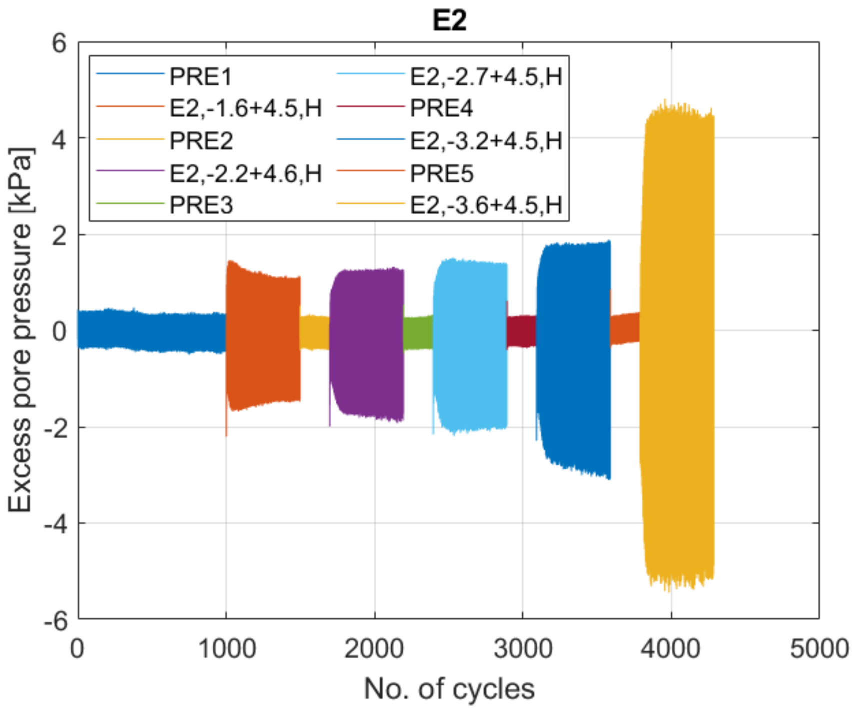

Figure D.258: Pore pressure at tip transducer P2

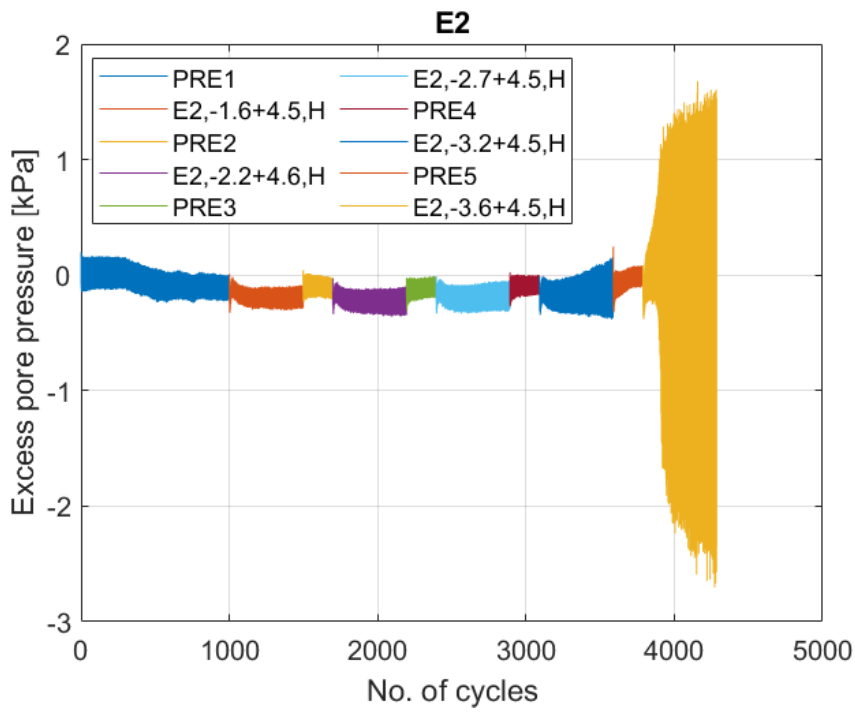

Figure D.259: Pore pressure at tip transducer P8

Force VS displacement

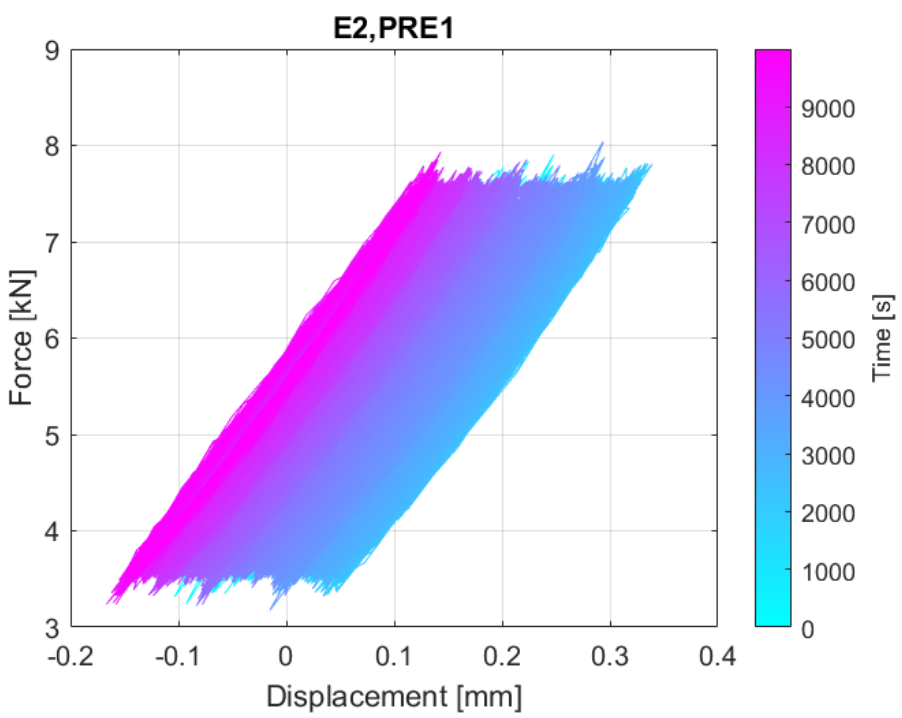

Figure D.260: Force VS absolute displacement

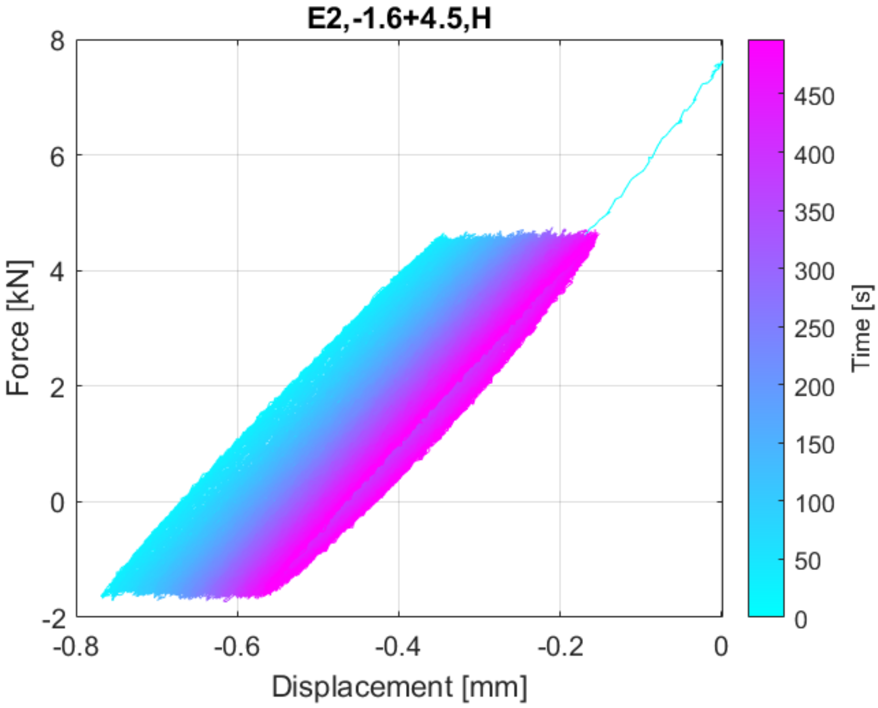

Figure D.261: Force VS absolute displacement

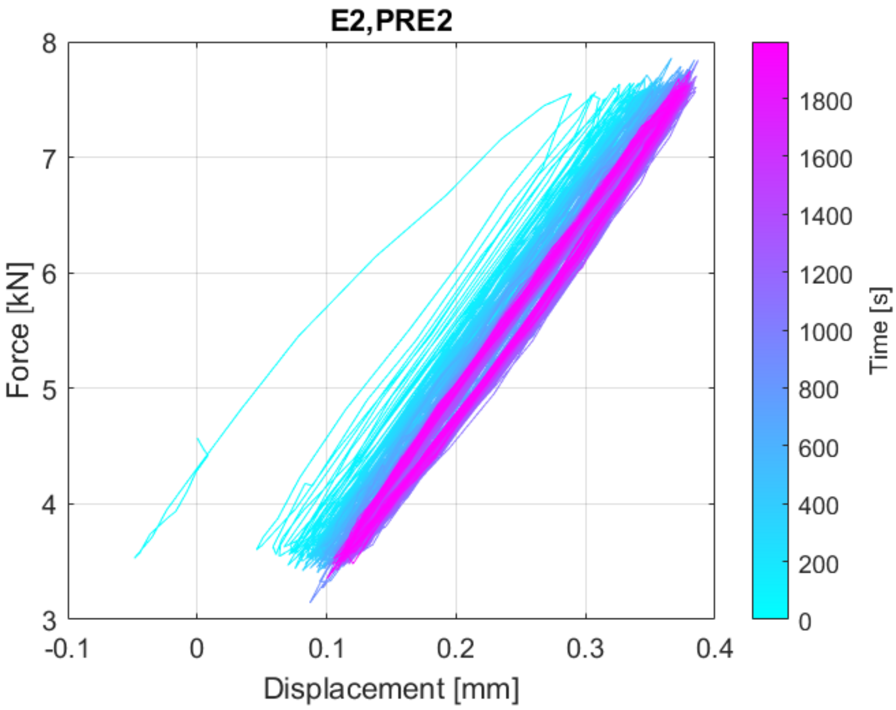

Figure D.262: Force VS absolute displacement

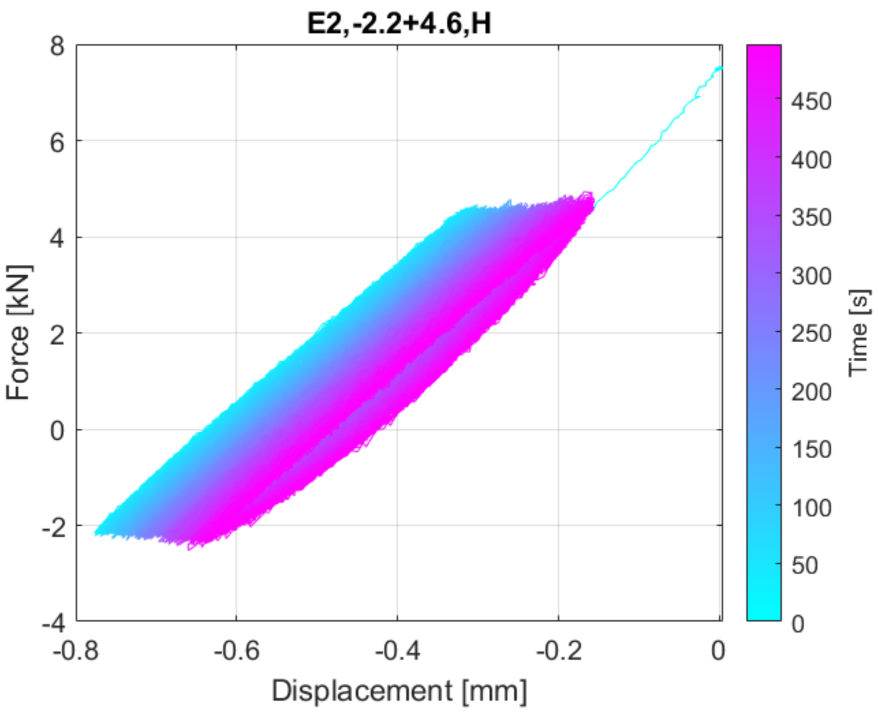

Figure D.263: Force VS absolute displacement

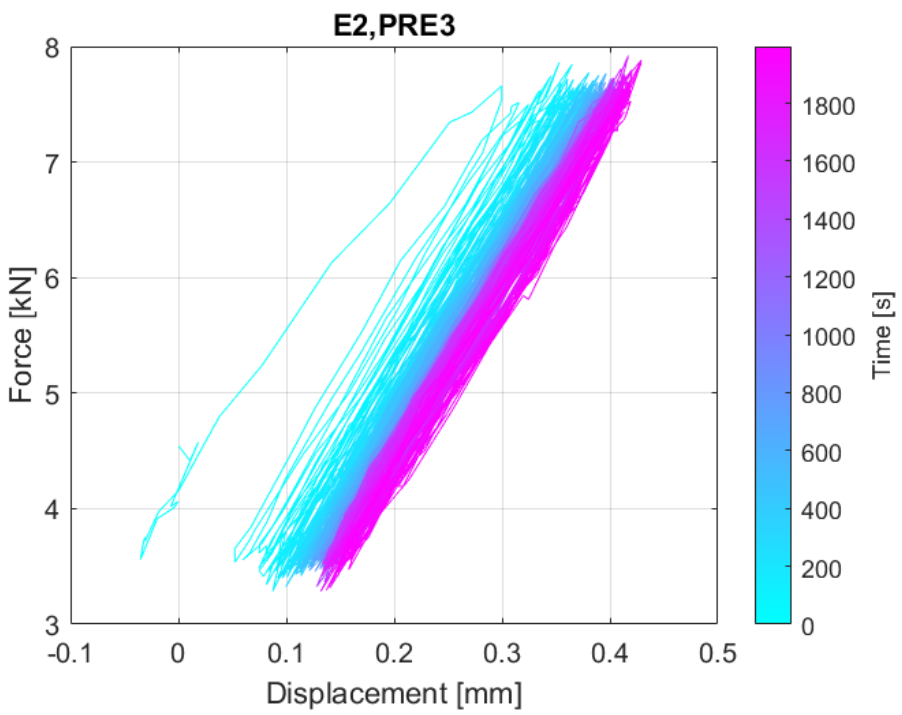

Figure D.264: Force VS absolute displacement

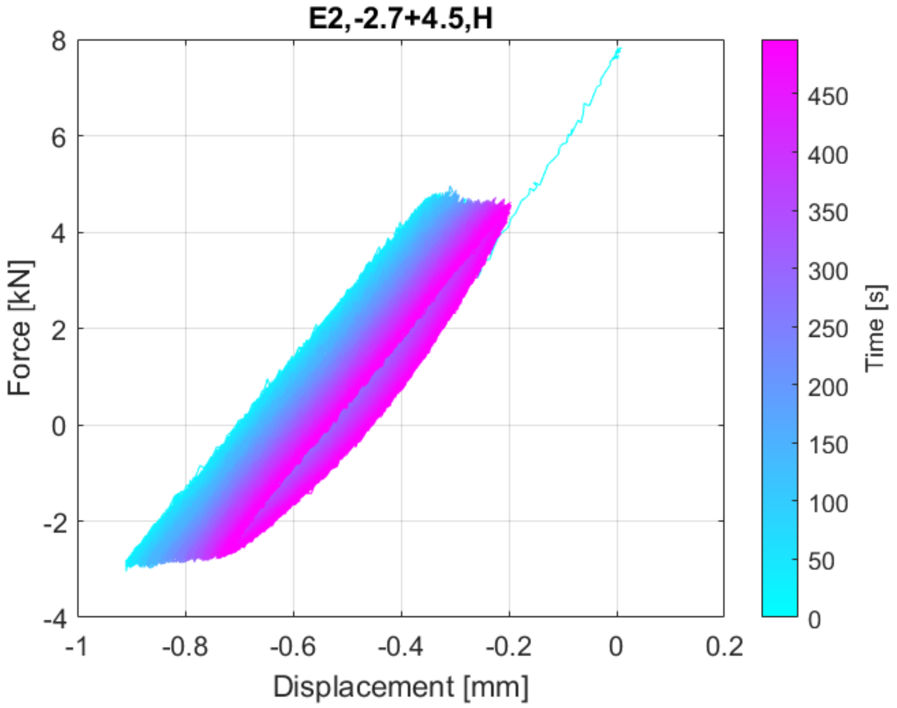

Figure D.265: Force VS absolute displacement

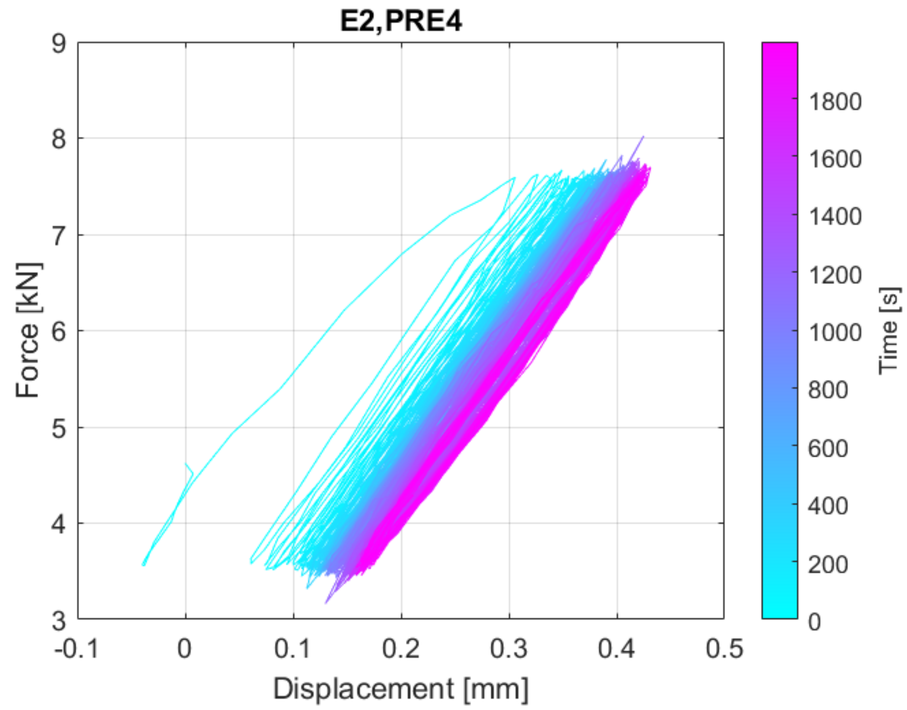

Figure D.266: Force VS absolute displacement

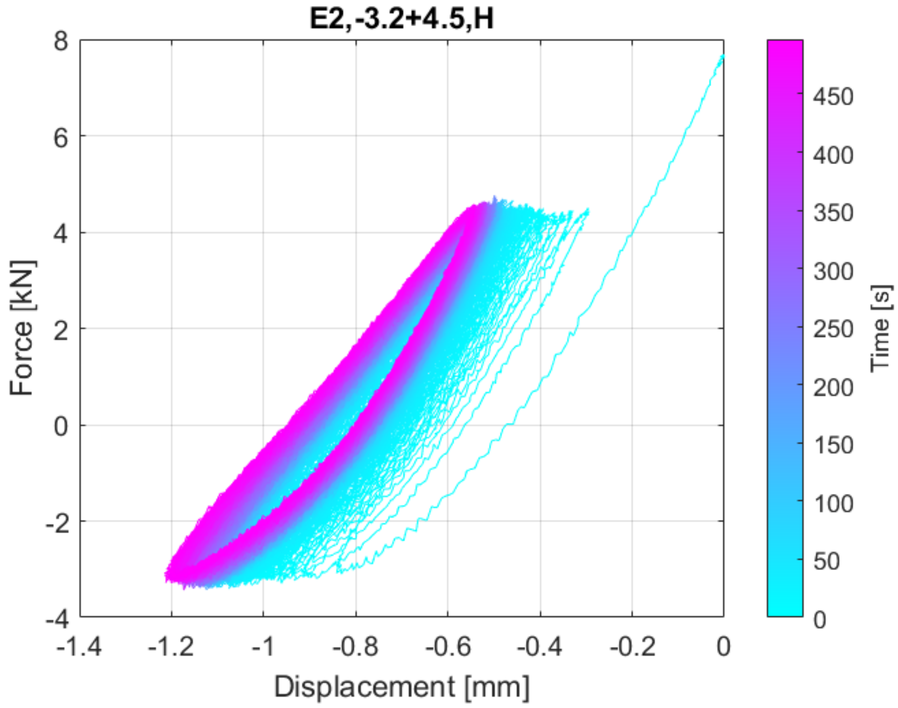

Figure D.267: Force VS absolute displacement

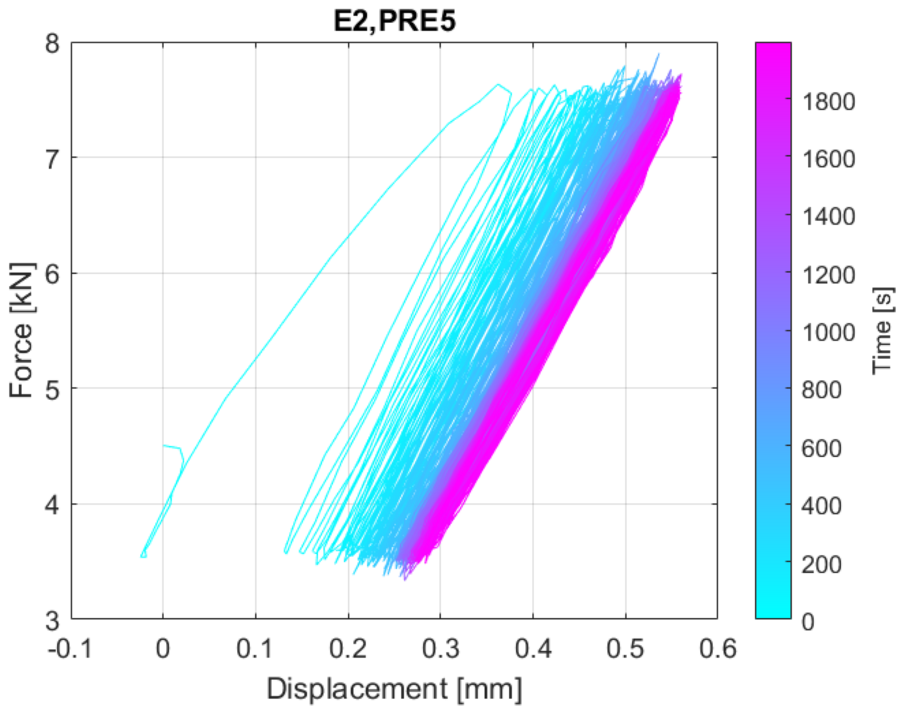

Figure D.268: Force VS absolute displacement

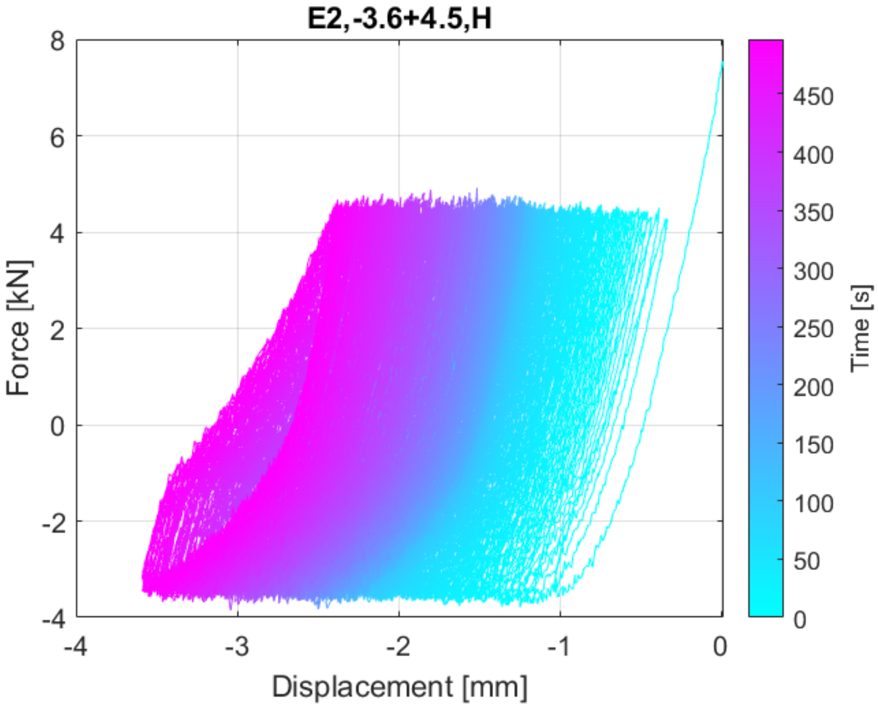

Figure D.269: Force VS absolute displacement

D.6.3 Test subgroup E3 - 0.5 Hz

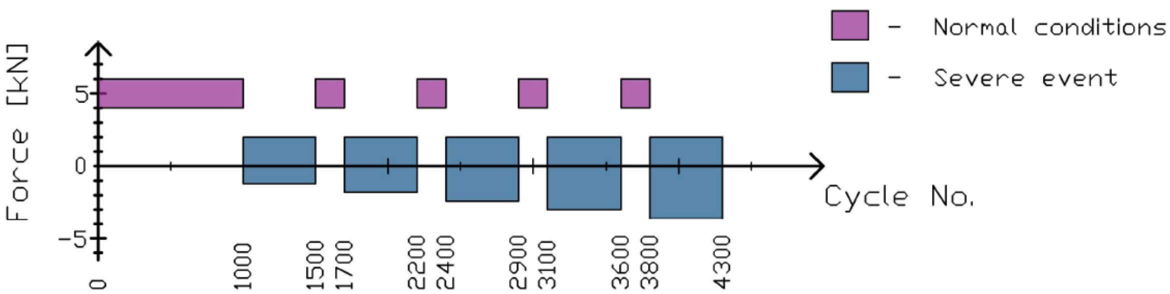

Figure D.270: Actual loading plan for Test subgroup E3

CPT

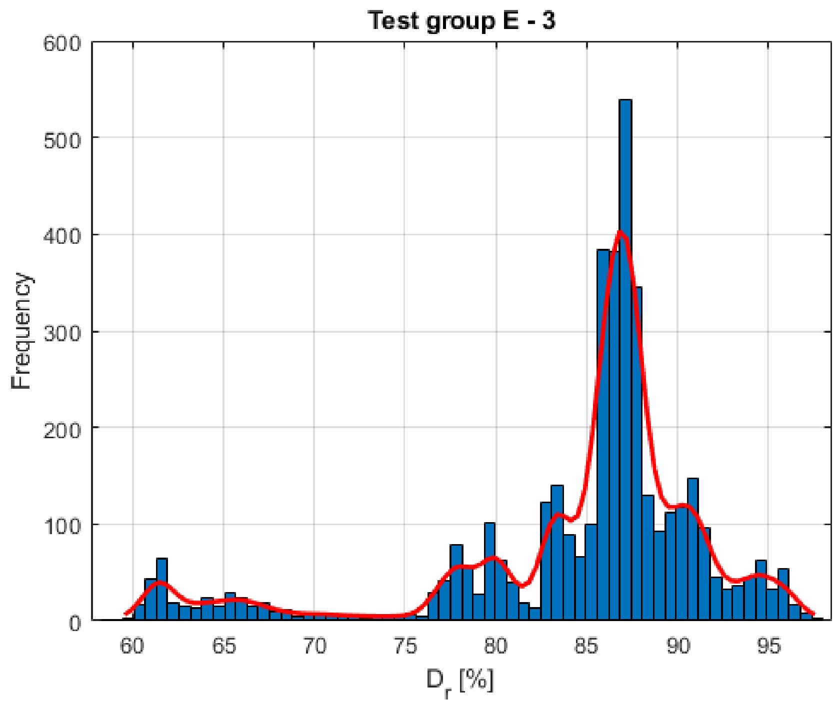

Figure D.271: Dr histogram with distribution fit for test subgroup E3

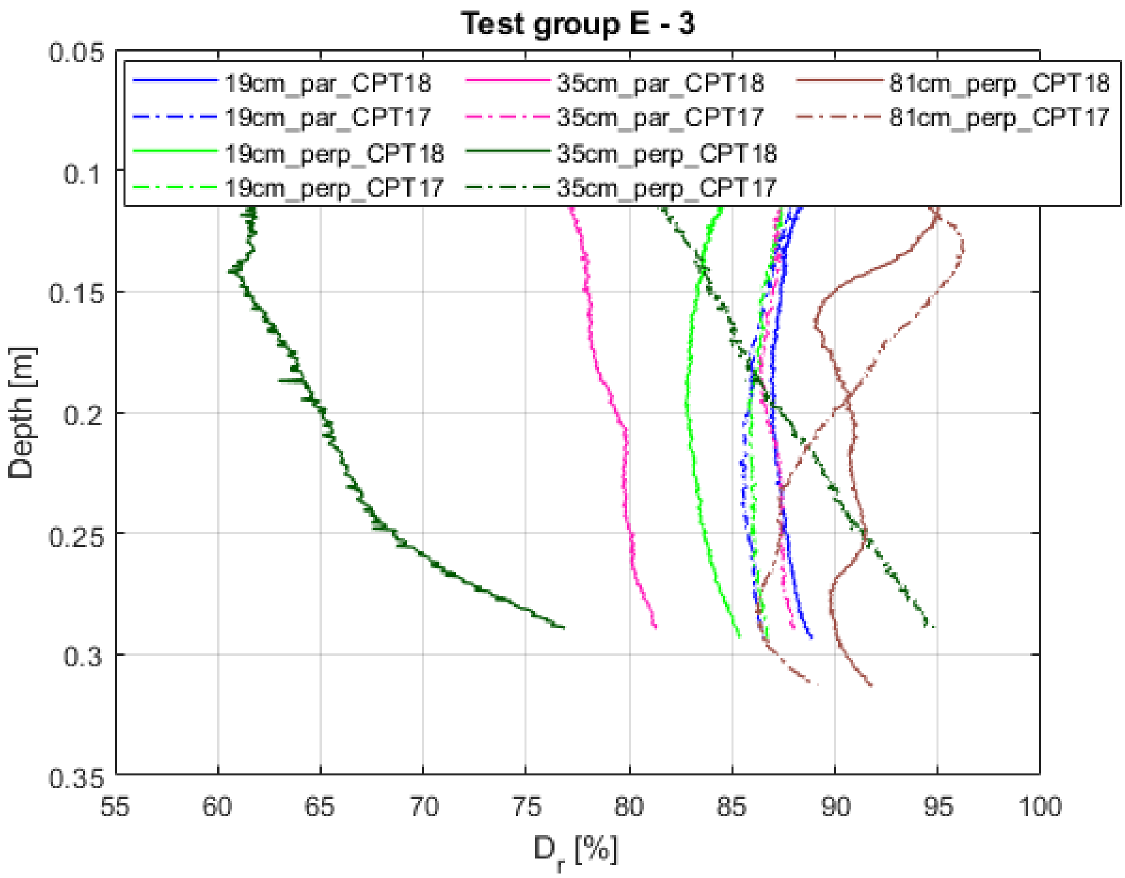

Figure D.272: Test-specific Dr results for CPT test subgroup E3

Force and displacement

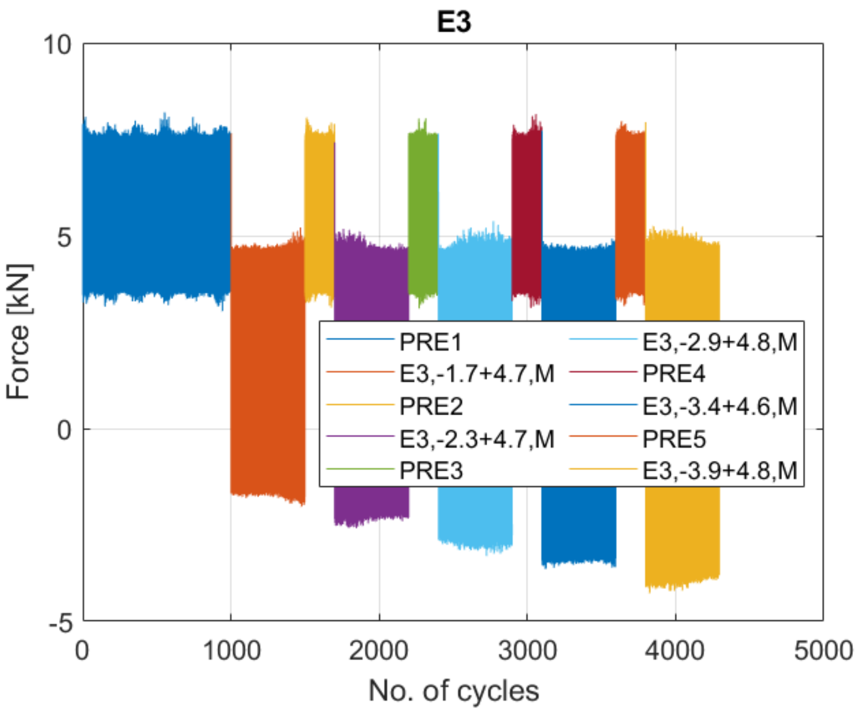

Figure D.273: Force VS No. of cycles

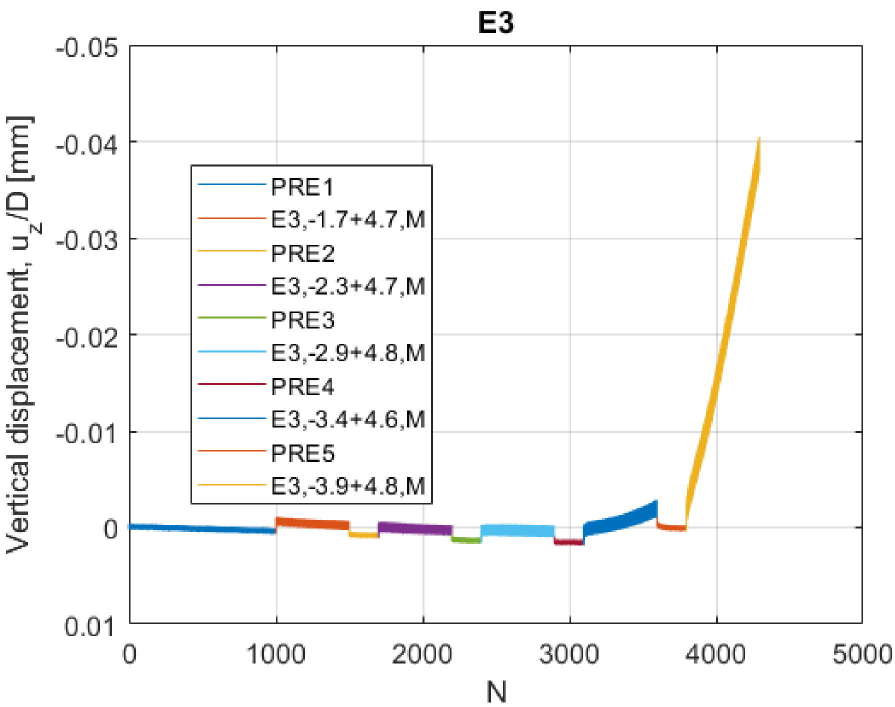

Figure D.274: Displacement VS No. of cycles

Lid Transducers

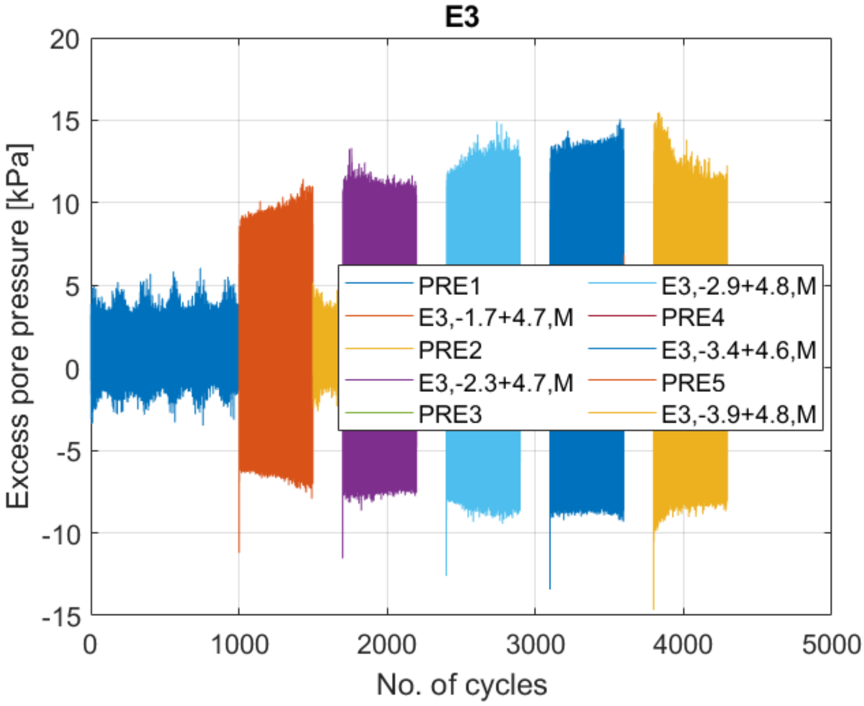

Figure D.275: Pore pressure at lid transducer P6

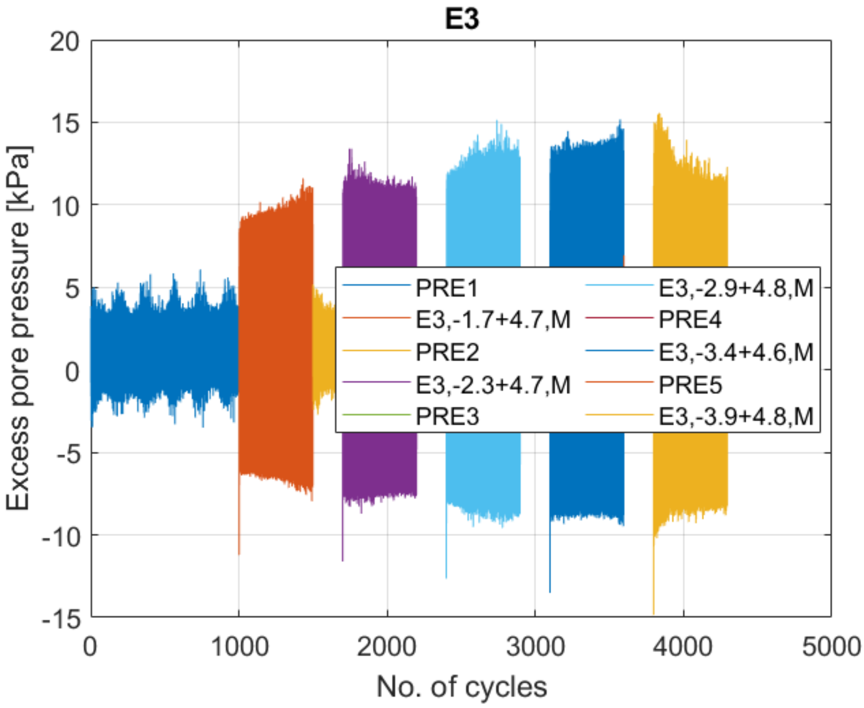

Figure D.276: Pore pressure at lid transducer P10

1st Level Transducers

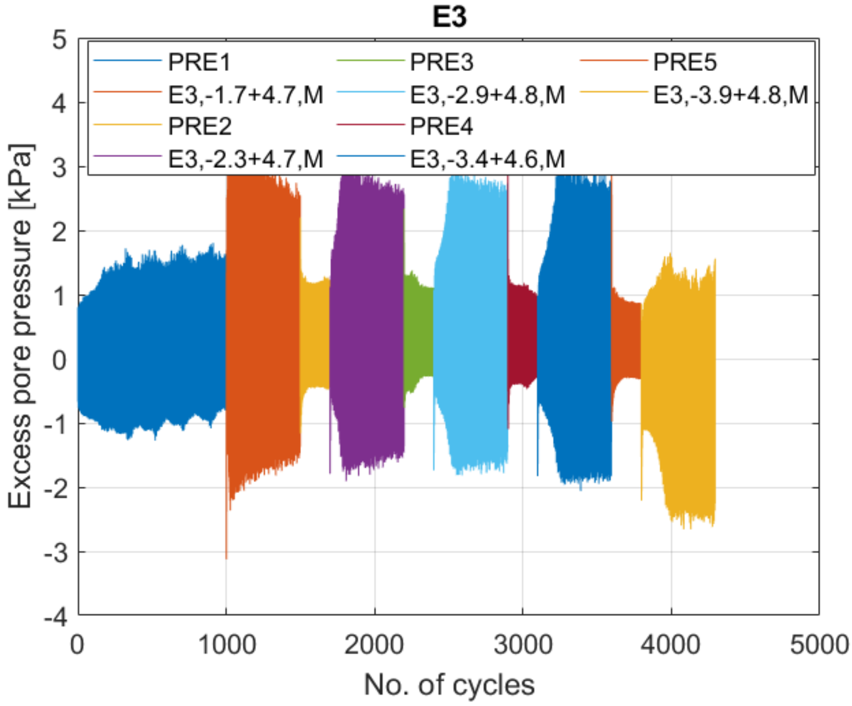

Figure D.277: Pore pressure at 1st level inner side transducer P4

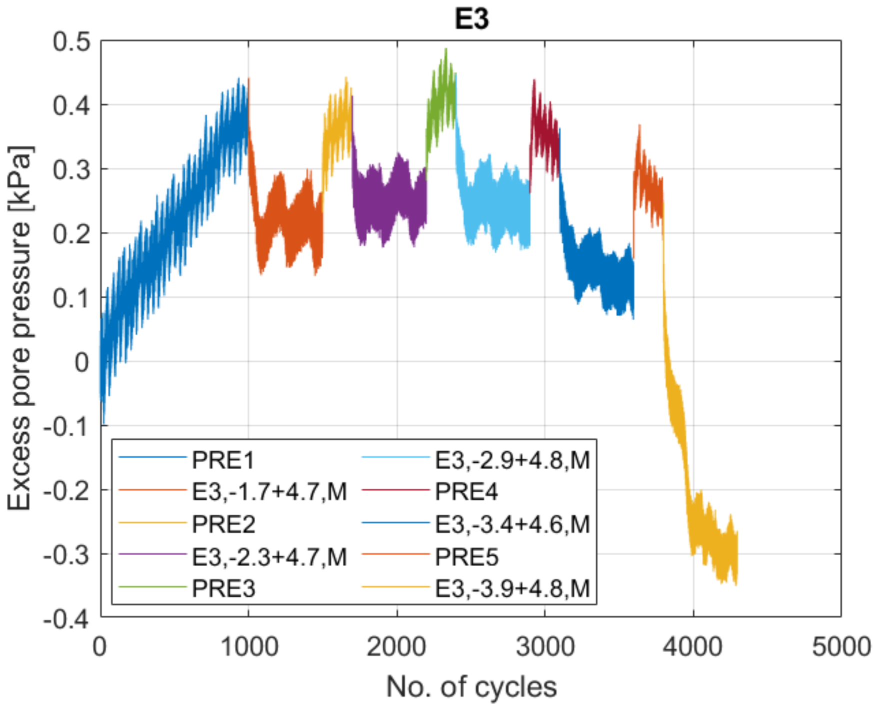

Figure D.278: Pore pressure at 1st level inner side transducer P11

2nd Level Transducers

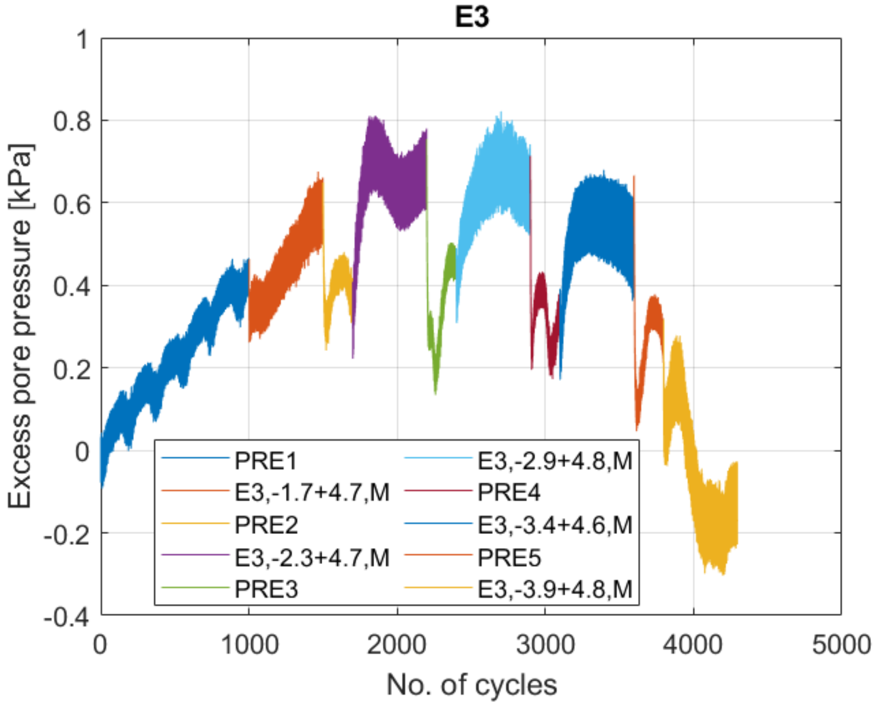

Figure D.279: Pore pressure at 2nd level inner side transducer P5

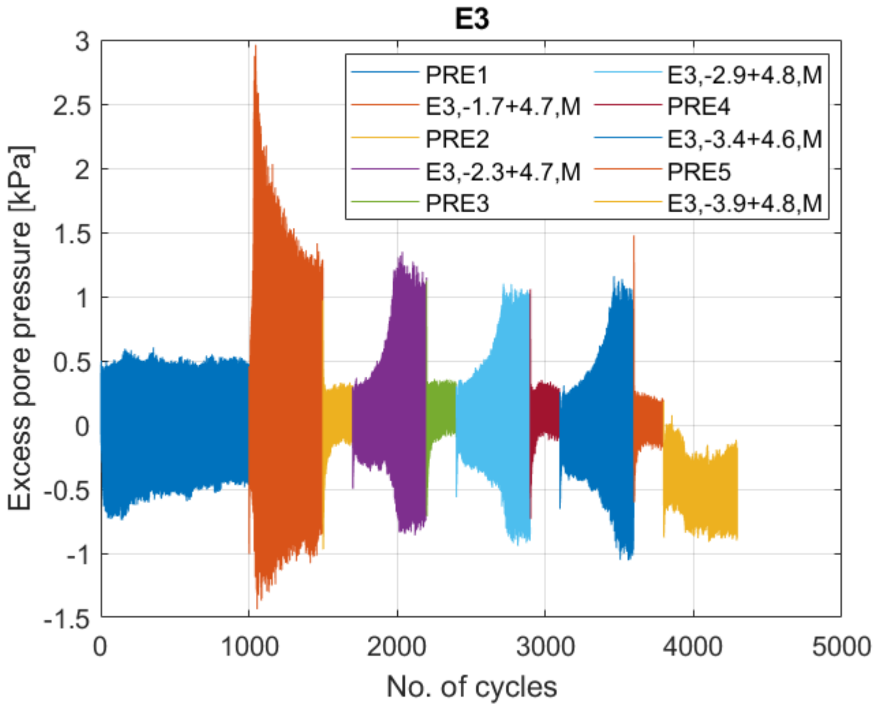

Figure D.280: Pore pressure at 2nd level inner side transducer P12

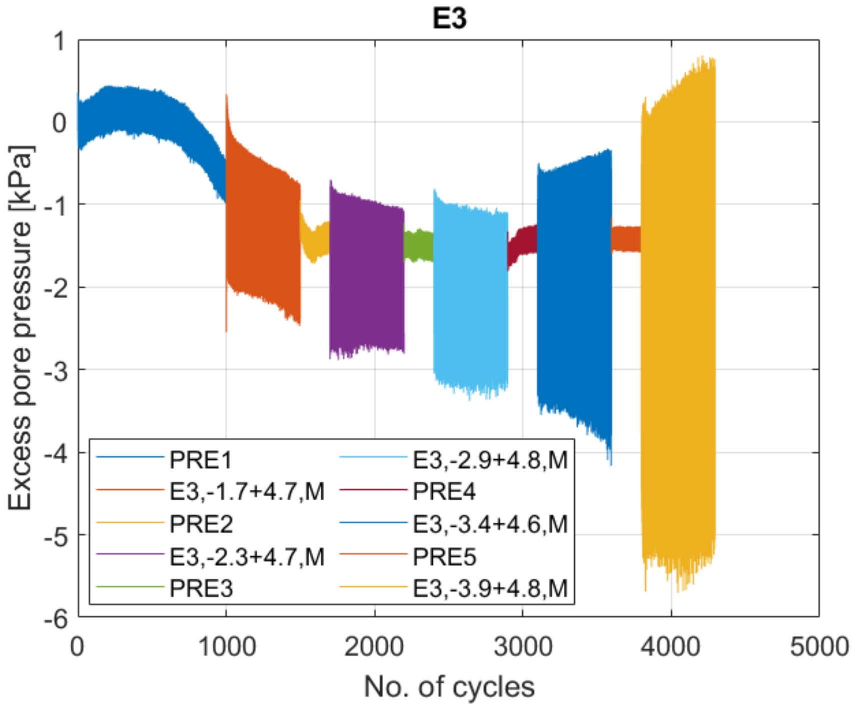

Figure D.281: Pore pressure at 2nd level outer side transducer P1

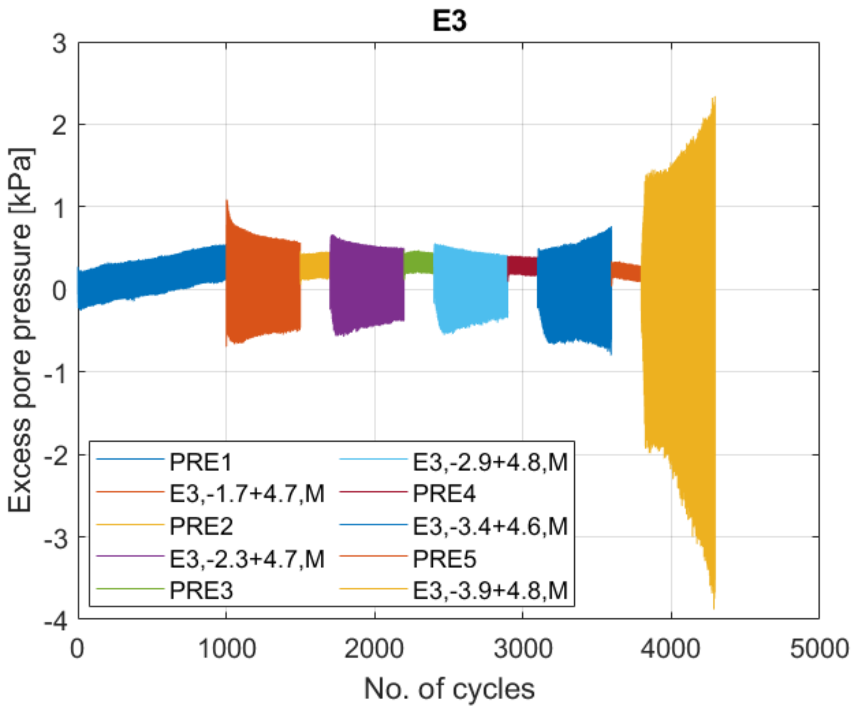

Figure D.282: Pore pressure at 2nd level outer side transducer P9

Skirt Tip Transducers

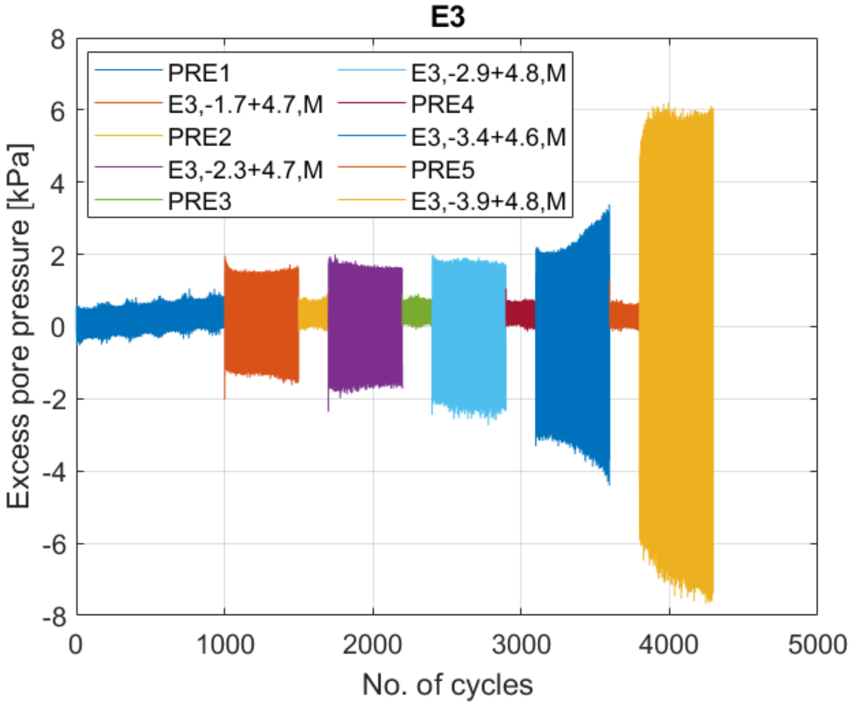

Figure D.283: Pore pressure at tip transducer P2

Force VS absolute displacement

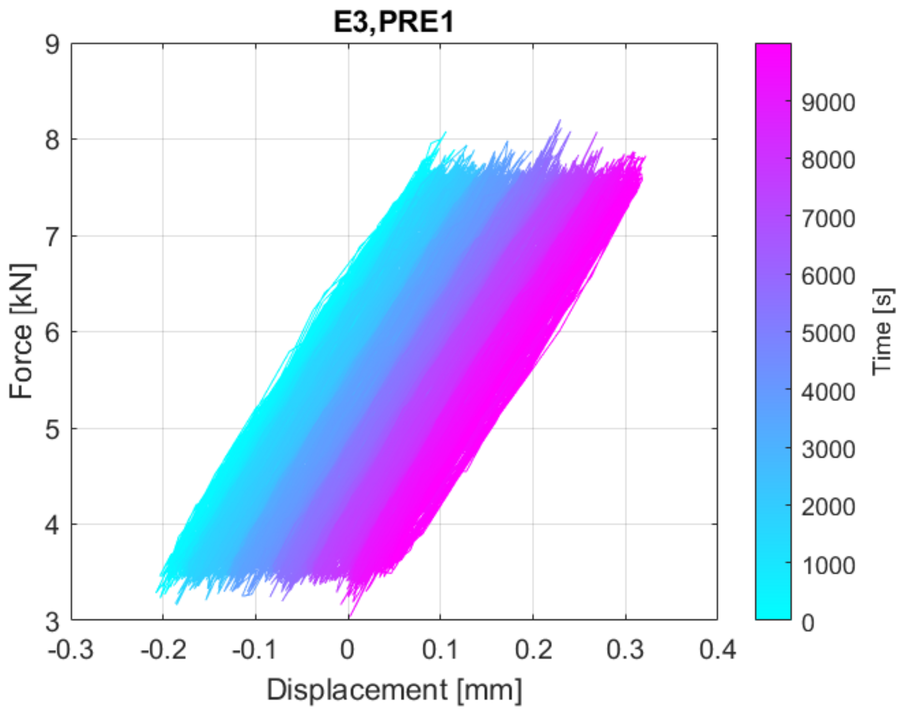

Figure D.284: Force VS absolute displacement

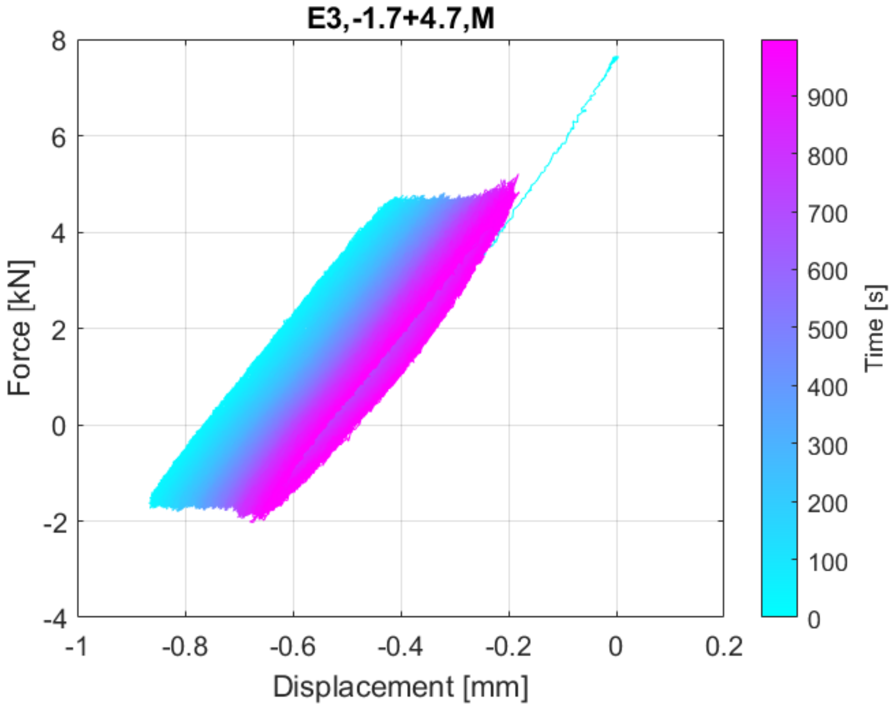

Figure D.285: Force VS absolute displacement

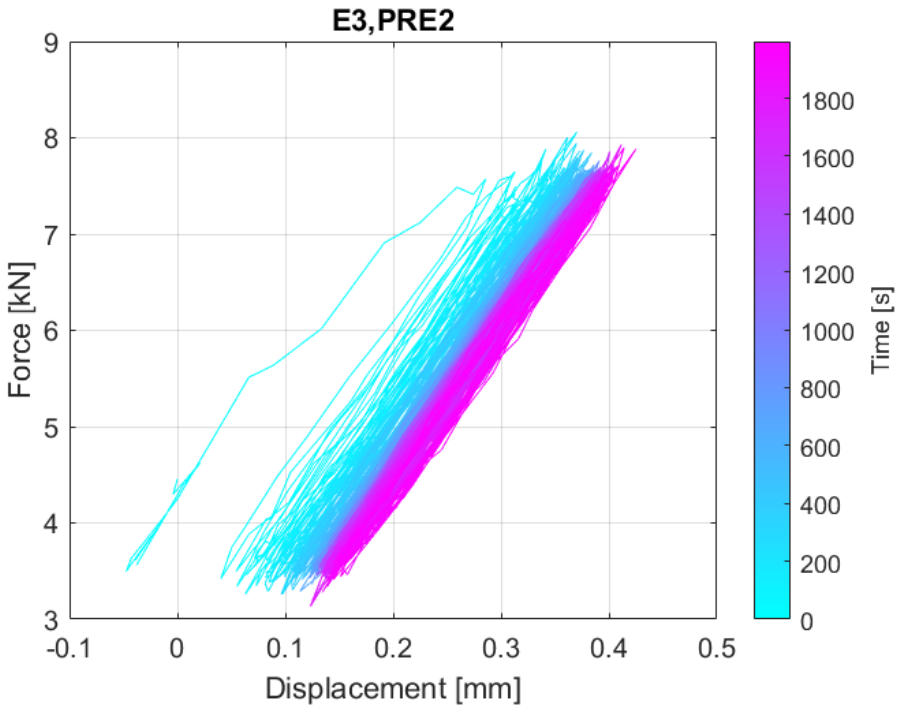

Figure D.286: Force VS absolute displacement

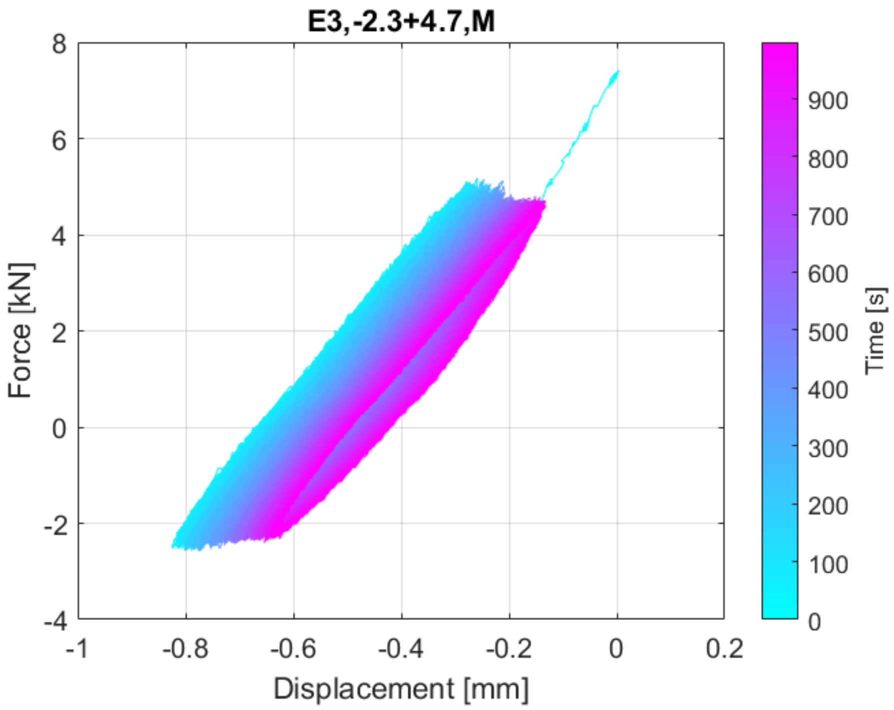

Figure D.287: Force VS absolute displacement

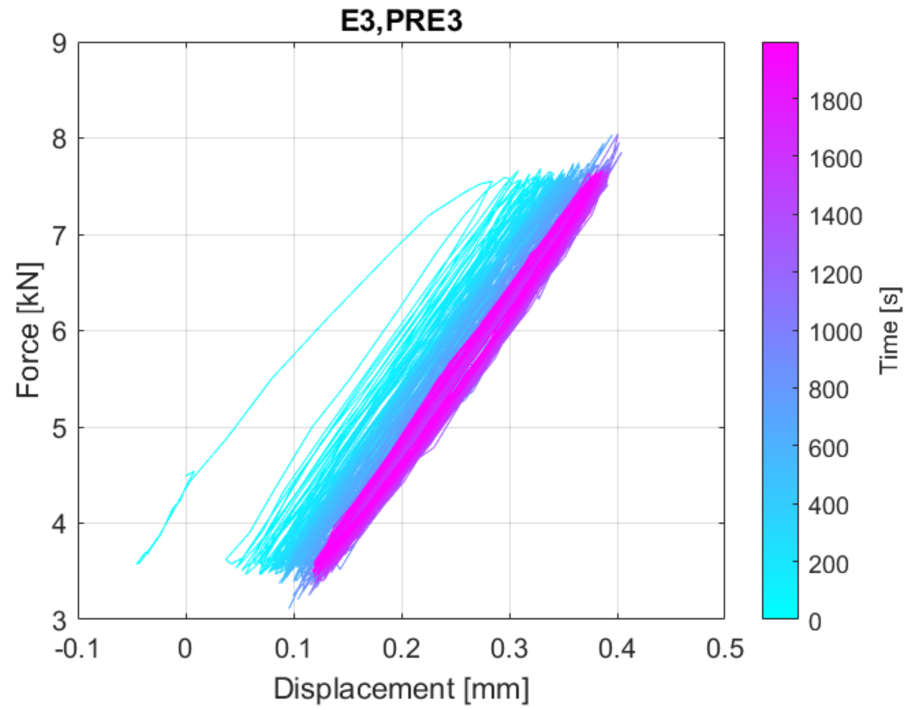

Figure D.288: Force VS absolute displacement

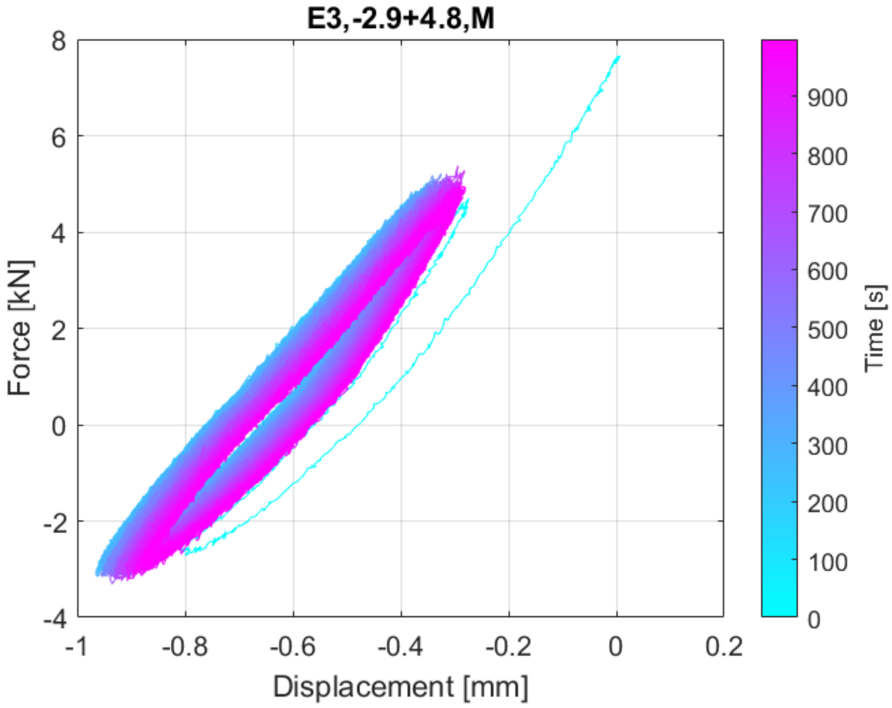

Figure D.289: Force VS absolute displacement

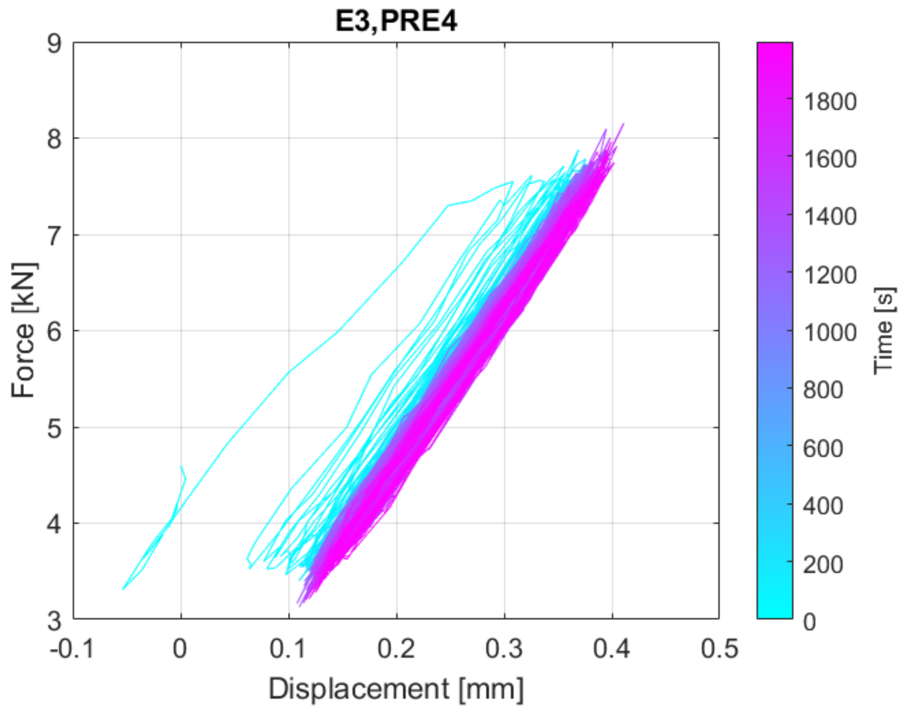

Figure D.290: Force VS absolute displacement

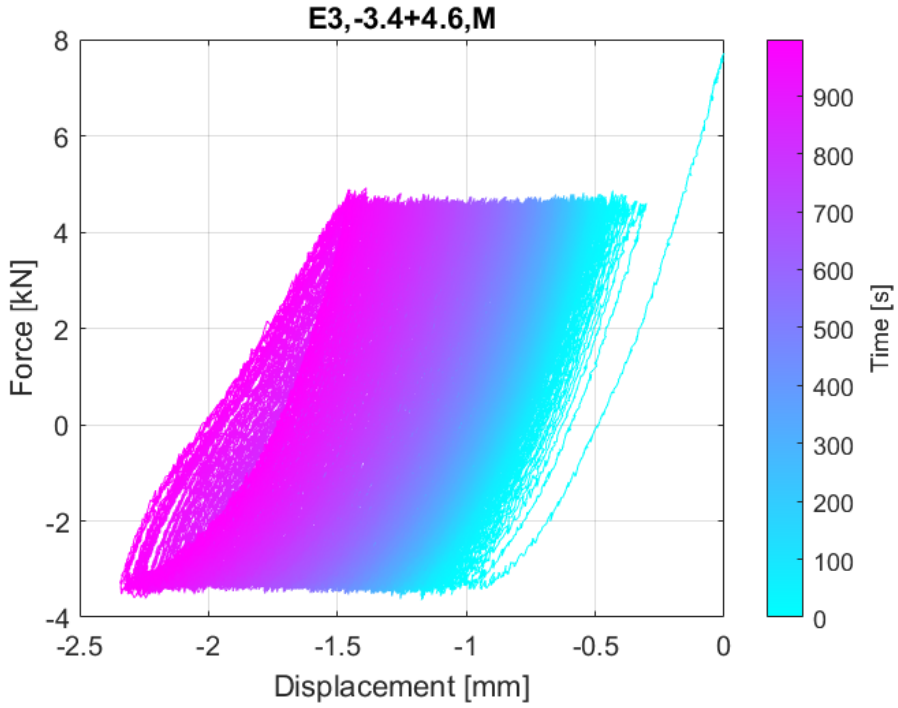

Figure D.291: Force VS absolute displacement

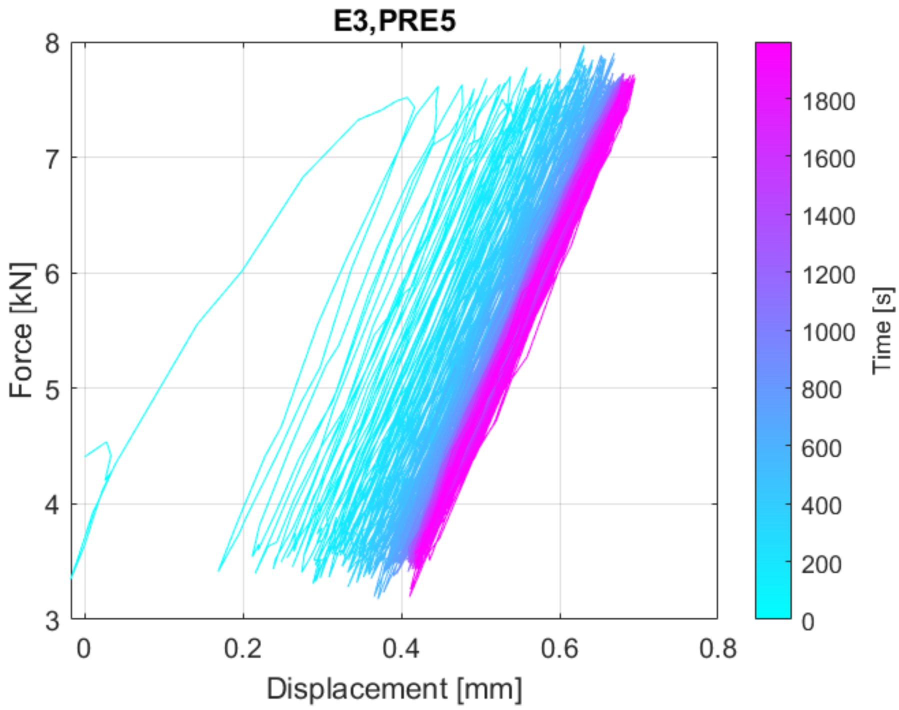

Figure D.292: Force VS absolute displacement

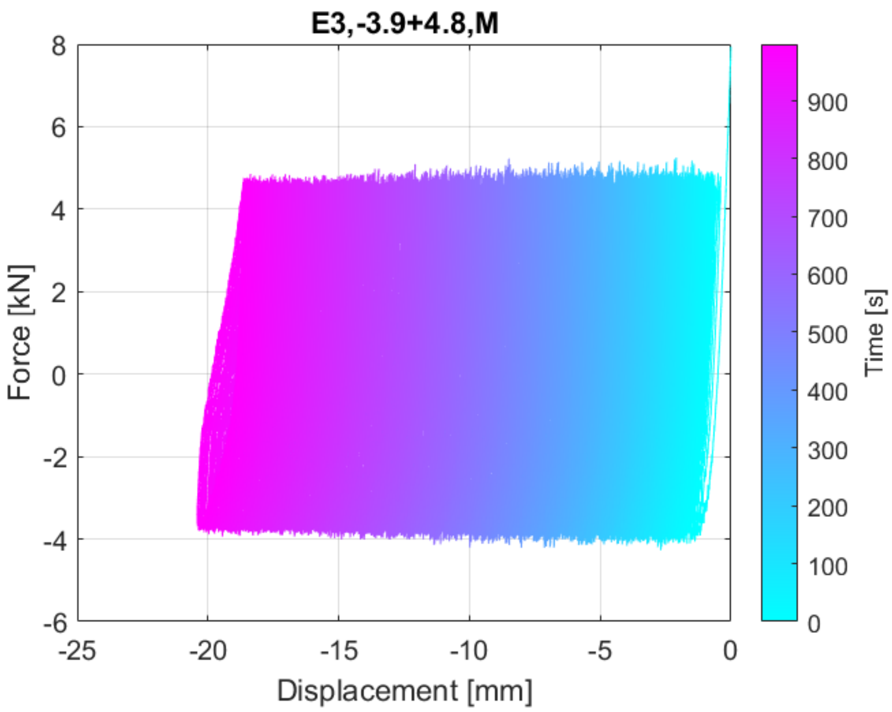

Figure D.293: Force VS absolute displacement

D.7 Test group F

Similar to the test conducted in section D.6 two way loading is tested. In the following results the compression force is changed to 7 kN, and ratio between tensile and compression for each event is kept as D.5 to investigate if the force has an influence on the bucket. 2 tests have been carried out where the following frequencies are used 0.1 Hz and 1 Hz, the precycle is kept with a frequency of 0.1 Hz. The loading plan for both tests are shown in table D.7 as well as in figure D.294.

Table D.8: Loading plan for 'Test group F'

Packet No.	Conditions	Force command F_{min} [kN]	F_{max} [kN]	Force ratio	Cycle No.	Frequency [Hz]
1	Normal	4.0	6.0	0.67	1000	0.1
2	Severe	-2.8	7.0	-0.40	500	0.1, 1.0
3	Normal	4.0	6.0	0.67	200	0.1
4	Severe	-4.2	7.0	-0.60	500	0.1, 1.0
5	Normal	4.0	6.0	0.67	200	0.1
6	Severe	-5.6	7.0	-0.80	500	0.1, 1.0
7	Normal	4.0	6.0	0.67	200	0.1
8	Severe	-7.0	7.0	-1.00	500	0.1, 1.0
9	Normal	4.0	6.0	0.67	200	0.1
10	Severe	-8.4	7.0	-1.20	500	0.1, 1.0

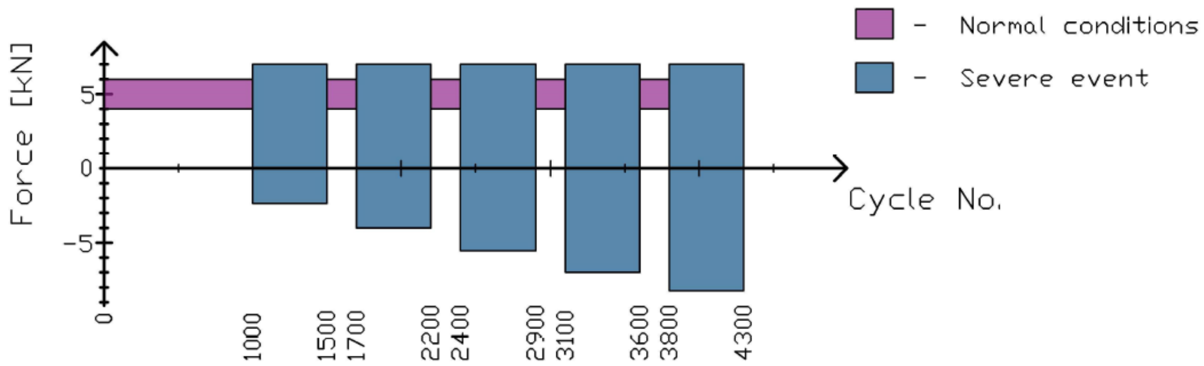

Figure D.294: Scheduled loading plan for Test group F

D.7.1 Test subgroup F1 - 0.1 Hz

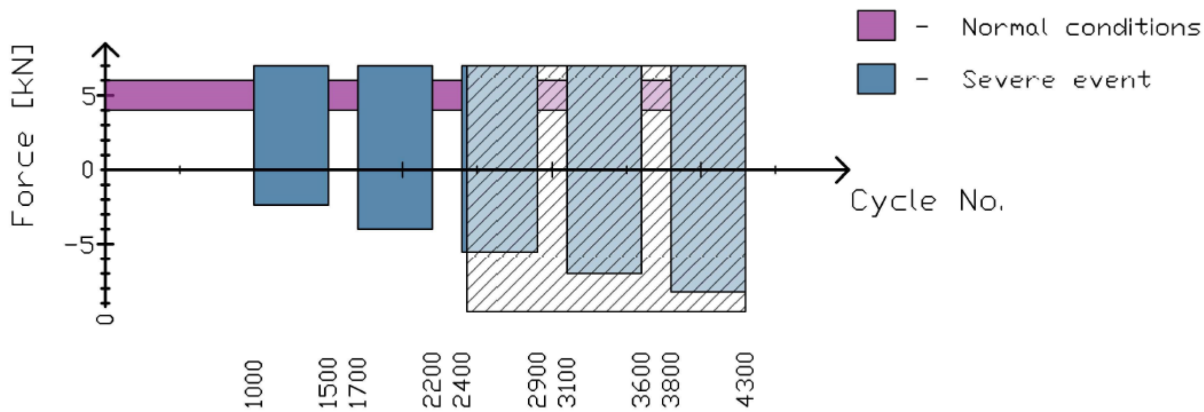

Figure D.295: Actual loading plan for test subgroup F1

CPT

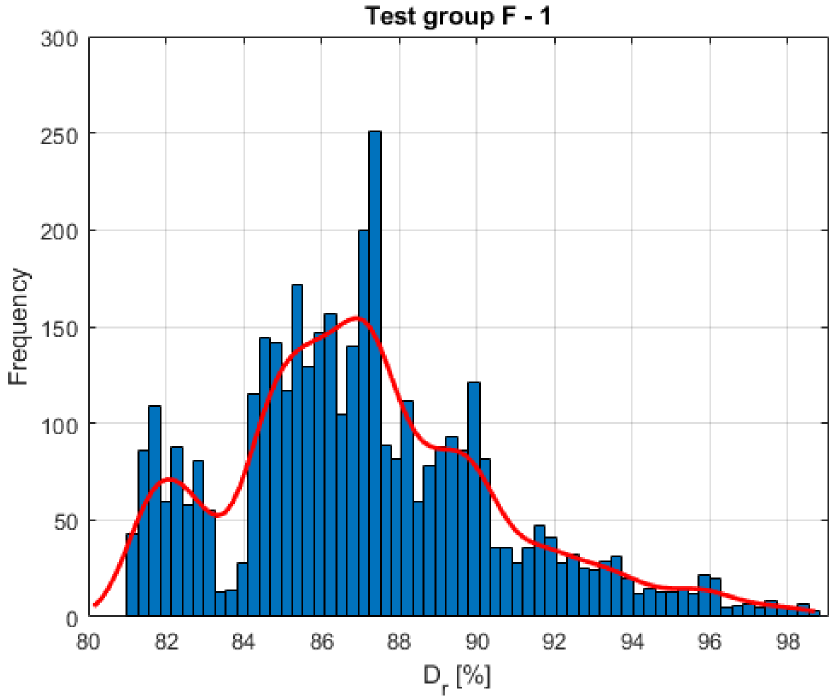

Figure D.296: Dr histogram with distribution fit for test subgroup F1

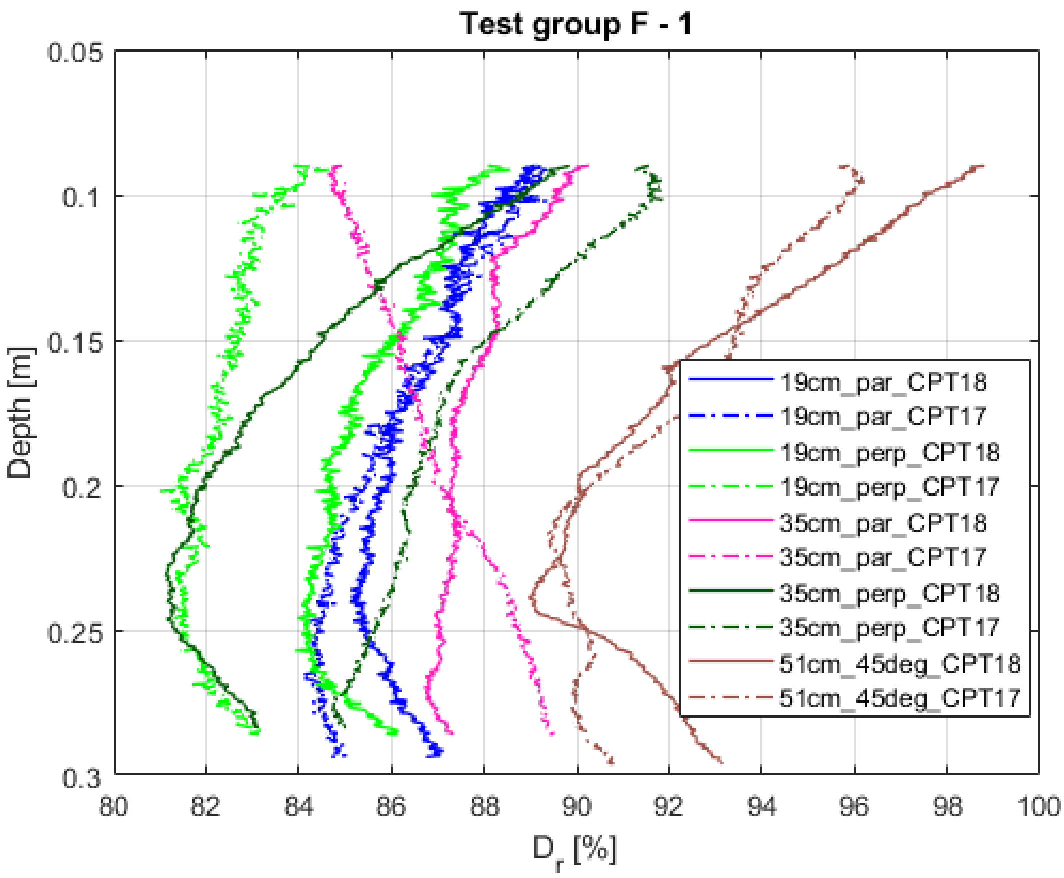

Figure D.297: Test-specific Dr results for CPT test subgroup F1

Force and displacement

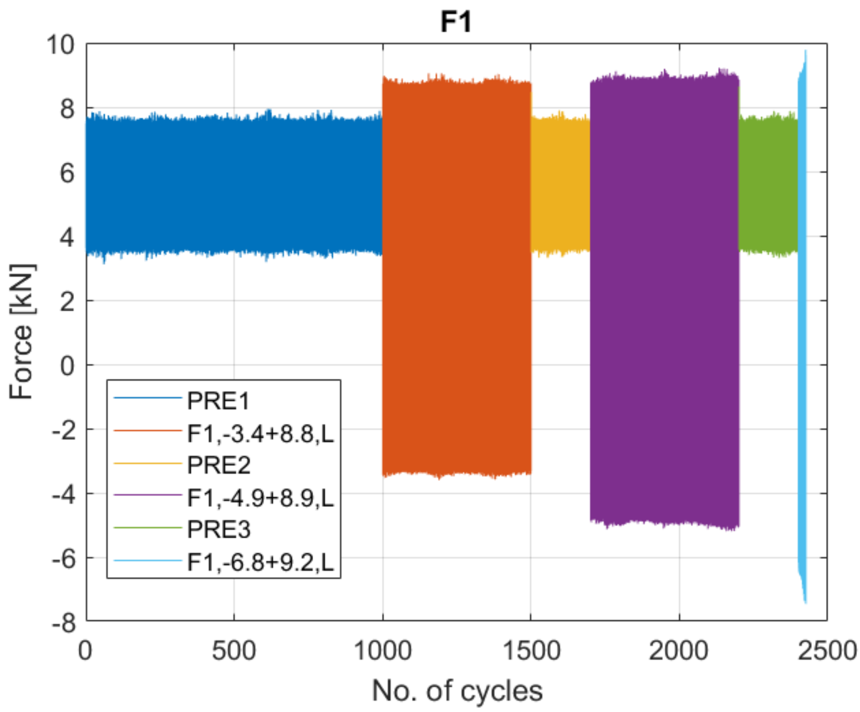

Figure D.298: Force VS No. of cycles

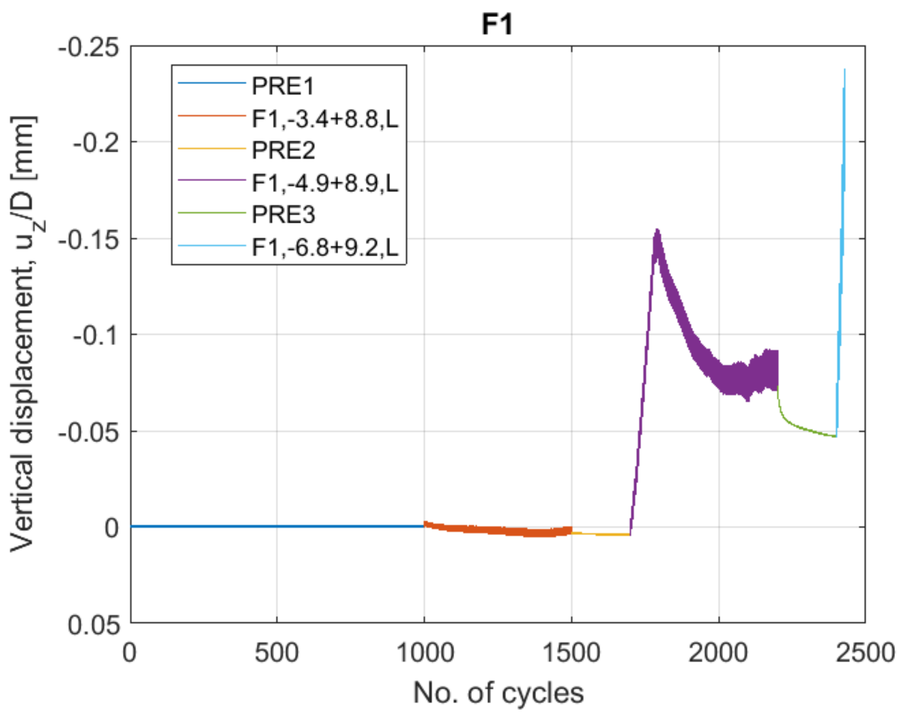

Figure D.299: Displacement VS No. of cycles

Lid Transducers

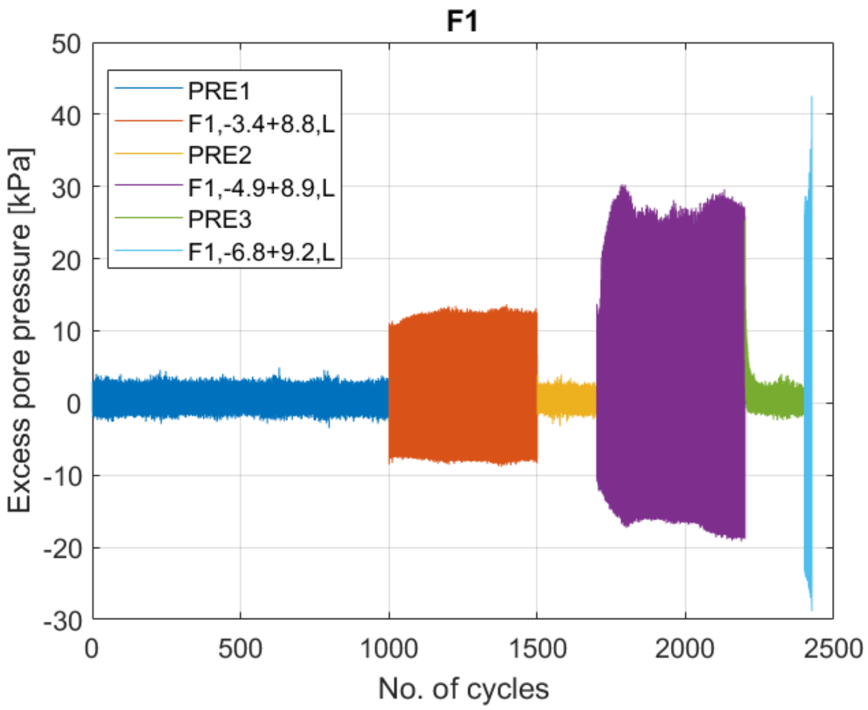

Figure D.300: Pore pressure at lid transducer P6

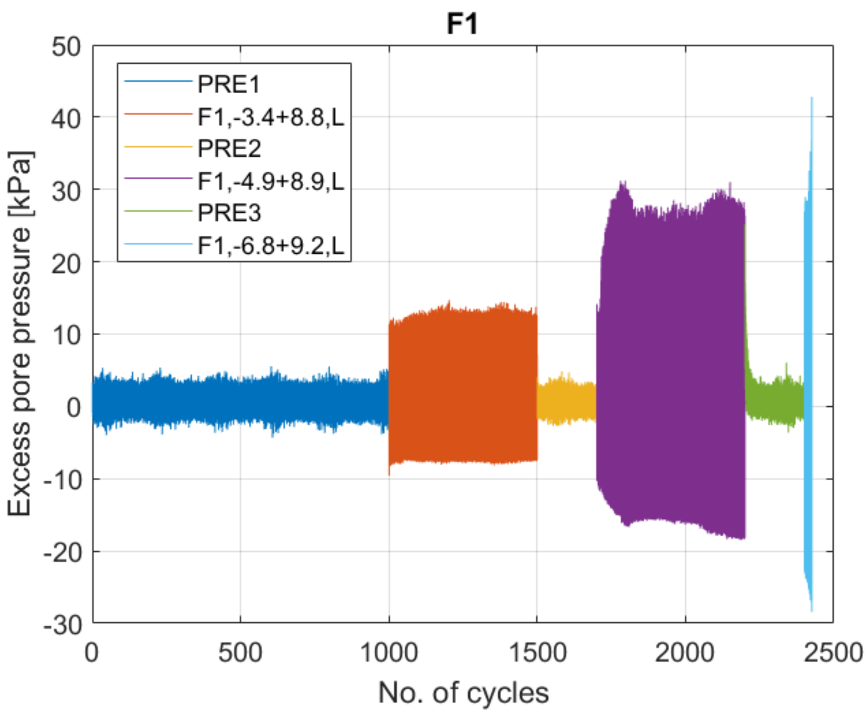

Figure D.301: Pore pressure at lid transducer P10

1st Level Transducers

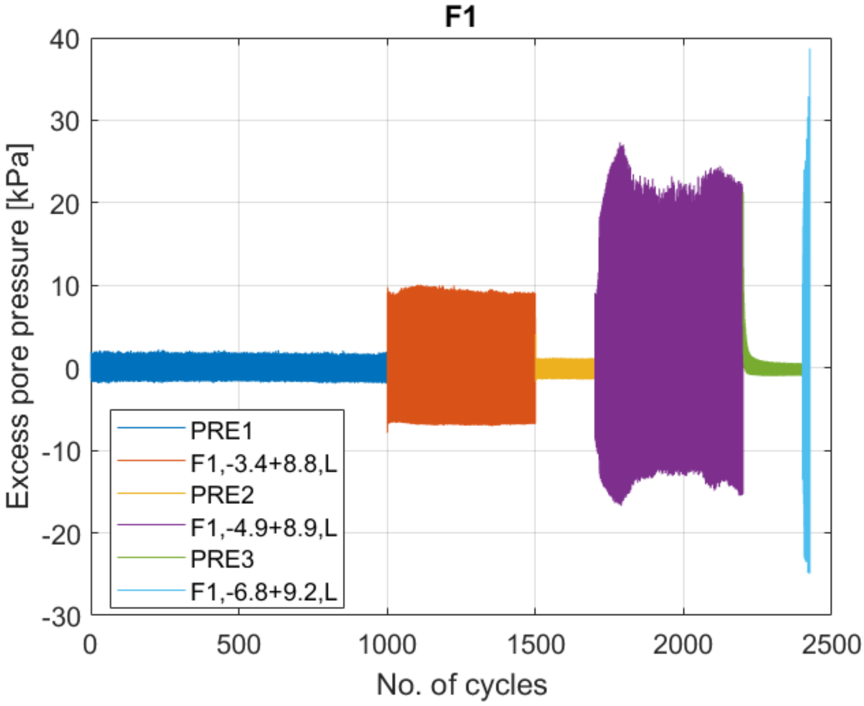

Figure D.302: Pore pressure at 1st level inner side transducer P4

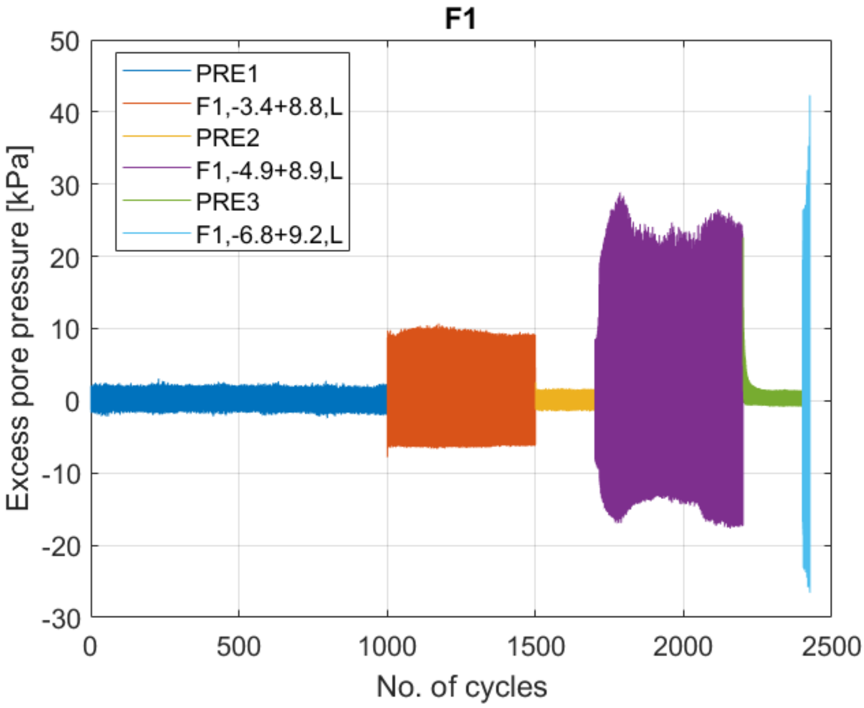

Figure D.303: Pore pressure at 1st level inner side transducer P11

2nd Level Transducers

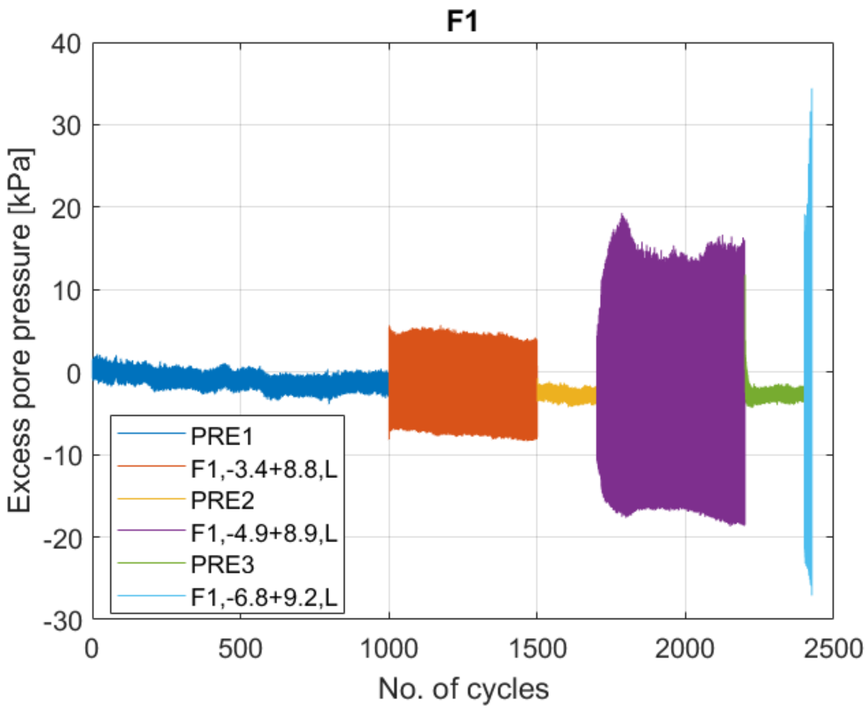

Figure D.304: Pore pressure at 2nd level inner side transducer P5

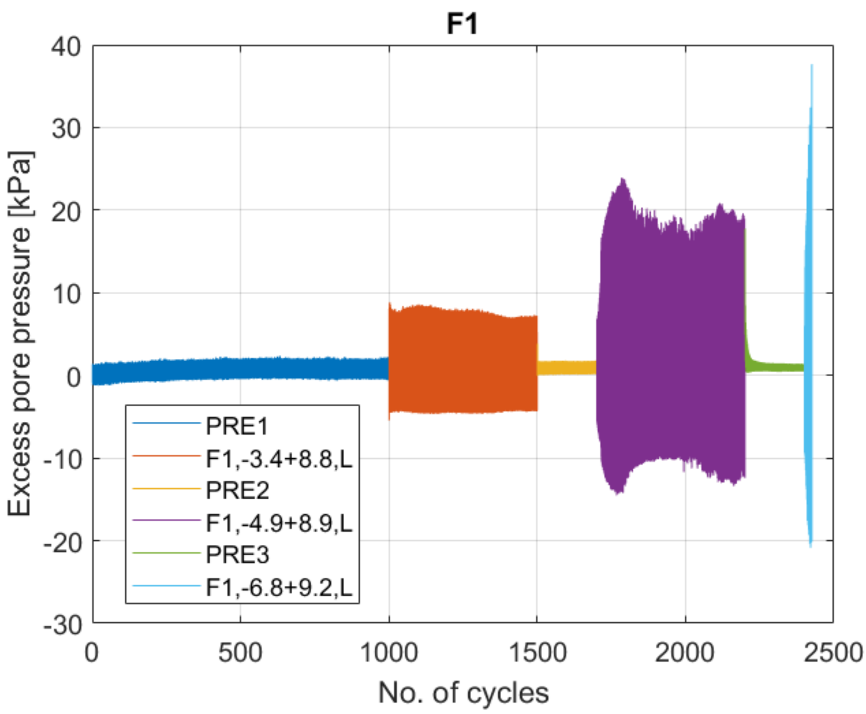

Figure D.305: Pore pressure at 2nd level inner side transducer P12

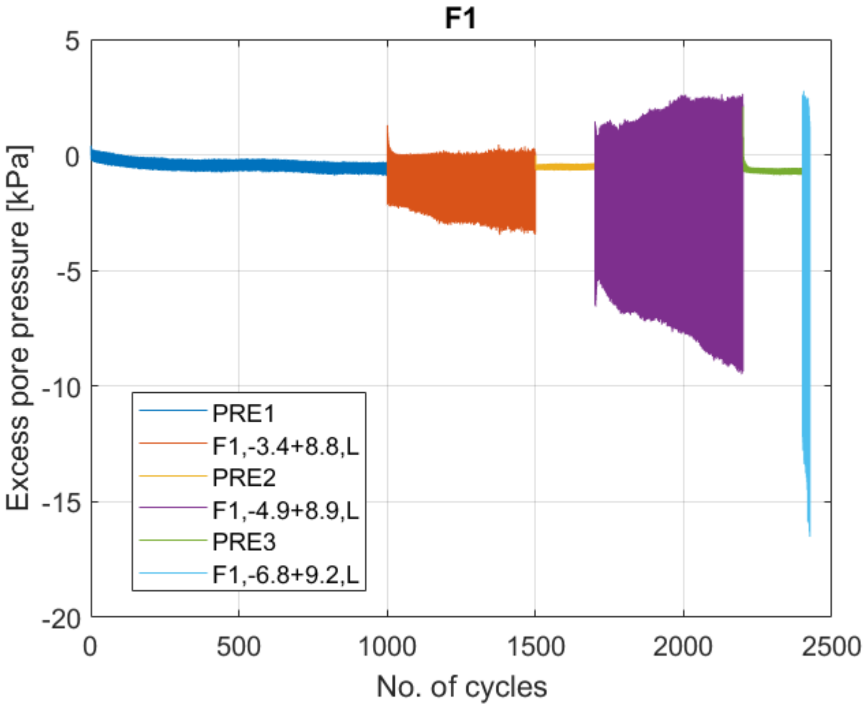

Figure D.306: Pore pressure at 2nd level outer side transducer P1

Skirt Tip Transducers

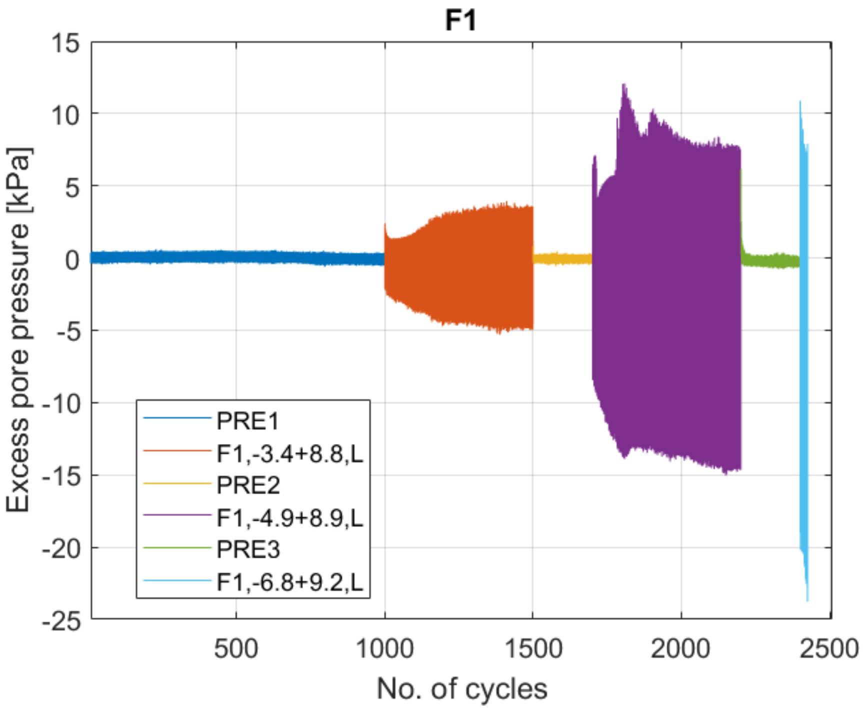

Figure D.307: Pore pressure at tip transducer P2

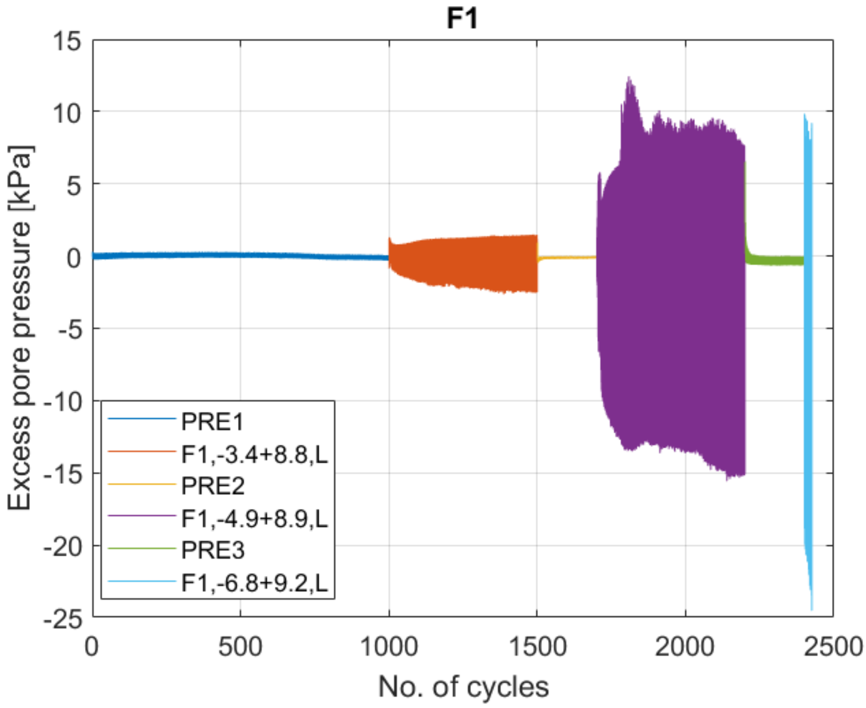

Figure D.308: Pore pressure at tip transducer P8

Force VS displacement

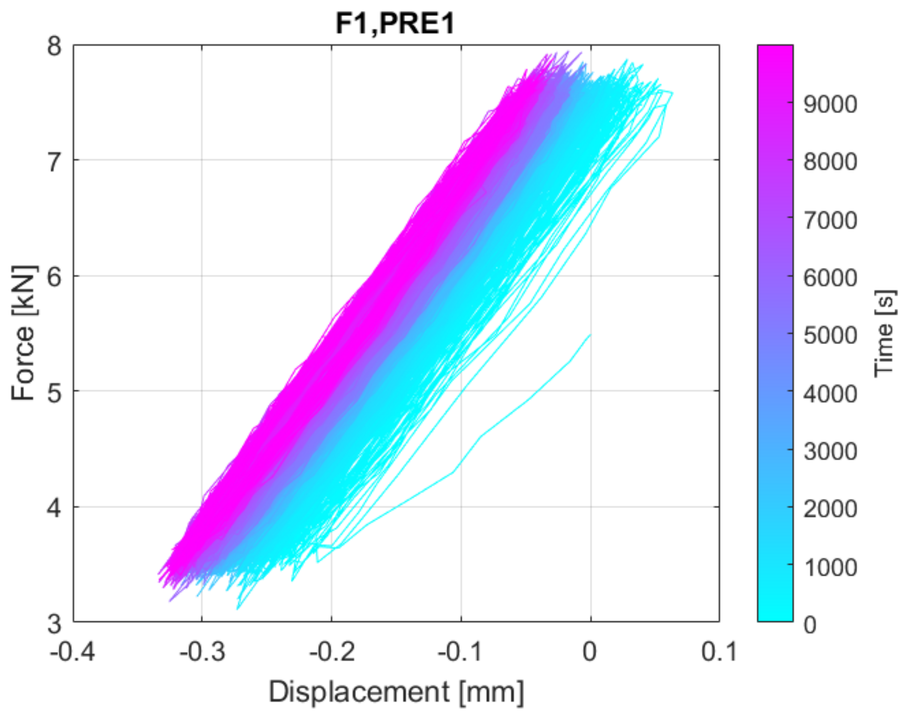

Figure D.309: Force VS absolute displacement

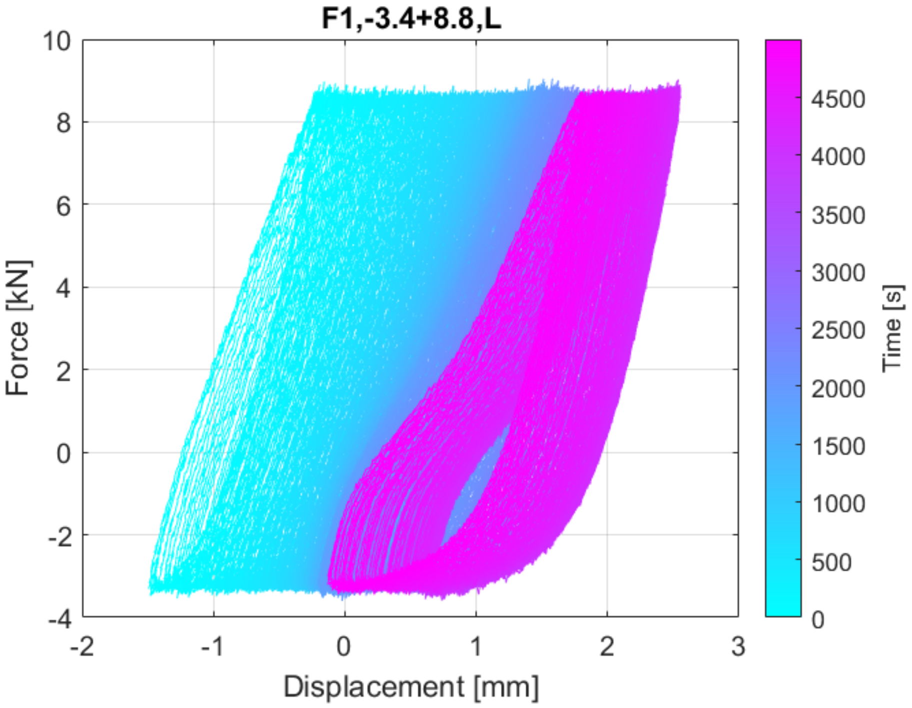

Figure D.310: Force VS absolute displacement

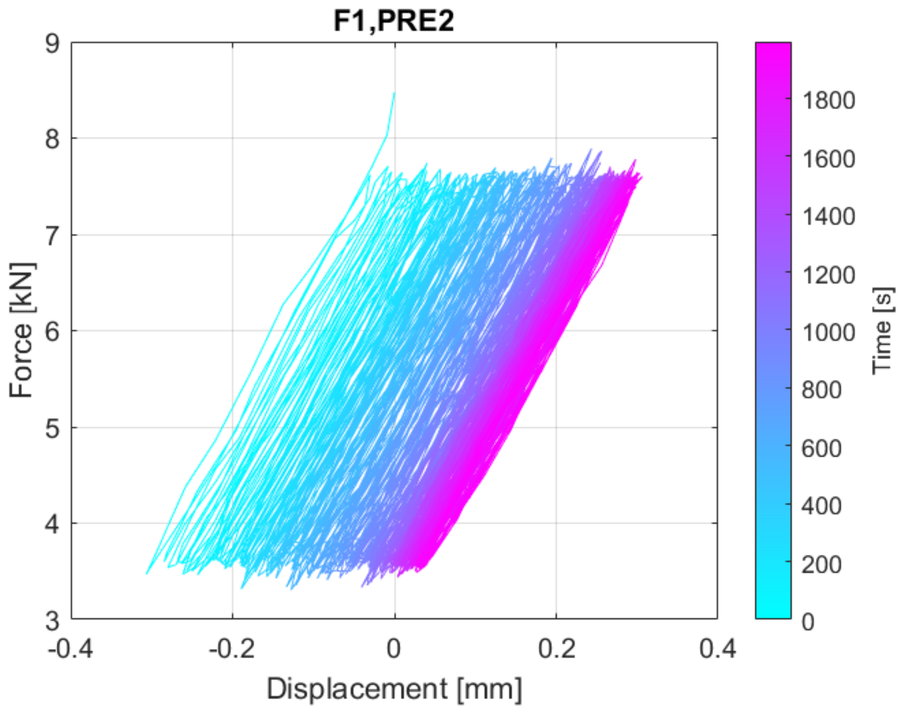

Figure D.311: Force VS absolute displacement

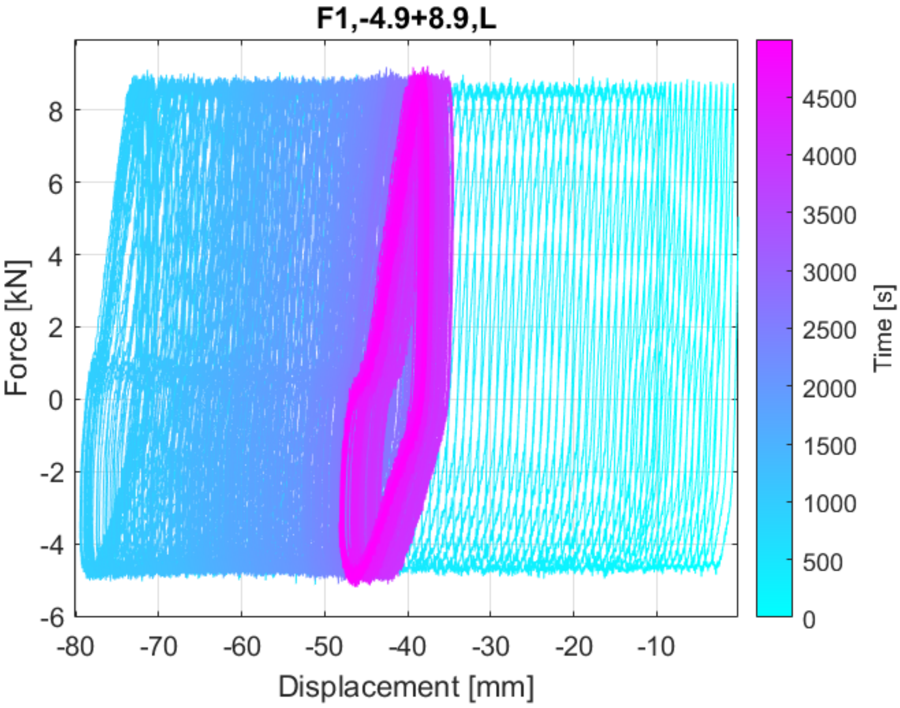

Figure D.312: Force VS absolute displacement

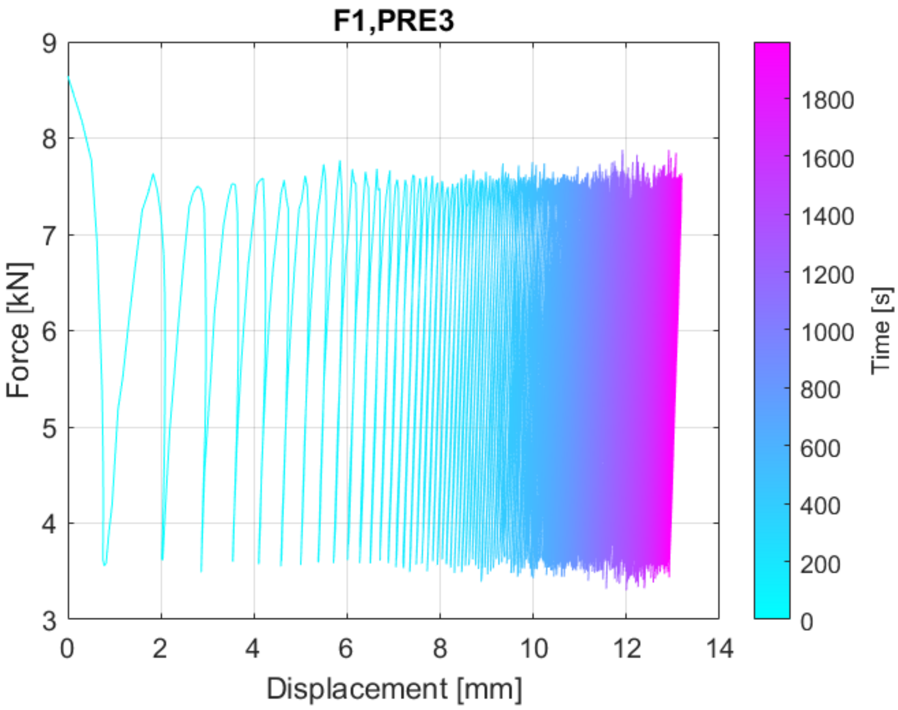

Figure D.313: Force VS absolute displacement

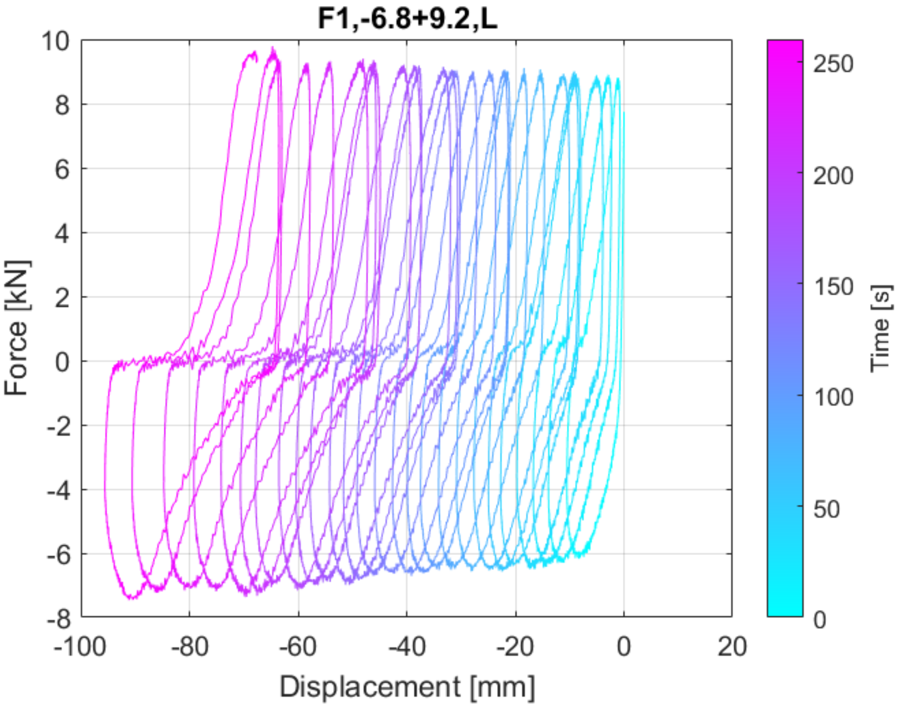

Figure D.314: Force VS absolute displacement

D.7.2 Test subgroup F2 - 1.0 Hz

Figure D.315: Actual loading plan for test subgroup F2

CPT

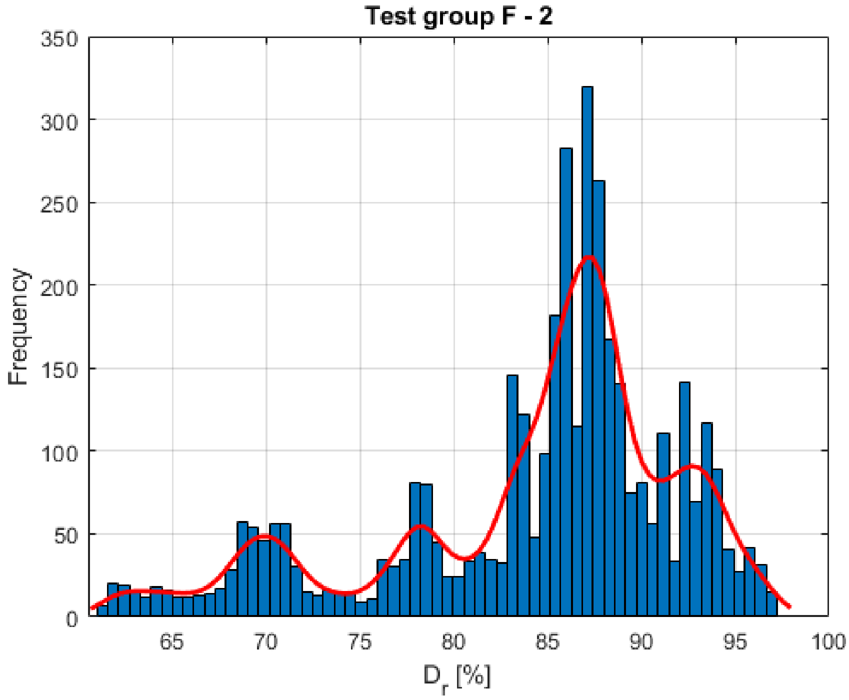

Figure D.316: Dr histogram with distribution fit for test subgroup F2

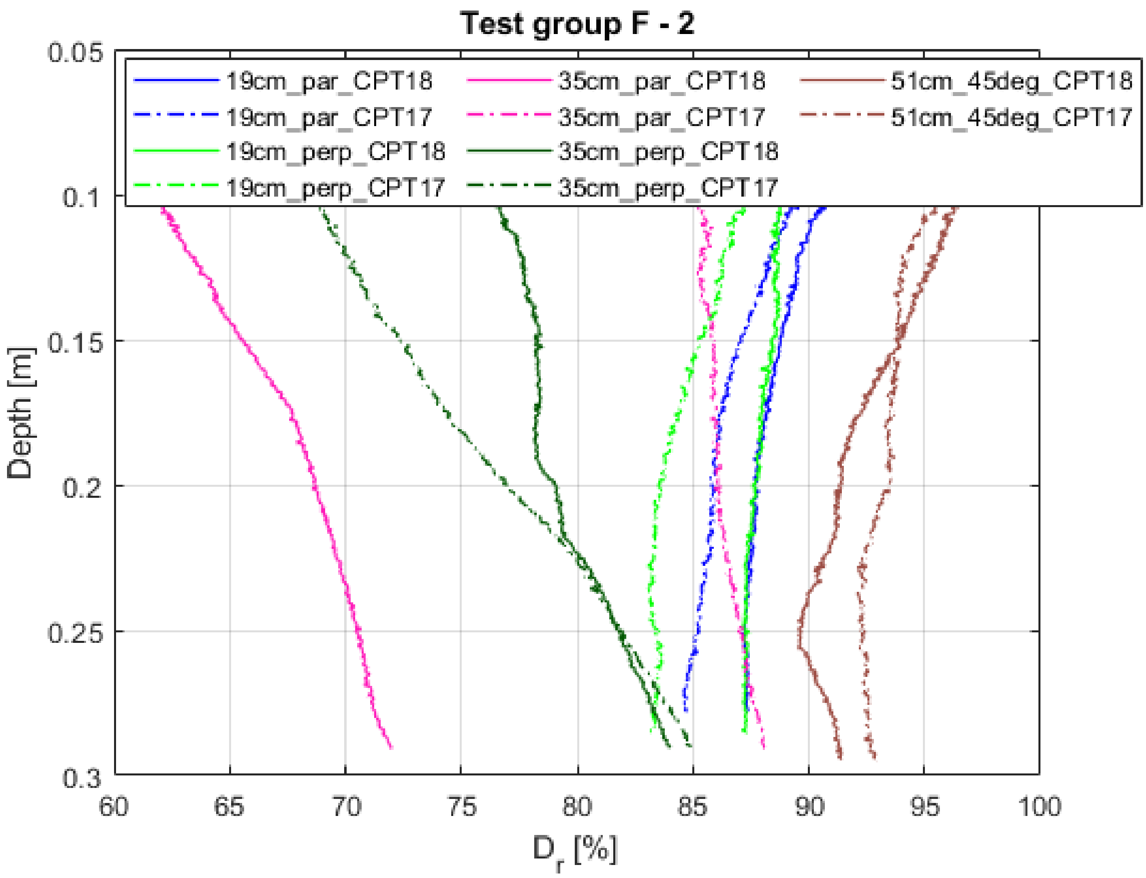

Figure D.317: Test-specific Dr results for CPT test subgroup F2

Force and displacement

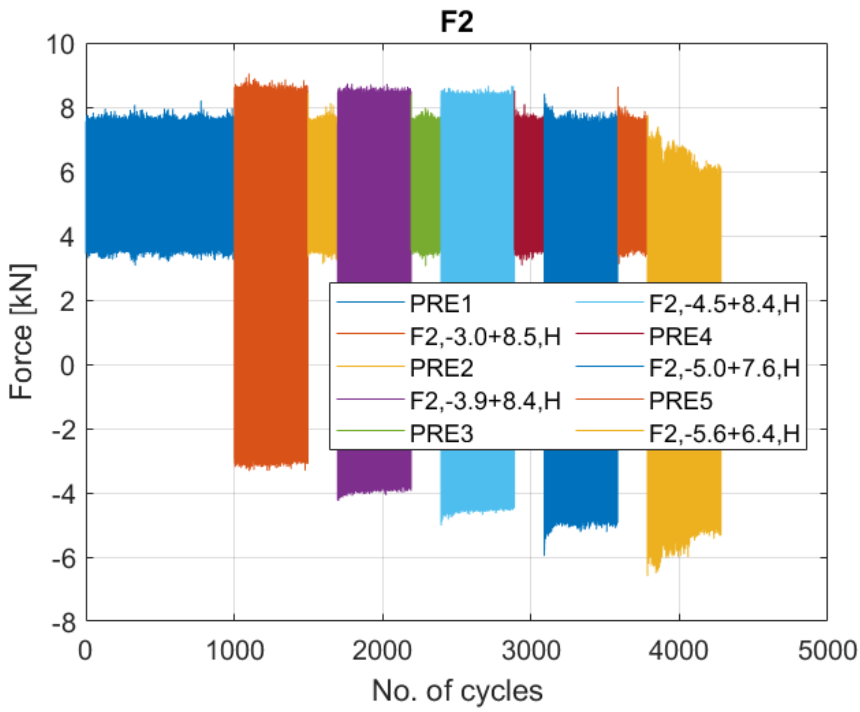

Figure D.318: Force VS No. of cycles

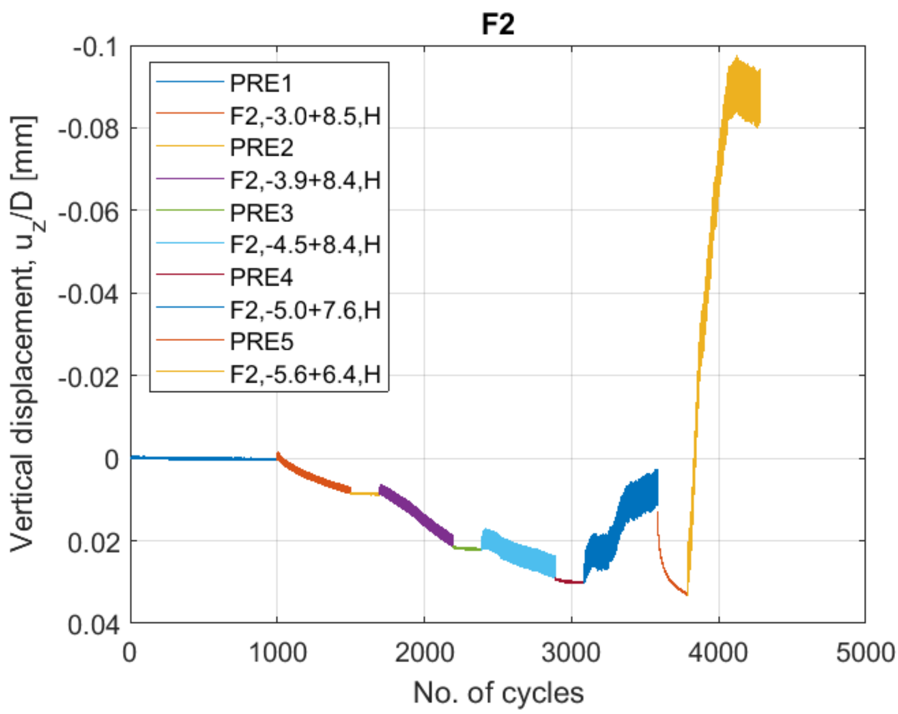

Figure D.319: Displacement VS No. of cycles

Lid Transducers

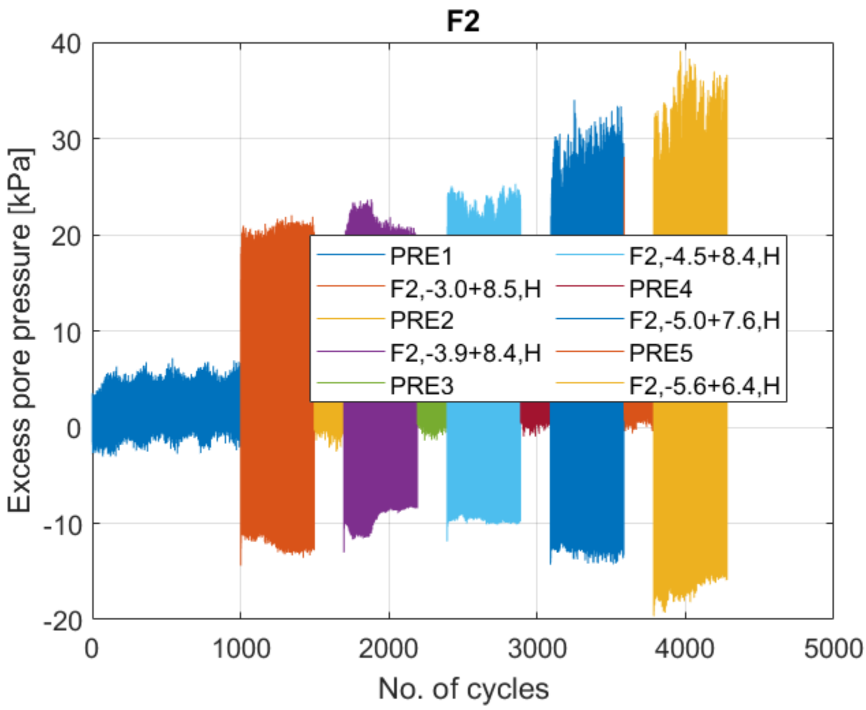

Figure D.320: Pore pressure at lid transducer P6

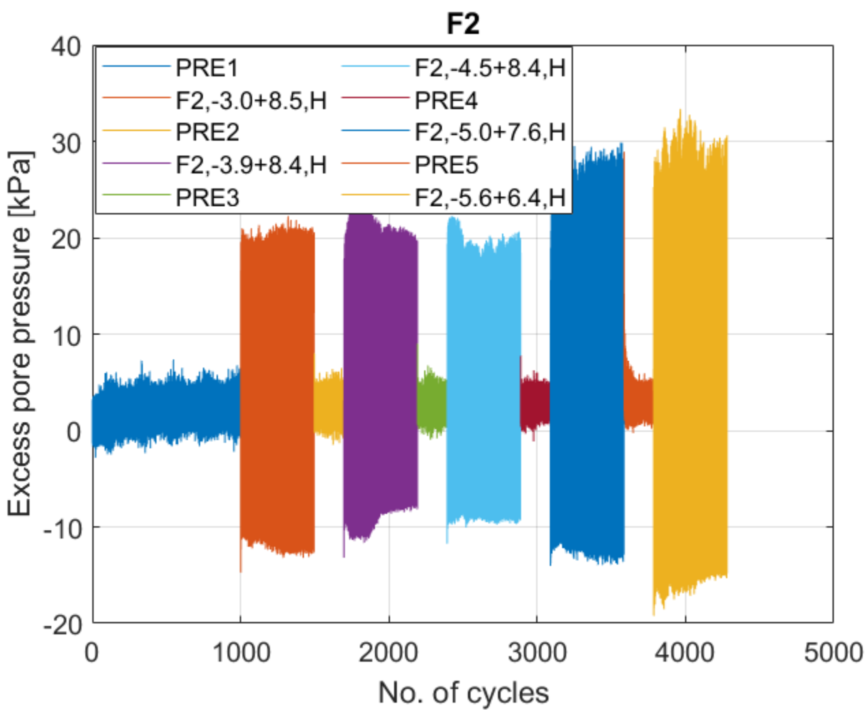

Figure D.321: Pore pressure at lid transducer P10

1st Level Transducers

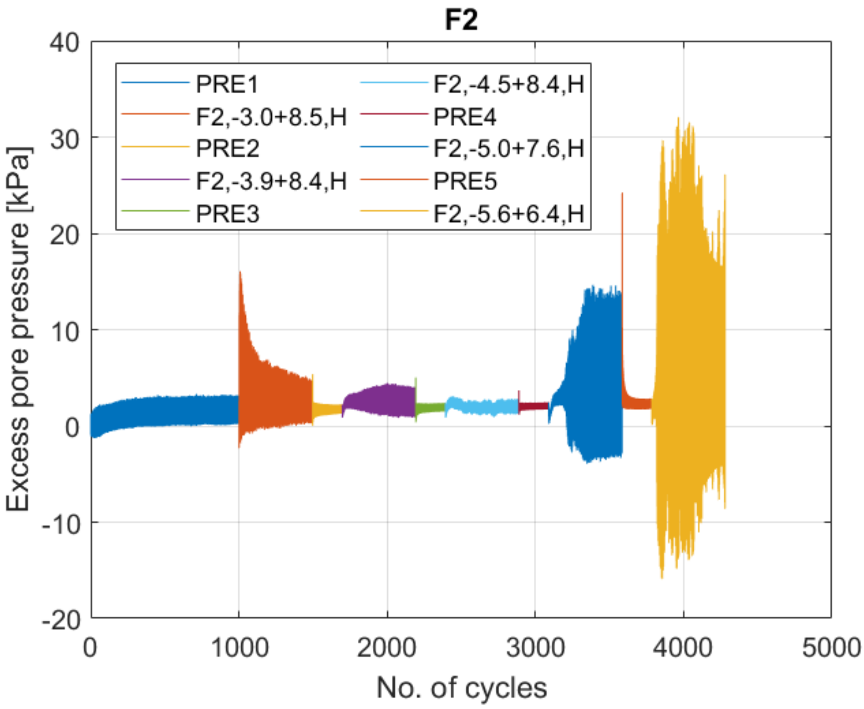

Figure D.322: Pore pressure at 1st level inner side transducer P4

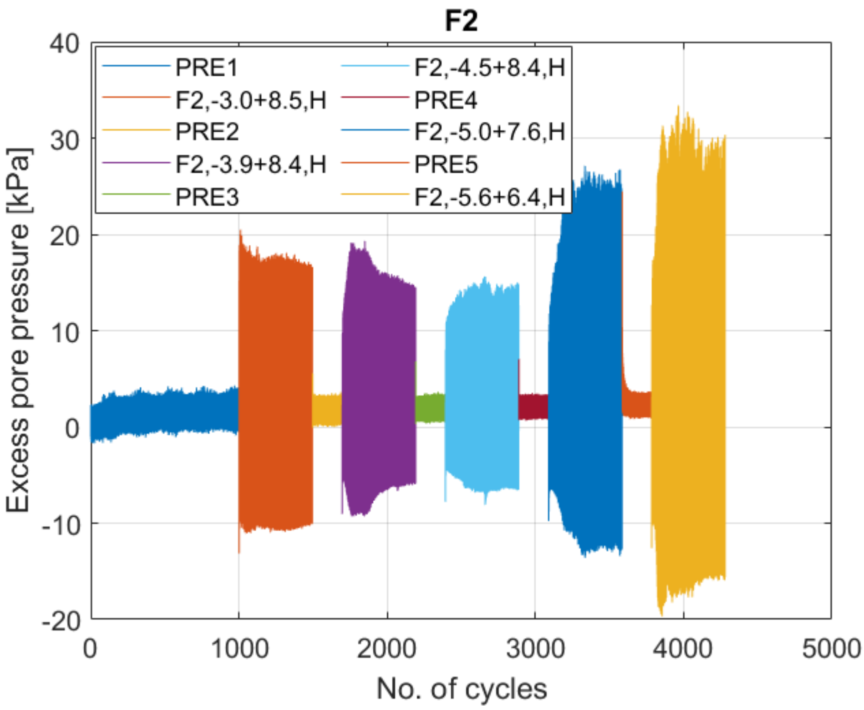

Figure D.323: Pore pressure at 1st level inner side transducer P11

2nd Level Transducers

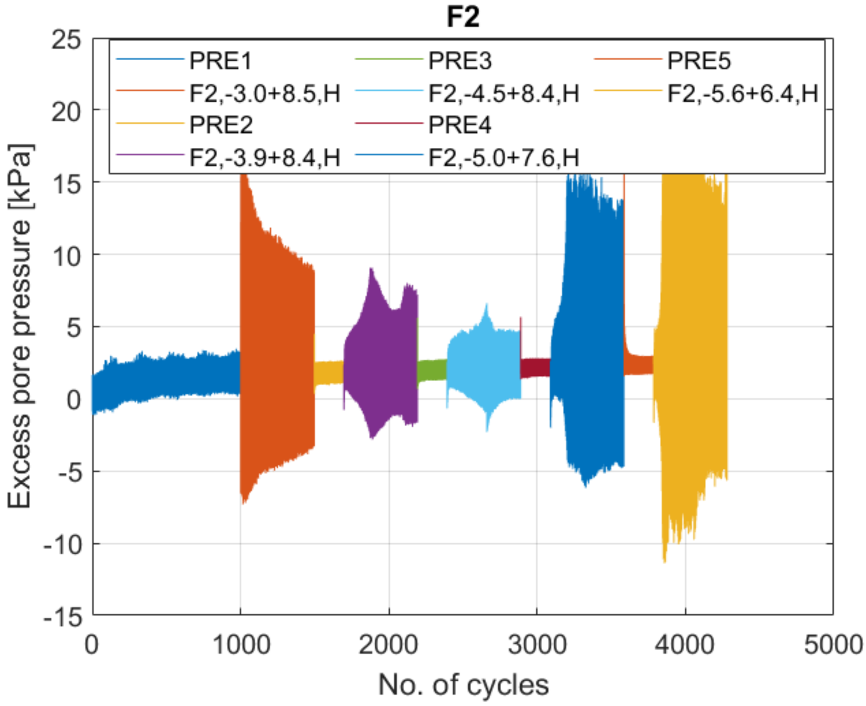

Figure D.324: Pore pressure at 2nd level inner side transducer P12

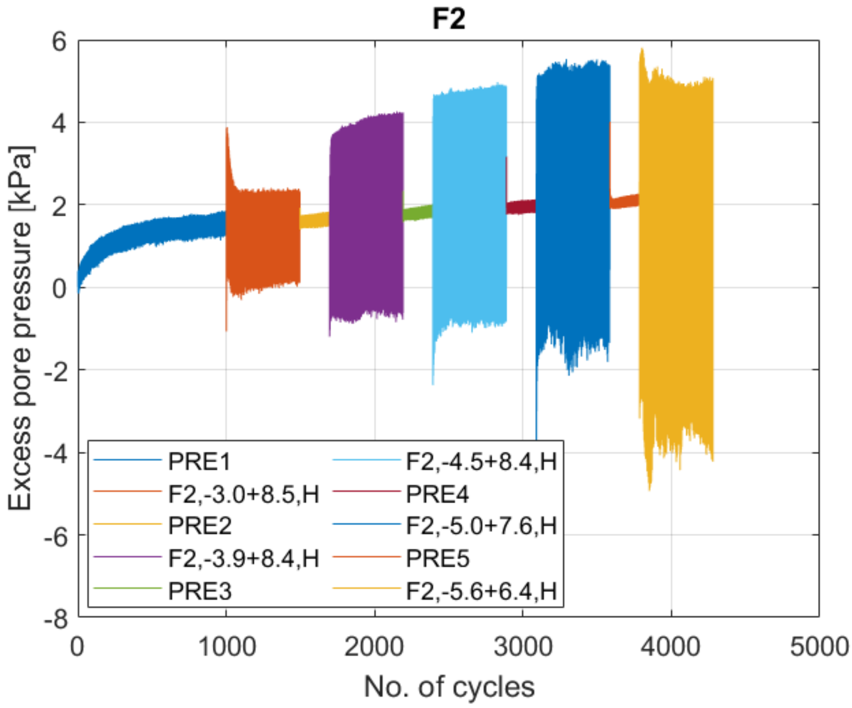

Figure D.325: Pore pressure at 2nd level outer side transducer P1

Skirt Tip Transducers

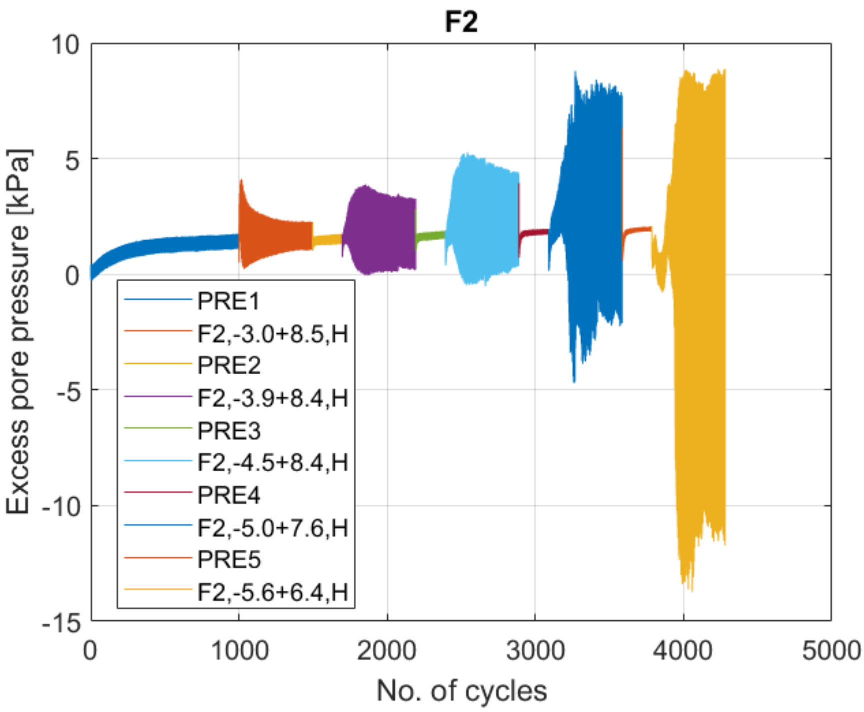

Figure D.326: Pore pressure at tip transducer P2

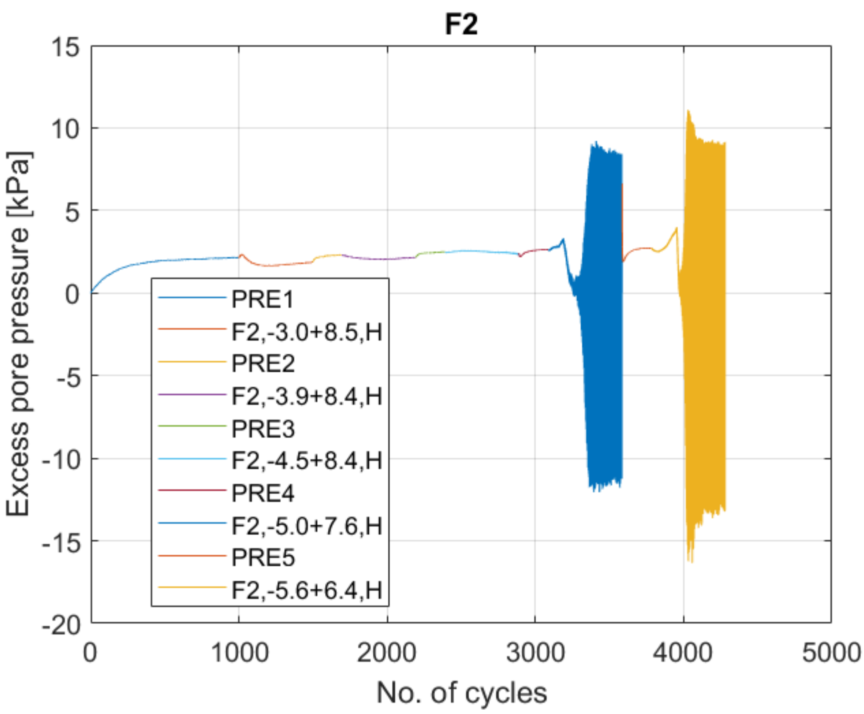

Figure D.327: Pore pressure at tip transducer P8

Force VS displacement

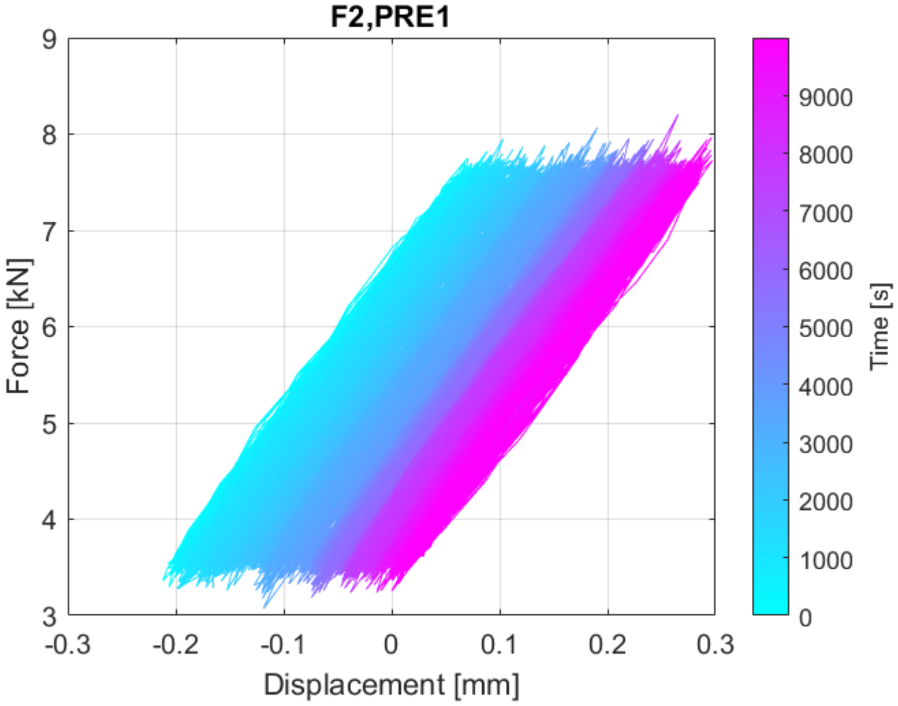

Figure D.328: Force VS absolute displacement

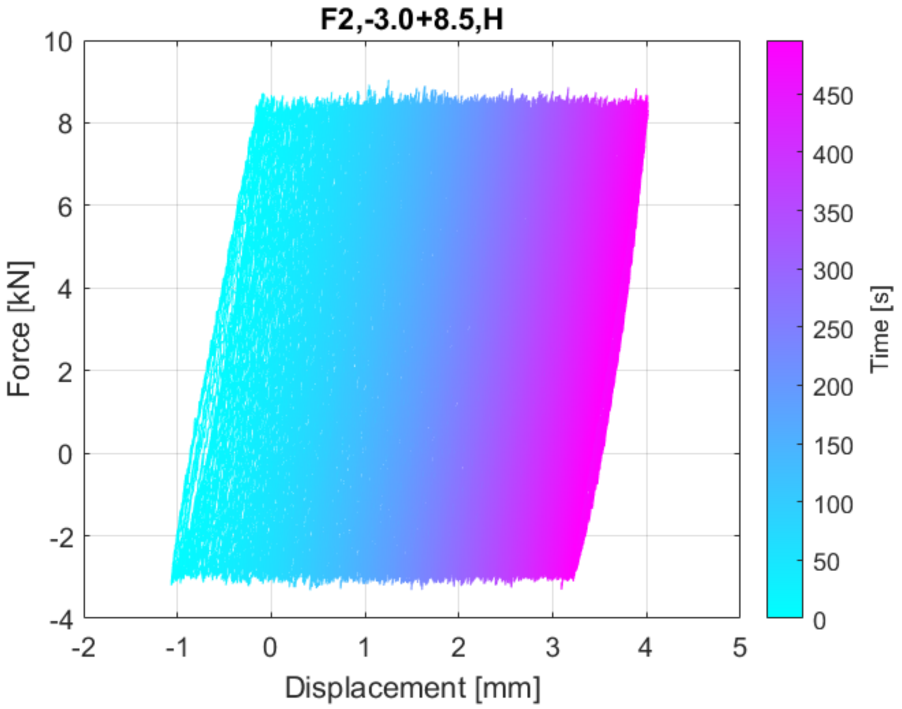

Figure D.329: Force VS absolute displacement

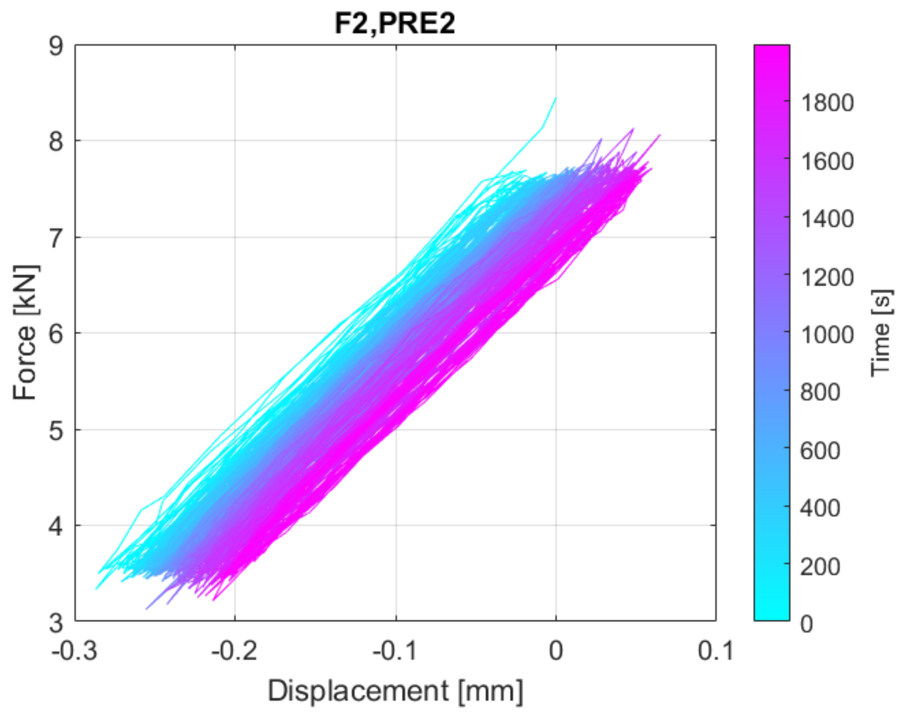

Figure D.330: Force VS absolute displacement

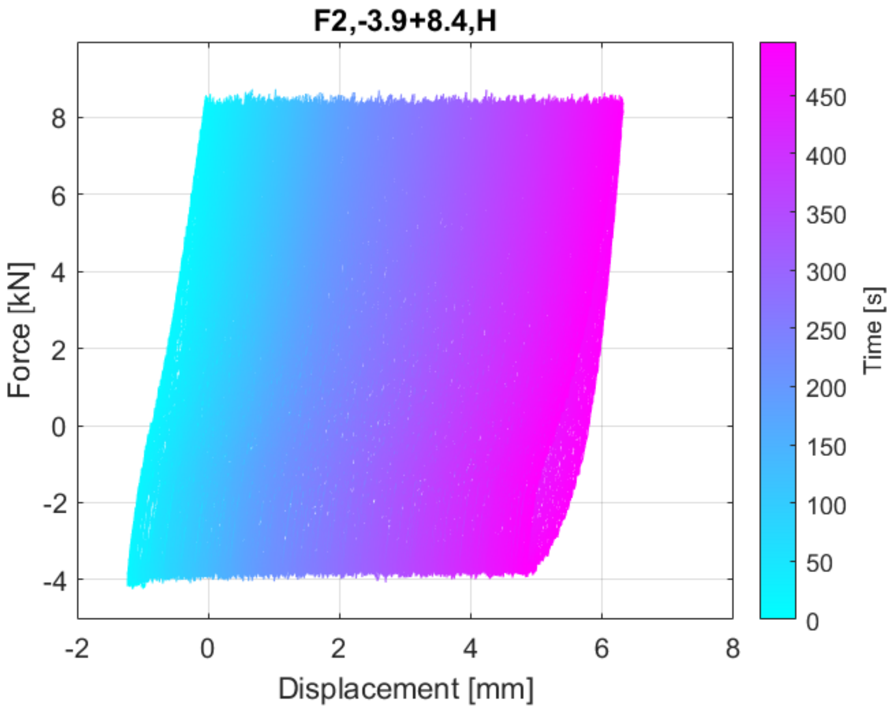

Figure D.331: Force VS absolute displacement

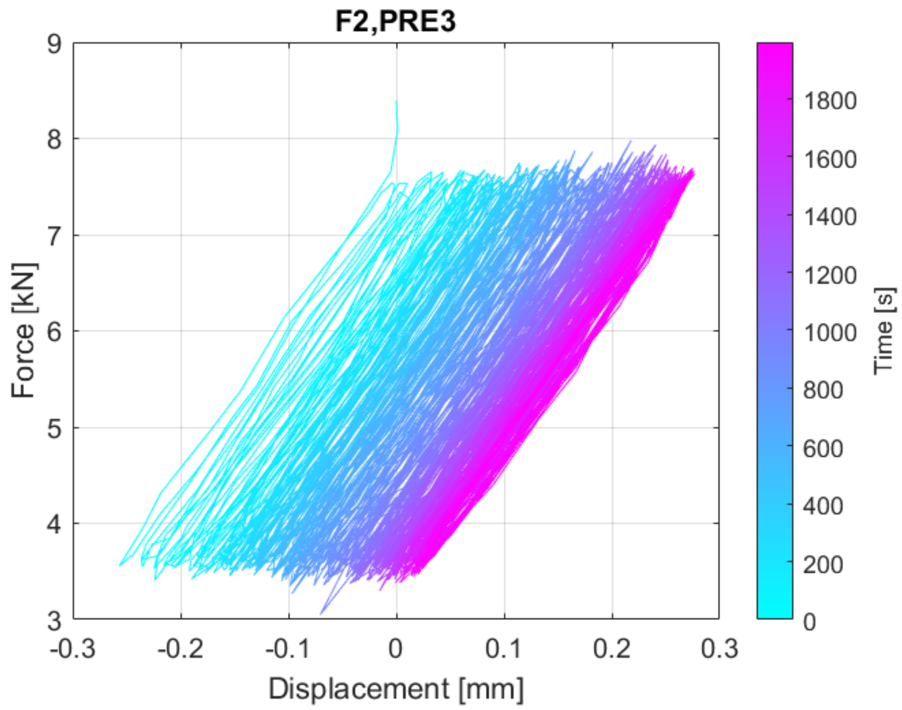

Figure D.332: Force VS absolute displacement

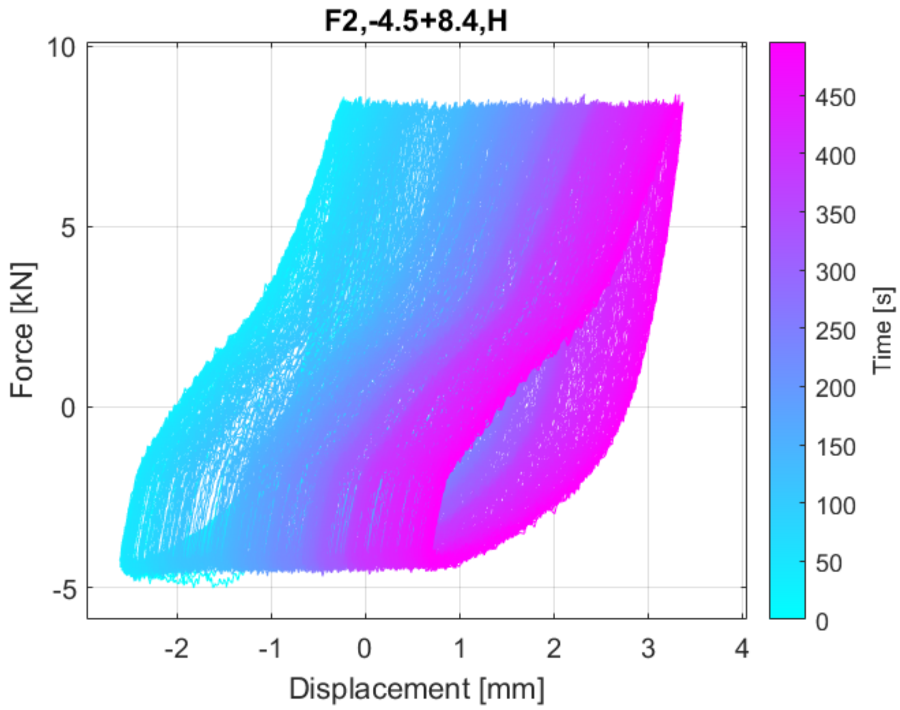

Figure D.333: Force VS absolute displacement

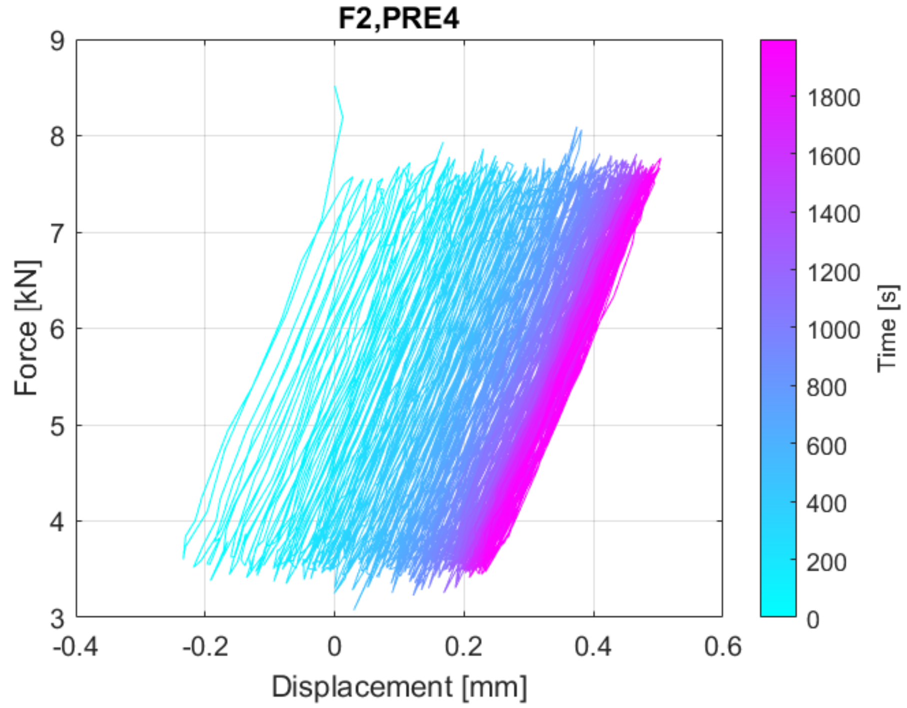

Figure D.334: Force VS absolute displacement

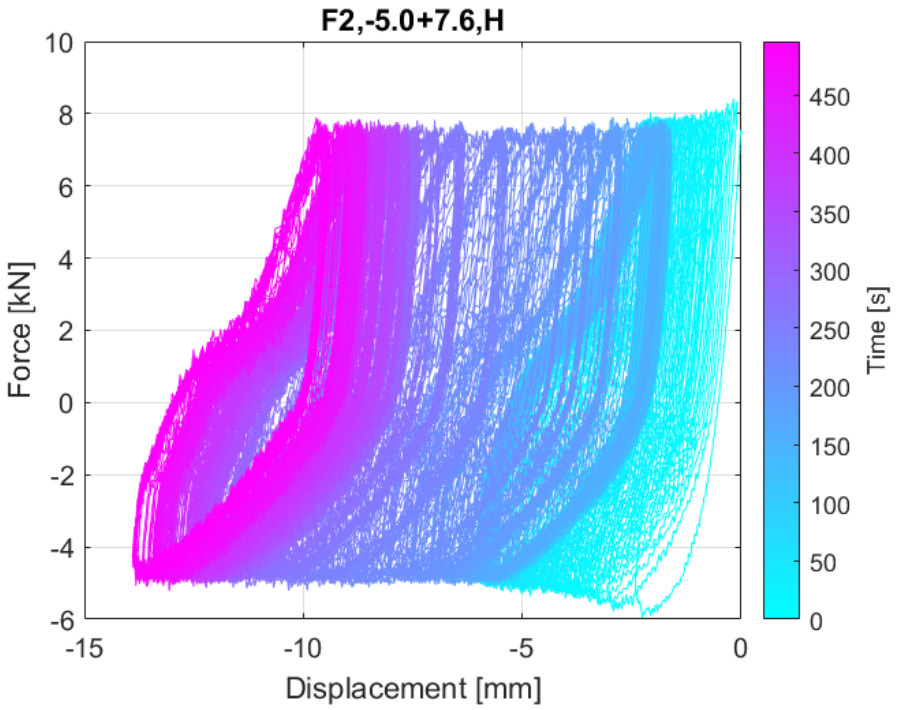

Figure D.335: Force VS absolute displacement

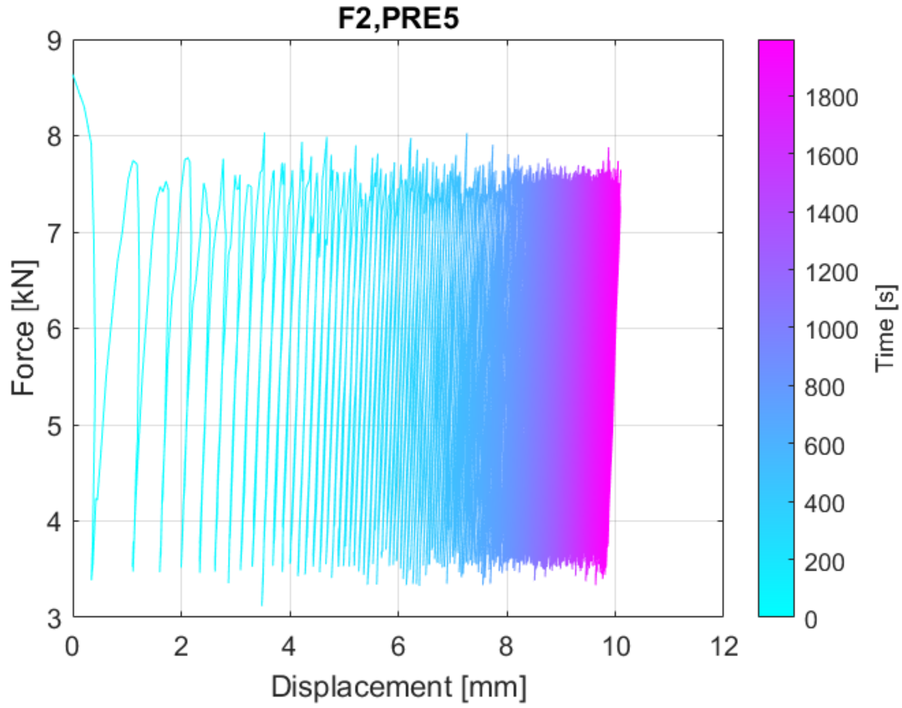

Figure D.336: Force VS absolute displacement

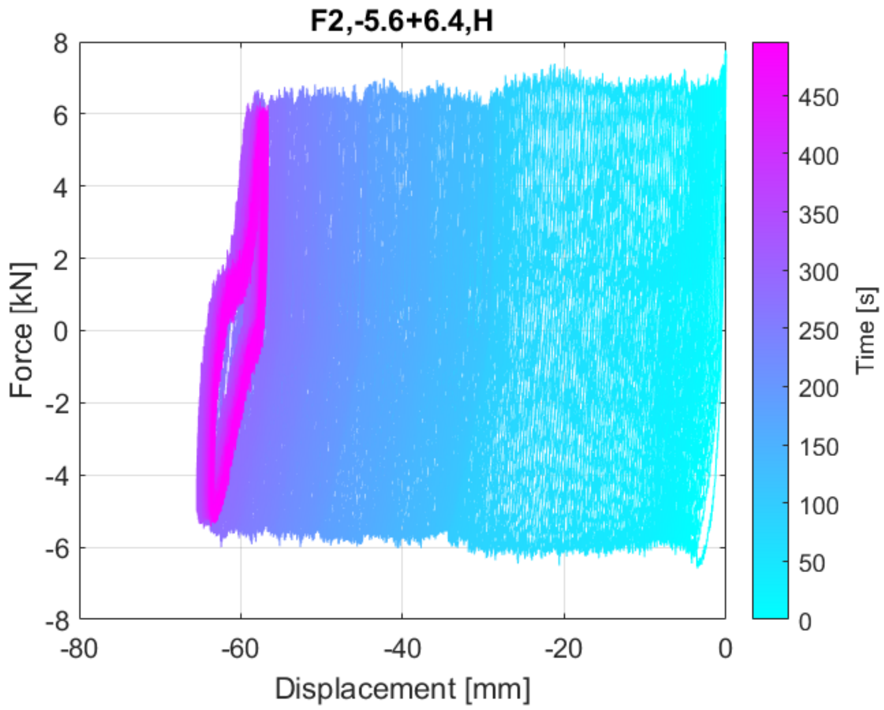

Figure D.337: Force VS absolute displacement

Appendix E | Displacement Based Test

This appendix contains results from displacement based test in order to investigate influence of loading frequency to the build-up of excess pore water pressure.

This test was done in order to confirm or deny the hypothesis about the influence of cyclic load frequency to the development of the excess pore water pressure and the behaviour of the suction bucket under these loads which is discussed in chapter 5. It was noticed that majority of the test subjected to the upwards displacement were loaded with 0.1 Hz loading frequency. To investigate if there is any pattern here test which is summarized in E.1 were performed. Idea behind this test is to keep amplitude of the displacement as a constant and step-by-step increase loading frequency while recording the development of the excess pore water pressure.

Table E.1: Summary of the displacement based test

No. of cycles	Frequency [Hz]	Amplitude [mm]
3000	0.1 0.2 0.3 0.4 0.5 1.0 2.0 5.0 10.0	± 1

As it can be seen from the figure E.1 in order to achieve the same displacement - force needed to be increased with increased loading frequency

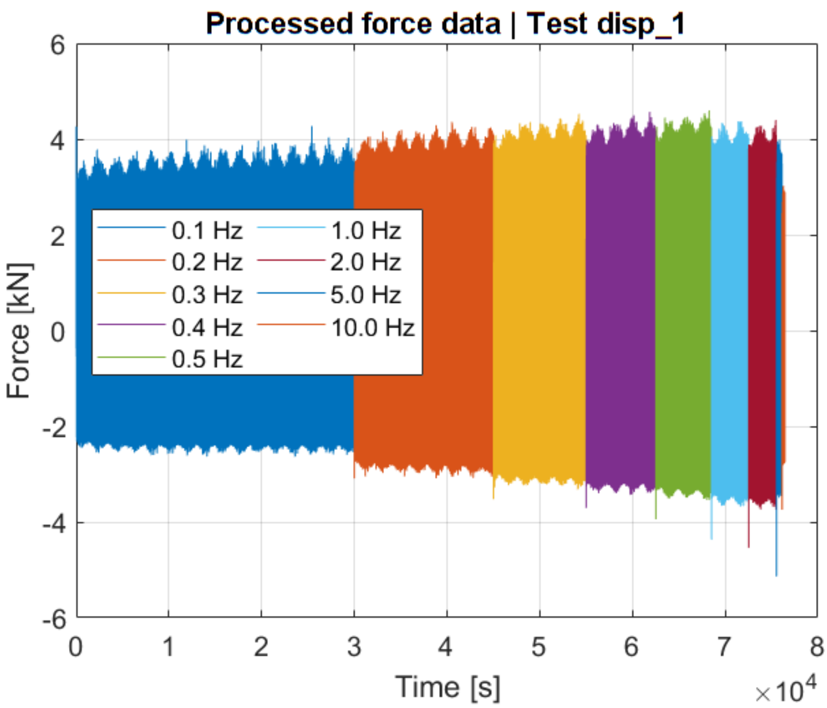

Figure E.1: Force vs time

As it is seen from the figure E.2 amplitude of the displacement remain constant until loading frequency was raised to 5.0 Hz and higher. That could be explained by the limitations of the machinery used, it is simply not capable of moving with such high frequency. For the sake of this investigation results with loading frequency lower than that is used for comparison.

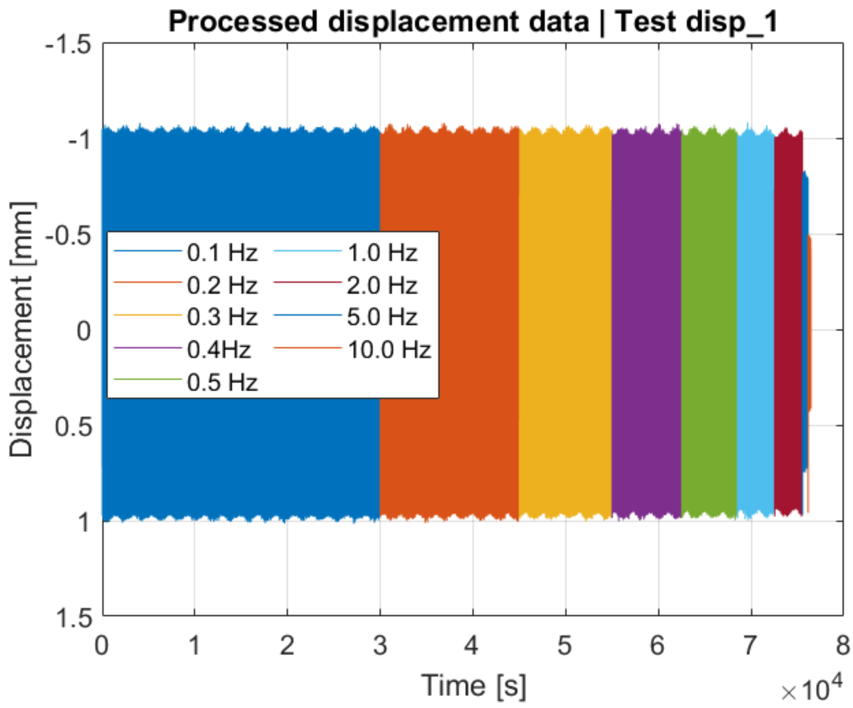

Figure E.2: Displacement vs time

Unloading / reloading stiffness can be seen in figure E.3 and it is clear to see that stiffness increase with increased loading frequency. Bigger fluctuation is observed for higher frequencies, but that could be explained by the earlier mentioned fact that hydraulic piston was not able to move that fast and follow given commands.

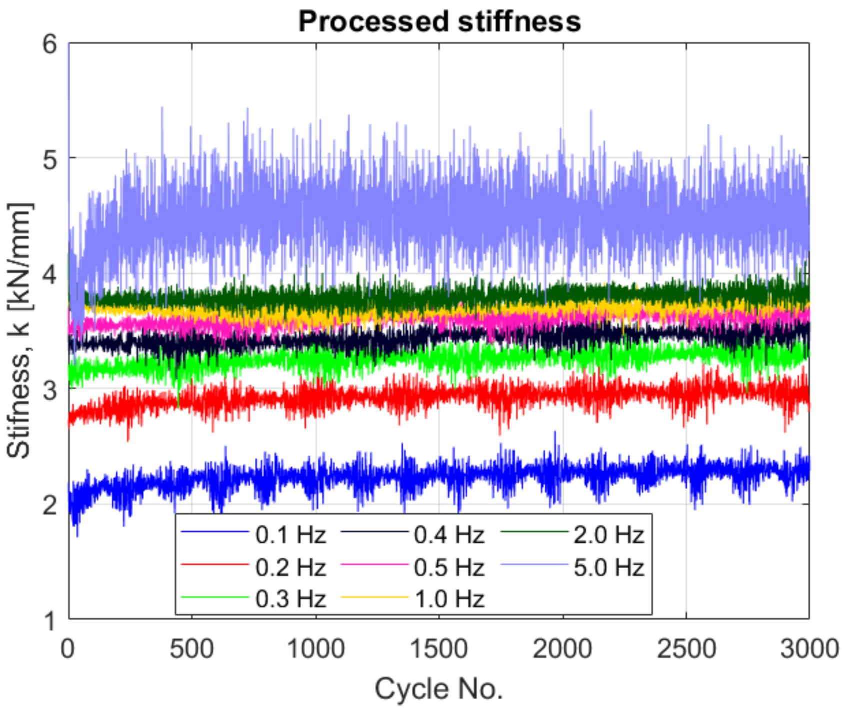

Figure E.3: Unloading/reloading stiffness vs No. of cycles

Development of excess pore water pressure can be seen in E.4 where significant build-up of EPP is observed. It can be argued that it is influenced by the increasing cyclic forces as it is presented in E.1. However, during the test cyclic forces were increasing only for the loading scenarios with $0.1 - 0.5$ Hz, while build-up of EPP in both positive and negative direction was observed during entire test. Explanation for that could be related with the time needed to dissipate of EPP and it is discussed more detailed in chapter 5.

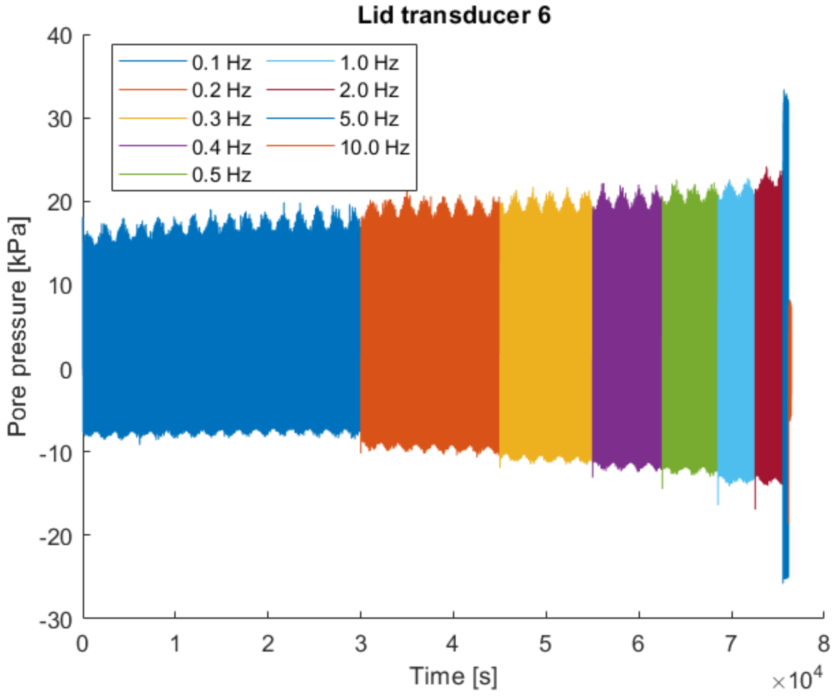

Figure E.4: Pore pressure at lid transducer P6

Appendix F | Excess Pore Pressure Development

This appendix is continuation of chapter 5 where tests grouping according to their displacement were introduced.

In tables below comparison of excess pore pressure development is presented for all three groups exposed to: pulled-up, stable and pushed-down displacements respectively. Comparison is made by comparing values at the 1st cycle with the values at 500th cycle. These values are chosen because they are most common number used in most of the tests. Some test failed before reaching 500 cycles, for such cases values are given to their last cycle which is written in () right after the test name are being used.

- Max PP - Maximum value of excess pore pressure in each cycle
- Min PP - Minimum value of excess pore pressure in each cycle
- Range of PP - Range of excess pore pressure in each cycle between the maximum and minimum values.
  $Range = PP_{max} - PP_{min}$
- Ratio of PP - Ratio of excess pore pressure in each cycle between the maximum and minimum values.
  $Ratio = \frac{PP_{max}}{PP_{min}}$

Table F.1: Changes in pore pressure, first group (Pulled up)

Test	Max PP			Min PP			Range of PP			Ratio of PP		
	1st	500th	Δ %	1st	500th	Δ %	1st	500th	Δ %	1st	500th	Δ %
C2,-2.8+5.5,H	1.82	9.11	400.55	-14.18	-14.31	0.92	16.00	23.42	46.38	-0.13	-0.64	396.00
C3,-4.1+3.2,H (433)	6.90	12.63	83.04	-11.91	-12.01	0.84	18.81	24.64	30.99	-0.58	-1.05	81.52
C4,-4.6+0.9,H (161)	13.26	18.81	41.86	3.71	4.81	29.65	9.55	14.00	46.60	3.57	3.91	9.41
D1,-4.4+5.8,H	2.35	12.55	434.04	-23.94	-22.12	-7.60	26.29	34.67	31.88	-0.10	-0.57	477.98
D2,-4.2+6.4,H	10.77	10.29	-4.46	-21.23	-17.67	-16.77	32.00	27.96	-12.63	-0.51	-0.58	14.79
D2,-4.4+5.6,H	6.25	14.58	133.28	-21.56	-19.45	-9.79	27.81	34.03	22.37	-0.29	-0.75	158.59
D3,-3.7+6.9,L	9.72	13.03	34.05	-8.04	-13.45	67.29	17.76	26.48	49.10	-1.21	-0.97	-19.87
D3,-4.7+6.9,L (87)	14.59	22.77	56.07	-16.06	-21.19	31.94	30.65	43.96	43.43	-0.91	-1.07	18.28
E1,-3.0+4.8,L	6.06	8.53	40.76	-7.95	-9.73	22.39	14.01	18.26	30.34	-0.76	-0.88	15.01
E1,-3.6+4.9,L (148)	8.83	13.90	57.42	-11.90	-15.29	28.49	20.73	29.19	40.81	-0.74	-0.91	22.52
E3,-3.9+4.8,M	4.37	4.90	12.13	-18.68	-14.84	-20.56	23.05	19.74	-14.36	-0.23	-0.33	41.14
F1,-4.9+8.9,L	9.66	23.17	139.86	-14.73	-22.65	53.77	24.39	45.82	87.86	-0.66	-1.02	55.99
F1,-6.8+9.2,L (25)	22.88	32.70	42.92	-27.31	-31.38	14.90	50.19	64.08	27.67	-0.84	-1.04	24.38
F2,-5.0+7.6,H	9.71	21.42	120.60	-22.03	-21.31	-3.27	31.74	42.73	34.63	-0.44	-1.00	128.05
F2,-5.6+6.4,H	20.00	28.56	42.80	-27.70	-23.91	-13.68	47.70	52.47	10.00	-0.72	-1.19	65.44

Number of cycles varies from test to test. Comparison is made for the most common number of cycles - 500. If test stopped before reaching this value, number of cycles is provided in ()

Table F.2: Changes in pore pressure, second group (Stable)

Test	Max PP			Min PP			Range of PP			Ratio of PP		
	1st	500th	Δ %	1st	500th	Δ %	1st	500th	Δ %	1st	500th	Δ %
C1,1.9+6.9,H	5.30	7.83	47.74	-7.96	-7.48	-6.03	13.26	15.31	15.46	-0.67	-1.05	57.21
C1,-0.7+7.3,H	6.91	8.85	28.08	-6.83	-6.69	-2.05	13.74	15.54	13.10	-1.01	-1.33	30.76
C2,-2.7+6.6,H	6.47	9.43	45.75	-11.11	-8.84	-20.43	17.58	18.27	3.92	-0.58	-1.07	83.18
D1,-2.3+6.6,H	11.38	12.74	11.95	-13.49	-10.77	-20.16	24.87	23.51	-5.47	-0.84	-1.18	40.22
D1,-3.2+6.6,H	8.89	16.83	89.31	-10.57	-13.59	28.57	19.46	30.42	56.32	-0.84	-1.24	47.24
D1,-3.7+6.5,H	14.62	15.80	8.07	-15.46	-10.61	-31.37	30.08	26.41	-12.20	-0.95	-1.49	57.47
D1,-4.2+6.4,H	11.84	17.27	45.86	-13.85	-10.77	-22.24	25.69	28.04	9.15	-0.86	-1.60	87.57
D2,-3.2+6.5,H	15.03	16.03	6.65	-20.55	-12.49	-39.22	35.58	28.52	-19.84	-0.73	-1.28	75.48
D3,-2.7+6.9,L	9.82	7.53	-23.32	-8.39	-6.19	-26.22	18.21	13.72	-24.66	-1.17	-1.22	3.93
E1,-1.8+4.8,L	4.00	1.85	-53.75	-7.86	-6.71	-14.63	11.86	8.56	-27.82	-0.51	-0.28	-45.82
E1,-2.4+4.8,L	2.96	4.80	62.16	-7.25	-8.42	16.14	10.21	13.22	29.48	-0.04	-0.57	39.63
E2,-1.6+4.5,H	5.84	8.54	46.23	-10.48	-9.05	-13.65	16.32	17.59	7.78	-0.56	-0.94	69.34
E2,-2.2+4.6,H	6.83	10.13	48.32	-11.48	-10.62	-7.49	18.31	20.75	13.33	-0.60	-0.95	60.33
E2,-2.7+4.5,H	8.50	11.39	34.00	-12.76	-11.24	-11.91	21.26	22.63	6.44	-0.67	-1.01	52.12
E2,-3.2+4.5,H	9.18	12.88	40.31	-13.62	-11.79	-13.44	22.8	24.67	8.20	-0.67	-1.09	62.08
E2,-3.6+4.5,H	10.21	11.33	10.97	-14.65	-9.39	-35.90	24.86	20.72	-16.65	-0.70	-1.21	73.14
E3,-1.7+4.7,M	5.36	-8.95	-266.98	-8.93	-8.90	-0.33	14.29	-0.05	-100.35	-0.60	1.01	-267.54
E3,-2.3+4.7,M	8.65	8.47	-2.08	-10.23	-9.54	-6.74	18.88	18.01	-4.61	-0.85	-0.89	5.00
E3,-2.9+4.8,M	8.33	10.79	29.53	-10.78	-10.67	-1.02	19.11	21.46	12.30	-0.77	-1.01	30.87
E3,-3.4+4.6,M	8.40	12.24	45.71	-11.81	-10.55	-10.67	20.21	22.79	12.77	-0.71	-1.16	63.12
F1,-3.4+8.8,L	9.68	11.11	14.77	-8.80	-9.74	10.68	18.48	20.85	12.82	-1.10	-1.14	3.70
F2,-3.0+8.5,H	16.59	18.77	13.14	-14.04	-13.96	-0.57	30.63	32.73	6.86	-1.18	-1.34	13.79
F2,-4.5+8.4,H	19.38	22.39	15.53	-12.55	-11.29	-10.04	31.93	33.68	5.48	-1.54	-1.98	28.43

Number of cycles varies from test to test. Comparison is made for the most common number of cycles - 500. If test stopped before reaching this value, number of cycles is provided in ()

Table F.3: Changes in pore pressure, third group (Pushed down)

Test	Max PP			Min PP			Range of PP			Ratio of PP		
	1st	500th	Δ %	1st	500th	Δ %	1st	500th	Δ %	1st	500th	Δ %
A1.-0.2+28.7.H	48.19	24.60	-48.95	-16.28	-22.99	41.22	64.47	47.59	-26.18	-2.96	-1.07	-63.85
A2.-3+35.1.H	28.36	4.57	-83.89	-7.85	1.05	-86.62	36.21	3.52	-90.28	-3.61	4.35	-220
A3.-3+32.1.H	67.18	31.73	-52.77	-26.19	-8.92	-65.94	93.37	40.65	-56.46	-2.57	-3.56	38.68
C1,-2.9+10.0,H	13.77	17.36	26.07	-9.54	-7.77	-18.55	23.31	25.13	7.81	-1.44	-2.23	54.79
F2,-3.9+8.4,H	14.37	12.73	16.20	-14.48	-11.71	-19.13	28.85	27.91	-3.26	-0.99	-1.38	39.40

Number of cycles varies from test to test. Comparison is made for the most common number of cycles - 500. If test stopped before reaching this value, number of cycles is provided in ()

F.1 Pulled up - Overburden pressure build up

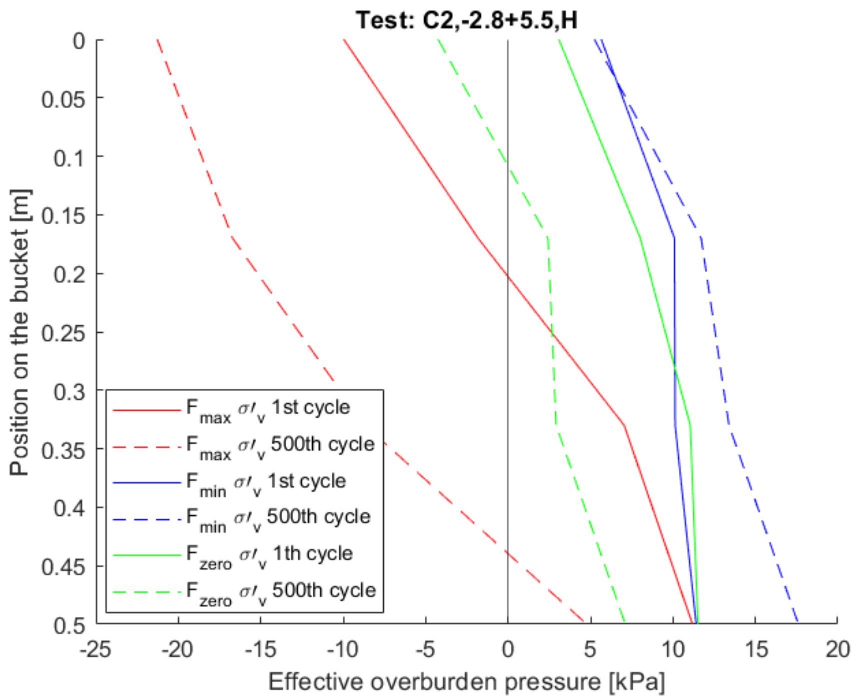

Figure F.1: Overburden pressure build up from 1st to 500th cycle.

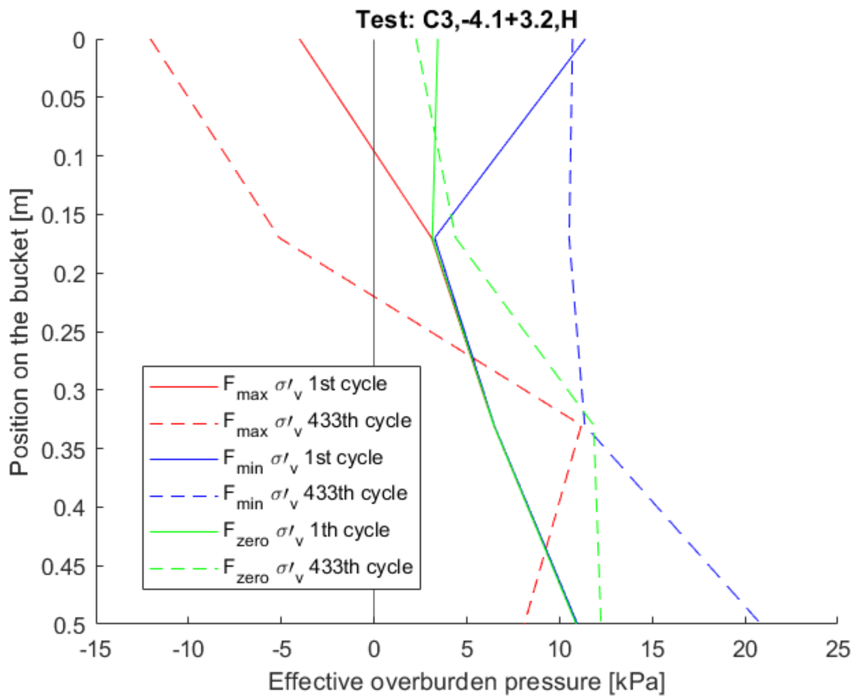

Figure F.2: Overburden pressure build up from 1st to 433th cycle.

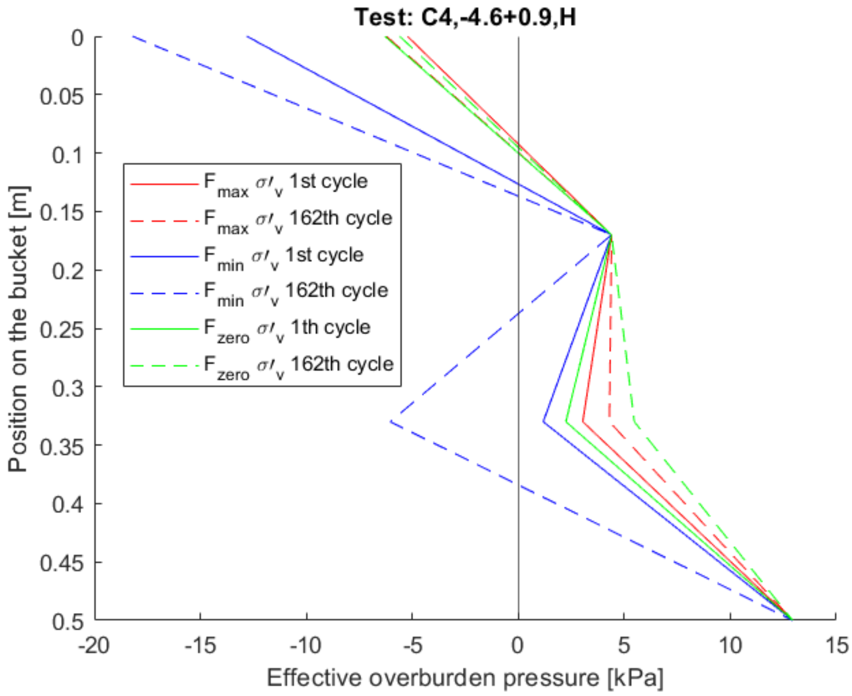

Figure F.3: Overburden pressure build up from 1st to 162th cycle.

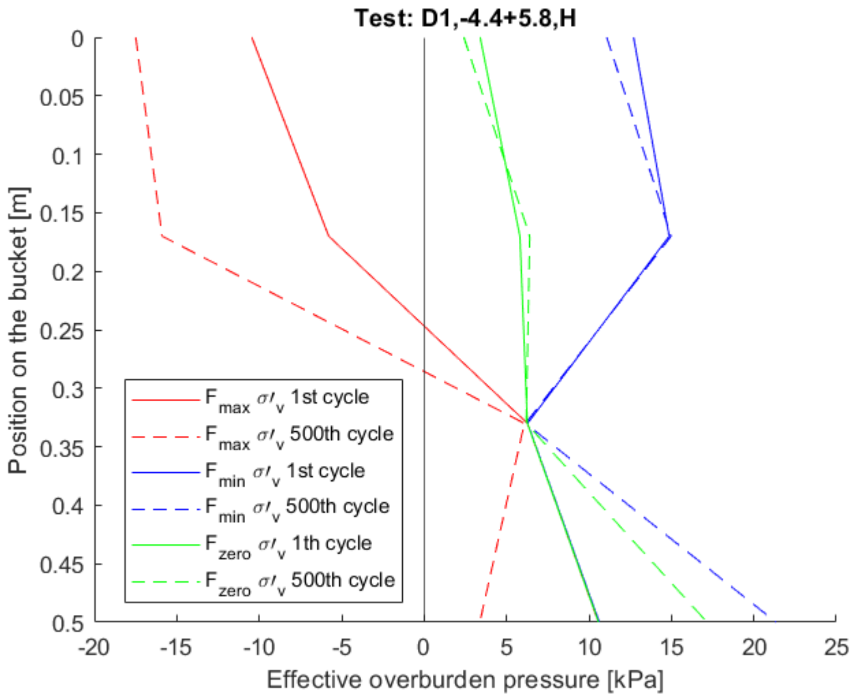

Figure F.4: Overburden pressure build up from 1st to 500th cycle.

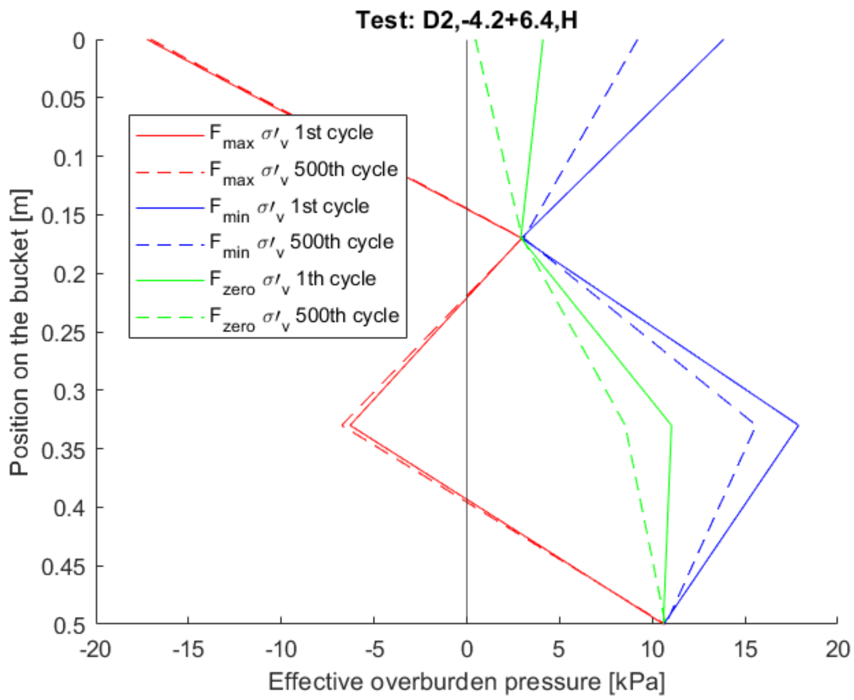

Figure F.5: Overburden pressure build up from 1st to 500th cycle.

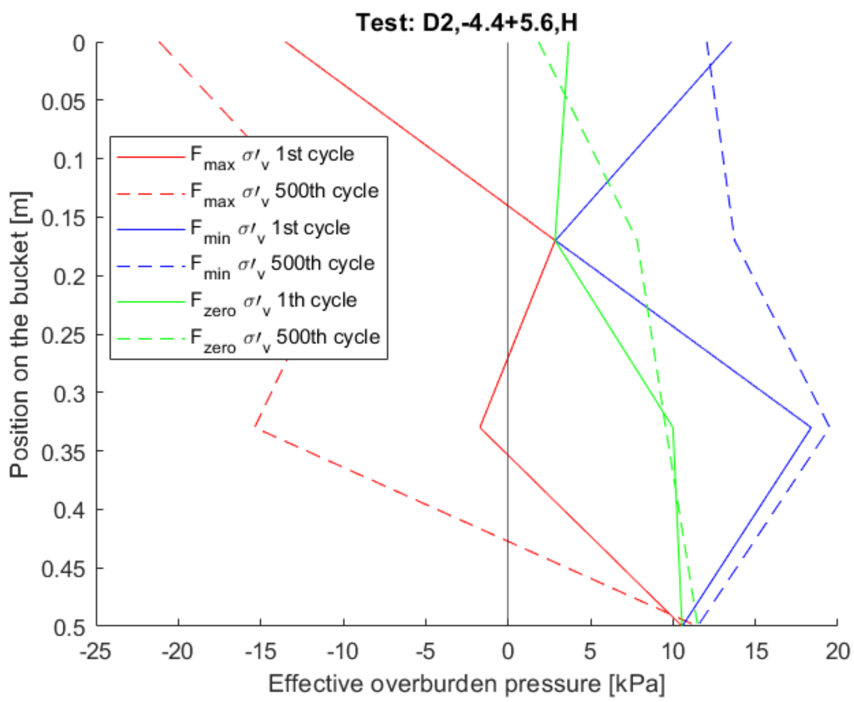

Figure F.6: Overburden pressure build up from 1st to 500th cycle.

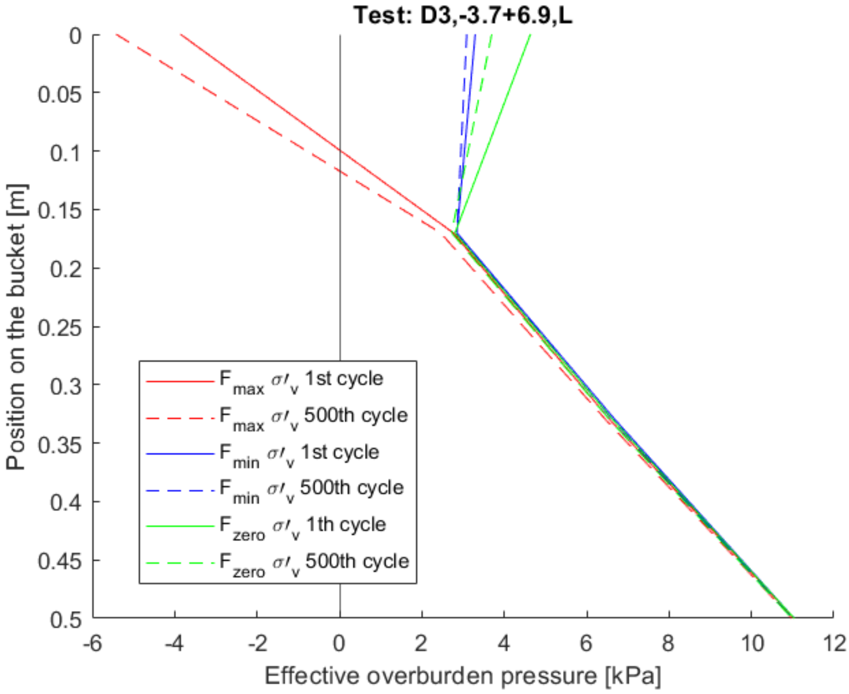

Figure F.7: Overburden pressure build up from 1st to 500th cycle.

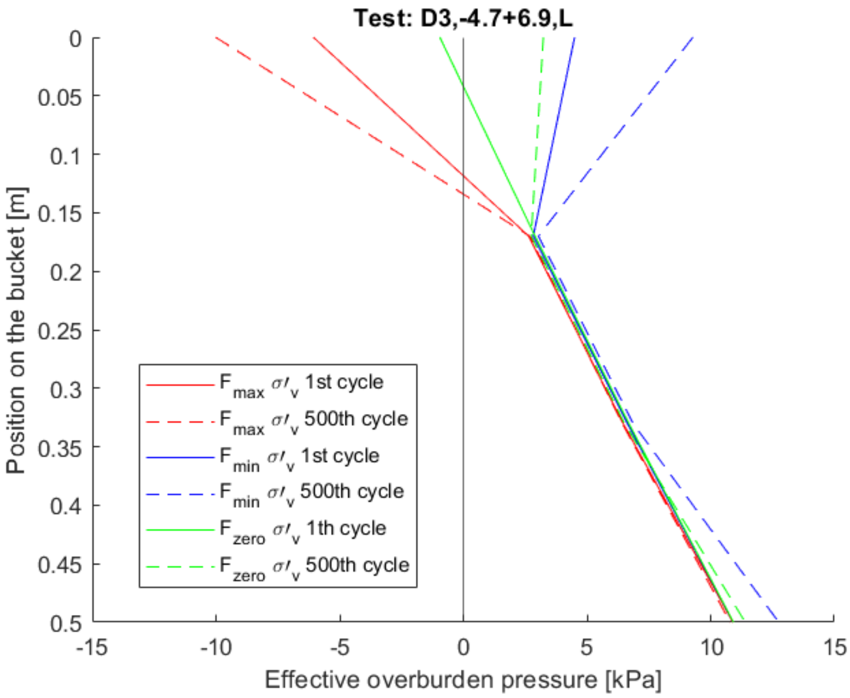

Figure F.8: Overburden pressure build up from 1st to 500th cycle.

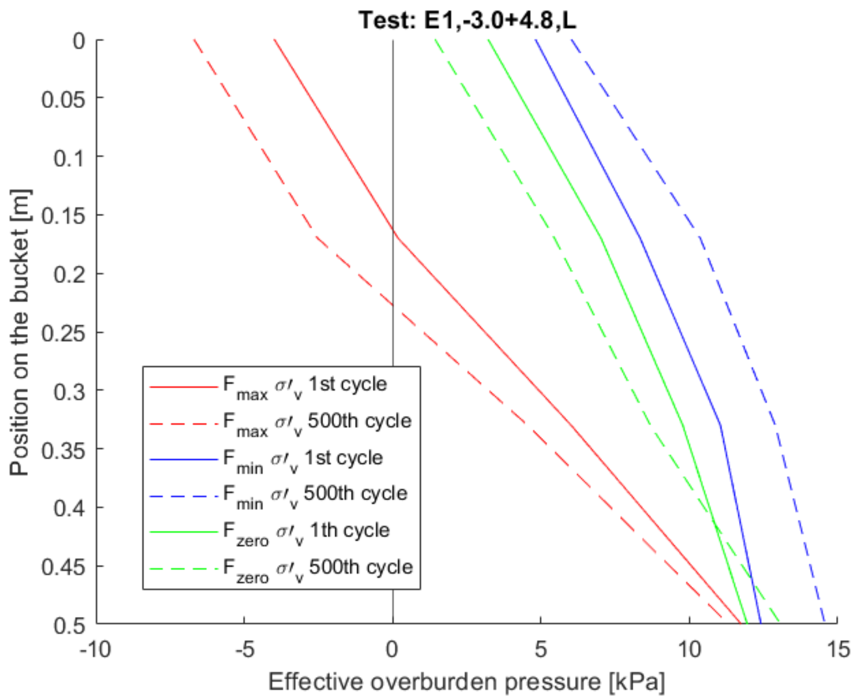

Figure F.9: Overburden pressure build up from 1st to 500th cycle.

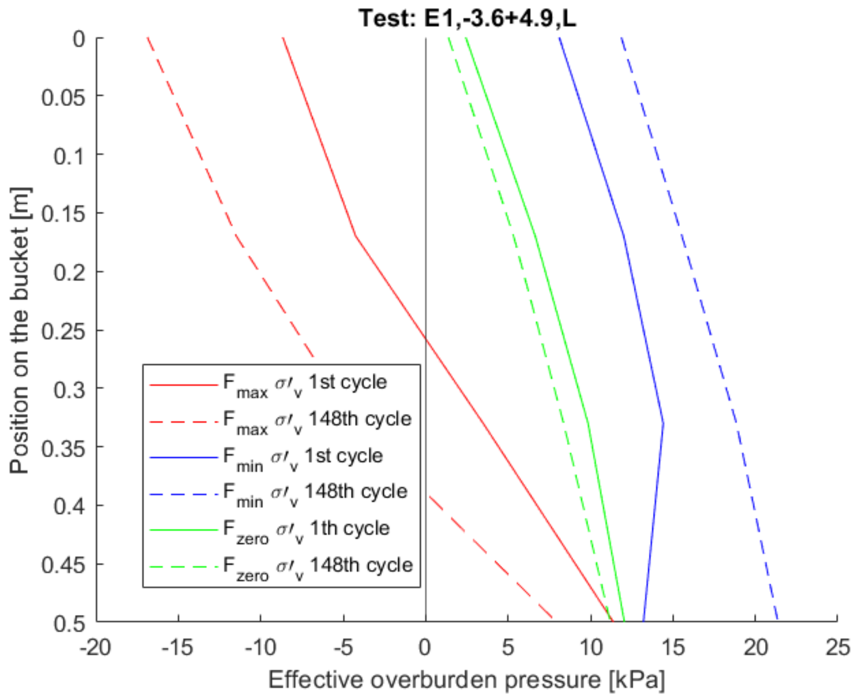

Figure F.10: Overburden pressure build up from 1st to 148th cycle.

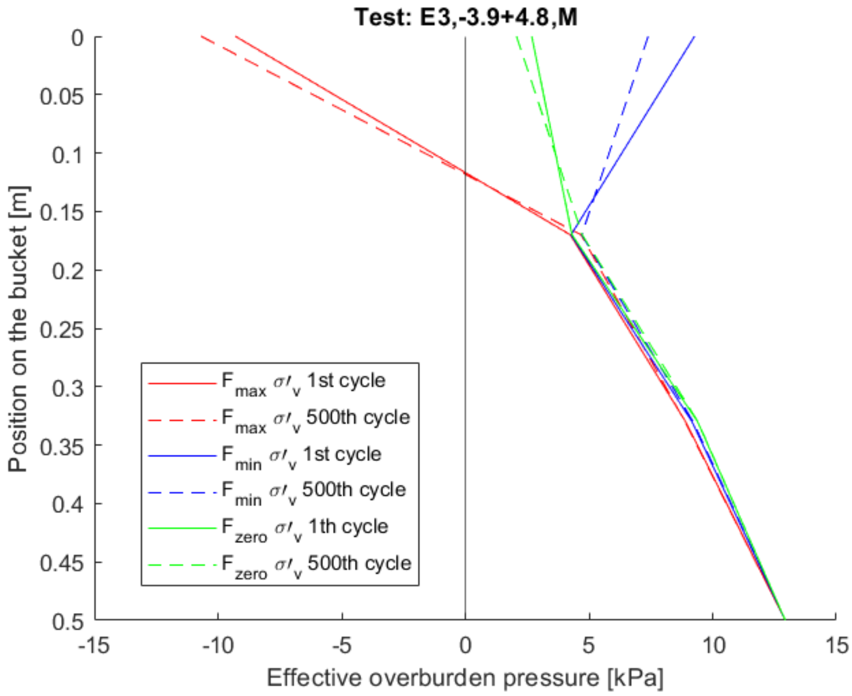

Figure F.11: Overburden pressure build up from 1st to 500th cycle.

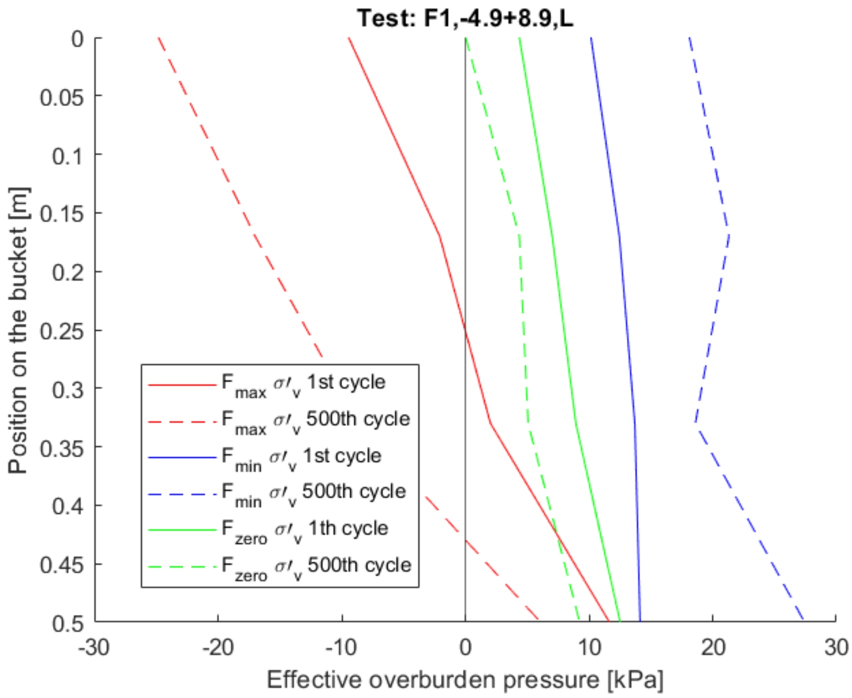

Figure F.12: Overburden pressure build up from 1st to 500th cycle.

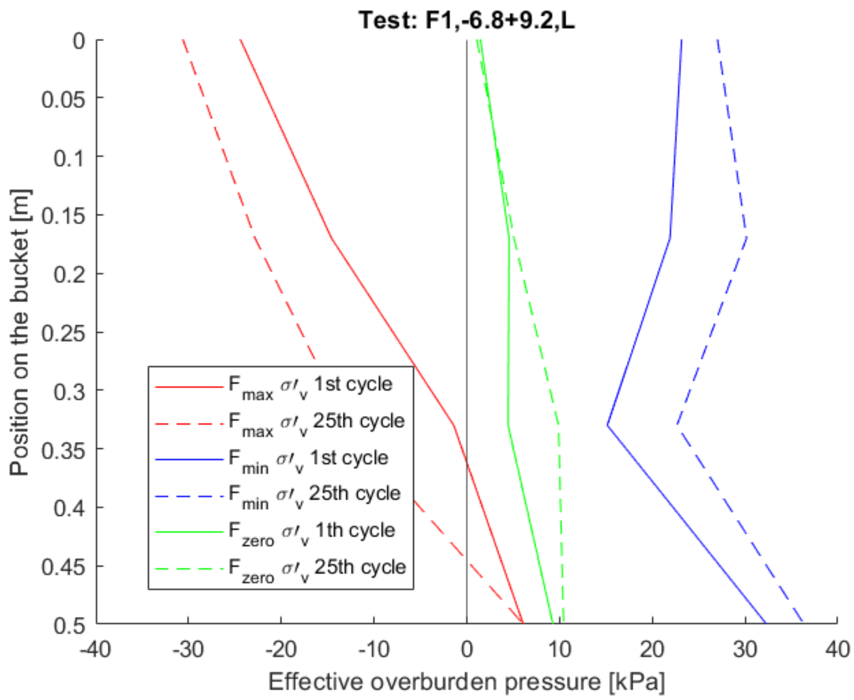

Figure F.13: Overburden pressure build up from 1st to 25th cycle.

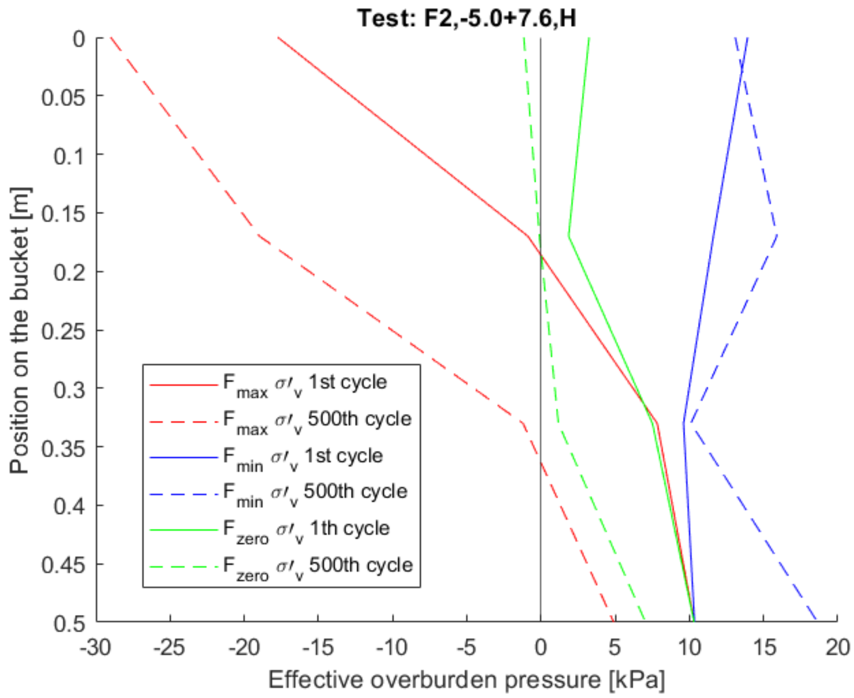

Figure F.14: Overburden pressure build up from 1st to 500th cycle.

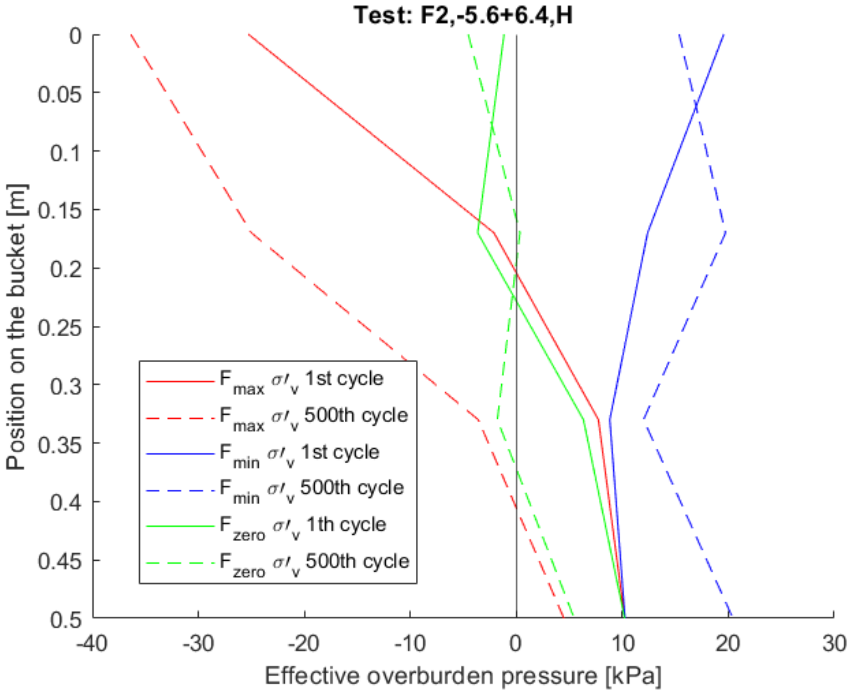

Figure F.15: Overburden pressure build up from 1st to 500th cycle.

F.2 Stable - Overburden pressure build up

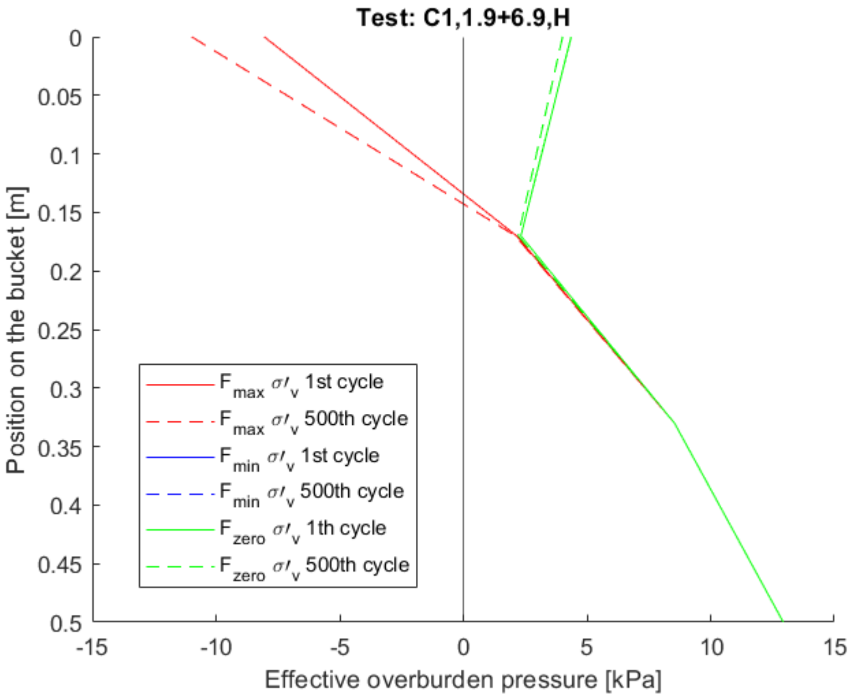

Figure F.16: Overburden pressure build up from 1st to 500th cycle.

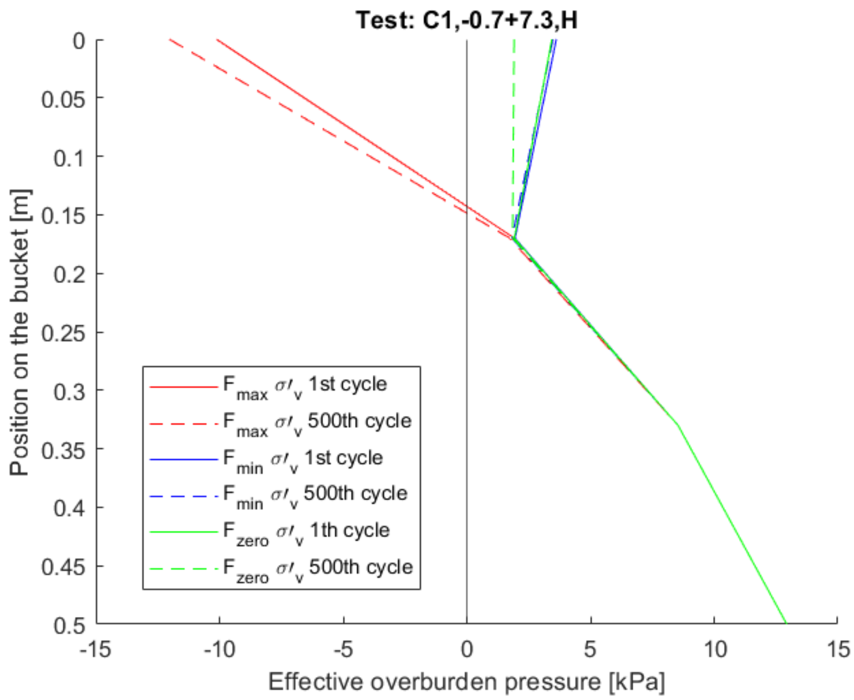

Figure F.17: Overburden pressure build up from 1st to 500th cycle.

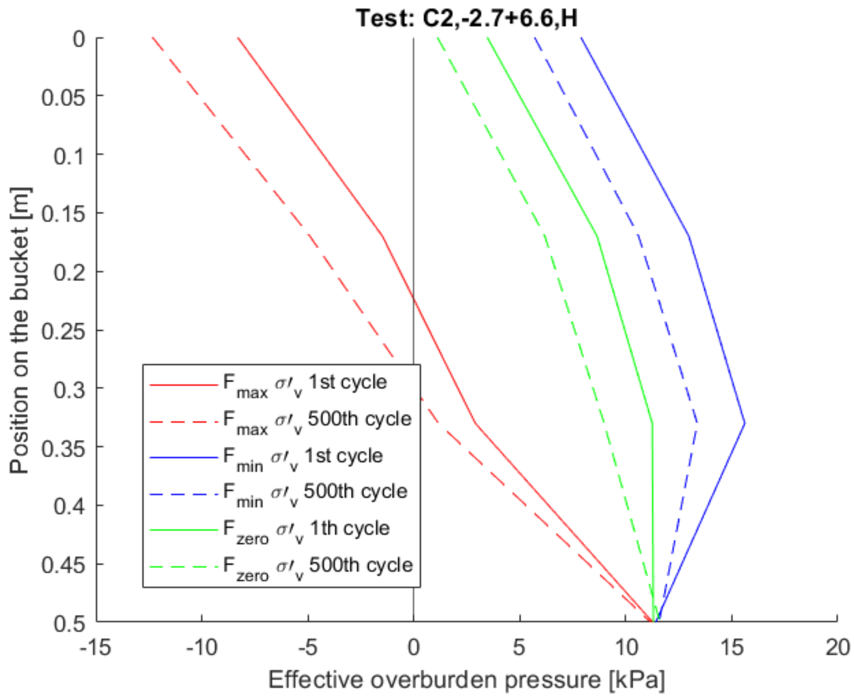

Figure F.18: Overburden pressure build up from 1st to 500th cycle.

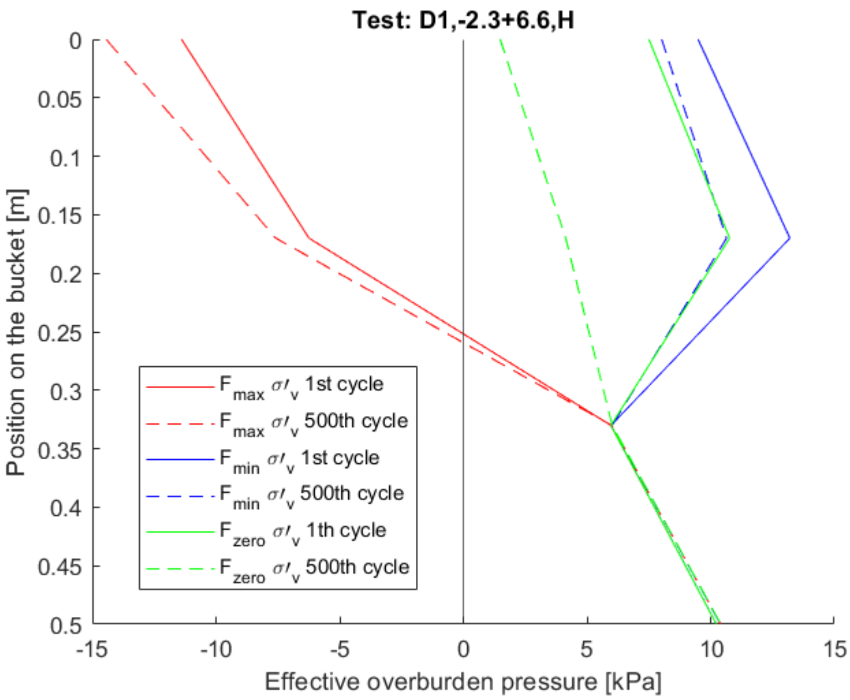

Figure F.19: Overburden pressure build up from 1st to 500th cycle.

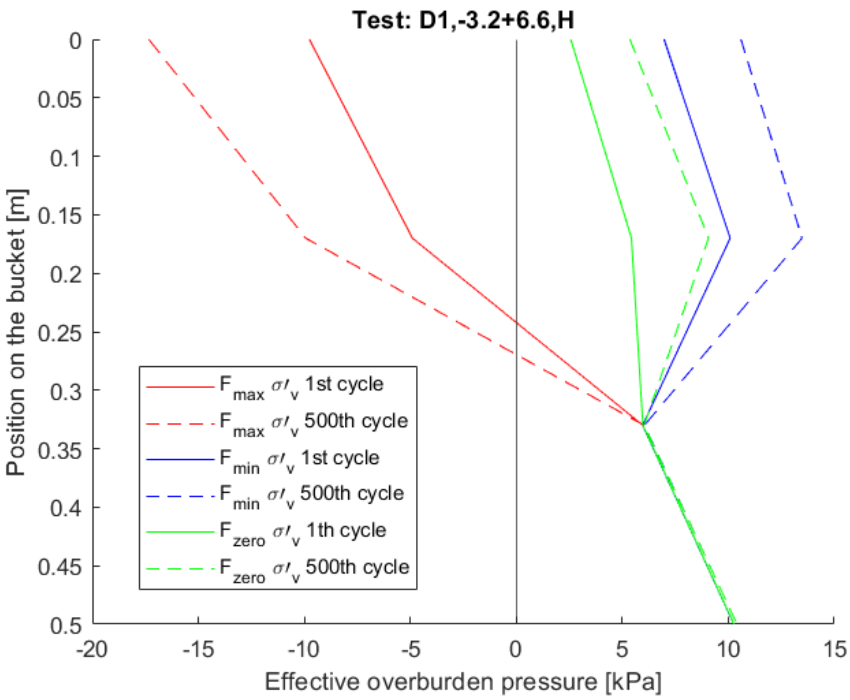

Figure F.20: Overburden pressure build up from 1st to 500th cycle.

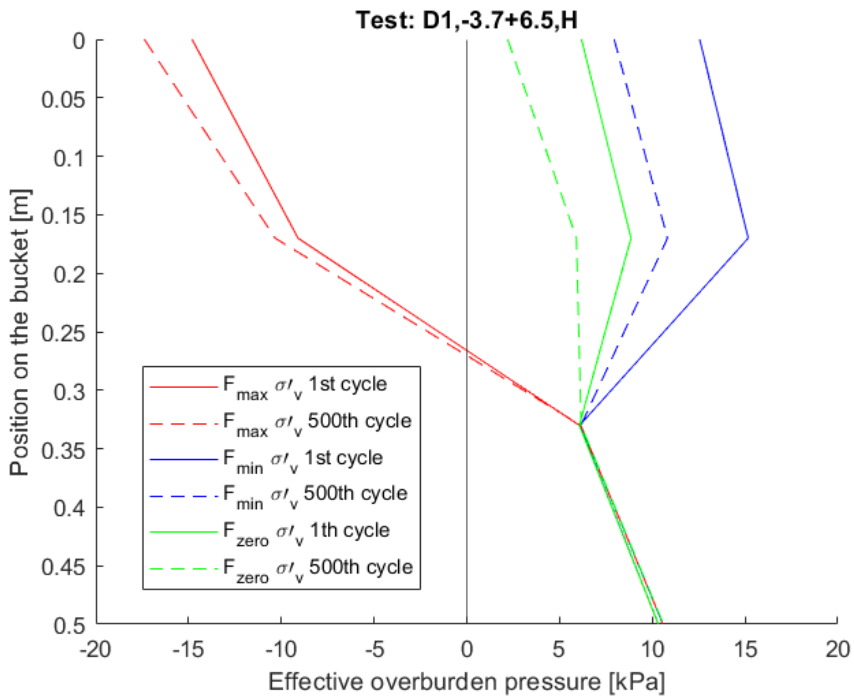

Figure F.21: Overburden pressure build up from 1st to 500th cycle.

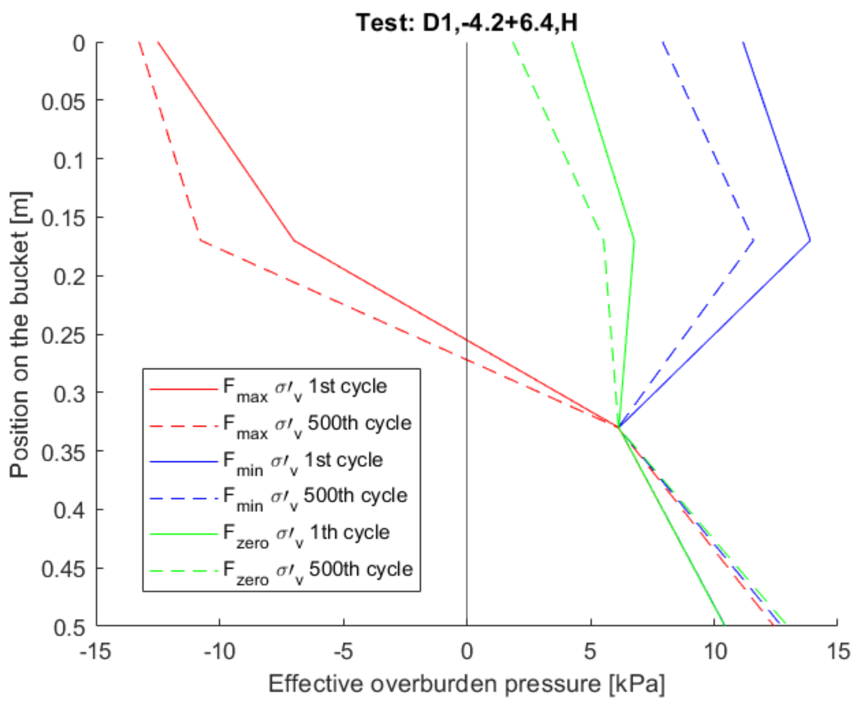

Figure F.22: Overburden pressure build up from 1st to 500th cycle.

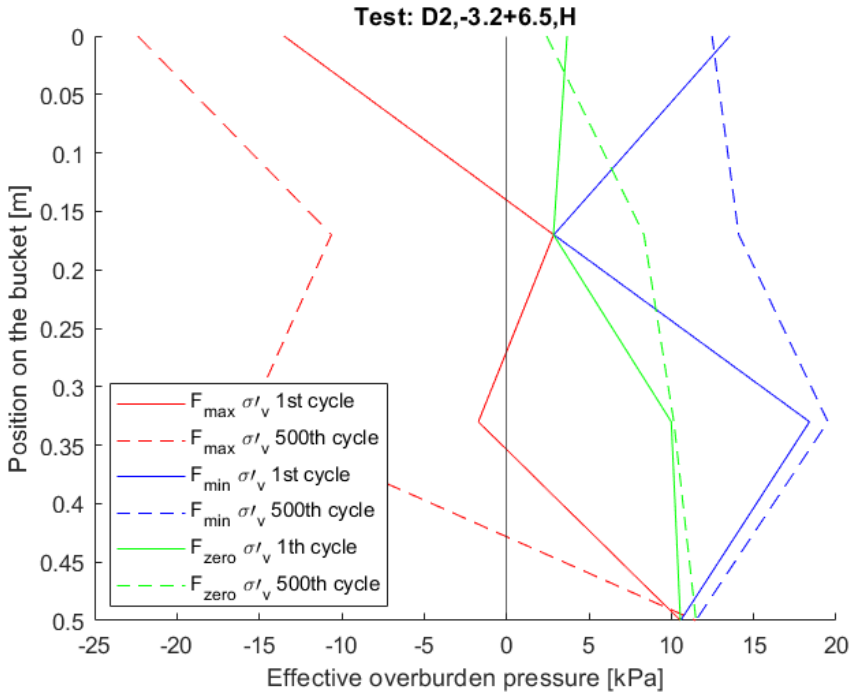

Figure F.23: Overburden pressure build up from 1st to 500th cycle.

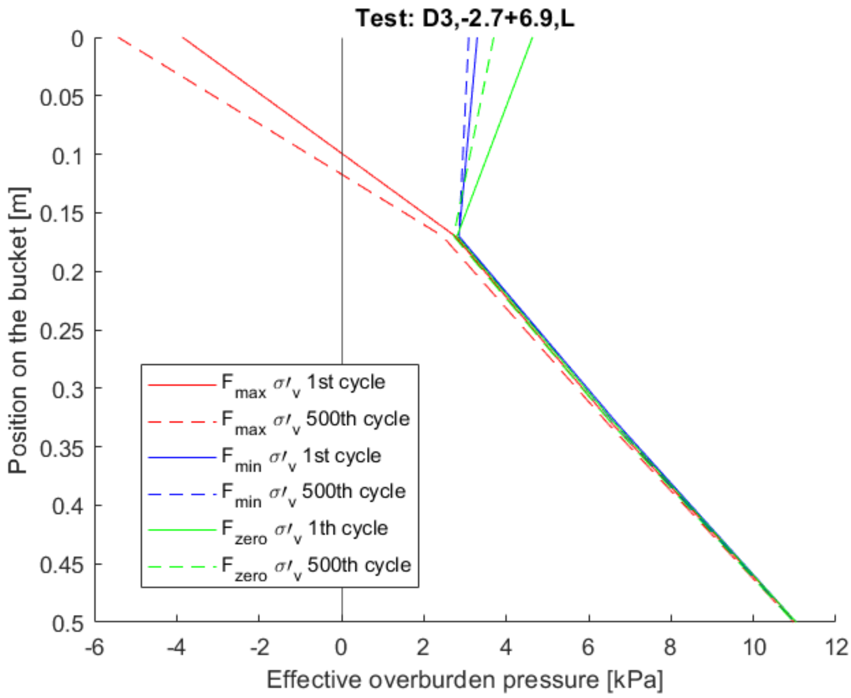

Figure F.24: Overburden pressure build up from 1st to 500th cycle.

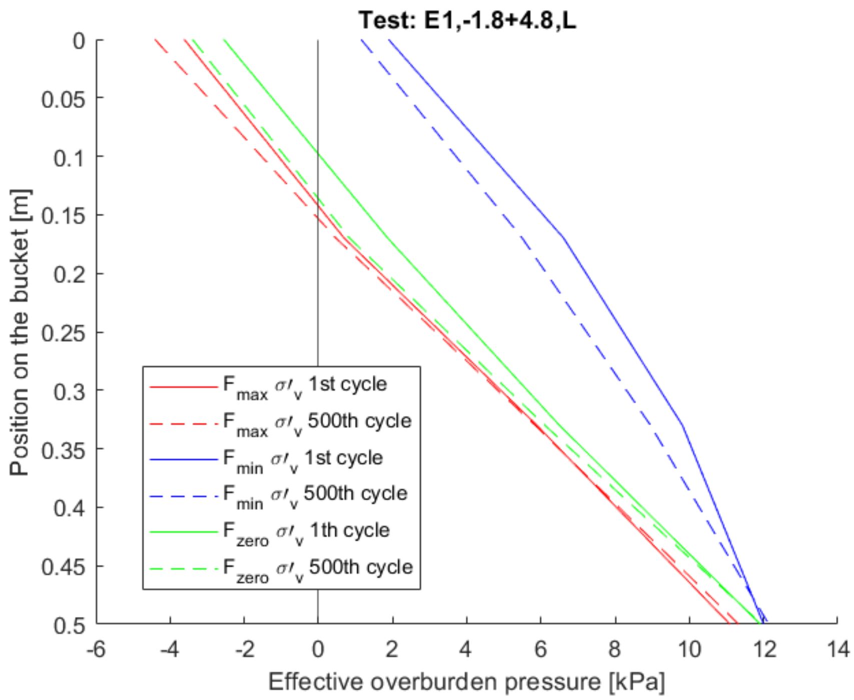

Figure F.25: Overburden pressure build up from 1st to 500th cycle.

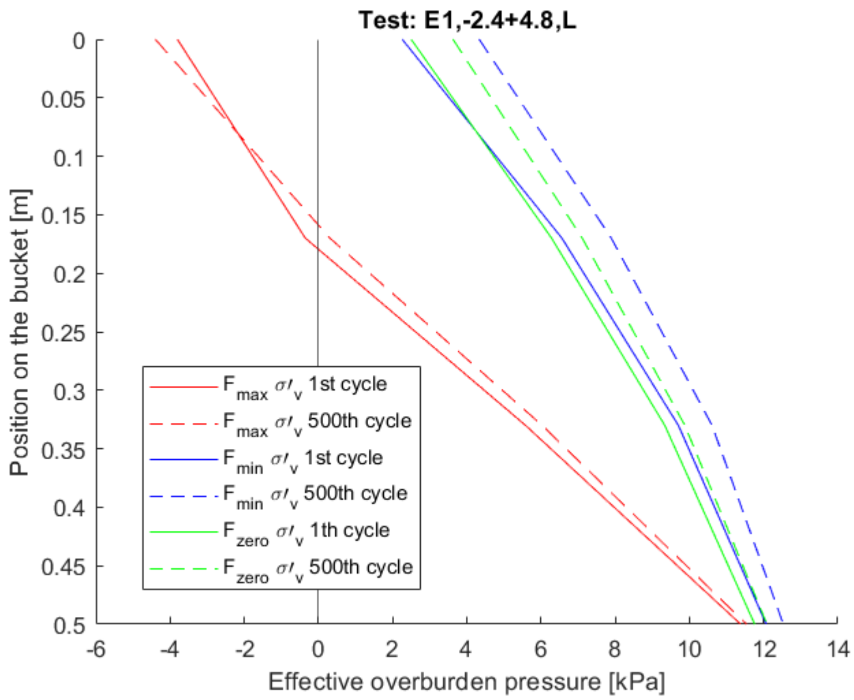

Figure F.26: Overburden pressure build up from 1st to 500th cycle.

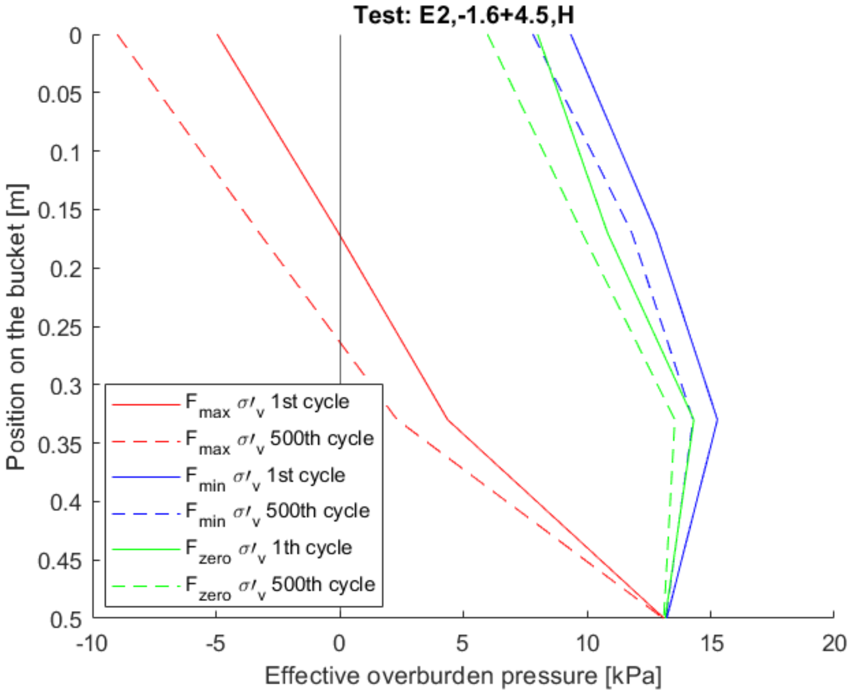

Figure F.27: Overburden pressure build up from 1st to 500th cycle.

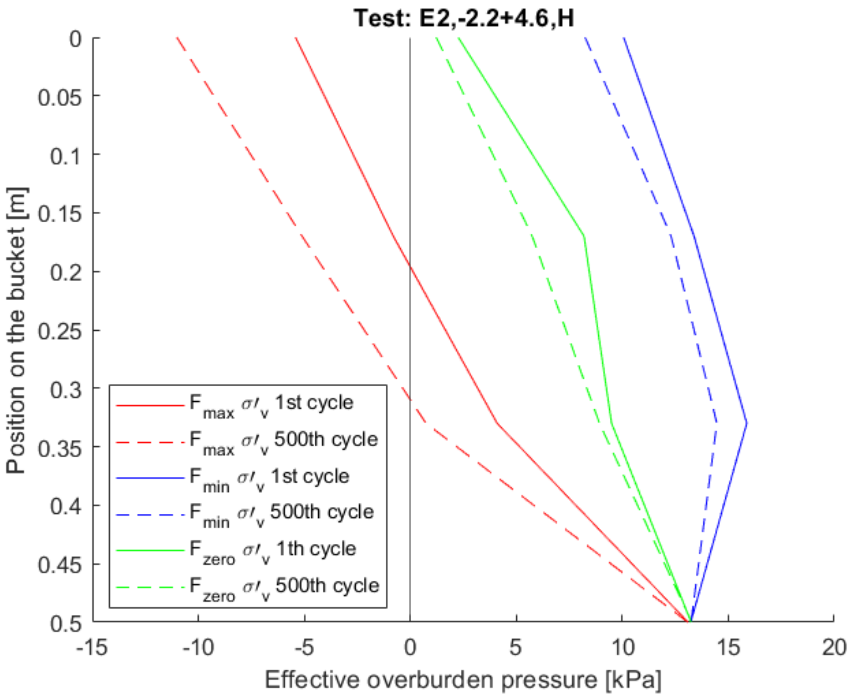

Figure F.28: Overburden pressure build up from 1st to 500th cycle.

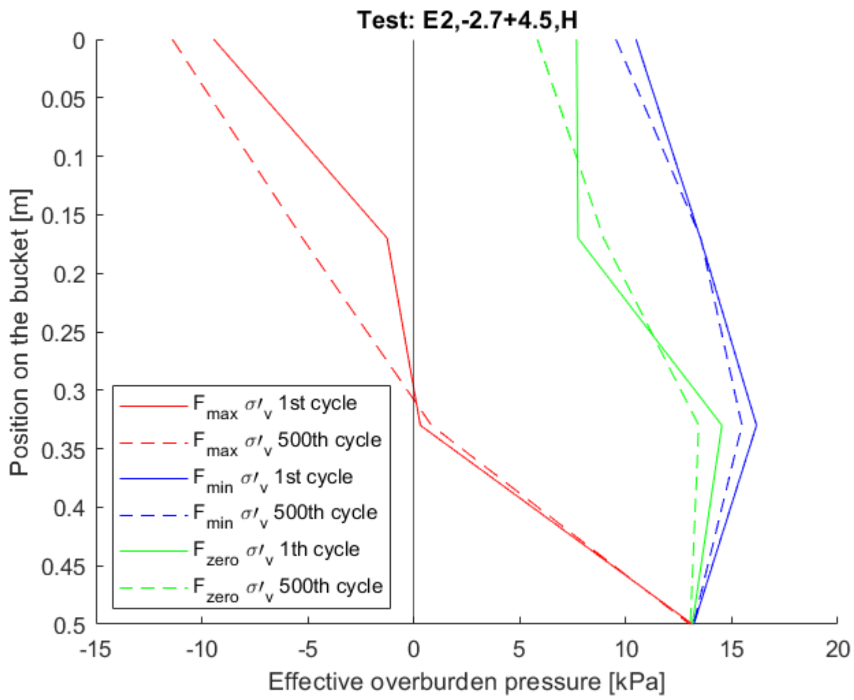

Figure F.29: Overburden pressure build up from 1st to 500th cycle.

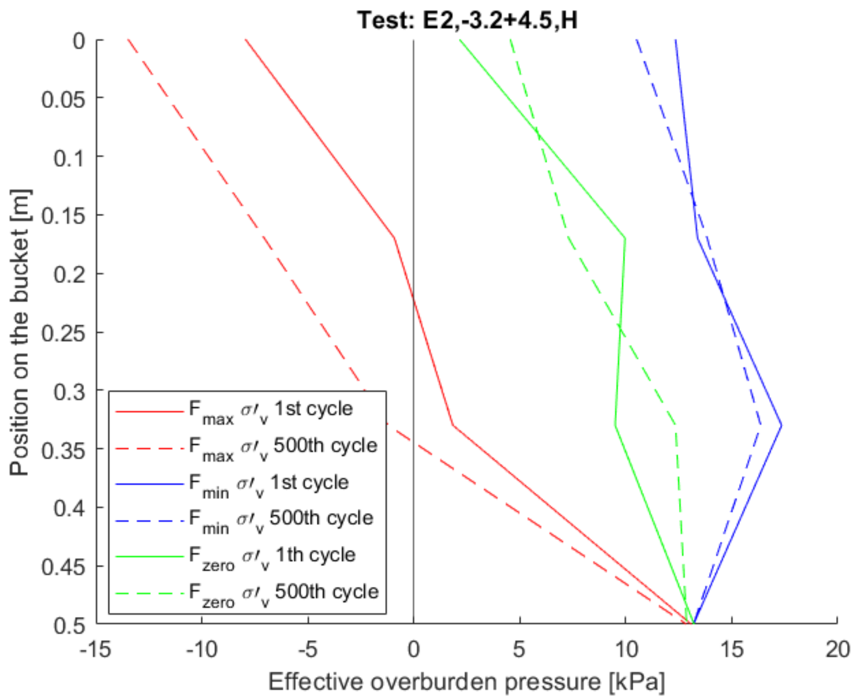

Figure F.30: Overburden pressure build up from 1st to 500th cycle.

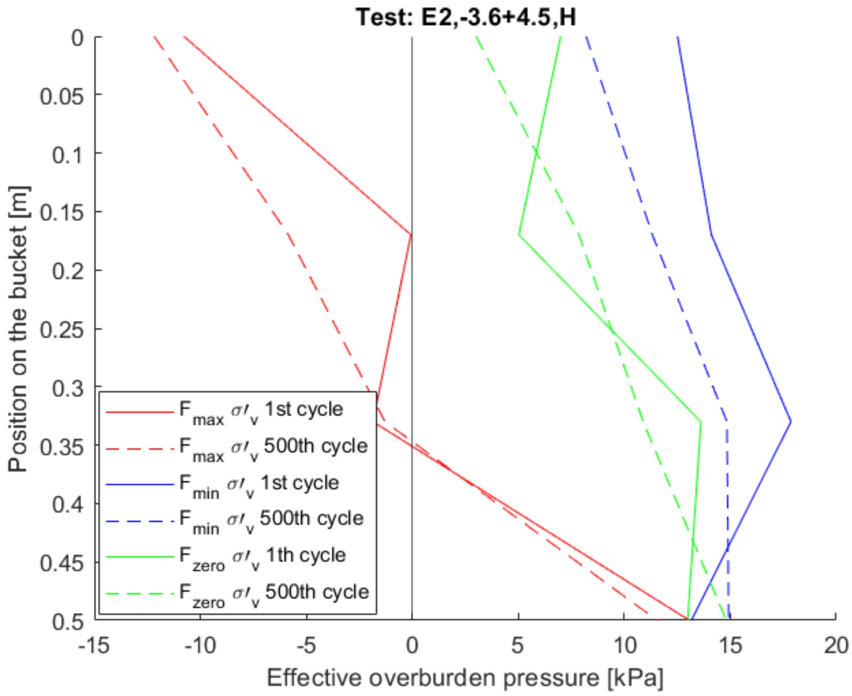

Figure F.31: Overburden pressure build up from 1st to 500th cycle.

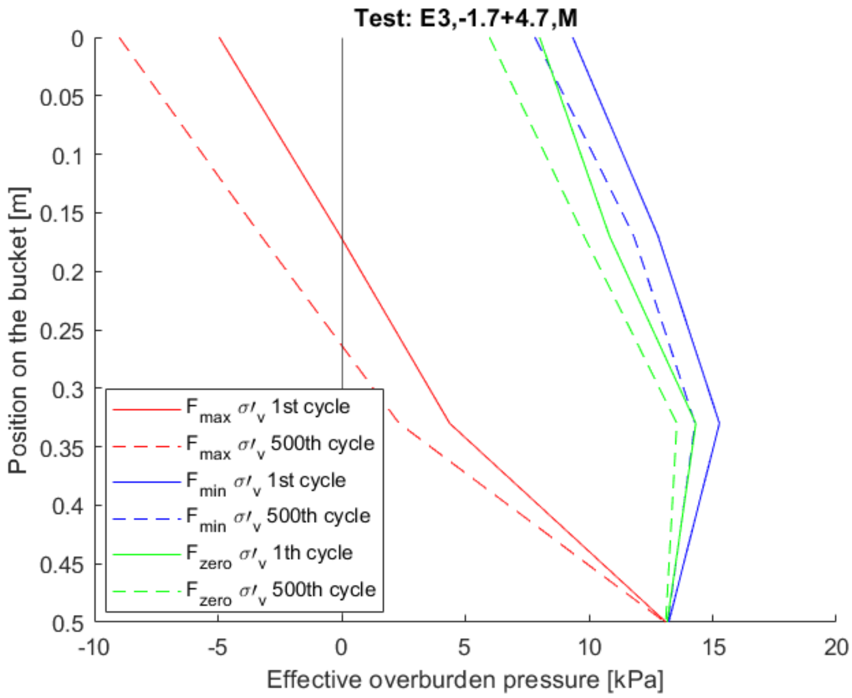

Figure F.32: Overburden pressure build up from 1st to 500th cycle.

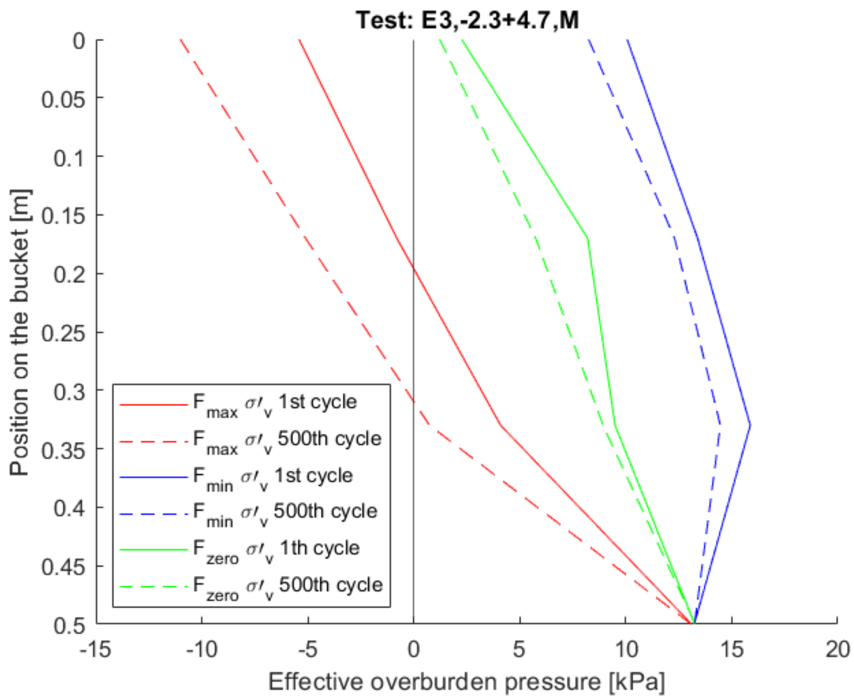

Figure F.33: Overburden pressure build up from 1st to 500th cycle.

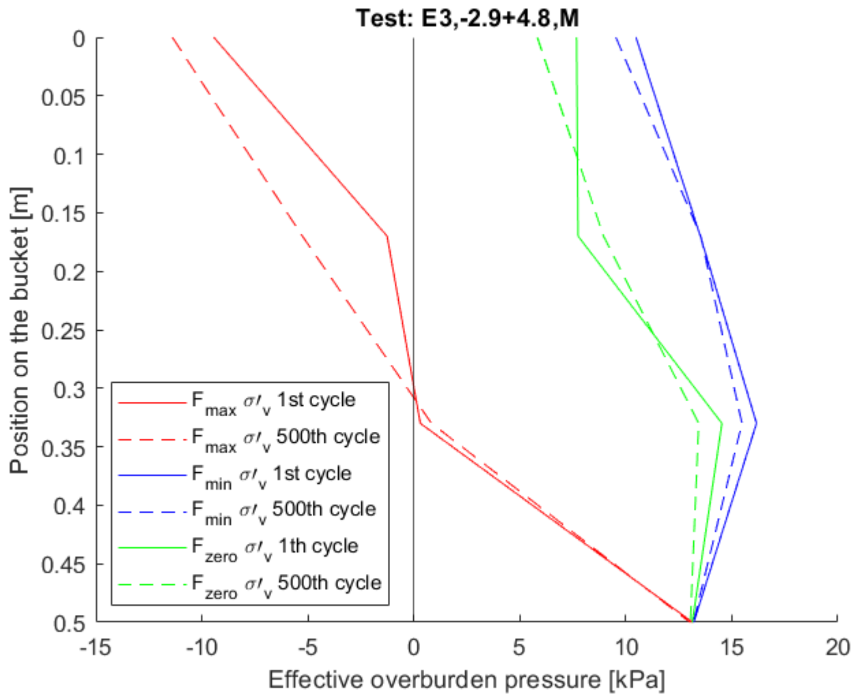

Figure F.34: Overburden pressure build up from 1st to 500th cycle.

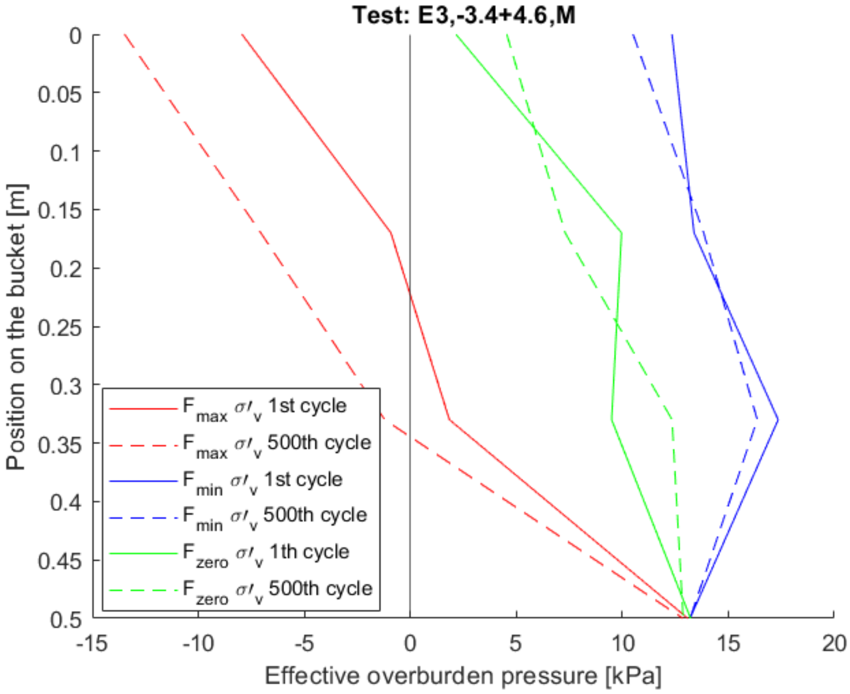

Figure F.35: Overburden pressure build up from 1st to 500th cycle.

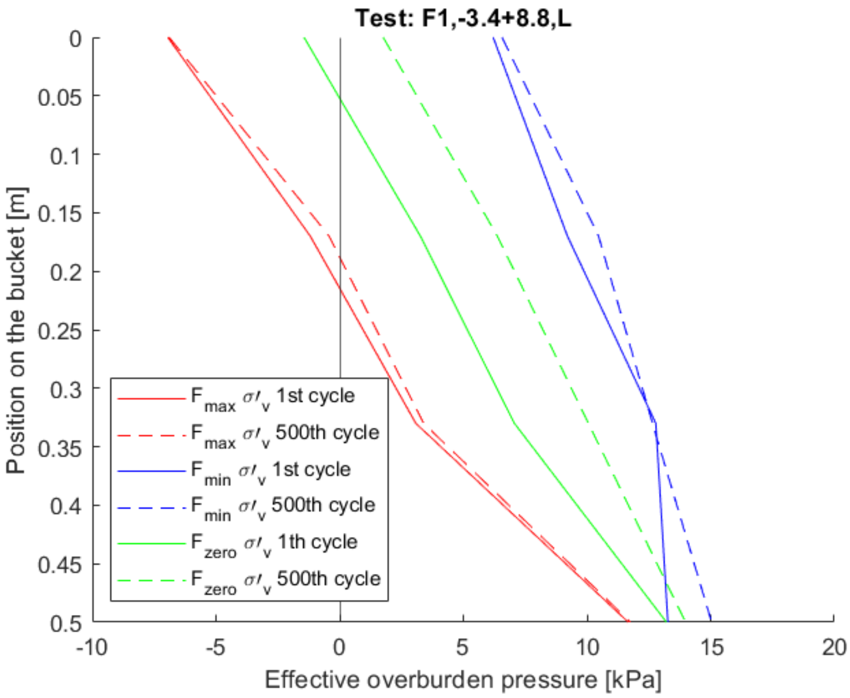

Figure F.36: Overburden pressure build up from 1st to 500th cycle.

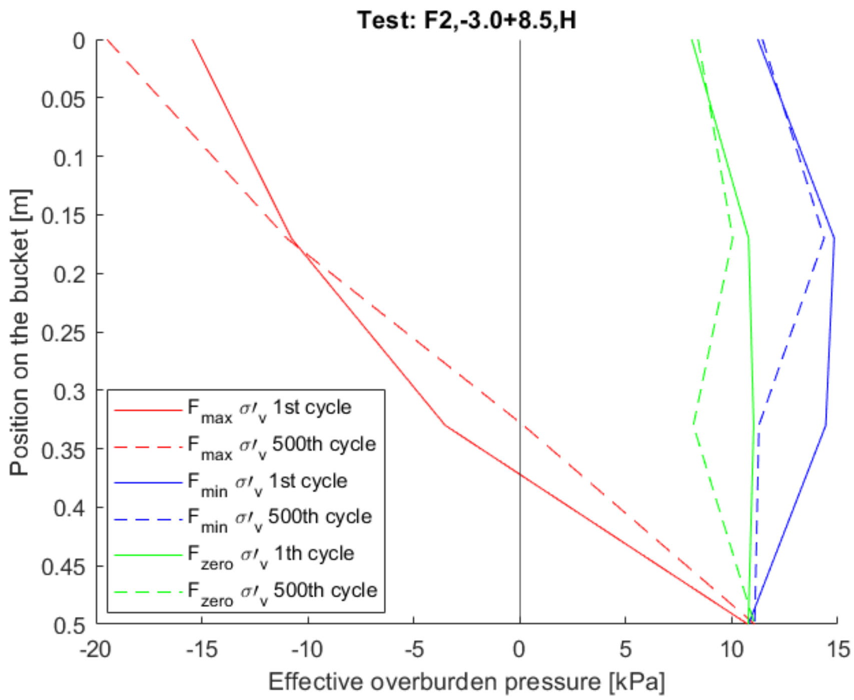

Figure F.37: Overburden pressure build up from 1st to 500th cycle.

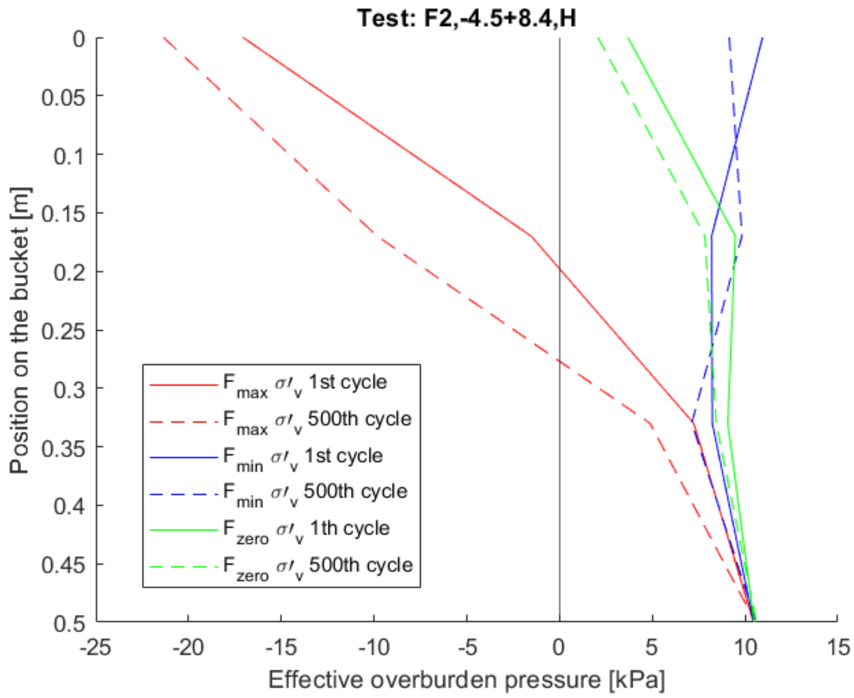

Figure F.38: Overburden pressure build up from 1st to 500th cycle.

F.3 Pushed down - Overburden pressure build up

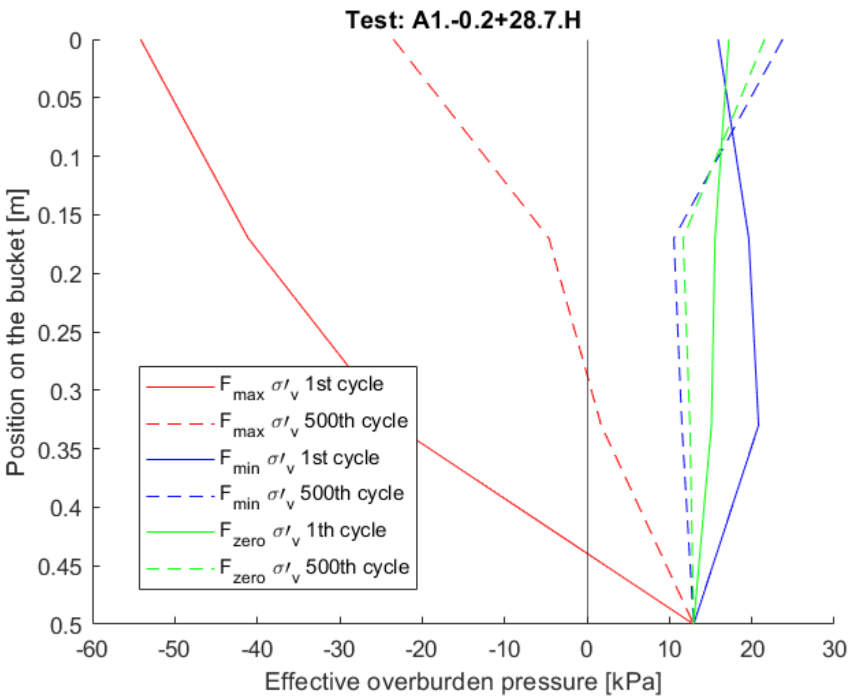

Figure F.39: Overburden pressure build up from 1st to 500th cycle.

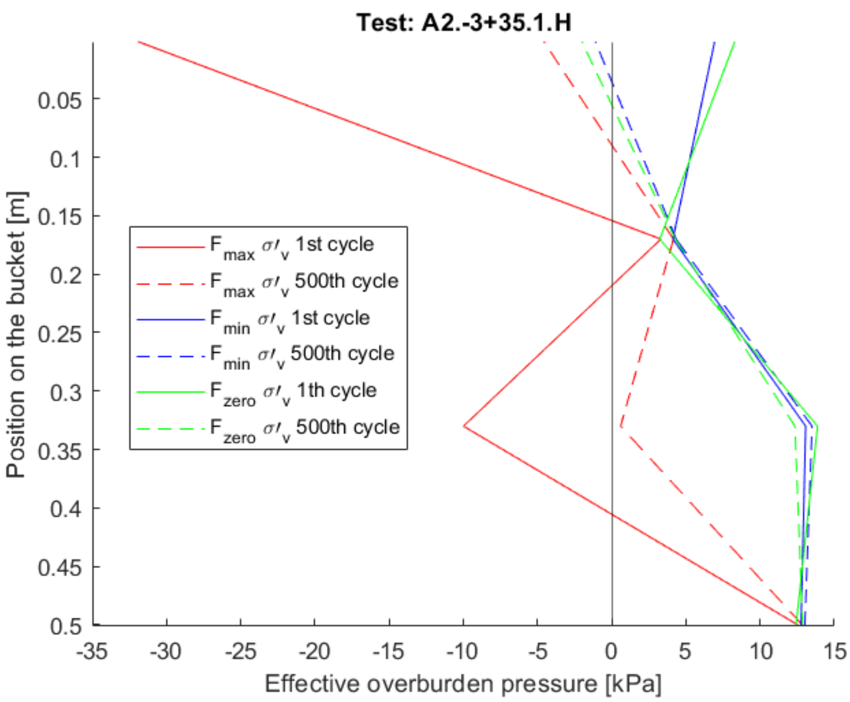

Figure F.40: Overburden pressure build up from 1st to 500th cycle.

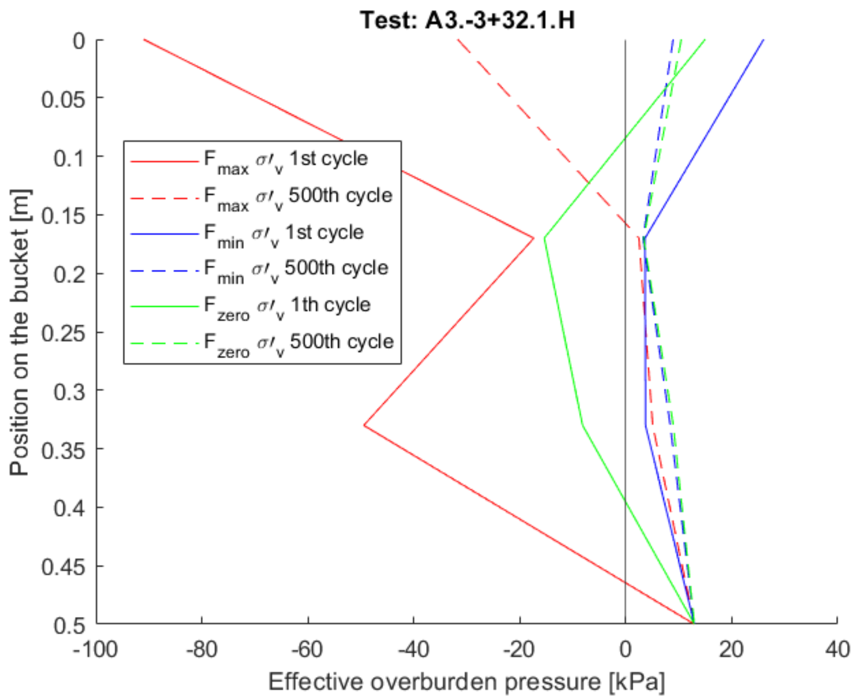

Figure F.41: Overburden pressure build up from 1st to 500th cycle.

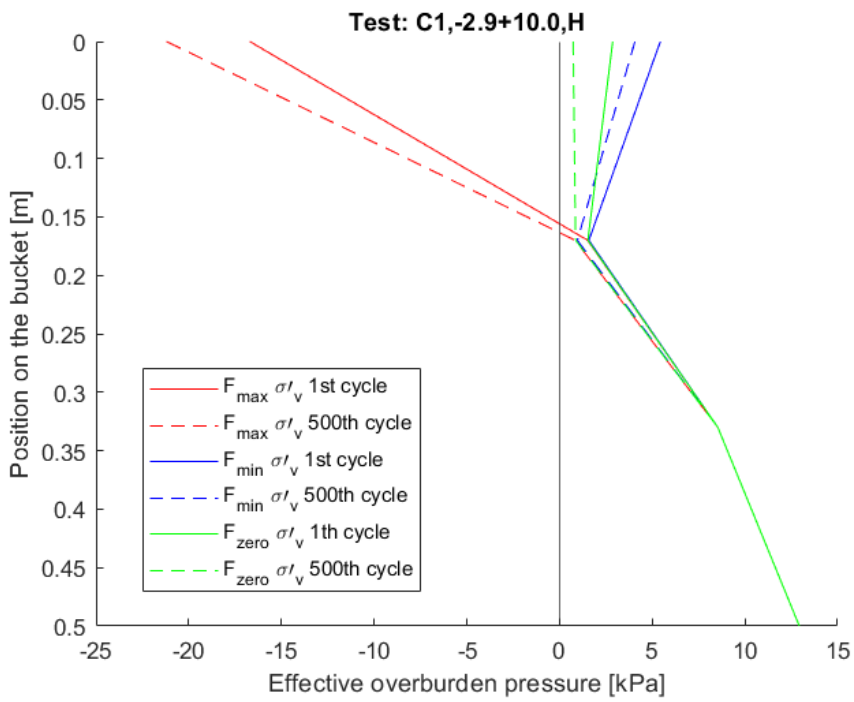

Figure F.42: Overburden pressure build up from 1st to 500th cycle.

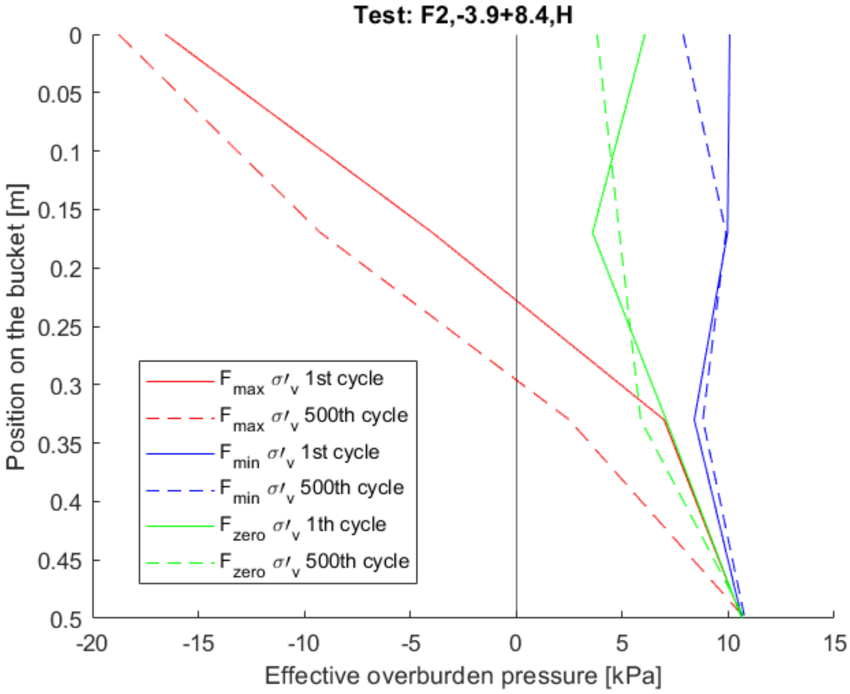

Figure F.43: Overburden pressure build up from 1st to 500th cycle.

Appendix G | Unloading / Reloading Stiffness

This appendix is a continuation of section 5.4 on page 52 where unloading / reloading stiffness of all three groups of tests were introduced, but plots with stiffness of only first 500 cycles were presented. Here stiffness over entire tests can be seen.

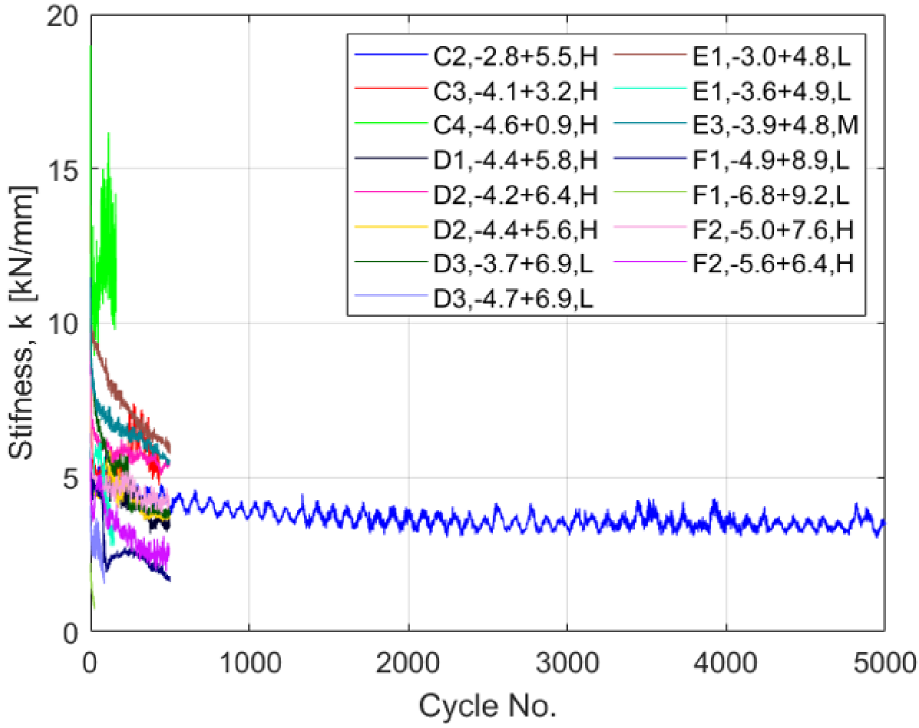

Figure G.1: Unloading/reloading stiffness of first group of tests

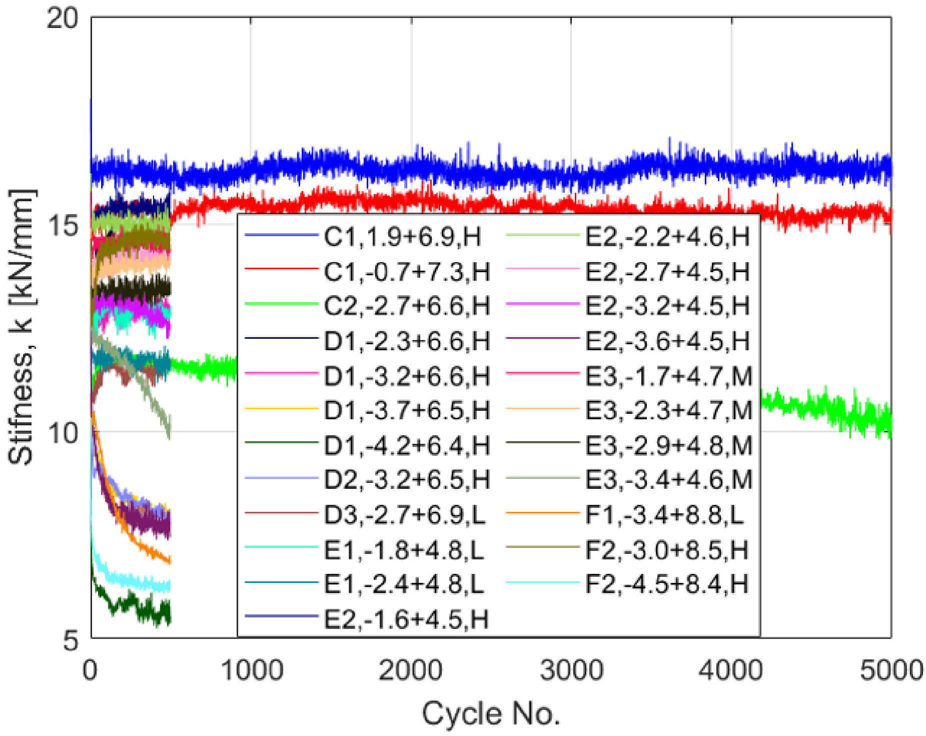

Figure G.2: Unloading/reloading stiffness of second group of tests

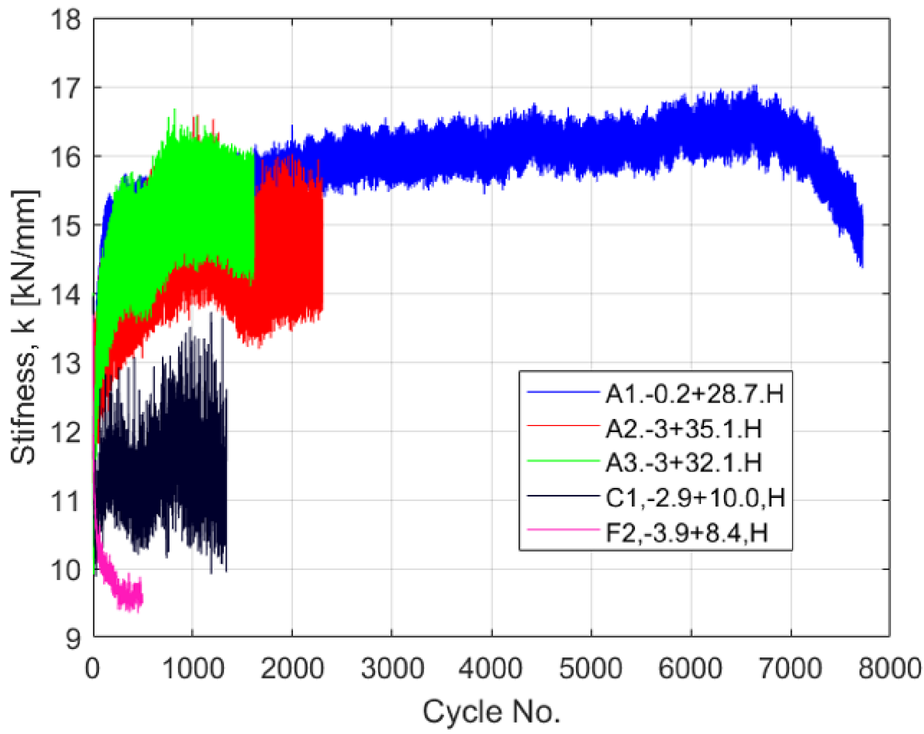

Figure G.3: Unloading/reloading stiffness of third group of tests

Appendix H | Displacement Tendencies

H.1 Force ratio vs displacement

When looking at the group which got pulled up, it is noticed that there is a correlation between force ratio and the displacement, by the first look in figure H.1 it seems like when the force ratio decreases then the displacement increases for instance from test 1 to test 3, and then again from test 3 to 5 the force ratio increases, but with negative signs, then the displacement decreases. This tendency is also seen for the other two scenarios for the neutral group and pushed down group, and can be seen in figure H.2 and H.3. It is of course hard to see a clear tendency for the pushed down tests, since only 5 tests resulted in the bucket being pushed down.

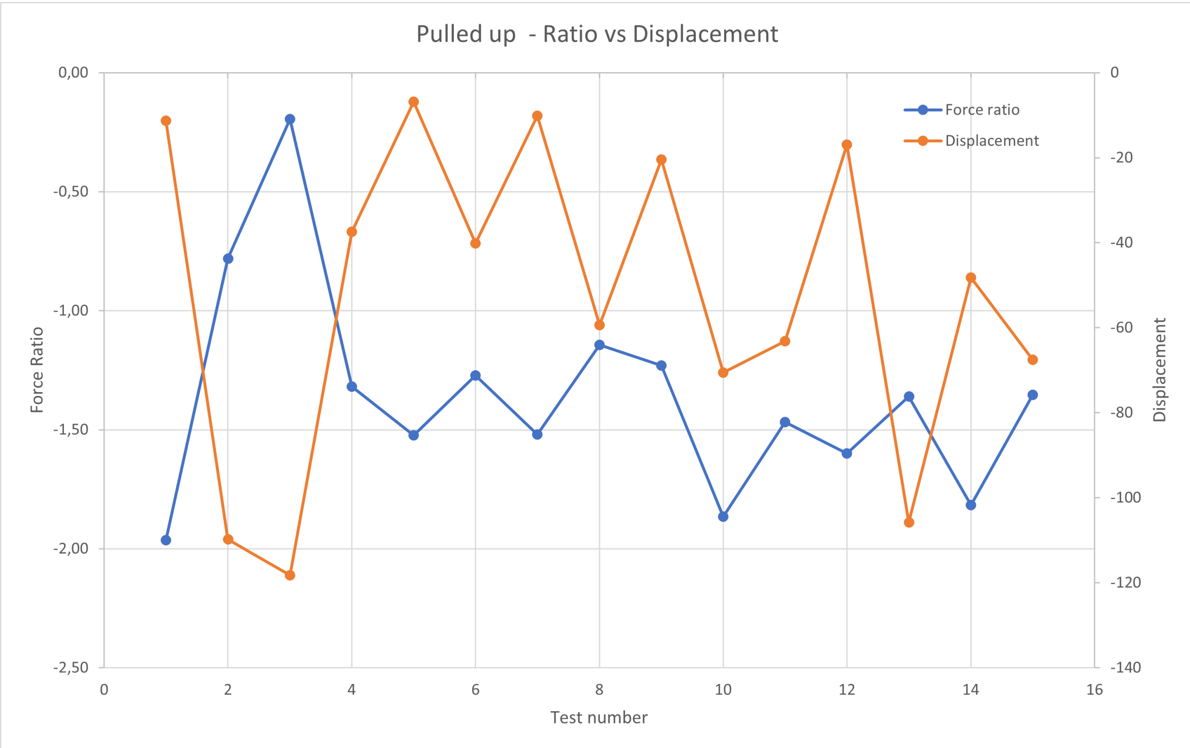

Figure H.1: Comparison of force ratio and displacement

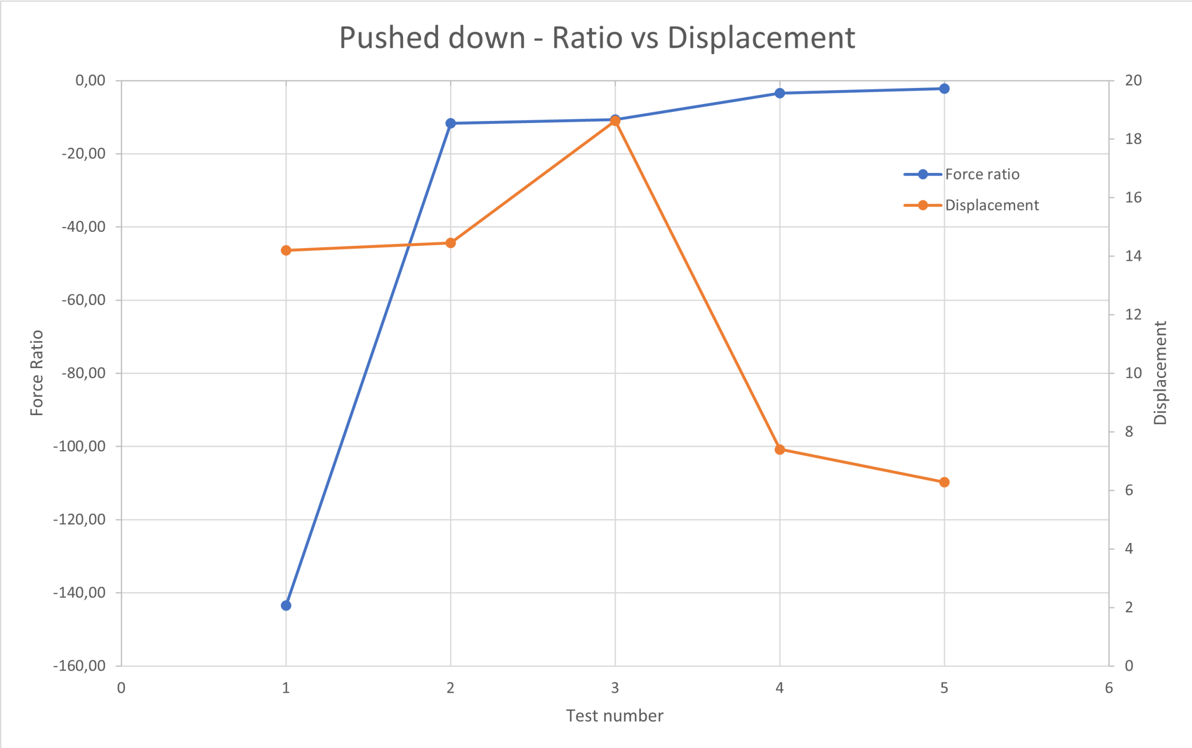

Figure H.2: Comparison of force ratio and displacement

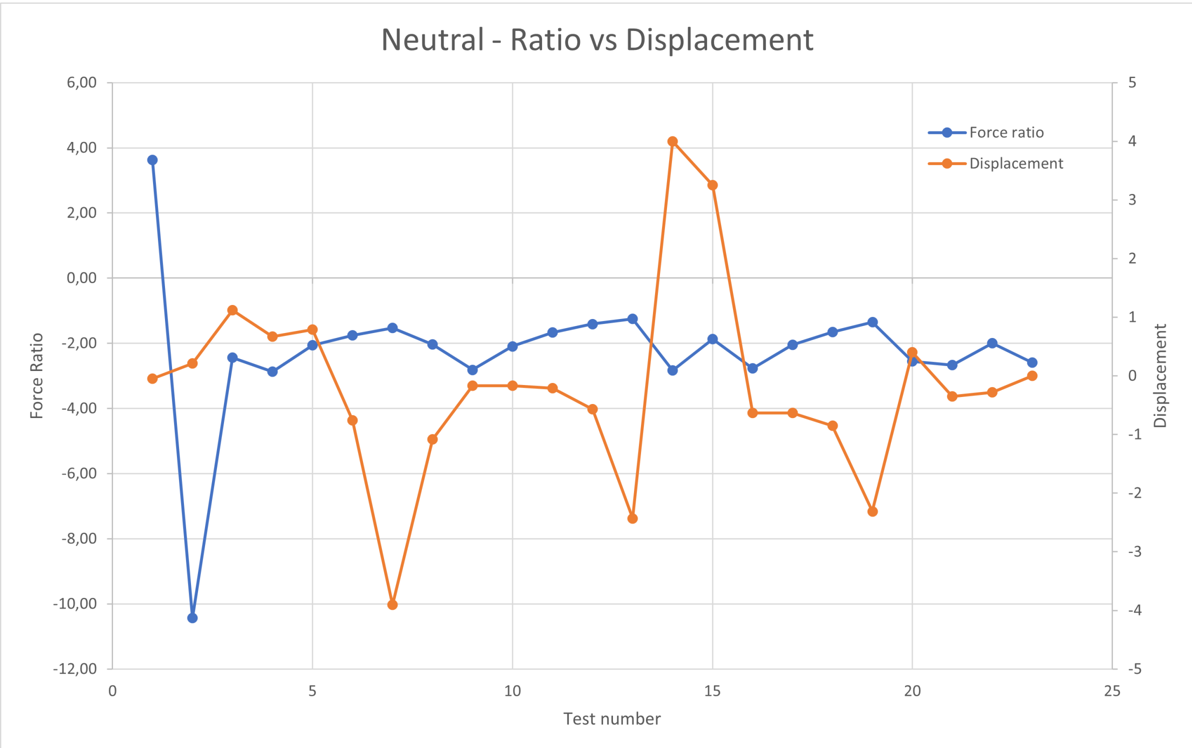

Figure H.3: Comparison of force ratio and displacement

H.2 Max force vs displacement

From figures H.5, H.5 and H.6 the displacement and compression force is plotted together. From the three investigated groups correlated follows some that each other in movement.

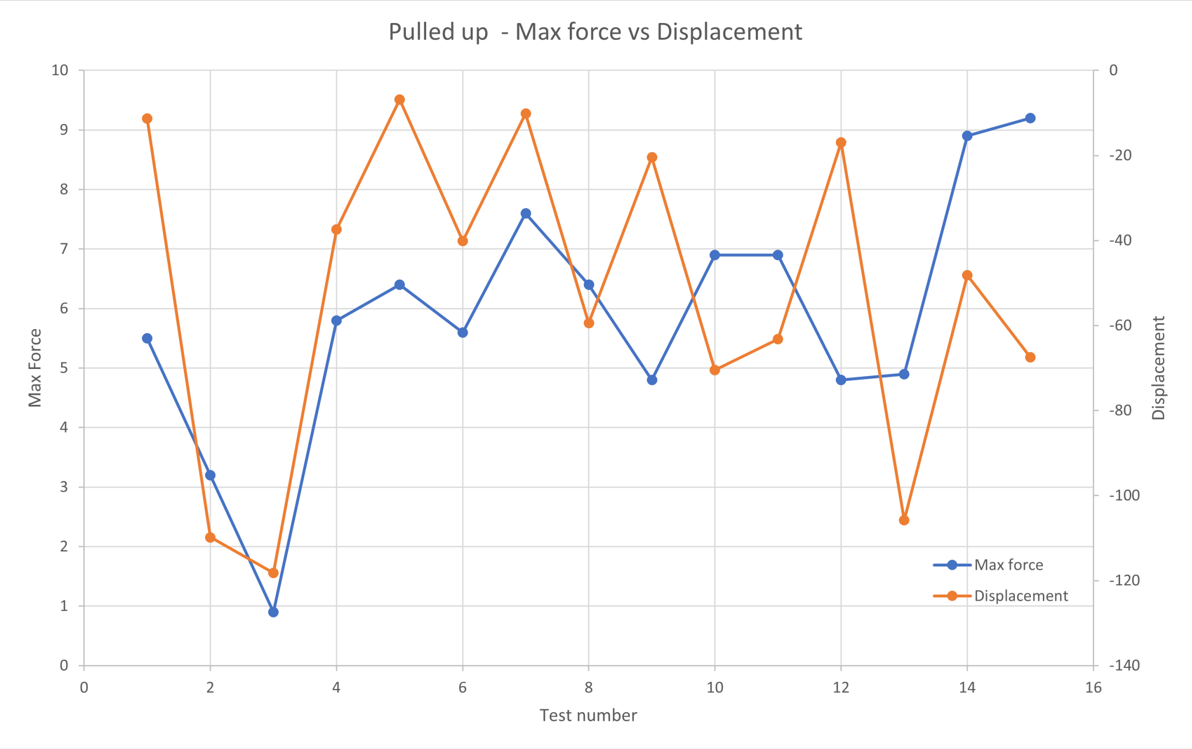

Figure H.4: Comparison of compressive force and displacement

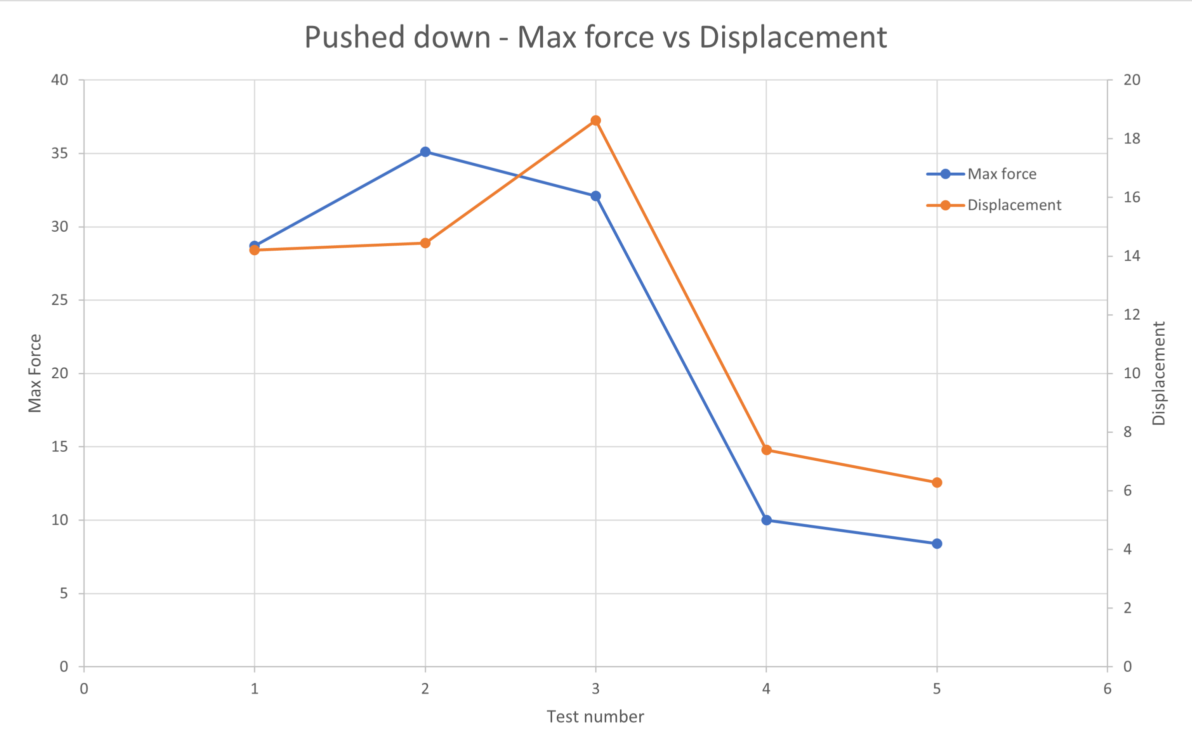

Figure H.5: Comparison of compressive force and displacement

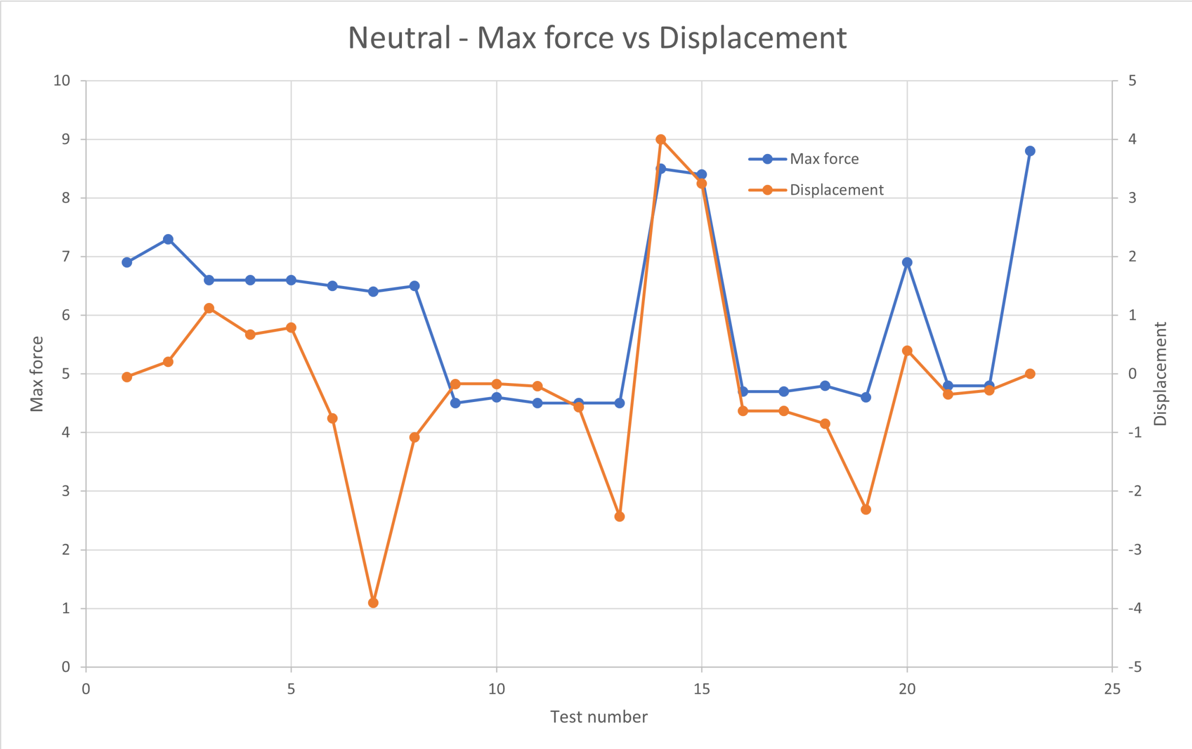

Figure H.6: Comparison of compressive force and displacement

Min force vs displacement

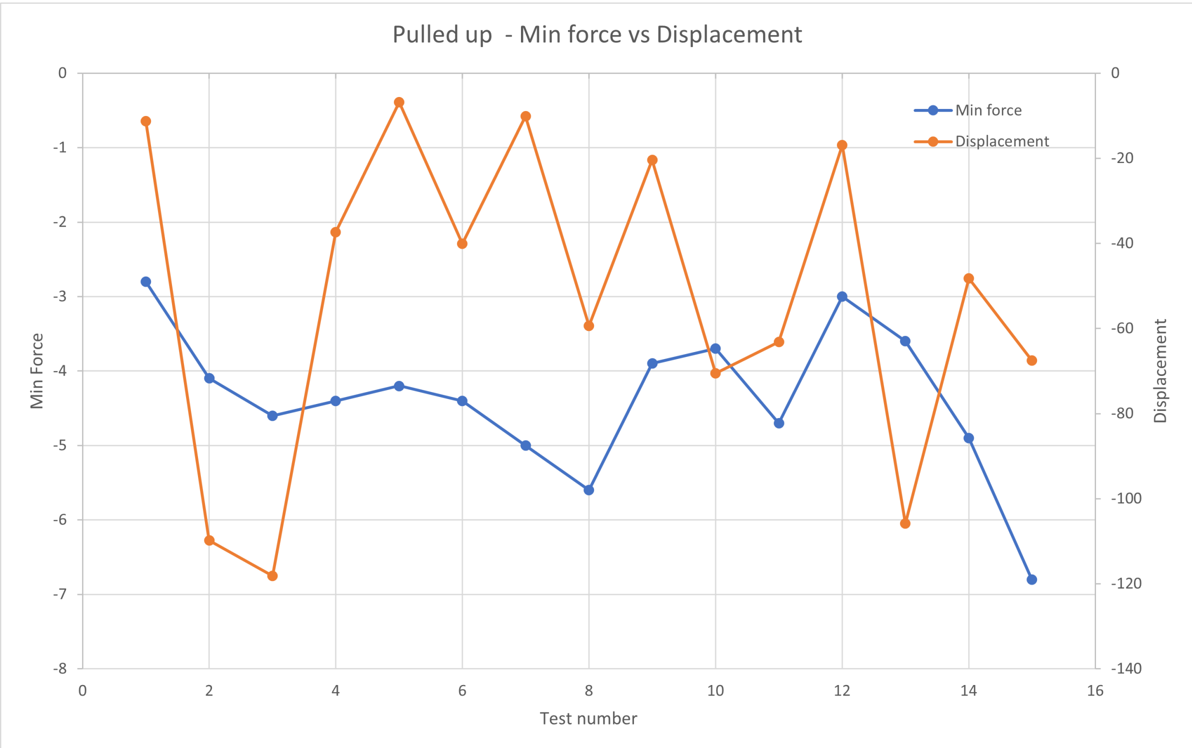

Figure H.7: Comparison of tensile force and displacement

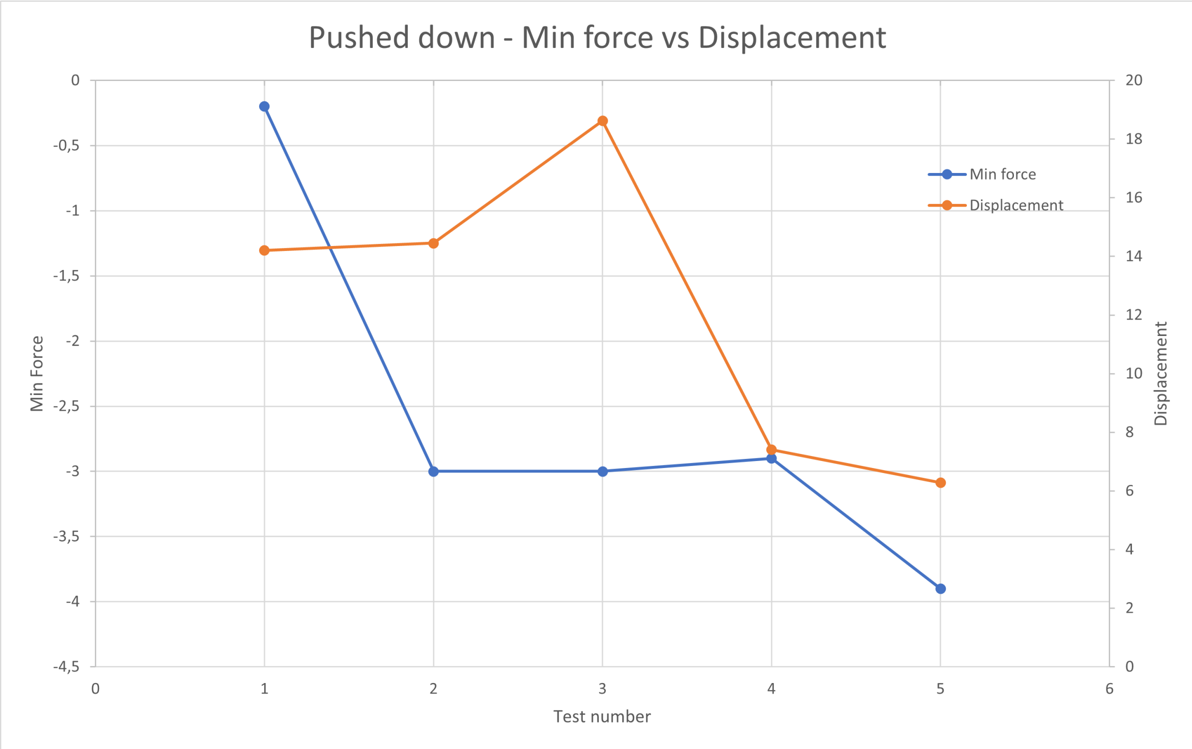

Figure H.8: Comparison of tensile force and displacement

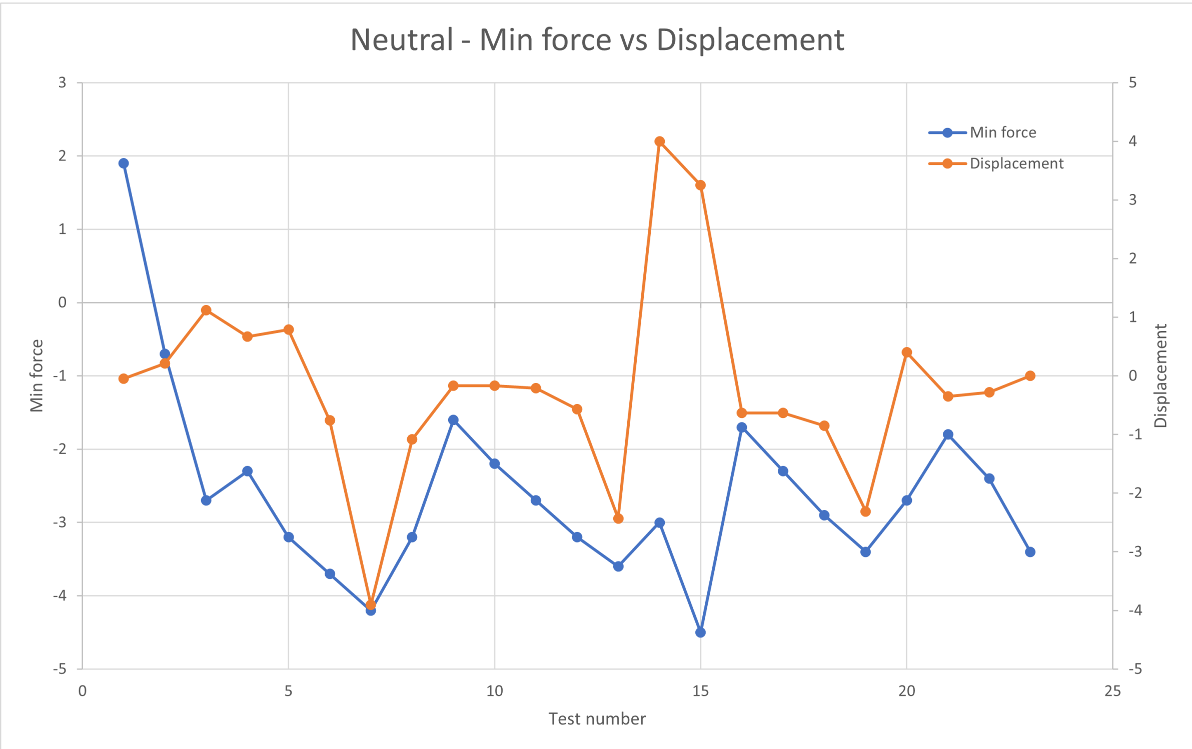

Figure H.9: Comparison of tensile force and displacement